PROCEEDINGS OF THE ELEVENTH RADIATION PHYSICS AND PROTECTION CONFERENCE

Atomic Energy Authority Headquarter

Nasr City, Cairo - Egypt

(25-28 November 2012)

Organized by

Atomic Energy Authority
National Network of Radiation Physics

Contents of the Eleventh Radiation Physics and Protection Conference Proceedings

Fukushima Nuclear Accident, the Third International Severe Nuclear Power Plant Accident

Samia M. Rashad
Nuclear and Radiological Regulatory Authority
Cairo, Egypt

ABSTRACT

Japan is the world's third largest power user. Japan's last remaining nuclear reactor shutdown on Saturday 4th of May 2012 leaving the country entirely nuclear free. All of 50 of the nation's operable reactors (not counting for the four crippled reactors at Fukushima) are now offline. Before last year's Fukushima nuclear disaster, the country obtained 30% of its energy from nuclear plants, and had planned to produce up to 50% of its power from nuclear sources by 2030.

Japan declared states of emergency for five nuclear reactors at two power plants after the units lost cooling ability in the aftermath of Friday 11 March 2011 powerful earthquake. Thousands of (14000) residents were immediately evacuated as workers struggled to get the reactors under control to prevent meltdowns.

On March 11th, 2011, Japan experienced a sever earthquake resulting in the shutdown of multiple reactors. At Fukushima Daiichi site, the earthquake caused the loss of normal AC power. In addition it appeals that the ensuing tsunami caused the loss of emergency AC power at the site. Subsequent events caused damage to fuel and radiological releases offsite. The spent fuel problem is a wild card in the potentially catastrophic failure of Fukushima power plant. Since the Friday's 9.0 earthquake, the plant has been wracked by repeated explosions in three different reactors.

Nuclear experts emphasized there are significant differences between the unfolding nuclear crisis at Fukushima and the events leading up to the Chernobyl disaster in 1986. The Chernobyl reactor exploded during a power surge while it was in operation and released a major cloud of radiation because the reactor had no containment structure around to. At Fukushima, each reactor has shutdown and is inside a 20 cm-thick steel pressure vessel that is designed to contain a meltdown. The pressure vessels themselves are surrounded by steel-lined, reinforced concrete shells. Chernobyl disaster was classified 7 on the International Nuclear and Radiological Event Scale (INES). The release of I-131 and CS-137 alone corresponds to a 500.000 T Bq I-131 equivalent. Taken all Fukushima Daichi reactors into consideration this is obviously an INES 7event.

In this paper a summary of events at Fukushima will be given, review of the risks that seaside reactors face from natural disasters, roadmap of environmental remediation activities, Japanese earthquake and tsunami

implications for the UK Nuclear Industry and the US-NRC recommendations for enhancing reactor safety in the 21Th century.

1- INTRODUCTION

The IAEA Incident and Emergency center received Information from the International seismic safety center (ISSC) at around 8:15 CET 11 March morning about the earthquake of magnitude 8.9 near the coast of Honshu, Japan. Japan's nuclear and Industrial Safety Agency (NISA) has heightened State of alerts has been declared at Fukushima Dainchi NPP. NISA says the plant has been shut down and no release of radiation has been detected. Onagawa, Fukushima Daini and Tokai NPPs were also shut down automatically, and no radiation release has been detected. The IAEA received information from it's international seismic safety center that a second earthquake of magnitude 6.5 has stuck Japan near the Coast of Honshu, near the Tokai plant. The earthquake and tsunami caused problems with Fukushima Dainichi 1 Nuclear power reactors. The reactor are boiling water reactors, three of the six reactors at the site were in operation when the earthquake hit.

The reactors are designed to shutdown automatically when a quake strikes, and emergency diesel generators began the task of pumping water, around the reactors to cool them down. However stopped about an hour later. The failure of the back up generators has been blamed on tsunami flooding DC power from batteries was consumed after approximately 8 hours. At that point the plant experienced a complete blackout (no electric power at all). Hours passed as primary water inventory was lost and core degradation occurred (through some combination of zirconium oxidation and clad failure). Portable diesel generators were delivered to the plant site. AC power was restored allowing for a different backup pumping system to replace inventory in the reactor pressure vessel.

Considering the extremely wide use of radiation in the medical, industry, power and research reactors, radiological accidents are somewhat rare. Nevertheless the statistics reported by the US Departments of Energy REAC/TC organization clearly show that radiological accidents are not something that we can ignore. According to DOE-REAC/TC from 1944 to March 2000: 414 major accidents, 133742 persons involved, 2998 significantly exposed, and 127 fatalities. These statistics include Chernobyl Accident. The 414 major radiation accidents include: Criticalities: 22, Radiation devices: 307, and Radioisotopes: 85. Depending upon the Criteria used there have been only 6 to 12 accidents involving research or power reactors.

Since 16 March at the Fukushima Dainichi nuclear plant, radiation levels spiked three times since the earthquake, but have stabilized since 16 March at levels which are, although significantly higher than the normal levels, were within the range that allows workers to continue onsite recovery measures.

The spent fuel problem is a wild card in the potentially catastrophic failure of Fukushima power plant. Since the Friday's 9.0 earthquake, the plant has been wracked by repeated explosions in three different reactors. Spent fuel removed from a nuclear reactor is highly radioactive and generates intense heat. This fuel needs to be actively cooled for one to three years in pools that cool the fuel, shield the radioactivity and keep the fuel in the proper position to avoid fission reactions IF the cooling is lost, the water can boil and fuel rods can be exposed to the air, possibly leading to severve damage and a large release of radiation. In addition to pools in each of the plant's reactor buildings, there is another facility, the common use spent fuel pool-where spent fuel is stored after cooling at least 18 months the reactor buildings. The fuel is much cooler than the assemblies stored in the reactor buildings.

Katsuhiko who is professor of urban safety at kobe University, has highlighted three incidents at reactors between 2005 and 2007 atomic plants at Onagawa, Shika, and Kashiwazaki - Kariwa were all struck by earthquakes that triggered tremors stronger than those to which the reactor had been designed to survive. In the case of the incident at the Kushiwazaki reactor in northwestern Japan, a 6.8 Scale earthquake on 16 July 2007 set off a fire that balzed for two hours and allowed radioactive water to leak from the plant. However no action was taken in the wake of any of these incidents despite Katsuliko's warning at the time that the nation's reactors had fatal flaws in their design.

On 18 March, Japan assigned an INES rating of 5 to units 1, 2, 3 and INES rating of 4 to the site, take all Fukushima Daiichi reactors into consideration this is obviously INES 7 event.

2- Japanese Earthquake/Tsunami; Problems with Nuclear Reactors 3/12/2011

The Japanese earthquake and tsunami are natural catastrophes of historic proportions. The death toll is likely to be in the thousands. While the information is still not complete at this time, the tragic loss of life and destruction caused by the earthquake and tsunami will likely dwarf the damage caused by the problems associated with the impacted Japanese nuclear plants. Here is the best understanding of the sequence of events at the Fukushima I-1 power station.

- The plant was immediately shut down (scrammed) when the earthquake first hit. The automatic power system worked.
- All external power to the station was lost when the sea water swept away the power lines.
- Diesel generators started to provide backup electrical power to the plant’s backup cooling system. The backup worked.
- The diesel generators ceased functioning after approximately one hour due to tsunami induced damage, reportedly to their fuel supply.
- An Isolation condenser was used to remove the decay heat from the shutdown reactor.

- Apparently the plant then experienced a small loss of coolant from the reactor.
- Reactor Core Isolation Cooling (RCIC) pumps, which operate on steam from the reactor, were used to replace reactor core water inventory, however, the battery[7] supplied control valves lost DC power after the prolonged use.
- DC power from batteries was consumed after approximately 8 hours.
- At that point, the plant experienced a complete blackout (no electric power at all).
- Hours passed as primary water inventory was lost and core degradation occurred (through some combination of zirconium oxidation and clad failure).
- Portable diesel generators were delivered to the plant site.
- AC power was restored allowing for a different backup pumping system to replace inventory in reactor pressure vessel (RPV).
- Pressure in the containment drywell rose as wetwell became hotter.
- The Drywell containment was vented to outside reactor building which surrounds the containment.
- Hydrogen produced from zirconium oxidation was vented from the containment into the reactor building.
- Hydrogen in reactor building exploded causing it to collapse around the containment.
- The containment around the reactor and RPV were reported to be intact.
- The decision was made to inject seawater into the RPV to continue to the cooling process, another backup system that was designed into the plant from inception.
- Radioactivity releases from operator initiated venting appear to be decreasing.
- While there are risks associated with operating nuclear plants and other industrial facilities, the chances of an adverse event similar to what happened in Japan occurring in the US is small.
- Since September 11, 2001, additional safeguards and training have been put in place at US nuclear reactors which allow plant operators to cool the reactor core during an extended power outage and/or failure of backup generators – “blackout conditions.”

Japanese authorities are working as hard as they can, under extremely difficult circumstances, to stabilise the nuclear power plants and ensure safety."

3- THE RISKS WITH SEASIDE REACTORS

But the risks that seaside reactors like Fukushima face from natural disasters are well-known. Indeed, they became evident six years ago, when the Indian Ocean tsunami in December
2004 inundated India's second-largest nuclear complex, shutting down the Madras power station.

Many nuclear-power plants are located along coastlines, because they are highly water-intensive. Yet natural disasters such as storms, hurricanes, and tsunamis are becoming more common, owing to climate change, which win also cause a rise in ocean levels, making seaside reactors even more vulnerable.

For example, many nuclear-power plants located along the British coast are just a few metres above sea level. In 1992, Hurricane Andrew caused significant damage at the Turkey Point nuclear-power plant on Biscayne Bay, Florida, but, fortunately, not to any critical systems.

As global warming brings about a rise in average temperatures and ocean levels, inland reactors will increasingly contribute to, and be affected by, water shortages. During the record-breaking 2003 heatwave in France, operations at 17 commercial nuclear reactors had to be scaled back or stopped because of rapidly rising temperatures in rivers and lakes. Spain's reactor at Santa Maria de Garona was shut for a week in July 2006 after high temperatures were recorded in the Ebro river.

During the 2003 heat wave, Electricite de France, which operates 58 reactors the majority on ecologically sensitive rivers such as the Loire - was compelled to buy power from neighboring countries on the European spot market. The state-owned EDF, which normally exports power, ended up paying 10 times the price of domestic power, incurring a financial cost of €300m. Similarly, although the 2006 European heatwave was less intense, water and heat problems forced Germany, Spain, and France to take some nuclear power plants offline and reduce operations at others.

Nuclear plants located by the sea do not face similar problems in hot conditions, because ocean waters do not heat up anywhere near as rapidly as rivers or lakes. And, because they rely on seawater, they cause no freshwater scarcity. But as Japan's reactors have shown, coastal nuclear-power plants confront more serious dangers.

When the Indian Ocean tsunami struck, the Madras reactor's core could be kept in safe shutdown condition because the electrical systems had been ingeniously installed on higher ground than the plant itself. And, unlike Fukushima, which bore a direct impact, Madras was far away from the epicenter of the earthquake that unleashed the tsunami.

Fukushima is likely to stunt the appeal of nuclear power in a way similar to the accident at the Three Mile Island plant in Pennsylvania in 1979 did, not to mention the far more severe meltdown of the Chemobyl reactor in 1986. If the fallout from those incidents is a reliable guide, however, nuclear power's advocates will eventually be back.

4- SUMMARY OF EVENTS AT FUKUSHIMA DAI-ICHI

4-1 The condition at Fukushima

At 14:46 Japan standard time on March 11, 2011, the Great East Japan Earthquake-rated a magnitude 9.0-occurred at a depth of approximately 25 kilometers (15 miles), 130

kilometers (81 miles) east of Sendai and 372 kilometers (231 miles) northeast of Tokyo off the coast of Honshu Island. This earthquake resulted in the automatic shutdown of 11 nuclear power plants at four sites along the northeast coast of Japan (Onagawa 1, 2, and 3; Fukushima Dai-ichi 1, 2, and 3; Fukushima Dai-ni 1, 2, 3, and 4; and Tokai 2). The earthquake precipitated a large tsunami that is estimated to have exceeded 14 meters (45 feet) in height at the Fukushima Dai-ichi Nuclear Power Plant site. The earthquake and tsunami produced widespread devastation across northeastern Japan, resulting in approximately 25,000 people dead or missing, displacing many tens of thousands of people, and significantly impacting the infrastructure and industry in the northeastern coastal areas of Japan.

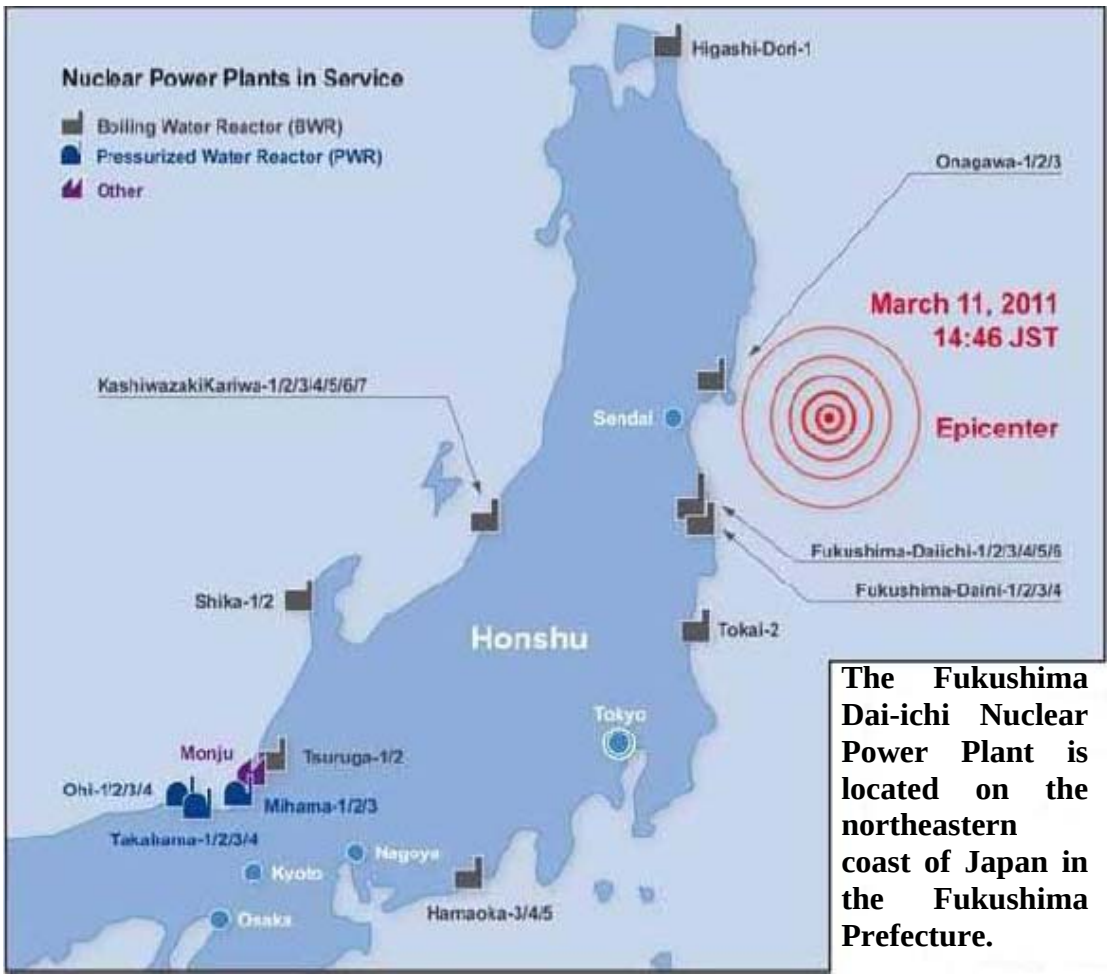

The Fukushima Dai-ichi Nuclear Power Plant is located on the northeastern coast of Japan in the Fukushima Prefecture.

Figure 1: Nuclear Power Plants in Japan

Fukushima Dai-ichi Units 1 through 4 are located in the southern part of the station and are oriented such that Unit 1 is the northernmost and Unit 4 is the southernmost. Fukushima Dai-ichi Units 5 and 6 are located farther north and at a somewhat higher elevation than the Unit 1–4 cluster, and Unit 6 is located to the north of Unit 5.

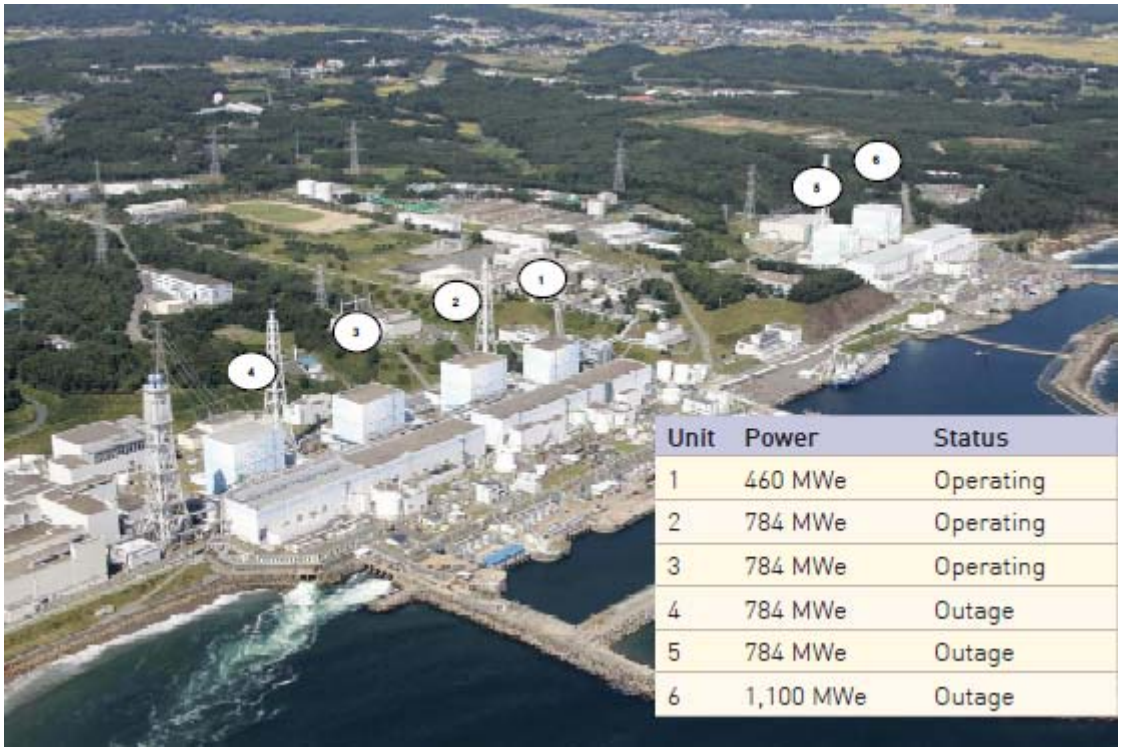

Figure 2: Fukushima Dai-ichi Nuclear Power Plant (status before earthquake)

The Fukushima Dai-ichi site includes six boiling water reactors (BWRs).

Table 1: Reactors at the Fukushima Dai-Ichi Nuclear Power Plant

Unit	Net MWe*	Reactor, Containment, and Cooling Systems**
1	460	BWR-3, Mark I, IC, HPCI
2	784	BWR-4, Mark I, RCIC, HPCI
3	784	BWR-4, Mark I, RCIC, HPCI
4	784	BWR-4, Mark I, RCIC, HPCI
5	784	BWR-4, Mark I, RCIC, HPCI
6	1,100	BWR-5, Mark II, RCIC, HPCS

* MWe-megawatts electric

** IC-isolation condenser, HPCI-high-pressure coolant injection system, RCIC-reactor core isolation cooling system, HPCS-high-pressure core spray system

On March 11, 2011, Units 1, 2, and 3 were in operation, and Units 4, 5, and 6, were shut down for routine refueling and maintenance activities; the Unit 4 reactor fuel was offloaded to the Unit 4 spent fuel pool. As a result of the earthquake, all of the operating units appeared to experience a normal reactor trip within the capability of the safety design of the plants. The three operating units at Fukushima Dai-ichi automatically shut down, apparently inserting all control rods into the reactor. As a result of the earthquake, offsite power was lost to the entire

facility. The emergency diesel generators started at all six units providing alternating current (ac) electrical power to critical systems at each unit, and the facility response to the seismic event appears to have been normal. Approximately 40 minutes following the earthquake and shutdown of the operating units, the first large tsunami wave inundated the site followed by multiple additional waves. The estimated height of the tsunami exceeded the site design protection from tsunamis by approximately 8 meters (27 feet). The tsunami resulted in extensive damage to site facilities and a complete loss of ac electrical power at Units 1 through 5, a condition known as station blackout (SBO). Unit 6 retained the function of one of the diesel generators.

The operators were faced with a catastrophic, unprecedented emergency situation. They had to work in nearly total darkness with very limited instrumentation and control systems. The operators were able to successfully cross-tie the single operating Unit 6 air-cooled diesel generator to provide sufficient ac electrical power for Units 5 and 6 to place and maintain those units in a safe shutdown condition, eventually achieving and maintaining cold shutdown.

Despite the actions of the operators following the earthquake and tsunami, cooling was lost to the fuel in the Unit 1 reactor after several hours, the Unit 2 reactor after about 71 hours, and the Unit 3 reactor after about 36 hours, resulting in damage to the nuclear fuel shortly after the loss of cooling. Without ac power, the plants were likely relying on batteries and turbine-driven and diesel-driven pumps. The operators were likely implementing their severe accident management program to maintain core cooling functions well beyond the normal capacity of the station batteries. Without the response of offsite assistance, which appears to have been hampered by the devastation in the area, among other factors, each unit eventually lost the capability to further extend cooling of the reactor cores.

At that time the current condition of the Unit 1, 2, and 3 reactors is relatively static, but those units have yet to achieve a stable, cold shutdown condition. Units 1, 2, 3, and 4 also experienced explosions further damaging the facilities and primary and secondary containment structures. The Unit 1, 2, and 3 explosions were caused by the buildup of hydrogen gas within primary containment produced during fuel damage in the reactor and subsequent movement of that hydrogen gas from the drywell into the secondary containment. The source of the explosive gases causing the Unit 4 explosion remains unclear. In addition, the operators were unable to monitor the condition of and restore normal cooling flow to the Unit 1, 2, 3, and 4 spent fuel pools.

4-2 Sequence of Events

Below is a sequence of events early in the accident for the six Fukushima Dai-ichi reactors. This sequence of events provides only the level of detail necessary for the near-term assessment of insights and the recommendation of actions for consideration at U.S. nuclear facilities. When available, times indicated are in Japan standard time.

Unit 1 Sequence of Events	
March 11	
14:47	Earthquake, loss of offsite ac power, and plant trip
14:52	Isolation condenser operated to cool reactor
15:03	Isolation condenser stopped operating
15:37	Tsunami and total loss of ac power—SBO
15:37	Loss of ability to inject water to the reactor
~17:00	Water level below top of fuel
--:--	Partial core damage (several hours after tsunami)
March 12	
14:30	Vent primary containment
15:36	Explosion results in severe damage to the reactor building (secondary containment)

Figure 3: Damage to Unit 1

Unit 2 Sequence of Events	
March 11	
14:47	Earthquake, loss of offsite ac power, and plant trip
~14:50	RCIC manually operated to inject water to reactor
15:41	Tsunami and total loss of ac power at site—SBO
March 13	
--:--	RCIC continued to be used to cool reactor
~11:00	Vent primary containment
March 14	
13:25	RCIC stopped operating
~18:00	Water level below top of fuel
--:--	Partial core damage (approximately 3 days after tsunami)
--:--	Blowout panel open on side of reactor building
March 15	
~06:00	Explosion; suppression chamber pressure decreased indicating the possibility that primary containment was damaged

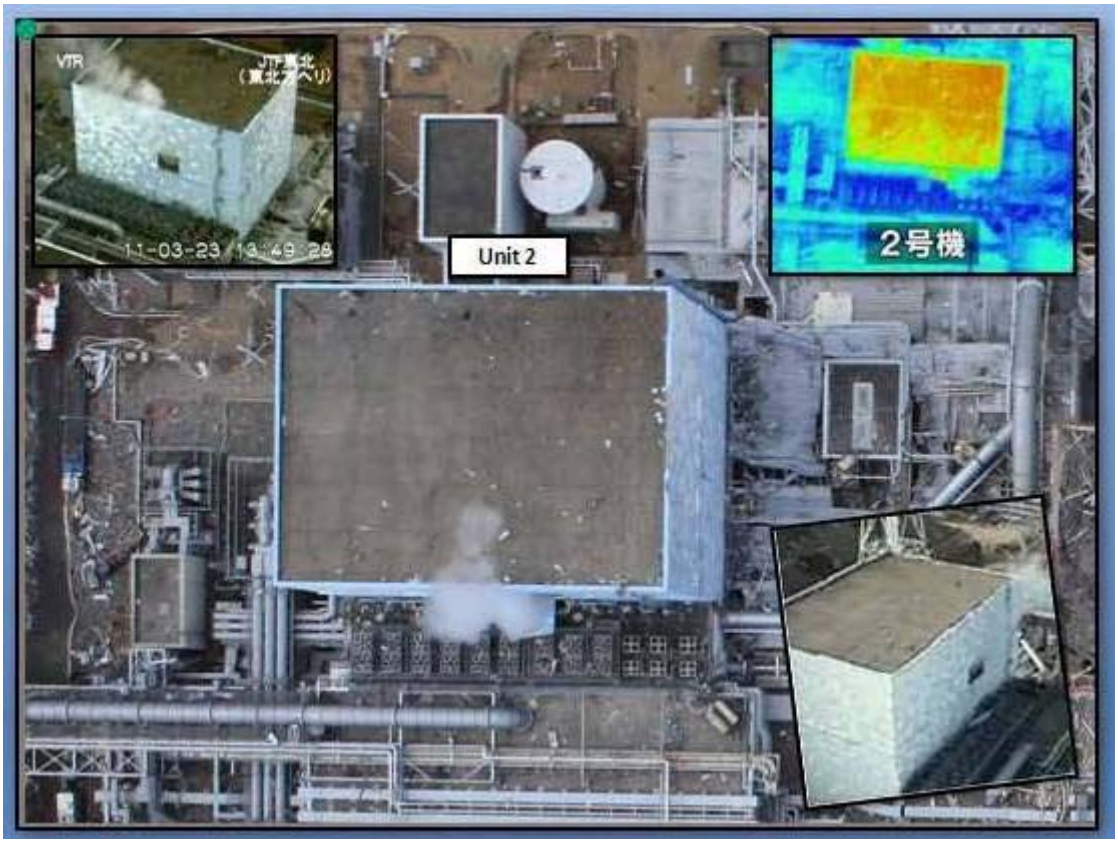

Figure 4: Damage to Unit 2

Unit 3 Sequence of Events	
March 11	
14:47	Earthquake, loss of offsite ac power, and plant trip
15:05	RCIC manually started to inject water into reactor
15:41	Tsunami and total loss of ac power at site—SBO
March 12	
11:36	RCIC stopped operating
12:35	HPCI automatically started injecting water into reactor
March 13	
02:42	HPCI stopped operating
~08:00	Water level below top of fuel
--:--	Partial core damage (approximately 2 days after tsunami)
March 14	
05:20	Vent primary containment
11:01	Explosion results in severe damage to the reactor building (secondary containment)

Figure 5: Damage to Unit

Unit 4 Sequence of Events (Unit 4 reactor was defueled)	
March 11	
14:46	Earthquake and loss of offsite ac power
15:38	Tsunami and total loss of ac power at site—SBO
March 15	
~06:00	Explosion in reactor building

Figure 6: Damage to Unit 4

Unit 5 & 6 Sequence of Events (Both units were shut down for periodic inspection)	
March 11	
14:46	Earthquake and loss of offsite ac power
15:41	Tsunami and total loss of ac power at site—SBO
March 20	
14:30	Unit 5 enters cold shutdown
19:27	Unit 6 enters cold shutdown

Protective Action Recommendations at Fukushima Dai-ichi	
March 11	
	Evacuation of residents within 3 kilometers (1.9 miles) and shelter-in-place for residents within 10 kilometers (6.2 miles)
March 12	
	Evacuation of residents within 20 kilometers (12.4 miles)
March 15	
	Evacuation of residents within 30 kilometers (18.6 miles)
April 11	
	"Planned Evacuation Areas" and "Evacuation Prepared Area" established in the areas beyond 20 kilometers (12.4 miles)
April 21	
	Restricted area within 20 kilometers (12.4 miles) established to allow temporary access and exclusion area of 3 kilometers (1.9 miles) established for members of the public

Figure 7: Fukushima Dai-ichi Units 1-4 following explosions

The tsunami was more disruptive than the earthquake, with inundation reaching many kilometres inland and affecting an area of up to 500km^2. The buildings and infrastructure of many towns and villages have been completely destroyed, with debris scattered over a large area. This, combined with the earthquake damage created significant problems in the first few days following the events for access to the Fukushima-1 site for specialist equipment and personnel.

Fuel Assemblies Cooling Ponds

Reactor Units 1, 2 and 3 were operating at power when the earthquake struck while the Reactor Units 4, 5 and 6 were already shutdown. Reactor Unit 4's fuel had been off-loaded to

its pond, while Reactor Units 5 and 6 had a full complement of fuel in their respective reactor pressure vessels despite being shutdown. The inventory in the respective ponds is shown below:

Table 2: Number of Fuel Assemblies in Cooling Ponds at Fukushima-1

Unit	Capacity	Irradiated Fuel Assemblies	Unirradiated (new) Fuel Assemblies	Most Recent Additions of Irradiated Fuel
1	900	292	100	March 2010
2	1240	587	28	September 2010
3	1220	514	52	June 2010
4	1590	1331	204	November 2010
5	1590	946	48	January 2011
6	1770	876	64	August 2010

Despite the loss of power, the reactors at the Fukushima-1 site had a number of ways to provide cooling for a short period time following the tsunami. These systems described in more detail below required no AC power, plant service and instrument air, or external cooling systems to deliver their function. However, they did require DC battery power to operate. It is believed that the batteries were only rated for 8 hours which was an insufficient time for this event for alternative power sources to be restored.

4-3 Key Events over the First few Days

Reactor Unit 1

- Containment venting started at 10:17am local time on 12 March 2011.
- Hydrogen explosion in the upper structure at 3:36pm local time on 12 March 2011.
- Sea-water injection into the reactor pressure vessel at 8:20pm local time on 12 March 2011.
- Sea-water injection stopped due to lack of water at 1:10am local time on 14 March 2011. Restarted several hours later.

Reactor Unit 2

- Containment venting started at 11:00am local time on 13 March 2011.
- Blowout panel opened in reactor building following explosion in Unit 3 at 11:00am local time on 14 March 2011.
- Sea-water injection into the reactor pressure vessel at 4:34pm local time on 14 March 2011.
- Reactor vented at 0:02am local time on 15 March 2011.
- Explosion heard and suppression chamber/torus pressure decreased at 6:20am local time on 15 March 2011. Containment assumed to be damaged from this point.

Reactor Unit 3

- Containment venting started at 8:41am local time on 13 March 2011.

- Sea-water injection into the reactor pressure vessel at 11:55am local time on 13 March 2011.
- Sea-water injection stopped due to lack of water at 1:10am local time on 14 March 2011. Restarted several hours later.
- Reactor vented at 5:20am local time on 14 March 2011.
- Containment vessel pressure rose at 7:52am local time on 14 March 2011 ahead of a large (presumed hydrogen) explosion at 11:01am local time.

NISA press releases suggest that the initial sea-water injection through the "Fire Extinguish Line" was limited to about $2m^3$/hr. Without active cooling and/or sufficient water injection, the reactor fuel elements in the cores would have become uncovered, over-heat, lose their geometry and integrity, and release radioactive gases and particles previously contained by the zircaloy fuel cladding. In addition, once zircaloy is no longer covered with water but is in a hot steam atmosphere, hydrogen can be produced with the resulting explosion risk. Indications of the water level in the reactor pressure vessel reported since 15 March 2011 indicate that the fuel in Reactor Units 1 to 3 has consistently been only half to two thirds covered (Ref. 14, IAEA fax to authorities, 15 March 2011 at 5:40pm local time). The hydrogen explosions from 12 March 2011 indicate that the fuel was actually uncovered much earlier than 15 March 2011.

Sea-water injection was not increased from $2m^3$/hr until 23 March 2011 (Reactor Unit 1) and not replaced with freshwater until 25 March 2011 (Ref. 13). Pumps on fire trucks were initially used for the water injection. Pumping started to be switched to temporary motor driven pumps from 27 March 2011 (Reactor Unit 1 from 29 March 2011, Unit 2 from 27 March 2011 and Unit 3 from 28 March 2011). To mitigate the risk of a further hydrogen explosion in Reactor Unit 1, TEPCO started to inject nitrogen into the containment vessel from 7 April 2011.

4-4 Radiation Levels:

The Japanese authorities have informed the IAEA that the following radiation dose rates have been observed on site at the main gate of the Fukushima Daiichi Nuclear Power Plant. At 00:00 UTC on 15 March a dose rate of 11.9 millisieverts (mSv) per hour was observed. Six hours later, at 06:00 UTC on 15 March a dose rate of 0.6 millisieverts (mSv) per hour was observed. These observations indicate that the level of radioactivity has been decreasing at the site. As reported earlier, a 400 millisieverts (mSv) per hour radiation dose observed at Fukushima Daiichi occurred between Units 3 and 4. This is a high dose-level value, but it is a local value at a single location and at a certain point in time. The IAEA continues to confirm the evolution and value of this dose rate. It should be noted that because of this detected value, non-indispensible staff was evacuated from the plant, in line with the Emergency Response Plan, and that the population around the plant is already evacuated.

Initially Japan implemented a 3 Km radious evacuation zone and 10 Km radius shelter zone, this was quickly extended to 10 Km radius evacuation zone and 20 Km radius shelter zone, and then later to a 20 Km radius evacuation zone and 30 Km radius shelter zone. The Japanese do not pre-distribute potassium iodate tablests to those within the predetermined emergency planning zone. In response to Fukushima emergency, potassium iodate tablets

were distributed to evacuation centers within three days. Tablets were not distributed to evacuees until nine days into the accident.

About 150 persons from populations around the Daiichi site have received monitoring for radiation levels. The results of measurements on some of these people have been reported and measures to decontaminate 23 of them have been taken. The IAEA will continue to monitor these developments. Evacuation of the population from the 20 kilometre zone is continuing.

The Japanese have asked that residents out to a 30 km radius to take shelter indoors. Japanese authorities have distributed iodine tablets to the evacuation centres but no decision has yet been taken on their administration.

Based on a press release from the Japanese Chief Cabinet Secretary dated 16 March 2011, the lAEA can confirm the following information about human injuries or contamination at the Fukushima Daiichi nuclear power plant.

4-5 Injuries

The reported number of injuried person as of 16 March 2011 include:

- 2 TEPCO employees have minor injuries;
- 2 subcontractor employees are injured, one person suffered broken legs and one person whose condition is unknown was transported to the hospital;
- 2 people are missing;
- 2 people were "suddenly taken ill";
- 2 TEPCO employees were transported to hospital during the time of donning respiratory protection in the control centre;
- 4 people (2 TEPCO employees, 2 subcontractor employees) sustained minor injuries due to the explosion at Unit 1 on 11 March and were transported to the hospital; and
- 11 people (4 TEPCO employees, 3 subcontractor employees and 4 Japanese civil defense workers) were injured due to the explosion at Unit 3 on 14 March.

4-6 Radiological Contamination

About only 20 Employees are Suffering Radiological Contamination:

- 17 people (9 TEPCO employees, 8 subcontractor employees) suffered from deposition of radioactive material to their faces; but were not taken to the hospital because of low levels of exposure;
- One worker suffered from significant exposure during "vent work," and was transported to an offsite center;
- 2 policemen who were exposed to radiation were decontaminated; and
- Firemen who were exposed to radiation are under investigation.

4-7 Evacuation of Populations:

On 12 March, the Japanese Prime Minister ordered the evacuation of residents living within 10 kilometres of the Fukushima Daini nuclear power plant and within 20 kilometres of the Fukushima Daiichi nuclear power plant.

Japan's Nuclear and Industrial Safety Agency (NISA) has reported that about 185 000 residents had been evacuated from the towns listed below as of 13 March 2011, 17:00 (JST). Populations of Evacuated Towns Near Affected Nuclear Power Plants were:

Hirono-cho	5 387
Naraha-cho	7 851
Tomioka-cho	15 786
Okuma-cho	11 186
Futaba-cho	6 936
Namie-cho	20 695
Tamura-shi	41 428
Minamisouma-Shi	70 975
Kawauchi-mura	2 944
Kuzuo-mura	1 482
Total	184 670

Iodine Distribution

Japan has distributed 230000 units of stable iodine to evacuation centers from the area around Fukushima Daiichi and Fukushima Daini NPPs. The Japanese do not pre-distribute iodine tablets to those within the predetermined emergency planning zone. In response to the Fukushima emergency, the tablets were distributed to evacuation centres within three days. Tablets were not distributed to evacuees until nine days into the accident. The UK provided potassium iodate tablets to the British Embassy in Japan.

4-8 Doses to Intervention Personnel

With regard to the Japanese response to the nuclear emergency at the Fukushima-1 site, it has been necessary for the operator’s staff and emergency services, in seeking to restore cooling, to incur radiation exposures considerably in excess of the 100mSv emergency dose limit that is applied in Japan. For this work doses up to 250mSv have been authorised, and 30 people closely involved with the emergency have received doses between 100-250mSv.

4-9 Monitoring, Decontamination and Medical Assistance of Evacuees and Casualties

Monitoring and decontamination units were employed at evacuation centres to identify those who may have been contaminated and to provide reassurance monitoring to those who were not. It is believed that contamination was identified on a few evacuees who were successfully decontaminated at the evacuation centre. During the emergency, there were a few workers who received significant skin doses to their feet or lower legs (believed to be 2-3Sv) and were taken to hospital for medical treatment and later discharged.

4-10 Radiological Monitoring of the Environment

Widespread environmental monitoring of the environment was implemented across Japan, including measurements of air concentrations, ground deposition, water and foodstuffs within a few days of the earthquake. Radiation monitoring during and after a nuclear emergency plays an important role in providing an input to decision making and in the provision of information to the public and to official bodies. Monitoring undertaken might

relate to the immediate impact of the accident on people and the potential future impact resulting from environmental contamination.

4-11 Taking Agricultural Countermeasures, Countermeasures against Ingestion and Longer Term Protective Actions

In Japan, milk, leafy green vegetables and drinking water were found to exceed regulation values in some localized areas and restrictions were implemented. Discharges to sea of contaminated water resulted in fishing bans within 30km of the Fukushima-1 site being implemented along with a change to the regulation value of iodine-131 in fishery products being implemented.

4-12 Recent Developments at the Fukushima Daiichi Nuclear Power

On 1 February 2012 and continuing until 17 February TEPCO was actively monitoring a temperature increase at a sensor located at the bottom of the Unit 2 Reactor Pressure Vessel (RPV). Throughout this period TEPCO continuously provided updated information showing that the temperature increase was isolated to this single sensor.

Between 13 and 17 February, TEPCO investigated whether a malfunction of this specific temperature sensor was the cause of the increased temperature measurements. Based on a combination of results from the initial testing performed on 13 February and continuous monitoring, TEPCO stated that this entire event is likely caused by damage to this specific sensor.

5- Road Map of Environmental Remediation Activities

5-1 Remediation Activities and Strategy

On 26 January the Ministry of the Environment released the "Road Map of Environmental Remediation Activities". This Road Map covers the environmental remediation strategy to be employed in the Deliberate Evacuation Area and the Restricted Area. By the end of March, these areas are to be re-categorized as follows (by the Nuclear Emergency Response Headquarters as decided on 26 December 2011):

- The area prepared to call off the evacuation instruction, which will include those areas with estimated doses to the public of less than20 mSv/yr;
- The area to restrict residency, which will include those areas with estimated doses to the public between 20 mSv/yr and 50 mSv/yr; and
- The area with difficulty of return, which will include those areas with estimated doses to the public of greater than 50 mSv/yr.

The following is a general overview of the remediation approach that has been proposed:

- land/house owners will be identified;
- Public meetings will be held for transparency and to increase the local population's understanding of the remediation process;

- Permission from land/house owners will be obtained so that remediation teams can access land and houses for initial surveying;
- Field surveys (for radiation monitoring and earthquake and tsunami damage inspection) will take place;
- The best environmental remediation process for each area will be determined;
- Permission from land/house owners will be obtained again before implementation of any remediation actions;
- Remediation of sites will take place;
- Radiation monitoring will confirm the effectiveness of the remediation activities; and
- Results of the remediation activities will be provided to the land/home owners.

The following is an approximate remediation schedule of activities to take place in the re-categorized areas:

- In areas with estimated doses to the public of less than20 mSv/yr;
  - For those areas with 10 to 20 mSv/yr and schools with more than 5 mSv/yr remediation activities are planned to be completed by December 2012;
  - For those areas with 5 to1 0 mSv/yr remediation activities are planned to be completed by the end of March 2013; and.
  - For those areas with 1 to 5 mSv/yr remediation activities are planned to be completed by the end of March 2014.
- In areas with estimated doses to the public between 20 mSv/yr and50 mSv/yr remediation activities are planned to be completed by the end of March 2014; and
- In areas with estimated doses to the public of less than50 mSv/yr remediation demonstration projects will be conducted. When the demonstration projects are completed a review and discussion of the results will take place to decide the best way forward in these areas.

The Road Map states that in March in-depth action plans for environmental remediation for each municipality are planned to be developed. Finding appropriate locations to temporarily store any removed material (soil, concrete, etc.) and organizing appropriate manpower to conduct remediation activities is an on-going priority.

5-2 Radiation Doses to Workers

Table 3: Combined external and internal radiation doses to workers at Fukushima Daiichi

Dose (mSv)	March	April	May	June	July	August	September
Greater than 250	6	0	0	0	0	0	0
200-250	2	0	0	0	0	0	0
150-200	13	0	0	0	0	0	0
100-150	77	0	0	0	0	0	0
50-100	309	3	0	0	0	0	0

20-50	859	81	19	16	6	0	7
10-20	1041	310	133	96	69	21	28
Less than 10	1434	3214	2854	1997	2043	1080	1011
Total personnel	3742	3608	3017	2111	2118	1101	1046
Max (mSv)	670.36	69.28	41.61	39.62	31.24	18.27	30.81
Average (mSv)	22.58	3.83	2.85	2.26	1.85	1.46	1.80

On 17 October, a TEPCO employee was working with water injection equipment on the second floor of the reactor building for Unit 1. When his work was completed, contamination was discovered around his mouth. However, a whole body counter measurement identified no internal contamination.

TEPCO had previously reported that 65 personnel (all sub-contractors) who worked at the Fukushima plant during the initial response had not undergone whole body counting. Several have been identified since that time and an investigation to identify remaining personnel is on-going. At present there are 20 persons outstanding from this identification process. Nine of them have been identified as not being applicable for whole body counting, seven are still under investigation to obtain their contact details and four have been unable to be found through their provided contact information.

On29 October two workers were injured onsite. An accident occurred during the disassembly of a crane used to construct the Unit 1 reactor building cover. A bundle of wires fixed by the bank wire on the base released and struck workers engaged in dismantling work. One worker broke both of his legs and the other worker sustained injury to both his shoulders and other areas of his body. The worker with broken legs was transported via helicopter to the Fukushima Medical University Hospital immediately after the accident where he had surgery and was transferred to an Intensive Care Unit. The other worker was transported to the Sogo lwaki Kyoritsu Hospital approximately 4 hours after first receiving treatment at the medical unit at J-Village. The cause of the accident is currently being investigated.

On 1 November TEPCO announced that due to the reduction of the airborne concentration of contamination onsite, requirements for wearing facemasks onsite are being reduced. These new rules come into effect on 8 November.

5-3 Latest Information Regarding Protective Measures for the Public

On 20 February Fukushima Prefecture released preliminary results from their project to estimate external doses to residents who were in the surrounding area for the first four months following the accident, Le. from 11 March to 11 July 2011. The table below shows the estimated external doses to those members of the public that were in Namie Town, Kawamata Town (in Yamakiya district) and litate Village. [Please note that these external dose estimates have been put together based on a survey of when and where people were during the months that followed the accident. When the full survey is released it will likely include a substantial discussion of the estimation process.]

Table 4: Estimated external doses to 9747 members of the public from Namie Town, Kawamata Town and Iitate Village from 11 March to 11 July 2011

Estimate dose (mSv)	Number of people*
0-1	5636
1-2	2081
2-3	825
3-4	387
4-5	290
5-6	203
6-7	130
7-8	62
8-9	46
9-10	16
10-11	26
11-12	14
12-13	8
13-14	6
14-15	7
>15	10
Total	9747
* Please note the figures apply only to members of the public in the surrounding areas. They do not include radiation workers who lived in the area and worked onsite in this time period.	

5-4 Investigation Committee on the Accidents at the Fukushima Nuclear Power Station

The Investigation Committee on the Accident at the Fukushima Nuclear Power Stations was established by the Japanese Government after the accident occurred in March 2011. This committee is currently producing an independent review of the accident and will publish a full document on this topic during this summer. On 26 December 2011 the committee released an interim report providing their preliminary findings.

5-5 Updated Mid and Long Term Roadmap on Decommissioning of Fukushima Daiichi Nuclear Power Plant

On 23 January METI updated the Roadmap document titled the "Mid-and-long-Term Roadmap towards the Decommissioning of Fukushima Daiichi Nuclear Power Station Units 1-4, TEPCO" which outlines the proposed decommissioning process. This document was originally finalized during a meeting on 21 December 2011 between the Agency of Natural Resources and Energy (ANRE), METI, NISA and TEPCO. An updated summary document is also available online.

The decommissioning Roadmap employs three distinct phases which are quoted here:

- "Phase 1: From the completion of Step 2 to the start of fuel removal from the spent fuel pool (target is within two years). In addition to work preparing to start removing

fuel from the spent fuel pool, this phase will include research and development necessary for the removal of fuel debris, the start of site investigations, and other tasks in a period of intensive preparation for decommissioning.

- Phase 2: From the end of Phase 1 to the start of fuel debris removal (target is within ten years). Within this phase, we will step up many research and development tasks towards the removal of fuel debris, and tasks such as reinforcement of PCV. This phase will be further divided into three steps: early, mid, and late, as a guideline for judging progress within the phase.
- Phase 3: From the end of Phase 2 to the end of decommissioning (target is 30-40 years). This is the phase for implementation of tasks from fuel debris removal to the end of decommissioning."

5-6 Research and Development Roadmap Document

On 23 January METI released the document titled the "Research and Development Road Map for Decommissioning Units 1-4 at TEPCOs Fukushima Daiichi Nuclear Power Plant" which was previously released on 21 December and only available in Japanese. This road map document was drafted between ANRE, TEPCO, MEXT, JAEA, and Toshiba and Hitachi / Hitachi-GE Nuclear Energy Ltd.

This document is comprised of the fundamental research and development (R&D) philosophy, the R&D plan, the R&D framework and the ideal state of international cooperation for R&D.

The R&D areas have been divided into:

- R&D related to removal of fuel from spent fuel pools;
- R&D related to preparation for removal of fuel debris;
- R&D related to processing and disposal of radioactive waste, and;
- R&D concerning remote control devices.

R&D for each of these areas is described within the plan based on the phases introduced in. the mid and long term decommissioning plan. This document introduces a number of technical issues which need to be resolved during the R&D program. It discusses prospective technologies that could be introduced to help solve these challenges.

6- Uk Office for Nuclear Regulation Activities:

6-1 Evaluation and Conclusions:

The UK office of Nuclear Regulation (ONR) the situation was kept the situation under review at the highest level in Government. The health and Safety Executive's Nuclear Directorate (which became the office for Nuclear Regulation (ONR), an Agency of the Health and safety Executive – on 1 April 2011, provided authoritative advice on nuclear aspects throughout the crisis. An interim report was prepared responds to the secretary of state for Energy and Climate Change to examine the circumstances of the Fukushima accident to see what lessons could be learnt to enhance the safety of the UK nuclear industry.

The direct causes of the nuclear accident, a magnitude 9 earthquake and the associated 14 metre high tsunami, are far beyond the most extreme natural events that the UK would be expected to experience. We are reassuringly some 1000 miles from the edge of a tectonic plate, where earthquake activity is more common and severe. Design provisions at the Fukushima-1 site appear to only have been made to protect against a 5.7 metre high surge in sea level, and there is a history of large tsunamis hitting this coast of Japan. It is reported that over the 150 years Japan has experienced along its east coast several tsunamis of height greater than six metres, some greater than 20 metres. However, we have been unable to identify the specific history of tsunamis at the Fukushima-1 site.

UK nuclear power plants, both operational and those planned, are of a different design to the BWR reactors at the Fukushima-1 site. In addition, our approach to design basis analysis requires designers and operators to demonstrate that adequate protection is in place for natural events of a very remote nature, based on an extrapolation from the historical record. We then require them to demonstrate that there are no "cliff-edge" effects or that more could not be reasonably done to protect against very remote events. This leads them to conclude that:

Conclusion 1: In considering the direct causes of the Fukushima accident there is no reason for curtailing the operation of nuclear power plants or other nuclear facilities in the UK. Once further work is completed any proposed improvements will be considered and implemented on a case by case basis, in line with the normal regulatory approach.

Conclusion 2: In response to the Fukushima accident, the UK nuclear power industry has reacted responsibly and appropriately displaying leadership for safety and a strong safety culture in its response to date.

Conclusion 3: The Government's intention to take forward proposals to create the Office for Nuclear Regulation, with the post and responsibilities of the Chief Inspector in statute, should enhance confidence in the UK's nuclear regulatory regime to more effectively face the challenges of the future.

Conclusion 4: To date, the consideration of the known circumstances of the Fukushima accident has not revealed any gaps in scope or depth of the Safety Assessment Principles for nuclear facilities in the UK.

Conclusion 5: With considerations of the events in Japan, and the possible lessons for the UK, has not revealed any significant weaknesses in the UK nuclear licensing regime.

Conclusion 7: There is no need to change the present siting strategies for new nuclear power stations in the UK.

Conclusion 8: There is no reason to depart from a multi-plant site concept given the design measures in new reactors being considered for deployment in the UK and adequate demonstration in design and operational safety cases.

Conclusion 9: The UK's gas-cooled reactors have lower power densities and larger thermal capacities than water cooled reactors which with natural cooling capabilities give longer timescales for remedial action. Additionally, they have a lesser need for venting on loss of cooling and do not produce concentrations of hydrogen from fuel cladding overheating.

Conclusion 10: There is no evidence to suggest that the presence of MOX fuel in Reactor Unit 3 significantly contributed to the health impact of the accident on or off the site.

Conclusion 11: With more information there is likely to be considerable scope for lessons to be learnt about human behaviour in severe accident conditions that will be useful in enhancing contingency arrangements and training for such events.

6-2 UK Interim Report Recommendations

From the consideration of the events at the Fukushima-1 site various matters should be reviewed to determine whether there are any reasonably practicable improvements to the safety of the UK nuclear industry. In formulating the interim report recommendations a trial is made to group them into logical categories and to identify those who are expecting to follow up the recommendations. The recommendations in full are listed below.

Table 5: UK Interim Report Recommendations

General	
International Arrangements for Response	**Recommendation 1:** The government should approach IAEA, in co-operation with others, to ensure that improved arrangements are in place for the dissemination of timely authoritative information relevant to a nuclear event anywhere in the world.
National Emergency Response Arrangements	**Recommendation 2:** The Government should consider carrying out a review of the Japanese response to the emergency to identify any lessons for UK public contingency planning for widespread emergencies, taking account of any social, cultural and organisational differences. **Recommendation 3:** The Nuclear Emergency Planning Liaison Group should instigate a review of the UK's national nuclear emergency arrangements in light of the experience of dealing with the prolonged Japanese event.
Openness and Transparency	**Recommendation 4:** Both the UK nuclear industry and ONR should consider ways of enhancing the drive to ensure more open, transparent and trusted communications, and relationships, with the public and other stakeholders.

Relevant to the Regulator	
Safety Assessment Approach	**Recommendation 5:** Once further detailed information is available and studies are completed, ONR should undertake a formal review of the Safety Assessment Principles to determine whether any additional guidance is necessary in the light of the Fukushima accident, particularly for "cliff-edge" effects.

Relevant to the Regulator	
Emergency Response Arrangements and Exercises	**Recommendation 6:** ONR should consider to what extent long-term severe accidents can and should be covered by the programme of emergency exercises overseen by the regulator. **Recommendation 7:** ONR should review the arrangements for regulatory response to potential severe accidents in the UK to see whether more should be done to prepare for such very remote events.

Relevant to the Nuclear Industry	
Off-site Infrastructure Resilience	**Recommendation 8:** The UK nuclear industry should review the dependency of nuclear safety on off-site infrastructure in extreme conditions, and consider whether enhancements are necessary to sites' self sufficiency given for the reliability of the grid under such extreme circumstances.
Impact of Natural Hazards	**Recommendation 9** : The UK nuclear industry should initiate a review of flooding studies, including from tsunamis, in light of the Japanese experience, to confirm the design basis and margins for flooding at UK nuclear sites, and whether there is a need to improve further site-specific flood risk assessments as part of the periodic safety review programme, and for any new reactors. This should include sea-level protection.
Multi-reactor Sites	**Recommendation 10** : The UK nuclear industry should ensure that safety cases for new sites for multiple reactors adequately demonstrate the capability for dealing with multiple serious concurrent events induced by extreme off-site hazards.
Spent Fuel Strategies	**Recommendation 11**: The UK nuclear industry should ensure the adequacy of any new spent fuel strategies compared with the expectations in the Safety Assessment Principles of passive safety and good engineering practice.
Site and Plant Layout	**Recommendation 12** : The UK nuclear industry should review the plant and site layouts of existing plants and any proposed new designs to ensure that safety systems and their essential supplies and controls have adequate robustness against severe flooding and other extreme external events.
Fuel Pond Design	**Recommendation 13** : The UK nuclear industry should ensure that the design of new spent fuel ponds close to reactors minimises the need for bottom penetrations and lines that are prone to siphoning faults. Any that are necessary should be as robust to faults as are the ponds themselves.
Seismic Resilience	**Recommendation 14** : Once detailed information becomes available on the performance of concrete, other structures and equipment, the UK nuclear industry should consider any implications for improved understanding of the relevant design and analyses.

Relevant to the Nuclear Industry	
Extreme External Events	**Recommendation 15 :** When considering the recommendations in this report the UK nuclear industry should consider them in the light of all extreme hazards, particularly for plant layout and design of safety-related plant.
Off-site Electricity Supplies	**Recommendation 16 :** The UK nuclear industry should undertake further work with the National Grid to establish the robustness and potential unavailability of off-site electrical supplies under severe hazard conditions.
On-site Electricity Supplies	**Recommendation 17 :** The UK nuclear industry should review any need for the provision of additional, diverse means of providing robust sufficiently long-term independent electrical supplies on sites, reflecting the loss of availability of off-site electrical supplies under severe conditions.
Cooling Supplies	**Recommendation 18 :** The UK nuclear industry should review the need for, and if required, the ability to provide longer term coolant supplies to nuclear sites in the UK in the event of a severe off-site disruption, considering whether further on-site supplies or greater off-site capability is needed. This relates to both carbon dioxide and fresh water supplies, and for existing and proposed new plants. **Recommendation 19 :** The UK nuclear industry should review the site contingency plans for pond water make up under severe accident conditions to see whether they can and should be enhanced given the experience at Fukushima.
Combustible Gases	**Recommendation 20 :** The UK nuclear industry should review the ventilation and venting routes for nuclear facilities where significant concentrations of combustible gases may be flowing or accumulating to determine whether more should be done to protect them.
Emergency Control Centres, Instrumentation and Communications	**Recommendation 21 :** The UK nuclear industry should review the provision on-site of emergency control, instrumentation and communications in light of the circumstances of the Fukushima accident including long timescales, wide spread on and off-site disruption, and the environment on-site associated with a severe accident. **Recommendation 22 :** The UK nuclear industry, in conjunction with other organisations as necessary, should review the robustness of necessary off-site communications for severe accidents involving widespread disruption.

Human Capabilities and Capacities	**Recommendation 23 :** The UK nuclear industry should review existing severe accident contingency arrangements and training, giving particular consideration to the physical, organisational, behavioural, emotional and cultural aspects for workers having to take actions on-site, especially over long periods. This should take account of the impact of using contractors for some aspects on-site such as maintenance and their possible response.
Safety Case	**Recommendation 24 :** The UK nuclear industry should review, and if necessary extend, analysis of accident sequences for long-term severe accidents. This should identify appropriate repair and recovery strategies to the point at which a stable state is achieved, identifying any enhanced requirements for central stocks of equipment and logistical support.
Way Forward	
Way forward	**Recommendation 25 :** A response to the various recommendations in the interim report should be made available within one month of it being published. These should include appropriate plans for addressing the recommendations. Any responses provided will be compiled on the ONR website.

7- Usnrc: Enhancing Safety in the 21st Century

In the days following the Fukushima Dai-ichi nuclear accident in Japan, the U.S. Nuclear Regulatory Commission (NRC) directed the staff to establish a senior-level agency task force (the Task Force) to conduct a methodical and systematic review of the NRC's processes and regulations to determine whether the agency should make additional improvements to its regulatory system and to make recommendations to the Commission for its policy direction. The Policy Statement on Safety Goals sets forth two qualitative safety goals, which are supported by two quantitative supporting objectives. The following are the qualitative safety goals:

> Individual members of the public should be provided a level of protection from the consequences of nuclear power plant operation such that individuals bear no significant additional risk to life and health. Societal risks to life and health from nuclear power plant operation should be comparable to or less than the risks of generating electricity by viable competing technologies and should not be a significant addition to other societal risks.

7-1 Quantitative Supporting Objectives:

The risk to an average individual in the vicinity of a nuclear power plant of prompt fatalities that might result from reactor accidents should not exceed one-tenth of one percent (0.1 percent) of the sum of prompt fatality risks resulting from other accidents to which members of the U.S. population are generally exposed. The risk to the population in the area near a nuclear power plant of cancer fatalities that might result from nuclear power plant operation should not exceed one-tenth of one percent (0.1 percent) of the sum of cancer fatality risks resulting from all other causes.

In the Policy Statement on Safety Goals, the Commission emphasized the importance of features such as containment, siting, and emergency planning as "integral parts of the defense-in-depth concept associated with its accident prevention and mitigation philosophy." A cursory review of documents discussing the agency's approach to defense-in-depth provides a range of explanations and applications.

The Commission's policy on probabilistic risk assessment (PRA) ("Use of Probabilistic Risk Assessment Methods in Nuclear Regulatory Activities," dated August 16, 1995), states the following:

> Defense-in-depth is a philosophy used by the NRC to provide redundancy for facilities with "active" safety systems, e.g. a commercial nuclear power [plant], as well as the philosophy of a multiple-barrier approach against fission product releases.

The decision described defense-in-depth as encompassing the following requirements:

(1) require the application of conservative codes and standards to establish substantial safety margins in the design of nuclear plants;

(2) require high quality in the design, construction, and operation of nuclear plants to reduce the likelihood of malfunctions, and promote the use of automatic safety system actuation features;

(3) recognize that equipment can fail and operators can make mistakes and, therefore, require redundancy in safety systems and components to reduce the chance that malfunctions or mistakes will lead to accidents that release fission products from the fuel;

(4) recognize that, in spite of these precautions, serious fuel-damage accidents may not be completely prevented and, therefore, require containment structures and safety features to prevent the release of fission products; and

(5) further require that comprehensive emergency plans be prepared and periodically exercised to ensure that actions can and will be taken to notify and protect citizens in the vicinity of a nuclear facility.

The Task Force has found that the defense-in-depth philosophy is a useful and broadly applied concept. It is not, however, susceptible to a rigid definition because it is a philosophy. For the purposes of its review, the Task Force focused on the following application of the defense-in-depth concept:

- protection from external events that could lead to fuel damage
- mitigation of the consequences of such accidents should they occur, with a focus on preventing core and spent fuel damage and uncontrolled releases of radioactive material to the environment
- emergency preparedness to mitigate the effects of radiological releases to the public and the environment.

Many of the elements of such a regulatory framework already exist in the form of rules regarding station blackout, anticipated transient without scram, maintenance, combustible gas control, aircraft impact assessment, beyond-design-basis fires and explosions, and alternative treatment. Other elements, such as severe accident management guidelines, exist in voluntary

industry initiatives. The Task Force has concluded that a collection of such "extended design-basis" requirements, with an appropriate set of quality or special treatment standards, should be established.

The Task Force applied this conceptual framework during its deliberations. The result is a set of recommendations that take a balanced approach to defense-in-depth as applied to low-likelihood, high-consequence events such as prolonged station blackout resulting from severe natural phenomena. These recommendations, taken together, are intended to clarify and strengthen the regulatory framework for protection against natural disasters, mitigation, and emergency preparedness, and to improve the effectiveness of the NRC's programs.

7-2 Task Force's Recommendations

Clarifying the Regulatory Framework

1. The Task Force recommends establishing a logical, systematic, and coherent regulatory framework for adequate protection that appropriately balances defense-in-depth and risk considerations.

Ensuring Protection

2. The Task Force recommends that the NRC require licensees to reevaluate and upgrade as necessary the design-basis seismic and flooding protection of structures, systems, and components for each operating reactor.
3. The Task Force recommends, as part of the longer term review, that the NRC evaluate potential enhancements to the capability to prevent or mitigate seismically induced fires and floods.

Enhancing Mitigation

4. The Task Force recommends that the NRC strengthen station blackout mitigation capability at all operating and new reactors for design-basis and beyond-design-basis external events.
5. The Task Force recommends requiring reliable hardened vent designs in boiling water reactor facilities with Mark I and Mark II containments.
6. The Task Force recommends, as part of the longer term review, that the NRC identify insights about hydrogen control and mitigation inside containment or in other buildings as additional information is revealed through further study of the Fukushima Dai-ichi accident.
7. The Task Force recommends enhancing spent fuel pool makeup capability and instrumentation for the spent fuel pool.
8. The Task Force recommends strengthening and integrating onsite emergency response capabilities such as emergency operating procedures, severe accident management guidelines, and extensive damage mitigation guidelines.

Strengthening Emergency Preparedness

9. The Task Force recommends that the NRC require that facility emergency plans address prolonged station blackout and multiunit events.
10. The Task Force recommends, as part of the longer term review, that the NRC pursue additional emergency preparedness topics related to multiunit events and prolonged station blackout.

11. The Task Force recommends, as part of the longer term review, that the NRC should pursue emergency preparedness topics related to decision making, radiation monitoring, and public education.

Improving the Efficiency of NRC Programs

12. The Task Force recommends that the NRC strengthen regulatory oversight of licensee safety performance (i.e., the Reactor Oversight Process) by focusing more attention on defense-in-depth requirements consistent with the recommended defense-in-depth framework.

IAEA NUCLEAR SAFETY ACTION PLAN

12 Point Plan

Adopted by Board of Governers

Endorsed by all Member States

- **Regulatory Bodies**
- **Operating organization**
- **IAEA Safety Standards**

MAKING NUCLEAR POWER SAFER

The IAEA Action Plan

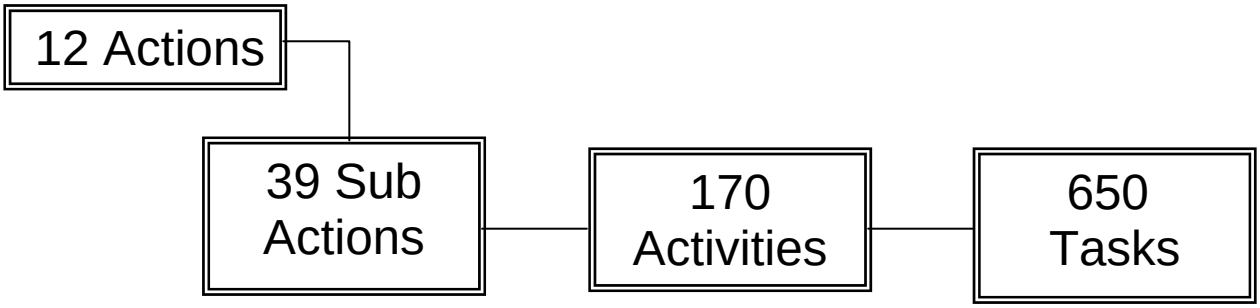

- Assessment of Safety Vulnerabilities.
- IAEA PEER Reviews.
- Strengthen Emergency preparedness and Response.
- Strengthen the Effectiveness of National Regulatory Bodies.
- Strengthen effectiveness of operating organizations.
- Review and Strengthen IAEA Safety Standards.
- Improve Effectiveness of International Legal Framework.
- Member States Embarking on Nuclear Power Program.
- Strengthen and Maintain Capacity building.
- Protection of People+ Environment from Ionizing Radiation.
- Communication Dissemination of Information.
- International Expert's Meeting Reactor and spent fuel safety.
- Research and Development.

8- Evaluation and Conclusions

International cooperation and coordination is needed including the following:

- Participation collaborative, international efforts to determine and analyze the Fukushima accident sequence of events.
- Participation in international efforts to update IAEA Fundamental safety standard [NSR-1] and other related standards to reflect insights from the Fukushima event.
- Continued cooperation and coordination between national regulatory authorities on insights from the Fukushima event as well as their plans, actions and findings. According to the given information in this paper, the following technical issues have priority for further examination:
  - External event issues (seismic, flooding, fires, sever weather).
  - Station blackout.
  - Severe accident measures (combustible gas control, emergency operating procedures, severe accident management guidelines).
  - Strategies intended to maintain or restore core cooling, containment, and spent fuel pool cooling capabilities under the occurrence of explosions or fire to include strategies in the following areas.
    (i) fire fighting (ii) operations to mitigate fuel damage, and (iii) Actions to minimize radiological release.
  - Emergency preparedness (emergency communications, radiological protection, emergency planning zones, dose projections and modeling, protective actions).

Abbreviations

AEC	Atomic Energy Commission (Japan)
BWR	Boling Water Reactor
C&I	Control and Instrumentation
CSF	Critical Safety function
DBA	Design Basis Analysis
DG	Diesel Generator
EOP	Emergency Operating Procedures
HPA	Health Protection Agency
HPA-CRCE	Health Protection Agency Centre for Radiation Chemical and Environmental Hazards
HPCI	High Pressure Coolant Injection
HSE	Health and Safety Executive
IAEA	International Atomic Energy Agency
ICRP	International Commission on Radiological Protection
LOCA	Loss of Coolant Accident
LWR	Light Water Reactor
METI	Ministry of Economy Trade and Industry (Japan)
MEXT	Ministry of Education Culture Sport Science and Technology (Japan)

MOX	Mixed Oxide Fuel
NEA	Nuclear Energy Agency (of the OECD)
NISA	Nuclear and Industrial Safety Agency (Japanese nuclear safety regulator)
NPP	Nuclear Power Plant
OECD	Organization for Economic Co-operation and Development
ONR	Office for Nuclear Regulation (formerly the Nuclear Directorate of the HSE)
PSA	Probabilistic Safety Analysis
RCIC	Reactor Core Isolation Cooling
RCS	Reactor Coolant System
RHR	Residual Heat Removal
SAM	Severe Accident Management
SAMG	Severe Accident Management Guidelines
SBO	Station Blackout
SRV	Safety Relief Valve
TEPCO	The Tokyo Electric Power Company
US NRC	Nuclear regulatory Commission (United States of America)
WANO	World Association of Nuclear Operators
WHO	world Health Organization

BIBLIOGRAPHY

1- HM chief Inspector of Nuclear Installations, Japanese earthquake and tsunami: Implications for the Nuclear Industry, office of Nuclear Regulation, 18 May 2011.

2- Charles Miller et al., Recommendations for Enhancing Reactor safety in the 21th century, The Near Term Task Force, Review of Insights from the FUKUSHIMA DAI-ICHI Accident, US. NRC, 12 July 2011.

3- IAEA. Orge, Fukushima Nuclear Accident update log, Daily updates 11 March – 2 June 2011.

4- IAEA, International Atomic Energy Agency, Atoms for Peace, Fukushima Daiichi status Report, 27 Oct. 2011, 2 November 2011, 13 Feb. 2012, 30 March 2012, 27 April 2011, 2 May 2012.

5- Reducing Risks, Protecting People: HSE's Decision Making Process. HSE Books 2001. ISBN 0 7176 21510. www.hse.gov.uk/risk/theory/r2p2.pdf.

6- Safety Assessment Principles for Nuclear Facilities. 2006 Edition Revision 1. HSE January 2008. www.hse.gov.uk/nuclear/saps/saps2006.pdf.

7- The nuclear crisis in Japan. D Okimoto, A Hanson, K Marvel, 21 March 2011. http://iis--db.stanford.edu/evnts/6615/March21 JapanSeminar.pdf.

8- "Preparedness and Response for a Nuclear or Radiological Emergency", IAEA Safety Standards Series No. GS-R-2, IAEA, 2002.

9- ICRP (2007). The 2007 Recommendations of the International Commission on Radiological Protection. ICRP Publication 103.

10- ICRP (2008). Application of the Commission's Recommendations for the Protection of People in Emergency Exposure Situations. ICRP Publication 109.

11- ICRP (2009). Application of the Commission's Recommendations for the Protection of People living in long-term Contaminated Areas after a Nuclear Accident or a Radiation Emergency. ICRP Publication 111.

12- Rashad S.M., Survey of Selected Accidents in Production, Research, Experimental Nuclear Reactors, NRSC/R-1 1.88, Nuclear Regulatory and Safety Center, Atomic Energy Authority, Cairo, Jan. 1988.
13- Hammad F.H. and Rashad S.M., Study of Some Published Severe Accidents At Nuclear" Power Plants up to April 1986. NRSC/R - 2.88 Nuclear Regulatory and Safety Centre, Atomic Energy Authority, Cairo, Jan. 1988.
14- Rashad S.M., and Hammad F.H., A Study of Selected Severe Accidents in Central Nuclear Power Plants. 12th Congress for Statistics, Computer Science, Social and Demographic Research, Ain Shams University, Cairo, March 1987.
15- Rashad S.M., Nasser O.S., and Hammad F.H., Probabilistic Analysis of Fire Events in Nuclear Power Plants, Proceeding of the International ENS/ANS Conference on Thermal Reactor Safety "NUC safe 88", Avignon, France, Oct. 1988.
16- S.M. Rashad and F .H. Hammad, Review and Analysis of Some Nuclear and Radiological Accidents, 5th Conf. Nucl. Sc., Appl., Vol. 1, Cairo, 1992.
17- S.M., Rashad and F.B. Hammad,. Abnomal Occurrences at US NPPs, Proceedings of Al Azhar Engineering Third International Conference, Cairo, Dec. 1993.
18- S.M., Rashad, the International Nuclear Event Scale (INES) and Its Application to Nuclear Facilities Accidents, ARE - AEA - Int. Rep 169, 1995.
19- IAEA Safety Series No. 75 - INSAG-4 Safety Culture, IAEA, Vienna, 1991.
20- Eisenhut D.G. et ai, "TMI Plus 5: Nuclear Power on the Ropes" IEEE Spectrum, April 1984, Volume 21, Number 4.
21- Wyckoff. H, "Losses of off Site Power at U.S. Nuclear Power Plants - All Years Through 1988, "NSAC /144, April 1989.
22- Long R.L. and Crimimine T.M., "Three Mile Inland Accident Technical Support", Nuclear Technology Vol. 45, Aug. 1981.
23- Chernobyl: The Soviet Report, Nuclear News, Sept., 1986.
24- The International Chernobyl Project, Assessment of Radiological Consequences and Evaluation of Protective Measares, Technical Report, IAEA, August 1991.

Comogenic Radionuclides in the Atmosphere: Origin and Applications

Abdalla A. Abdel Monem
Nuclear Materials Authority, Cairo, Egypt

ABSTRACT

The primary cosmic radiation arriving at the top of the atmosphere comprise mainly positively charged particles: protons (~87%), alpha -particles (~12%) and heavier nuclei such as Li, Be, B, C, O and F. Their energy spectrum peaks are in the vicinity of 1-2 GeV, but may extend up to 10^{18}eV. They are believed to be of galactic origin and to have been accelerated to their present energies by intersteller magnetic fields.

The low energy particles ionize the atmosphere and are stopped. All other particles undergo collision with the nuclei of the atmosphere gases and produce new particles by a fragmentation process called "spallation". During nuclear spallation reactions in the atmosphere, particles are produced which may be either fragments of the target nucleus or newly created by collision. The particles produced are nuclei of H and He particularly ^{2}H, ^{3}H and ^{3}He as well as neutrons.

The neutrons that are involved in these processes are captured by ^{14}N to produce ^{14}C ($t_{1/2}$ =5730y). Also, produced by interaction with atmospheric N are: ^{3}H, ^{3}He, ^{7}Be and ^{10}Be. All these nuclides can also be formed by interaction with O as well as ^{14}C. Interaction with ^{40}Ar produces ^{26}AI, ^{36}CI, ^{38}CI, ^{39}CI, ^{32}Si, ^{37}Ar, ^{39}Ar, ^{22}Na, 24Na, ^{35}S, ^{33}P and ^{32}P. Interaction with Kr produces ^{81}Kr and ^{85}Kr. With the exception of ^{3}He, all these nuclides are unstable. They either remain in the atmosphere for substantial periods of time or are rapidly removed by precipitation.

Several of the cosmogenic radionuclides have reasonable long half-lives to be useful for the study of geological processes. The cosmogenic^{14}C forms $^{14}CO_2$ which is rapidly mixed with the atmosphere. Living organisms contain constant level ^{14}C, but when dead, the activitydue to ^{14}C decreases with a half-life of 5730y. Hence, it can be used to measure ages of C- containing materials.

Tritium ($t^{1/2}$=12.33y) in the atmosphere is removed with the meteoric precipitation, which under favorable conditions can be used to date groundwater and study circulation of water in the ocean.

The cosmogenic noble gases nuclides ^{37}Ar, ^{39}Ar, ^{81}Kr and ^{85}Kr have long residence time in the atmosphere. The other cosmogenic ones, ^{10}Be, ^{26}AI and ^{32}Si, rapidly removed from the atmosphere by precipitation are deposited in marine or lacustrine sediments and in the polar ice sheets, where they are used to measure the rate of deposition of marine sediments. The group ^{10}Be,^{26}AI and ^{36}CI are suitable for glaciological studies together with ^{14}C, ^{31}CI and ^{81}Kr which occur in air bubbles trapped in glacial ice. Also, the cosmagenic^{10}Be, ^{26}AI and ^{36}CI accumulate in rocks exposed to cosmic rays at

the surface of the Earth, which makes them useful to measure erosion rates and exposure ages.

The existence of ^{10}Be in young volcanic rocks in island arcs and subduction zones has been attributed to the melting of deep sea sediments in the down-going slab of oceanic crust. Similarly, the presence of ^{10}Be in tektites from Indochina and Australia can be attributed to melting of continental sediments containing ^{10}Be produced in the atmosphere.

The use of these radionuclides for the study of geologic phenomena has been enhanced by ultra-senstive mass spectrometers. This equipment may enable to detect time-dependent variations in the production rates of certain radionuclides that could be attributed to past fluctuations of the solar activity or of the geomagnetic field.

COSMIC RAYS

The primary cosmic radiation arriving at the top of earth s atmosphere consists mainly of positively charged particles mostly protons.The energy spectrum is nearly l-2GeV, but may extend to 10^{15} or10^{18}eV.Heavier nuclei are also present: per 1000 protons are about 150 nuclei of helium, about 8 nuclei in the range of carbon-nitrogen-oxygen and about 3-4 heavier nuclei. Their energy spectra per nucleon are the same as the proton spectrum.

The cosmic rays incident on the earth's atmosphere are believed to be of galactic origin and to have been accelerated to their high energies by interstellar magnetic fields. The low energy (lGeV) component of the cosmic ray flux, is arriving from the sun especially during solar flares.

The intensity of the cosmic ray flux increases greatly with increasing altitude, at 6-9 km above the surface of the earth, it is 30 times greater than at ground level. Also, the high latitudes have a much stronger level of cosmic ray flux than low latitudes by a factor of five.The high altitude greater intensity is explained by the lower density of air and much less interactions, whereas the latitudinal effect is explained by the earth" s magnetic field.In the first case, the atmospheric air .pressure is very much reduced at higher altitudes (~50 mbar at 20km above sea level), so the absorption of cosmic rays by collisions with atmospheric atoms is much less.In the second case, the solar wind (a continual flow of protons and electrons) acts to press the magnetic lines of force on the side nearest to sun and the magnetic field is intensified, whereas on the opposite side of the earth the magnetopause is drawn far off the earth causing the lines of force to be attenuated and giving the entire magnetosphere the shape of a "Comet". The protons and electrons as well as the products of the cosmic shower are entrapped between the magnetic lines of force by being turned back and forth following sinuous paths. Thus, they are held far from the earth at the magnetic equator, but can reach down close to the ground in the magnetic polar regions.(Fig.) This geometry explains the latitudinal variation in cosmic flux back ground.

The energy of more than 50% of the cosmic flux particles is between 0.5 and 5 GeV. When high energetic protons hit target nuclei, it emits one or several nucleons and forms a product nucleus of lower atomic number. Such spallation reactions occur in the atmosphere of the earth when the cosmic ray protons and secondary particles interact with atoms of oxygen, nitrogen and argon.(Fig.) The resulting cosmogenic radionuclides either remain in the atmosphere for a long period of time or are rapidly removed from it by precipitation depending on their chemical properties.

Several of the cosmogenic radionuclides have sufficiently long half-lives to be useful for the study of geologic processes. The most important such radionuclides are ^{3}H, ^{7}Be, ^{10}Be, ^{14}C, $^{26}A1$,^{32}Si, $^{36}C1$,^{39}Ar, ^{81}Kr, ^{85}Kr.

THE C-14 DATING

^{14}C is produced in the atmosphere by interaction of cosmic rays produced neutrons with the stable isotopes of oxygen, nitrogen and carbon. The most important reaction is that between slow neutrons and nitrogen

$$^{14}N\ (n, p)^{14}C$$

The atoms of ^{14}C are then incorporated into $^{14}CO_2$ molecules which are rapidly mixed throughout the atmosphere and the hydrosphere and attain constant levels of concentration representing a steady state. This state is attained by the rate of production of ^{14}C in the atmosphere on one hand and its decay on the other according to the equation

$$^{14}C \rightarrow {}^{14}N + \beta^{-} + \upsilon^{-} + Q$$

Where the value of Q is 0.156 MeV to the ground state of ^{14}N and noɣ-ray is emitted.

The radioactivity of carbon extracted from plant or animal tissue that died t years ago is given by

$$A = A_0 e^{-\lambda t}$$

Where

A =^{14}C measured in dpm per gram carbon

A_0= ^{14}C in the same specimen when plant or animal were alive. The best estimate of the specific activity of ^{14}C in equilibrium with the atmosphere (A_0) is 13.56± 0.07 dpm/g

$t_{1/2}$ = 5730± 40y

$\lambda = 0.693/5730 = 1.209 \times 10\text{-}^{4}y^{-1}$

Solving the above equation for t

$$t = l/\lambda \ln(Ao/A)$$
$$= 19.035 \times 10^{3} \log (A_0/A) \text{ years}$$

However, it was observed that wood of the 18th and 19th centuries have ^{14}C activities ~2% higher than the wood of the 20thcentury, which was attributed to the massive introduction of dead CO_2 into the atmosphere by combustion of fossil fuel since the beginning of the industrial revolution. This became known as the "Suess Effect". Also, the Nuclear tests in the atmosphere in the fifties and the sixties and the operation of nuclear reactors and particle accelerators have greatly increased the level of ^{14}C activity on the surface of the earth. The Bomb-produced ^{14}C has been detected in the oceans and in the biosphere including humans.

The distributions of both cosmogenic and anthropogenic ^{14}C have been used to study the interaction of the atmosphere with the surface water layer and the deep waters of the ocean.

The development of tandem accelerator mass spectrometers, such ultrasensitive instruments enabled measurement of ^{14}C in small milligram size samples. Also, it is capable of measuring short lived cosmogenic isotopes.

A wide variety of materialsare datable by this method, Table, including calcium carbonate of mollusk shells. However, bio-genic or inorganically precipitated calcium carbonate may have anomalously low ^{14}C contents due to the presence of dead carbon released by the dissolution of limestone or due to aging of oceanic bottom waters.

TRITIUM

Following the discovery by Urey (1933) that natural hydrogen is composed of two isotopes, protium and deuterium, the search for heavier isotopes of hydrogen began.

The Norwegian Hydro-Electric Establishment, Oslo, Norway, electrolyzed 13,000 tons of ordinary water to 11c.c. and sent the sample to Lord Rutherford (1937) and the sample was analyzed by the newly developed mass spectrograph by Aston. This showed that the (T atoms : D atoms) was still less 50,000. Later, it was shown the T is radioactive and 31 years half-life was assigned to it. This paved the way to more sensitive methods of analysis, radioactive counting.

Naturally occurring T was detected in molecular hydrogen in the atmosphere. The T: H ratio was 4×10^{15}. This data supported a suggestion by Libby (1946) that T is produced by cosmic rays.

Tritium is a β^- emitter with an energy maximum of 18 KeV and half-life of 12.262± 0.004 years. It emits no gamma ray.

Cosmic ray produced tritium takes place by reactions like (n,t), (p,t) or (μ,t) on ^{14}N or ^{16}O. Based on the energy of the incident particle and the nuclear cross section, the production rate ranges between.

In addition ^3H is formed due to the explosion of nuclear devices in the atmosphere and by the operation of nuclear reactors and particle accelerators.

Tritium is rapidly incorporated into water molecules and is removed from the atmosphere by precipitation. The residence time of tritiated water in the lower stratosphere is 1-10 years. Once it reached the lower troposphere, its half-residence time is 35 days.

The concentration of H in meteoric water is measured in Tritium Units (T.U.), which the abundance of one ^3H atom per 10 hydrogen atoms and is equivalent to 7.1 disintegrations of ^3H per minute per liter of water, However, the concentration of ^3H in meteoric water depends on number of factors:

1) The natural production rate in the stratosphere, estimated to be 0.5± 0.3 atoms of $^3H/cm^2/sec$.
2) The decay of ^3H by beta emission to stable ^3He with a half-life of 12.26 y.
3) The second injection of ^3H from the stratosphere into the troposphere.
4) The presence of bomb-produced ^3H.
5) The presence of ^3H locally produced by nuclear reaction and particle acceleration.

It was observed that ^3H contents in meteoric precipitation in the northern hemisphere fluctuated between values less than 25(T.U.) prior to 1953 to 2200 (T.U.) in 1964 following the extensive testing of nuclear devices in the atmosphere.

The presence of the bomb-produced ^3H can serve as a tracer to study atmospheric, hydrologic and oceanic processes. However, the continuing decay of bomb-produced ^3H, its unequal global distribution and the local injection of anthropogenic ^3H, all interfer with the

use of this nuclide to trace the movement of water in the subsurface and to date its last exposure to the atmosphere.

An alternative method to date water is based on ^{3}He, the stable daughter of ^{3}H. The presence of ^{3}He from the atmosphere and old ground water may be corrected for by measurement of the $^{3}He/^{4}He$ ratio. The atmosphere value for this ratio is 1.384×10^{-6}. The existence of excess ^{3}He in the oceans has been confirmed.

^{7}Be and ^{10}Be

The cosmogenic Be-isotopes are formed by spallation reactions of high-energy protons with oxygen and nitrogen atoms .The global production rate of ^{10}Be is (1.5-3.0) $\times10^{-2}$ atoms/cm^2/sec. The ^{7}Be and ^{10}Be are rapidly removed from the atmosphere by precipitation and are transferred to the sediments at the bottom of the oceans and to the continental ice sheets of Greenland and Antarctica.

The short half-life (35 days) of ^{7}Be makes it useful for the study of atmospheric processes, surface ocean water and mixing of sediments in near shore marine and lacustrine environments .

The long lived ^{10}Be ($t_{½}=1.5\times10^{6}$ y) is useful in dating marine sediments which not only the time elapsed since deposition but also the secular variation of its production rate and the rate of sediment deposition

^{26}Al

It is produced from ^{40}Ar atoms in the atmosphere by spallation reactions caused by cosmic-ray protons. The production rate of ^{26}Al is about 1.1×10^{-4} atoms/cm^2/sec. The ^{26}Al is rapidly removed from the atmosphere and enters the oceans by precipitation and rapidly removed from the surface layer of the ocean by adsorption on particles of biological origin.

Also, ^{26}Al has been used to measure the growth rate of Mn-nodules. Both radionuclides (^{10}Be and ^{26}Al) are used to date continental ice sheets of Greenland and Antarctica which are considered geological reservoirs of cosmogenic radionuclide that form in the atmosphere. The most suitable ones: ^{10}Be, ^{26}Al, ^{32}Si and ^{36}Cl which have short residence time in the atmosphere and are deposited on the ice sheets within one year of their formation or less.

^{36}Cl

The ^{36}Cl has shown some promise for geological and hydrological studies. The radionuclide ^{36}Cl is produced by spallation reactions caused by cosmic-ray protons interactions with ^{40}Ar atoms. About ⅔of the production is in the stratosphere and ⅓ in the troposphere. The ^{36}Cl is also produced by irradiation of sea water (^{35}Cl) with neutrons released during nuclear explosions. After short residence time of about one week, ^{36}Cl is removed from the atmosphere by rain and snow.

The fraction of ^{36}Cl that enters the ocean remains in the solution until it decays because of the long residence time of chlorine (1×10^{8}y). However, chloride-bearing evaporate deposits and chloride mineral deposits in desert basins on land should contain cosmogenic^{36}Cl whose concentration can be used to date these deposits. Also, ^{36}Cl that is deposited on land remains in solution and may be used to date groundwater or trace its migration in the subsurface. The ^{36}Cl deposited in snow and ice sheets in Greenland and Antarctica is used to date these ice sheets and detect any variations in its production rate in the atmosphere

^{32}Si

The ^{32}Si use to date ice sheets and groundwater is limited because the deposition of ^{32}Si by meteoric precipitation appears to vary seasonally. Also, a correlation between ^{32}Si and bomb-

produced ^{90}Sr in air samples was found during the period 1960-1964 which indicated the presence of excess bomb-produced ^{32}Si in the air.

^{39}Ar

It is produced primarily from ^{40}Ar by several nuclear reactions, the most important of which is ^{40}Ar (n,2n) ^{39}Ar. Its concentration in the atmosphere is 0.112 ppm per liter of Ar, less than 5% of which is contributed by nuclear weapon tests in the atmosphere. The concentration of ^{39}Ar in the atmosphere is probably constant both in terms of time and geographic location on the Earth because it has a long residence time in the atmosphere which evens out fluctuations in its production rate. For this reason the radionuclide is well suited for the dating of glacial ice and groundwater.

^{81}Kr and ^{85}Kr

These cosmogenic radionuclides are produced by spallation reactions involving protons and by (n,ɣ) reactions from stable ^{80}Kr and ^{84}Kr respectively. The ^{85}k ($t_{½}$ = 10.6y) is produced also by nuclear fission. The ^{81}Kr ($t_{½}$ = 2.13×10^{5}y) is not a fission product but only a cosmogenic radionuclide that occurs in the atmosphere, in groundwater that has been in contact with the atmosphere and in bubbles trapped in glacial ice, hence suitable for dating such materials.

DATING MARINE SEDIMENTS

The abundance of cosmogenic radionuclide in a terrestrial reservoir such as ice sheets or sediments is controlled by:

1) The production rate of the radionuclide in the atmosphere, which depends on the cosmic ray flux, the strength of the Earth`s magnetic field, the concentration of target atoms in the atmosphere, and the nuclear cross-sections for the spallation reaction.
2) The sedimentation rate which in inversely proportional to the concentration of radionuclide, because a high sedimentation rate tends to dilute the concentration of the radionuclide.
3) The magnetic latitude of the site and the extent to which latitude dependent variation of the production rate are smoothed out by mixing during transport in the atmosphere, within the surface layer of the oceans, and bioturbation of sediment or flow deformation of ice.
4) The time elapsed since deposition.

The cosmogenic radionuclides ^{10}Be and ^{26}Al initially enter the ocean in ionic form and mix with their stable isotopes ^{9}Be and ^{27}Al respectively. Owing to their high ionic potentials (ratio of charge to radius), a significant fraction of both ions is rapidly removed from the surface layer by adsorption on particles of inorganic or biological origin.

The residence time of ^{10}Be and ^{26}Al in the surface layer of the ocean is estimated at ~16y which is comparable to the horizontal mixing time in this layer.The residence time of ^{10}Be and ^{26}Al in the deep ocean is very important it determines the time scale for variation in the production rate. It has been estimated ~630y for the scavenged species, whereas it is for the dissolved ionic species 1600y for ^{10}Be and 1400y for ^{26}Al which is comparable to the mixing time of the oceans taken to be 1000y. This implies that the deposition of ^{10}Be and ^{26}Al should be uniform throughout the oceans.
For dating sediments, it is assumed that the disintegration rate of (^{10}Be or ^{26}Al) varies only with time, according to

$$^{10}Be=^{10}Be_i\, e^{-\lambda t}$$

Where ^{10}Be is the disintegration rate atomic abundance, $^{10}Be_i$ is the same at time of deposition (t=0), λ of ^{10}Be is (0.462×10^{-6}ɣ$^{-1}$), and t is the time elapsed since deposition

If $^{10}Be_i$ is invariant with time and sedimentation rate is constant and equal to (a=h/t) where h is depth below top of the sediments, then the above equation can be rewritten as:

$$^{10}Be=^{10}Be_i\ e^{-(\lambda h/a)}$$

$$\ln{}^{10}Be=\ln{}^{10}Be_i - \lambda h/a$$

The last equation is a staright line in the coordinates $\ln{}^{10}Be$ and h whose slope $m=-\lambda/a$ and whose intercept on the ordinate is $\ln{}^{10}Be_i$

When both ^{10}Be and ^{26}Al are measured in the same samples (Fig.4), the ratio of their disintegration rates decreases with time according to the equation

$$^{26}Al/^{10}Be = (^{26}Al/^{10}Be)_I\ e^{-t(\lambda Al-\lambda Be)}$$

$$= (^{26}Al/^{10}Be)_I\ e^{-t\lambda`}$$

Where $\lambda`=0.506\times10^{-6}\ y^{-1}$ corresponding to $t_{1/2}=1.37\times10^6$y, and the straight line equation takes the form

$$\ln (^{26}Al/^{10}Be) = \ln(^{26}Al/^{10}Be)_I - \lambda`h/a$$

The advantage of thisgeochronometer is that time-dependent variations in the production rates and geochemical pathways of the two nuclides tend to cancel out.

VOLCANIC ROCKS

^{10}Be has been observed and measured in lavas extruded by volcanoes associated with subduction zones and island arcs. Also, the cosmogenic^{53}Mn ($t_{1/2}$ = 3.7 $\times10^6$y) may be detectable in island arc volcanics . The relatively high and uniform concentration of ^{10}Be, lead to the conclusion that the ^{10}Be in lava flows of island arcs results from the incorporation of deep-sea sediments at the source. This confirms that magma originates, at least in part, by melting within the down-going slab of the oceanic crust.

DATING OF CONTINENTAL ICE SHEETS AND GROUNDWATER

The continental ice sheets of Greenland and Antarctica are geological reservoirs of cosmogenic radionuclides that form in the atmosphere. The first group of these nuclides (^{10}Be, ^{26}Al, ^{36}Cl and ^{32}Si) have short residence times in the atmosphere and are deposited on the sheets within one year of their formation.

The second group oflong livedcosmogenic radionuclides associated with ice sheets have long residence time in the atmosphere because they are either noble gases (^{39}Ar, ^{81}Kr) or form gaseous compounds (^{3}H, ^{14}C). They occur trapped with air bubbles during conversion of snow to glacial ice. Therefore, their abundances are relatively insensitive to fluctuations in their production rates, hence, more suitable for dating.

A more reliable method of dating glacial ice is based on the ratio ($^{36}Cl/^{10}Be$). The relevant equation is

$$^{36}Cl/^{10}Be = (^{36}Cl/^{10}Be)_I\ e^{-\lambda`t}$$

Where $\lambda`=(\lambda_{Cl}-\lambda_{Be}) = 1.788\times10^{-6}y^{-1}$

Corresponding to effective $t_{½} = 3.87\times10^5$years

BIBLIOGRAPHY

Libby, W. F., 1955. Radiocarbon Dating (2nd ed.) University of Chicago press, Chicago, 175p.
Suess, h. E., 1955. Radiocarbon concentration in modern wood. Science, 122, 415-417.
Suess, h. E., 1969.Tritium geophysics as an international research project. Science, 163,1405-1410.
Craig,H and Lal, D., 1961. The production rate of natural rtritium. Tellus,13, 85-105.
Faur, G., 1986. Principle of Isotope Geology, (2nded) John Wiley and Sons, Newyork, 589p.
Strahler, A.N. and Strahler, A.H. 1973.Environmental Geoscience: InteractionBetween Natural Systems and Man. John Wiley and Sons In., NEW YORK, 511p.
Giletti, Bruno, 1956. The geochemistry of tritium. Ph. D. Thesis, Columbia University, 153p.

Table (1): Principal long-lived cosmogenic radionuclides.

Nuclide	$T_{1/2}$	λy^{-1}
^{10}Be	1.5×10^{6} y	0.462×10^{-6}
^{14}C	5730±40 y	0.1209×10^{-3}
^{26}Al	0.716×10^{6} y	0.968×10^{-6}
^{32}Si	276±32 y	0.251×10^{-2}
^{36}Cl	0.308×10^{6}y	2.25×10^{-6}
^{39}Ar	269 y	0.257×10^{-2}
^{53}Mn	3.7×10^{6} y	0.187×10^{-6}
^{59}Ni	8×10^{4} y	$0.086\times10^{-}4$
^{81}Kr	0.21310^{6} y	3.25×10^{-6}

Table (2): Material suitable for dating by the C-14 method.

Amount required In grams	Material
25	Charcoal and wood
25	Grains, seeds, nutshells, Grasses, twigs, cloth, Paper, hide, burned bones
50-300	Organic material Mixed with soil
50-200	Peat
50	Ivory
300	Bones (charred)
100 or more	Bones (collagen)
100	Shells (inorganic carbon)
several kilograms	Shells (organic carbon)
variable	Lake marl and deep-sea Or lake sediment
2-to5 kg	Pottery and iron

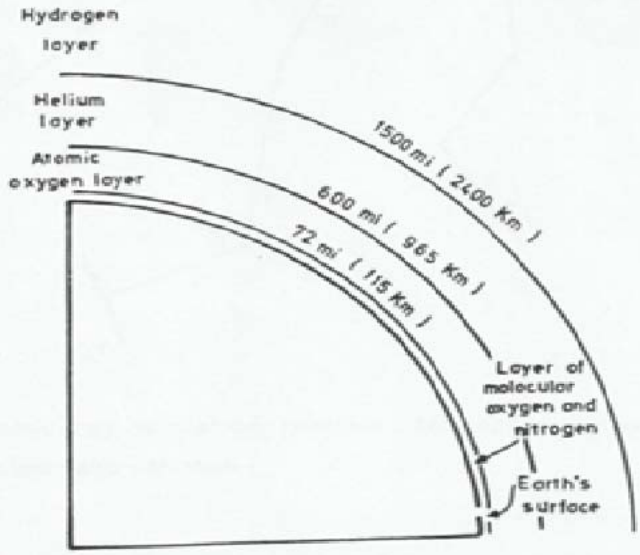

Fig. 1 Schematic diagram of the atomic helium and hydrogen layers of the earth's outer atomsphere.

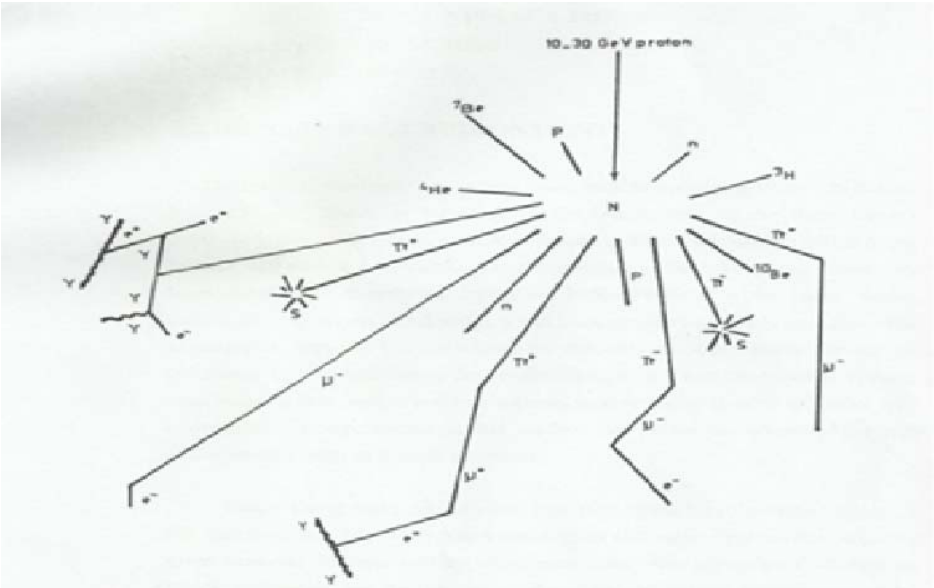

Fig. 2 Cosmic ray spallation reaction. Interaction between proton and N atom.

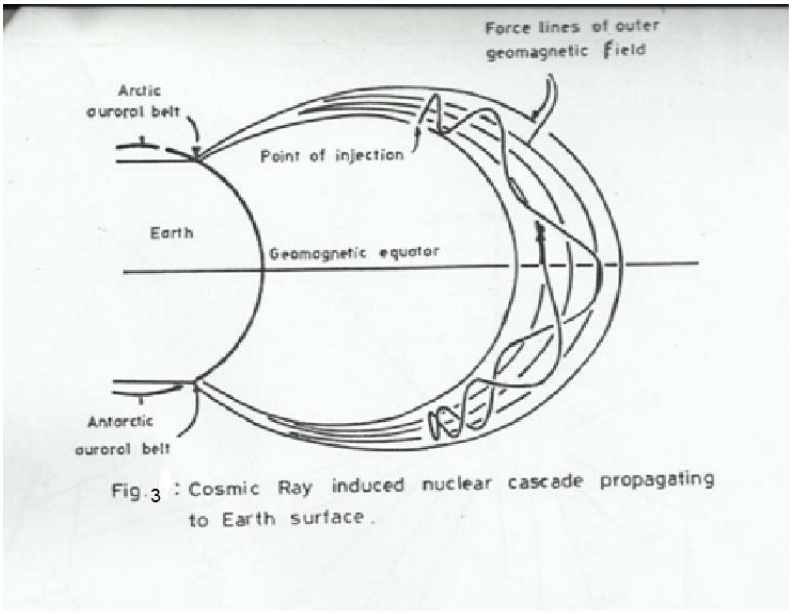

Fig. 3 : Cosmic Ray induced nuclear cascade propagating to Earth surface.

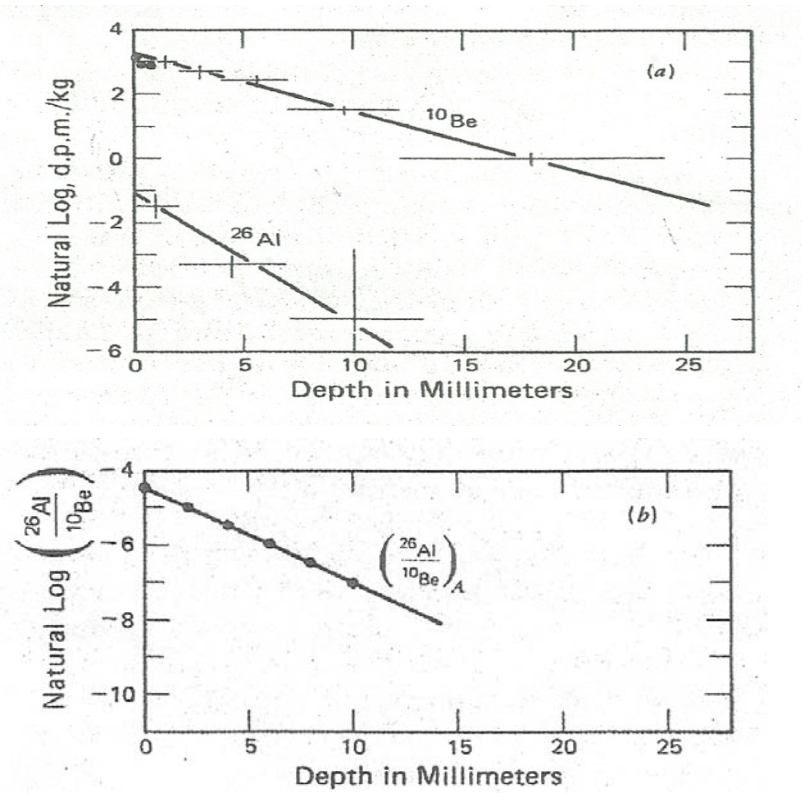

Fig. 4 a) The decay rate of cosmogenic ^{10}Be and ^{26}Al in manganese nodules from the Pacific Ocean. b) the decay rate of the isotopic ratio ^{26}Al/^{10}Be shows that the effective half-life is 1.37x10^{6} years.

Overview on the Multinational Collaborative Waste Storage and Disposal Solutions

C. A. MARGEANU
Reactor Physics, Nuclear Safety and Nuclear Fuel Performances Dept.,
Institute for Nuclear Research Pitesti, Romania
e-mail: cristina.margeanu@yahoo.com

ABSTRACT

The main drivers for a *Safe, Secure and Global Energy future* become clear and unequivocal: *Security of supply* for energy sources, *Low-carbon electricity generation* and *Extended nuclear power* assuring economic nuclear energy production, safe nuclear facilities and materials, safe and secure radioactive waste management and public acceptance. Responsible use of nuclear power requires that – in addition to safety, security and environmental protection associated with NPPs operation – credible solutions to be developed for dealing with the radioactive waste produced and especially for a responsible long term radioactive waste management. The paper deals with the existing multinational initiative in nuclear fuel cycle and the technical documents sustaining the multinational/regional disposal approach. Meantime, the paper far-reaching goal is to highlight on: What is offering the multinational waste storage and disposal solutions in terms of improved nuclear security?

***Key words*:** Global security and safety/multinational initiative approach and cooperation/multinational disposal/regional disposal/improved nuclear security

INTRODUCTION

Nowadays it becomes clear and unequivocal that a SAFE, SECURE and GLOBAL energy future will be driven by: ***Security of supply for energy sources*** and ***Low-carbon electricity generation*** that lead to ***Extended nuclear power*** assuring economic nuclear energy production, safe nuclear facilities and materials, safe and secure radioactive waste management and public acceptance that all previously mentioned conditions are guaranteed.

The radioactive waste management key goals can be expressed in the terms of the capability to ensure the SAFETY of future generations, to enhance short and long term world wide SECURITY, and to make safe and secure the proposed solutions for all nuclear nations. Last decades marked the nuclear security as a growing concern based on a couple of „sensitive points", such as:

- diversion of fissile materials separated during civil reprocessing of spent fuel (essentially means Pu stockpiles amounting up to hundreds of tonnes; Pu stockpiled inventories are still growing indicating that the owners do not know what to do with it),
- clandestine reprocessing of spent fuel to produce weapons materials (by states signatories of the Non-Proliferation Treaty, by states who not signed NPT or by terrorist groups; social and political dramatic changes or disruptions on decades can change the trusty status of a country and today's trusty guardian may be tomorrow's unpredictable regime),

- diversion of radioactive wastes with the intention of dispersion and contamination (radioactive dispersal devices terrorist attacks leading to massive social and economic impacts, even if the actual health hazards might be relatively low being involved small quantities of LLW),
- disruption of radioactive waste storage facilities in terrorist attacks, war or, recently, natural catastrophic conditions (a monster earthquake followed by a vast subsequent tsunami leads to the crisis at Fukushima Dai-ichi NPP in March, 2011).

All of the security problems previously mentioned are relevant for any country being already or entering into the nuclear power arena, and all of the possible solutions should be considered at the national level. The global evolution of the Spent Fuel (SF) amount is presented in the figure below, [1].

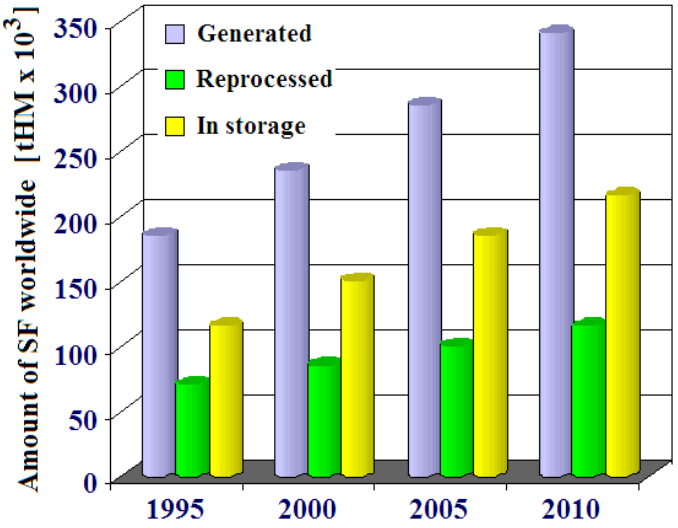

Responsible use of nuclear power requires that – in addition to safety, security and environmental protection measures associated with NPPs operation – credible solutions to be developed for dealing with the radioactive waste produced that include the spent fuel (if regarded as waste), High Level Waste (if reprocessing is carried out), and all other radioactive waste produced in nuclear fuel cycle activities. A full and credible solution to responsible long term radioactive waste management implies a technological and safety approach for spent fuel disposition strategy, an institutional framework to allow its implementation and the scientific, technical and industrial capabilities to carry out needed activities.

The radioactive waste management still centres on national strategies, not only for collection, interim storage and treatment, but also for disposal. The tendency towards unilateral action mainly reflects that radioactive waste represents a sensitive political issue, making difficult the cooperation among countries. It is a well-known, general accepted principle that a country enjoying the nuclear energy or nuclear technology use benefits, should also take full ethical and legal responsibility for managing the generated radioactive waste. This principle, however, does not necessarily imply that each country should exclusively develop its own national repositories, regardless of the technical, economic, financial and institutional implications. There are countries whose radioactive waste volumes do not easily justify a national repository, and/or countries that do not dispose of corresponding resources or favourable natural conditions for waste disposal to begin a national repository project or would prefer to collaborate in shared initiatives because of their

economic advantages. In such cases it may be appropriate encouraging of a multinational collaborative effort to ensure the access to a common repository, in order that the partner countries can fulfil the responsibility for their managing wastes safely.

VIABILITY OF THE MULTINATIONAL INITIATIVE AND COLLABORATION

The multinational and regional collaboration for spent fuel and high level waste disposal beneficiate by the International Atomic Energy Agency support based on technical documents on multinational/regional disposal approach (1998, IAEA TECDOC-1021 outlines the important factors to be taken into account in the process of realizing multinational disposal options, [2]; 2004, IAEA TECDOC-1413, key technical document for Member States potentially interested in multinational repository concepts as hosting, partner or third party countries, [3]; 2005, IAEA TECDOC-1482, report on multinational storage developments discussed in the terms of relevant technical, economic/financial, institutional, socio-political, and ethical infrastructural issues, [4]; 2011, IAEA TECDOC-1658, updated overview of earlier multinational initiatives for spent fuel storage and disposal, including a SWOT - strengths, weaknesses, opportunities and threats – analysis of recent initiatives and their impacts on the viability of implementing multinational disposal facilities in the future, [5]), Director General public statements (Dr. M. ElBaradei in 2003, 2008), establishment of a Multinational Approaches Expert Group which released in 2005 "Multilateral Approaches to the Nuclear Fuel Cycle" strategic study looking at how multilateral approaches throughout the nuclear fuel cycle can enhance global safety and security, [6].

The ***multinational repository concept***, according to IAEA TECDOC-1413, ***assumes that waste originating from more than one country is being disposed in a common repository***. The country hosting the repository, "host country", accepts waste from one or more other countries, "partner countries" or "customer / client countries". Apart from the host and partner countries other countries, "third party countries", may also have interest in the multinational repository. For example, a third party country may be a transit country for the shipment of the waste from the partner country to the host country. The multinational repository concept suggests that any country regardless of geographical location may participate in such a collaborative scheme.

Above mentioned IAEA report, [3], also deals with the terms of "regional repository concept" and "international repository concept". The regional repository concept is applied to multinational concepts in which the host country and the partner countries are located in the same geographic region of the world. The international repository concept implies that the waste disposal is organised under the authority of a supra-national body, such as the United Nations for instance.

Three main scenarios were identified as potentially feasible and were described in the IAEA TECDOC-1413, together with an additional concept - Fuel Leasing, as follows, [3]:

- *The Add-on Scenario*: a host country, having already implemented a national repository, offers, in some later stage, to complement its national inventory of wastes for disposal by wastes imported from other countries. Such a decision could be based on economic (share or decrease the disposal costs) or safety and security reasons. The repository remains effectively a *national repository*, but with a part of the nuclear waste inventory arising from abroad. However, the national infrastructural framework would have to be amended to enable the acceptance of foreign radioactive waste.

This type of scenario is characterised by the availability of all necessary resources and capabilities in the hosting country. In this case, a national repository programme would first be developed and implemented and then, at a later stage, disposal services might be offered to potential partner countries. It requires that the hosting country have the political will, the technical and financial resources and the natural conditions (geology) to develop a repository.

The host country motivation for participating in such scenario can arise from various reasons: straightforward business initiative; desire to share repository development costs; willingness to help neighbours (in the context of a regional repository scenario); interest in reducing global security risks; commitment to reduce the number of disposal sites worldwide; opportunity to trade its offer to take radioactive waste from its partners for some other national goal to which all partner countries can contribute.

- *The Cooperation Scenario*: a shared repository is developed by a group of partner countries (two or more) joining in a mutual agreement on building a repository in one or more of the participating countries, rather than having a national facility in each and every country. If the partner countries belong to the same geographical region, the repository is called *regional repository*; otherwise, it is called *multinational repository*.

The contribution of the partner countries will logically depend on the capabilities and demands of the hosting country and on their own capabilities. Potential contributions could include technical assistance (including regulatory assistance), advance funding or political support. Various cooperation scenarios can be developed, as in following examples:

▪ *Several industrialised countries, with relatively small nuclear energy programmes and extensive national experience, cooperate for the disposal of their radioactive waste in a host country satisfying all necessary technical requirements*.

The countries in such group would be attracted to the multinational concept because of the prospect of reducing the number of waste sites and saving resources by not developing individual repositories and by benefiting from economies of scale.

▪ *Several countries with small quantities of radioactive wastes and in varying stages of development seek assistance from each other and cooperate to ensure that one of them acquires all necessary technology and institutional structures*.

A good example for such scenario could be the cooperation between a significant number of IAEA's member states operating only research reactors and/or one or very few nuclear power reactors. These countries might all face similar difficulties in implementing a self-sufficient national disposal concept for all types of radioactive waste and particular for HLW and SNF. In these conditions, the multinational cooperation seems to be a logical consequence. The partners would cooperate to ensure that the finally chosen host or hosts, by the time of implementation, will satisfy all technical and institutional requirements.

Another good example could be several countries whose sole use of nuclear materials is in the industrial, research reactors and medical area.

▪ *Repositories specialized for specific types of waste, possibly combined with arrangements for international exchanges.*

This approach could be useful in the case when certain countries were specialized in disposal of specific types of waste. These countries could accept wastes of a certain type from other countries either as part of a commercial arrangement or, conceivably, as part of an agreement involving exchange of waste types. Examples could be the following: the collection of spent sealed sources for disposal in only a few countries, the exchange of heat generating waste against non-heat generating transuranic waste (TRU) or of L/ILW against HLW. Such

exchanges would require agreement among parties on waste equivalence and on measures for waste characterization, quality assurance and quality control.
The cooperation in this light illustrates the viability of multinational cooperation as a pre-stage for the development of multinational repositories. It could also lead to the development and implementation of specialised repositories as a multinational cooperative effort.

- *The International or Supra-national Scenario*: implementing a higher level of control and supervision, the operation of such a repository (or network of repositories) would be fully in the hands of an international body. Each host country would cede control of the necessary site to the specified international body.

A couple of additional complications are making this scenario unlikely in the near-term future, namely: creation of an extraterritorial framework and development of a financial model appealing to the host country and solving the multiple technical problems associated with opening a geological repository. However, increasing global concerns over proliferation and nuclear security may make countries more willing to cooperate thus give more credible chances to the international or supranational approach.

The scenarios previously described are end-point scenarios and could be interesting to discuss on the mechanisms which could lead to the successful development of each scenario.

The Type I scenario is host country driven and requires only one potential host to achieve the necessary level of national agreement and then to make an offer to partner countries. The most obvious candidates for host country are large countries with significant national waste inventories. An important additional driver for such potential hosts with a nuclear history, giving rise to legacy wastes, can be the availability of funding to enable remediation efforts to progress. The obvious partners are those with small nuclear waste inventories and/or complex geological environments.

The Type II scenarios are more partner country driven and states that a group of countries may get together, without, in the first instance, identifying potential hosts. These countries can work on agreeing a transparent and equitable framework for a multinational approach and thereafter seek potential hosting offers — either from within their own group or from third party countries who would subsequently become a member of the group. An interesting possibility in the partner-driven scenario is "a reverse auction" scenario possibility. It involves the "buyers" (the potential repository users) making open offers of financial and other benefits in the hope of attracting a potential host. If first iterations fails, the benefits offered are progressively raised until one (or more) hosting offers is received. This development scenario would ensure that the key acceptance issues were settled before investing the time and resources needed for development of a state of the art, safe repository.

For Type III scenarios the most plausible driver might be the global drive to combat the terrorism and thus to ensure that radioactive materials are as inaccessible as possible.

Fuel leasing Concept: assuming that the uranium producer or fuel fabricant does not transfer title of the delivered fuel to the user. Instead, the fuel is leased for use in the reactor and returned to the supplier when discharged from the reactor. Such promising approach would allow all countries (even with small nuclear programmes) to enjoy nuclear power benefits without challenging with the spent fuel management and providing the necessary infrastructure by itself. However, in order to provide fuel leasing services, the supplier must be in a country that will accept the spent fuel return from other countries.

The fuel leasing concept was part of the Global Nuclear Energy Partnership (GNEP) launched in 2006, in order to restrict the spread of sensitive technologies such as enrichment, but it did not come to fruition under that program. Of all the nuclear suppliers, Russia has expressed the most support for fuel leasing and take-back.

The IAEA TECDOC-1482 presents the results of an analysis applied to the Regional Spent Fuel Storage Facility by taking into account, under the light of ethical considerations, the following: technical requirements (safety criteria and standards, safeguards and physical protection, fuel acceptance criteria, long term stability of systems and stored fuel, site selection, infrastructure issues, storage technology, licensing, operations in the repository, spent fuel transportation, decommissioning of the facility, R&D), economic and financial considerations (financial sources and conditions, economic evaluation, potential host country and customers), institutional issues (organizations, legal aspects), political and public acceptance considerations.

The regional spent fuel storage concept is a part of the overall nuclear fuel cycle, as shown in figure below, [4], and therefore should not be seen in isolation.

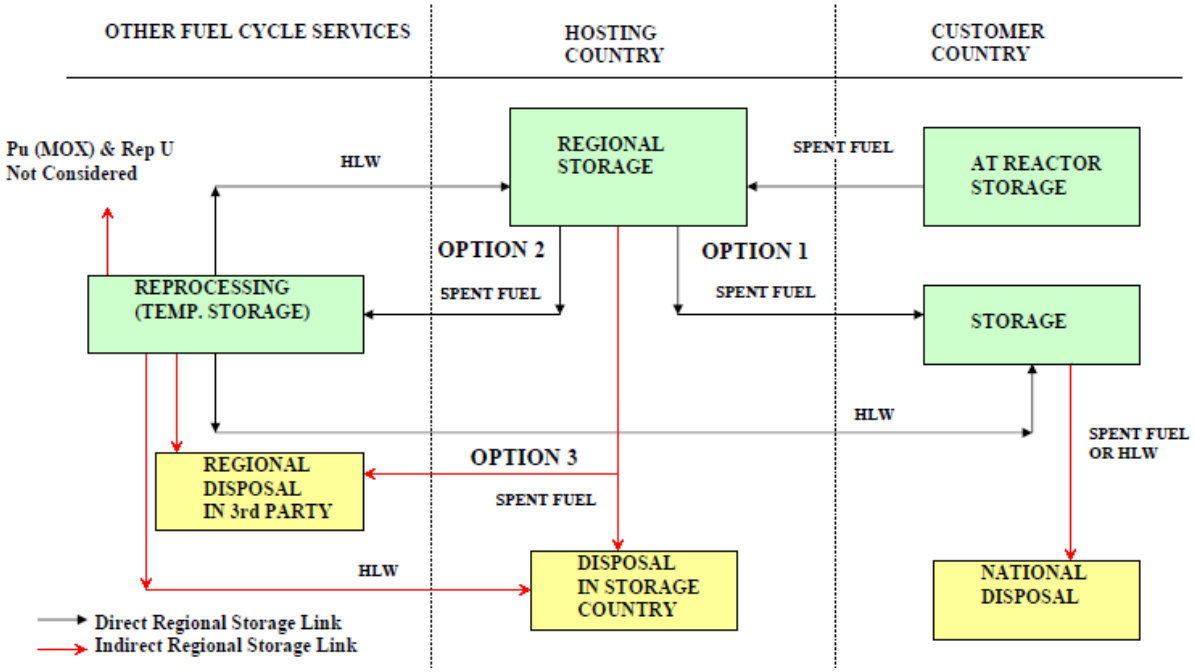

There are three categories of stakeholders involved in a regional spent fuel storage system, namely: ***hosting country*** offering a regional spent fuel storage service, ***customer countries*** sending their spent fuel to the hosting country for storage, and ***third party countries*** having an interest in the storage system.

The host country offering a regional spent fuel storage service has, basically, three options: Option 1 – the spent fuel is stored in the regional storage facility for a specified period determined at the beginning of the storage agreement. The storage being the only service offered, the customer country agrees to take back the spent fuel at the end of this period. There may be an acknowledged possibility of the spent fuel remaining in the regional storage facility beyond the termination date, if agreed by both the parties, and also the possibility to let the storage period open-ended.

Option 2 – the spent fuel is stored in the regional facility for a specified (or unspecified) period, after which it will be sent for reprocessing. It is possible again to extend the storage period as agreed among the parties. Reprocessing services can be available in the hosting country or be obtained from another country. The reprocessing service is assumed to be based on the undertaking that HLW will be returned either to the customer country directly, or to the regional storage facility or to a disposal facility if the latter is available within the hosting country or in a multinational repository in a third country. The disposal possibility for the HLW is not considered to form a direct link to the regional storage system. The other materials resulting from reprocessing do not form part of this management system.
Option 3 – the spent fuel is stored for a specified (or unspecified) period in the regional storage facility, after which it will be transferred to a regional disposal facility in the hosting country or in a multinational repository as mentioned in Option 2. The direct disposal for spent fuel is also not considered to form a direct link to the regional storage facility.

The IAEA TECDOC-1482 conclusions sustained the technical feasibility and viability of the regional spent fuel storage concept, based on the potential safeguards and security benefits coming from the spent fuel storing in a few safe, reliable, secure facilities. There have been suggestions that multinational storage schemes might be more easily implemented than final disposal projects with indefinite timescales. However, public and political opposition to accepting foreign fuel for storage represent also a strong driver, unless definite agreements for sending the material back to the owner are in place.

IAEA TECDOC-1658 succeeded to offer a valuable updated overview of changing global attitudes towards nuclear power and of potential developments in the nuclear fuel cycle, assessing how and when these changes may influence the viability of establishing multinational disposition approaches for spent fuel. The report addressed in more detail the key open technical and strategic issues (identified already in earlier IAEA works) that strongly affect the probability of multinational approaches success, identifying areas in which further work could be done to advance the progress of multinational approaches towards the final disposition of spent nuclear fuel.

In choosing the national policies for the peaceful use of nuclear energy, states make decisions exercising their sovereign rights, taking into account also their international treaty commitments under, for example the Non-Proliferation Treaty. They may, in principle, choose to pursue national nuclear programmes under their exclusive control to meet their nuclear energy generation requirements. However, must restrict the further spread of sensitive technologies that could give a capability for weapons production to additional countries. IAEA refers to "sensitive technological areas" relevant to the application of safeguards as being: (a) Uranium enrichment; (b) Spent fuel reprocessing; (c) Heavy water production; (d) Plutonium handling, including manufacture of Pu and Mixed Uranium/Plutonium fuel, [5].

The interest increase in using nuclear power and the goal of managing the expansion in ways that reduce risks of proliferation and terrorism are strong drivers for implementation of shared spent fuel disposition facilities.

The developments in reactor and fuel cycle technologies will directly impact on disposal, in both technical level and strategic manner. At *technical level*, the advanced approaches will change the long-lived radioactive wastes nature and volume. Shorter toxic lifetimes can result in making easier the problems of finding suitable repository sites and developing expensive, long-lived engineered barriers. The variety of fuel and waste types will imply polyvalent

handling and disposal facilities. Most of the technological developments come as arguments in favour of shared repositories that avoid the necessity for all nuclear power programmes, however small, to develop all of the required technologies. The new possibilities opened by reactor and fuel cycle developments influence strategic as well as technical thinking on disposition options. Disposal strategies may change; spent fuel may become less of a liability and more of an asset, so that direct disposal will become less attractive. A key point still remains as long as they do not eliminate the need for geological disposal. There are extensive inventories of existing spent fuel or wastes where new technologies cannot be retroactively applied. Furthermore, none of the advanced treatments will eliminate all long-lived wastes resulting from nuclear power generation. Lastly, other nuclear technologies also produce long-lived wastes that must be emplaced in geological repositories.

In the above mentioned IAEA report, [5], recent initiatives are described and their impacts on the viability of implementing multinational disposal facilities in the future are assessed. The assessment is based on examination of the strengths of the proposals and the opportunities they provide for advancing multinational initiatives. It considers also their weaknesses and the threats that they might pose for national disposition programmes or for multinational cooperation prospects.

The selected key issues for assessment are as follows: siting strategies; regulatory and legal aspects; liabilities and long term rights; fair funding mechanisms; safety and security; timing for repository implementation; political attitudes and public acceptance; potential impact on the national nuclear programmes.

Talking further on multinational initiative in nuclear fuel cycle it must be mentioned:

- *Global Nuclear Power Infrastructure (GNPI)*: Russian initiative, based on possible *Add-on and fuel leasing scenarios*, is centred on proposals to establish multinational facilities providing shared ownership for enrichment, reprocessing and eventually disposal. Establishment of a network of International Nuclear Fuel Cycle Centres (INFCC), including enrichment services, under IAEA safeguards, was a key element of such an infrastructure, capable of providing access to the benefits of nuclear energy to all interested countries in strict compliance with non-proliferation requirements. To be noted that Russia mentioned the potential follow-up stages of GNPI-INFCC implementation that include organizing a timely solution of spent fuel management by reprocessing and disposal of residual waste using modern fast reactor and spent fuel management technologies.

- *Global Nuclear Energy Partnership (GNEP)*: originally proposed by USA in 2006, based on possible *Add-on and fuel leasing scenarios,* represents a far-reaching effort aimed to promote the global expansion of nuclear power while decreasing risks of proliferation and nuclear terrorism and addressing the challenges of disposal, by encouraging States to rely on assured fuel services rather than acquiring indigenous enrichment and reprocessing capabilities. Success in GNEP would result in a small number of suppliers that provide assured supplies of fresh fuel and spent fuel disposition services for the rest of the world. GNEP anticipated a fuel cycle arrangement under which assistance and assurances of supply of fresh fuel would encourage States to build and operate nuclear power reactors and return their spent fuel to GNEP recycling centres, where the spent fuel would be processed and separated into constituent streams. A key feature of GNEP is the coordinated research and development programme to develop the enabling transuranic partitioning and transmutation technologies required to fulfil the global GNEP spent fuel disposition commitments. The expansion of GNEP to many countries beyond the original group that would like to supply

fuel cycles services is a positive development, but still remains long way ahead to be successful. The key elements of GNEP are shown in the figure below, [5].

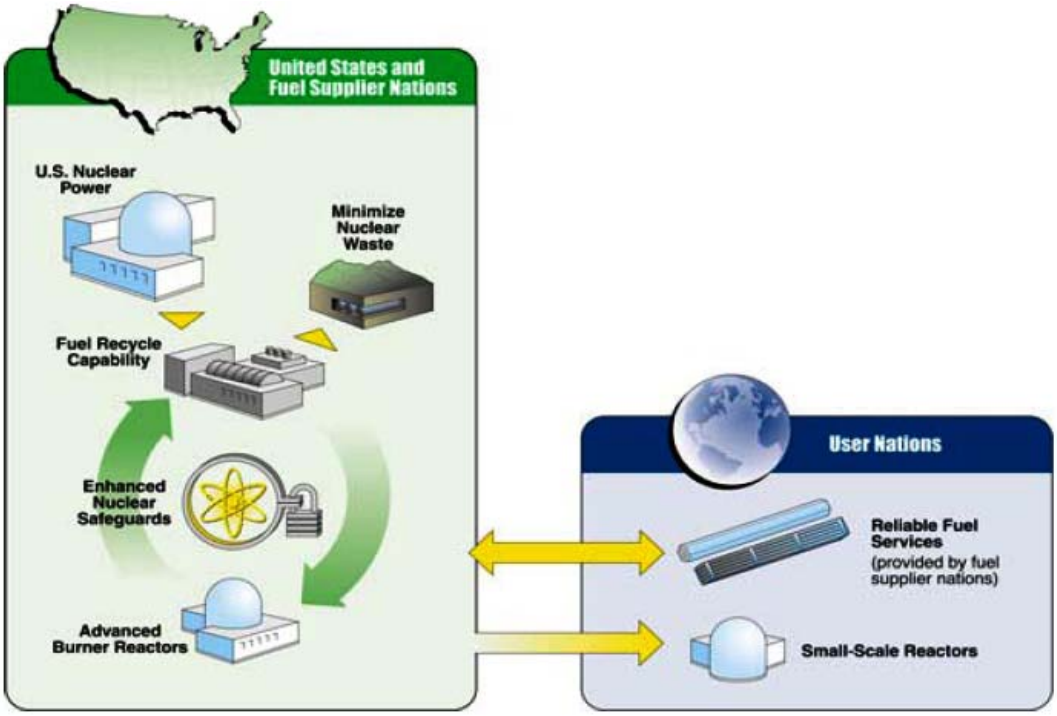

- *SAPIERR (Strategic Action Plan for Implementation of European Regional Repositories) Projects*, [7]: based on European Commission funds, is leadership the credible *cooperation approaches* to provide multinational disposal facilities that could increase global security, as well as bringing economic and environmental benefits. SAPIERR-I, 2003-2005, involved 14 European countries, being devoted to pilot studies on the feasibility of shared regional storage facilities and geological repositories, for use by European countries. It was designed to help the EC clarify basic questions, legal aspects affecting the issue and to identify new research and technical developments that may be needed to implement regional solutions to European radioactive waste disposal. SAPIERR-II, 2006-2008, as follow-up project was built on the pilot studies of SAPIERR-I to develop options for organizational frameworks and project plans that could lead to the establishment of a European Repository Development Organization (ERDO) for European regional repositories. To clarify issues related to the potential ERDO structure and future programme, a series of specific studies were carried out on organizational structures, legal liabilities, economics, safety and security and public and political acceptability. At the end of the project, SAPIERR shared storage and disposal concept had been developed to a level where political level buy-in was necessary for further progress.

- *ERDO-WG (European Repository Development Organization Working Group)*: includes representatives nominated by the governments of ten countries working together on a shared solution for radioactive waste to establish the basis for a commonly owned, not-for-profit organisation that could develop and implement shared solutions. First stage of the ERDO-WG work, already completed, was to produce a model structure and plan for the ERDO (see figure below, according to information available on ERDO-WG web site, [8]). The second part is to present its model structure and plan for ERDO to the governments of potentially interested

Member States in order to establish which countries wish to go ahead with the formal establishment of a jointly owned ERDO. Establishing ERDO, with a clear development plan and associated work schedule, would fulfil part of the requirements placed on its owner countries by EU Council Directive 2011/70/EURATOM. The other associated element of these requirements is that ***a shared solution should not be pursued on its own; it should lie within the framework of a national plan and programme in each country. This approach has become known as a "dual track" approach.*** If ERDO initiative will be successful, it may act as a role model for regional cooperation in other parts of the world, such as Arabian Gulf, South East Asia, Central and South America or North Africa. ERDO represents a major step forward in Europe.

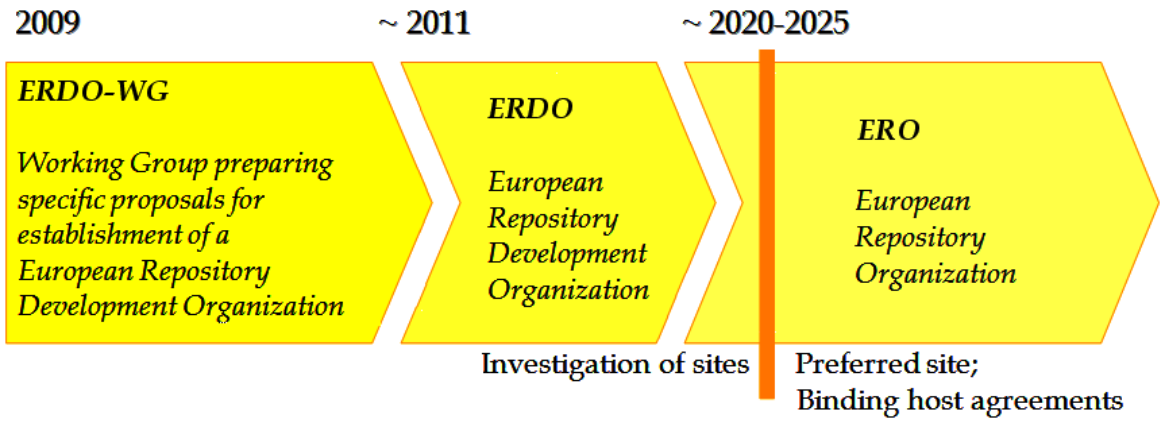

- *ARIUS (Association for Regional and International Underground Storage)*, [1]: formed in 2002 and based on *cooperation scenarios*, aims to organize studies of technical, legal, political and societal issues associated with multinational storage and disposal options, and to ensure that these options remain a topic for discussions on the world stage and are recognized as a feasible future choice for countries that express their option for this strategy. ARIUS is also a key driving organization behind the SAPIERR projects. ARIUS undertakes a number of studies to find answers to some of the principal questions surrounding international solutions.

THE MULTINATIONAL WASTE STORAGE AND DISPOSAL SOLUTIONS ON THE WAY TO IMPROVED NUCLEAR SECURITY

The most commonly posed question when the issue of shared repositories is raised is *"which country will be the host?"*. "You will never find that a country is willing to host a repository for other people's waste … but there is a way forward, modelled on the best international practice being pursued today", [8].

In practice, multinational sitting strategies can be modelled directly on successful, modern, national sitting approaches since both approaches face very similar challenges. National and multinational disposal projects both have to go through the same technical and stakeholder involvement steps; they may take many years to achieve sitting successfully, avoiding the premature selection of potential sites. A successful sitting programme must be consensual and inclusive from the outset, must assure the transparency for all aspects of the repository project, must allow active inclusion of local communities at all stages.

The expected global security and safety benefits were recognized as major arguments for supporting the concept of multinational repositories and encouraging potential host countries to offer their cooperation to interested partner countries.

Providing a proper disposal facility accessible also to countries that may not be in a position to implement a state of the art national repository may contribute to safety and security on a global scale.

It may also reduce proliferation concerns. Emplacing the SNF deep underground inside a facility that is highly monitored, with numerous engineered and administrative controls, can enhance both physical security and safeguards relative to most surface storage facilities.

In addition the multinational repository approach could be useful in further reducing the environmental impacts for small countries with limited resources. With a multinational approach the environmental risks associated with under-funded or marginally-funded repositories that might result in some countries could be avoided.

For the host country a multinational repository implementation could incur a negative incremental long term environmental impact because it will become the disposal site for radioactive material generated by partner countries. Such potentially greater environmental impacts require that the benefits of cooperation are equitably shared between host and partner, and fees paid to the host by partner country are to be assumed.

The SAPIERR-II report on safety and security concludes that the required safety and security standards are achievable for multinational facilities and confirms that a shared project presents no technical issues that will not have to be overcome in national projects.

International treaties and conventions, and the comprehensive system of international guidance, national regulations and control mechanisms, ensure that a shared regional repository and associated waste management system will be at least as safe and secure as any national repository and waste management system. Indeed, a shared waste management system and final repository offers a potential safety advantage over separate smaller national systems primarily as a result of the pooled financial and human resources that can be invested to ensure implementation to high technical standards.

A shared final repository also offers a security advantage in the long-term against proliferation of nuclear materials, since the number of sites at which nuclear material is held is reduced. Furthermore, since the combined efforts of several countries may give better prospects for joint realisation of a project at an earlier time than if national projects proceed independently, this presents a small but tangible benefit due to a reduction in the average time that spent fuel is stored at national facilities.

What is offering the multinational waste storage and disposal solutions in terms of improved nuclear security? In the following, some key issues are summarized:

▪ *a limited number of storage/disposal facilities to be secured* – enhancing security; replacing disconnected organisations with different standards and financial capabilities; making easier to control activities and, for public, more transparent to monitor;

▪ *enhanced engineered and institutional security measures* – ensuring the highest standards of safety & security for a few multinational repositories; encouraging in the same time the harmonisation of individual countries standards;

▪ *enhanced level of international oversight* – benefit of a simpler safeguards surveillance on a few multinational repositories, with activities carried out stringently, but more economically; the international oversight guaranteed not only by the normal IAEA mechanisms but also by the insight required by the nations sharing the disposal facility;

▪ *improved financing arrangements* – general economic advantages of sharing well-known / economy of scale; easier finding funds for long-term disposal projects; reducing chances that the funds intended to provide waste disposal security could be diverted to more pressing needs in times of national crisis; a closer financial control and oversight.
▪ *availability of earlier underground disposal for smaller countries*, with new nuclear power programs and/or no realistic repository options in their programs.

The IAEA plays a central role in encouraging and facilitating progress in multinational waste storage and disposal. The IAEA assists Member States in examining the issues concerning shared facilities for spent fuel disposition, by developing best approaches and implementing sound spent fuel disposition strategies, publishing guidelines and facilitating the promulgation of best practices.

REFERENCES

[1] Association for Regional and International Underground Storage (ARIUS) official website, www.Arius-world.org
[2] "Technical, Institutional and Economic Factors Important for Developing a Multinational Radioactive Waste Repository", IAEA TECDOC-1021 (1998)
[3] "Developing multinational radioactive waste repositories: Infrastructural framework and scenarios of cooperation", IAEA TECDOC-1413 (2004)
[4] "Technical, economic and institutional aspects of regional spent fuel storage facilities", IAEA TECDOC-1482 (2005)
[5] "Viability of Sharing Facilities for the Disposal of Spent Fuel and Nuclear Waste", IAEA TECDOC-1658 (2011)
[6] "Multilateral Approaches to the Nuclear Fuel Cycle", IAEA, INFCIRC/640 (2005)
[7] The SAPIERR Projects official website, www.sapierr.net
[8] European Repository Development Organization Working Group official website, www.erdo-wg.eu

International Regulations for Transport of Radioactive Materials, History and Security

R.M.K.EL-Shinawy
Radiation Protection Dept. NRC,
Atomic Energy Authority, Cairo, Egypt.

ABSRACT

International Regulations for the transport of radioactive materials have been published by International Atomic Energy Agency (IAEA) since 1961. These Regulations have been widely adopted into national Regulations. Also adopted into different modal Regulations such as International Air Transport Association (IATA)& International Martime Organization (IMO). These Regulations provide standards for insuring a high level of safety of general public, transport workers, property & environment against radiation, contamination, criticality hazard & thermal effects associated with the transport of radioactive wastes & materials.

Several reviews conducted in consultation with Member States (MS) & concerned international organizations, resulted in comprehensive revisions till now.

Radioactive materials are generally transported by specialized transport companies & experts. Shippers & carriers have designed their transport operations to comply with these international Regulations.

About 20million consignments of radioactive materials take place around the world each year. These materials were used in different fields such as medicine, industry, agriculture, research, consumer product & electric power generation.

After September 11,2001, the IAEA & MS have worked together to develop a new guidance document concerning the security in the transport of radioactive materials. IAEA have initiated activities to assist MS in addressing the need for transport security in a comprehensive manner. The security guidance & measures were mentioned & discussed. The transport security becomes more developed & integrated into national Regulations of many countries beside the safety Regulations. IAEA & other International organizations are working with MS to implement transport security programs such as guidance, training, security assessments & upgrade assistance in these fields.

Key words: ***Transport, Radioactive material, Safety, Security, Training***

INTRODUCTION

The use of radioactive material is an important part of modern life and technology. Radioactive material is used extensively in medicine, industry, agriculture, research, consumer products and electrical power generation. Tens of millions of packages containing radioactive material are consigned for transport each year throughout the world[(1)]. The quantity of radioactive material in these packages varies from very small quantities in

shipments of consumer products to very large quantities in shipments of irradiated nuclear fuel.

The Regulations for safe transport of radioactive material establish standards of safety which provide an acceptable level of control of the radiation, criticality and thermal hazards to persons, property and the environment that are associated with the transport of radioactive material.

These Regulations are supplemented by hierarchy of Safety Guides and Safety Practices including "Advisory Material for the IAEA Regulations for the Safe Transport of Radioactive Material" IAEA Safety Standards Series No ST-2[(2)]; Planning and Preparing for Emergency Response to Transport Accidents Involving Radioactive Material" IAEA Safety Standard Series No.ST-3;[(3)]" Compliance Assurance for the Safe Transport of Radioactive Material" IAEA Safety Series No.112[(4)]; " Quality Assurance for the Safe Transport of Radioactive Material", IAEA Safety Series No.113[(5)] and others.

The IAEA first published Safety Series No.(6) in 1961[(6)] for application to the national and international transport of radioactive material by all modes of transport. Several reviews, conducted in consultation with Member States and the international organizations concerned, resulted in seven comprehensive revisions being published in 1964, 1967, 1973,1985,1996,2005 and 2009[(7)].

Through the worldwide adoption of the IAEA's Regulations for all modes of transport, a very high level of safety during transport has been achieved.

Nuclear fuel cycle facilities are located in various parts of the world and materials of many kinds need to be transported between them. Many of these are similar to materials used in other industrial activities. However, the nuclear industry's fuel and waste materials are radioactive, and it is these 'nuclear materials' about which there is most public concern.

The highly radioactive wastes (especially fission products) created in the nuclear reactor are segregated and recovered during the reprocessing operation. These wastes were transported using a specially designed ships (Purpose – built ships). See Fig (1).

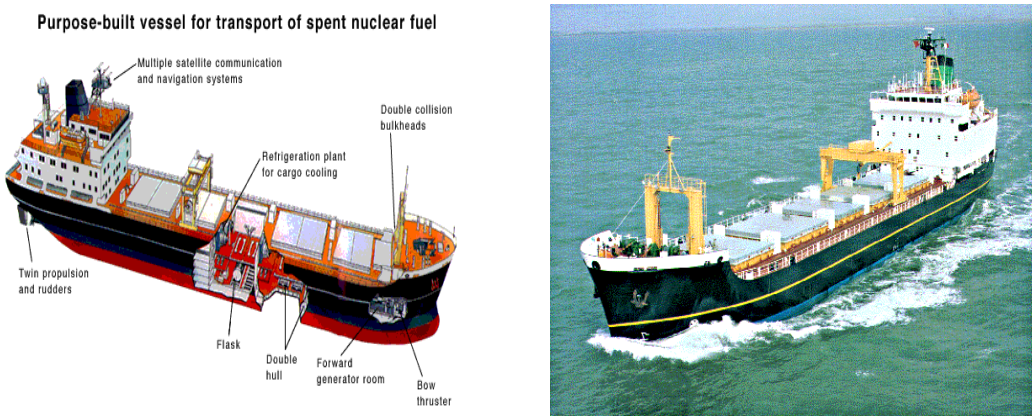

Fig.1

The transport ships are designed to withstand a side-on collision with a large oil tanker. If the ship did sink, the casks will remain sound for many years and would be relatively easy to recover since instrumentation including location beacons would activate and monitor the casks.

The British Company, Pacific Nuclear Transport Ltd, (PNTL) fleet has successfully completed more than 170 shipments over 30 years. About 8 million kilometers were covered without any accident resulting in release of radioactivity.

Except for some fissile materials (also called nuclear material in international instruments), the security of radioactive materials during transport was not a major concern prior to September11, 2001. Normal commercial practices were considered adequate to prevent loss of the material, and there was little concern that anyone would want to acquire the material for malicious purposes. That belief has been disproven by the revelation that adversaries not only have examined the possibility of using radioactive materials for malicious acts, but also have planned such acts and demonstrated a willingness to use all means at their disposal to carry them out. The IAEA and Member States have worked cooperatively to develop a new guidance document "Security in the Transport of Radioactive Material[8] and have initiated activities to assist Member States in addressing the need for transport security in a complete manner.

IAEA REGULATIONS, HISTORY AND DEVELOPMENT

Although radioactive material has been used for more than a century, significant use for beneficial purposes only began in the later 1940s and early 1950s. At that time, since the utilization of this material was increasing dramatically, it was recognized that safe and effective transport arrangements were required in order to properly protect man and his environment.

Since 1957, the IAEA has exerted efforts towards developing and maintaining its Regulations for the Safe Transport of Radioactive Material .

The result of this effort was the publication of the IAEA`s Regulations for the Safe Transport of Radioactive Materials, 1961 Edition, Safety Series No.[6]. This first edition of the Regulations established basic prescriptions in terms of packaging standards and package make-up for the containment of radioactive material and for the prevention of criticality when the material is fissile.

Since the Regulations were first issued, the IAEA has hardly worked with its Member States and relevant international organizations to update the Regulations, taking advantage of experience in the application of the Regulations and of advances in technology and knowledge. Consequently, the IAEA has issued several revisions to the Regulations.

The 1996 Edition of the Regulations was issued with a new nomenclature. It was identified as "IAEA Safety Standards Series, Requirements, No.ST-1[9], " rather than Safety Series No.6. In 2000 a revised edition of ST-1 was issued and was identified as IAEA Safety Standards Series Requirements, No.ST-R-1" (ST-1 Revised)[10].

The Standing Advisory Group on the Safe Transport of Radioactive Material (SAGSTRAM) was established by the IAEA in 1978 to advise on the IAEA`s transport safety programme and on the development and implementation of the Regulations. Safety Standards Committee (TRANSSAC) was formed in 1996 (and renamed to TRANSSC in 2000) replacing the function of SAGSTRAM. This advisory body ultimately endorses the text for a revision to the Regulations, and recommends submission of that text to the IAEA Board of Governors for approval.

Regulations Philosophy

The Regulations are fundamentally based on the philosophy that radioactive material being transported should be adequately packaged to provide protection against the hazards of the material under all conditions of transport including foreseeable accidents.

Therefore, the philosophy of the Regulations is that, as far as possible:

(1) Packages of radioactive material should be dealt with in the same way as other hazardous goods;
(2) Safety depends primarily upon the package and not on operational control;
(3) The consignor should be responsible for ensuring safety during transport through proper characterization of the contents proper packaging of those contents, and proper operational actions.

Regulations Scope and Objective

The scope of the Regulations is clearly specified and applied to:

(1) The transport of radioactive material by all modes on land, water or in the air,
(2) Any transport which is incidental to the use of the radioactive material.

In this context, transport comprises all operations conditions associated with, and involved in the movement of the radioactive material including the:

(1) Design of the package;
(2) Manufacture, maintenance and repair of the packaging; and
(3) Preparation, consigning, loading, carriage (including in –transit storage), unloading and receipt at the final destination of loads of radioactive material and packages.

In this Regulations there are three general performance levels that relate to the design of the package:

(1) Routine conditions of transport (incident free),
(2) Normal conditions of transport (minor mishaps), and
(3) Accident conditions of transport.

On the other hand, these Regulations do not apply to the following types of material:

(1) Radioactive material that is an integral part of the means of transport (such as depleted uranium counterweights in a aircraft);
(2) Radioactive material moved within an establishment that is subject to appropriate safety Regulations in force in the establishment and where the movement dose not involve public roads or railways;
(3) Radioactive material implanted or incorporated into a person or live animal for diagnosis or treatment (such as a cardiac pacemaker, or radionuclides injected into a person for medical purposes);
(4) Radioactive material in consumer products that have received regulatory approval, following their sale to the end user (such as smoke detectors);
(5) Natural material and ores containing naturally occurring radionuclides which are not intended to be processed for use of these radionuclides provided that the activity concentration of the material dose not exceed certain limits.

The objective of the Regulations is to protect people and the environment from the effects of radiation during the transport of radioactive material.

Protection is achieved by:

- containment of radioactive contents;
- control of external radiation levels;
- prevention of criticality; and
- prevention of damage caused by heat.

The fundamental principle applied to the transport of radioactive material is that the protection comes from the design of the package, regardless of how the material is transported.

PACKAGES, PACKAGING AND CATEGORIES

By package is meant the packaging together with is radioactive contents as presented for transport. Packaging may, in particular, consist of one or more receptacle, absorbing materials, spacing structure, radiation shielding and devices for cooling, for absorbing mechanical shocks and for thermal insulation. There are six types of packaging.

1- Excepted Package

Is a packaging containing excepted radioactive material, empty package and may be transported provided that:

- It is in a good condition and securely closed.
- Any labels which may have been displayed on it, are no longer visible.

2- Industrial packages

These are packages designed to contain low specific activity materials (LSAM) or surface contaminated objects (SCO), are of three different Types, IP-1, IP-2 and IP-3.

3- Type (A) package

It is designed to withstand the normal conditions of transport and minor possible accidents.

4- Type (B) package

It is designed to withstand the normal conditions of transport and severe accident conditions.

There are two classes namely:

- Type $B_{(U)}$, requiring unilateral approval (*competent authority of the country of origin*).
- Type $B_{(M)}$, requiring multilateral approval (*competent authorities of all the countries through or into which the package may pass*).

5- Type (C) package

It is designed to withstand severe crush, puncture and fire tests as well as impact with high speed (90m/sec). It is used to transport large quantities of radioactive material by air.

6- Packages containing fissile materials

These packages must be designed to ensure criticality safety during normal and accident conditions of transport.

Categories For Packages And Overpacks

To protect the public and transport workers against radiation emitted by the material during transport, the radiation level in the vicinity of the packages is limited. With regard to the shielding provided, packages are classified in three categories, I-WHITE, II-YELLOW AND III-YELLOW (see Fig.2&3). Each is associated with specified maximum radiation levels at the external surface of the package (0.005mSv/h), (0.005-0.5mSv/h) (0.5-2mSv/h) and at a distance of one meter from the surface (TI)(0), (0-1) &(1-10) respectively. The TI is determined by multiplying the radiation level at one meter by 100, i.e. RL_{1m} (mSv/h)x100

While most of the pure alpha and beta-emitters could be transported as white packages, it would be economical to transport gamma emitters as yellow packages. Otherwise considerable amounts of shielding would be required to bring the radiation levels to those corresponding to white packages. All fissile materials are packed and shipped in such a manner that criticality cannot be reached under any foreseeable circumstances of transport.

Marking, Labelling And Placarding

1- Marking

- Each package of gross mass exceeding 50kg shall have its permissible gross mass legibly and durably marked on the outside of the packaging.
- Each package which conforms to a type A package design shall be legibly and durably marked on the outside of the package with "Type A".
- Each package conforms to type B package design shall be legibly and durably with identification mark allocated to that design by the competent authority, serial number of the design and marked with either Type $B_{(U)}$ or Type $B_{(M)}$ as required.
- Each package marked type $B_{(U)}$ or type $B_{(M)}$ shall be plainly marked by embossing, stamping or other means resistant to the effect of fire and water with the trefoil symbol.

2- Labelling:

- Each package, overpack, tank of freight container bear labels according to the appropriate category (see Fig 2&3). Any labels which do not relate to contents shall be removed or covered. Additional labels describing other dangerous properties shall be added.
- The labels shall be affixed to two opposite sides of the outside of a package or overpack or on the outside of all four sides of a freight container or tank.
- Each label shall be completed with, Contents., Activity Curies (Ci) or Becquerels, (Bq) or in units of grams (g) for fissile material, A criticality safety Index, (CSI) is used.

3- Placarding

- Large freight containers carrying packages other than excepted packages and tanks shall bear four placards (see Fig.3).
- The united Nations Number (UNN) for the consignment shall also displayed on the placards (lower half) or on a separate one shown in Fig.(4) which shall be affixed adjacent to the main placard in all four sides of the freight container.

Fig.2

Category I- White

Fig.3

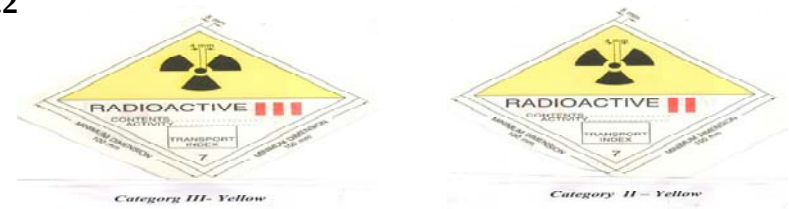

Category III- Yellow *Category II – Yellow*

Fig.4

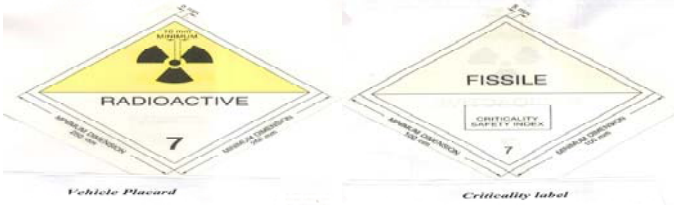

Vehicle Placard *Criticality label*

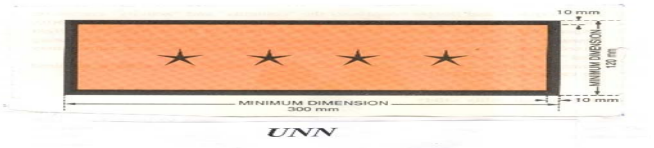

UN

STORAGE OF RADIOACTIVE MATERIALS

Radioactive materials except those in category I-WHITE packages, shall be kept separated from living accomodations, from regularly occupied working spaces that may be continually occupied by passengers or the public. A dose of 5mSv/h and 1mSv/h were used for calculation of the segregation distances for transport workers and general public respectively. They shall also be separated from undeveloped photographic films or plates so that these are not expected to be more than 0.1mSv/h consignment. The appropriate segregation distance shall be derived on the basis of these assumptions.

Packages of radioactive material shall not be stored near dangerous goods with which common loading or storage is prohibited. The number of category II-YELLOW and III-YELLOW packages stored in one place, shall be so limited that the total sum of the transport indices in any individual group of such packages dose not exceed 50. Undelivered packages shall be placed in a safe location and the appropriate competent authority shall be informed as soon as possible and a request made for instructions on further action.

CUSTOMS OPERATIONS

Customs operations involving examination of the contents of a package containing radioactive materials should be carried out in a place where adequate means of radiation exposure control are provided, and in the presence of persons qualified to deal with radioactive materials. Any packages opened on customs should, before being forwarded to the

consignee to its final instructions destination, be restored to its original packaging specifications so that all radiation protection requirements are restored.

GENERAL ACCIDENT PROVISIONS

In the event of a package of radioactive materials breaking or leaking, or becoming involved in a crash or fire, the affected area should be suitably segregated and no person should be allowed to enter or to remain within the segregated area until qualified persons are available to check radiation and contamination levels and supervise subsequent operation including salvage operations. However, the presence of radioactive materials should not be considered to prevent rescue operations or fighting of fires by qualified persons. All persons who may have become contaminated with radioactive materials should be subject to immediate examination and appropriate decontamination measure.

Any conveyance, building, location equipment or part thereof which has become contaminated as a result of an accident in the course of transport of radioactive materials should be decontaminated by qualified persons as soon as possible. Finally, a complete accident report should be submitted to the competent authority for further actions.

TRAINING

As one means of promoting safety in transport as well as encouraging harmony in regulatory control, the IAEA has from time to time organized training courses with the co-operation of Member State Governments and Organizations. These have been aimed at individuals from developing countries with appropriate responsibilities in the area of the transport Regulations and their implementation. The programme started with individual training courses to specific Member States in the early 1980 and regional training course for other countries in 1984. Beginning in 1987 formal regional and interregional training courses have been held about once per year at different Member States.

In order to encourage further training, the IAEA found it desirable to develop a basic course text on the safe transport of radioactive material it was therefore decided that the lecture notes from the 1987 course would form the basis of this text, and that it would be focused on the 1985 Edition of the Regulations [(11)]. The result was the IAEA`s Training Course Series No.1 which was updated to a second edition in 1991[(12)] because the consignor has overall responsibilities for the proper packaging and preparation of radioactive material for transport, detailed knowledge of the Transport Regulations is imperative. The IAEA has an in-depth training course available that can assist Member States and other involved in the transport of radioactive material in understanding and applying the Transport Regulations[(13)] While the course is primarily intended for regulatory authorities, it can also assist consignors and carriers in recognizing their responsibilities and provide them with a detailed understanding of how to comply with the Transport Regulations.

The purpose of a regional or inter-regional training course is to provide guidance to regulatory and key industrial personnel on the Regulations and practices for the safe transport of radioactive material. The objective of each IAEA training course is to ensure that the participants thoroughly understands the philosophy principles, and application of the of the provision of the transport Regulations.

The purpose of the training is to provide a rational method for convening a training course and to foster high quality training. The manual serves as a tool for instructors to use in

presenting subjects pertaining to the Regulations in a logical and understandable manner. It also allows training course participants to become knowledgeable about the Regulations.

TRANSPORT SECURITY

Security of nuclear (fissile) material, including during international transport, has been addressed since 1979 under the umbrella of the Convention on the Physical Protection of Nuclear Material[14]. States that are party to the Convention are obligated to abide by the security provisions specified in it. However, the same situation dose not exist for security of non-fissile radioactive material during transport. Heightened awareness of the need to secure such materials during transport has led to a series of developments aimed at defining and supporting uniform implementation of transport security requirements.

DANGEROUS GOODS TRANSPORT SECURITY

Recognizing the need for increased security following the events of September 11,2001, the UN Committee of Experts introduced measures to enhance security for the transport of all dangerous goods in the 12th revised edition of the Model Regulations.

RADIOACTIVE MATERIAL AS CLASS 7 DANGEROUS GOODS

Beginning with the early versions of the Transport Regulations, there has been a threshold for denoting what constitutes a "large quantity" of radioactive material. In the current Transport Regulations, this is 3,000 A_1 for special form material and 3,000A_2 for non-special form material, with the observation that the dangerous goods security requirements should not apply to nuclear (fissile) material that is already subject to physical protection requirements during transport as a result of the Convention on the Physical Protection of Nuclear Material and the supporting guidance in INFCIRC/225[15]. These recommendations provided the basis for the Class 7 (radioactive material) requirements in the Model Regulations.

IAEA TRANSPORT SECURITY GUIDANCE

Although the security measures and definition of high consequence radioactive material added to the Model Regulations were recognized as a very positive step, the IAEA initiated a review of these provisions to ensure they were technically sound and consistent with other approaches used in nuclear and radioactive material security.

The recommendations of the Technical Meeting to Review Guidance for Security in the Transport of Radioactive Material held at the IAEA headquarters in Vienna, provided a good summary of the conclusions of this series of meetings.

1. Some radioactive materials, such as excepted packages, low specific activity materials, and surface contaminated objects that can be shipped unpackaged, do not warrant security measurers above prudent management practices.
2. Two categories of security measures, basic and enhanced (differentiated by a radioactivity threshold) are sufficient for specifying appropriate measures and are consistent with the approach used for other dangerous goods in the UN Model Regulations.

3. The threshold for high consequence radioactive material should be revised to take into account analyses done on the consequences of intentional dispersal and developments in the safety and security of radioactive sources.
4. While the security requirements in the Model Regulations are an adequate set of baseline measures, there are additional measures that Member States might wish to consider when the national Design Basis Threat indicates it might be appropriate, in situations of increased threat, or for particularly attractive material.

These recommendations result in three groups of security measures which are illustrated in as follows:

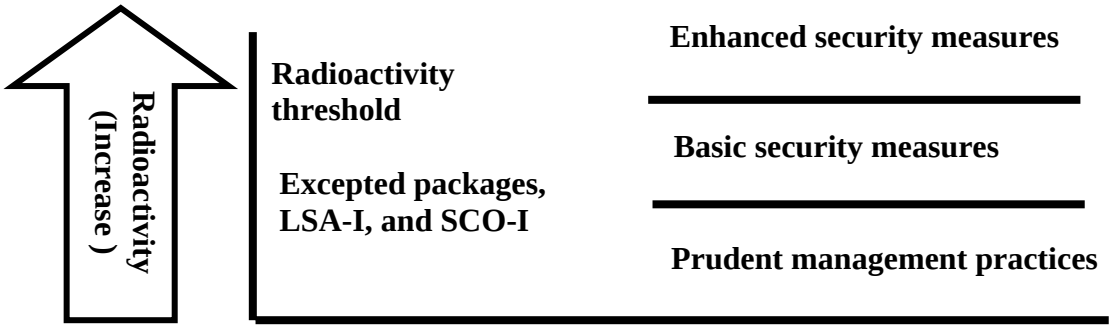

Exceptions from security requirements

Malicious use of radioactive material could involve exposure to radiation (a radiation exposure device) or dispersal of the radioactive material (a radiological dispersal device). Small quantities of radioactive and low activity concentration material would not be very effective in such applications because the consequences of their use would be low. Therefore, the draft guidance recommends that no transport security measures above prudent management practices be required for the following:

- excepted packages with contents limited to the activity allowed for non-special form material,
- low specific activity material in category LSA-I that can be shipped unpackaged, and
- surface contaminated objects in category SCO-I that can be shipped unpackaged.

Two categories of security measures

Radioactive materials present a very wide spectrum of attractiveness for malicious use. Materials and packages with potentially significant but limited consequences such as Type A packages, LSA-II, LSA-III, and SCO-II have some attractiveness. By contrast packages containing high activities such as large sealed sources or large quantities of radionuclides (especially in dispersible form) could be very attractive for malicious use.

Tow security categories were recommended-basic level and enhanced level. The specific security measures recommended for each level were drawn from the model Regulations and, where necessary, tailored for application to radioactive material shipments.

At the basic level the security measures include security awareness training and periodic retraining, maintenance of training records, use of known or identified carriers, and use of properly secured in transit storage areas.

Enhanced level security measures include recommendations that consignors, carriers, and others develop, adopt, implement, and comply with a security plan that addresses the following:

- allocation of responsibilities and authority to fulfill these responsibilities;
- material transport records;
- reviews of operations and assessments of vulnerabilities;
- clear statement of measures to be used to reduce security risks;
- procedures for reporting and dealing with security threats, breaches, and incidents;
- testing, periodic review, and updating of security plans; and
- security of information including limiting distribution of it.

Threshold for enhanced level of security

Extensive discussions were held on how the threshold for the enhanced level of security should be defined. From a strict security standpoint, there are advantages to using per-conveyance basis as this best identifies conveyances that are carrying a total quantity of material that should be protected. From an operational standpoint, a per-package basis is much more feasible to implement because it dose not require carriers to keep a record of the activity on the conveyance. It was concluded that the per-package basis was acceptable, and a radioactivity threshold was then defined to identify those packages that should be subject to the enhanced security measures.

Because the transport of nuclear (fissile) material is already subject to security requirements as specified in the Convention for the Physical Protection of Nuclear Material and the supporting guidance in INFCIRC/225[15], there is some overlap between the two sets of recommendations. A comparison of INFCIRC/225 and the draft transport guidance shows that for :

- *Category I nuclear material*, the security measures of INFCIRC/225 are more stringent than the enhanced security measures (e.g., requiring escorts), but this is appropriate given the much greater potential consequences that an improvised nuclear device could have when compared to a radiological dispersal device;
- *Category II nuclear material*, the security measures of INFCIRC/225 are roughly comparable to the enhanced security measures; and
- *Category III nuclear material*, the security measures of INFCIRC/225 are roughly comparable to the basic security measures.

Consequently, if Category III nuclear material with an activity per package that exceeds the radioactivity threshold for the enhanced level of security is being transported, the shipment should meet the enhanced measures because of its radiological potential for malicious use.

The IAEA Code of Conduct on the Safety and Security of Radioactive Sources (the Code)[16] is being implemented by many countries. Ninety-two countries have notified the IAEA of their intent to implement the Code. Among other requirements, the Code and its supplement, Guidance on the Import and Export of Radioactive Source[17], require certain measures such as notification and consent before the import or export of Category I and II radioactive sources.

Additional Security Measures

While the basic and enhanced security measures are generally consistent with the Model Regulations, there may be instances when a country feels that the security situation calls for additional measures. For example, additional measures may be warranted in elevated threat conditions, when the Design Basis Threat for the country indicates measures are appropriate,

or when the attractiveness of the material is high. The guidance document provides a list of possible additional security measures that countries might wish to consider imposing when appropriate. Such measures include:

- additional training for transport personnel,
- licensing of transport operators,
- real time tracking of shipments and the use of a transport control centre,
- guards,
- specially designed conveyances, and
- additional measures to protect the confidentiality of information.

TRANSPORT SAFETY AND SECURITY INTERFACES

Transport safety is a deterministic based discipline. Specific tests and limitations are applied on the assumption that certain conditions and events may occur during transport. It is not assumed these will occur during any given transport, but each package must be designed, tested, and prepared for transport as if it is expected that they will occur .

Transport security is a threat based discipline. It is not feasible to establish a single set of security measures that are suitable for use in all situations without seriously overdesigning the security system for anything but be highest threat conditions. This would be very costly and ineffective. Instead, the recommendations are intended to provide an appropriate level of security under normal threat conditions, and provisions are included that allow the adjusting of the measures to meet current threat conditions.

There are avoidable interactions between some safety and security measures in transport planning, preparation, and operations. These can be categorized on the basis of whether they are complementary or potentially conflicting. That is, some measures provide benefits in both areas, whereas some measures may benefit one while having a potentially adverse effect on the other, requires which careful consideration by the regulatory authorities, consignors, and carriers to develop approaches that provide appropriate levels of protection in each area.

This can be illustrated with the major components of transport safety as follows:

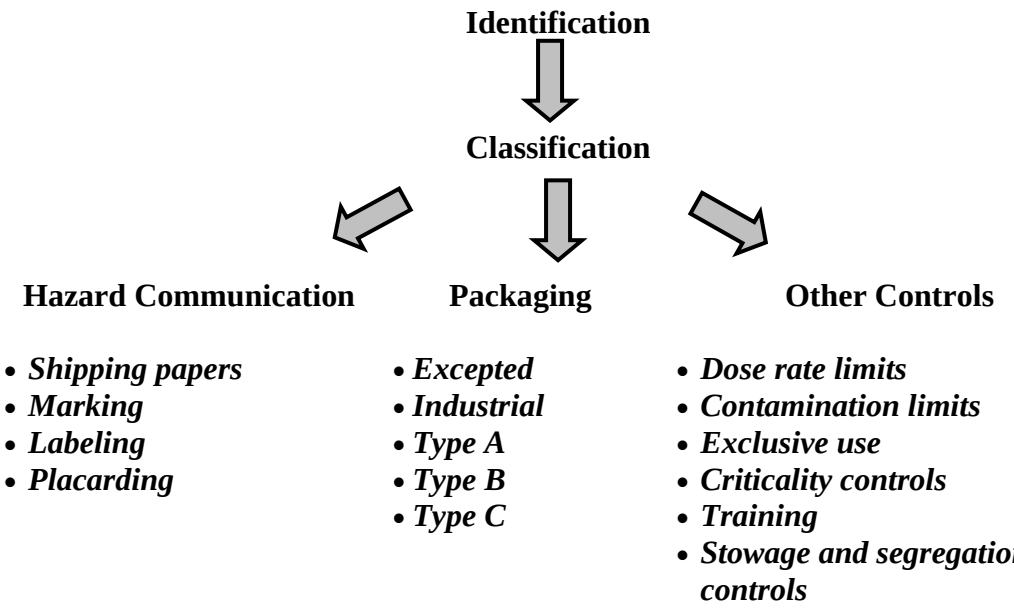

Identification

Identification of the material being transported is required for both safety and security. This step collects information on the material being transported that is necessary to determine what specific safety or security provisions apply based on the hazards (safety) or potential adverse consequences of malicious use (security).

Classification

In general, higher hazard radioactive materials require more stringent safety and security measures. However, this is not always the case. For example, a special form capsule of an alpha-emitting radionuclide presents a low safety hazard because the encapsulation is robust (containment), and no shielding is needed. At the same time, this material may be very attractive to an adversary because of its potential use in a radiological dispersal device. Consequently, safety and security need to be considered separately to determine what set of measures should be applied.

Hazard Communication

Hazard communication (safety) and information security (security) have conflicting objectives. From a safety perspective, it is desirable to warn workers, the public, and emergency responders of the presence of radioactive material. Marking, labeling, placarding, and shipment documentation are designed to clearly indicate the presence of radioactive material and the degree of caution that should be exercised. This can also be considered as advertising to adversaries " here is the good stuff" and is contrary to maintaining a key element in transport security- unpredictability in when and where shipments are being made.

Some countries have developed pragmatic approaches to ensuring security while also ensuring that the functions supported by hazard communication can still be performed. For example, when escorts accompany a shipment, they can provide the communication to emergency responders that placards ordinarily do.

Packaging

Packaging is an area in which safety may or may not provide substantial security benefits. For example, large, heavily shielded Type B packages provide security benefits through delay (increasing the adversary task time) and sabotage resistance. The mass and construction of the packages provide protection of the contents, and the robust closures often require specialized tools and techniques to open the packages. However, lightweight drum-type Type B packages may contain material with the potential for very high radiological consequences and yet be easily moved by a person. Some transport packages are internationally designed for portability (well logging sources and radiography cameras). In these cases specific security measures are needed that take into account the speed and ease with which an adversary could complete acquisition of a package.

Other Controls

Most of the other transport safety controls have little bearing on security. An exception is when exclusive use of the conveyance is required for safety purposes as this gives the consignor control over loading and unloading, routing, scheduling, and other operational aspects of the transport. While these safety controls are primarily focused on radiation

protection (dose rate, contamination limits, etc.) security must address both access removal of the packages from the conveyance and the seizure of the conveyance.

The Transport Regulations specify that " These Regulations do not specify controls such as routeing or physical protection which may be instituted for reasons other than radiological not detract from the standards of safety which these Regulations are intended to provide. " Thus, a consignor should consider the possible impact of security measures on the safety measures required by Transport Regulations, and vice versa.

CONCLUSION

Transport safety and security for radioactive material have very different histories and often require differing approaches to ensure accomplishment of their objective.
The IAEA Regulations for safe transport of radioactive material (STRAM) are widely adopted and provide standards for insuring a high a high degree of safety. As transport security becomes more fully developed and integrated into the national regulatory frameworks of more countries, the regulatory authorities, consignors, carriers, and receivers of radioactive material shipments will be challenged to fully implement programs that address not only the well recognized requirements for safety, but also those for security. The IAEA, and other international partners are working with Member States to implement transport security programs and resources such as guidance, training programs, security assessments, and upgrades assistance are available. The international community can ensure that this critical need is addressed if working together.

REFERENCES

1) R,B,POPE, J.D., Mc CLURE, "Estimated" annual worldwide shipments of radioactive material" packaging and Transportation of Radioactive Materials, (Proc.Symp. Vienna, 1987), IAEA STI/PUB/781, IAEA, Vienna (1987)459-468.
2) Advisory Material for the IAEA Regulations for the safe transport of Radioactive Material (1996 Radiation), Safety Standards Series, No. TS-G1.1(ST-2) iaea, Vienna(2002).
3) IAEA, Planning and Preparing for Emergency Response to Transport Accidents Involving Radioactive Material "Safety Standards Series No.TS-G-1-2 (ST-3), IAEA, Vienna (2002)
4) IAEA Compliance Assurance for the Safe Transport of Radioactive Material Safety Series No.112, IAEA Vienna (1994).
5) IAEA Quality Assurance for the Safe Transport of Radioactive Material Safety Series No.113,IAEA,Vienna (1994).
6) IAEA Regulations for the Safe Transport of Radioactive Materials, 1961 Edition, Safety Series. No.6 IAEA, Vienna (1961).
7) IAEA Regulations for the Safe Transport of Radioactive Material, Safety Standard Series TS-R-1, IAEA, Vienna (2009).

8) IAEA, Security in the Transport of Radioactive Material, Implementing Guide, IAEA, Vienna (2008).
9) IAEA Regulations for the Safe Transport of Radioactive Materials 1996 Edition Safety Standard Series No.ST-1, IAEA Vienna (1996).
10) IAEA Regulation for the Safe Transport of Radioactive Material, 1996 Edition (Revised), Safety Standards Series, No.TS-R-1 (ST-1 Revised), IAEA Vienna (2000).
11) IAEA Regulations for the Safe Transport of Radioactive Material, 1985 Edition, Safety Series No.6,IAEA, Vienna (1985).

Measurement of Natural Radioactive Nuclide Concentrations and the Dose Estimation of Workers Originated from Radon in Manganese Ore Mine

N. A. Mansour, Nabil M. Hassan and M. R. Blasy*

Zagazig University, Faculty of Science, Physics Department, Zagazig – Egypt

Zagazig University, Faculty of Science, Geology Department, Zagazig – Egypt

ABSTRACT

Manganese ore is widely used in many industries. Such as ore contain natural radioactive nuclides at various concentrations. If this ore contain high concentrations of natural radioactive nuclides, workers handling them might be exposed to significant levels of radiation. Therefore it is important to determine the radioactive nuclides in this ore. Also the regulation of radon concentration at workplaces has gained an accentuated importance in all countries. Nevertheless, at this time there is no globally accepted workplace protocol that sets out safe radon concentration values. In this study the radon concentration measured by using an Alpha Guard radon monitor, the equilibrium factor which was greater than the value given in literature, effective radiation dose, which are necessary for the exact estimation of the radiation dose originating from radon. The regulation of radon concentration at workplaces has gained an accentuated importance in all countries. Approach: The natural radionuclides (^{238}U, ^{232}Th and ^{40}K) contents of manganese ore samples collected from Umm Bogma, southwest Sinai and from the mountain access Hamid South Eastern Desert, Egypt have been determined by low background spectroscopy using hyper-pure germanium (HPGe) detector. Results: The mean activities due to the three radionuclides (^{238}U, ^{232}Th and^{40}K) were found to be 1500±65, 490±65 and 364±45 Bqkg^{-1}, respectively. The absorbed dose rate due to the natural radioactivity in samples under investigation ranged from 1522±45 → 1796±43 nGyh^{-1}. The radium equivalent activity varied from 3807±114→ 4446±133 Bqkg^{-1}.The representative external hazard index values for the corresponding samples are also estimated. Conclusion: The results of this assessment obtained by the gamma-ray spectroscopic analysis, have indicated that the levels of natural radioactivity were lower than the international recommended limits.

Keywords: *Natural radionuclides / Dose estimation and assessment / Radiation protection / Manganese ore mine / Equivalent activity / radiation hazard index / gamma spectrometer / Radon / Alpha-Guard .*

1- INTRODUCTION

Manganese from the transition elements, as it is located between the chromium and iron. In spite of the limitations of what was known about it and its uses in a pure case. The manganese is great of an importance in practice and that is basic component in steel industry in the form of Ferro manganese (manganese, which contains almost (80%) manganese). Also manganese dioxide is used as a dryer, or as a catalyst in paint, varnish and remover of color in the glass

industry, and in the dry batteries, remover of colors in oils, and as a catalyst for oxidation in analytical chemistry. Also introduces the components of manganese within the composite for agriculture, and within the components of animal foods. Manganese melts at the temperature 1244 ± 3 °C, and boils at 2095 °C. It is oxidation in the air and as the temperatures increased is cover by brown oxide. A manganese minerals like that Pyrolusite, which occurs in all ore deposit and represent the most abundant manganese mineral. It is found as new prismatic crystals with transversal cracks which is the result of decrease in unite cell dimensions due to the loss of the hydroxyl group of manganite as a result of dehydration of manganese and transformation into pyrolusite. Psilomelane(Ba- bearing manganese oxide) and cryptomelane(K-bearing manganese oxide) are similar to each other in their X-ray differaction patterns. It has been possible to distinguish between them by spectrographic analysis where psilomelane shows strong Ba lines and cryptomelane show strong K lines. In general pyrolusite and polianite are similar in their crystal lattice and accordingly to their X-ray powder patterns. Gangue minerals in the manganese ore include calcite, gypsum, goethite, hematite and barite. The most important producing countries are: Russia, China, South Africa, India, Indonesia and Morocco. An established fact that all the construction material contains trace amount of natural radioactivity. This activity in a major source of external and internal radiation exposure to the occupants of the industry. The most commonly radio nuclides in the construction materials from gamma-radiation are uranium and thorium series together with potassium (Luigi et al., 2000). Research on health risks caused by the naturally occurring radioactive noble gas radon and its progenies has gained great attention, in particular those aspects related to controlling high radon concentrations (ICRP65, 1994; USEPA, 2004) and to regulating the air quality in workplaces (SSI, 1999; Gooding and Dixon, 1992; Risica, 2001). Since workers spend an average of approximately 2400 h per year at their workplaces, the radiation exposure from radon in the workplace could be significant in cases when the radon concentration is relatively high (Scivyer and Gregory, 1995; Dixon et al., 1996).

Radon isotopes are amongst the members of radioactive series of Uranium and Thorium and are practically inert and have the properties of gases under conditions of geological interest.

Radionuclides are present always in the natural environment. Natural radiation is usually classified as either cosmic or terrestrial radiation (El-Zakla et al., 2007). Large variations in dose rates of both cosmic and terrestrial radiation are found depending on where the measurements are made (Shenber, 1997). Measurements of natural radioactivity in environmental samples, especially in raw materials produced by mining are very important to determine the amount of change of the natural background activity with time as a result of any radioactive release (Iwaoka et al., 2009). Emanation of radon (^{222}Rn), for example is associated with the presence of radium and its ultimate precursor uranium in the ground (Bossew and Lettner, 2007). The inhalation of its short-lived daughter produces is a major contributor to the total radiation dose to exposed subjects (UNSCEAR, 1993). Many studies have investigated the radioactive elements in different ore samples (Chau et al., 2008); however few studies have investigated the radioactive content of manganese (Mn) ore. Manganese is an essential trace element in the metabolism of all living organisms, animals or plants. Normally it is found in human blood with concentration <320 nmol L-1 and functions as a cofactor for some enzymes. Exposure of man to high levels of manganese leads to hyper manganese anemia (high Mn levels in blood) and defect in its metabolism with its accumulation in the liver and the basal ganglia is lethal (Tuschl et al., 2008). Also, manganese intoxication has been described in children on long term parenteral nutrition presenting with liver and nervous system disorders (Kafritsa et al., 1998). In adults, together with occasional

oral intake and product contamination with the element can lead to brain accumulation and neurotoxicity (Hardy et al., 2008). Manganese exposure is usually via inhalation (the risk varying with the manganese species involved and with particle size). There are specific measures to protect those working in manganese-related industry (or mining) such as reducing exposure levels and time of exposure and the use of exhaust ventilation (Kavasi et al., 2009). In addition to the risk of exposure to high doses, manganese provides another risk factor if the ore contains residual radioactive elements. This arises the our interest to investigate the potential of existence of residual radioactive elements in manganese ore, particularly with the increasing demand of using this ore in many industries including the steel industry in Egypt. The aim of this work is to determine the concentration of natural radioactivity uranium, thorium and potassium in manganese ore produced by one of the local companies working in manganese mining. and to measure the surface radiation dose rate and the radium equivalent activity and radiation hazard index.

Wherever the manganese ore samples are used in many industrial purposes, consequently there are specific measures to protect the working in the manganese ore samples related industry such as reducing exposure levels and time of exposure and the use of exhaust ventilation. The determination of the elements presented in manganese ore samples by using X-ray florescence techniques (XRF). Describes the use of simultaneous TDA/TGA to measure the moisture content in manganese dioxide. TGA measurement at partial vacuum can accurately determine quantitative analysis in manganese dioxide and aid in determing the required heating and drying conditions for the chemical.

In this work presents some of the difficulties encountered in determining the average radon concentration, as well as the radiation dose originating from radon to the workers in a manganese mine in Egypt. Manganese oxides, due to their structure, have good adsorption characteristics, and are therefore widely used in nuclear measurement techniques as well as for the selective enrichment of different radionuclides (Moore and Reid, 1973).

1.1. Geological Origin

The manganese ore samples are collected from some ore mines . The ore mines in Oleikat, Marahil and Um Sakran localities(West Central Sinai) and at Wade Kalahil(South Eastern Desert). The manganese ore minerals include pyrolusit, psilomelane and manganese. These minerals are associated with small amount of gangue minerals as calcite, barite, gypsum, salt, quartz and iron oxides. Manganese ore is found as lntricular bodies, veins and cavity filling. Most manganese minerals represent the core of the masses with iron- minerals forming the peripheries. The host rocks are of calcaries sediment of Carboniferous age. The origin of manganese minerals is deposition from thermal water rich in Mn and Fe elements during Oligocene to late Miocene . These elements have been leached from basaltic sheets of Tertiary volcanism in the West Central Sinai, or from the acidic igneous rock of Basement complex of southern Sinai (El Shazly et al., ca63).

U and Th are present in the earth's crust at an average concentration of 4.2 and 12.5 ppm, respectively (Wollenberg and Smith, 1990). When a geological formation containing ^{238}U and ^{232}Th has not been disturbed (closed system) for more than a million years, the members of the individual decay series will have the same activity (Bq/kg) which is known as Secular Equilibrium. However, when the geological formation is not closed to radionuclide migration, ^{226}Ra can migrate and be deposited somewhere outside the formation. Then secular equilibrium will not exist and the growth of ^{226}Ra by radioactive decay of its ancestors will not occur. ^{226}Ra is said to be unsupported.

2. MATERIALS AND METHODS

Five manganese ore samples were collected from different places at Um Bogma area[Oleikat, Marahil and Um Sakran localities(West Central Sinai) and at Wade Kalahil(South Eastern Desert)]. Samples were stored for 30 days before its counting radioactivity to ^{224,226}Ra period to achieve the secular equilibrium $\lambda_B >> \lambda_A$ between radium and its products and then measure the samples 3600 sec. The energy and intensity of various gamma-ray lines have been measured using a system consist of Canberra coaxial High-Purity Germanium detector (HPGe) which has a photo peak efficiency of 70% . The energy resolution of 2 keV Full-Width at Half Maximum (FWHM) for the 1332 keV gamma-ray line of ^{60}Co. A cylindrical lead shield of 5 cm thickness, which contains inner concentric cylinder of Cu with thickness of 10 mm, was used to shield the detector and to reduce the effect of background. The detector was cooled to liquid nitrogen temperatures and coupled to a PC-based 8K multichannel analyzer and an ADC with Genie 2000 for data acquisition and analysis. The calibration of the detector was carried out by using standard point sources ^{60}Co (1173.2 and 1332.5 keV), ^{133}Ba (356.1 keV) , ^{137}Cs (661.9 keV) and ^{22}Na (1368.6keV) besides ^{226}Ra (186.2keV). Absolute efficiency calibration curves are calculated for activity determination of the sample by using standard ^{226}Ra, contained in the same cylindrical bottles as the samples. The samples were prepared with a uniform geometry. An empty bottle with the same geometry was measured for subtracting the background. The gamma-ray transitions of energies 1120.3 keV (^{214}Bi) and 1764 keV (^{214}Bi) were used to determine the concentration of the ^{238}U series. The gamma-ray transitions of energies 911.1 keV (^{228}Ac) and 2614 keV (^{208}Tl) were used to determine the concentration of the (^{232}Th) series. The 1460 keV gamma-ray transition of ^{40}K was used to determine the concentration of ^{40}K in the samples as shown in Table (1) and their intensities. The spectra of the samples were perfectly analyzed using a special PC Genie 2000 software to calculate the concentrations of ^{238}U, ^{232}Th and ^{40}K and their decay products.

2.1. **Gamma-Ray Spectrometer System:**

The instrumentation used to measure γ-rays from radioactive samples consists of a HPGe semiconductor detector, associated electronics, and a computer-based multichannel analyzer [H.R. Verma, 2007] as shown in Fig. (1)

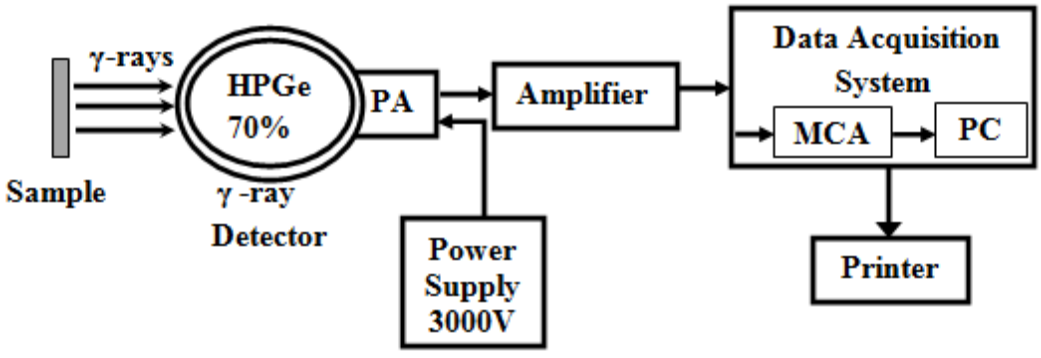

Fig.1: Blocked diagram of HPGe γ-ray spectrometer system.

2.2. **SAMPLE COLLECTION AND PREPARATION**

Samples were collected from different places in one of the work sites of Egyptian manganese mine location (Um Oleikat West Central Sinai. And from the Wade Kalahin South Eastern

Desert). Each sample, ~ 500 - 1000g, was packed in a plastic container, sealed well and stored for 30 days before analysis this allow the in-growth of uranium and thorium decay products and prevent the escape of radiogenic gases ^{222}Rn and ^{220}Rn and allow secular equilibrium of ^{238}U and it's decay products see Table (1).

Table (1): The natural radionuclides, their gamma lines used and their intensities [VIENNA, 1990].

Parent	Max. Activity	Daughter	γ-ray energy	Abundance
^{238}U	130 Bq/Kg	^{226}Ra	186.2	3.29
		^{214}Pb	295.2	18.7
		^{214}Pb	351.9	35.8
		^{214}Bi	609.3	45.0
		^{214}Bi	1120.3	14.9
		^{214}Bi	1764.5	16.0
		^{214}Bi	2204.1	5.0
^{232}Th	85 Bq/Kg	^{212}Pb	238.6	45.0
		^{208}TI	583.1	30.0
		^{228}Ac	911.1	29.0
		^{228}Ac	968.6	17.5
		^{208}Tl	2614.7	36.0
^{40}K	1600 Bq/Kg		1460	10.67

3. RESULTS AND DISCUSSION

3.1. Natural specific activity measurement

The activity levels for radionuclides in the measured samples are computed using the following equation [Amrani D(2001)]

$$A = (cps)_{net} / \varepsilon_{ff} I_{\gamma} m \quad (1)$$
$$(cps)_{net} = (cps)_{sample} - (cps)_{B.G}$$

Where:
A = The activity level of a certain radionuclide (Bq/ kg)
$(cps)_{net}$ = The net count rate of the sample (counts / seconds)
ε_{ff} = The detector efficiency for the specific gamma ray energy
$I\gamma$ = The intensity of gamma-line in a radionuclide
m = The dried sample mass in kilograms.

Activities due to the presence of ^{226}Ra, ^{232}Th and ^{40}K radio nuclides have been determined in the samples. The minimum, maximum and mean activity values of ^{226}Ra, ^{232} Th and ^{40}K found in these samples are listed in Table 2. As may be seen in this table the measured values of activity in the samples due to ^{232}Th vary from 490 Bqkg^{-1} to 6 Bqkg^{-1}, ^{226}Ra activities

vary from 1500 Bqkg^{-1} to 100 Bqkg^{-1} and variation in ^{40}K activities ranges from 364 Bqkg^{-1} to 116 Bqkg^{-1}.
The activity concentration is shown in Table 2 where all activity is lower than world average except value.

Table 2: Minimum, maximum and mean activity concentration values for manganese ore samples.

Radionuclide	Minimum (Bq / kg)	Maximum (Bq / kg)	Medium (Bq / kg)
^{238}U	100	1500	650
^{232}Th	6	490	248
^{40}K	116	364	240

For ^{238}U activity concentration was determined by measuring the 295.2 keV (18.7 %) and 351.9 keV (35.8.1 %) gamma-rays from ^{214}Pb and the 609.3 keV (45 %) and 1120.3 keV (14.9 %) gamma-rays from ^{214}Bi. ^{232}Th activity was determined from the gamma-rays of 238.6 keV (45 %) from ^{212}Pb and 338.4 keV (12 %), 911.1 keV (29 %) and 968.6 keV (17.5 %) from ^{228}Ac and 583.1 keV (30 %) gamma-rays from ^{208}Tl. ^{40}K concentration was measured from its 1460 keV (10.67 %) gamma-ray line. The obtained spectrum of the background gamma radiation was subtracted from the measured gamma ray spectra of the samples. The characteristic gamma-ray emitters are marked above the corresponding peaks. A selected spectrum for manganese ore sample is shown in the following figure.

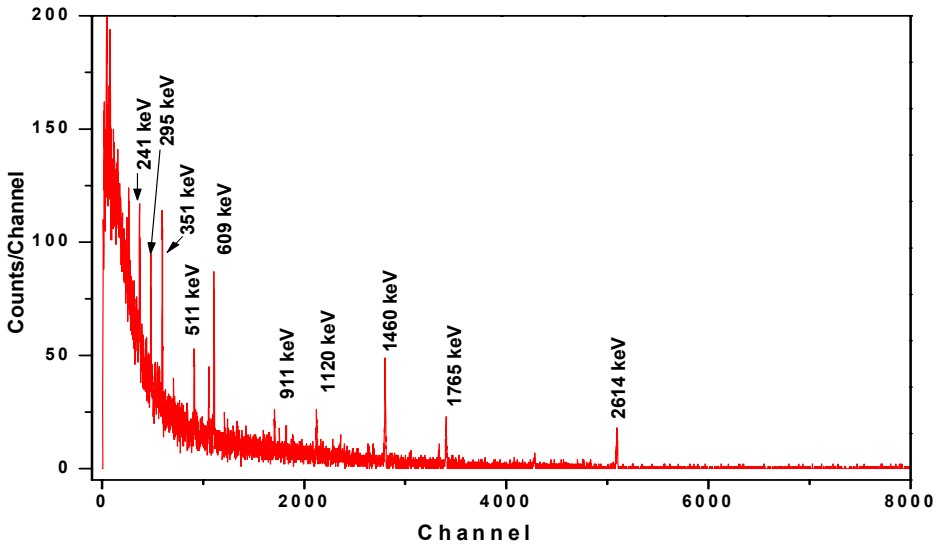

Fig. 2: Portion of Gamma ray spectrum for manganese ore sample code 2.

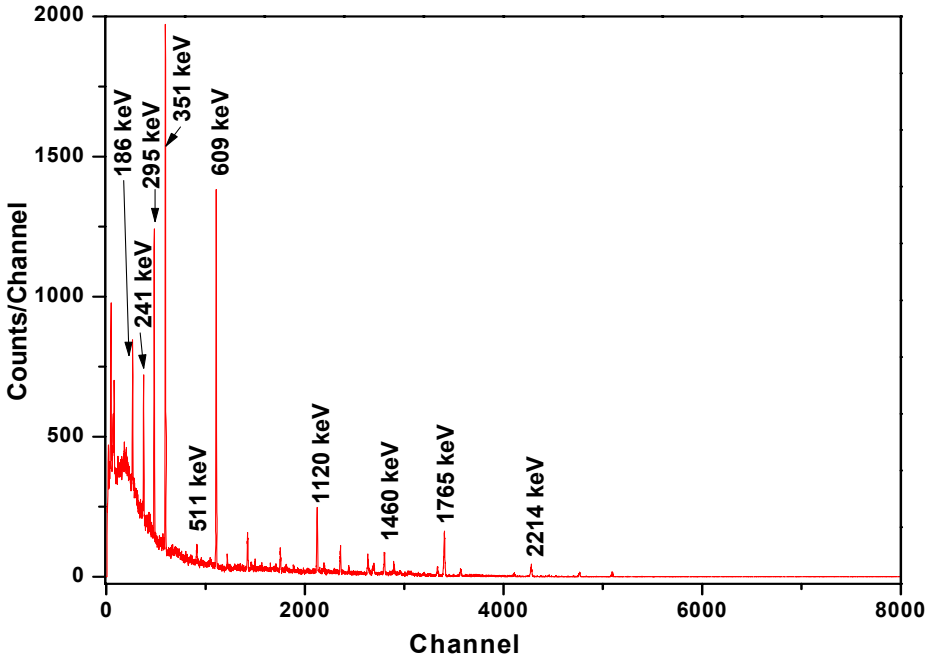

Fig. 3: Portion of Gamma ray spectrum for manganese ore sample code 4.

To assess the radiological hazard of the manganese ore samples, it is useful to calculate an index called the radium equivalent activity, Ra_{eq}, defined according to the estimation that 1 Bq / kg of ^{226}Ra, 1.43 Bq / kg of ^{232}Th and 0.077 Bq / kg of ^{40}K produce the same γ-ray dose [Amrani D(2001)]. This index Ra_{eq} is given as:

$$\mathbf{Ra_{eq} = C_{Ra} + 1.43\ C_{Th} + 0.077\ C_K} \qquad \mathbf{(2)}$$

Where C_{Ra}, C_{Th} and C_K are the activity concentration in $Bqkg^{-1}$ of ^{226}Ra, ^{232}Th and ^{40}K, respectively. The maximum value of Ra_{eq} in manganese ore samples must be less than 370 $Bqkg^{-1}$ for safe use (UNSCEAR, 1993), i.e., to keep the external dose below 1.5 mSv y^{-1}. The values of Ra_{eq} are higher than criterion limit. In manganese ore samples, the Ra_{eq} activity are not within the recommended safety limit when used in industry. The calculated values of the radium equivalent Ra_{eq} for the studied manganese ore samples are given in Table 3.

Another radiation hazard index, the representative level index, $\mathbf{H_{in}}$, used to estimate the levels of

γ-radiation hazard associated with the natural radionuclides in specific samples, is defined as [KAFALA S. I., 2007].

$$\mathbf{H_{in} = (C_{Ra} / 150) + (C_{Th} / 100) + (C_K / 1500)} \qquad \mathbf{(3)}$$

Where C_{Ra}, C_{Th} and C_K are the activity concentrations in Bq/kg of ^{226}Ra, ^{232}Th and ^{40}K respectively. The values of $\mathbf{H_{in}}$ for the studied samples are given in table 3.

Table (3): Radium equivalent activity ($Bqkg^{-1}$), External Annual dose (mSv/y), Gamma-Radiation external and internal hazard (H_{ex}, H_{in}), Absorbed dose (nGy/h) and the Annual Effective Dose (μSvy^{-1}).

Sample code	Ra_{eq}	H_{ex}	H_{in}	Dose Rates (nGy/h)	EAD ($\mu Sv\ y^{-1}$)
1	4446±133	12.01±.35	93.145	1796±43	2.02±0.06
2	3951±118	10.67±.31	914.903	1586±51	1.94±0.05
3	4259±127	11.50±.34	91.089	1718±51	2.10±0.06
4	3807±114	10.47±.31	574.220	1522±45	1.90±0.05

3.2. Radiation Hazard Index

This factor is used to estimate the level of gamma radiation hazard associated with natural radionuclides in specific manganese ore samples. The external hazard index is obtained from Ra_{eq} expression through the assumption that its maximum value allowed corresponds to the upper limit of Ra_{eq} (370 $Bqkg^{-1}$) according to UNSCEAR, 1993. This index value must be less than unity in order to keep the radiation hazard insignificant; then, the external hazard index (H_{ex}) can be defined as the potential radiological hazard posed by the different samples was calculated using the following equation [Ngachina M, 2007],

$$H_{ex} = 0.0027C_{Ra} + 0.00386C_{Th} + 0.000208C_{K} \quad (4)$$

Where C_{Ra}, C_{Th} and C_K are the specific activities of ^{226}Ra, ^{232}Th and ^{40}K (in $Bq.kg^{-1}$) were calculated for the investigated samples to indicate different levels of external γ-radiation due to different combinations of specific natural activities in specific manganese ore samples. In addition to the external hazard, radon and its short-lived products are also hazardous to the respiratory organs. The internal exposure to radon and its daughter products is quantified by the internal hazard index (H_{in}) which was given by the formula (3) (Beretaka and Mathew, 1985).

3.3. External Annual Dose

The external annual effective dose (EAD) is calculated for a room with dimensions of 4 m × 5 m × 2.8 m, estimated that the samples is put. The equation used to calculate the annual effective dose may be defined as [H. H. Hussain et.al, 2010 and Ngachina M, 2007], The external annual effective dose (EAD) is calculated,

$$EAD = (0.92\ C_{Ra}+1.1\ C_{Th}+0.08\ C_K) \times 10^{-9}\ (Gy/\ h) \times (0.7\ Sv/\ Gy)\ (24 \times 365 \times 0.8\ /y) \quad (5)$$

Where, 0.92, 1.1 and 0.08 are the specific dose rates of Ra, Th and K, respectively; with an estimated indoor occupancy factor of 0.8.

The variation of the activity concentration (Bq/kg) of ^{238}U, ^{232}Th and ^{40}K radionuclides in the collected samples in location of manganese ore samples Company is represented in Table (3).

It is well known that the acceptable total absorbed dose rate (D) due to gamma radiations and absorbed by the staff operators surrounded by materials containing radionuclides of ^{226}Ra, ^{232}Th and ^{40}K should not exceed the average world value of 0.055 mGy/h (UNSCEAR, 1993). Therefore, dose rate in outdoor air at 1 m above the ground was calculated as

$$D = R_{Ra} C_{Ra} + R_{Th} C_{Th} + R_{K} C_{K} \qquad (6)$$

The absorbed dose in tissues are calculate using the conversion factor in (nGy/h) , which are Known to be R_{Ra} = 0.427 for ^{226}Ra (^{238}U-series), R_{Th} = 0.662 for ^{232}Th and R_{K} = 0.0437 for ^{40}K. The equivalent dose rate is calculated by

$$D = (0.427\, C_{Ra} + 0.662\, C_{Th} + 0.043\, C_{K}) \times 10^{-3} \qquad (7)$$

Where C_{Ra} , C_{Th}, and C_{K} are the activities (Bq/kg) of ^{226}Ra (^{238}U-series), ^{232}Th and ^{40}K, respectively expressed in Bq/ kg.

The U-238, Th-232 and K-40 in NORM samples activity concentration values reported in this study are less than the international recommended limits.

3.4. Radon Emanation Coefficient and Radon Exhalation Rate of the Manganese Ore Samples (Active Method)

The active method for measuring radon exhalation rate is carried out in Zagazig University, Faculty of Science, Physics Department by using the pulse type ionization chamber (Alpha Guard, Genitor Instruments, Frankfurt, Germany). Alpha Guard was calibrated in Egyptian National Institute for Standard. Each sample and Alpha Guard monitor were placed together at the same time in the Alpha Guard chamber as shown Fig. 9. Alpha Guard chamber is a container consisting of a firm corrosion-resisting stainless steel container with a removable gas-tight lid. The container dimensions were 45.0 cm diameter and 31.7 cm height. Its volume was 50.4 liters. The lid was equipped with three gas-tight electric ducts. One duct server, together with a special charger, was used as a power supply for the radon analyzer or monitor. The second duct was used to connect the fan in the middle of the inner side of the lid to the power supply, by means of a power adapter. The fan was used to ensure an even distribution of the radon exhalation from the sample in the interior of the container. The third duct provided communication between the Alpha Guard in the interior of the container and an external PC. The concentration of radon emanated from each sample inside the exhalation container was allowed to build up with time and, was measured in every one hour in diffusion mode of Alpha Guard monitor system to avoid thorn gas concentration effect for an average time of 3 days. For the Alpha Guard (diffusion mode), the sensitivity for thorn is about 10% of radon sensitivity T. ISHIKAWA; (2004). Moreover, the typical manganese ore samples show the radium concentration is higher than thorium. Even if we assume the radon and thorn exhalation rate are the same, the effects of thorn on measured concentrations can be neglected. A direct measurement

concentration at a time t during the growth of radon inside the chamber. From the radon

radon concentration in the sealed space which is the expected concentration at t >30 days) can be estimated. The radon exhalation rate of any sample, is defined as the flux of radon released from the surface of material, was also calculated.

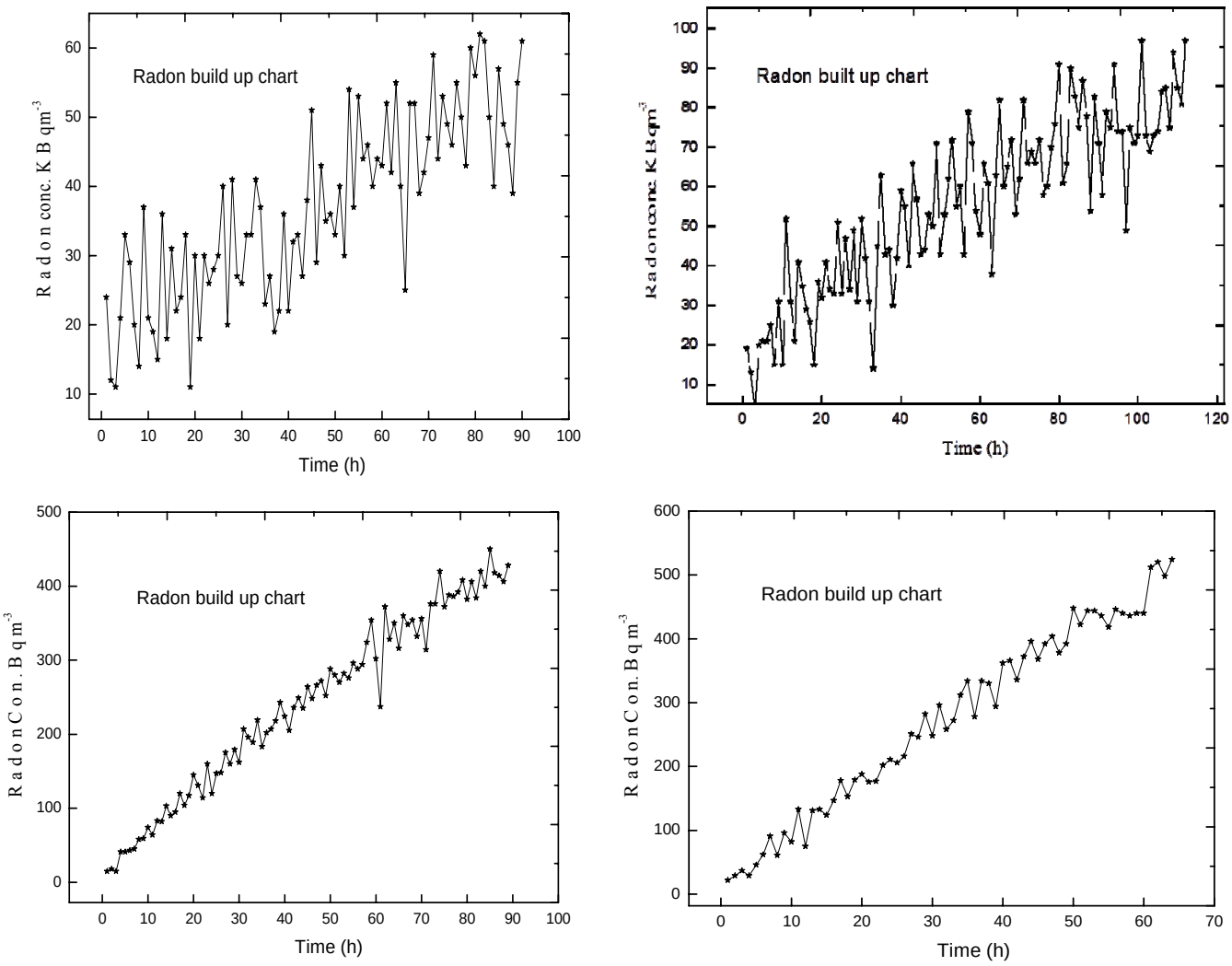

Fig. (4): Radon growth curve for Manganese ore sample code number 1, 2, 3 and 4 respectively.

For manganese ore sample 2, 3, as an example, the Equilibrium Radon Conc. = 107 Bq, 1365±35 Bq and the Radon emanation coefficient (EC) =0.0743±0.0146, 0.0296±0.00076 gmm^{-3} and radon exhalation rate =4.2693E^{-06}, 4.87305E^{-05} $Bqm^{-2}s^{-1}$respectively.

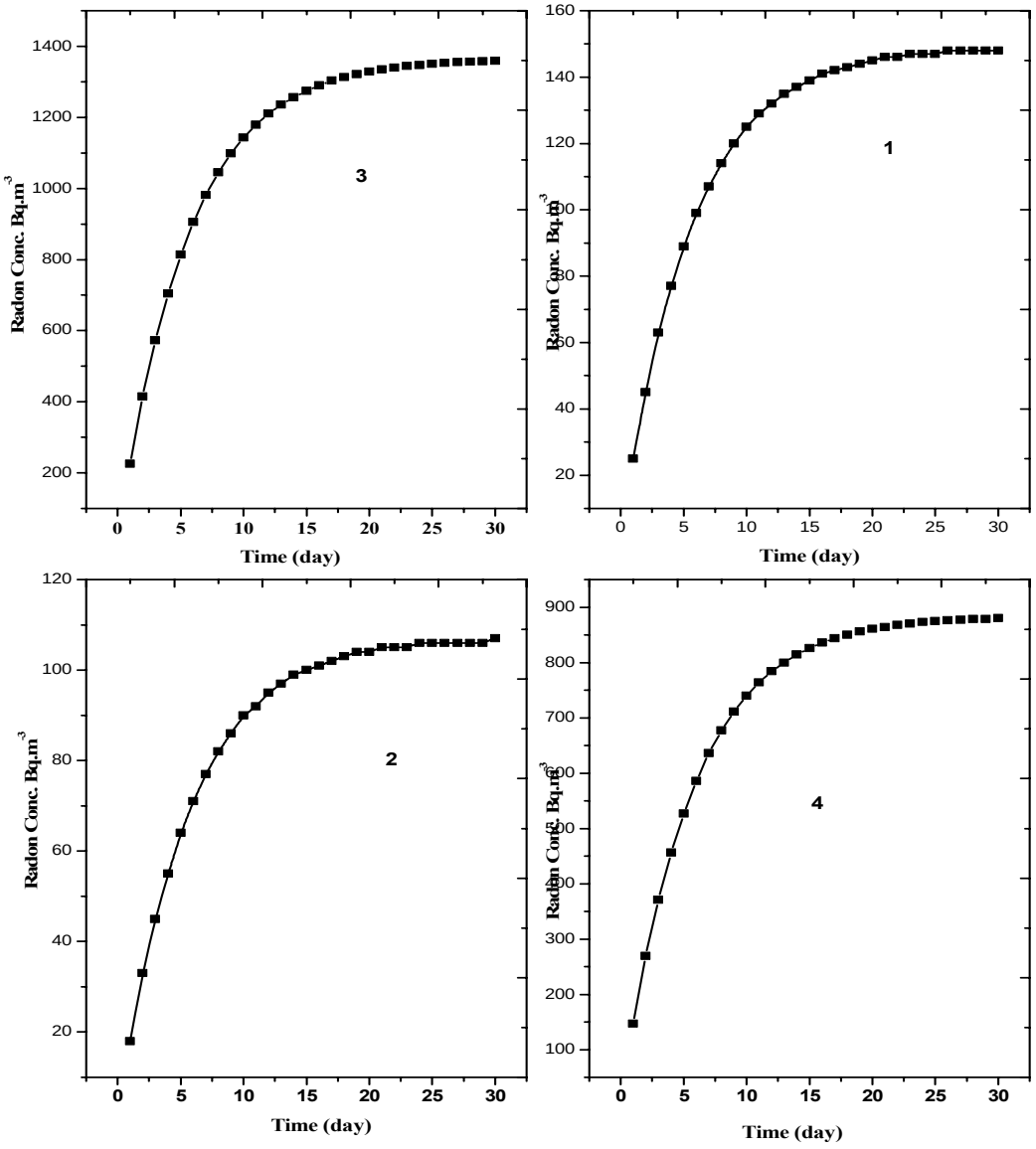

Fig. (5): Daily average Radon (^{222}Rn) concentration curve in four manganese ore samples.

The radon concentration of all samples was measured with ALPHA GUARD (active method) which as a very simple and reliable technique for exhalation rate measurements. The radon concentration is measured as a function of time directly from the software of ALPHA GUARD which set to the PC control system. The equilibrium radon concentration of the manganese ore samples was calculated and ranged from high radon concentration of manganese ore samples with code number 1, 2 to lower radon concentration of samples with code number 3, 4 .

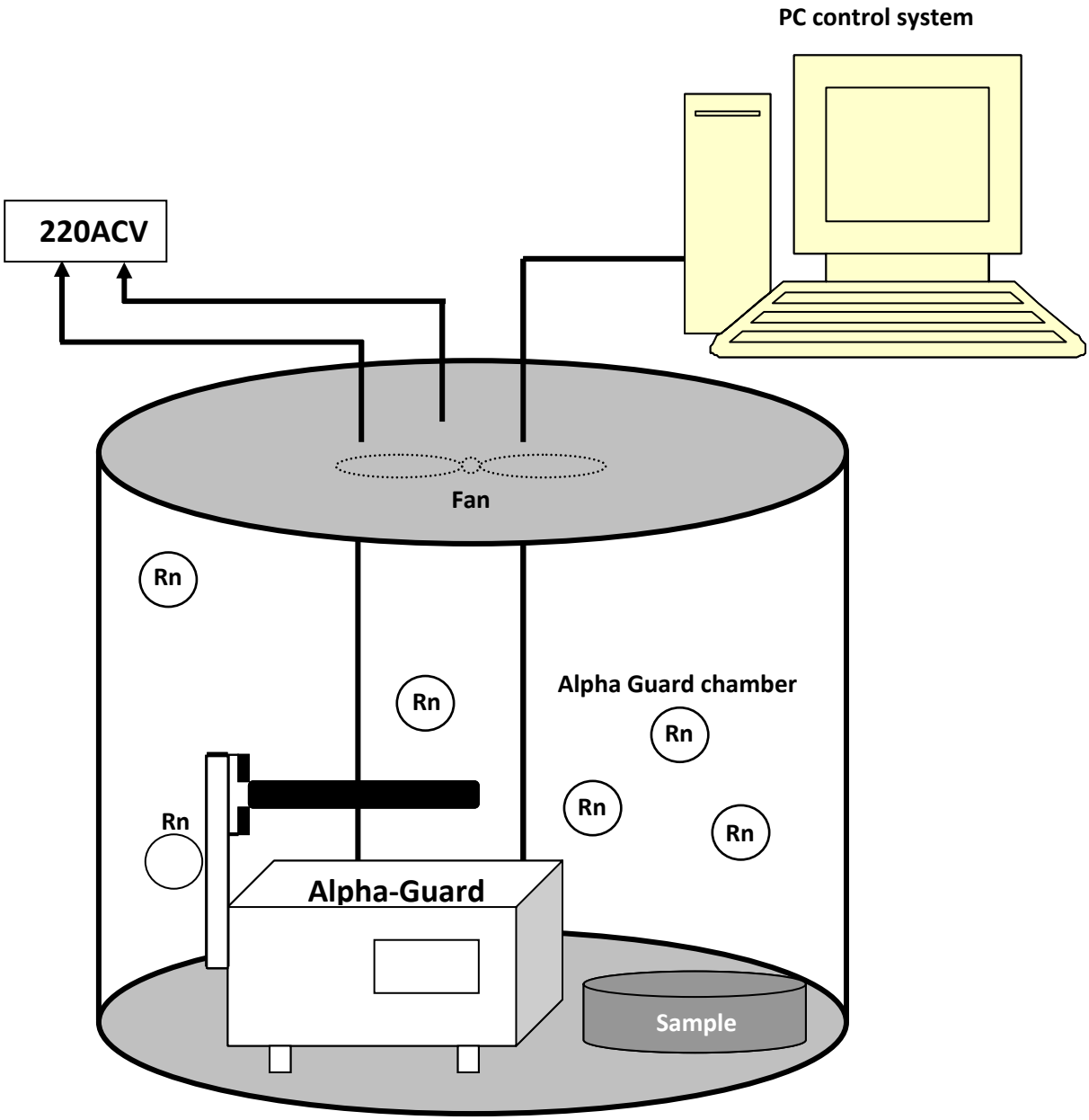

Fig. (6): Schematic diagram showing the active setup used for the exhalation measurements of samples with ALPHA GUARD.

To determine the radon (^{222}Rn) emanation coefficient (EC), the samples code number 2 were initially counted for 3 days, and counted again after reaching the radioactive equilibrium between ^{222}Rn decayed from ^{226}Ra and its respective short-life daughters. The ^{222}Rn(EC) was determined using the formula described by (White and Rood, 2001; El Afifi and Awwad, 2005)

$$^{222}\mathbf{Rn\ (EC)} = \mathbf{N_{Rn} \times m\ /\ (N_{Ra} \times V)} \qquad \mathbf{(8)}$$

$$\mathbf{E = N_{Rn} \times V \times \lambda\ /\ sample\ surface\ area} \qquad \mathbf{(9)}$$

where ^{222}Rn (EC) is the radon emanation coefficient, N_{Rn} is the equilibrium Radon concentration , N_{Ra} is the Radium concentration, λ is radon decay constant (2.1×10^{-6} s^{-1}), V is the Sample volume, m is the mass sample and E is the radon exhalation rate. The value of Rn(Ec) for sample with code 2, 3 is equal to (EC) =0.0743±0.0146 gm m^{-3}, 0.0296±0.00076 gm m^{-3} respectively.

3.5. XRF analysis

Table (4) and Fig. (7) represents the analysis of the manganese ore samples using the XRF technique. The data showed major elements Ca, Mn, Fe, Zn, Sr, Rh, Ba, and La (Qualitative Analysis), Fitting Coefficient: 0.1327.

Table (4): Results of analysis of the manganese ore samples using XRF-technique (Quantitative Analysis).

Element	٪ms	٪mol	Sigma	Intensity	K ratio
^{20}Ca	0.7740	1.0824	0.5180	1481	.0074169
^{25}Mn	90.2710	92.0925	0.1585	453611	0.6615427
^{26}Fe	4.7080	4.7248	0.1337	28851	.0374311
^{30}Zn	0.6971	0.5977	0.2467	2836	.0026239
^{38}Sr	0.2613	0.1672	0.1453	3122	.0022423
^{45}Rh				8707	.0232775
^{56}Ba	1.8791	0.7668	0.5005	5981	.0460195
^{57}La	1.4094	0.5687	0.4439	4810	.0341303

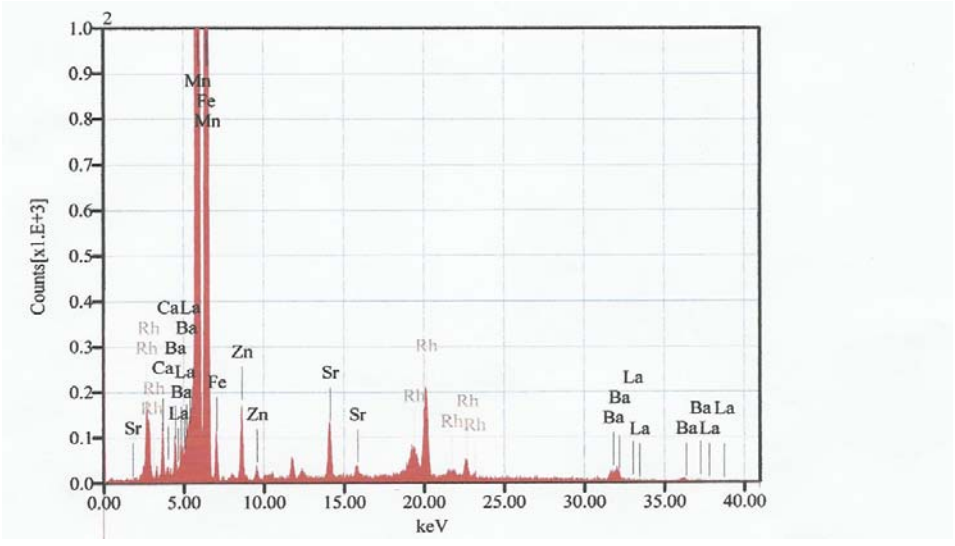

Fig. (7): Illustrates the analysis in one of the manganese ore sample by XRF Techniqu

3.6. Differential thermal analysis (DTA) and Thermo gravimetric analysis (TGA)

DTA as a method of material investigation and its curve Figs. (8-11) can record the transformations where the heat is either absorbed or released. It used as a finger print for identification purposes. It was made for the examination of different materials and helpful for

better understanding of given results by x-ray diffraction, chemical analysis and microscopy. DTA can also be used for quantitative measurements (enthalpy measurements). The area under a DTA peak can be to the enthalpy change and is not a detected by the heat capacity of the sample. The obtained sample was analyzed by differential thermal analysis (DTA) and thermo gravimetric analysis (TGA) using analyzer (Shimadzu TGA- 50H) in Physics Department Faculty of Science Cairo University was carried out in the temperature range 30 – 800°C at a heating rate of 10°C/min in N_2 atmosphere, which provides both mass losses Fig. (10) and thermal information Fig. (11). For this testing, a small powder sample of the manganese ore (3.047mg) is being heated continuously up to 800°C, and during this process the samples relative loss in weight (weight change sensitivity of 0.01 mg) is being measured over the time Fig. (8, 10). In Fig. (8) there are two endothermic peaks at temperatures of 318.50 °C and 627.42 °C. The first one corresponds to decomposition of OH and the second correspond to decomposition of O.

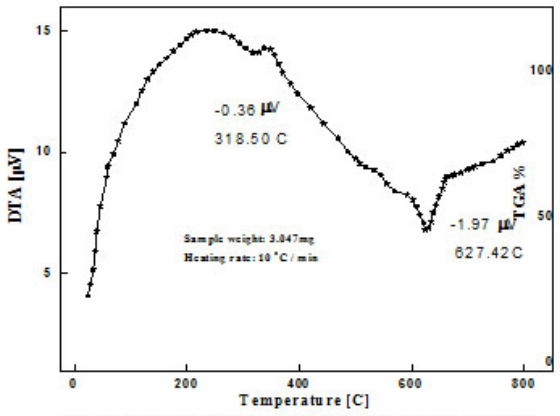

Fig. (9): DTA analysis shows the endothermic peaks with the manganese ore sample under N_2 atmosphere.

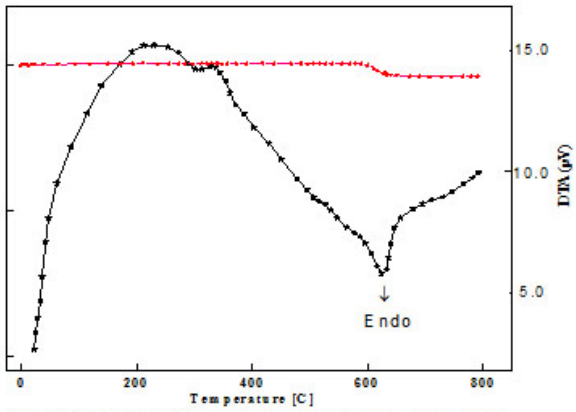

Fig. (8): TGA and DTA curves of manganese ore sample under N_2 atmosphere which shows the endothermic peaks.

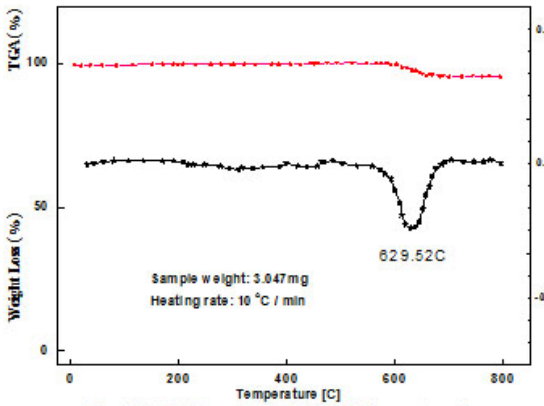

Fig. (11): TGA analysis and DrTGA spectra of manganese ore at N_2atmosphere .

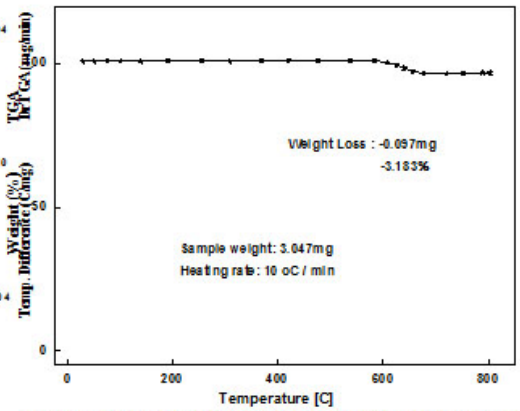

Fig. (10): TGA curve is displayed from left to right. The descending TGA thermal curve indicates a weight loss occurred by -0.097mg.

All the manganese oxides underwent phase transformation twice at 318.5 and 627.42 °C, accompanying endothermic reactions. No sharp variation in the TGA graph indicates the absence of sudden phase changes due to material weight loss.

4. CONCLUSION

An investigation was carried out to find the concentration of Naturally Occurring Radioactive Materials (NORMs) in manganese ore samples which collected at different from some ore mines, Activity concentrations of ^{238}U, ^{232}Th and ^{40}K in manganese ore samples were determined using an HPGe gamma spectrometric system. Concentrations ranged from 100 to 1500 Bq kg−1 for ^{238}U, 6 to 490 Bq kg−1 for ^{232}Th and 116 to 364 Bq kg−1 for ^{40}K. While NORM-contaminated equipment has been a concern in the manganese ore mines, the results of this investigation show that NORM contamination of Egypt equipment is significant. From the present results, it may be concluded that, for the studied samples NORM around location of manganese ore mines, the level of natural radioactivity and hazard parameters are less than the international recommended limits.

Since radon and their progenies contribute with greater than the radiation dose received from natural and man made radiation sources [W. Zahorowski; (1996)], it is important to understand the generation process of radon from different materials, their migration from this material and finally their entering process into outdoor atmosphere and indoor to our working places. Radon problem needs so much effort to solve, not only it is scientifically challenging but also due to its potential relevance to the quality of human life. Although the public interest in this problem is not as much as might be, a lot of efforts of many scientists all over the world have been done to complete characterize indoor radon concentrations and to reduce excessive level. The radon concentration of all samples was measured with Alpha GUARD (active method) which as a very simple and reliable technique for exhalation rate measurements. The radon concentration is measured as a function of time directly from the software of Alpha GUARD which set to the PC control system. The equilibrium radon concentration of the manganese ore samples was calculated and ranged from high radon concentration of manganese ore samples with code number 1, 2 to lower radon concentration of samples with code number 3, 4 which shows a typical growth of the radon.

5. ACKNOWLEDGEMENT

I would like to thank Prof. Dr. Tarik El-Sayed Amer, Head of Pilot Plant (Ores Processing), Experimental Department, Nuclear Materials, Authority of Egypt for his helping in preparation the manganese ore samples and assistance and Prof. Dr. Mohamed Fayez Hassan, Head of Experimental Nuclear Physics Department, Egyptian Atomic Energy Authority of Egypt (EAEA), for his helping during the measurement, useful comments and assistance.

REFERENCES

(1) Wollen berg, H.A., Smith, A.R., 1990. A geochemical assessment of terrestrial g-ray absorbed dose rates. Health Phys. 58, 183–189.

(2) El-Zakla, T., H.A. Abdel Ghany and A.M. Hassan, 2007. Natural radioactivity of some local fertilizers. Rom. J. Phys., 52: 731-739. http://www.nipne.ro/rjp/2007_52_57/0731_0740.pdf.

(3) United Nations Scientific Committee on the Effects of Atomic Radiation (UNSCEAR), 1993. Ionizing radiations: sources and biological effects of atomic radiation (UNSCEAR). Report to the General Assembly with annexes, Vienna.

(4) Tuschl, K., P.B. Mills, H. Parsons, M. Malone and D. Fowler et al., 2008. Hepatic cirrhosis, ystonia, polycythaemia and hypermanganesaemia-A new metabolic disorder. J. Inherit. Metab. Dis., 31: 151-163. PMID: 18392750.

(5) Shenber, A.M., 1997. Measurements of natural radioactivity levels in soil in Tripoli. Appli. Radiat. Isot., 48: 147-148. DOI: 10.1016/50969- 8043(96)00065-6.

(6) Luigi, B., B. Maurizio, M. Giorgio, M. Rento and R. Serena, 2000. Radioactivity in raw materials and end products in the Italian Ceramics industry Environ. Radioactiv., 47: 171-181. DOI: 10.1016/s0265-931x(99)00026-0.

(7) Kavasi, N., J. Somlai, T. Vigh, S. Tokonami and T. Ishikawa et al., 2009. Difficulties in the dose estimate of workers originated from radon and radon progeny in a manganese mine. Radiat. Measure., 44: 300-305. DOI: 10.1016/J.radmeas.2009.03.014.

(8) Iwaoka, K., K. Tagami and H. Yonehara, 2009. Measurement of natural radioactive nuclide concentrations in various metal ores used as industrial raw materials in Japan and estimation of dose received by workers handling them. J. Enviorn. Radioactiv., 100: 993-997. DOI: 10.1016/J.Jenvrad.2009.08.004.

(9) Kavasi, N., Vigh, T., Sorimachi, A., Ishikawa, T., Tokonami, S., Hosoda, M., 2010. Effective dose of miners due to natural radioactivity in a manganese mine in Hungary. Radiat. Prot. Dosim. 141 (4), 32e435.

(10) ICRP, 1987. International Commission on Radiological Protection. Lung Cancer Risk from Indoor Exposures to Radon Daughters. ICRP Publication 50, Oxford.

(11) ICRP, 1991. International Commission on Radiological Protection. Recommendations of the International Commission on Radiological Protection. ICRP Publication 60, Oxford.

(12) ICRP, 1994a. International Commission on Radiological Protection. Protection against 222Rn at Home and at Work. ICRP Publication 65, Oxford.

(13) ICRP, 1994b. International Commission on Radiological Protection. Human Respiratory Tract Model for Radiological Protection. ICRP Publication 66, Oxford.

(14) Kavasi, N., Somlai, J., Vigh, T., Tokonami, S., Ishikawa, T., Sorimachi, A., Kovacs, T., 2009. Difficulties in the dose estimate of workers originated from radon and radon progeny in a manganese-mine. Radiat. Meas 44 (3), 300e305.

(15) Moore, W.S., Reid, D.F., 1973. Extraction of radium from natural waters using manganese- impregnated acrylic fibers. J. Geophys. Res. 78 (36), 8880–8886.

(16) Polga´ ri, M., Szabo´ , Z., Szederke´nyi, T., 2000. Manga´ne´rcek Magyarorsza´ gon. MTA Szegedi Akade´miai Bizottsa´ g, Szeged.

(17) Risica, S., 2001. Italian basic safety standards legislation. J. Radiol. Prot. 21, 81. Scivyer, C.R., Gregory, T.J., 1995. BRE (Building Research Establishment) Radon in the workplaces.
(18) SSI (Swedish Radiation Protection Institute), 1999. Radon legislation and national guidelines. Åkerblom, G., ISSN: 0282-4434.
(19) Dixon, D.W., Gooding, T.D., McCready-Shea, S., 1996. Evaluation and significance of radon exposures in British workplace buildings. Environ. Int. 22, S1079–S1082.
(20) USEPA (United States Environmental Protection Agency), 2004. A Citizen's Guide to Radon: the Guide to Protecting Yourself and Your Family from Radon. 402-K-02-006.
(21) Wollenberg, H.A., Smith, A.R., 1990. A geochemical assessment of terrestrial g-rayabsorbed dose rates. Health Phys. 58, 183–189.
(22) H.R. Verma "Atomic and Nuclear Analytical Methods" Verlag Berlin Heidelbe York,(2007).
(23) VIENNA 1990 Tables for Practical aspects of operating neutron activation an laboratory; No.564, IAEA, VIENNA.
(24) Amrani D., (2001) Tahta M; Appl. Radiat.and Iso.; 54, 687.
(25) KAFALA S. I., (2007), MACMAHON T. D.; J. Radioanl.Nucl. Chem., 271(2) 507. Ngachina M. (2007), Garavaglia M., Giovani C., Kwato Njock M.G. and Nourreddine A; Radiat.Measur.; 42, 61.
(26) Ngachina M. (2007), Garavaglia M., Giovani C., Kwato Njock M.G. and. Nourreddine A; Radiat.Measur.; 42, 61.
(27) Bareteka, J., Mathew, P.J., 1985. Natural radioactivity of Australian building materials,
(28) industrial waste and by-products. Health Physics 48, 87–95.
(29) H. H. Hussain , R. O. Hussain , R. M. Yousef and Q. Shamkhi "Natural radioactivity of some local building materials in the middle Euphrates of Iraq" J Radioa. Nucl. Chem., 284, 43–47, (2010).
(30) T. ISHIKAWA; (2004). Effects of thoron on a radon detector of pulse-ionization chamber type, Radiat. Prot. Dosim., 108, 327, 330.
(31) White, G.J., Rood, A.S., 2001. Radon emanation from NORM contaminated pipe scale and soil at petroleum industry sites. Journal of Environmental Radioactivity 54, 401e413.
(32) El Afifi, E.M., Awwad, N.S., 2005. Characterization of the TE-NORM waste associated with oil and natural gas production in Abu Rudeis, Egypt. Journal of Environmental Radioactivity 82, 7e19.
(33) W. Zahorowski and S. Whitt lest one; (1996). A fast portable manometer for field measurement of radon and thoron flux, Radiat. Prot. Dosim., 67, 109–120 .

Assessment of natural radioactivity and radiation hazard indices in different soil samples from assiut governorate

Shams A.M. Issa[a], M.A.M. Uosif[a], M.A. Hefni[b], A.H. El-Kamel[b] and Nesreen A. A.[b]
[a]*Physics Department, Faculty of Sciences, Al-Azhar University (Assiut branch), Egypt*
[b]*Physics Department, Faculty of Sciences, Assiut University, Egypt*
shams_issa@yahoo.com

ABSTRACT

Natural radioactive materials under certain conditions can reach hazard radiological levels. So, it becomes necessary to study the natural radioactivity levels in soil to assess the dose for the population in order to know the health risks and to have a baseline for future changes in the environmental radioactivity due to human activities. Determine the radioactivity concentration of ^{226}Ra, ^{232}Th and ^{40}K in surface and 20 cm soil samples collected beside Assiut fertilizer plant, Assiut government in south Upper Egypt, to assess their contribution to the external dose exposure. The contents of natural radionuclides ^{226}Ra, ^{232}Th and ^{40}K were measured in investigated samples by using gamma spectrometry [NaI (Tl) 3"x 3"]. The total absorbed dose rate, annual effective dose rate, radium equivalent, excess lifetime cancer risk and the external hazard index, which resulted from the natural radionuclides in soil, were calculated.

Key word: *Natural radionuclides, soil and hazard index*

INTRODUCTION

Natural radioactivity is common in rocks, soil, beach sand, sediment and riverbed soil, in rivers and oceans, and even in our building materials and homes. Radioactive isotopes concentration in soil is an indicator of radioactive accumulation in the environment, which affects humans, plants and animals. Naturally occurring radioactive materials generally contain terrestrial origin radionuclides (primordial radionuclides), left over since the creation of the earth (1). The natural radioactivity in soil is derived mainly from the ^{238}U and ^{232}Th parent series and natural ^{40}K. Natural environmental radioactivity and the associated external exposure due to gamma radiation depend primarily on the geological and geographical conditions. The sources of radioactivity in soils other than those of natural origin are mainly due to extensive use of fertilizers rich in phosphates for agricultural purposes (2). Study of soil radioactivity can provide reference data in observing possible future anthropomorphic impact and associated radiological risk to human health. The activity concentrations of radionuclides in the ^{238}U and ^{232}Th decay chains and from ^{40}K were determined through gamma-rays spectrometry in a low background configuration (3).

MATERIALS AND METHODS

Sampling and sample preparation

Eighteen samples were collected from different places at the area surrounding the company for fertilizers in assiut. Ten samples were collected from the surface. Eight samples were collected from the depth 30 cm. Each sample was dried in an oven at about 110°C to ensure that moisture was completely removed. The samples were crushed, homogenized and sieved through a 200 μm, which is the optimum size enriched in heavy minerals. Weighed samples were placed in polyethylene beaker, of 197 cm^3 volumes each. The beakers were completely sealed for 4 weeks to reach secular equilibrium where the rate of decay of the progeny becomes equal to that of the parent (radium and thorium). This step is necessary to ensure that radon gas confined within the volume and the Progeny will remain in the sample (4, 5).

Instrumentation and calibration

Activity measurements were performed by gamma ray spectrometer, employing a scintillation detector 3×3 inch. It is hermetically sealed assembly, which includes a NaI (Tl) crystal, coupled to PC-MCA Canberra Accuspes. To reduce gamma ray background, a cylindrical lead shield (100 mm thick) with a fixed bottom and movable cover shielded the detector. The lead shield contained an inner concentric cylinder of copper (0.3 mm thick) in order to absorb X rays generated in the lead. In order to determine the background distribution in the environment around the detector, an empty sealed beaker was counted in the same manner and in the same geometry as the samples. The measurement time of activity or background was 43 200 s. The background spectra were used to correct the net peak area of gamma rays of measured isotopes. A dedicated software program Genie 2000 from Canberra has carried out the online analysis of each measured gamma ray spectrum (6).

RESULTS AND DISSECTION

Radioactivity

The results for the activity concentrations of natural radionuclides ^{226}Ra, $^{232}Th$and ^{40}K together with their average values and range in 10 surface soil samples and 8 soil samples taken at depth 30 cm were reported in Table1 and Table2 respectively. All values are reported as $Bqkg^{-1}$ dry weight. As can be seen in table 1, the concentrations of ^{226}Ra and ^{232}Th and

Table 1: Activity concentration (Bqkg^{-1}) of ^{226}Ra, ^{232}Th and ^{40}K in surface soil samples.

Sample No.	^{226}Ra	^{232}Th	^{40}K
1	44±2.2	1±0.02	327±16.4
2	77±3.9	63±3.2	290±14.5
3	44±2.2	47±2.3	214±10.7
4	60±3.0	40±2.0	195±9.8
5	7±0.6	10±0.5	118±5.9
6	11±0.5	9±0.4	108±5.4
7	122±6.1	154±7.7	346±17.3
8	37±2.1	51±2.5	202±10.1
9	30±1.5	14±0.7	183±9.1
10	12±0.8	5±0.3	126±6.3
Range	**7 - 122**	**1 - 154**	**108 - 346**
Average	**40.4±2.3**	**39.5±2**	**211±10.6**

Table 2: Activity concentration (Bqkg^{-1}) of ^{226}Ra, ^{232}Th and ^{40}K in soil samples at depth 30 cm.

Sample No.	^{226}Ra	^{232}Th	^{40}K
1	118±5.9	119±5.9	261±13.1
2	107±5.4	37±1.8	259±12.9
3	53±2.6	133±6.6	315±15.8
4	61±3.1	58±2.9	229±11.4
5	145±7.2	165±8.3	368±18.4
6	153±7.6	170±8.5	424±21.2
7	194±9.7	187±9.4	464±23.2
8	39±2.0	37±1.8	111±5.5
Range	**39 - 194**	**37 - 187**	**111 -464**
Average	**108.8±5**	**113.3±5**	**304±15**

^{40}K for surface soil samples were ranged from 7±0.6 to 122±6.1 Bqkg^{-1}, from 1±0.02 to 154±7.7 Bqkg^{-1} and from 108±5.4 to 346±17.3 Bqkg^{-1}, respectively.

Table 2 shows that, the activity concentration of ^{226}Ra and ^{232}Th and ^{40}K for soil samples at 30 cm depth were ranged from 39±2 to 194±9.7 Bqkg^{-1}, from 37±1.8 to 187±9.4 Bqkg^{-1} and from 111±5.5 to 464±23.2 Bqkg^{-1}, respectively. The world average concentrations are 35, 30 and 400 Bqkg^{-1} for ^{226}Ra, ^{232}Th and ^{40}K respectively. The average activity concentrations of

^{226}Ra and ^{232}Th in surface and depth soil samples of investegated area were higher than the world figures reported in (2).

Radium equivalent activity (Ra_{eq})

It was calculated through the following relation (7):

$$Ra_{eq} = A_{Ra} + 1.43A_{Th} + 0.077A_K \quad (1)$$

where, A_{Ra}, A_{Th} and A_K are the activity concentrations of ^{226}Ra, ^{232}Th and ^{40}K in Bqkg^{-1},respectively. It has been assumed that 370 Bqkg^{-1} of ^{226}Ra, 259 Bqkg^{-1} of ^{232}Th and 4810 Bqkg^{-1} of ^{40}K produce the same gamma dose rate. The maximum value of Ra_{eq} in all soil samples is required to be less than the limit value of 370 Bqkg^{-1} recommended by the Organization for Economic Cooperation and Development for safe use, i.e., to keep the external dose below 1.5 mSvy^{-1}. Table 3 and 4 show that, the values of Ra_{eq} in surface and at depth 30 cm are less than the 370 Bqkg^{-1}.

Absorbed dose rates (D)

The external terrestrial γ-radiation absorbed dose rate in air at a height of about 1m above the ground was calculated by using the conversion factor of 0.0414 nGyh^{-1}/Bqkg^{-1} for ^{40}K, 0.461 nGyh^{-1}/Bqkg^{-1} for ^{226}Ra and 0.623 nGyh^{-1}//Bqkg^{-1} for ^{232}Th (8)

Table (3): Radium equivalent, the dose rate, hazard index, annual effective dose rate and excess lifetime cancer risk for surface soil samples.

Sample No.	Ra_{eq} Bqkg^{-1}	D nGyh^{1-}	H_{ex} nGyh^{-1}	A. Eff. μSvy^{-1}	ELCR
1	70.6	34.6	0.2	42.0	1.5E-04
2	189.4	85.7	0.5	104.0	3.6E-04
3	127.7	57.6	0.3	70.0	2.4E-04
4	132.2	60.0	0.4	72.8	2.5E-04
5	30.4	14.2	0.1	17.2	6.0E-05
6	32.2	15.0	0.1	18.2	6.4E-05
7	368.9	163.8	1.0	198.8	7.0E-04
8	125.5	56.3	0.3	68.4	2.4E-04
9	64.1	29.9	0.2	36.3	1.3E-04
10	28.9	13.8	0.1	16.8	5.9E-05
Average	**117**	**53.1**	**0.3**	**64.5**	**2.3E-04**

assuming that ^{137}Cs, ^{90}Sr and the ^{235}U decay series can be neglected as they contribute very little to the total dose from environmental background (9).

$D = 0.427C_{Ra} + 0.662\ C_{Th} + 0.043\ C_K$ nGyh^{-1}, (2)

Where C_{Ra}, C_{Th} and C_K are the concentration in ($BqKg^{-1}$) of radium, thorium and potassium, respectively. Table 3 and table 4 give the results for the absorbed dose rate in air for surface and depth soil samples.

External radiation hazard (H_{ex})

The external hazard index H_{ex} can be calculated by the following equation (10):

$$H_{ex} = C_{Ra}/370 + C_{Th}/259 + C_K/4810 \quad (3)$$

Table (4): Radium equivalent, the dose rate, hazard index, annual effective dose rate and excess lifetime cancer risk for soil samples at depth 30 cm.

Sample No.	Ra_{eq} $Bqkg^{-1}$	D $nGyh^{1-}$	H_{ex} $nGyh^{-1}$	A. Eff. μSvy^{-1}	ELCR $\times 10^{-4}$
1	308.3	137.3	0.8	166.6	5.8
2	179.9	82.6	0.5	100.2	3.5
3	267.4	118.0	0.7	143.2	5.0
4	161.6	72.8	0.4	88.3	3.1
5	409.3	182.0	1.1	220.9	7.7
6	428.7	191.0	1.2	231.9	8.1
7	497.1	221.9	1.3	269.4	9.4
8	100.5	45.0	0.3	54.6	1.9
Average	**294.1**	**131.3**	**0.8**	**159.4**	**5.6**

where C_{Ra}, C_{Th} and C_K are the activity concentrations of ^{226}Ra, ^{232}Th and ^{40}Kin $Bqkg^{-1}$, respectively. The value of this index must be less than the unity in order to keep the radiation hazard to be insignificant. Table 3 and table 4 show the average values of H_{ex} in soil sample are less than the unity.

Annual effective dose (A. eff.)

Annual estimated average effective dose equivalent received by a member was calculated using a conversion factor of 0.7 $SvGy^{-1}$, which was used to convert the absorbed rate to human effective dose equivalent with an outdoor occupancy of 20% and 80% for indoors (8). The annual effective dose was determined as follows:

$$\text{Annual effective dose rate} = D \times T \times F \quad (4)$$

Where D is the calculated dose rate (in $nGyh^{-1}$), T is the outdoor occupancy time (0.2x24 h x365.25 d≈1753 hy^{-1}), and F is the conversion factor ($0.7x10^{-6}$ $SvGy^{-1}$). The experimental results of annual effective dose rate are presented in table 3 and table 4. The International Commission on Radiological Protection (ICRP) has recommended the annual effective dose

equivalent limit of 1 $mSvy^{-1}$ for the individual members of the public and 20 $mSvy^{-1}$ for the radiation workers (11).

Excess lifetime cancer risk (ELCR):

Excess lifetime cancer risk (ELCR) was calculated using the following equation and presented in Table 3 and table 4.

$$ELCR = AEDE \times DL \times RF \quad (5)$$

where AEDE, DL and RF is the annual effective dose equivalent, duration of life(70 years) and risk factor (Sv^{-1}), fatal cancer risk per sievert. For stochastic effects, ICRP60 uses values of 0.05 for the public (12).

CONCLUSION

The specific radioactivity values of ^{226}Ra, $^{232}Th$and ^{40}K measured in soil samples determined by gamma-ray spectrometer. For each sample in this study, the specific activity, radium equivalent activity, annual radiation dose, external hazard and excess lifetime cancer risk have been determined to assess the radiological hazards from the soil samples. The calculated average radium equivalent activity (Ra_{eq}) values for all the soil samples examined are lower than the recommended maximum level of radium equivalent of 370 $Bqkg^{-1}$.

The average external (H_{ex}) hazard index has been determined to be less than the recommended value. The values obtained in the study are with in the recommended safety limit, showing that the soil samples do not pose any significant radiation hazard. This study can be used as a reference for more extensive studies of the same subject in future.

ACKNOWLEDGMENT

This work was carried out using the nuclear analytical facilities at the Physics Department, Faculty of Sciences, Al-Azhar University, Assiut, Egypt.

REFERENCES

(1) UNSCEAR, United Nations Scientific Committee on the Effects of Atomic Radiation. Sources, effects and risks of ionizing radiation. Report to the General Assembly, with annexes, United Nations, New York, (1982).
(2) UNSCEAR, United Nations Scientific Committee on the Effect of Atomic Radiation. Sources and Effects of Ionizing Radiation. Report to General Assembly, with Scientific Annexes, United Nations, New York, (2000).
(3) A. El-Gamal, et al.; Radiat. Meas; 42, 457, (2007).
(4) IAEA, Uranium deposits in metamorphic rocks. International atomic energy agency, Vienna, (1989).
(5) Manazul I.,Alam M.N., Hazari S.K.S; Radiat. Isotopes; 51, 747-755, (1999).

(6) Shams A. M. Issa, M. A. M. Uosif and L. M. Abd El-Salam; Radiation Protection Dosimetry; 150, 488-495, (2011).
(7) Yu. K.N, Z.J,Guan., M.J, Stoks., E.C, Young; J.Environ. Radioactivity; 17, 931, (1992).
(8) UNSCEAR, United Nations Scientific Committee on the Effects of Atomic Radiation. Exposure from natural sources of radiation.UN,NewYork, (1993).
(9) Leung, K.C., Lau, S.Y., Poon, C.B.; J. Environ. Radioact; 11, 279–290, (1990).
(10) Beretka, J., Mathew, P.J.; Health Phys; 48, 87–95, (1985).
(11) International Commission on Radiological Protection (ICRP). ICRP Publication 65, Annals of the ICRP 23(2). Pergamon Press, Oxford, (1993).
(12) V. Ramasamy, G.Suresh , V.Meenakshisundaram and V.Ponnusamy; Applied Radiation and Isotopes; 69 184–195, (2011)

^{226}Ra, ^{232}Th and ^{40}K analysis in water samples from Assiut, Egypt.

Hany El-Gamal[(1)], Marwa Abdel Hamid[(2)], A.I. Abdel Mageed[(1)], A. L. El-Attar[(1)]
[(1)] Physics department, Assiut university, Egypt.
[(2)] South Egypt cancer Institute, Assiut university, Egypt.
e-mail:elgamal99@yahoo.com

ABSTRACT

The activity concentrations of ^{226}Ra, ^{232}Th and ^{40}K were determined in water samples, using 2"x2" NaI(Tl) scintillation detector. Water activity ranges from 0.07 to 0.59 BqL^{-1} for ^{226}Ra, 0.05 to 0.37 BqL^{-1} for ^{232}Th and 3.25 to 8.72 BqL^{-1} for ^{40}K with mean values of 2.64, 2.22 and 119.50 BqL^{-1}, respectively. As far as the measured gamma radionuclides is concerned, the mean annual effective doses for all analyzed samples of water are in the range of 0.02–0.08, 0.03-0.17 and 0.03-0.10 mSv yr^{-1} for infants, children and adults, respectively, all being lower than the reference level of the committed effective dose recommended by the WHO.

Key words: *Natural radioactivity, Upper Egypt, Ground water, annual effective dose.*

INTRODUCTION

Measurements of natural radioactivity in drinking water have been performed in many parts of the world, mostly for assessment of the doses and risk resulting from consuming water. Potential health hazards from natural radionuclides in consuming water have been considered adopting the guideline activity concentration for drinking water quality recommended by WHO[(1)]. It was observed that an important source of natural radioactivity in water is radium. It is a naturally occurring isotope, found in the earth's crust, a member of the uranium ^{238}U decay series. The predominant radium isotopes in groundwater are ^{226}Ra, an alpha emitter with a half-life of 1600 years, and ^{228}Ra, a beta emitter with a half life of 5.8 years [(2-4)]. Many salts of radium are soluble in water, and therefore surface, drinking and mineral waters may be enriched in radium and its descendant radon. Radium- 226 is an earth alkaline element sharing the metabolic pathways of calcium in the human body. Thus, an appreciable fraction of radium is preferentially deposited in bone, the remaining fraction being distributed almost uniformly in soft tissues [(5)]. Due to their radiotoxicity, especially those of ^{226}Ra, a contamination hazard for human beings exists even at low concentration levels [(6)].

Potassium is a major element widely distributed in crustal rocks [(7)]. Thus, potassium occurs in various minerals and clays, from which it may be dissolved through weathering processes and transferred into the liquid phase. ^{40}K decays directly to ^{40}Ca beta emission; it also decays through electron capture [(8)] to ^{40}Ar followed by a prompt 1.46 MeV gamma emission. As a consequence of water/rock–soil interactions, ^{40}K is released to water bodies, contributing to the presence of radioactive constituents of drinking water.

The present study attempts to understand the occurrence and distribution of natural radionuclides ^{226}Ra, ^{232}Th and ^{40}K in water samples from Assiut governorate, Upper Egypt, to assess the concentration of ^{226}Ra, and to estimate the radiation doses received by humans living in this area.

Materials and methods

Sample collection and preparation techniques

Fifteen water samples were collected from Assiut, Upper Egypt and prepared for gamma analysis as follows:
-13 water samples were collected from open wells (used for drinking and for agriculture purposes).
- 2 drinking water samples were taken from the tap water system.

The water samples were collected in standard (1 liter) polyethylene Marinelli beakers, which also used as a measuring container. Before use, the containers were washed with dilute hydrochloric acid and rinsed with distilled water. Each beaker was filled up to brim and a tight cap was pressed on, so that the air was completely removed from it. Samples were acidified by adding 0.5 ml of conc. HNO_3 per liter, to prevent any loss of radium isotopes around the container walls, and to avoid growth of micro- organisms [9]. The samples were stored in the laboratory for a minimum of 1 month to allow daughter products to come into radioactive equilibrium with their parents ^{226}Ra and ^{232}Th before radiometric analysis.

Gamma-ray detection system

Each sample was measured with a gamma-ray spectrometer consisting of a NaI(Tl) detector and multichannel analyzer of 8192 channel, with the following specifications: Resolution (FWHM) at 1.33 MeV ^{60}Co is 60 keV – relative efficiency at 1.33 MeV ^{60}Co is 7.5 %. The detector is shielded in a chamber of two layers starting with stainless steel (10 mm thick) and lead (30 mm thick). This shield serves to reduce different background radioactivity.
To minimize the effect of scattered radiation from the shield, the detector is located in the center of the chamber. The sample was placed above the detector and measured for at least 24 h. The spectra were either evaluated with computer software program Maestro (EG&G ORTEC), or manually using a spread sheet (Microsoft Excel) to calculate the natural radioactivity. ^{226}Ra activity of the samples was determined via its daughters (^{214}Pb and ^{214}Bi) through the intensity of the 295.22, 351.93 keV, for ^{214}Pb Gamma-lines and 609.31, 1120, 1764.49 keV, for ^{214}Bi Gamma-lines. ^{232}Th activity was determined from the daughters (^{228}Ac), (^{212}Pb) and (^{208}Ti) through the intensity of 209.25, 338.32, 911.2 keV Gamma-lines for (^{228}Ac), (^{212}Pb) emissions at 238.63 keV and (^{208}Ti) emissions at 583.19, 2614 keV Gamma-lines. ^{40}K activity determined from the 1460.7 keV Gamma-line.

RESULTS AND DISCUSSION

The activity concentrations of ^{226}Ra, ^{232}Th and ^{40}K in water samples from different location in Assiut are presented in Table 1. As seen, the concentrations of ^{226}Ra, ^{232}Th and ^{40}K varied from 0.07 to 0.59 BqL^{-1}, 0.05 to 0.37 BqL^{-1} and from 3.25 to 8.72 BqL^{-1}, respectively. It should be noted that in all samples except (Sa1 and Sa6), the concentrations of ^{226}Ra is higher than that of ^{232}Th and this reflects the fact that radium is more soluble in groundwater than its thorium and uranium precursors, and its solubility is enhanced by: the common-ion effect (when dissolved solids are high), an oxygen-poor environment, and the fragmentation of

uranium-bearing minerals [10]. Samples Sa1and Sa6 have not the same symmetry like the rest of samples. This may be explained by the different origins of these water, these waters come from different depths and pass through different geological layers.

Table 1 shows variations in radionuclide concentrations in ground waters from one sample to another; these variations depend on the minerals derived from aquifer rocks. The abundance of ^{40}K activity observed in all samples, may be due to agricultural activities going on in the area that involve the use of potassium fertilizers which may have been transported to the groundwater, given that ^{40}K is a highly soluble element [10]

Sample code	Activity concentration in BqL^{-1} ^{226}Ra	^{232}Th	^{40}K
Sa1	0.17±0.09	0.37±0.23	5.06±3.42
Sa2	0.314±0.12	0.13±0.07	4.19±2.33
Sa3	0.23±0.15	0.08±0.07	5.73±1.97
Sa4	0.14±0.11	0.07±0.05	5.42±2.5
Sa5	0.54±0.35	0.10±0.08	6.55±1.93
Sa6	0.29±0.16	0.50±0.28	8.72±4.32
Sa7	0.22±0.13	0.12±0.09	3.25±2.09
Sa8	0.13±0.06	0.12±0.06	3.51±1.09
Sa9	0.32±0.12	0.11±0.05	3.71±1.39
Sa10	0.13±0.10	0.07±0.03	7.21±2.32
Sa11	0.13±0.07	0.06±0.03	6.02±1.90
Sa12	0.10±0.04	0.08±0.06	4.43±2.36
Sa13	0.07±0.05	0.05±0.04	5.20±2.35
Sa14	0.09±0.02	0.07±0.03	7.07±4.06
Sa15	0.19±0.12	0.08±0.07	3.39±2.13

Table 1: The activity concentration in BqL^{-1} of water samples and the estimated annual effective doses in mSv $year^{-1}$ due to ingestion of ^{226}Ra, ^{232}Th and ^{40}K for different age groups.

Radiation dose estimation

The annual effective doses have been calculated according to the equation introduced by (11) and (12). Several factors must be addressed for proper dose evaluation due to the radionuclides in drinking water, these factors are: the weighted average activity concentration in (Bq/L), the amount of water intake by person in one year, the dose coefficient for radionuclides ingestion by humans (mSv/Bq). Doses were estimated by considering a consumption rate (150, 350 and 500 l $year^{-1}$) for infants, children and adults, respectively.The conversion factors for ^{226}Ra, ^{232}Th and ^{40}K as reported by ICRP [13], IAEA [14] and WHO [15] are (9.6×10^{-7}, 4.5×10^{-7} and 5×10^{-9} Sv Bq^{-1}) for infants, (8×10^{-7} , 2.9×10^{-7} and 5×10^{-9} Sv Bq^{-1}) for children and (2.8×10^{-7}, 2.3×10^{-7} and 5×10^{-9} Sv Bq^{-1}) for adults.

The calculated effective doses for different age groups infants, children and adults are presented in table 2. It should be noted that doses were ranged from 0.02–0.08 mSv $year^{-1}$ for infants, 0.03-0.17 mSv $year^{-1}$ for children and 0.03-0.10 mSv $year^{-1}$ for adults. Figure 1 shows that doses received by children are higher than that received by infants and adults and doses received by adults are higher than that recevied by infants.

The doses obtained in our study are much lower than the recommended reference level of 0.26, 0.2 and 0.1 mSv year^{-1} for effective doses for infants, children and adults, respectively which published by WHO [15], IAEA [14] and UNSCEAR [16], from one year consumption of drinking water, and consequently, it can be recommended that, the investigated waters are suitable for life-long human consumption.

Table2: Estimates of annual effective doses in mSv year^{-1} due to ingestion of ^{226}Ra, ^{232}Th and ^{40}K for different age groups and due to the total ingestions.

Sample code		^{226}Ra			^{232}Th			^{40}K		Total dose		
	Infants	Children	adults	Infants	children	adults	Infants	children	adults	Infants	children	adults
Sa1	0.024	0.024	0.003	0.0476	0.037	0.008	0.023	0.042	0.012	0.053	0.094	0.079
Sa2	0.045	0.008	0.003	0.087	0.013	0.007	0.043	0.014	0.010	0.057	0.108	0.069
Sa3	0.033	0.005	0.004	0.064	0.008	0.010	0.032	0.009	0.014	0.042	0.082	0.055
Sa4	0.020	0.004	0.004	0.039	0.007	0.009	0.019	0.008	0.013	0.028	0.055	0.041
Sa5	0.077	0.006	0.004	0.151	0.010	0.011	0.075	0.011	0.016	0.089	0.172	0.103
Sa6	0.041	0.033	0.006	0.081	0.050	0.015	0.040	0.057	0.021	0.082	0.147	0.119
Sa7	0.031	0.008	0.002	0.061	0.012	0.005	0.030	0.013	0.008	0.042	0.079	0.052
Sa8	0.018	0.008	0.002	0.036	0.012	0.006	0.018	0.013	0.008	0.029	0.054	0.040
Sa9	0.046	0.007	0.002	0.089	0.011	0.006	0.044	0.012	0.009	0.056	0.107	0.066
Sa10	0.018	0.004	0.005	0.036	0.007	0.012	0.018	0.008	0.018	0.028	0.056	0.044
Sa11	0.018	0.004	0.004	0.035	0.006	0.010	0.017	0.006	0.015	0.026	0.051	0.039
Sa12	0.014	0.005	0.003	0.028	0.008	0.007	0.014	0.009	0.011	0.023	0.043	0.034
Sa13	0.010	0.003	0.003	0.0196	0.005	0.009	0.009	0.005	0.013	0.017	0.033	0.028
Sa14	0.012	0.004	0.005	0.025	0.007	0.012	0.012	0.008	0.017	0.022	0.044	0.038
Sa15	0.027	0.005	0.002	0.053	0.008	0.005	0.026	0.009	0.008	0.035	0.067	0.044

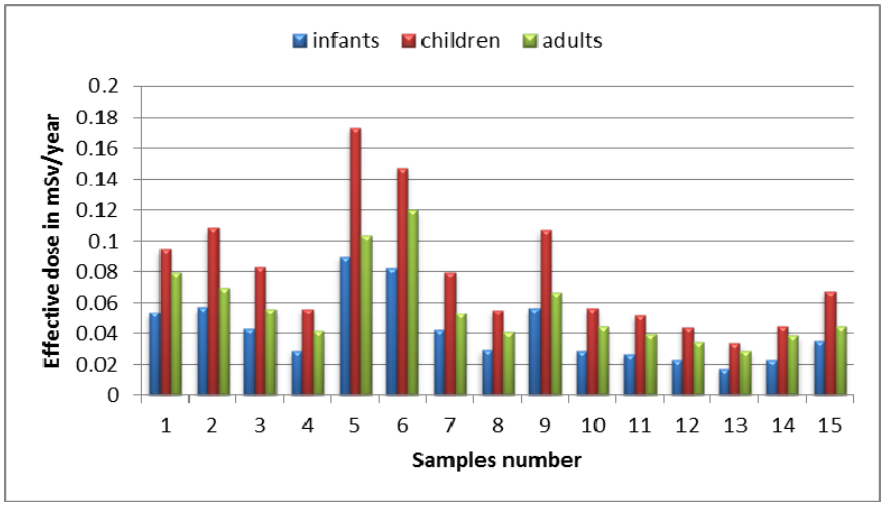

Figure 1: The mean annual effective doses for infants, children and adults in mSv year^{-1} due to the total ingestions.

Comparison of results with similar in other countries

The values of ^{226}Ra, ^{232}Th and ^{40} K concentrations from the present work are compared with those from other countries and they listed in table 3. ^{226}Ra values from the present work are higher than that reported by (17-18) in Egypt and Sudan respectively. It has values lower than

that reported by (10, 19-22) in Yemen, Brazil, China, Sweden and Finland respectively. The activity concentrations of ^{232}Th is lower than that reported by (10) and higher than the concentrations reported from other countries. The values of ^{40}K concentrations presented in this work seem to be much higher than that reported from other countries.

Table3: The activity concentration of ^{226}Ra, ^{232}Th and ^{40}K in BqL^{-1} of the investigated samples in comparison with other countries.

Country	^{226}Ra	Activity concentration in BqL^{-1} ^{232}Th	^{40}K	Reference
Egypt	Mean 0.20	Mean 0.13	Mean 5.29	Present work
Yemen	2.01-6.55	1.07-2.93		(10)
Egypt(Qena)	Mean 0.08	Mean 0.04		(17)
Sudan	0.007-0.014	0.001-0.039		(18)
Brazil	0.01-3.79			(19)
China	Max 0.93			(20)
Sweden	0.016-4.9			(21)
Finland	0.01-49			(22)

CONCLUSIONS

The natural radioactivity levels of ^{226}Ra, ^{232}Th and ^{40}K have been measured in water samples from Assiut, Egypt using gamma ray spectroscopy. The activity profiles of the radionuclides have clearly showed low activity concentrations across the study area. The total effective doses due to all radionuclides are 0.04, 0.07 and 0.06 for infants, children and adults respectively, which are %15, %35 and %60 of the values of 0.26, 0.2 and 0.1 mSv for the recommended reference level of committed effective dose from 1 year's consumption of drinking water for infants, children and adults, respectively. From this one can recommended that, the investigated water are acceptable for life-long human consumption.

REFERENCE

(1) WHO, World Health Organization, Guidelines for Drinking Water Quality, Vol. 3 Chapter 9 Draft, Geneva, Switzerland. (2003).

(2) Iyengar, M.A.R. (1990).The Natural Distribution of Radium. The Environmental Behavior of Radium,Technical Reports Series No. 310, IAEA, 1, 9-128.

(3) Marovic, G., Sencar. J., Franic. Z., Lokobaner. N. (1996).Radium-226 in Thermal and mineral Springs of Croatia and Associated Health Risk. J. Environ. Radio., 33, 309-317.

(4) Sidhu. K.S., and Breithart. M.S. (1998).Naturally Occurring Radium-226and Radium-228 in Water Supplies of Michigan. Bull. Environ. Contam. Toxicol., 61, 722-729.

(5) Wrenn. M.E ., Durbin. P.W., Howard. B., Lipsztein. J., Rundo. J., Still. E.T., Willis. D.I. (1985).Metabolism of Ingested U and Ra. Health Phys., 48, 601-633.

(6) Sheppard. M.I. (1980). The environmental behaviour of radium.AECL-6796". Atomic Energy of Canada, Ltd.
(7) Cox. P.A. (1991).The Elements: Their Origin, Abundance and Distribution. Oxford University Press, Oxford.
(8) Adams. J.A.S., Gasparini. P. (1970). Gamma Ray Spectrometry of Rocks. Elsevier,Amsterdam.
(9) Navratil. J.D., Greenwell. R.D., Macasek. F. (1997). Radioactive waste management and environment restoration, Proc. Int. Conf. Singapore; Oct. 12–16, 1997.
(10) Abd El-Mageed. A.I., El-Kamel. A., Abbady. A., Harb.S., Saleh. I.I. (2011). Natural radioactivity of ground and hot spring water in some areas in Yemen. Desalination , In Press, Corrected Proof, Available online 30 November 2011.
(11) EPA, Final draft for the drinking water criteria document on radium, US Environmental Protection Agency, Washington, Dc, 1999 Tr-1241-85.
(12) Meltem. D., Gursel. K.(2010). Natural radioactivity in various surface waters in Adana. Turkey, Desalination 261,126–130
(13) ICRP, 72, Age-dependent doses to members of the public from intake of radionuclides: Part 5, Compilation of Ingestion and Inhalation Dose Coefficients, Annals of the ICRP, 26 (1), ICRP Publication 72, Pergamon Press, Oxford, (1996).
(14) IAEA, International basic safty standards for protection against ionizing radiation and for the safety of radiation sources. Safety series 15, Vienna, (1996).
(15) WHO (World Health Organization). Guidelines for drinking water quality: radiological aspects, /http://www.who.int/water_sanitation_health/dwq/gdwq3/en/S. (2004).
(16) UNSCEAR. Report to General Assembly. Annex B: Exposure from Natural Radiation Sources. and, Report to General Assembly. With Scientific Annexes. Sources and Effects of Ionizing Radiation. United Nations Sales Publications No. E.00.IX.3 Volume I: Sources and No. E.00.IX.4 (Volume II: Effects). United Nations, New York, 1220 Pp. (2000).
(17) Ahmed, N.K. (2004). Natural radioactivity of ground and drinking water in some areas of upper Egypt, Turk. J. Eng. Environ. Sci. 28: 345–354.
(18) Alfatih, A.A., Isam, S., Ibrahim, A., Saif El Din, Siddeeg, M.B., Eltayeb Hatem, Idriss Hajo, Hmza Walid, Yousif, E.H. (2006). Investigation of natural radioactivity levels in water around Kadugli, Sudan, Appl. Radiat. Isot. 66:1650–1653.
(19) Godoy, J.M., Godoy, M.L.(2006). Natural radioactivity in Brazilian groundwater, J. Environ. Radioact. 85:71–83.
(20) Zhuo, W., Lida, T., Yang, X.(2001) Occurrence of $_{222}$Rn, ^{226}Ra, ^{228}Ra and U in groundwater in Fujian Province, China, J. Environ. Radioact. 53:111–120.
(21) Isam Saleh, M.M., Pettersson, H.B.L., Lund, E.(2002). Uranium and thorium series radionuclides in drinking water from drilled bedrock wells: correlation to geology and bedrock radioactivity and dose estimation, Radiat. Prot. Dosim. 102 (3): 249–285.
(22) Salonen,L.(1994). ^{238}U series radionuclides as a source of increased radioactivity in groundwater originating from finish bedrock. 71–84, in: J. Soukko (Ed.), Future Groundwater Resources at Risk, IAHS Publication No. 222. IAHS Press, Oxfordshire

Radioactivity And Dose Assessment Of Rock And Soil Samples From Homa Mountain, Homa Bay County, Kenya

D. Otwoma[1,2,*], J. P. Patel[2] , S. Bartilol[3] and A.O.Mustapha[4]
[1] *Ministry of Energy, P. 0. Box 30582, Nairobi, Kenya*
[2] *Department of Physics, University of Nairobi, P. O. Box 30187, Nairobi, Kenya*
[3] *Institute of Nuclear Science, University of Nairobi, Nairobi, Kenya*
[4] *Department of Physics, Federal University of Agriculture, Abeokuta, Nigeria*
[*] Corresponding author: otwoma@uonbi.ac.ke *and* otwooma@gmail.com

ABSTRACT

The in situ measured average outdoor absorbed dose rate in air was found to vary from 108.4 to 1596.4 nGy h^{-1} at Homa Mountain area in southwestern Kenya. Rock and soil samples collected gave average values of the radioactivity concentrations of ^{40}K, ^{226}Ra and ^{232}Th of 915.6, 195.3 and 409.5 Bq kg^{-1}, respectively. The range of the annual effective dose for a person living in Homa Mountain area calculated varied from 28.6 to 1681.2, with a mean of 470.4 µSv. These results imply Homa Mountain have elevated levels of natural radioactivity thus the region is a high background radiation area.

INTRODUCTION

External irradiation from radionuclides naturally present in the environment is an important component of the exposure of human populations. Inescapable feature of life on earth include radiation exposure due to terrestrial from natural occurring radioactive material (NORM), cosmic and internal sources. The main sources of NORM are ^{40}K, ^{238}U (^{226}Ra) and ^{232}Th and are present in various degrees in all media in the environment, including the human body itself. In terms of NORM, the igneous rocks of granitic, carbonatite and alkaline composition are enriched in K, Th and U, compared to rocks of basaltic[1,2,3,4]. These exposures originate primarily from gamma radiation arising from decay of these radionuclides at locations outside the human body. Since these radioisotopes are not uniformly distributed in nature, knowledge of their dispersal in rocks and soils plays an important role in radiation protection and measurement. Owing to the health risks associated with the exposure to indoor radiation, many governmental and international bodies such as the International Commission on Radiological Protection (ICRP)[5] have adopted measures at minimizing such exposures.

In Kenya, Mustapha[2], Hashim[6] and Achola[7] determined the radionuclide content of NORM in building materials and radiation dose rates.

The aim of this study is to determine the activity levels of radionuclides in rock and soil around Homa Mountain area in southwestern Kenya. The annual effective dose equivalent (AEDE) from terrestrial radiation were calculated and compared to those measured in situ. The results obtained are compared with national and world average. Local authorities can use the results of this study to limit the use of building materials that can cause a significant increase in radiation exposure due to higher level external gamma exposure. This is the first study to assess the level of the background radiation in Homa Mountain area.

SURVEY AREA AND SAMPLING

Homa Mountain is a large carbonatite complex that forms a broad peninsula on the eastern shores of Lake Victoria. It is bound by latitude 0^0 30' N and 0^0 20' N and longitude 33^0 26' E and 34^0 34' E. The complex is defined as a series of cone sheets of carbonatites and breccias intrusions in the oldest rock in the Nyanzian series composed of shattered Nyanzian and ijolites as described by Le Bas[8] and Mulaha[9]. Increased human habitation is encroaching on the carbonatite hills surrounding Homa Mountain and satellite hills.

Field measurements and sample collection

Radioactivity measurements were carried out in the field using Radiagem hand held survey meters that could be coupled with NaI (Tl). The study area, shown in green in Figure 1, was traversed on foot, and ambient dose equivalent rates in air were measured 1 meter (gonad height) from the ground at suitable sites including around dwellings, farmlands, water sources and yet to be settled areas currently used for growing crops, grazing cattle or recreation. The coordinates of the readings were determined by global positioning system. At chosen sites soil was scooped while rock pieces were chipped from outcrops and transferred to the laboratory. A total of 44 samples were taken.

MATERIALS AND METHODS

Calibration of the Radiagem was done by comparing its readings to similar equipment exposed to known X-ray and ^{137}Cs gamma sources. Gamma spectroscopy was used to determine the activities of ^{40}K, ^{226}Ra and ^{232}Th with a p-type intrinsic hyper pure germanium (HpGe) coaxial detector mounted vertically and coupled to a 3 kV digital high voltage source. The HpGe detector was calibrated for energy and relative efficiency using calibration sources containing ^{133}Ba, ^{22}Na, ^{137}Cs, ^{54}Mn and ^{60}Co. A performance test using IAEA[10] standard reference material Soil-375, RGU, RGTh and RGK was used for checking the efficiency of the calibration of the system as done by Mustapha[2], Achola[7] and Hisham[6].

Sample Preparation and Analysis

In the laboratory, these samples were dried in air and then pulverized, homogenized and sieved through 100 μm mesh. 200 g samples were carefully weighed and packed in standard plastic containers which were properly tightened and hermetically sealed with aluminum foil to prevent escape of gaseous ^{220}Rn and ^{222}Rn and stored for 30 days to allow secular equilibrium between thorium and radium and their decay products.

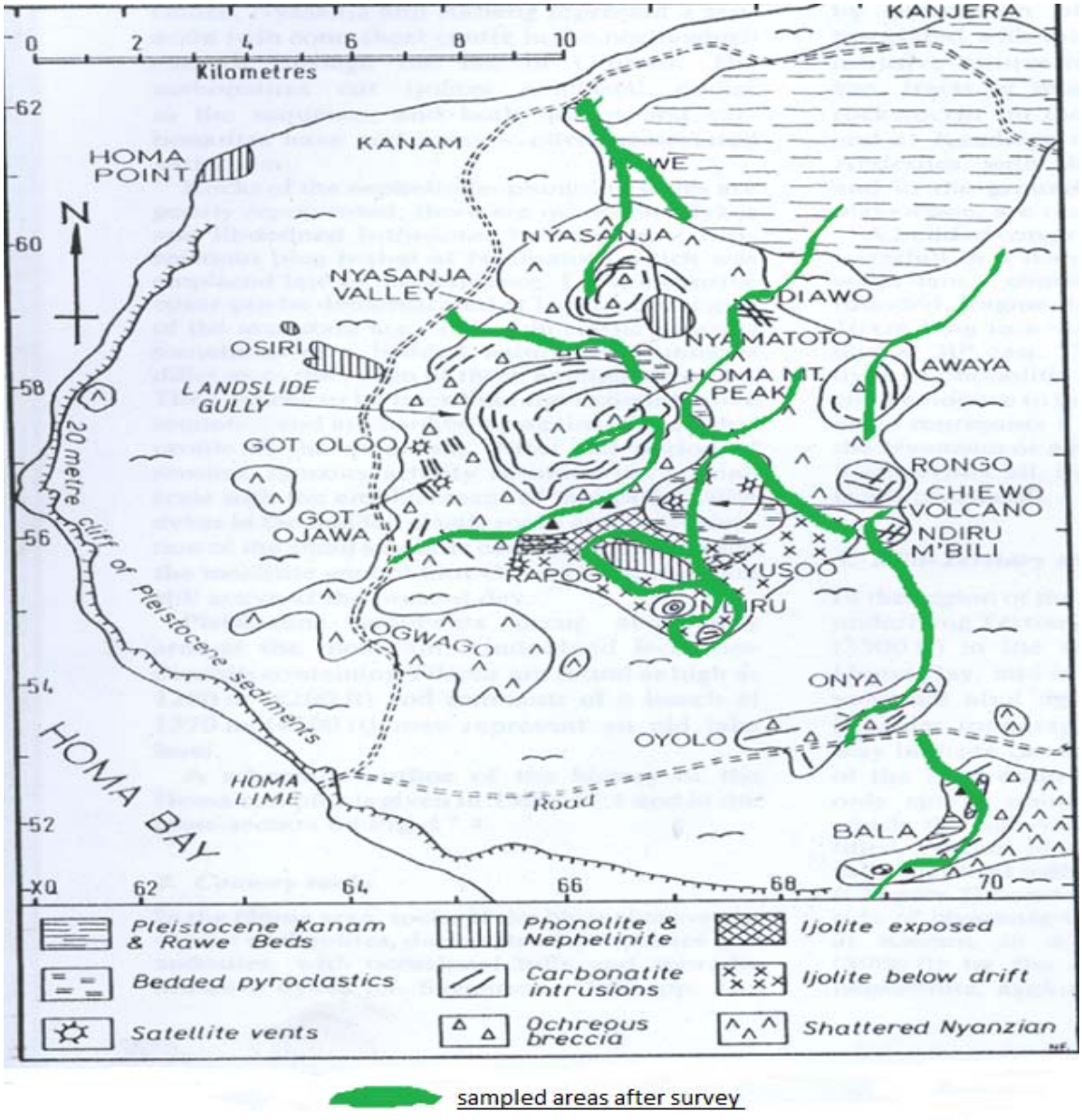

Figure 4. Sketch map of Homa Mountain area east of Homa Bay with green showing sampled areas after survey meter measurements

Radiometric and indicative Dose Analysis

The activity concentrations of ^{226}Ra and ^{232}Th were calculated assuming a secular equilibrium with their decay products. The gamma transition energies of 351.9 keV of ^{214}Pb and 609.2 keV of ^{214}Bi were used to determine the concentrations of the ^{238}U (^{226}Ra) series. The gamma transition energies of 238.6 keV of ^{212}Pb, 583.1 keV of ^{208}Tl and 911 keV of ^{228}Ac were used to determine the concentrations of the ^{232}Th series. The activity concentration of ^{40}K was determined from the peak areas of 1460 keV.

The contribution of natural radioisotopes to absorbed dose rate in air (ADRA) depends on the concentrations of the radioisotopes in the rock and soil. The contribution of terrestrial

gamma radiation to absorbed dose rate in air at 1 m above the ground (ADRA) can be calculated using the following formula[1, 3, 4, 11] .

$$\mathbf{ADRA = 0.043C_K + 0.427C_{Ra} + 0.666C_{Th}} \quad \mathbf{(1)}$$

where C_K, C_{Ra} and C_{Th} are the activity concentrations of ^{40}K, ^{226}Ra and ^{232}Th, respectively, in the rock and soil samples in units of Bq kg^{-1}. The world average annual effective dose equivalent (AEDE) from outdoor terrestrial gamma radiation for Homa Mountain region was calculated as recommended by UNSCEAR[1, 4]:

$$\mathbf{AEDE = ADRA \times DCF \times OF \times T} \quad \mathbf{(2)}$$

Where DCF is dose conversion factor (0.7 Sv Gy^{-1}), OF is outdoor occupancy factor (0.2) and T is the time factor (8766 h) taking leap year into account.

RESULTS AND DISCUSSIONS

Air Absorbed Dose Rate in Air Results from Survey in Situ Measurements

Table 1 shows the important descriptive from 210 points in and around Homa Mountain area where the Radiagem was used. This dose rates were measured directly at the sites and the survey meter gave values in n/μSv h^{-1}. The mean ADRA was 493.3 nSv h^{-1} is higher than the estimate of average global terrestrial radiation which ranges 24 to 160 nGy h^{-1}[1]. The maximum level of 1596.4 nSv h^{-1} translates to an annual dose of 14 mSv for a resident living there and possibly 70 mSv in 5 years.

Table 1. Descriptive of the Data of Absorbed Dose Rates using hand held survey meters.

Dose Rate Descriptive	**Statistic**
Mean	493.3
> 160 nGy h^{-1} (112 nSv h^{-1})	90.5%
24 to 160 nGy h^{-1} (16.8-112 nSv h^{-1})	9.5%
Median	418.7
Variance	85063.2
Standard Deviation	250.3
Minimum	108.4
Maximum	1596.4
Range	1488.0
Kurtosis	2.14

Activity Concentration, Absorbed Dose Rate And Annual Effective Dose Equivalent

The average activity concentrations in the 44 rock and soil samples from locations in and around Homa Mountain and the corresponding ADRA and AEDE are summarized in Table 2.

Table 2. Average radioactivity concentrations of ^{40}K, ^{226}Ra and ^{232}Th rock and soil samples and absorbed dose from gamma radiation

Region	^{40}K Bq kg^{-1} (mg/kg)	^{226}Ra Bq kg^{-1}	^{232}Th Bq kg^{-1}	ADRA nGy h^{-1}	AEDE µSv y^{-1}
Bala					
24b	496.0±4	80.8±5.3	439.6±1	241.57	296.5
25	2064.5±2	454.4±2	444.3±2	578.70	710.2
26b	63.9±27.1	124.3±5	ND	60.01	73.6
27	454.8±7	44.0±15.0	695.5±1	501.54	615.5
28b	872.2±3	27.5±10.6	67.4±4.1	94.13	115.5
29b	867.9±3	40.0±9.9	74.8±4.6	104.21	127.9
30b	2260.5±3	351.8±3	232.8±4	402.46	493.9
Ndiru	**Chiewo**	**Rongo**	**Awaya**	**Complex area**	
5b	1139.5±3	97.8±5.3	318.9±1	303.14	372.0
15b	514.7±4	52.4±8.2	231.0±2	198.35	243.4
16b	1279.5±2	ND	178.2±4	180.31	221.3
31	1596.4±2	85.1±11.8	140.5±3	198.55	243.7
2b	267.2±7	41.7±10.2	65.3±5.5	72.78	89.3
1b	1411.9±2	37.7±11.1	309.9±1	283.20	347.5
3b	1231.2±4	111.4±8	242.1±3	261.74	321.2
4b	197.0±11	ND	17.1±8.7	23.31	28.6
8b	1092.3±3	49.1±9.9	156.0±3	171.83	210.9
9b	216.4±13	1567.5±0	1005.4±0	1348.22	1654.6
10b	323.2±6	49.3±6.8	45.5±6.9	65.25	80.1
11b	1468.5±3	ND	111.6±4	137.47	168.7
13b	661.6±4	47.5±10.2	568.8±1	427.55	524.7
14b	279.6±9	83.5±7.8	524.9±1	397.26	487.5
22b	1253.6±2	ND	994.8±0	724.04	888.6
23b	1818.1±3	50.6±13	212.9±2	348.60	427.8
12	1405.2±3	113.2±6	421.1±1	389.21	477.6
Rawe					
6b	2672.9±2	166.3±5	564.5±2	561.9	689.6
7b	1674.2±2	95.5±6.4	456.0±1	416.46	511.1
17	186.8±11	54.3±11.2	675.1±1	480.83	590.1
18	260.1±9	44.5±13.8	476.3±2	347.4	426.3
19b	161.8±15	220.2±4	559.6±1	473.67	581.3
20b	1392.7±2	623.0±1	271.7±2	506.85	622.0
21	573.3±6	487. 9±1	564.4±1	608.87	747.2

Homa	**Mountain**				
32b	108.3±20	174.7±6	75.1±7.8	129.27	158.6
33b	138.0±18	376.9±1	54.0±7.4	202.83	248.9
34	183.5±12	421.3±5	582.4±1	283.20	347.5
35	1174.9±3	24.4±16.6	203.1±2	196.20	240.8
36	1341.2±2	124.8±4	538.8±1	469.80	576.6
38	3017.8±1	312.1±2	189.0±3	388.90	477.3
39	ND	1398.8±1	1160.1±1	1369.91	1681.2
40	333.5±6	36.8±17.2	74.0±3.3	79.33	97.3
41	920.8±3	38.3±16.0	1153.8±1	824.37	1011.7
42	670.4±4	ND	1447.0±1	992.52	1218.1
43	559.3±6	76.4±11.9	648.1±1	488.3	599.3
44	300.0±12	84.8±9.4	507.7±2	387.23	475.2
45	1382.9±2	ND	117.7±2	145.24	178.2
sum				16625.15	20403.0
mean	915.6±3	195.3±8	409.5±4	383.33	470.4
Max	3017.8±1	1567.5±0	1447.0±1	1369.91	1681.2
Min	63.9±27.1	27.5±10.6	17.1±8.7	23.32	28.6
St Dev	733.1	322.6	342.6	302.06	370.7

ND = non detectable

The cumulative mean activity concentration for the 44 Homa Mountain samples of ^{40}K, ^{226}Ra and ^{232}Th (915.6, 195.3 and 409.5 Bq kg^{-1}, respectively) are higher than the world average (400, 35 and 30 Bq kg^{-1}, respectively[(1)]). The standard deviations depict the spatial variation of the activity concentrations of the natural radionuclides in each rock and soil type. This ranged from non detectable (ND) to highest levels of 3017.8 ± 1.5, 1567.5 ± 0.4 and 1447.0 ± 0.8 Bq kg^{-1}, respectively. Uncertainties of ^{40}K, ^{232}Th and ^{226}Ra (^{238}U) activity concentrations range from 0.05 % to 31.01%.

About 80% of the rock and soil collected at Homa Mountain show ^{226}Ra (^{238}U) activity concentration that is higher than the world average value of 35 Bq kg^{-1} [(1)], and the average ^{226}Ra activity concentration value of 195.3 Bq kg^{-1} is more than 5.58 times the world average value. In 95% of the samples, the ^{232}Th activity concentrations exceed the world average value of 30 Bq kg^{-1}, and the mean ^{232}Th activity concentration value of 409.5 Bq kg^{-1} obtained in this work is 13.65 times higher than the world average value. The mean activity concentrations of ^{40}K of 915.6 Bq kg^{-1} is more than 2 times the world average value of 400 Bq kg^{-1} reported by UNSCEAR[(1)]. The highest ^{238}U (^{226}Ra) activity concentration of 1567.5 ± 0.4 Bq kg^{-1} (44 times the world average) was found from the top of Got Chiewo. The highest ^{232}Th activity concentration of 1447 ± 0.8 and highest ^{40}K activity concentration 3017.8 ± 1.5 came from carbonatite rock samples taken on top of Homa Mountain. It is about 48 times the world average for ^{232}Th and 7.5 times the world average for ^{40}K.

The average AEDE from the calculated outdoor terrestrial gamma radiation at 1 m above the ground in Homa Mountain was found to vary from 0.029 to 1.68 with the mean value of 0.47 mSv y^{-1} and a standard deviation of 0.37 mSv y^{-1}. Only one sample had a value less than

70 μSv y^{-1} which is the world average[1] out of the 44 samples showing that Homa Mountain area qualifies to be a High Background Radiation Area (HBRA). 43 samples are by a factor of 6.71, above the world average value of 0.07 mSv y^{-1}. It compares to those reported by Mustapha[3] from natural stone ranging from 0.155 to 1.559 with an average of 0.509 mSv y^{-1}.

Correlation Between In Situ And Laboratory Followed By Calculation Measurements

Calculations using equation 2 after inserting HpGe measured concentration values, yielded the mean ADRA of 383.36 nGy h^{-1} a value 6 times higher than average global terrestrial radiation. The maximum level of 1.37 μSv h^{-1} which translates to 12 mSv y^{-1} for a resident living there is way beyond the dose limit of 1 mSv y^{-1} for the general public and compares with the 20 mSv y^{-1} for radiation workers[4, 5,12].

A good correlation between the ambient dose equivalent measured with the survey meter and those estimated from the radioactivity concentrations of ^{40}K, ^{226}Ra and ^{232}Th in rock/soil samples was observed. It was noted that the estimated values, are however, lower than the measured. UNSCEAR[1] explains that data from different parts of the world showed that absorbed dose rates in air inferred from concentrations of radionuclides in soil can differ from those obtained through direct measurements by up to 50%. Several factors do influence the direct measurements of absorbed dose rates[1], the most relevant to the present study are presence of radon and its gamma emitting decay products in the atmosphere and the ground roughness. Radon and its decay products which emit gamma are dispersed in the atmosphere and will contribute to direct dose measurements, whereas the dose conversion factors used to convert the radioactivity concentrations of radionuclides to dose do not take into consideration the radon presence in air. Also the terrain around and on Homa Mountain comprises of hills, sloppy valleys, plateaus, escarpments, troughs etc., which make the ground surface quite rough rather than flat. On the average the survey meter sees more source volume than the flat interface models assumed in the dose conversation factors derivation. These factors could have contributed to making the results from direct measurements in the present study higher than those calculated. Nevertheless, both sets of results indicate the study area is a HBRA.

Comparisons with Recent Results on Natural Gamma Radioactivity

Numerous studies such as those undertaken by Nyamai[13], Mulaha[7], Patel[14], Mustapha[15], Oladele[17], Shanthi[18, 19] and Otansev[20] have shown the presence of radioactive minerals such as zircon, allanite, apatite and monazite in the rocks together with high potassium fledspar correlate well with the high activity measured comparable to the values in Homa Mountain area. A comparison of the mean activity concentration values obtained in this study with values from other regions of the world is presented in Table 3.

Table 3. Comparison of Mean Activity Concentration values (Bq kg^{-1}) of Rock and Soil Samples from different Countries

Sample ID	^{40}K	^{226}Ra	^{232}Th	Reference
Mean for 44 samples from Homa Mt area	915.6	195.3	409.5	This Study
Kenya (national average)	255.7	28.7	73.3	Mustapha[2]
Kenya (Carbonatites)	185.6	179.0	950.2	Mustapha[15]
Southwestern Region(Nigeria)	286.5	54.5	91.1	Oladele [17]
Turkey, Kestanbol	1,207.0	115.0	192.0	Otansev[20]
Turkey, Rize	105-1235	11-188	10-105	Merdanoglu[21]
HBRA, India	1585	44	215	Shanthi[18]
Kenyakumari, India	940	20	114	Shanthi[19]
Yemen (granite and gneiss)	1,742.8 and 2,341	53.6 and 22	27 and 121	AbdEl-Mageed[22]
Spain (national average)	650.0 (48 – 1570)	46.0 (13 – 165)	49.0 (7 – 204)	Baeza[23]
Punjab Province (Pakistan)	615.0	35.0	41.0	Tahir[24]
Bangalore (India)	635.1	26.2	53.1	Prasad[25]
Bangladesh	833	42	81	Chowdhury[26]
Saudi Arabia	1099	76.4	81	Alharbi[3]
World's average	400	35	30	UNSCEAR[1]

Some are the national averages while others are of specific geological rock base or an area of interest. Table 3 shows that the mean activity concentration values obtained in this study are higher than those obtained in all the countries considered, while they are lower than those obtained in India, Yemen, Saudi Arabia and Turkey for ^{40}K only. Homa Mountain area thus qualifies to join the ranks of high background radiation areas in the world. Compared with the worldwide average concentration in soils and rocks, the present study results are higher for most of the analyzed samples indicating a possible accumulation of ^{238}U (^{226}Ra), ^{232}Th and ^{40}K in Homa Mountain region, which may be due to geochemical processes.

CONCLUSION

Background radiation investigations, a major issue of environmental monitoring studies, have been done all over the world in order to determine the radioactivity in rock and soil samples. This study determined that the average activity concentrations of Homa Mountain area samples were much higher than worldwide averages. It was observed that the common geological characteristics of the areas with the high background radiations were the carbonatites of the Homa Mountain.

.

REFERENCES

(1) UNSCEAR (2000) United Nations Scientific Committee on the Effects of Atomic Radiation, Exposures from natural radiation sources, United Nations, New York.
(2) Mustapha, A.O., Patel, J.P. and Rathore, I.V.S., (1999) Assessment of human exposure to natural sources of radiation in Kenya, Radiat. Prot. Dosim, **82**, 285-292, Oxford University Press
(3) Alharbi W. R., J. H. AlZahrani and Adel G. E. Abbady (2011) Assessment of Radiation Hazard Indices from Granite Rocks of the Southeastern Arabian Shield, Kingdom of Saudi Arabia. Australian Journal of Basic and Applied Sciences, 5(6): 672-682
(4) UNSCEAR, (1988) United Nations Scientific Committee on Effects of Atomic Radiation, Sources, Effects and Risks of Ionizing Radiation, Report to the General Assembly, United Nations, New York
(5) ICRP (1984) *Principles for Limiting Exposure of the Public to Natural Sources of Radiation*. International Commission on Radiological Protection Publication 39, Annals of the ICRP **14**(1)
(6) Hashim N. O., I. V. S. Rathore, A. M. Kinyua and A. O. Mustapha (2004) Natural and artificial radioactivity levels in sediments along the Kenyan coast. Radiation Physics and Chemistry (71) pp 805 – 806
(7) Achola S. O., J. P. Patel, A. O. Mustapha and H. K. Angeyo (2012) Natural Radioactivity in the High Background Radiation Area of Lambwe East, Southwestern Kenya, Radiation Protection Dosimetry, pp 1-6, Oxford University Press
(8) Le Bas, Michael John (1977) Carbonatite – Nephelinite Volcanism. An African Case History, John Wiley & Sons Ltd, United Kingdom
(9) Mulaha Timothy O. (1989) The Ndiru Hill Carbonatite, South Nyanza District, Western Kenya. MSc thesis in Geology and Mineralogy, Department of Geology, University of Helsinki, Unpublished
(10) International Atomic Energy Agency (1987) Preparation and Certification of IAEA Gamma Spectrometry Reference Materials. IAEA/RL/148, IAEA, Vienna
(11) Kapdan E., A. Varinlioglu and G. Karahan (2012) Outdoor Radioactivity and Health Risks in Balikesir Northwestern Turkey, Radiation Protection Dosimetry, Vol. 148, No. 3, pp 301-309
(12) Kenya Government (1982) The Radiation Protection Act Cap 243 Laws of Kenya. Government Printers. Nairobi
(13) Nyamai Christopher M. (1989) The Mineralogy of Uncompahgrites and Turjaites from South Rangwa Complex, Western Kenya. MSc in Geology and Mineralogy, Department of Geology, University of Helsinki, Unpublished
(14) Patel, J.P. (1991) Environmental radiation survey of the area of high natural radioactivity of Mrima hill of Kenya, Discovery and Innovation, Vol. 3, No. 3, P 31-36
(15) Mustapha, A. O (1999) Assessment of Human Exposures to Natural Sources of Radiation in Kenya, PhD thesis, University of Nairobi, Unpublished
(16) Jibiri N. N., S. K. Alausa and I. P. Farai (2009) Assessment of external and internal doses due to farming in high background radiation area in old tin mining localities in Jos-plateau, Nigeria, Radioprotection Vol 44 139-151

(17) Oladele Samuel Ajayi (2009) Measurement of activity concentration of ^{40}K, ^{226}Ra and ^{232}Th for assessment of radiation hazards from soils of the southwestern region of Nigeria, Radiat Environ Biophys **(48)** 323-332

(18) Shanthi G., C. G. Maniyan, A. G. Raj and T. K. Thampi (2009) Radioactivity in Food Crops from High Background Radiation Area in South West India, Curr. Sci. 97(p), 1331 – 1335

(19) Shanthi G., J. Thampi, T. Kumaran, G. A. G. Raj and C.G. Maniyan (2010) Measurement of Activity Concentration of Natural Radionuclides for the Assessment of Radiological Indices. Radiation Protection Dosimetry Vol. 141 No. 1 90 - 96

(20) Otansev P., G. Karaha, E. Kan, I Barut and H. Taskin (2012) Assessment of Natural Radioactivity Concentration and Gamma Dose Rate Levels in Koyseri, Turkey. Radiation Protection Dosimetry Vol. 148 No. 2 227 – 236

(21) Merdanoglu, B and Altinsoy, N. (2006) Radioactivity concentrations and dose assessment for soil samples from Kestanbol, granite area. Radiation Protection Dosietry. 121 399-405

(22) Abd El-Mageed A.I., A.H. El-Kamel, A. Abbady, S. Harb, A. M. M. Youssef and I. I. Saleh (2010) Assessment of Natural and Anthropogenic Radioactivity levels in rocks and soils in the environs of Juban town in Yemen, Tenth Radiation Physics & Protection Conference, 27-30 November 2010, Nasr City, Egypt

(23) Baeza, A., del Rio, M., Mir, C., Paniagua, J.M.(1992) Natural Radioactivity in Soils of the Province of Caceres, Spain, Radiation Protection Dosimetry **(45)** 261-263

(24) Tahir, S. N. A., Jamil, K., Zaidi, J. H., Arif, M., Ahmed, N. and Ahmad S. A. (2005) Measurement of activity concentration of naturally occurring radionuclides in soil samples from Punjab Province of Pakistan and Assessment of Radiological hazards, Radiation Protection Dosimetry 113(4), 421 -427

(25) Prasad Shiva N. G., N. Nagaiah and N. Karunakara (2008) Concentrations of 226Ra, 232Th and 40K in the Soils of Bangalore Region, India. Health Physics (**94**) pp 264 – 271

(26) Chowdhury M. I., M. Kamal, M. N. Alam, Saleha Yeasmin and M. N. Mostafa (2005) Distribution of Naturally Occurring Radionuclides in Soils of the Southern Districts of Bangladesh. Radiation Protection Dosimetry, pp 1-5

Design and Implementation of Head and Neck Perspex Phantom for Intensity Modulated Radiation Therapy

*** K.M. Radaideh[a], L.M. Matalqah[b,c] , A.A. Tajuddin[d]**

*[a)] School of Physics, Universiti Sains Malaysia, 11800 Minden, Penang, Malaysia, *khaldoonmah1@yahoo.com*
[b)] School of Pharmaceutical Sciences, Universiti Sains Malaysia, 11800 Minden, Penang, Malaysia,
[c)] School of Pharmacy, Allianze University College of Medical Sciences (AUCMS, 13200, Kepala Batas, Penang, Malaysia
[d)] Campus Director, Engineering Campus, Universiti Sains Malaysia (USM), 14300 Nibong Tebal, Penang, Malaysia, draat@usm.my

ABSTRACT

The aims of this study are to design, construct and evaluate the applicability of a head and neck Perspex phantom for dosimetric verification of intensity modulated radiation therapy (IMRT). Thermoluminescent dosimeters (TLDs) was used in this study. Consistency of the fabricated phantom readings was checked by multiple IMRT irradiations. The inter-fraction standard deviation among all TLDs' measurement was 3.7%, and the averages of all repetitive measurements at OAR and PTV were comparable with TPS with a percentage variation of 4.8% (SD 8.1) and P value > 0.05 (95% CI). These findings suggest the consistency and the reproducibility of the phantom and its applicability for IMRT treatment verification.

Keywords: *IMRT / verification / head and neck / phantom*

INTRODUCTION

Head and neck region is a challenging site for treatment with intensity modulated radiotherapy (IMRT).[1] Due to the complexity of this technique and high dose gradient region, significant inconsistencies between doses calculated by IMRT treatment planning systems (TPS) and those measured through *in vivo* dosimetry especially in the vicinity of critical structures have been reported.[2] Hence, this technique demands a high level of dosimetric accuracy, the verification of these dose distributions is a prerequisite for a safe and efficient application. Other approaches have been used to verify patient IMRT treatment fields prior to delivery.[3]

Many dosimeters have been used for *in vivo* dosimetry, include semiconductor diodes and thermoluminescent dosimetry.[4] Thermoluminescent dosimeters (TLD) are often more suited to point dose measurements in high gradient region due to their relative small size compared to ion chambers. TLDs also allow measurement of multiple points simultaneously. However, the accuracy of the measurement depends heavily on the quality control of the TLD's reading and calibration procedures and their use requires careful and time-consuming handling and annealing procedures.[5] With careful handling and attention to standardized annealing and readout protocols, TLD dosimetry have been shown to achieve an accuracy of 2%.[6]

The purposes of this study were to design and construct a head and neck phantom and to test its applicability for dosimetric verification of IMRT plans.

MATERIALS AND METHODS

A. Phantom methodology

The anatomically realistic phantom of head, neck and shoulder regions was designed from Perspex materials (Figure 1). The CT images of a standard size patient's head and neck region obtained through SIEMENS CT Scanner (SOMATOM Sensation Open, Germany) were used for construction of the Perspex slices. Eight organs at risks (OAR) were selected, these included right and left eyes, optic chiasm, right and left optic nerves, brainstem, left parotid gland, and larynx, in addition to the both sides of planning target volumes (PTV) included the borderline. On each slice, holes of 1.5x8 mm^2 size were drilled into points of interest within OARs and PTV. These holes were at least 1cm apart for placement of TLDs. Total of 110 TLDs were used in this study (Figure 2). A CT scan was then performed for the fabricated phantom for contouring the OAR and PTV regions and to check the position of TLDs.

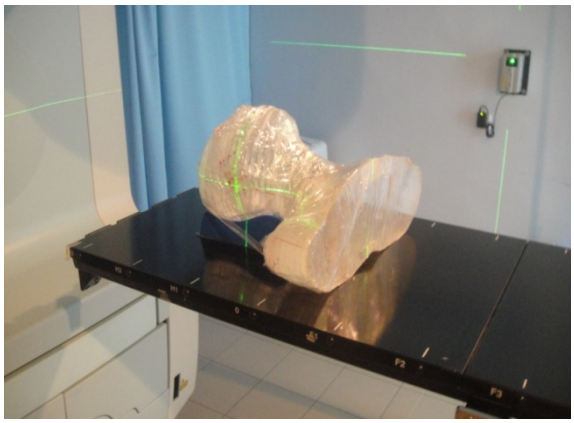

Figure 1: Designed head and neck phantom from Perspex material for IMRT dose verification

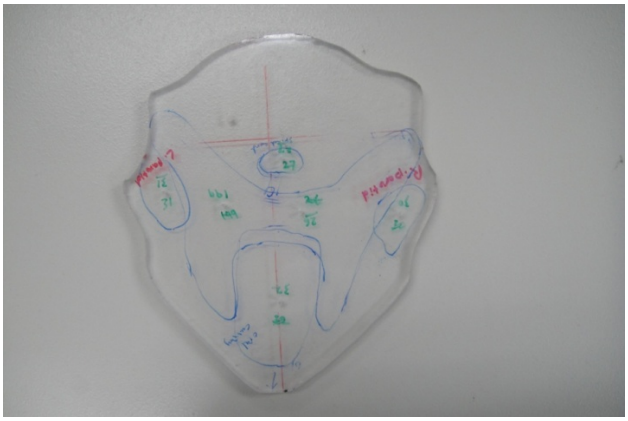

Figure 2: A slide of phantom shows delineated OAR and PTV with drilled holes in varies point of interest.

B. TLDs calibration

The TLDs used in this study were selected from a batch of Rod-shaped LiF;Mg:Ti (TLDs) with dimensions of 1.0 x 1.0 x 6.0 mm^3 as obtained from the manufacturers (Bicron NE, USA). Siemens Mevatron MD2 LINAC (Siemens Inc, USA) was the radiation source in this study.

TLD-100 were annealed using a thermal cycle: 1 h at 400 °C , cooling for 2h, 24 h at 80 °C to associate the dipoles into trimmers, thus removing low temperature TL peaks and reducing fading when integrating intensity measurements.[7,8] A Nabertherm oven (Nabertherm, Germany) was used for annealing procedure and a Harshaw model 3500 (Harshaw, USA) was used as TLD reader. The TLDs were selected after a careful

initialization procedure.[9] The reading profile was as follows: Preheat temperature of 50 ºC for 0 sec, acquire temperature rate 12 ºC/sec, acquire maximum temperature of 300 ºC for 33 ⅓ sec , and annealing temperature of 300 ºC for 0 sec. The TLDs were selected with sensitivity within 3%.

For TLDs calibration, Solid Water Phantom and a FC65-G (Wellhofer, Germany) ionization chamber were used and Percentage Depth Dose (PDD) curve and a correction factor were obtained.[10] The slabs were inserted in between the Solid Water Phantom (Nuclear Associates, Chicago, IL) at d_{max} for calibration. The 6MV photon beams from a Siemens Mevatron MX2 linear accelerator (Siemens Inc, USA) was used to irradiate TLDs at a nominal SSD of 100 cm with a (10 x 10 cm²) field size. The accuracy of TLD measurements depends on the reproducibility of the results [8,9,11] as measured by the standard deviation of each individual calibration factor. Five subsequent calibration cycles were carried out to establish individual calibration factors at d_{max}.[12]

C. Percentage Depth Dose Curve

PDD curve study was performed by exposing the TLDs and Ion Chamber at different depths (ranged from 0 to 20 cm) and 10 cm thickness as full backscatter in the Solid Water Phantom at reference settings. The PDD curves using TLDs in Perspex phantom and ion chamber in water phantom are presented in Figure 3. The $K_{correction}$ value found was 1.05 ± 0.0003 to 6MV LINAC This correction replace all corrections for sensitivity, phantom material, field size, and fading.

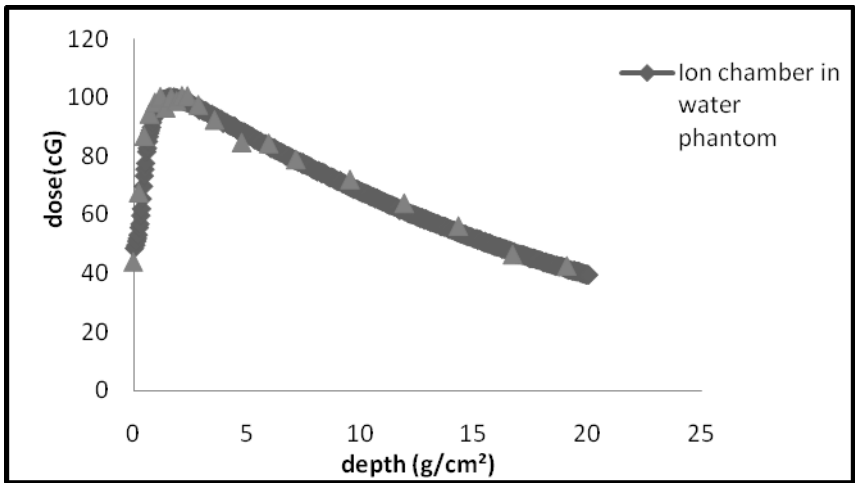

Figure 3: PDD curve using Ion Chamber in Water Phantom and TLDs in Perspex Phantom

D. Phantom verification

According to the reproducibility of calibration's results, out of 240 TLDs only 110 were chosen for our study distributed into OAR and PTV regions. A thermoplastic mask with three fixation points, used during the patient's treatment, was used during phantom irradiation. Three fractions of an IMRT treatment were applied to the fabricated phantom. The TLDs were placed into various locations of interest and then were read out after each treatment. The

measured doses at OAR and PTV regions for the three fractions were then compared to the point dose recorded at similar locations from the TPS using the live dose evaluation function.

E. Phantom application in IMRT verification using patients' plans

Two head and neck patients' treatment plans were chosen and performed on the designed phantom. The treatment plans were transferred to the phantom by matching the isocenter points of phantom after installing TLDs at points of interest.

RESULTS AND DISCUSSION

The reproducibility of the TLDs was checked and an excellent consistency was obtained for repetitive measurements (Figure 4). The inter-fraction standard deviation among TLDs' measurement was 3.7%, and the averages of the three repetitive measurements of TLDs at OAR and PTV also were comparable with TPS, with percentage variation of 4.8% (SD 8.1). Analysis using the ANOVA test showed no significant statistical differences between measured and calculated doses with P value > 0.05 (95% CI). These findings suggest the consistency and the reproducibility of our phantom as measured by TLDs using IMRT treatment.

Agreement between the TLDs doses of patients' plans transferred to phantom and TPS doses was found at OAR points with percentage variation of 7.2% (SD 4.5) and 12.3% (SD 10.1) and 1.3% (SD 0.6) and 5.5% (SD 1.9) at PTV points, for both patients and p value > 0.05 (Figure 5). However, it was observed that TPS overestimated the doses value with 3% at PTV and 8% at OAR for the first patient, 5.8% at PTV and 19% at OAR for the second patient. The dosimetric accuracy of IMRT treatment-planning systems has been studied. One of the studies [13] that attempted to address the accuracy of calculated dose for the total plan transferred to a phantom compared with measurements for a series of patients, accepted discrepancies within 5% as the criterion for treatment verification approval in the QA of IMRT. In agreement with another study [14] where ion chamber measurements are usually within 4% of the calculations at high dose region (PTV) and more than 10% (OAR) deviations in low-dose regions was registered in some hybrid phantom plans, we found that the average percentage variation was 9.8% at OAR and 3.4% at PTV. Previous study has also proposed a confidence level of 3% in high-dose, low-gradient areas, and 10% in high-dose and high-gradient areas of IMRT dose distribution as an acceptance criterion.[15]

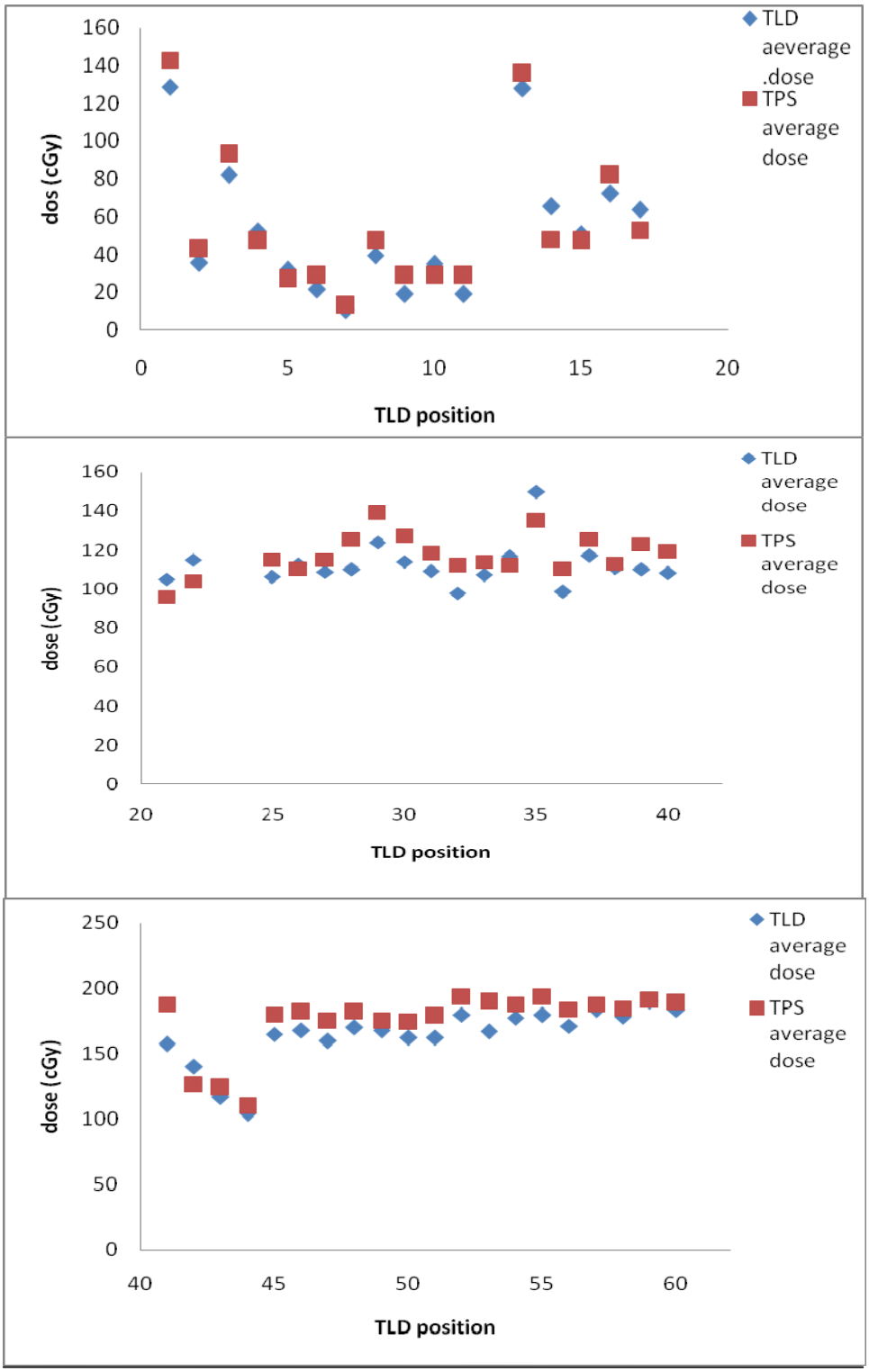
dos (cGy)
TLD position
TLD aeverage .dose
TPS average dose
dose (cGy)
TLD position
TLD average dose
TPS average dose
dose (cGy)
TLD position
TLD average dose
TPS average dose

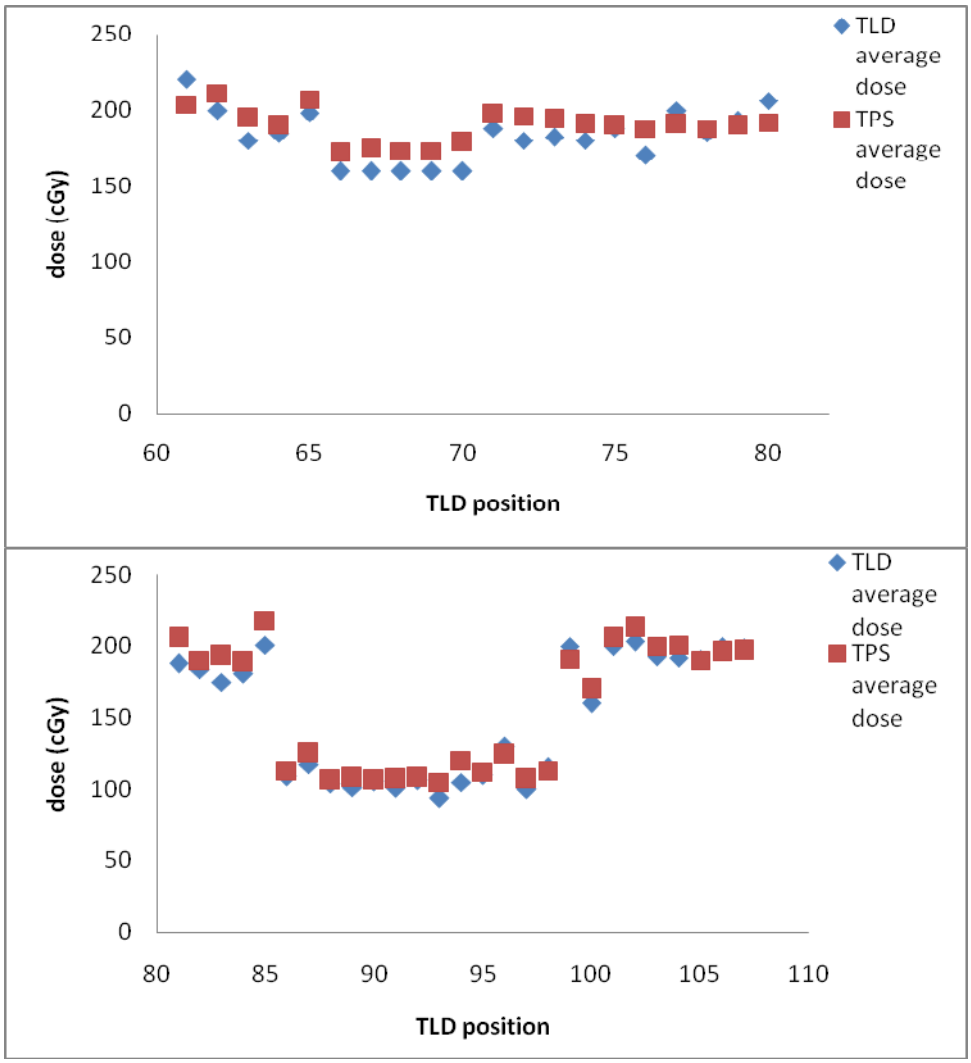

Figure 4: Phantom verification TLDs' readings (cG) for the three irradiation fractions compared to

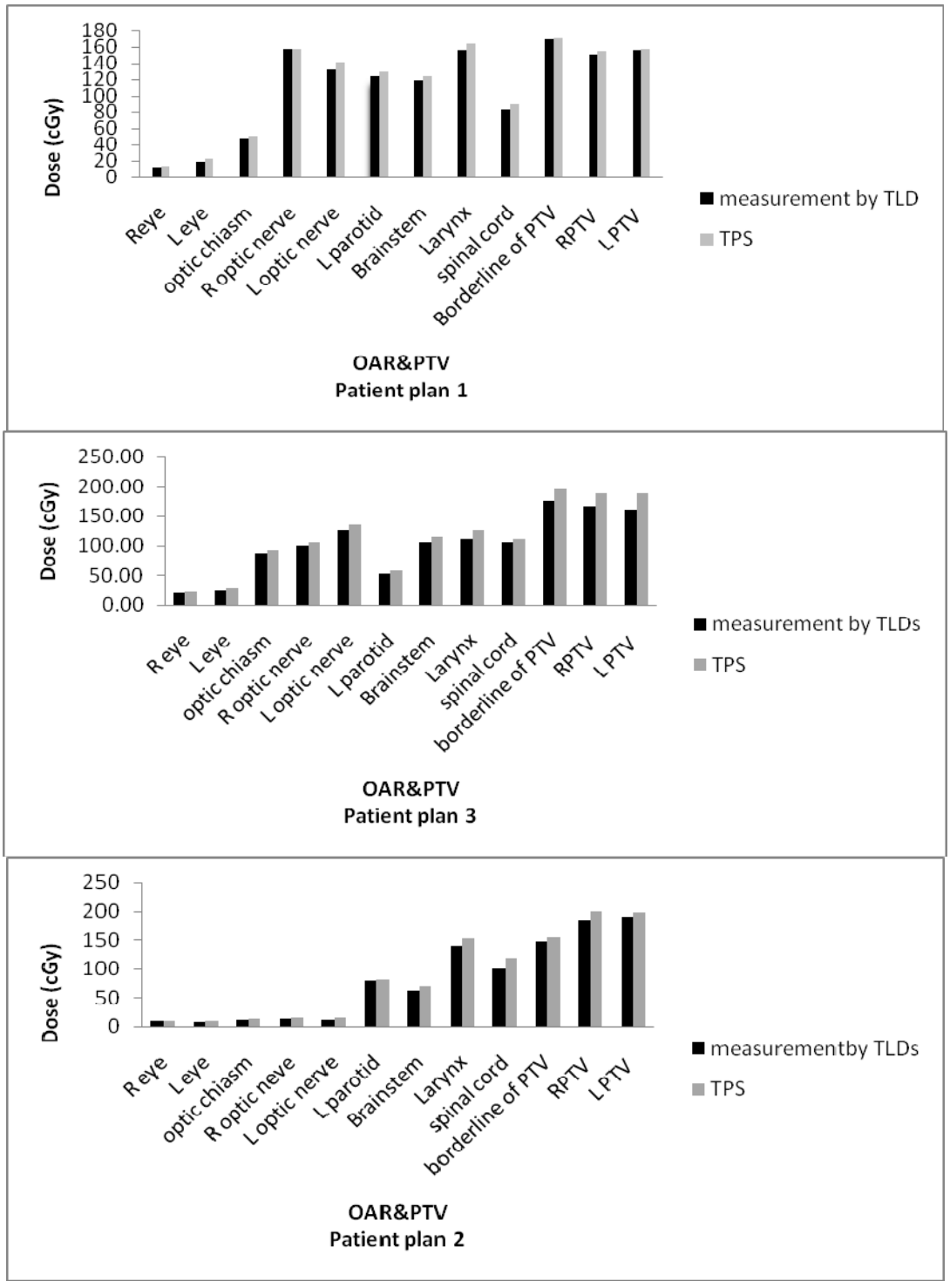

Figure 5: Measured doses at organs at risk (OAR) and Planning Target Volume (PTV) for the three patients repectively, treated by IMRT compared to doses calculated by Treatment Planning system (TPS)

CONCLUSION

The results suggested that our phantom is applicable for IMRT treatment dose verification. Furthermore, TLDs can be used as accurate and reproducible detectors for IMRT to measure the doses at any point of interest. In addition, our result highlighted the fact that TPS may not give accurate dose values at PTV with an overestimated of an average of 4.4 % at PTV and 13.5% at OAR. This ratio should be considered in clinical practice as it may cause sub-therapeutic dose at PTVs.

REFERENCES

(1) M.K.M. Kam, R. Chau, J. Suen, P.H.K. Choi, and P.M.L. Teo, "Intensity-modulated radiotherapy in nasopharyngeal carcinoma: dosimetric advantage over conventional plans and feasibility of dose escalation* 1," Int J Radiat Oncol* Biol* Phys **56** (1), 145-157 (2003).

(2) H. Chung, H. Jin, J.F. Dempsey, C. Liu, J. Palta, T.S. Suh, and S. Kim, "Evaluation of surface and build-up region dose for intensity-modulated radiation therapy in head and neck cancer," Med Phys **32**, 2682 (2005).

(3) S. Gillis, C. De Wagter, J. Bohsung, B. Perrin, P. Williams, and B.J. Mijnheer, "An inter-centre quality assurance network for IMRT verification: results of the ESTRO QUASIMODO project," Radiother Oncol **76** (3), 340-353 (2005)

(4) RA Kinhikar, R. Upreti, S. Sharma, CM Tambe, and DD Deshpande, "Intensity modulated radiotherapy dosimetry with ion chambers, TLD, MOSFET and EDR2 film," Australas.Phys. Eng.Sci.Med **30** (1), 25-32 (2007)

(5) A. Van Esch, J. Bohsung, P. Sorvari, M. Tenhunen, M. Paiusco, M. Iori, P. Engström, H. Nyström, and D.P. Huyskens, "Acceptance tests and quality control (QC) procedures for the clinical implementation of intensity modulated radiotherapy (IMRT) using inverse planning and the sliding window technique: experience from five radiotherapy departments," Radiother Oncol **65** (1), 53-70 (2002)

(6) G.A. Ezzell, J.M. Galvin, D. Low, J.R. Palta, I. Rosen, M.B. Sharpe, P. Xia, Y. Xiao, L. Xing, and C.X. Yu, "Guidance document on delivery, treatment planning, and clinical implementation of IMRT: Report of the IMRT subcommittee of the AAPM radiation therapy committee," Med phys **30**, 2089 (2003)

(7) J.M. Galvin, G. Ezzell, A. Eisbrauch, C. Yu, B. Butler, Y. Xiao, I. Rosen, J. Rosenman, M. Sharpe, and L. Xing, "Implementing IMRT in clinical practice: a joint document of the American Society for Therapeutic Radiology and Oncology and the American Association of Physicists in Medicine," Int J Radiat Oncol* Biol* Phys **58** (5), 1616 (2004)

(8) T. Kron, "Applications of thermoluminescence dosimetry in medicine," Radiation protection dosimetry **85** (1-4), 333 (1999); WPM Mayles, S. Heisig, and HMO Mayles, "Treatment verification and in vivo dosimetry," Radiother Phys, 227-251 (2000)

(9) D. Huyskens, R. Bogaerts, J. Verstraete, M. Lööf, H. Nyström, C. Fiorino, S. Broggi, N. Jornet, M. Ribas, and DI Twaithes, "Practical guidelines for the

implementation of in vivo dosimetry with diodes in external radiotherapy with photon beams (entrance dose)," ESTRO Physics Booklets (2001)

(10) J. VanDam and G. Marinello, Methods for in vivo dosimetry in external radiotherapy. (Garant Publ., 2006).

(11) JJ Wood and WPM Mayles, "Factors affecting the precision of TLD dose measurements using an automatic TLD reader," Phys Med Biol **40**, 309 (1995)

(12) T. Kron, M. Butson, F. Hunt, and J. Denham, "TLD extrapolation for skin dose determination in vivo," Radiother Oncol **41** (2), 119-123 (1996)

(13) T. Kron, M. Butson, T. Wong, and P. Metcalfe, "Readout of thermoluminescence dosimetry chips using a contact planchet heater," Australas.Phys. Eng.Sci.Med **16** (3), 137 (1993).

(14) P. McGhee, S. Humphreys, and P. Dunscombe, "An efficient approach to routine TL dosimetry," Med Dosi: **18** (4), 187 (1993)

(15) EJ Fairbanks and LA DeWerd, "Thermoluminescent characteristics of LiF: Mg, Ti from three manufacturers," Med Phys **20**, 729 (1993).

(16) Y.S. Horowitz, "Thermoluminescence and Thermoluminescent Dosimetry, v. 1," (1984).

(17) S.W.S. McKeever, M. Moscovitch, and P.D. Townsend, Thermoluminescence dosimetry materials: properties and uses. (Nuclear Technology Publishing, 1995).

(18) C. Furetta and P.S. Weng, Operational thermoluminescence dosimetry. (World Scientific Pub Co Inc, 1998).

(19) F.H. Attix, "Introduction to radiological physics and radiation dosimetry," (1986).

(20) N. Yazici, "The influence of heating rate on the TL response of the main glow peaks 5 and 4+ 5 of sensitized TLD-100 treated by two different annealing protocols," Nuclear Instruments and Methods in Physics Research Section B: Beam Interactions with Materials and Atoms **215** (1-2), 174-180 (2004).

(21) K.M. Radaideh and A.S. Alzoubi, "Factors impacting the dose at maximum depth dose (d_{max}) for 6 MV high-energy photon beams using different dosimetric detectors," Bioheal Sci Bullet **2**(2),38-42 (2010).

(22) D. Tsai Ph, "Dosimetric verification of the dynamic intensity-modulated radiation therapy of 92 patients," Int J Radiat Oncol* Biol* Phys **40** (5), 1213-1230 (1998).

(23) P. Xia and C. Chuang, "Patient-specific quality assurance in IMRT," Intensity-Modulated Radiation Therapy, AAPM, Med Phys Monog **29**, 495-514 (2003).

(24) A. Kapulsky, E. Mullokandov, and G. Gejerman, "An automated phantom-film QA procedure for intensity-modulated radiation therapy," Med Dosi **27** (3), 201-207 (2002).

Evaluation of Patient Radiation Dose during Orthopedic Surgery

H. Osman[1], A. Sulieman[3], A. Elzaki[1,4], A. K. Sam[2]
1Taif University college of applied medical science
2Sudan University of science and technology
3Sudan Atomic Energy Commission
Corresponding author: Hamid Osman Hamid Email: hamidsssan@yahoo.com

ABSTRACT

The number of orthopedic procedures requiring the use of the fluoroscopic guidance has increased over the recent years. Consequently the patient exposed to un avoidable radiation doses. The aim of the current study was to evaluate patient radiation dose during these procedures.37 patients under went dynamic hip screw (DHS) and dynamic cannulated screw (DCS) were evaluated using calibrated Thermolumincent Dosimeters (TLDs), under c-arm fluoroscopic machines ,in three centers in Khartoum-Sudan. The mean Entrance Skin Dose (ESD) was 7.9 mGy per procedure. The bone marrow and gonad organ exposed to significant doses. No correlation was found between ESD and Body Mass Index (BMI), or patient weight. Well correlation was found between kilovoltage applied and ESD. Orthopedic surgeries delivered lower radiation dose to patients than cardiac catheterization or hysterosalpingraphy (HSG) procedures. More study should be implemented to follow radiation dose before surgery and after surgery

Key words :*Radiation dose, patient ,TLDs, orthopedic surgery*

1-INTRODUCTION

The number of orthopedic procedures requiring the use of the fluoroscopic guidance has increased over the recent years (1). It is now accepted that closed operative procedures are the treatment of choice in many types of complex fractures because of their lower infection, smaller incision wounds and relatively low morbidity at implant removal (2), so fluoroscopic guided procedure in orthopedic surgeries now is common and favorite practice. However, patients exposed to un avoidable radiation exposure during these procedures, consequently radiation dose to radiosensitive organ just like bone marrow or gonads organs, which addressed as an important issue that must be taken into consideration. Moreover, most of those patients are subjected to additional exposure before surgery for diagnosis and after surgery for follow up. However, if the practice is justified and the protection optimised, the dose to the patient will be as low as reasonably achievable (ALARA) and compatible with the medical purpose(3).

The radiation beam in interventional fluoroscopy procedures is typically directed at a relatively small patch of skin for a substantial length of time. This area of skin receives the highest radiation dose of any portion of the patient's body. The dose to this skin area may be high enough to cause a sunburn-like injury, hair loss, or in rare cases, skin necrosis (5). Therefore, there is an imperative need to optimise the radiation dose and to assess the

radiation risk per procedure, since tissue reactions (stochastic effects) are involved, in order to encourage the staff for further optimisation of patient doses. Optimisation of patient dose could be achieved by selection of modern equipment, adoption of good radiographic technique, well-trained personnel and well-defined Diagnostic Reference Level (DRL) in order to avoid unnecessary exposure to the patient(3,4).Patient entrance skin dose (ESD) is significant parameter which has been used to report patient doses, and this has been studied in many parts of the world (5,6,7,8,18). In Sudan, as far as authors know, no study has been published in open literature regarding patient radiation doses during orthopedic procedures. This might be attributed to the lack of adequate monitoring facilities, lower infrastructure in health care and the generally low level of interest among orthopedic surgeons as users of ionizing radiation. Therefore this will seek to provide first-hand data on patients ESD , and hence extrapolated effective dose *E* from the ESD value.
The current study intends to; (I) evaluate radiation dose to patients in three different orthopedic centers and (II) estimate patient organs doses .

2-MATERIALS and Methods

2-1 Patients dose measurements

A total of 37 patients were examined, and evaluated in this study. Patients were divided into two groups according to type of orthopedic procedure (18 underwent Dynamic hip screw , fixation of the proximal end of the femur [DHS] and 19 dynamic cannulated screw, fixation of the distal end of the femur [DCS].
The indications for the investigations included the trauma fracture and pathologic fractures, which had been well diagnosed in the emergency department and out clinics. Ethics and research committee at each targeted orthopedic center approved the study and informed consent was obtained from all patients prior to the procedure. TLDs were packed on a thin envelope made of transparent plastic foil to protect the TLDs from any contamination, and at the same time not to appear in the final image or produce any image artifact . Each envelope contained three TLDs. The envelope kept in place at beam entry site with adhesive tape during the procedure.

For each patient, the following parameters were recorded i.e. fluoroscopic data: tube voltage, tube current and total screening time and patient data: name, age, weight, height, clinical indication and surgeon name, start and end time of the procedure.

2-2 X-Ray machines

Three different x-ray machines were used throughout this study, All machines were not equipped with Kerma air product (KAP), but have ability to be operated in continuous beam and pulse fluoroscopy modes (0.2 sec/ pulse) during different procedures.

Table 1: The technical specifications of the C-arm machines used in this study

Machine	Origin country	Model	Max kVp	Generator type	Beam Filtration AL(mm)	Installation date	Last image hold
Siemens	Germany	Siremobil 2000	120	HF	2.5	2009	Yes
Siemens	Germany	Siremobil 4K	120	HF	2.7	2004	Yes
Wolverson	Italy	TCA3M9/6	140	HF	2.5	1999	Yes

HF=High Frequency

2-3 Dosimeters

Thermo luminescence dosimeters (TLD-GR200A) of lithium fluoride (LiF:Mg,Cu,P).TLD calibrated under reproducible reference condition using C arm machine Siemens siremobil mentioned in table one at72Kv , one mA and three pulses of pulsed fluoroscopy. against ionization chamber PTW.CONNY II connected to radiation monitor controller at standard distance of focal spot and image intensifier of the C-arm (this approach the average energy used during most orthopedic procedures encountered in the study) .

2-5 Estimation of organ dose and effective dose

ESD was used to assess the equivalent organ dose for selected organs during orthopedic procedures. Organ dose (mGy) estimation was made using computer software provided by the National Radiological Protection Board (NRPB-SR262)(9). Organs doses from DHS and DC S were obtained from the average value of conversion factors for anteroposterior pelvis view. The organ or tissue-specific weighting factor accounts for the variations in the risk of cancer induction or other adverse effects for the specific organ.

3- RESULTS

Thirty seven patients were included in this study. The main indications for orthopedic surgery was trauma cases (75.7%),pathologic fracture (24.3%).all of the patients have examined with conventional x-ray prior to surgery procedure, and also have imaged after surgery procedure directly. And 57% have done two to three x-ray image as follow up (all pathologic fracture patients) Patients demographic data (height, age , weight, BMI), screening time per procedure and number of fluoroscopic images are presented in Table 2. Table 3 presents the minimum , median, mean third quartile and maximum values of the ESD. Effective Organs radiation dose (mSv) was estimated using computer soft ware provided by the National radiological protection Board (NRPB SR 262) (9), as showed in Table 4.
The mean fluoroscopic factor for both procedure was 74 ±2.07 kV,1.12±0.2mA and 0.62 ±0.16 mins. DHS showed higher exposure factor (mean 74 ±2.2 kV,1.15±0.2mA and 0.64 ±0.18 mins) compared to DCS (72.3 ±1.9 kV,1.09±0.18mA and 0.6 ±0.14 mins). Moreover more fluoroscopic image were obtained during DHS compared to DCS, which will result in more ESD delivered to patient in DHS technique (ESD were 8.2 and 7.9 mGy for DHS and DCS procedure respectively).

Table 2 Patients physical characteristics (height, age, weight and BMI), screening time per exposure and number of fluoroscopic exposure (mean and the range in the parentheses.

Group	N	Height (cm)	Patients age	Weight (Kg)	BMI	Screening time per exposure	No of fluoroscopic images
All	37	163.4 (151-179)	49.5 (29-67)	69.6 (50-89)	25.9 (21.4-30.1)	0.6 (0.2-0.9)	6 (3-7)
DHS	18	166.2 (151-177)	46.7 (29-62)	71.8 (58-89)	25.8 (22.9-27.8)	0.7 (0.4-0.9)	5.8 (4-7)
DCS	19	1160.7 (152-179)	52.2 (35-67)	67.5 (50-80)	26 (21.4-30.1)	0.5 (0.2-0.9)	4.5 (3-6)

Table 3 Minimum, median, mean, ,third quartile and maximum values of ESD (mGy)

Group	No	Minimum	Median	Mean	3rd quartile	Maximum
All	37	5.2	8.1	7.9	9.2	14.2
DHS	18	5.5	7.8	8.2	9.1	14.2
DCS	19	5.2	8.3	7.9	8.8	10.8

Table 4 Estimation of patient organ radiation dose

Tissue or organ	**Wt**	**E(mSv)**
Gonads	0.2	0.158
Bone marrow	0.12	0.0948
Bladder	0.05	0.0395
Breast	0.05	0.0395
Thyroid	0.05	0.0395
Bone surface	0.005	0.0395
Remainder	0.05	0.806
Total	1	**1.217**

4-DISCUSSION

Patient demographic data and exposure factors

The main factors affecting patients dose in fluoroscopic guided orthopedic surgery are: exposure factors, filtration, source to surface distance, collimation, pathology and complication of surgery. There were no significant differences between the two patients groups in terms of height, weight, BMI and fluoroscopic images.

A correlation was not found between ESD and patient weight and BMI (Figure 1 (a) and (b)),this might be attributed to complexity of procedure and number of exposure taken in each procedure. Correlation was found between kv applied and radiation dose (Figure 1 (c)) in which R^2 =0.9.

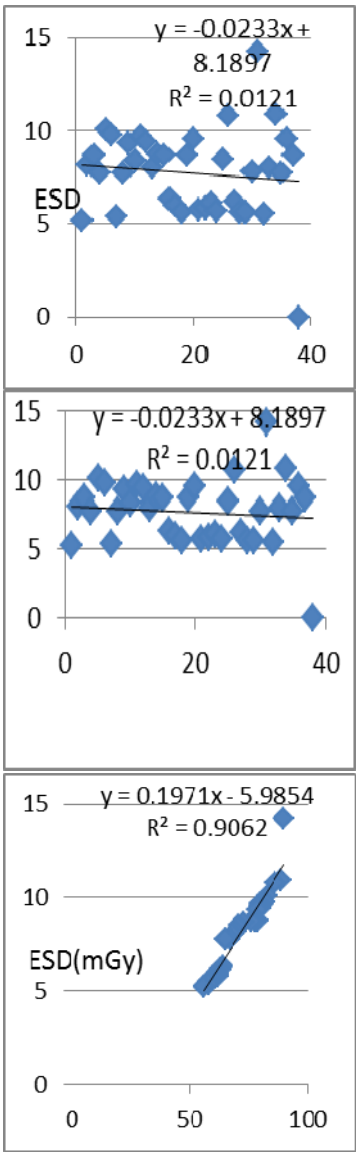

Figure 1 (a), (b) and (c) correlation between BMI , patient weight and Kv applied and ESD mGy.

Bone marrow and Gonad organ showed the higher organ dose compared to other organ and about 2% and 1.2% from ESD for aforementioned organs respectively.

In this study no dose area product DAP were used in all hospitals encountered throughout the study, however all of available literature DAP found to be an important tools in determining the ESD values for patients and hence extrapolated effective dose *E* from the ESD value, also as DAP is easy to assess.(10).

In a study carried by Crawely et al (11) , authors calculated the ESD using the formula

$$\mathbf{ESD = DAP/A_p}$$
$$\mathbf{A_p = A_{ii}(d_p/d_{ii})^2}$$

Where A_p is area irradiated at the patients input surface, A_{ii} is the field area at the intensifier input face, d_p is the distance from the x-ray tube focus to patients and d_{ii} is the distance from x-ray tube focus to the input image intensifier face. They revealed that the first, third quartiles and median of DAP (Gy-cm^2) for the patients in DHS were to be 1.7,3.7,2.6 (Gy-cm^2) respectively. and hence the average ESD for the aforementioned procedure was 4.76 mGy per procedure.

Compared the results of Crawely et al (11) to the current study, the current study showed higher value, and this could be attributed to varied x –ray C-arm machine used in each study and the type of practice used by different orthopedic surgeon. And the latter depend on the experience of the staff.

Table 5 Comparison of the average entrance radiation dose in this study and literature

Authors	No of Pt	Procedure type	Median	3rd quartile DAP or ESD	Mean ESD (mGy)	Effective dose (msV)
Sulieman et al (2007)(12)	37	HSG	3.40	4.94	3.60	0.43
Crawely et al(11)	43	Iorthopedic	2.58 Gy-cm^2	3.74 Gy-cm^2	N A	0.72
Sulieman et al (2011)(13)	57	I ERCP	44.79 mGy	86.10 mGy	75.6	4.16
Kirousis et al (2009)(14)	25	I ortho IMN	2.87Gy-cm^2	4.47 Gy-cm^2	4.1	N.A
Klaus et al (2007)(15)	60	TOCE IC	4.53 Gy-cm^2	12.3 Gy-cm^2	34.2	4.6
Mehdizadeh et al (2007)(16)	18	IC	2.56 mGy	3.24 mGy	2.97	N.A
Current study	37	I ortho	8.1 mGy	9.02 mGy	7.9	1.21

Pt=patients TOCE=Transarterial oily chemoembolization
I ortho= interventional orthopedic IMN=Intramedullary nailing
IC interventional cardiology HSG =Hysterosalipingography
ERCP= Endoscopic retrograde cholangio pancreatography

From the values of the mean entrance skin dose obtained during this study, and compared to values in the study carried by Klaus et al (2oo7) (15) for Transarterial oily chemoembolization in interventional cardiology, this study showed lower value and this might be attributed to different procedure in which during cardiology procedure cardiologist required a considerable number of images taken with increased mA value (Technique Known by photospot imaging(17)), in this technique mA value increased (pulsed fluoroscopy) to provide single spot image with adequate image quality with lower image noise, and this increase patient dose by 0.5 μGy for single shot which could result of patient irradiation

equivalent to two second of screening with typical image intensifier dose rate of 0.25 μGy/sec (17).Also mean ESD in Endoscopic retrograde cholangiography resulted in higher patient radiation dose than orthopedic procedure (> 11%) and this also might be due to different interventional procedures. As general any way most orthopedic procedure irradiate patient with lower radiation than in most cardiology or ERCP procedures.
Compared the results of this study with other studies in orthopedic procedures (11), this study showed higher value and this might be due to the physical of individual procedure, type of machine used and /or experience of surgeon.
In the study performed by Goldstone et al (18) the experiences of the staff play a gold role in the reduction of the radiation dose to both staff themselves and patient.

CONCLUSION

This study evaluated the patients radiation dose in orthopedic surgery under C arm fluoroscopic machines, using TLDs. The mean ESD was 7.9 mGy. And high organ dose was estimated for bone marrow and gonad organ (2% and 1.2% from ESD respectively. No correlation was found between ESD and BMI. Orthopedic procedure radiation dose depend mainly on orthopedist surgeon procedure, and delivered less radiation doses to patients than cardiac or hysterosalpingography procedures. More study should be implemented to follow radiation dose before surgery and after surgery.

REFERENCES

(1) Richards, A. M. and Putney, R. The risk from radiation exposure during operative X-ray screening in hand surgery. J. Hand Surg.19(3), 393–396 (1994).
(2) Bahari, S., Morris, S., Broe, D., Taylor, C., Lenehan, B. and McElwain, J. Radiation exposure of the hands and thyroid gland during percutaneous wiring of wristand hand procedures. Acta Orthop. Belg. 72(2), 194–198 (2006).
(3) International Commission of Radiological Protection. Recommendations of the International Commission of Radiological Protection. ICRP 60 (Oxford: Pergamon Press) (1991).
(4) European Union. Council Directive 97/43 Euratom, on health protection of individuals against the dangers of ionizing radiation in relation to medical exposure. Official Journal of the European Communities No. L 180, 9th July, 22–27 (1997).
(5) Mettler F, Koenig TR, Wagner LK, Kelsey CA. Radiation injuries after fluoroscopic procedures. Seminars Ultrasound, CT, MRI 2002; 23:428-42.
(6) Perisinakis K, Theocharopoulos N, Damilakis J, Katonis P, Papadokostakis G, Hadjipavlou A, Gourtsoyiannis N. Estimation of patient dose and associated radiogenic risks from fluoroscopically guided pedicle screw insertion. Spine. 2004; 29:1555-60
(7) Va˜no E, Gonzalez L, Fernandez JM, Alfonso F, Macaya C. Occupational radiation doses in interventional cardiology: a 15-year follow-up. Br J Radiol. 2006;79:383-8.
(8) Fitousi NT, Efstathopoulos EP, Delis HB, Kottou S, Kelekis AD, Panayiotakis GS. Patient and staff dosimetry in vertebroplasty. Spine. 2006;31:E884-9.

(9) Hart, D., Jones, D. G. and Wall, B. F. Normalised organ doses for medical X ray examinations calculated using Monte Carlo techniques. NRPB 262 (1998).
(10) 10.Mooney.R,Thomas.P.S.Dose reduction in a Paediatric X-Ray department following optimization of radiographic technique.BJR.1998;852-860
(11) Crawley .M.T,Roger .A.T. Dose – Area product measurements in A range of common orthopedic procedures and their possible use in establishing local diagnostic reference levels.BJR . 73 .2000;740-744.
(12) Sulieman .A et al . radiation dose optimisation and risk estimation to patients and staff during hysterosalpingography. Radiat. Prot. Dosim.128.2007;217-226
(13) Sulieman .A et al Reduction of radiation dose to patients and staff during endoscopic retrograde cholangiopancreatography.Saudi journal of Gastroenterology . 17.2011:23-29
(14) Kirousis.G, Delis.H, Megas.P, Lambiris.E, and Panayiotakis.G. Dosimetry during intramedullary nailing of the tibia Patient and occupational exposure . Acta Orthopaedica 80 .2009; 568–572
(15) Klaus .B, Evelien .B, Régine .L. Daniël De, Wolf and Thierens.H patient-specific dose and radiation risk estimation in pediatric cardiac catheterization**.** American Heart Association. Circulation.111.2005;83-89
(16) Mehdizadeh.S, Owrangi.M.A , Derakhshan.Sh. Patient dose measurements in interventional radiology. Asian J. Exp. Sci., 21, 2007;105-108
(17) Penelope Allisy-Robert,Jerry Williams. Farr's physics for medical imaging. 2nd edition.Saunders Elsevier 2008.
(18) Goldstone K E , Wright H , COHEN B. Radiation exposure to the hands of orthopaedic surgeons during procedures under fluoroscopic X-ray control. 1993, *The B J R, 66,* 899-901.

Potentiality of Melatonin as a Radiation Protector against Hemoglobin Damage in the Experimental Animals Due to Gamma Irradiation

Hamed Farag[1], Ramadan Ali Hassan[2], Shimaa Mohamed[3]
[1]*Nuclear Department, Faculty of Engineering, King Abdulaziz University Saudi Arabia*
[2]*Nuclear Medicine Unite, National Cancer Institute, Cairo University, Egypt.*
[3]*Microwave Unite, Physics Department, National Research Center, Egypt.*

ABSTRACT

Ionizing radiation causes serious damage in biological system. Some drugs and antioxidants are used to prevent such damage. In the present study two doses of melatonin (10 mg/kgand30mg/kg) were selected to be used for such purpose. The radioprotective effects of melatonin on hemoglobin of red blood cells from female mice was studied through UV absorption spectrum, ESR spectroscopy, dielectric measurements and relative viscosity .The results of Hemoglobin absorption indicate that a pronounced increase in the average value of peak position and width at half maximum W_{hmax} followed by a decrease in the absorbance of sort band, decrease in absorption ratio A_{578} / A_{540} in addition to disappearance of globin band at 275 nm. The free radicals which are expected to be formed after exposing to γ-irradiation are detected by electron spin resonance spectroscopy (ESR). The results indicate that the intensity of ESR signal for hemoglobin extracted from animals exposed to γ-irradiation is greater as compared with normal hemoglobin. Dielectric measurements indicate that there is an increase in dielectric permittivity (ε'), the dielectric loss (ε'') and the a.c conductivity (σ_{ac}) while some decrease is noticed in the viscosity measurements after exposing to irradiation. The data obtained from the whole studied parameters after treating animals with melatonin become closer to those for unirradiated samples.

Key word: *Melatonin, Radiation Protector, gamma radiation,*

INTRODUCTION

The aim of this study is to examine the potentiality of melatonin as radioprotective agent against oxidative damage induced by γ-irradiation. This study will be achieved by investigating the change in biophysical properties of hemoglobin from female mice through UV absorption spectrum, ESR spectroscopy, dielectric measurements and relative viscosity.

Radiation produces numerous biological perturbations in cells by direct ionization of DNA and other cellular targets such as proteins and lipid and by indirect effect through free radical production. Exposure to ionizing radiation produces oxygen derived free radical (ROS) in the tissue environment. These radicals include hydroxyl radicals (the most damaging radical), superoxide anion and other oxidants such as hydrogen peroxide. The intracellular generation and accumulation of these free radicals causes change in molecular

structure of proteins such as hemoglobin. According to these induced radiation effect, numerous antioxidants could be used for biological and medical safety.

The effect of both gamma rays and alpha particles on human erythrocytes to assess radiation induced membrane damage and hemoglobin oxidation and denaturation was studied [(1)]. The result indicated that alpha particles proved to be less efficient than the gamma rays. The time dependence of hemolysis showed clear differences with the gamma rays the process was faster than alpha particles.

Biological effect of short duration exposure to moderate and intense static magnetic field was studied by measuring absorption spectra of hemoglobin molecule and electric conductivity [(2)]. The result indicated that there is increase in the width at half the maximum of the sort band besides decrease in A_{578} /A_{542} ratio.

The effect of ionizing radiation on some bovine hemoglobin characteristics using electron paramagnetic resonance (EPR) spectroscopy and (IR) spectroscopy was studied[(3)]. It was found that the intensity of (EPR) signal which attributed to free radicals is greater in radiated sample than un-irradiated, this means that ionizing radiation may lead to increase of free radical production and decrease in α helices contents, which reflect the degradation of hemoglobin molecular structure

Protective effect of ascorbic acid on molecular behavior changes of hemoglobin induced by magnetic field was observed, by measuring the relative permittivity, dielectric loss, relaxation time, conductivity, radius and diffusion coefficient of hemoglobin solution [(4)]. The result indicted that exposure to magnetic field resulted in changes in the molecular behavior of Hb molecule while treatment with ascorbic acid afforded comparatively more significant amelioration in these molecular change.

The effect of gamma irradiation on the molecular properties of myogloin was studied[(5)]. The results indicated that irradiation caused initial fragmentation of the protein molecule and disrupted the hem group, result in decrease absorbance at (409 nm).Ascorbic acid protected against the degradation of Protein molecule by scavenging oxygen free radical that are Produced by irradiation

Protective effects of melatonin on the ionizing radiation induce DNA damage in the rat brain was studied [(6)]. The results indicated that significant increase in DNA damage was found in the radiation treated rat brain. Pre-treatment of rats with interaperitoneal dose of 100 mg/kg melatonin provided significant decrease in the DNA strand breakage and lipid peroxidation. Treatment with melatonin can protect brain cells from oxidative damage induced by ionizing radiation.

Protective effect of melatonin on spinal cord damage after gamma irradiation was studied [(7)]. The results indicated that melatonin may be useful in preventing spinal cord damage against radiation toxicity due to its potential of free radical scavenging.

Prophylactic role of melatonin against radiation induced damage in mouse cerebellum with special reference to purkinje cells was studied [8]. The results indicated that the antioxidative properties of melatonin resulting in its prophylactic property against radiation induced biochemical and cellular alternation in the cerebellum. The findings support the idea that melatonin may be used as an anti irradiation drug due to its potent free radical scavenging and antioxidative efficacy.

EXPERIMENTAL WORK

Materials:

Animals:

In this study 60 female mice having weight ranged between 20-25g maintained at animal house laboratory, National Research Center under the normal conditions of water and diet supply. The animals were divided into two main groups each group divided into three subgroups:

1- Control group (A):

A_1: Normal animals.

A_2 and A_3 Animals treated with 10 mg/kg and 30 mg/kg melatonin.

2- Irradiated group (C):

C_1: Animals exposed to γ-irradiation.

C_2 and C_3 Animals treated with 10 mg/kg and 30 mg/kg melatonin one day before exposing to γ –irradiation.

Melatonin treatment:

Melatonin (N-acetyl-5-methoxytryptamine) C_{13} H_{16} N_2 O_2 , MW 232.3and M.P.117.0-120.0 ^{o} C from Mallinckrodt Inc. ,Paris, Kentucky was used. The animals were injected with freshly prepared melatonin dose of 10 mg/kg and 30 mg/kg body weight one day before γ-irradiation. Melatonin was prepared in 0.9 % NaCl/ethanol (vol/vol, 20/1) .about 0.4 mg of melatonin dissolved in 1 ml of 0.9 % NaCl/ethanol. All injections were administrated intraperitoneally in volume of 0.025 ml/g body weight.

Irradiation facilities:

The animals were placed in a carton box W 20 × L 20 cm and depth of 5 cm many small holes were made in the box sides to enable the animals to alive during the experiment of irradiation. The dose delivered to the animals were calculated and adjusted in the middle of the box width (2.5 cm from the surface) in order to be sure that all the animals receive a uniform and homogenous field of irradiation the whole body animals were exposed to 6.0 Gy γ-irradiation emitted from linear accelerator cited in the radiotherapy department of the National Cancer Institute, Cairo University. The machine of irradiation was supplied from

Elekta Company having 6.0 MV photon rays production at different field areas at a 100.0 cm distance perpendicular to skin. Dose rate was about 400.0 cGy per monitor unit.

Experimental techniques:

Hemoglobin extraction:

The heparinized blood was centrifuged at 3500.0 r.p.m. for 10 minutes at 4oC.The packed red blood cells were washed with 5 volumes saline solution at 20.0^{o}C. Recentrifuge to separate the washed red blood cells. Steps 2 and 3were repeated 3 times. The clean red blood cells were lysed with four volumes of deionized water finally; the mixture was centrifuged at 7000.0 r.p.m. for 40.0 minutes at 4.0^{o}C to separate the hemoglobin.

Hemoglobin spectrum:

Hemoglobin spectrum was done through the use of the spectrophotometer (Jasco. UV/visible spectrometer typeV-570 (Germany) in the range from 250.0 nm to 700.0 nm.

***ESR spectroscopy*:**

DMPO (5,5-dimethyle-1-pyrroline N-oxide) from sigma-Aldrich chemie -Jmbh, Steinhein, Germany. Was added to hemoglobin solution .About 1.0 µ l of DMPO to 0.5 ml of hemoglobin solution in a quartz ESR flat cell and placed into the T_m cavity of a Bruker electron paramagnetic resonance E_{500} , Elxsys using super-X-band 9 GHz ESR spectrometer Germany. The sample was scanned starting within 2 min of the addition of (DMPO) using the following instrument parameters : modulation amplitude 4.0 G; modulation frequency 100.0 k Hz ; microwave power 20.0 mW ; gain 60.0; scan time 40.0 sec; time constant 0.02 sec.

Dielectric measurements:

Dielectric measurements were done in the frequency range from 100.0Hz to 1.0 MHz using computerized RLC HIOKI 3531 Z Hitester (E. E. Corporation, Japan)

The sample cell has two squared platinum black electrodes of area (1 x 1) cm^2 each with an interelectrode distance of 1.0 cm.

Measurement of viscosity:

The Measurements were performed at certain concentration (3.4×10^{-5}M) and constant temperature (25°C) with an AVS 350 automatic Ubbelohde-type capillary viscometer from schott-Geraete (Hofheim, Germany) which allows reproduction of the flow times with an accuracy of 0.03s. The instrument was also equipped with a model CT 1450 thermostat bath

ESULTS AND DISCUSSION

Absorption spectra:

Absorption spectra for hemoglobin (Hb) extracted from the animals of different subgroups are illustrated graphically in Figures (1) and (2) The obtained bands which characterize hemoglobin are as follows: 578 nm (hem-hem interaction band), 540.0 nm (Fe-N in porphyrine) nitrogen iron bonds in porphyrine, 414 nm (sort band), 340.0 nm (globin- hem interaction band) and 275.0 nm (protein band).These wave lengths are comparable with those found in literature[2,9 ,10].

The average values of peak height, peak position and the width at half maximum (W_{hmax}) of sort band and the absorption ratios of A_{578} / A_{540} in the absorption spectra for hemoglobin extracted from the animals of the two groups A and C are calculated and given in the following table .

Group	Peak hieght	Peak position	W_{hmax}	A_{578}/A_{540}
Group A				
A_1	3.30	414	40	1.007
A_2	3.33	414	40	1.010
A_3	3.36	414	40	1.020
Group C				
C_1	2.85	413	52	0.840
C_2	3.20	414	41	1.000
C_3	3.35	414	40	0.990

No detectable change is observed in absorption spectra for hemoglobin extracted from the animals of control group A either before or after treating with melatonin. Two doses of melatonin were selected (10.0 and 30.0 mg/kg) which are considered to be in the non-toxic rang[11].

Great differences are detected in heme parts at visible wave length for hemoglobin extracted from the animals exposed to γ-irradiation for the subgroups C_1, such as relatively disappearance of globin band at 280 nm. Moreover, there is an increase in the width at half maximum of the sort band beside decrease of the absorbance at sort band, decrease in heme–heme interaction band and decrease in A_{578}/ A_{540}.These results indicate a partial loss of molecule stability [10]. Irradiation disrupted the heme groups, resulting in decrease of the absorbance at sort band. It causes a slight breakdown of the polypeptide chain break covalent bonds and disrupts the ordered structure of proteins [5,12] as a result of the increase in the free radical production [3,8,14]. These free radicals contribute to hemoglobin denaturation and precipitation, leading to anemia [10, 13]. Also these free radicals (reactive oxygen species) induce deteriorating effect on antioxidant defensive system, decreases antioxidant capacity of the organism and depletes levels of know antioxidant [14]. This promoted oxy hemoglobin to met hemoglobin [2, 12]. In the presence of melatonin protective effect against γ-irradiation damage is observed. This finding is achieved by the studied parameters given in the table for the investigated animals treated with both doses of melatonin 10 mg/kg and 30 mg/kg before exposing to γ-irradiation (C_2, C_3). These parameters are found to become closer to those given of the control group A. Melatonin acts as direct free radical scavenger and detoxifies the highly cytotoxic $OH^{\bullet}$ and other radicals produced by ionizing radiation [8,14,15].Because of its rather small size and high lipophilicty, melatonin crosses biological membranes easily , thus reaching all compartments in the cell [16].

ESR spectra of DMPO spin adducts:

The free radicals which are expected to be formed by exposing the body to γ-irradiation is studied through the electron spin resonance ESR spectroscopy. It can detect spin adducts of

spin-trapping agent 5,5-dimethyl 1-pyrroline n-oxide (DMPO) with reactive oxygen radicals which are expected to be generated in hemoglobin extracted from the animals of two groups A and C. As shown graphically in Figures (3) to (5).

As shown in Figure (3), no signal is detected for hemoglobin of control group except after the addition of DMPO to hemoglobin as shown in Figure (3(c)) in comparable with Figures (3- (a)) and (3- (b)).

When the spin-trapping agent (DMPO) is added to hemoglobin in the presence of hydrogen peroxide radical (H_2O_2), DMPO radical adduct has been detected which is assigned to peroxyl radical at tyrosin-103. This provides an evidence for unpaired electron density [17].

As shown in Figure ESR spectra consist of the three sharp, differentially broadened lines, which is characteristic of nitro oxide spin labels [18,20].

DMPO spin adducts signal intensity of oxygen radical in hemoglobin extracted from animals of control subgroups (A_1, A_2 and A_3) are not changed by treating with melatonin doses 10 mg/kg and 30 mg/kg as shown in Figure (4).

Figure (5) illustrates that the DMPO spin adducts signal intensity of oxygen radicals in hemoglobin extracted from animals of irradiated subgroups (C_1) is much greater than the control subgroup (A_1) and those for the subgroups (C_2andC_3) which are treated with melatonin doses before exposing to γ-irradiation due to the increase in the free radical which are expected to be formed as a result of irradiation.

From Figure (5) it is also seen that treatment with melatonin decreases the signal intensity. So it could be conclude that melatonin is a power full scavenger for O_2 and H_2O_2 [8, 14, 15].

Finally, ESR is considered to be a sensitive tool to support the other investigated tools to detect the free radicals.

Dielectric measurements:

The dielectric permittivity ε' ,the dielectric loss ε'' as well as the electrical conductivity σ_{ac} for hemoglobin extracted from the animals of control group (A) and γ- irradiated group were measured in the frequency range $10^2 - 10^6$ Hz and illustrated graphically in Figures (6) and (7). No detectable change is noticed when the animals from the control group (A) are treated with both doses of melatonin. On the other hand it is noticed that there is some increase in ε', ε'' and σ_{ac} of sub group C_1 as compared with those of control sub group A_1. This could be a good evidence for the increase of free radicals which are expected to be formed by exposing to γ- irradiation. By treating with melatonin all these values become closer to those of control subgroup A_1.

So, it could be conclude that the dielectric spectroscopy is considered to be a good tool to support the trend given by UV spectra and confirmed by ESR spectroscopy.

Viscosity measurements:

The dynamic viscosity (η) of hemoglobin extracted from animals of different subgroups is measured at certain concentration (3.4×10^{-5}M) and temperature (30°C). The data obtained are given in the following table.

C_3	C_2	C_1	A_1	**Group**
0.764	0.759	0.756	0.77	**η(CP)**

These values indicate that there is a slight decrease in the dynamic viscosity for hemoglobin of group exposed to γ–irradiation (C_1) as it compared with control group (A_1). By treatment with melatonin (C_2 and C_3) subgroups, the viscosity values become closer to those of control group (A_1). The decrease in viscosity by exposing to γ–irradiation (even it is very small) indicates some changes in dimensional and shape of hemoglobin molecule [12,19].

CONCLUSION

Exposing hemoglobin to gamma irradiation causes disrupted in the heme groups, slight breakdown of the polypeptide chain and break covalent bond. The study is carried out on female mice depending on the change in the biophysical and biochemical properties which are expected to be happened under the effect of the ionizing radiation. These changes were studied through UV absorption spectra, ESR spectroscopy, dielectric and viscosity measurements. A pronounced increase in the average value of peak position and width at half maximum W_{hmax} followed absorption ratio A_{578} / A_{540} was noticed. An increase in the intensity of ESR signal was noticed which is considered to be an evidence for the formation of free radicals. These changes were also studied through the increase in the dielectric parameter and decrease in the viscosity measurements after exposing to irradiation.The studied changes which are obtained as a result of exposing to irradiation are found to be eliminated by treating with 10 mg/kg and 30 mg/kg melatonin.

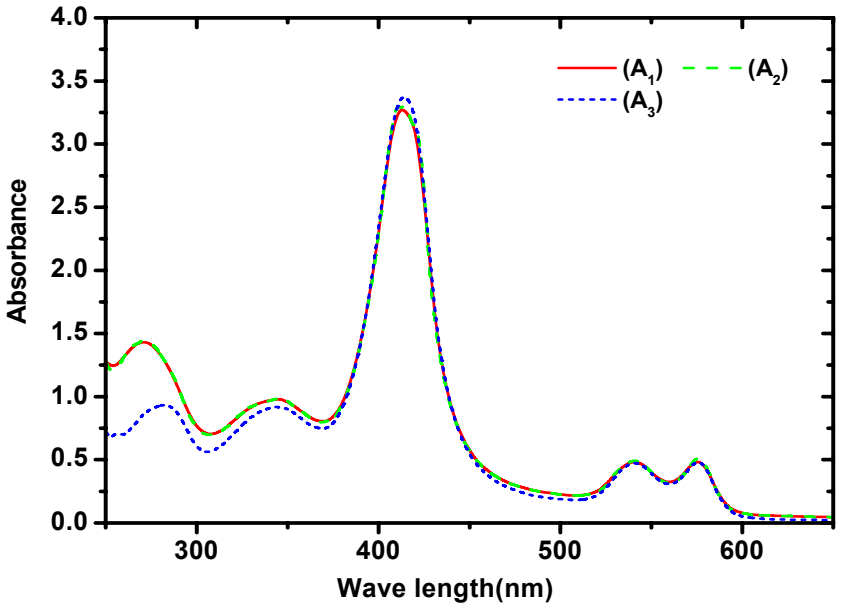

Figure (1): Absorption spectra of hemoglobin extracted from animals of control group A: (A_1) normal animals. (A_2) and (A_3) animals treated with 10 mg/kg and 30 mg/kg melatonin.

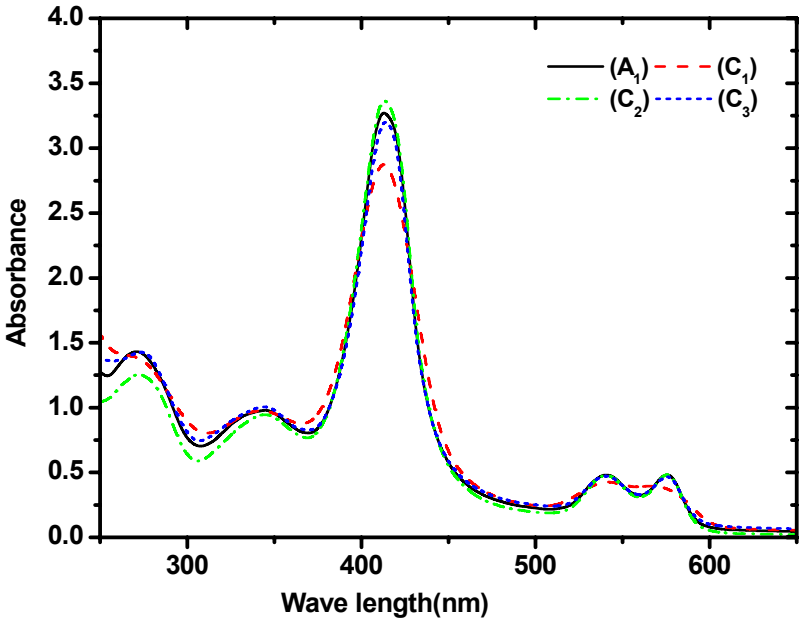

Figure(2): Absorption spectra for hemoglobin extracted from animals of whole body irradiated group C: (C_1) animals with whole body exposed to γ-irradiation, (C_2) and (C_3) animals treated with 10 mg/kg and 30 mg/kg melatonin

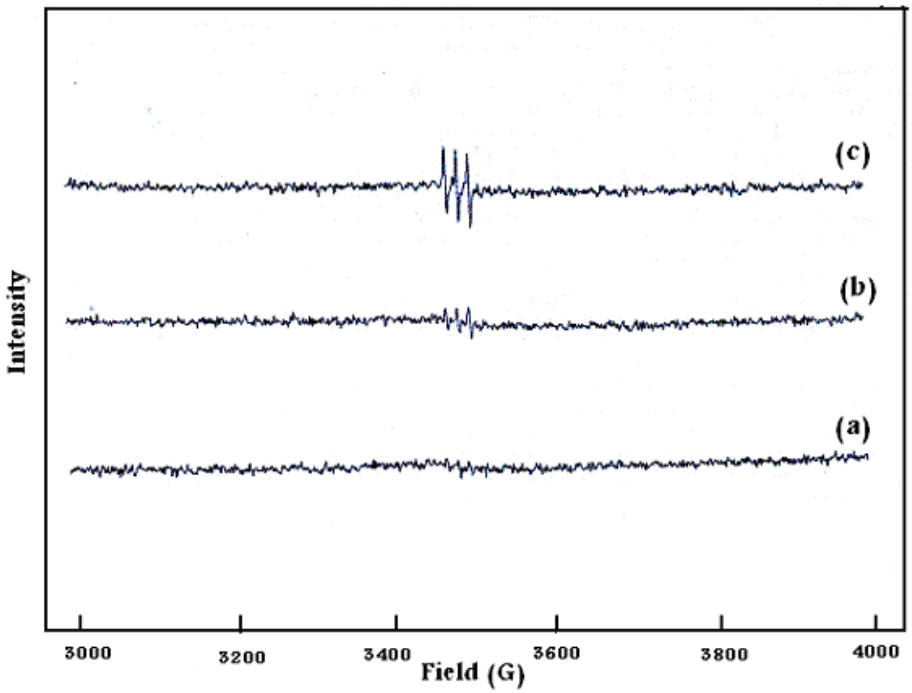

Figure (3): ESR spectra of hemoglobin extracted from animals of control group (a), DMPO (b) and DMPO- hemoglobin mixture (c)

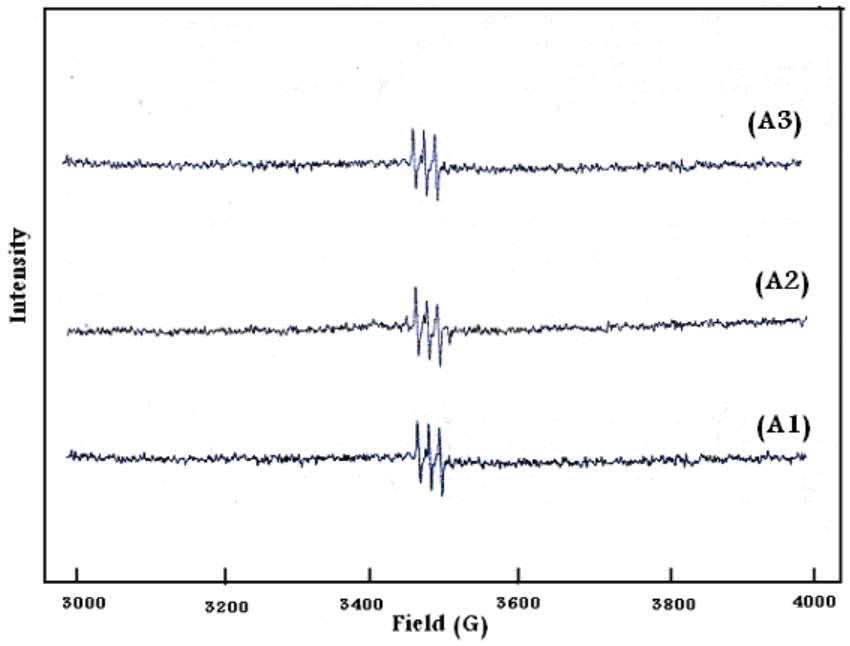

Figure (4): ESR spectra of hemoglobin extracted from animals of control group (A): (A_1) normal animals, (A_2) and (A_3) animals treated with 10 mg/kg and 30 mg/kg melatonin.

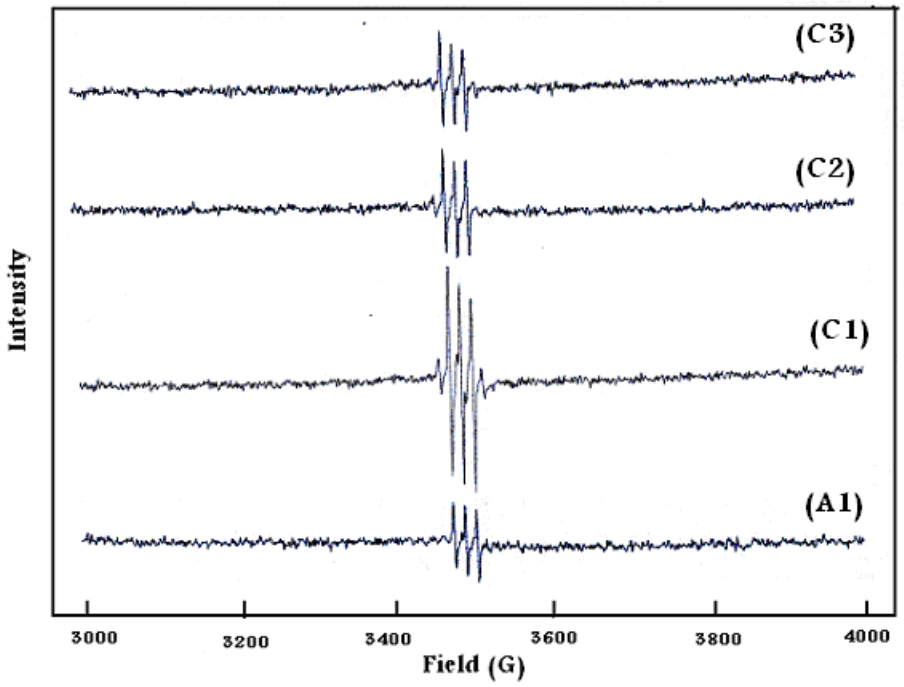

Figure (5): ESR spectra of hemoglobin extracted from animals of irradiated group (C). (C_1) irradiated animals, (C_2) and (C_3) animals treated with 10 mg/kg and 30 mg/kg melatonin

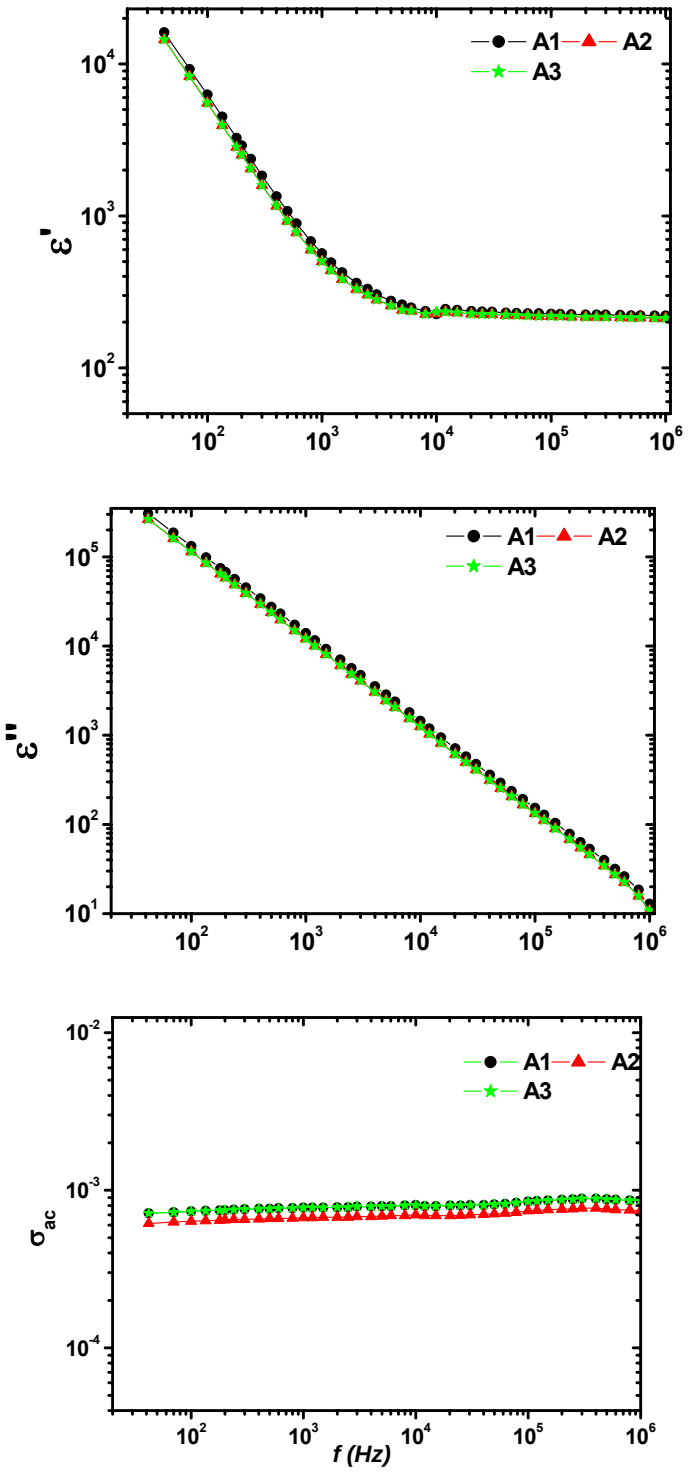

Figure (6): The variation of dielectric permittivity ε', dielectric loss ε'' and electrical conductivity σ_{ac} as a function of the frequency for hemoglobin extracted from animals of control group A.

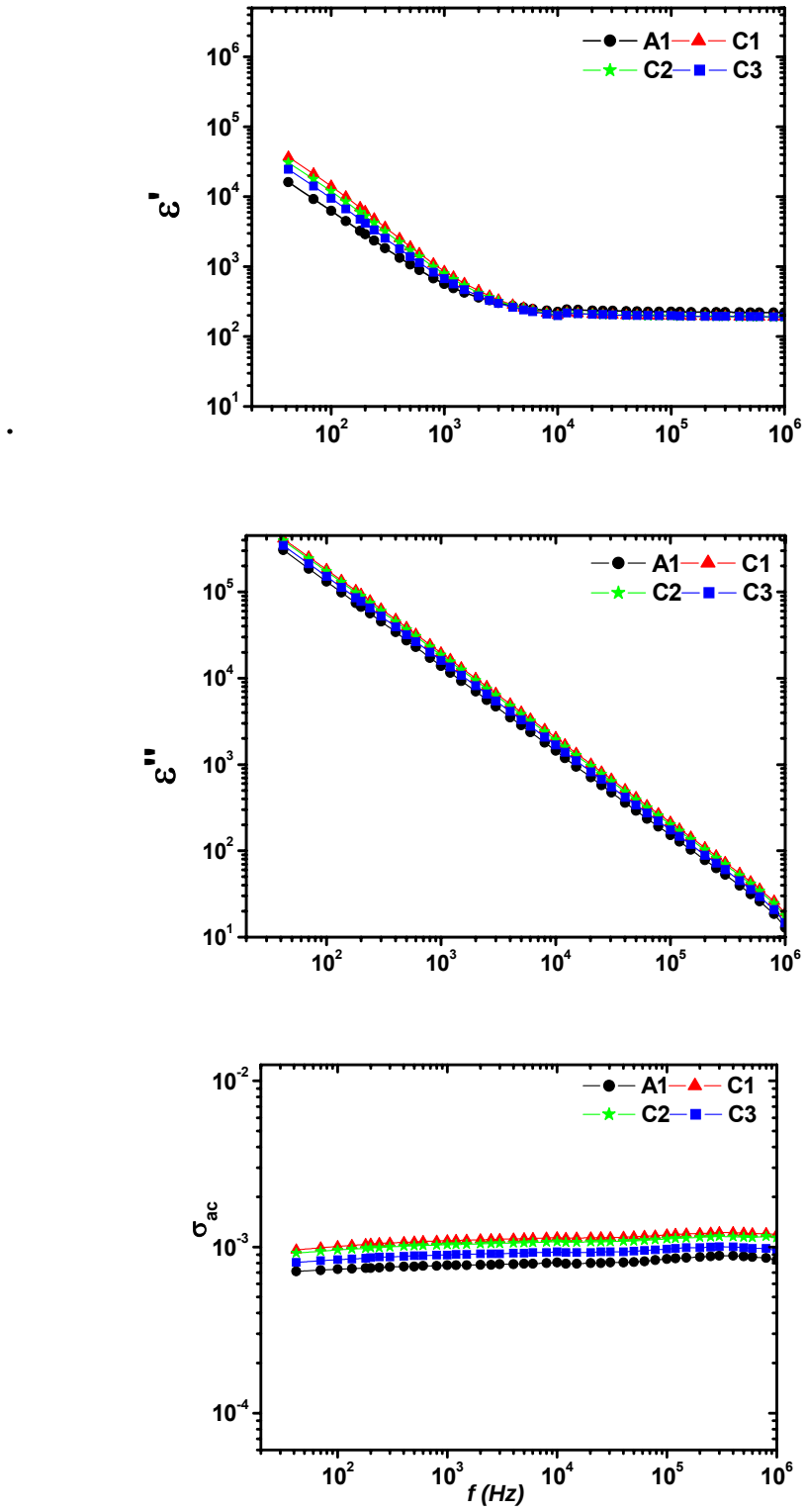

Figure (7): The variation of dielectric permittivity ε', dielectric loss ε'' and electrical conductivity σ_{ac} as a function of the frequency for hemoglobin extracted from animals of whole body irradiated group C

REFERENCES

(1) M. Puchala, Z. S. Lewandowska and J. Kiefer. J. Radiat. Res., 45(2), 275-279 (2004).
(2) N.S. Hassan and S.A. Abdelkawi. Egypt.J.Biophys. Biomed.Engng. 7(2), 233-243 (2006).
(3) A. M. Maghraby, M. A. Ali. Radiation Physics and Chemistry, 76, 1600-1605 (2007).
(4) N.S. Hassan, and T.H.M. Abou-Aiad, Journal of Applied Sciences, 7(9), 1279-1285 (2007).
(5) Y. Lee and K. B. Song. Journal of Biochemistry and Molecular Biology, 35(6), 590-594 (2002).
(6) U. Undeger, B. Giray, A.F. Zorlu, K. Oge and N. Bacaran, Exp. Toxic. Pathol. , 55, 379-384 (2004).
(7) S. Aghazadeh, M. Azarria, S. R. Mahdavi, A. Shirazi and B.M. Zangii. Japanes Society for Alternatives to Animal Experiments, AATEX 14, 535-538 (2008).
(8) R. Segovia, S. Kumari, R. K. Verma, and A.l. Bhatia. J. Radiol. Prot. 26, 227-234 (2006).
(9) L.S Johhav,A.R Rogas, H.A Lekic, S.G Martin. Acta Neurochir Sppl.102,367-371(2008).
(10) T.E. Shalaby and M.M. Shawki. Romanian J. Biophys. 16(3), 169-180 (2006).
(11) S.A. Mousa and S.A. Bashandy. Rom. J. Biophys. 18 (2) (2008).
(12) A. A. Saad El Din, O. S. Desouky, A. Z. El Behay and A. A. El Sayed. Radiat. Phys. Chem. 5, 755-757 (1996).
(13) Z. Jozwiak and Z. Helszer. Radiaton Research, 88, 11-19 (1981).
(14) H.G. El-Sokkary, B.M. Khidr and A.H. Younes. European Journal of Pharmacology, 540, 107-114 (2006).
(15) R.J. Reiter. FASEB J., 9, 526-533 (1995).
(16) G. Senera, N. Jahovicb, O. Tosuna, B. M. Atasoyc and B. Yeg˘enb. Life Science, 74, 563-572 (2003).
(17) R.G. Michael, R. A. Tschirrent-Guth, H. Ewa Witkowska, Y. C. Fann, D. P. Barr, P. R. Ortiz Montellano and R. P. Mason. Biochem .J. 330, 1293-1299(1998).
(18) E.M.K. Hedin, K. Hult, O.G. Mouritsen, P. Hoyrup. J.Biochem.Biophys. Methods 60, 117-138(2004).
(19) G. Sancheti and P.K. Goyal, Radiation & Cancer Biology Laboratory, Department of Zoology, University of Rajasthan, Jaipur – 302 004 (2011).
(20) G. Sancheti, and P. K. Goyal, (2007): Afr. J. Trad. CAM (2007) 4 (2): 165 - 172

Thorium Fuel Performance in a Tight Pitch LWR Lattice

S. S. Mostafa[**] E. A. Amin[*] I. I. Bashter[**] and A.M.Reda**
** Nuclear & Radiological Regulatory Authority, Cairo, Egypt.*
***Faculty of Science, Zagazig University, Zagazig, Egypt.*

ABSTRACT

The aim of this work is to study the utilization of thorium-based fuels in the intermediate neutron spectrum of a tight pitch LWR lattices. The analysis was performed using MCNP-5 and the WIMSD5 codes. *For the sake of showing* the potential benefits of using thorium in LWR fuel, a thorium fueled benchmark was analyzed. Comparison was made between the state-of-the-art codes, MCNP-5 and the WIMSD5. Eigenvalue and isotope concentrations were compared for a PWR pin -cell model up to high burnup (60GWd/ton). The first step of the investigation of the thorium fuel cycle is the validation of the results obtained from the codes for this particular type of fuel. To complete this first task we performed calculation of the benchmark announced by IAEA. The benchmark was based on a simplified PWR model of the assembly with reduced fuel composition. This calculation was focused on the comparison of the methods and basic nuclear data. The calculated and compared values are criticality and fuel composition as a function of burn up. The results showed that thorium-based fuels in the intermediate spectrum of tight pitch LWR have considerable advantages in terms of conversion ratio, reactivity control, non-proliferation characteristics and a reduced production of long-lived radiotoxic wastes. Due to the high conversion ratio of thorium-based fuels in intermediate spectrum reactors, the total fissile inventory required to achieve a given fuel burnup is only 11% to 17%higher than that of ^{238}U fertile fuels. However, unlike ^{238}U fertile fuels, the void reactivity coefficient with thorium-based fuels is negative in an intermediate spectrum reactor. This provides motivation for replacing ^{238}U with ^{232}Th in advanced high conversion intermediate spectrum LWRs (AHCLWR), such as the RMWR or SCR reactors.

INTRODUCTION

The use of thorium in current or advanced light water reactors (LWRs) has been of interest in recent years. These interests have been associated with the need to increase nuclear fuel resources and the perceived non-proliferation advantages of the utilization of thorium in the fuel cycle. Various options have been considered for the use of thorium in the LWR fuel cycle including;
(1) Its use in a once-through fuel cycle to replace non-fissile uranium or to extend fuel burnup due to its attractive fertile material conversion.(2) Its use for fissile plutonium burning in limited recycle cores.(3) Its advantage in limiting the transuranic elements to be disposed of in a repository (if only Th/^{233}Ufuel is used). The possibility for thorium utilization in multirecycle system has also been considered by various researchers, primarily because of the potential for near breeders with Th/^{233}U in the thermal energy range.
A recent study considered the use of Thorium-plutonium (Th/Pu) oxide fuels as an evolutionary way to simultaneously reduce plutonium volumes and capture energy from the

material [Björk 2009].In that work the neurotics properties of Th/Pu fuel and U/Pu mixed oxide (MOX) fuels with varying Pu isotope vectors were compared. For the supporting studies, burnup simulations using a lattice code were performed for a regular MOXPWR fuel assembly and for a Th/Pu PWR fuel assembly of the same geometry. The plutonium content of the two fuel types is chosen so that the same total energy release per fuel assembly is achieved. It was found that this requirement necessitated higher plutonium content in the Th/Pu case, because of the higher Th capture cross section than ^{238}U. For the two systems, reactivity coefficients and kinetics parameters were also calculated. The study indicated that the MOX and Th/Pu fuels have fairly similar neutronics properties in existing PWRs. The Th/Pu fuel was additionally found to offer an advantage over MOX fuel with regards to coolant void reactivity and plutonium consumption. It was concluded that introducing Th/Pu-fuel would improve these factors without imposing any major hurdles from a reactor physics point of view.

In1960-1980, fueling of LWRs with thorium was actively explored, including whole- and many benefits are obtained due to the use of thorium as a nuclear fuel instead of uranium core demonstrations in Indian Point I, Elk River, and the Shippingport Breeder. Thorium use was also extensively studied in the NASAP and INFCE programs but work was focused on recycle mode fuel cycles, using highly enriched $^{235}U$for startup, and burnup ~ 30 MWd/Kg. However, circumstances have changed since then: once-through fueling is assumed; a <20wt% ^{235}U anti-proliferation limitation has been imposed; and a discharge burnup approaching 60 MWd/Kg has been achieved in uranium-fueled LWRs, with further increases in prospect. In addition, an entirely new generation of codes and cross section sets has become available. Thus, a new round of computational benchmarks reflecting these new realities have been initiated.

Le Dai Dien, Ha Van Thong and GiangThanhHieu, for a purpose of proving the advantages of the thorium fuel cycle, *have performed* preliminary reactivity calculations for lattices of fuel rods containing ThO_2 and $(Th,U)O_2$ as well as UO_2 and MOX(?). The reactor would be water cooled and retains all design features of a LWR.They concluded that Th/^{233}U fuel cycle with the important advantages;

(1) Contribute into burning of plutonium stockpiles, and ^{239}Pu produced by this fuel cycle is much less than MOX or UO_2 fuel.(2)High radioactive waste with large lifetime is less than other fuel cycles.(3)High fuel burn-up.(4)Used for high temperature reactors (HTR).(5) Sustainable as compare with limited uranium resource.

In the present work, we performed a pin cell model for (Th-Pu) OX, and the obtained results such as k-infinity, fluxes, energy per fission, fuel composition, absorption and fission cross sections as a function of burnup are compared with the results present in the reference (1).

PROBLEM STATEMENT

MCNP5 and WIMS-D5 computer code systems were used to perform the neutronic analysis of the pin cell model of (Th-Pu) OX. MCNP5 is a computer code which uses the Monte Carlo method in the analysis of the neutron and other particle transport using several point cross section libraries.WIMS-D5is a general lattice cell computer code which uses transport theory (deterministic method) in the analysis of fuel pin. Both codes were used to calculate the

effective multiplication factor, total flux, energy per fission, different isotopes concentrations versus different stages of burnup**.**

Pin Cell Model

The present work reported here involves analysis of a PWR pin cell excised from a standard 17x17 pin Assembly typical of large Westinghouse PWRs. The usual all UO_2 fuel pellets were replaced by (Th-Pu) OX. The burnup calculations described in this study are based on this model. Since all actinides and fission products in the thorium and plutonium chains will be produced during burnup. Our analysis was done using WIMSD5 code with 69 groups WIMS library. The main objectives of this benchmark are to calculate the criticality as a function of burnup in the range of burnup from 0 to 60 GWd/tHM, fluxes, and the energy per fission, the fuel composition (major actinides and fission products), absorption cross sections and fission cross sections of the produced actinides and fission products as a function of burnup respectively. The calculations of burnup were performed for pin cell model of (Th-Pu) OX at a constant specific power of 37.7W/gHM (of initial heavy-metal).
The dimensions and the temperatures of the pin cell model are indicated in table 1.Table 2 shows the initial nuclide atom densities for the fuel and clad and moderator.

Tab.1: pin cell dimensions and temperatures of fuel, clad, moderator

Fuel pellet radius	0.47cm
Cladding radius	0.54cm
Radius of water	0.85cm
Temperature of fuel (K)	1023 K
Temperature of clad (K)	923 K
Temperature of water (K)	583K

Tab.2: initial nuclide densities in the cell (atoms / cm^3)

isotopes	Average in cell	Zone 1	Zone 2	Zone 3
Th-232	6.45E+21	2.11E+22		
Pu-238	2.97E+18	9.72E+18		
Pu-239	1.83E+20	5.99E+20		
Pu-240	7.10E+19	2.32E+20		
Pu-241	2.35E+19	7.69E+19		
Pu-242	1.46E+19	4.78E+19		
Cr	1.99E+20		8.14E+19	
Mn	1.26E+19			
Fe	5.20E+20		1.60E+20	
Ni	2.24E+20			
Zr	4.27E+21		4.37E+22	
C	1.60E+18			2.68E+18
H	2.86E+22			4.80E+22
O	2.78E+22	4.41E+22		2.40E+22

RESULTS AND DISSCUSION

The first important parameter calculated in this work is the neutron multiplication factor versus burnup.Figure1 shows K-infinity as a function of burn up in GWD/TON predicted by MCNP5 and WIMSD5 codes for pin cell model of thorium plutonium oxide. We can see that K-infinity for all cases decreases due to the depletion of fissile isotopes and the production of fission products and poisons. The remarkable decrease in the beginning is due to the production of Xe-135 which has a high neutron capture cross section and it has impact on thermal utilization factor and thus multiplication factor, so Xe-135 is considered an important poison in the reactor operation. The sharp decrease in the values of k-infinity at the end of burnup is due to the production of fission products which have high absorption cross sections which are not taken in consideration in the results of the reference (1).Our work represents the blue curve which is compared to the other curves of the reference results. The results obtained shows good agreement with the reference (1) results and the results obtained by ORIGEN-2code. The total results are shown in table 3.

Tab.3 k-infinity values of other different countries compared to our work

Burnup(GWD/TON)	0	30	40	60
k-infinity (Ref. 1)	1.12479	0.925198	0.887499	0.84756
k-infinity by ORIGEN-2 code	1.112	0.889	0.851	0.822
The present work by WIMSD5 code	1.127744	0.916267	0.873056	0.82698
Δk-infinity(Ref.1- present work)	- 0.0029	0.00857	0.0144	0.02058

The second calculated parameter is the total neutron flux of fuel, clad and moderator during different stages of burnup in GWD/TON. Figure.2 the average total neutron flux versus burnup for (Th-Pu) OX predicted by WIMSD5 code.table.4 shows a comparison of the total neutron flux of fuel, clad, and moderator of our present work and Ref.(1) results.

Tab. 4: comparison of total neutron flux for fuel, clad and moderator.

burnup	0	30	40	60
Fuel Ref(1)	2.9131317E+14	3.5005688E+14	3.6624260E+14	3.8775357E+14
fuel	3.04E+14	3.82E+14	4.01E+14	4.250E+14
Clad Ref(1)	2.9255918E+14	3.5062147E+14	3.6663592E+14	3.8785461E+14
clad	3.05E+14	3.83E+14	4.02E+14	4.2531E+14
Moderator Ref(1)	2.9300243E+14	3.5120984E+14	3.6725799E+14	3.8851187E+14
moderator	3.06E+14	3.84E+14	4.03E+14	4.2537E+14

It is obvious that the total average neutron flux is increasing during the burnup because the macroscopic fission cross section decreases mainly due to depletion of the fissile nuclides. This is a direct consequence of the constant linear power assumed. Fig.2 is shown that the

total neutron flux increases from $3.04\times10^{14}$to about 4.25×10^{14} cm-^{2}.sec^{-1} during burnup. The reference flux results begin from $2.9x10^{14}$ to $3.8x10^{14}$ which are near from the results obtained by WIMSD5 code in our present work.

The third calculated parameter is the average energy per fission which is the amount of energy produced per one fission. Figure .3: fission energy versus burnup for pin cell model of (Th-Pu) OX Predicted by WIMSD5 code. It is obvious that the average energy per fission decreases with burnup this is due to the change of fissile nuclides where the smooth transition from plutonium fissioning to ^{233}U fissioning causes the decrease in the average energy per fission .this is due to the fact that the fissile plutonium isotopes release about 200 MeV thermal energy per fission and ^{233}U only releases about 190 MeV thermal energy per fission. The results of energy per fission of Ref. (1) and our results obtained by WIMSD5 code are tabulated in table5.

Tab. 5: average energy per fission for reference values and our present work values:

Burnup(GWD/TON)	0	30	40	60
Energy per fission (Mev)) Ref(1)	207.891	205.775	204.411	202.009
Energy per fission (Mev) by WIMSD5 code	211.439	207.312	205.433	202.34

The fourth studied parameter in this work is calculating the atom densities of fission products and actinides versus different stages of burnup (0, 30, 40, 60) MWD/Kg for the pin cell model of thorium-plutonium oxide by using WIMSD5 library of 69 few groups.
The obtained results are compared with the results of Ref (1) and a good agreement is found between the two results and they are tabulated in table 6.the second column of each stage of burnup represents our present work.

Tab.6: The atom densities (atoms /barn x cm) of minor actinides and fission products at the different stages of burnup for Ref (1) values and our present work by WIMSD5 code.

symbol	0 MWd/kg	0 MWd/kg	30 MWd/kg	30 MWd/kg	40 MWd/kg	40 MWd/kg	60 MWd/kg	60 MWd/kg
Th-232	2.11E-02	2.11E-02	2.06E-02	2.07E-02	2.05E-02	2.05E-02	2.01E-02	2.01E-02
Pa- 231			2.06E-06	1.61E-06	2.32E-06	1.79E-06	2.38E-06	1.81E-06
Pa-233			2.26E-05	2.31E-05	2.48E-05	2.59E-05	2.79E-05	3.01E-05
u-232			9.24E-07	8.21E-07	1.49E-06	1.35E-06	2.55E-06	2.37E-06
U-233			2.54E-04	2.43E-04	2.99E-04	2.87E-04	3.37E-04	3.23E-04
U-234			2.40E-05	2.34E-05	3.76E-05	3.70E-05	6.73E-05	6.83E-05
U-235			3.60E-06	3.52E-06	6.79E-06	6.65E-06	1.47E-05	1.42E-05
U-236			2.35E-07	1.85E-07	5.91E-07	5.33E-07	2.26E-06	2.22E-06
U-237			6.22E-10	5.19E-10	1.58E-09	1.56E-09	6.02E-09	6.72E-09
U-238			3.32E-10	1.12E-10	6.92E-10	4.83E-10	3.06E-09	3.80E-09
Np-237			2.23E-08	1.68E-08	4.87E-08	4.10E-08	1.90E-07	1.88E-07
Np-239			1.68E-11	9.26E-14	2.17E-11	4.16E-13	3.10E-11	3.40E-12
Pu-238	9.72E-06	9.72E-06	8.18E-06	7.64E-06	8.54E-06	7.64E-06	8.18E-06	6.78E-06
Pu-239	5.99E-04	5.99E-04	7.08E-05	7.19E-05	2.34E-05	2.25E-05	2.74E-06	2.17E-06
Pu-240	2.32E-04	2.32E-04	1.62E-04	1.62E-04	1.06E-04	1.06E-04	2.41E-05	2.35E-05
Pu-241	7.69E-05	7.69E-05	1.00E-04	9.91E-05	7.58E-05	7.33E-05	2.91E-05	2.60E-05
pu-242	4.78E-05	4.78E-05	7.32E-05	6.80E-05	8.39E-05	7.62E-05	8.92E-05	7.51E-05
Am-241			5.19E-06	5.05E-06	4.46E-06	4.25E-06	1.98E-06	1.71E-06
Am-242			1.18E-08	8.12E-09	1.18E-08	8.19E-09	6.46E-09	4.17E-09
Am-242			7.79E-08	8.81E-08	6.60E-08	7.36E-08	2.81E-08	2.87E-08
Am-243			1.89E-05	2.27E-05	2.41E-05	2.89E-05	3.14E-05	3.71E-05
Cm-242			1.81E-06	1.49E-06	2.19E-06	1.83E-06	1.66E-06	1.36E-06
Cm-243			4.91E-08	3.80E-08	7.91E-08	6.16E-08	9.48E-08	6.98E-08
Cm-244			9.10E-06	1.13E-05	1.48E-05	1.84E-05	2.85E-05	3.54E-05

From the previous table, we can deduce that there is a change in the concentrations of fission Products and minor actinides; this will be illustrated in the following notes:

For plutonium isotopes, ^{239}Pu decreases with burnup, where its amount nearly has been burnt up at the end of burnup 60Mwd/kHz.^{241}Pu increases then decreases, this is due to that ^{241}Pu is produced via the capture of ^{240}Pu and on the other hand ^{241}Pu is depleted due to fissioning. For protactinium and uranium isotopes, the fissile nuclide ^{233}U increases with burnup due to neutron capture in ^{232}Th and subsequent decay of ^{232}Th to ^{233}Pa then to ^{233}U which participates more and more to the power.Pa-233 increases slightly with burnup due to increasing the total neutron flux.^{234}U also increases because it is produced via capture in ^{233}U and capture in ^{233}Pa and subsequent decay of ^{234}Pa.The slight increase in ^{233}U is due to its production from the capture in ^{234}U.^{232}U increases because it is formed by (n, 2n) reaction on^{233}U.For the concentrations of minor actinides, ^{243}Am and Cm-244 are the most abundant in the fuel.^{244}Cmincreases with burnup due to the neutron capture in ^{243}Am and subsequent decay of ^{243}Pu.The fifth aim of our calculations is studying the comparison between the absorption and fission cross sections of the produced fission products and actinides. The Ref.

(1) results are compared to our results obtained by WIMSD5 library of 69 groups. The second column in each stage of burnup represents our present work and a good agreement is found between the Ref. (1) results and our results.

The results are recorded in the table 7.

Tab.7: absorption and fission cross section for actinides and fission products:

	0 MWd/ kg HM				60 MWd/kg HM			
	sigma-absorption	sigma-absorption	sigma-fission	sigma-fission	sigma-absorption	sigma-absorption	sigma-fission	sigma-fission
symbol								
Th-232	8.49E-01	8.50E-01	2.64E-02	2.68E-02	1.13E+00	1.11E+00	2.34E-02	2.47E-02
Pa- 233	2.51E+00	2.52E+01	1.74E-01	1.68E-01	2.13E+01	2.15E+01	1.55E-01	1.55E-01
U-233	4.03E+01	3.91E+01	3.52E+01	3.42E+01	6.21E+01	5.98E+01	5.54E+01	5.34E+01
U-234	2.22E+01	2.19E+01	5.65E-01	5.32E-01	1.91E+01	1.81E+01	5.28E-01	5.10E-01
U-235	2.83E+01	2.77E+01	2.21E+01	2.13E+01	5.59E+01	5.36E+01	4.58E+01	4.35E+01
U-236	1.06E+01	1.02E+01	3.57E-01	2.20E-01	8.64E+00	8.65E+00	3.09E-01	2.05E-01
U-237	2.07E+01	2.04E+01	5.87E-01	5.84E-01	4.01E+01	3.86E+01	6.26E-01	6.21E-01
U-238	7.92E+00	8.17E+00	1.14E-01	1.09E-01	7.23E+00	7.20E+00	1.01E-01	1.01E-01
Np-237	2.77E+01	2.74E+01	5.63E-01	5.52E-01	3.42E+01	3.33E+01	5.09E-01	5.10E-01
Np-239	1.47E+01	1.61E+01	6.64E-01	6.44E-01	1.50E+01	1.78E+01	6.00E-01	5.94E-01
Pu-238	1.73E+01	1.69E+01	2.05E+00	1.93E+00	3.64E+01	3.52E+01	2.52E+00	2.36E+00
Pu-239	6.84E+01	6.69E+01	4.41E+01	4.32E+01	1.78E+02	1.75E+02	1.14E+02	1.12E+02
Pu-240	4.96E+01	4.90E+01	6.59E-01	5.81E-01	1.27E+02	1.18E+02	6.16E-01	5.51E-01
Pu-241	7.17E+01	6.89E+01	5.43E+01	5.17E+01	1.63E+02	1.55E+02	1.22E+02	1.15E+02
pu-242	2.36E+01	2.84E+01	4.98E-01	4.57E-01	1.78E+01	2.35E+01	4.46E-01	4.22E-01
Am-241	6.47E+01	6.13E+01	9.62E-01	8.83E-01	1.16E+02	1.10E+02	1.26E+00	1.13E+00
Am-242	3.52E+02	3.34E+02	2.87E+02	2.79E+02	8.71E+02	8.03E+02	7.06E+02	6.68E+02
Am-243	5.07E+01	5.10E+01	4.75E-01	4.71E-01	4.17E+01	4.22E+01	4.23E-01	4.33E-01
Cm-242	4.95E+00	4.24E+00	1.02E+00	4.55E-01	5.60E+00	4.78E+00	1.18E+00	5.48E-01
Cm-243	7.18E+01	8.07E+01	6.13E+01	7.23E+01	8.75E+01	1.03E+02	7.37E+01	9.33E+01
Cm-244	1.80E+01	1.80E+01	1.04E+00	9.90E-01	1.54E+01	1.54E+01	9.64E-01	9.16E-01

We can say that the change in the microscopic cross sections is due to the change in the neutron flux spectrum. The averaged microscopic absorption cross section increases from 0.85 barn at zero burnup to 1.11 at aburnup 60 Mwd/KgHM. The effect of the decrease in self shielding can be illustrated by the absorption cross section of Pu-239.At zero burnup sigma absorption=67 barn and at aburnup 60 Mwd/KgHM it equals 175 barn.

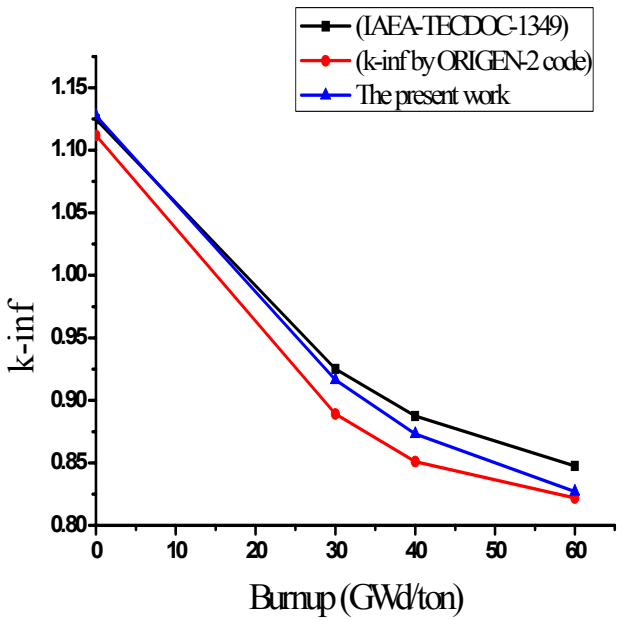

Figure .1:k-inf versus burnup for (Th-Pu) OX Predicted by WIMSD5 code

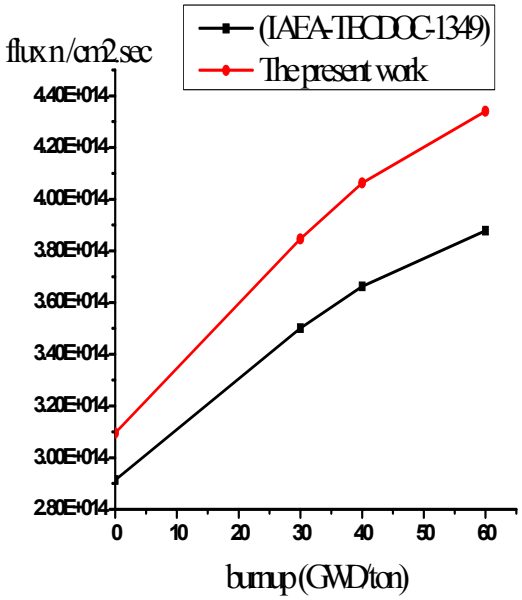

figure.2: flux versus burnup For (Th-Pu) OX Predicted by WIMSD5 code

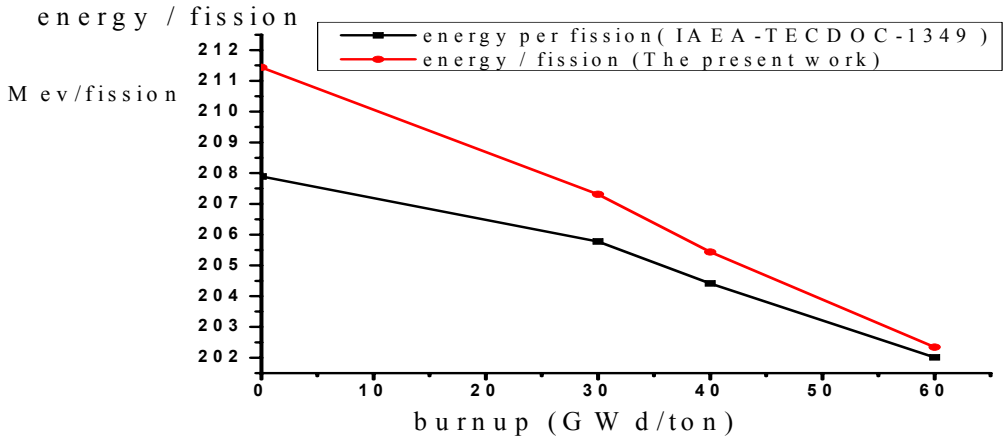

Figure .3: energy per fission versus burnup for pin cell model of (Th-Pu) OX Predicted by WIMSD5 code.

CONCLUSION

We can summarize the conclusion in the following points via the previous calculated parameters

1-MCNP5 and WIMSD5 codes are used for the calculation of a PWR fuel pin taken from 17X17 assembly in pressurized water reactor under specific condition of its operation.2-Pin

cell model is carried out for (Th-Pu) OX and many parameters have been calculated and the obtained results are compared with the results announced in Ref. (1) and a good agreement is found between the two results for all the calculated parameters. 3- The parameters calculated in this work involve k-infinity, fluxes, average energy per fission, the concentrations of fission products and actinides and the absorption and fission cross section(From Th-232 to Cm-244) versus burnup.4-For (Th-Pu) OX, Pu isotopes decrease with burnup but uranium isotopes increase with burnup and finally actinides as ^{243}Am and ^{244}Cm increase with burnup.

REFERENCES

(1) I A E A ; "Potential of thorium based fuel cycles to constrain plutonium and reduce long lived waste toxicity"; TECDOC-1349, April 2003.
(2) K.D.Weaver, X.Zaho, E.E. Pilat and P.Hejzlar; "A PWR Pin cell burnup benchmark"; May 7, 2000 – May 11, 2000.
(3) D.Yun, T.K.KimandT.A.TAiwo; "Th /U-233 multi recycles in PWR s"; August 11, 2010.
(4) I A E A ; "Thorium fuel cycle – Potential benefits and challenges"; IAEATECDOC-1450, May 2005.
(5) M. J. Halsall and C.J. Tubman; "The 1986 wims nuclear data library"; reactor physics division EEwinfrith, September 1986.

Pure-Triplet Scattering for Radiative Transfer in Semi-infinite Random Media with Refractive-Index Dependent Boundary

M. Sallah and **A. R. Degheidy**
Theoretical Physics Research Group, Physics Department, Faculty of Science, Mansoura University, Mansoura P. O. Box. 35516, EGYPT

ABSTRACT

Radiative transfer problem for pure-triplet scattering, in participating half-space random medium is proposed. The medium is assumed to be random with binary Markovian mixtures (e.g. radiation transfer in astrophysical contexts where the clouds and clear sky play and two-phase medium) described by Markovian statistics. The specular reflectivity of the boundary is angular-dependent described by the Fresnel's reflection probability function. The problem is solved at first in the deterministic case, and then the solution is averaged using the formalism developed by Levermore and Pomraning, to treat particles transport problems in statistical mixtures. Some physical quantities of interest such as the reflectivity of the boundary, average radiant energy, and average net flux are computed for various values of refractive index of the boundary.
Keywords: *Radiative transfer, Binary random media, Refractive index dependent Specular-reflecting boundary.*

INTRODUCTION

During the last two decades, the applications of diffusion theory to stochastic radiation transfer problems have become more fruitful, particularly in neutron transport problems. The review by Pomraning [1] summarizes the work on the transport of neutral particles in a random mixture of two immiscible, nonparticipating materials and provides an extensive list of references to earlier work. Applications can vary over a wide range from astrophysical clouds in the interstellar medium to pebble bed nuclear reactors [2]. In the case of pebble bed nuclear reactor [3], small spheres of uranium coated in carbon are randomly mixed in the reactor core. The neutron transport in boiling water reactors gives an interesting example of applications. The water, which acts as both a coolant and moderator, is in two-fluid random state (liquid and vapor). Also, the shielding calculations [4] need a statistical transport treatment to obtain an accurate measurement of the shield effectiveness.

Applying the appropriate boundary conditions to the transport equation led to awkward results [5]. For this purpose, the Fresnel's reflection probability function is applied on the boundary of the semi-infinite planar medium considered in this work. Furthermore, the solution of the one-speed neutron transport equation in a stochastic (random) semi-infinite participating medium is presented analytically. The binary random medium is assumed to consist of two randomly mixed immiscible fluids. That is, at any point in space and time one or the other component of the mixture is present in its pure state, according to some prescribed statistics which we assume to be described as a two-state homogeneous Markov process. We do not allow these two components to mix at the atomic level. Thus the physical

picture is that of a grainy background material making up randomly distributed chunks of random sizes and shapes of the two components of the mixture (such as the situation in the boiling water reactors). For any given physical realization of the statistics, the transport is described by the deterministic Boltzmann transport equation. The medium boundary is considered to have specular reflectivity described by the Fresnel's reflection probability function [6], and the medium is exposed to angular-dependent external incident flux. The deterministic solution is obtained in an exponential form and then averaged using the formalism obtained by Levermore et al. [7] and Pomraning [8]. The effect of anisotropy is very important in studying the radiation transfer problems. So in this work, we include a higher order of anisotropic scattering in a semi-finite random medium. This higher order of anisotropic scattering is called pure-triplet scattering, where the scattering of particles in the medium where the radiation is transferred considered as pure-triplet. The idea to present a pure-triplet radiation scattering instead of a linear anisotropic scattering is legitimate and motivated in the present work. Numerical results are computed for the average of reflectivity, radiant energy, and net flux, for different values of the single scattering albedo with varying the parameters that characterize the random medium, taking into account the effect of the refractive index of the medium boundary on the calculated physical quantities.

PROBLEM FORMULATION

This analysis begin with the monoenergetic radiative transfer equation in a planar participating medium [9], which is given by

$$\left[\mu\frac{\partial}{\partial z}+\sigma(z)\right]\Psi(z,\mu)=\frac{\sigma_s(z)}{2}\int_{-1}^{1}P(\mu,\mu')\Psi(z,\mu')d\mu' \tag{1}$$

$$0\le z\le b,\quad -1\le\mu\le 1$$

where $\Psi(z,\mu)$ is the radiation intensity with geometrical space variable z, and angular variable μ (directional cosine of the propagating radiation), $\sigma(z)$ is the total cross-section, $\sigma_s(z)$ is the scattering cross-section. The anisotropic scattering phase function, $P(\mu,\mu')$, can be expanded by terms of Legendre polynomials [10] as

$$P(\mu,\mu')=\sum_{n=0}^{\infty}a_nP_n(\mu)P_n(\mu')=1+a_1\mu\mu'+a_2P_2(\mu)P_2(\mu')+a_3P_3(\mu)P_3(\mu')+\cdots \tag{2}$$

with $P_n(\mu)$ is the n^{th} Legendre polynomial function and a_n are the anisotropy scattering coefficients with $a_0 = 1$. First term corresponds to the isotropic scattering ($a_1 = a_2 = a_3 = 0$) where probability of radiation scattering is equal for all directions. The second term gives the linearly anisotropic scattering ($a_1 \neq 0$, $a_2 = a_3 = 0$). The third term represents the quadratic scattering or Rayleigh scattering ($a_1 = 0$, $a_2 = 0.5$, $a_3 = 0$). The fourth term corresponds to the triplet scattering ($a_1 = a_2 = 0$, $a_3 \neq 0$). In this work, the scattering is considered as pure-triplet [11]. It is very important to include anisotropic scattering higher order for the collision treatment in radiation transfer to calculate the effective physical parameters.

It is more convenient to write Eq.(1) in terms of the optical depth space variable

$$x(z) = \int_0^z \sigma(z)dz\,, \qquad 0 \le \mathrm{x} \le \mathrm{L} \tag{3.a}$$

with medium optical thickness

$$L(b) = \int_0^b \sigma(z)dz \tag{3.b}$$

In terms of x, Eq.(1) becomes:

$$\left(\mu\frac{\partial}{\partial x}+1\right)N(x,\mu) = \frac{\omega}{2}\int_{-1}^{1} P(\mu,\mu')N(x,\mu')d\mu' \tag{4}$$

where

$$N(x,\mu) \equiv \Psi(z,\mu) \tag{5.a}$$

and the single scattering albedo, which is independent of z (homogeneous medium), is given by

$$\omega = \sigma_s / \sigma \tag{5.b}$$

The propagating radiation according to the transport equation (4) with radiation intensity function $N(x, \mu)$ are assumed to subject to the refractive-index-dependent boundary in the half-space medium ($L \to \infty$) as

$$N(0,\mu) = \Lambda(\mu) + \rho(\mu;n)N(0,-\mu), \tag{6.a}$$

$$\lim_{x\to\infty} N(x,\mu)e^{-\varepsilon x} = 0, \quad \varepsilon > 0. \tag{6.b}$$

where $\Lambda(\mu)$ is the angular-dependent external incident flux, and $\rho(\mu;n)$ is the refractive-index- dependent specular reflectively of the boundary, with n is the refractive index of the medium boundary. This specular reflectively is considered to be calculated from Fresnel's reflection probability function [12,13]

$$\rho(\mu;n) = \frac{1}{2}\left[\left(\frac{\mu - n\mu_0}{\mu + n\mu_0}\right)^2 + \left(\frac{\mu_0 - n\mu}{\mu_0 + n\mu}\right)^2\right] \tag{7}$$

The direction of the incident radiation beam after refraction is determined from Snell's law

$$\mu_0^2 = 1 - \frac{1-\mu^2}{n^2} \tag{8}$$

The behavior of Fresnel's reflection probability function is shown in Fig.(1), which indicates that the reflectivity increases as the refractive index of the medium boundary increase.

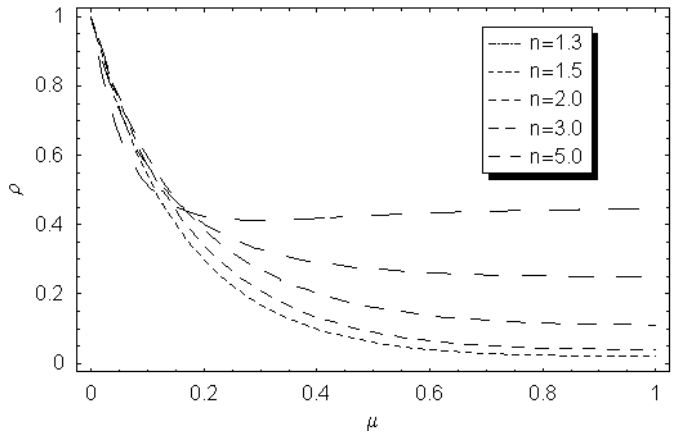

Fig.(1): The reflectivity $\rho(\mu;n)$ versus the directional cosine μ for different values of refractive index *n*

For pure-triplet scattering, we get Eq.(4) as

$$\left(\mu\frac{\partial}{\partial x}+1\right)N(x,\mu)=\frac{\omega}{2}\int_{-1}^{1}\left[1+a_3P_3(\mu)P_3(\mu')\right]N(x,\mu')d\mu' \tag{9}$$

The radiative transfer equation of the type given by Eqs.(9) admits separable exponential solutions of the form

$$N(x,\mu)=A\Phi(\mu,k)\exp(-kx) \tag{10}$$

where $\Phi(\mu,k)$ is a normalized function and A is the normalization constant to be determined.

Using of Eq.(10) in Eq.(9) yields

$$(1-k\mu)\Phi(\mu,k)=\frac{\omega}{2}\left[G_0(k)+a_3P_3(\mu)G_3(k)\right] \tag{11}$$

with

$$G_m(k)=\int_{-1}^{+1}P_m(\mu)\Phi(\mu,k)d\mu \tag{12}$$

Integrating Eq.(11) over $\mu\in[-1,+1]$ gives

$$(1-\omega)G_0(k)-kG_1(k)=0 \tag{13}$$

Multiplying Eq.(11) by μ and μ^2 and integrate over $\mu\in[-1,+1]$, one gets, respectively

$$G_1(k)-\frac{k}{3}\left[G_0(k)+2G_2(k)\right]=0 \tag{14}$$

$$\frac{1}{3}\left[(1-\omega)G_0(k)+2G_2(k)\right]-\frac{k}{5}\left[3G_1(k)+2G_3(k)\right]=0 \tag{15}$$

Dividing Eq.(11) by $(1-k\mu)$ and integrate over $\mu\in[-1,+1]$ we get

$$\left[1-\frac{\omega}{k}q_0\left(\frac{1}{k}\right)\right]G_0(k)-\frac{a_3\omega}{k}q_3\left(\frac{1}{k}\right)G_3(k)=0 \tag{16}$$

where we have defined the n^{th} order Legendre function of second kind, $q_n(y)$, as

$$q_n(y)=\frac{1}{2}\int_{-1}^{1}\frac{P_n(\mu)}{y-\mu}d\mu \tag{17}$$

with

$$q_0\left(\frac{1}{k}\right)=\frac{1}{2}\ln\left(\frac{1+k}{1-k}\right) \quad \text{and} \quad q_3\left(\frac{1}{k}\right)=\frac{1}{4k^3}\left(5-3k^2\right)\ln\left(\frac{1+k}{1-k}\right)-\frac{5}{2k^2}+\frac{2}{3} \tag{18}$$

Equations (13) – (16) constitute four linear homogeneous algebraic equations for the four unknowns G_0, G_1, G_2 and G_3. The corresponding vanishing of the coefficient determinant gives the characteristic equation (transcendental equation) satisfied by k, as

$$\begin{vmatrix} 1-\omega & -k & 0 & 0 \\ -\frac{k}{3} & 1 & -\frac{2k}{3} & 0 \\ \frac{1-\omega}{3} & -\frac{3k}{5} & \frac{2}{3} & -\frac{2k}{5} \\ 1-\frac{\omega}{k}q_0 & 0 & 0 & -\frac{a_3\omega}{k}q_3 \end{vmatrix}=0 \tag{19}$$

Now for normalized $\Phi(\mu,k)$ [i.e. $G_0(k)=1$], we have

$$G_1(k)=\frac{1}{k}(1-\omega) \tag{20}$$

$$G_2(k)=\frac{1}{2}\left[1-\frac{3}{k^2}(1-\omega)\right] \tag{21}$$

and

$$G_3(k)=\frac{5}{6k}-\left(\frac{5}{2k^3}+\frac{2}{3k}\right)(1-\omega) \tag{22}$$

Therefore, from Eq.(11) we obtain

$$\Phi(\mu,k)=\frac{\omega}{2(1-k\mu)}\left\{1+a_3P_3(\mu)\left[\frac{5}{6k}-(1-\omega)\left(\frac{5}{2k^3}+\frac{2}{3k}\right)\right]\right\} \tag{23}$$

and hence we obtain the solution in the form

$$N(x,\mu)=\frac{\omega A}{2(1-k\mu)}\left\{1+a_3P_3(\mu)\left[\frac{5}{6k}-(1-\omega)\left(\frac{5}{2k^3}+\frac{2}{3k}\right)\right]\right\}\exp(-kx) \tag{24}$$

The constant A can be determined by introducing a weight function $W(\mu)$ in order to force the boundary condition Eq.(6.a) to be fulfilled, as

$$\int_0^1 W(\mu)[N(0,\mu)-\Lambda(\mu)-\rho(\mu;n)N(0,-\mu)]d\mu=0 \tag{25}$$

this can give

$$A=\left(\frac{2}{\omega}\right)\frac{I_0}{I_+-I_-(n)} \tag{26}$$

where

$$I_0=\int_0^1 W(\mu)\Lambda(\mu)d\mu\ ,\qquad I_+=\int_0^1 W(\mu)J(+\mu)d\mu\ , \tag{27.a}$$

and

$$I_-(n)=\int_0^1 W(\mu)\rho(\mu;n)J(-\mu)d\mu \tag{27.b}$$

with

$$J(\pm\mu)=\frac{1}{(1\mp k\mu)}\left\{1+a_3P_3(\pm\mu)\left[\frac{5}{6k}-(1-\omega)\left(\frac{5}{2k^3}+\frac{2}{3k}\right)\right]\right\} \tag{28}$$

Hence, the solution is given by

$$N(x,\mu)=\frac{I_0}{I_+-I_-(n)}J(+\mu)\exp(-kx) \tag{29}$$

Equation (29) represents the explicit form of the deterministic analytical solution for the problem under consideration. Now, we can calculate the reflectivity at the boundary of the half-space medium as

$$R=\int_0^1 \mu N(0,-\mu)d\mu\ ,\quad \text{which gives}\quad R=\frac{I_0I_R}{I_+-I_-(n)}\quad \text{with}\quad I_R=\int_0^1 \mu J(-\mu)d\mu \tag{30}$$

Furthermore, we could calculate the radiant energy and the net flux of the propagating radiation, respectively, as

$$E(x)=\int_{-1}^1 N(x,\mu)d\mu\ ,\quad \text{which gives}\quad E(x)=\frac{I_0I_E}{I_+-I_-(n)}\exp(-kx) \tag{31}$$

and

$$F(x)=\int_{-1}^1 \mu N(x,\mu)d\mu\ ,\quad \text{which gives}\quad F(x)=\frac{I_0I_F}{I_+-I_-(n)}\exp(-kx) \tag{32}$$

where

$$I_E=\int_{-1}^1 J(\mu)d\mu\ ,\quad \text{and}\quad I_F=\int_{-1}^1 \mu J(\mu)d\mu \tag{33}$$

STATISTICAL ANALYSIS

For particle transport in binary statistical mixtures a pioneering approach was propounded by Levermore [7] and Pomraning [8]. The mixing statistics were assumed to be Markovian [7–9] with exponentially distributed chord lengths in each material.

Assuming that σ and σ_s obey the same statistics in the sense that $\omega=\sigma_s/\sigma$ (in Eq.(5.b)) is non-stochastic [9]. This means that ω takes the same value inside the two immiscible fluids of

the medium. Hence the transport problem described by equations (4) and (6) is only stochastic through the optical depth variable x and the optical size of the system L. The statistics of the problem are entirely described by the joint probability density $P(x;L;z;b)$, defined such that $PdxdL$ is the probability that for a given geometric position z and a given geometric system thickness b, the position z corresponds to an optical depth lying between x and $x + dx$ and the system thickness b corresponds to an optical thickness lying between L and $L+ dL$. The ensemble-averaged intensity is thus given by [7,9]

$$\langle \Psi(z,b,\mu) \rangle = \int_0^\infty dL \int_0^\infty dx P(x,L;z,b) N(x,\mu) \tag{34}$$

All of the statistical information are embodied in the joint probability function $P(x,L;z,b)$. In the special case of binary homogeneous Markov statistics, one has the near separable form [8] of this joint probability function denoting the two materials making up the binary mixture by subscripts 0 and 1

$$P(x,L;z,b) = \sum_{i=0}^{1} p_i f_i(x;z) f_i(L-x;b-z) \tag{35}$$

where p_i represents the probability of finding material i at any point in the system. In terms of mean slab thickness λ_i of the alternating slabs of the two materials making up the planar system, one has [9]

$$p_i = \frac{\lambda_i}{\lambda_0 + \lambda_1}, \quad i = 0,1 \tag{36}$$

The function $f_i(x;z)$ in Eq.(35) is the probability density function defined such that $f_i dx$ is the probability that the planar system has an optical depth lying between x and $x + dx$, given that the geometric depth is z and given that the point z lays in material i. For the case of homogeneous binary Markov statistics being discussed, the function $f_i(x;z)$ is known in closed analytic form [9]. In view of Eq.(35), Eq.(34) becomes

$$\langle \Psi(z,b,\mu) \rangle = \sum_{i=0}^{1} p_i \int_0^\infty dL f_i(L-x;b-z) \int_0^\infty dx f_i(x;z) N(x,\mu) \tag{37}$$

The above equation simplifies considerably if the problem under consideration is a half-space (semi-infinite) medium ($b \to \infty$). So, the system optical thickness L tends to infinity for each realization of the statistics, and N at any x is the same for each realization. That is for half-space problems, the solution $N(x,\mu)$ depends only upon the single random variable x. Thus N in Eq.(37) can be taken outside of the inner integration, and the remaining integration over L yields unity, since $f_i(L - x;b - z)$ is a probability density function, normalized to a unit integral. Consequently, Eq.(37) reduces to

$$\langle \Psi(z,\mu) \rangle = \sum_{i=0}^{1} p_i \int_0^\infty dx f_i(x;z) N(x,\mu) \tag{38}$$

Such an average is easily computed for homogeneous binary Markovian statistics. We consider a pure exponential in optical depth space variable, $\exp(-\nu\tau)$, with ν being a constant, and ask for the ensemble average of this exponential. If we denote this ensemble-average by the function $E_i(\nu;z)$, we shall have

$$E_i(\nu;z) = \int_0^\infty dx f_i(x;z) \exp(-\nu x) \tag{39}$$

It was found by Pomraning [9] that

$$E_i(\nu;z) = \gamma_i \exp(-r^+ z) + (1-\gamma_i) \exp(-r^- z) \tag{40}$$

with $E_i(Nk;0) = 1$, where

$$\gamma_i = \frac{\nu\sigma_j + (1/\lambda_c) - r^+}{r^- - r^+}, \quad i = 0,1, \quad j = 0,1, \quad i \neq j \tag{41}$$

and

$$2r^{\pm} = (\sigma_1 + \sigma_0)\nu + \frac{1}{\lambda_c} \mp \sqrt{(\sigma_1 - \sigma_0)^2\nu^2 - \frac{2\nu}{\lambda_c}(p_1 - p_0)(\sigma_1 - \sigma_0) + \frac{1}{\lambda_c^2}} \tag{42}$$

where

$$\lambda_c = \frac{\lambda_0\lambda_1}{\lambda_0 + \lambda_1} \tag{43}$$

AVERAGE SOLUTION

The above analysis can be used to evaluate the ensemble-average solution of the problem under consideration. The average solution can be obtained for the radiation intensity by substituting from Eq.(29) into the form (38) to have

$$\langle \Psi(z,\mu) \rangle \equiv \langle N \rangle = \frac{I_0}{I_+ - I_-(n)} J(\mu) \sum_{i=0}^{1} p_i E_i(k;z) \tag{44}$$

Then the corresponding average interesting physical quantities whose deterministic formulae are given by equations (32) – (33), can be obtained as

i) Average radiant energy:

$$\langle E(z) \rangle = \int_{-1}^{1} \langle N(x,\mu) \rangle d\mu \qquad \text{which gives} \qquad \langle E(z) \rangle = \frac{I_0 I_E}{I_+ - I_-(n)} \sum_{i=0}^{1} p_i E_i(k;z) \tag{45}$$

ii) Average net flux:

$$\langle F(z) \rangle = \int_{-1}^{1} \mu \langle N(x,\mu) \rangle d\mu \qquad \text{which gives} \qquad \langle F(z) \rangle = \frac{I_0 I_F}{I_+ - I_-(n)} \sum_{i=0}^{1} p_i E_i(k;z) \tag{46}$$

NUMERICAL CALCULATIONS

The externally-incident flux $\Lambda(\mu)$ is assumed to have the form

$$\Lambda(\mu) = \mu^{\ell}, \quad \ell = 0,1,2,\cdots \tag{47}$$

We use, for calculations [11,14], the special forms of the weight function

$$W_1(\mu) = \mu \ , \quad W_2(\mu) = \frac{\sqrt{3}}{2}\mu\left(1 + \frac{3}{2}\mu\right), \quad W_3(\mu) = \mu N^+(0,\mu) = \mu N(0,-\mu) \tag{48}$$

Table (1) shows the data of reflectivity R for isotropic scattering, $a_3 = 0$, and transparent medium, $\rho = 0$ (i.e. $n = 1$), with incidence $\Lambda(\mu) = 2$ for different values of single scattering albedo ω. In the semi-infinite medium the reflectivity is independent of the stochasticity of the random medium (see Eq.(30)). So our results can be compared with that calculated by the variational method [15]. The comparison shows good agreement between the data calculated by the different weight functions and also with the published data. While the variation of the reflectivity R on the refractive index n of the medium boundary is shown in Table (2) for pure-triplet scattering with $a_3 = 0.5$, using the weight function $W_1(\mu)$.

Table (1) The reflectivity *R* for isotropic scattering $a_3 = \rho = 0$, and $\Lambda(\mu) = 2$

ω	$W_1(\mu)$	$W_2(\mu)$	$W_3(\mu)$	Ref.[15]
0.40	0.09419	0.08180	0.10684	0.094
0.60	0.18608	0.16901	0.20180	0.182
0.80	0.35776	0.33795	0.37246	0.335
0.90	0.53137	0.51196	0.54256	0.475
0.95	0.69377	0.67627	0.70139	

Table (2) The reflectivity *R* for pure-triplet scattering $a_3 = 0.5$, and $\Lambda(\mu) = \mu$

ω	n = 1.3	n = 1.5	n = 2.0	n = 4.0
0.40	0.04366	0.04384	0.04423	0.04547
0.60	0.06633	0.06674	0.06766	0.07055
0.80	0.11427	0.11550	0.11829	0.12739
0.90	0.16234	0.16484	0.17060	0.19025
0.95	0.20541	0.20942	0.21882	0.25240

On the other side, we present, graphically, the calculations of the average radiant energy $\langle E(z) \rangle$ and the average net flux $\langle F(z) \rangle$ as functions of the space depth z inside the medium. All the plotted graphs are done by using the weight function $W_1(\mu)$ because of the comparable results obtained by using the other two weight functions. The average radiant energy and average net flux are computed for different values of the binary discrete random medium parameters λ_i , σ_i. The values of λ_i , σ_i are presented in Table (3) [8,16].

Table (3): Parameters λ_i and σ_i

Case	λ_0	λ_1	σ_0	σ_1
I	**99/100**	**11/100**	**10/99**	**100/11**
II	**99/10**	**11/10**	**10/99**	**100/11**
III	**101/20**	**101/20**	**2/101**	**200/101**

where the values given in table (3) correspond to an average cross section $\langle \sigma \rangle = 1$.

Figures (2) show the average radiant energy $\langle E(z) \rangle$ versus z for pure-triplet scattering $a_3 = 0.5$, $\Lambda(\mu) = \mu$, and $\omega = 0.95$: **(a)** with varying the refractive index for the first case of the random medium parameters given in table (3), and **(b)** for the different cases given in table (3) for $n = 1.5$. The corresponding data for the average net flux $\langle F(z) \rangle$ (as in Figs.(2)) are presented in Figures (3).

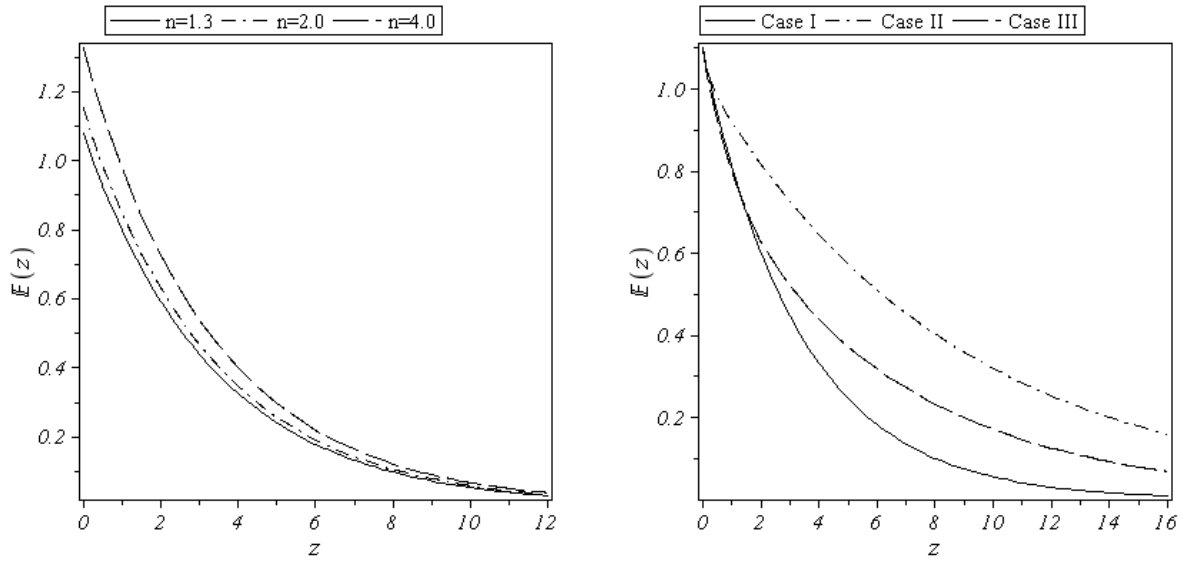

(a) varying the refractive index for *Case I* **(b)** for the Cases given in table (3) for *n = 1.5*.

Figs.(2): Average radiant energy vs. *z* for triplet scattering a_3 = 0.5, $\Lambda(\mu) = \mu$, and ω = 0.95

CONCLUSION

The reflectivity *R*, average energy $\langle E(z) \rangle$ and the average flux $\langle F(z) \rangle$ are calculated for the monoenergetic radiative transfer problem in a binary discrete random semi-infinite medium. The medium is assumed to have specular-reflecting boundary exposed to an angular-dependent external incident flux. The specular reflectivity of the boundary is described by the Fresnel's reflection probability function for the purpose of realizing the boundary conditions to obtain awkward results. In this work, we included the pure-triplet scattering, where the idea to present a pure-triplet scattering instead of a linear anisotropic scattering is legitimate and motivated in the present work. After obtaining the deterministic solutions, the average quantities have been computed for different values of the binary random medium parameters (λ_i and σ_i). The average quantities calculations are more effective at large depth, while at small depth there is no effect for the randomness. The situation is different for the effect of the medium boundary refractive index. The difference between the calculated results (*E* & *F*) can be seen easily for small depth but at higher depth *E* and *F* for different n tend to the same values. The comparison with published data show good acceptable results. The average radiant energy and average net flux depend mainly on the parameters (λ_i and σ_i) characterizing the binary discrete random medium, especially at large depth *z* inside the medium.

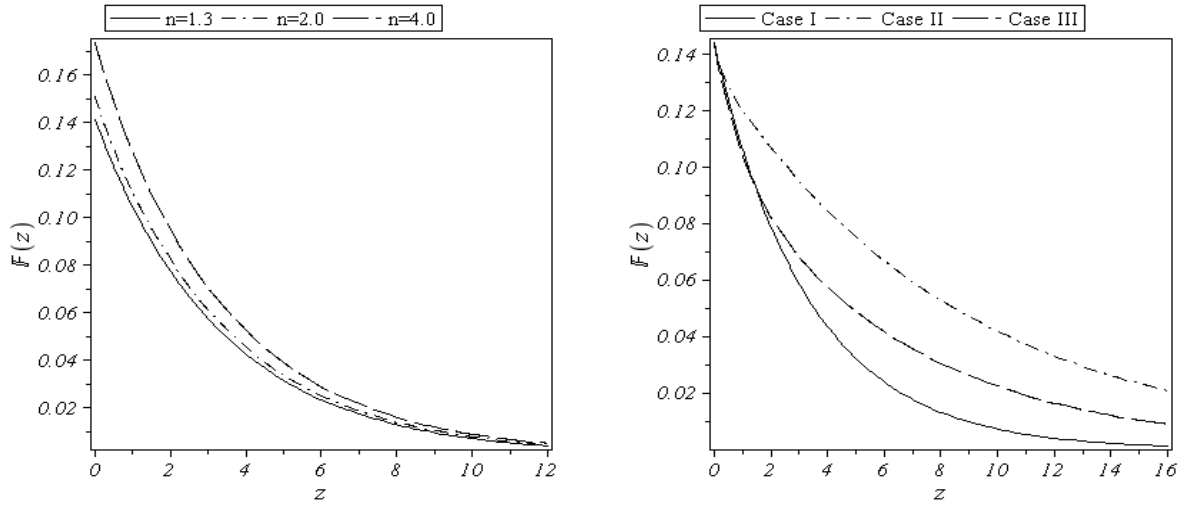

(a) varying the refractive index for *Case I* **(b)** for the Cases given in table (3) for *n = 1.5*.

Figs.(3): Average net flux vs. *z* for triplet scattering $a_3 = 0.5$, $\Lambda(\mu) = \mu$, and $\omega = 0.95$

REFERENCES

(1) Pomraning G.C., *Transp Theory Stat Phys* **27**, 405 (1998).
(2) Olson G.L., Miller D.S., Larsen E.W. and Morel J.M., *J. Quant. Spectrosc. Rad. Transf.* **101**, 269 (2006).
(3) Valko J., Tsvetkpov P.V., Hoogenboom J.E., *Nucl. Sci. Eng*. **135**, 304 (2000).
(4) Price B.T., Horton C.C., Spinney K.T., *Radiation shielding*, Oxford: Pergamon Press (1957).
(5) Ishimaru A., *Wave propagation and scattering in random media*. NY, Oxford: IEEE Press, Oxford University Press (2002).
(6) Degheidy A.R., Abdel Krim M.S., *J. Quant. Spectrosc. Rad. Transf.* **61**, 751 (1999).
(7) Levermore C.D., Pomraning G.C., Sanzo D.L., Wong J., *J. Math. Phys*. **27**, 2526 (1986).
(8) Pomraning G.C., *J. Quant. Spectrosc. Rad. Transf.* **40**, 479 (1988).
(9) Pomraning G.C., *Linear Kinetic Theory and Particle Transport in Stochastic Mixtures*, World Scientific, Singapore (1991).
(10) Mengüç M.P., Viscanta R, *J. of Quant. Spectro. & Radiative Transfer* **29**, 381 (1983).
(11) Sallah M., Degheidy A.R., *Annals of Nuclear Energy* **35**, 708 (2008).
(12) Roux, J.A., Smith A.M., *Prog. Astron. Aeronaut.* **35**, 3 (1974).
(13) Hecht E., *Optics*, Addison-Wesley, San Francisco (2002).
(14) El-Wakil S.A., Aboulwafa E.M., Degheidy A.R., Radwan N.K., *Waves Random Media* **4**, 127 (1994).
(15) Pomraning G.C. *Astrophys. J.* **159** 119 (1970).
(16) Adams M.L., Larsen E.W., Pomraning G.C., *J. Quant. Spectrosc. Rad. Transf.* **42**, 253 (1989).

Cross-sections of spallation residues produced in Proton –Induced reactions

A. Al-Haydari[(1)], A. A. Khan[(1)], G. S. Hassan [(2)], A. Abdul Ganai [(1)]
(1)*Physics Department, Faculty of Applied Science, Taiz University, Yemen*
(2)*Physics Department, Faculty of Science, Assiut University, Egypt*
a_alhaydari@yahoo.com

ABSTRACT

The recent available GSI data for proton-induced spallation reactions by using inverse kinematics at different energies are analyzed for different reactions in terms of the percola- tion model together with the intranuclear cascade model (MCAS). The simulation results obtained for the cross sections of production of light ions and isotopes as a function of mass and charge number is calculated. Results of calculations are in good agreement with experiment.

Keywords*: Spalltion, Lattice Model, Cross Section, Mass Distribution, Multifragmentation.*

INTRODUCTION

In the last decades, a great number of studies on spallition reactions were made both experimen- tally and theoretically due to their wide applications in material science [1], biology[2], surgical therapy [4], space engineering[5] and cosmography [6]. Interest in the spallation reactions has recently been renewed because of the importance of intense neutron sources for various applications, such as spallation neutron sources for condensed matter and material science [7–9] , accelerator-driven systems (ADS) for incineration of nuclear waste incineration[10; 11], or energy production[12], as well as for medical therapy. Further applications were also foreseen like the production of radioactive beams[13]. More traditional was also the astrophysical interest for the spallation reactions on hydrogen, which is the major reaction in the interstellar matter encountered by the cosmic rays during their flights [14]. So that, recently a large effort has been devoted at the Fragment Separator(GSI, Darmstadt) to the measurements of evaporation residues and fission fragments in fission and spallation reactions induced by proton and deuteron [15], using inverse kinematics, were able to supply the identification of all the isotopes produced in spallation and fission reactions[15]. The data obtained can be considered as a crucial benchmark for the theoretical and phenomenological models used in the ADS technology. The precision of these models to estimate residue production cross sections is still far from the accuracy required for technical applications, as it was shown in Refs[15; 16].

In this situation, theoretical studies of spallation and fission in the proton induced

reactions give us some helpful information about estimating of reaction products. Conventionally, the theoretical studies of spallation and fission in the proton induced reactions have been performed by different theoretical models[15]. The precision of these models to estimate residue production cross sections is still far from the accuracy required for technical applications. In the present work we will analyze the cross section of the fragments produced in proton- induced spallation reactions in wide range of incident energy and mass of target nuclei using MCAS model to investigate the validity of this model. The paper includes the following parts. In section 2, we briefly describe the model adopted in this work. In section 3, we present the calculation results and the comparison with experimental data. Asummary and conclusions are presented in section 4.

BASIC PHYSICSAL ASSUMPTIONS OF THE MODEL

2.1 Multifragmentation in spallation reactions

Since many years spallation reactions of medium and high energy protons with atomic nuclei are still of interest for many reasons. First of all, because knowledge of the reaction mechanism is still not complete. This is interesting both from theoretical and experimental point of view. Spallation reactions are generally described by a two-step mechanism. The first stage, intranuclear cascade in which the nucleon-nucleon collisions inside the nucleus induce the loss of a few high-energy nucleons and lead to the formation of excited prefragments[17; 18]. The incoming nucleon sees the substructure of the nucleus, i.e., a bundle of nucleons, due to its reduced wavelength. This fast stage of the nucleon-nucleon scattering interaction leads to the ejection of some of the nucleons and to the excitation of the residual nucleus, which will cool itself afterwards in the second stage [3]. This de-excitation mechanism has been explained as γ -ray, nucleon or cluster evaporation in competition with fission or even multi-fragmentation. The de-excitation process does not end with the ending of g ray emission. In fact the nucleus resulting after ag decay is often radioactive, which will continue to decay until a corresponding stable nucleus is reached [3]. However, experimental data indicate that, at intermediate energies, a third competing process, multifragmentation, comes into play, in which excited remnants break up into intermediate mass fragments (IMF). There are two approaches for theoretical description of multifragmentation: dynamical and statistical. In statistical multifragmentation models, it assumes that the excited remnant achieves thermal equilibrium state and then expands, eventually reaching the freeze-out volume. At this point it fragments into neutrons, light charged particles and IMFs. In dynamical models IMFs are formed at the fast stage of nuclear collision via dynamical forces between nucleons during the evolution of the total system of interacting projectile and target. In this case the whole system is break-up in multiple fragments which never pass through states of thermal equilibrium. There is one more approach for description of the process of multifragmentation: percolation theory. Percolation models treat the nucleus as a lattice with nucleons located at nodes of the lattice. It has been found that results of percolation calculations depend significantly upon the details of the lattice structure. For reasons of computational convenience, the simple cubic lattice has been most frequently used in multifragmentation simulations, but several studies have found [2, 3] that the face-centered-cubic lattice more accurately

reproduces the experimental distributions of fragment masses and their energy spectra[20]. That is, lattices were employed more as computational techniques rather than as formal nuclear models.

2.2 implementation of lattice in the cascade model

The most attractive lattice model is the face-centered-cubic (FCC) model proposed by Cook and Dallacasa[21] because it brings together shell, liquid-drop and cluster characteristics, as found in the conventional models, within a single theoretical framework. Unique among the lattice models, the FCC reproduces the entire sequence of allowed nucleon states as found in the shell model. The(FCC) lattice arrangement of nucleons for the colliding nuclei, is implemented in the modified Cascade Model(MCAS)[20].

Calculations of multifragmentation channels are performed on the basis of the bond-site model of percolation theory [20]. Acording to this model the neucleons are occupying lattice sites in alternating layers, can be seen as consisting of four interpenetrating cubes. A nearest-neighbor distance of about 2.0262 fm reproduces the known core density of nuclei (0.17 nucleons/fm^3).

It is known that a nucleon's distance from the center of the nucleus determines its principal quantum number n. The distance of the nucleon from the"nuclear spin axis" determines its total angular momentum (quantum number j). Finally, the distance of each nucleon from the $y - z$ plane determines its magnetic quantum number m. The inherent simplicity of the FCC model is evident in the FCC definitions of the eigenvalues:

$$\mathbf{n} = (|x| + |y| + |z| - 3)/2, \quad (1)$$

$$\mathbf{j} = (|x| + |y| - 1)/2, \quad (2)$$

$$|\mathbf{m}| = |x|/2, \quad (3)$$

Where the sign of the m value is determined by the intrinsic spin orientation of the nucleon in the antiferromagnetic lattice (spin up = 1/2 and spin down= -1/2). Conversely, the coordinate values can be determined solely from the nucleon eigenvalues:

$$\mathbf{x} = |2\mathbf{m}|\,(-1)^{\mathbf{m}+1/2} \quad (4)$$

$$\mathbf{y} = (2\mathbf{i}+1-|\mathbf{x}|\,)(-1)^{\mathbf{i}+\mathbf{j}+\mathbf{m}+1/2} \quad (5)$$

$$\mathbf{z} = (2\mathbf{n}+3-|\mathbf{x}|-|\,\mathbf{y}|)(-1)^{\,\mathbf{i}+\mathbf{n}-\mathbf{j}-1} \quad (6)$$

Where i is the isospin quantum number. Therefore, knowing the full set of eigenvalues for a given set of nucleons, the configuration of those nucleons in 3–D space relative to the nuclear center can be determined unambiguously. Using the fermi coordinates of each nucleon, the mean radius of the nucleus with A nucleons is defined as

$$R[A] = R_{nucleon} + \frac{1}{A}\sum^{A} r_j \quad (7)$$

Where r is the Euclidean distance of each nucleon, $\sqrt{x_j^2 + y_j^2 + z_j^2}$, from the origin. While $R_{nucleon}$ is the nucleon radius.

2.3 modified cascade with percolation model

In the modified intranuclear cascade-evaporation code, (MCAS)[20]. The percolation procedure is applying at the end of the cascade stage or at the nuclear surface for outgoing Particles. It used to describe fragment size distributions, as an outcome of nuclear fragmentation process. The nucleon coordinates equations(4-6) for the target or projectile nucleus are generated in accordance with the algorithm [19]. For each nuclear collision, lattices of target and projectile nuclei are oriented randomly in relation to the collision axes. This random orientation of the nuclear lattice in 3D space mimics the Woods-Saxon distribution of nuclear density for medium and heavy nuclei. Nucleons are characterized by a momentum distribution that is isotropic in the momentum space: $W(p)dp = p^2 dp,\ 0 \le p \le p_f \equiv p_f(r)$.

The maximum value of the local Fermi momentum depends on the nuclear density $\rho(r)$:

$$p_f(r) = \hbar[3\pi^2 \rho(r)]^{1/3} \qquad \textbf{(8)}$$

For nuclei with the mass number $A \le 16$ the nuclear density is approximated by the oscillatory distribution with parameters derived from experimental data:

$$\rho(r) = \frac{2}{z\pi^{3/2}a^3}\{1 + \frac{z-2}{3}(\frac{r}{a})^2\}Exp(-\frac{r^2}{a^2}) \qquad \textbf{(9)}$$

For nuclei with $A > 16$

$$\rho = \frac{\rho_0}{1 + Exp(\frac{r-c}{a})} \qquad \textbf{(10)}$$

where c is the half-density radius, $C = 1.07\ A^{1/3} fm$; the diffuseness parameter a is equal to 0.545 fm. Single nucleons are distributed inside the nucleus according to the condition $d \ge 2r_c$, where d is the distance between nucleon centers, and $r_c = 0.4fm$ is the nucleon radius. The inelastic interaction of two nuclei is treated as the superposition of two-body nucleon-nucleon and pion-nucleon interactions that can be referred to four main groups: Group A: Elastic and inelastic collisions of projectile nucleons with nucleons of the target nuclei. All secondary particles produced in any group of interactions are considered as cascade particles. Group B: Elastic and inelastic collisions of projectile nucleons with nucleons of the target nuclei. Group C: Elastic and inelastic collisions of secondary pions and nucleons with nucleons of the projectile nuclei. Group D: The so called "cascade-cascade" interaction, i.e. elastic and inelastic collisions of cascade particles with each other.

A fast incident nucleon may interact with any target nucleon located in its path with a cylindrical cut-off cross section area $\pi(r_0 + \lambda_D)^2$, where r_0 is the parameter related to the radius of strong interaction(almost equal to twice the value of the strong interaction range and is taken to be 1.3 fm) and λ_D is the De Broglie

wavelength. Thus, the probability of the interaction at the k^{th} nucleon without interaction with $(k-1)$ nucleons, is given by the binomial distribution:

$$w_k = \prod_{i=1}^{k} (1-q_i) q_k \qquad (11)$$

The partial probability $q_i\left(=1,2,\ldots\ldots(k-1)\right)$ expressed using cross-sections of the interaction with the i^{th} nucleon, σ_i , $q_i = \frac{\sigma i}{\pi(r_0+\lambda_D)}$.

Tracing the time evolution of the considered system, at fixed instant time, *t*, all possible collisions are sampled, i.e. for each of four collision groups (A,B,C, and D) the collision partners are identified. Then the effective collision occurring prior to others is determined (Δt = min{t_i}) and the positions of target nucleus and secondary particles are shifted to new instant of time $t \rightarrow t + \Delta t$. For selected two-body collision the characteristics of the reaction are sampled and the Pauli blocking is applied for the system at rest of both nuclei. During the evolution of the system, the produced resonances may decay before their sub- sequent interactions. A check is made whether the Pauli principle is satisfied both for all interactions and for the decay of resonances. The cascade stage of particle generation is completed when all cascade particles have left both nuclei or have been partly absorbed by them. In this way, the first fast stage of multiparticle production of the nuclear collision has been completed. After the fast cascade stage the FCC lattice is applied.

2.4 properties of residual nuclei after the first stage of the reactions.

As result of the first stage of the reaction, beside emitted particles, an excited nucleus remains. It differs from the initial target, in average, by only a few nucleons in mass number. Properties of the residual nucleus(i.e. mass (A_R), charge (Z_R) are evaluated, in the frame of the MCAS with lattice model. The number and total charge of the remaining nucleons in each remnant specify the mass and charge numbers of the residual nuclei. In general, remnants are in ex- cited states and possess angular momentum. The excitation energy of each remnant nucleus is determined by the energy of the absorbed particles and the ”holes” remaining after nucleons have been knocked out during the intranuclear cascade process. The momentum and angular momentum of the residual nucleus are evaluated applying the conservation of momentum and sequentially followed for each intranuclear interaction. Thus, there are three competing processes for the disintegration of the excited remnant nucleus: evaporation, fission and multi- fragmentation. The multifragmentation is implemented on the basis of the percolation theory and to determine the relative weights of the above three competing processes by applying the site-bond percolation model [20]. according to this model the nucleons occupying the lattice sites are assumed to be connected with their neighbors via bonds which schematically represent two body nuclear forces. In the first fast stage, during the development of the intranuclear cascade, some nucleons occupying the sites of the FCC lattice of the target (projectile) nucleus are knocked out, leaving ”holes” at those sites. These sites are said to be broken. The ratio of the number of broken sites to the total number of sites (the mass number of the target or projectile) characterizes

the degree of destruction of the target (projectile) nucleus after the cascade stage. This ratio depends on the collision energy, the mass numbers of the colliding nuclei and, particularly, on the impact parameter of the collision. In peripheral collisions, mainly peripheral nucleons are knocked out, meaning that, with high probability, the remaining nucleons form one cluster in which all sites are occupied. In collisions with more centrality, corresponding to intermediate or small impact parameters, nucleons are knocked out mainly from the nuclear interior and the target (projectile) remnant represents the lattice with some sites broken. As mentioned above, remnants, in general, are in excited states. The larger the impact parameter, the smaller is the number of broken sites and the less is the excitation energy of the remnant. This initial condition is preferable for equilibration and thermalization of the excited nuclear media and allows one to use evaporation and fission mechanisms for subse- quent disintegration of the excited remnant. With the increasing centrality of the collision, the number of broken sites increases (large destruction), leading to increasing excitation energy of the remnant nucleus. For this case, there is no conventional understanding of the mechanism of disintegration of an excited remnant (thermal break-up with statistical multifragmentation, liquid-gas phase transition, sequential evaporation, cold shattering break-up, etc.). However, it is obvious that when there is a considerable destruction of the remnant, there is no possibility for equilibration and thermalization over the whole volume of the remnant. For the excited remnant disintegration, the bond breaking probability is specified as an input parameter $p(b)$; in the form of impact parameter dependence:

$$p(b) = \frac{p_0}{1 + \left[b - \frac{R_A + R_B}{a}\right]} \qquad \textbf{(12)}$$

Where $p_0 = p(b = 0)$, R_A and R_B are the radii of the colliding nuclei, a=1.0fm, is a diffuseness parameter[29]. The cluster counting algorithm, developed by [20], looks for clusters (fragments): whether neighboring nucleons are connected via bonds or not. Only first-nearest and second-nearest neighbors are taken into account in the counting algorithm. In the initial FCC lattice, each nucleon has 12 first-nearest neighbors at a distance of 2.0262 fm and 6 second-nearest neighbors at 2.8655 fm. As a result of this counting algorithm, the mass and charge distribution of the fragments are obtained. Although this approach is statistical and the probability of any bond to be broken does not depend on its position, the probability of disintegration of the remnant on multiple clusters (fragments) will be higher in the vicinity of the regions with many broken sites. From this, it follows that the process of the multifragmentation is influenced by the dynamics of the collision. Next, the energetic characteristics of the radiated fragments are specified. In general, in its proper frame the remnant possesses rotational energy, E_{rot}, and excitation energy, E^* which are used in the summation of the rotational, E_{fr}^{rot} ,

$$E^{rot} + E^* = \sum E_i^{rot} \sum E^{kin}(A_i, Z_i) + \sum E^*(A_i, Z_i) + \frac{1}{2}\sum \frac{Z_i Z_j}{r_{ij}} \qquad \textbf{(13)}$$

In the standard intranuclear cascade model the contribution of rotational energy, E^{rot}, is small compared with other terms, at least for light nuclei, as projectiles. Large rotational energies could be realized in this approach if nuclear viscosity is included. In the current

calculations, the first term is neglected. Moreover, for the computational convenience additional simplifications are done in (Eq.13). Since the Coulomb repulsion of the charged fragments increases their kinetic energies, the resulting kinetic energies of the fragments are defined as follows:

$$E_{fr}^{kin} + E_{fr}^{coul} = \sum E^{kin}(A_i, Z_i) + \frac{1}{2}\sum \frac{Z_i Z_j}{r_{ij}} = \sum \varepsilon_i(A_i, Z_i) \qquad \textbf{(14)}$$

Another simplification concerns the excitation of the fragments: it is assumed that only one fragment among others is excited, the mass number of which is maximal. This is justified, particularly, when comparing the model with the data obtained through the inverse kinematics because the experimental setup registers a majority of radioactive fragments as well. Therefore, the excitation energy of the remnant, E^*, is converted into the kinetic energies of the fragments and the excitation energy of the fragment with a maximal mass:

$$E^* = \sum \varepsilon_i(A_i, Z_i) + E^*(A_{\max}, Z_{\max}) \qquad \textbf{(15)}$$

With these simplifications we generate the energy distribution of fragments applying considerations proposed in reference [30]. Before the collision the nucleons have a momentum distribution that is uniform inside the Fermi sphere of radius p_F. After the collision the distribution in the vicinity of the beam propagation is wider because of intranuclear interactions accompanied by local excitation of the nuclear medium. This can be written in the form:

$$n(\varepsilon)\alpha 1/\left\{1+\exp\left[\frac{\varepsilon-\varepsilon_F}{T_{eff}}\right]\right\} \qquad \textbf{(16)}$$

where $\varepsilon = p^2/2m$, and ε_F is the boundary Fermi energy. The"effective temperature" is given by;

$$T_{eff} = cE^*/N_{br}, \qquad \textbf{(17)}$$

where c is an adjustable parameter and N_{br} is the number of broken sites. Kinetic energies of nucleons composing the fragment are generated according to distribution (Eq.16), and, summing up all vector momenta directed randomly in 3-D space, we obtain the momentum of the fragment. In such a way, we generate momenta of all produced fragments. The remaining part of the remnant excitation energy, (Eq.15), is assigned to the fragment with maximal mass number. And, of course, we take into account the conservation of energy and momentum for the whole reaction. Results of calculations for reactions on various target nuclei, at different values of incident energy in range from 0.5 GeV to about 6 GeV, are discussed below.

2.6 results of calculations

In the present work, we have simulated the mass and charge distributions of the products resulting from various interactions at intermediate and high energies. The investigations of residues emerging from spallation reactions are usually performed in

direct kinematics which still remains a difficult task. Collision of protons and light nuclei with heavy ions performed at GSI in inverse kinematics allows one to determine the production of residues prior to β decay. This provides a good opportunity to compare the available data with theoretical models to achieve a better understanding of the mechanisms of reactions, which is far from satisfactory. Until now, calculations have been performed by different versions of intranuclear cascade followed by the evaporation model. As we discussed previously, the model used here is includes multifragmentation channels in the framework of the percolation approach.

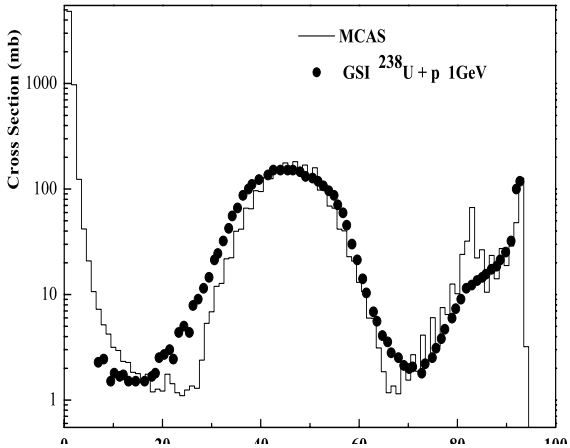

Figure 1: Charge distribution of residues in the reaction ^{238}U+p at 1 A GeV; p_{bond} = 0.57. Data are taken from paper[25].

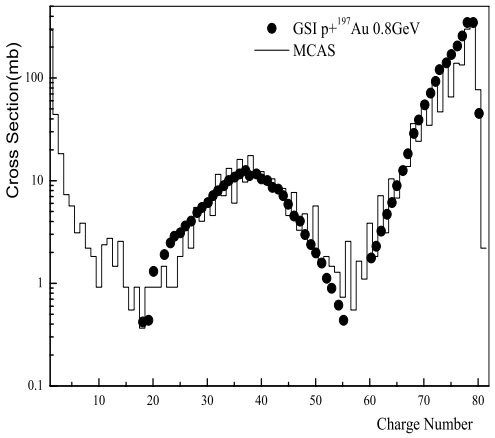

Figure 2: Charge distribution of residues in the reaction 197Au + p at 0.8 A GeV; *pbond* =0.56 Data are taken from paper[22].

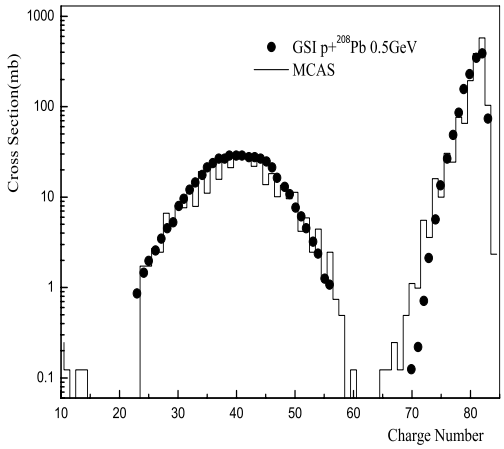

Figure 3: Charge distribution of residues in the reaction ^{208}Pb + p at 0.5 A GeV; p_{bond} = 0.57. Data are taken from paper[23].

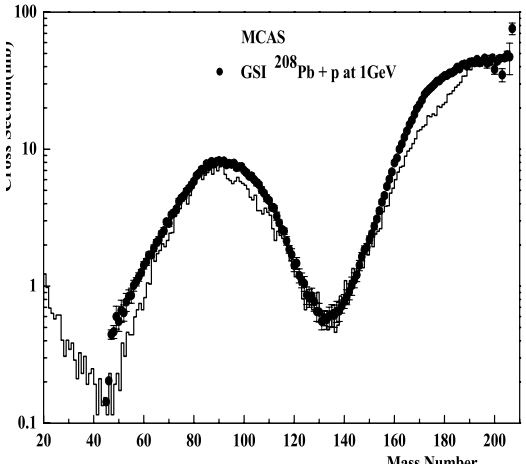

Figure 4: Mass distribution of residues in the reaction ^{208}Pb + p at 1 A GeV; p_{bond} = 0.57. Data are taken from paper[26].

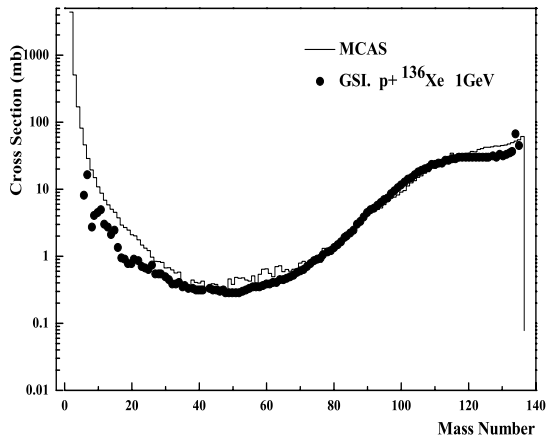

Figure 5: Mass distribution of residues in the reaction ^{136}xe+1 1 A GeV; *pbond* = 0.62. Data are taken from paper[24].

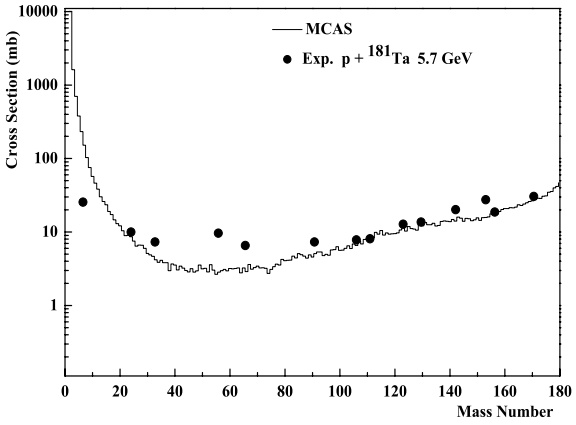

Figure 6: Mass distribution of residues in the reaction p+181Ta at 1 A GeV; *pbond* = 0.79. Data are taken

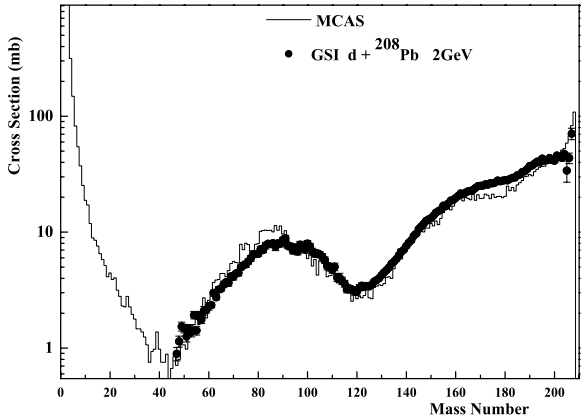

Figure 7: Mass distribution of residues in the reaction d+^{208}Pb at 2 A GeV; *pbond* = 0.63. Data are taken from paper[27].

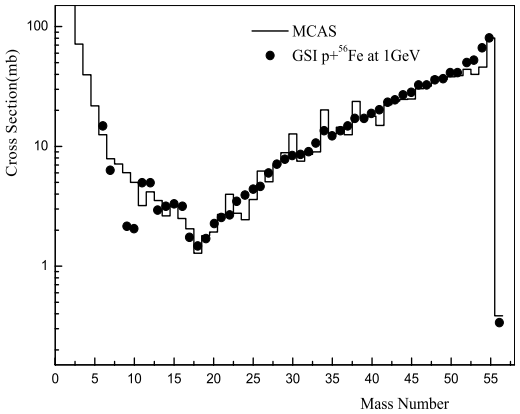

Figure 8: Mass distribution of residues in the reaction ^{56}Fe + p at 1 A GeV; *pbond* = 0.60. Data are taken from paper[26].

2.6 CONCULSIONS

At present work, the MCAS model which includes multifragmentation channels in the framework of the percolation approach is used to investigate the mass and charge distribution proton-induced reactions. The MCAS model can reproduce well the spallation and fission products of the fragment, we can conclude that the MCAS model can be applied to analyze fragment dis- tributions of proton induced at different energies successfully. However, there is still some work to be done in order to achieve a universal description for spallation reactions with arbitrary targets and arbitrary incident energy.

REFERENCES

(1) W. Gudowski. *Nucl. Phys.*, A 654:436c,(1999).
(2) M. Casolinno et. al. *Nature.,* 422 680 ,(2003).
(3) S. T. Mongelli et al. *Braz. J. Phys.*, 35, 894 ,(2005).
(4) C.A.Tobias,H.O.AngerandJ.H.Lawarence Am. J. *Roentgenol.Radiat.*67,1,(1952).
(5) J. H. Trainor *Adv. Space Res.* 14, 685,(1994).
(6) M. S. Smith and K. E. Rehm *Annu. Rev. Nucl. Part. Sci.* 51,91,(2001).
(7) G. S. Bauer *Proc. of the 2nd Int. Conf. on Accelerator Driven Transmutation Technologies (Kalmar, Uppsala University)* p159,(1996).
(8) *Department of Energy 1997 Tech. Rep. No. DOE/Er-0705*
(9) J. M. Carpenter *Nucl. Instrum. Methods* 145,91,(1977).
(10) C .D . Bowman, et al., *Nucl. Instrum. Methods Phys. Res. A* 320,336,(1992).
(11) T. Takizuka *Proc. of the International Conference on Accelerator-driven Transmutation Technologies and Application (Woodbury, NY: AIP Press)* p64,(1995).
(12) C . Rubbia, et al., *rapport CERN/AT/95-44/(ET)*,(1995).
(13) W . F. Henning *Nucl. Inst. Meth. B* 126,1,(1997).
(14) R. Rossi, et al. *Z. Phys.* 82,151,(1933).
(15) Li Ou, et al. *J. Phys. G: Nucl. Part. Phys.* 36,125104,12pp,(2009).
(16) Ignatyuk, A. V.; Kulagin, N. T.; Lunev, V. P.; Shubin, Yu. N.; Titarenko, N. N.; Batyaev, V. F.; Titarenko, Yu. E.; Zhivun, V. M.. *AIP Conference Proceedings.*,Volume 769, pp. 1307-1312 ,(2005).
(17) Y . Yariv, et al. *Phys. Rev. C.*20,2227,(1979). *Phys. Rev. C.*24,488,(1981).
(18) H .W . Bertini *Phys. Rev.* 131,1801,(1963).
(19) N.D. Cook, J. Phys. G: Nucl. Part. Phys. 23, 1109,(1997).
(20) G. Musulmanbekov and A.Al-Haidary *Physics of Atomic Nuclei, Vol.* Vol.66,9, pp. 167-1679, (2003).
(21) N.D. Cook, Atomkernenergie 28,195,(1976) ; V. Dallacasa, Atomkernenergie 37143,(1981); V. Dallacasa and N.D. Cook, Nuovo Cim. A97 157,(1987); N.D. Cook and V. Dallacasa, Phys. Rev. C351883,(1987).
(22) F. Rejmund et al., Nucl. Phys. A683540,(2001); J. Benlliure et al., Nucl. Phys. A683,513,(2001).
(23) B.Fernandez-Dominguez et al., *Nucl. Phys.* A 747,227,(2005), L.Audouin et al., *Nucl.Phys.* A 768, 1,(2006).
(24) C. Paradela,L.Giot *International Conference on Nuclear Data for Science and Technology, DOI: 10.1051/ndata:07772*,(2007).
(25) J. Taieb et al., *Nucl. Phys.*A 724,413,(2003).
(26) P . Napolitani et al. *Phys. Rev. C* ,70, 054607,(2004), E . Le Gentil et al., *Phys. Rev.* A562, 743-746,(2006).
(27) T.Enqvist et al., *Nucl. Phys. A*686,481,(2001), Enqvist T et al., *Phys. Rev. Lett.* 84,5736,(2000).
(28) J. Robb Grover, *Phys. Rev.* 126, 1540,(1962).
(29) W. Bauer U. Post, D. R. Dean, U. Mosel, *Nucl. Phys.* A452 699,1986
(30) X. Campi and J. Desbois, *Proc. 23th Int. winter Meeting on Nucl. Phys.*Bormio, p.707,1985

Calculation of FEPE of Scintillation Detector Using an Empirical Formula Based on Experimental Measurements

Mohamed. S. Badawi[a], , Ahmed. M. El-Khatib[a], Mohamed. A. Elzaher[b] and Abouzeid. A. Thabet[c]

[a] *Physics Department, Faculty of Science, Alexandria University, 21511 Alexandria, Egypt.*
[b] *Department of Basic and Applied Sciences, Faculty of Engineering, Arab Academy for Science, Technology and Maritime Transport, Alexandria, Egypt.*
[c] *Department of Medical Equipment Technology, Pharos University , Alexandria, Egypt.*
ms241178@hotmail.com

ABSTRACT

The full energy peak efficiency (FEPE) curves of the (3*3 in) NaI(Tl) detector at different seven axial distances from it, were measured in a wide energy range from 59.53 up to 1408 keV using calibration point sources. The distinction was based on the effects of the source energy and the source-to-detector distance. This work provides an empirical formula to calculate the (FEPE) for different detectors using the effective solid angle derived from experimental measurements. Comparison between the calculated and the measured efficiency values for the detectors due to the source-to-detector distances of 20, 25, 30, 35, 40, 45 and 50 cm observed that, the calculated values are in agreement with that of the experimental ones.

Key words: *Scintillation Detectors, Full Energy Peak Efficiency (FEPE) and Effective Solid Angle***.**

INTRODUCTION

NaI(Tl) radiation detectors is robust, low cost spectrometric system (detector and associated electronics) for spectra acquisition and it is used at room temperature (no refrigeration), therefore, it can be used in various applications in the field under unfavorable weather conditions [1].

This work is concerned with studying the effect of the distance and energy on the full energy peak efficiency (FEPE) within the energy range of interest. The (FEPE) is calculated by using the efficiency transfer principle which based on an empirical formula to calculate the effective solid angle ratio.

Efficient transfer is considered to be a popular method for calculating the full-energy-peak efficiencies (FEPE) of gamma-ray detectors where, a sample of interest on the basis of an experimental efficiency curve measured in the same detector, but with a calibrated sample of different size, geometry, density or composition [2]. The procedure saves time and resources, since the sample- specific experimental calibration is avoided. It has proven especially useful in environmental measurements [3],

It is based on the assumption that, the detector efficiency at a reference position, P_o, is the combination of the detector intrinsic efficiency, $\varepsilon_i(E)$, depending on both the photon energy and the measurement geometry [4]:

$$\varepsilon(E,P_o)=\varepsilon_i(E).\Omega_{eff}(E,P_o) \quad \textbf{(1)}$$

Where $\Omega_{eff}(E,P_o)$ is the effective solid angle between the source and the detector, which must include absorbing factors, taking into account the attenuation effects on the materials between the source and the detector active part. Thus, for any point source P, the efficiency can be expressed as a function of the reference efficiency, known at the same energy E, [4]:

$$\varepsilon(E,P)=\varepsilon(E,P_o)\frac{\Omega_{eff}(E,P)}{\Omega_{eff}(E,P_o)} \quad \textbf{(2)}$$

The conversion Ratio (R) of the effective solid angles is defined as:

$$R=\frac{\Omega_{eff}(E,P)}{\Omega_{eff}(E,P_o)} \quad \textbf{(3)}$$

Where, the effective solid angle subtended by the detector and the radioactive point source is calculated as reminding hereafter.

MATHEMATICAL TREATMENT

Selim and co-workers using the spherical coordinate system to derivative direct analytical elliptic integrals in order to calculate the detector efficiencies (total and full-energy peak) for any source-detector configuration, Badawi [5].

The pure solid angle subtended by the detector and the radioactive point source is defined as [6]:

$$\Omega=\int_{\theta}\int_{\varphi}\sin\theta d\varphi d\theta \quad \textbf{(4)}$$

By taking into account all absorbers between the source and detector, we will obtain the effective solid angle, (Ω_{eff}), as the following:

$$\Omega_{eff}=\int_{\theta}\int_{\varphi}f_{att}.\sin\theta d\varphi d\theta \quad \textbf{(5)}$$

Where, f_{att}, factor determines the photon attenuation by all absorbers materials between the source and the detector and it is expressed as:

$$f_{att}=e^{-\sum_i \mu_i\delta_i}$$

Where, μ_i, is the attenuation coefficient of the, i^{th}, absorber for a gamma-ray photon with energy, E_γ, and, δ_i, is the average gamma photon path length through the, i^{th}, absorber.

For an arbitrarily positioned axial radioactive point source at height, h, from the detector of radius, R, and side length, L, the polar, θ, and the azimuthal, φ, angles at the point of entrance of the detector is defined as, Badawi [5].

The extreme values of the polar angles are:

$$\theta_1 = \tan^{-1}\left(\frac{R}{h+L}\right)$$

$$\theta_2 = \tan^{-1}\left(\frac{R}{h}\right) \quad \textbf{(6)}$$

In this situation, the lateral distance is equal to zero, and according to the present symmetry the maximum azimuthal angles, φ, are equal to 2π.

Therefore the effective solid angle of axial point source can be expressed as:

$$\Omega_{eff} = \int_0^{\theta_1}\int_0^{2\pi} f_{att} \sin\theta d\varphi \, d\theta + \int_{\theta_1}^{\theta_2}\int_0^{2\pi} f_{att} \sin\theta d\varphi \, d\theta \quad \textbf{(7)}$$

The previous integration is calculated numerically using the trapezoidal rule in a basic program.

1. Experimental setup:

In this study (3*3) NaI (Tl) scintillation detector was used. The details of this detector setup parameter with acquisition electronics specifications supported by the serial and model number were listed in Table 1.

The (FEPE) has been measured using standard point sources (^{241}Am, ^{133}Ba, ^{152}Eu, ^{137}Cs and ^{60}Co) gamma-ray emitters, which obtained from the Physikalisch -Technische Bundesanstalt (PTB) in Braunschweig and Berlin.

The certificates which show the sources activities and their uncertainties for PTB sources are listed in Table 2. The data sheet states the values of half-life photon energies and photon emission probabilities per decay for all radionuclides used in the calibration process are listed in Table 3, which is available at the National Nuclear Data Center Web Page or on the IAEA website.

The homemade Plexiglas holder is used to measure these sources at seven different axial distances starting from 20 cm up to 50 cm with step 5 cm from the detector surface. The holder is placed directly on the detector entrance window as an absorber. In most cases the accompanying x-ray was soft enough to be absorbed completely before entering the detector. The source-detector separations start from 20 cm to neglect the coincidence summing correction.

The spectrum was recorded as P_4 where P refers to the source type (point) measured at distance number (4) which equal 20 cm, so P_5 means that the point source measured at 25cm and so on.

The spectrum acquired by (winTMCA32 software) which made by ICx Technologies and analyze by (Genie 2000 data acquisition & analysis software which made by Canberra), using the automatic peak search and the peak area calculations, along with

changes in the peak fit using the interactive peak fit interface when necessary to reduce the residuals and errors in the peak area values. The live time, the run time and the start time for each spectrum are entered into the spreadsheets. These sheets were used to perform the calculations necessary to generate the experimental (FEPE) curves with their associated uncertainties.

EXPERIMENTAL EFFICIENCIES:

The experimental efficiencies calculated by using the previously described standard sources. The experimental efficiency at energy E, for a given set of measuring conditions can be computed by:

$$\varepsilon(E) = \frac{N(E)}{T \cdot A_S \cdot P(E)} \prod C_i \quad \textbf{(8)}$$

Where, N (E) is the number of counts in the full-energy peak, T is the measuring time (in second), P (E) is the photon emission probability at energy E, A_S is the radionuclide activity, and, C_i are the correction factors due to dead time and radionuclide decay.

For the measurements of the low activity sources, the dead time had been always less than 3%, so the corresponding factor was obtained simply using ADC live time. The statistical uncertainties of the net peak areas were smaller than 1.0%. Since the acquisition time was long enough to get the number of counts which was more than 10,000 counts. The decay correction C_d for the calibration source from the reference time to the run time is given by:

$$C_d = e^{\lambda \cdot \Delta T} \quad \textbf{(9)}$$

Where, λ is the decay constant and ΔT is the time interval over which the source decays corresponding to the run time. The uncertainty in the experimental full energy peak efficiency σε is given by:

$$\sigma_\varepsilon = \varepsilon \cdot \sqrt{\left(\frac{\partial \varepsilon}{\partial A}\right)^2 \cdot \sigma_A{}^2 + \left(\frac{\partial \varepsilon}{\partial P}\right)^2 \cdot \sigma_P{}^2 + \left(\frac{\partial \varepsilon}{\partial N}\right)^2 \cdot \sigma_N{}^2} \quad \textbf{(10)}$$

Where, σ_A, σ_P and σ_N, are the uncertainties associated with the quantities A_S, P(E) and N(E), respectively, assuming that the only correction made is due to the source activity decay.

RESULTS AND DISCUSSION

The experimental study is held at Younis. S. Selim laboratory for Radiation Physics, Department of Physics, Faculty of Science, Alexandria University, Egypt. This laboratory uses several co-axial NaI(Tl) scintillation detectors. (3"*3") NaI(Tl) scintillation detector is used in the present study. The detector was calibrated by measuring the lowest activity point sources.

Fig. 1. Show that the effective solid angle is decreased by increasing the height of the source.it also shows that P_4 has the largest effective solid angle and P_{10} is the smaller one. The effective solid angle below 121 kev is sharply increased then its values tend to be fixed at higher energies for each position.

By taking The experimental full energy peak efficiency value of P_4 listed in the table (4) as a reference efficiency. The effective solid angle ratio for conversion from P_4 refernce curve of (FEPE) to P_5 up to P_{10} of (FEPE) are listed in table (5) and plotted in Fig. 2. Which show that, it is approximately fixed for each position. The standard deviation for each position conversion ratios is calculated and found to be less than 0.003 as listed in the table (5).

The calculated (FEPE) of P_5 up to P_{10} is obtained by multiplying the reference efficiency by the average value (conversion Ratio) of the effective solid angle for each position.The percentage error between the calculated and the measured efficiencies is given using the vaules which tabulated in table (6) by:

$$\Delta\% = \frac{\varepsilon_{Cal} - \varepsilon_{meas}}{\varepsilon_{meas}} \times 100 \qquad \textbf{(11)}$$

Where, ε_{cal} and ε_{meas} are the calculated and measured efficiencies, respectively.

By plotting the source height from the detector surface versus the average value of the effective solid angle ratio, we obtained an exponential decay curve as shown in Fig. 3. The fitting equation of this curve is obtained from Origin 8 program and found to be as:

$$R_x = R_o + Ae^{-\left(\frac{x}{t}\right)} \qquad \textbf{(12)}$$

Where, R_x is the conversion ratio from, P_4 to, P_x , and x is the axial source height in cm.

Parameter	**Value**	**Error**
$\mathbf{R_o}$	0.12965	0.00939
A	5.30799	0.26577
t	11.03816	0.33699
$\mathbf{Chi^2}$	4.65629E-5	
$\mathbf{R^2}$	0.99964	

So the equation (2) will be:

$$\varepsilon(E,P) = \varepsilon(E,P_4)R_x \qquad \textbf{(13)}$$

CONCLUSION

From this work we reach for a simple method to calculate the (FEPE) of cylindrical NaI(Tl) scintillation detector using an empirical formula. This formula is valid through a wide energy range and at different axial distances from the detector. The discrepancies in general for all the measurements were found to be less than (7%) between the calculated (FEPE) and experimental values at all energy regions

Acknowledgment

The authors would like to express their sincere thanks to Prof. Dr. Mahmoud. I. Abbas, Faculty of Science, Alexandria University, for the very valuable professional guidance in the area of radiation physics and for his fruitful scientific collaborations on this topic.

Dr. Mohamed. S. Badawi would like to introduce a special thanks to The Physikalisch-Technische Bundesanstalt (PTB) in Braunschweig, Berlin, Germany for fruitful help by support the radioactive sources.

Table (1) Detector setup parameters with acquisition electronics specifications for (3*3) NaI(Tl) scintillation detector

Items	Detector (D2)
Manufacturer	Canberra
Serial Number	09L 652
Detector Model	802
Type	Cylindrical
Mounting	Vertical
Resolution (FWHM) at 661 kev	8.5%
Cathode to Anode voltage	+1100 V dc
Dynode to Dynode	+80 V dc
Cathode to Dynode	+150 V dc
Tube Base	Model 2007
Shaping Mode	Gaussian
Detector Type	NaI(Tl)
Crystal Diameter (mm)	76.2
Crystal Length (mm)	76.2
Top cover Thickness(mm)	Al (0.5)
Side cover Thickness(mm)	Al (0.5)
Reflector – Oxide (mm)	2.5
Weight (Kg)	1.8
Outer Diameter(mm)	80.9
Outer Length(mm)	79.4
Crystal Volume in (cm^3)	347.639

Table (2) PTB point sources activities and their uncertainties.

PTB-Nuclide	Activity(kBq)	Reference Date 00:00 Hr	Uncertainty(kBq)
^{241}Am	259.0	1.June 2009	± 2.6
^{133}Ba	275.3		± 2.8
^{152}Eu	290.0		± 4.0
^{137}Cs	385.0		± 4.0
^{60}Co	212.1		± 1.5

Table (3) Half lives, photon energies and photon emission probabilities per decay for the all radionuclides used in this work.

PTB-Nuclide	Energy (kev)	Emission Probability %	Half Life (Days)
^{241}Am	59.52	35.9	157861.05
^{133}Ba	80.99	34.1	3847.91
^{152}Eu	121.78	28.4	4943.29
	244.69	7.49	
	344.28	26.6	
	778.9	12.96	
	964.13	14.0	
	1408.01	20.87	
^{137}Cs	661.66	85.21	11004.98
^{60}Co	1173.23	99.9	1925.31
	1332.5	99.982	

Table (4) Experimental Full Energy peak Efficiency (P_4 Reference Efficiency)

Nuclide	Energy	Exp P4 (Reference Efficiency)	Uncertainty
Am-241	**59.53**	4.821E-03	3.27E-05
Ba-133	**80.99**	5.273E-03	3.85E-05
Eu-152	**121.78**	5.570E-03	4.46E-05
Eu-152	**244.69**	4.523E-03	3.31E-05
Eu-152	**344.28**	3.755E-03	2.84E-05
Cs-137	**661.66**	2.097E-03	1.17E-05
Eu-152	**778.9**	1.760E-03	1.28E-05
Eu-152	**964.13**	1.376E-03	1.03E-05
Co-60	**1173.23**	1.110E-03	4.75E-06
Co-60	**1332.5**	9.870E-04	4.22E-06
Eu-152	**1408.01**	9.467E-04	6.78E-06

Table (5) The effective solid angle ratio for conversion from refernce curve FEPE to P_5 up to P_{10} FEPE.

Nuclide	Energy	$\frac{\Omega_{p4}}{\Omega_{P4}}$	$\frac{\Omega_{F5}}{\Omega_{F4}}$	$\frac{\Omega_{p6}}{\Omega_{P4}}$	$\frac{\Omega_{p7}}{\Omega_{P4}}$	$\frac{\Omega_{p8}}{\Omega_{P4}}$	$\frac{\Omega_{p9}}{\Omega_{P4}}$	$\frac{\Omega_{p10}}{\Omega_{P4}}$
Am-241	59.53	1	0.67459577	0.47593187	0.36067983	0.27253869	0.22527844	0.18625224
Ba-133	80.99	1	0.67413828	0.47667748	0.36078635	0.27310921	0.22371524	0.18455660
Eu-152	121.78	1	0.67381807	0.47719200	0.36082051	0.27347602	0.22264413	0.18328681
Eu-152	244.69	1	0.67343479	0.47779082	0.36079398	0.27385917	0.22140006	0.18167494
Eu-152	344.28	1	0.67326424	0.47805419	0.36077399	0.27402235	0.22085366	0.18096040
Cs-137	661.66	1	0.67295483	0.47853462	0.36073645	0.27431883	0.21986319	0.17964951
Eu-152	778.9	1	0.67288335	0.47864536	0.36072795	0.27438721	0.21963560	0.17934993
Eu-152	964.13	1	0.67279370	0.47878478	0.36071763	0.27447357	0.21934984	0.17897222
Co-60	1173.23	1	0.67271674	0.47890443	0.36070776	0.27454705	0.21910475	0.17864820
Co-60	1332.5	1	0.67266884	0.47897834	0.36070177	0.27459268	0.21895294	0.17844865
Eu-152	1408.01	1	0.67264840	0.47901089	0.36070023	0.27461330	0.21888709	0.17836083
Mean (Average)		1	0.67326518	0.47804589	0.36074059	0.27399437	0.22088045	0.18092367
Standard deviation:		0	0.00066	0.00104	0.00005	0.00069	0.00216	0.00271

Table (6) Theoritical and Experimental FEPE and the Discrepancy percentage (Δ%) between them.

Nuclide	Energy	Exp P5	P5 (Cal)	Δ%	Exp P6	P6 (Cal)	Δ%	Exp P7	P7 (Cal)	Δ%
Am-241	59.53	3.249E-03	3.246E-03	-0.098%	2.285E-03	2.305E-03	0.883%	1.707E-03	1.739E-03	1.859%
Ba-133	80.99	3.552E-03	3.550E-03	-0.058%	2.521E-03	2.521E-03	-0.023%	1.907E-03	1.902E-03	-0.227%
Eu-152	121.78	3.760E-03	3.750E-03	-0.265%	2.651E-03	2.663E-03	0.463%	1.982E-03	2.009E-03	1.400%
Eu-152	244.69	3.046E-03	3.045E-03	-0.037%	2.158E-03	2.162E-03	0.208%	1.625E-03	1.632E-03	0.397%
Eu-152	344.28	2.549E-03	2.528E-03	-0.819%	1.798E-03	1.795E-03	-0.171%	1.368E-03	1.354E-03	-1.026%
Cs-137	661.66	1.401E-03	1.412E-03	0.751%	1.006E-03	1.002E-03	-0.385%	7.646E-04	7.565E-04	-1.062%
Eu-152	778.9	1.177E-03	1.185E-03	0.653%	8.460E-04	8.411E-04	-0.576%	6.425E-04	6.347E-04	-1.211%
Eu-152	964.13	9.249E-04	9.264E-04	0.158%	6.576E-04	6.578E-04	0.030%	5.030E-04	4.964E-04	-1.321%
Co-60	1173.23	7.452E-04	7.474E-04	0.303%	5.514E-04	5.307E-04	-3.760%	4.195E-04	4.005E-04	-4.533%
Co-60	1332.5	6.679E-04	6.645E-04	-0.510%	4.828E-04	4.718E-04	-2.275%	3.649E-04	3.561E-04	-2.434%
Eu-152	1408.01	6.369E-04	6.374E-04	0.083%	4.539E-04	4.526E-04	-0.278%	3.448E-04	3.415E-04	-0.952%
Nuclide	Energy	Exp P8	P8 (Cal)	Δ%	Exp P9	P9 (Cal)	Δ%	Exp P10	P10 (Cal)	Δ%
Am-241	59.53	1.311E-03	1.321E-03	0.762%	1.059E-03	1.065E-03	0.558%	8.795E-04	8.723E-04	-0.825%
Ba-133	80.99	1.452E-03	1.445E-03	-0.458%	1.175E-03	1.165E-03	-0.885%	9.589E-04	9.541E-04	-0.503%
Eu-152	121.78	1.516E-03	1.526E-03	0.679%	1.227E-03	1.230E-03	0.309%	1.002E-03	1.008E-03	0.557%
Eu-152	244.69	1.239E-03	1.239E-03	0.032%	1.000E-03	9.991E-04	-0.102%	8.226E-04	8.183E-04	-0.514%
Eu-152	344.28	1.043E-03	1.029E-03	-1.378%	8.345E-04	8.293E-04	-0.621%	6.883E-04	6.793E-04	-1.304%
Cs-137	661.66	5.880E-04	5.746E-04	-2.282%	4.773E-04	4.632E-04	-2.966%	3.887E-04	3.794E-04	-2.400%
Eu-152	778.9	4.948E-04	4.821E-04	-2.575%	3.971E-04	3.886E-04	-2.120%	3.232E-04	3.183E-04	-1.509%
Eu-152	964.13	3.875E-04	3.770E-04	-2.714%	3.136E-04	3.039E-04	-3.082%	2.563E-04	2.489E-04	-2.890%
Co-60	1173.23	3.204E-04	3.042E-04	-5.064%	2.612E-04	2.452E-04	-6.117%	2.128E-04	2.009E-04	-5.610%
Co-60	1332.5	2.821E-04	2.704E-04	-4.137%	2.278E-04	2.180E-04	-4.277%	1.859E-04	1.786E-04	-3.929%
Eu-152	1408.01	2.656E-04	2.594E-04	-2.335%	2.140E-04	2.091E-04	-2.303%	1.748E-04	1.713E-04	-2.007%

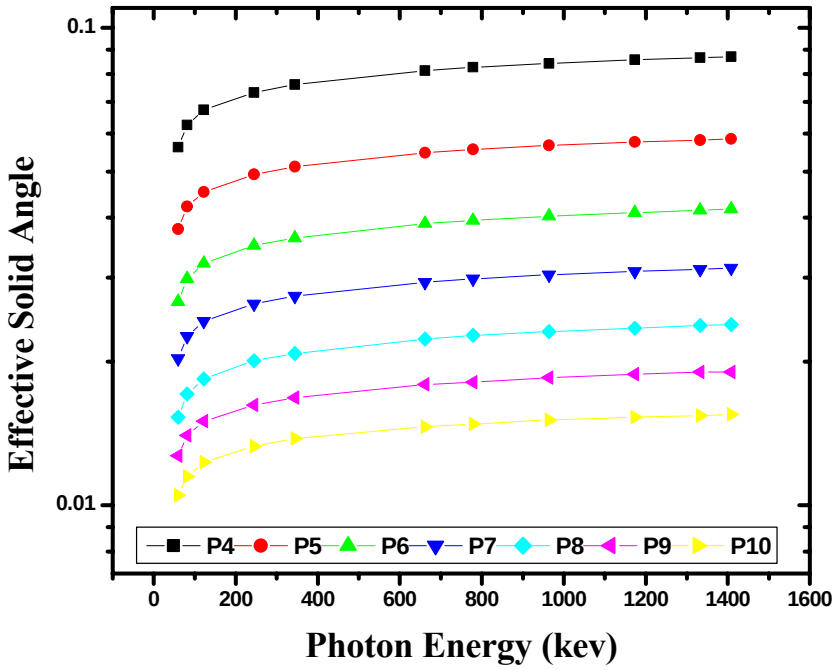

Figure 2 The effective solid angle ratio for conversion from P_4 refernce curve FEPE to P_5 up to P_{10} FEPE

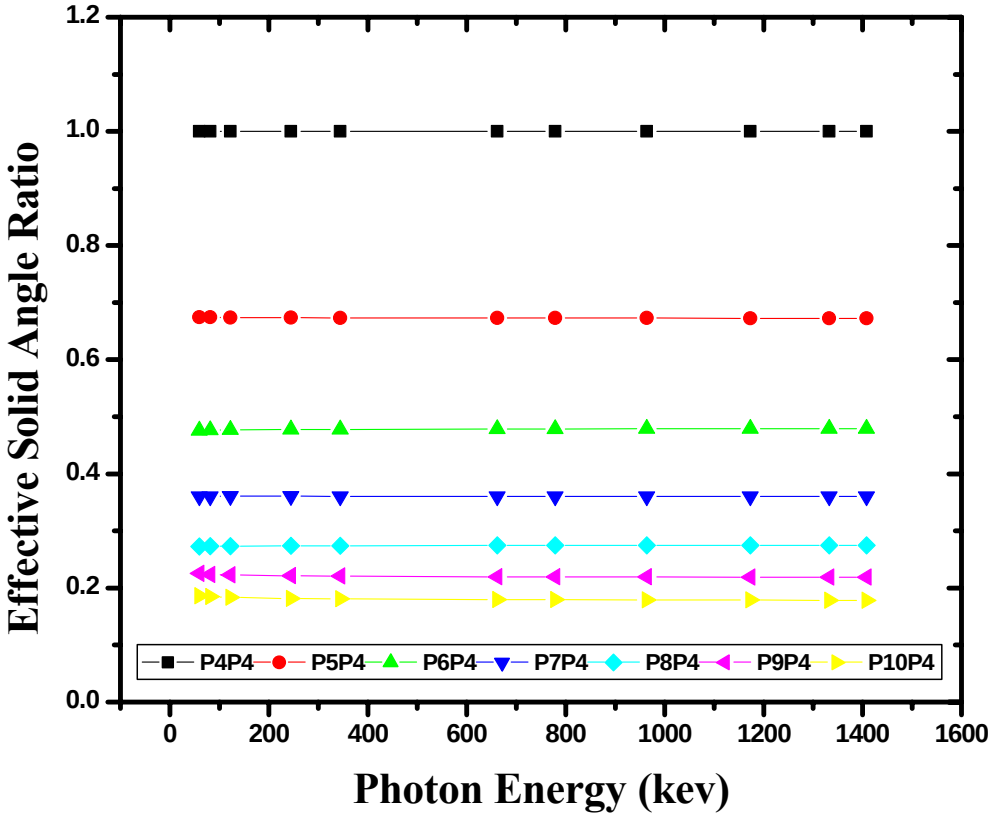

Figure 1 Comparison between the effective solid angles of P_4 up to P_{10}

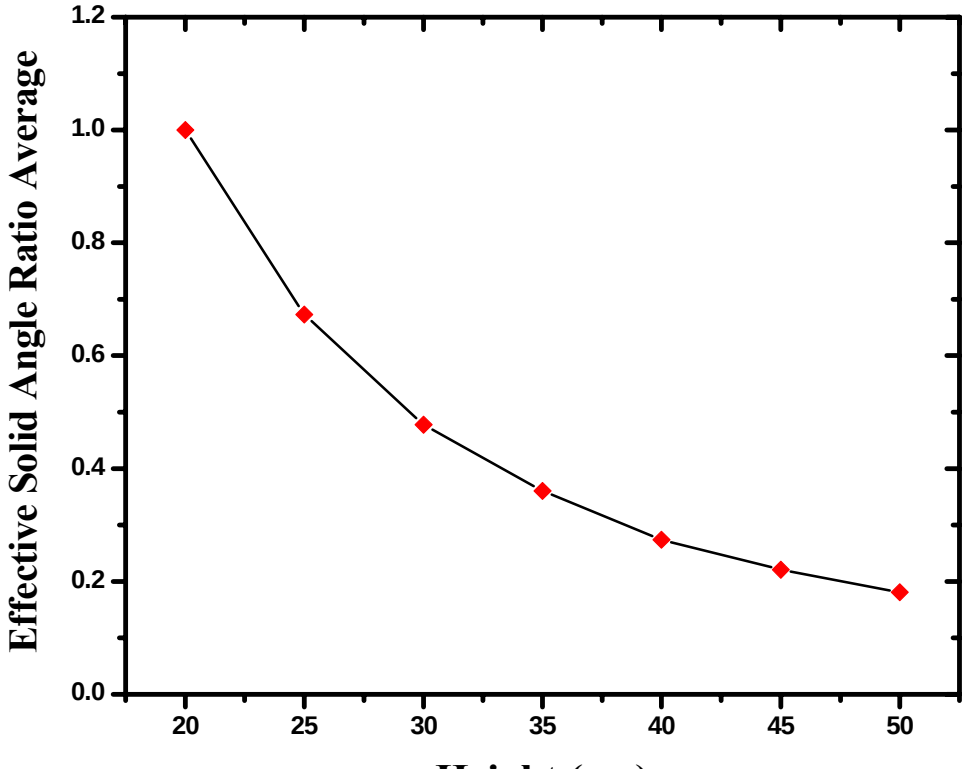

Figure 3 Relation between source height from the detector and the average value of the effective solid angle ratio

REFERENCES

(1) C.M. Salgado , L.E.B. Brandão, R. Schirru, C.M.N.A. Pereira, C.C. Conti, Validation of a NaI(Tl) detector's model developed with MCNP-X code. Progress in Nuclear Energy 59 (2012) 19-25

(2) T.Vidmar , N. Celik, N.CornejoDiaz, A.Dlabac, *et al,* Testing efficiency transfer codes for equivalence Applied Radiation and Isotopes 68 (2010) 355–359

(3) Gilmore, G.R., 2008. Practical Gamma-ray Spectrometry, second ed Wiley, New York.

(4) Marie-Christine Le´py_, Philippe Brun, Claude Collin, Johann Plagnard, Experimental validation of coincidence summing corrections computed by the ETNA software. Applied Radiation and Isotopes 64 (2006) 1340–1345

(5) Badawi, M.S., 2010. Comparative Study of the Efficiency of Gamma-rays Measured by Compact-and Well Type-Cylindrical Detectors. PhD. Thesis, Faculty of Science, Alexandria University, Egypt 2010.

(6) Pibida, L., S.S. Nafee, M. Unterweger, M.M. Hammond and L. Karam, et al., 2007. Calibration of HPGe gamma-ray detectors for measurement of radioactive noble gas sources. Applied Radiat. Isot. J. 65: 225-233.

Mass attenuation coefficients of Li_2O- B_2O_3 glass system at 0.662 and 1.25 MeV gamma energies

H.E. Donya*
Faculty of Science, Physics Department, Menoufia University, Egypt.
**Hossam Elsayed Donya (donyavip@menofia.edu.eg), Tel: 00201004164148*

ABSTRACT

Borate glasses are very promising materials for the radiation dosimetry applications in view of the fact that their effective atomic numbers (Z_{eff}) are very close to that of human tissue and having a high ability of hosting activators. The total mass attenuation coefficients, partial interactions and Z_{eff} of glass system (100-x)B_2O_3-xLi_2O (where x=5, 10, 15, 20, 25, 30, 35 and 40 mole %) have been calculated at photon energies 0.662 and 1.25 MeV using WinXCom software on the basis of mixture rule. Results indicated that the total mass attenuation coefficients showed a decrease with increasing the Li_2O content, due to a decrease in Compton scattering probability, which gave a dominant contribution to the total mass attenuation coefficients for the studied glass samples at both energies. However, the photoelectric absorption and coherent scattering showed an increase with increasing the Li_2O, concentrations at same energies. For a comparison, the total mass attenuation coefficients of the glass system had lower values at the energy 1.25 MeV than that at 0.662 MeV. Z_{eff} was found to increase linearly with the increase of Li_2O concentrations. It was concluded that low Li_2O concentrations in glass system, under study, have Z_{eff} closed to that of biological tissue (Z_{eff}=7.42) and have higher total absorption coefficients at energy of 0.662 MeV than that at 1.25 MeV. These results are very useful in designing gamma radiation detectors using thermoluminescence technique. Therefore, it is recommended to use low Li_2O content in Li_2O-B_2O_3 glass system which makes it suitable for radiation detection purposes in medical applications.

Keywords: *Borate glasses/Effective atomic number/Mass attenuation coefficients /Thermoluminescence.*

1. INTRODUCTION

New thermoluminescent (TL) materials are suitable for radiation detection in the last several years that have been produced and studied. Special attention was given to different glass systems by our group because of their high TL sensitivity and their negligible fading [1-3]. In our previous paper [1], it is showed that Li_2O-B_2O_3 glass system has good TL properties

to be considered as a new added candidate to the member of the currently being used dosimetric tree. The response of a thermoluminescent material to γ- ray detection depends on the atomic number of its constituents; then it is important to know first the effective atomic number of such material, Z_{eff}, for obtaining its expected TL response at different energies. This was carried out by calculating the strength of different interaction probabilities (cross-sections) between gamma rays and the studied materials (detectors) [4].

2. METHOD OF CALCULATION

The effective atomic number, Z_{eff} of a thermoluminescent material (a composite) can be calculated according to the following equation [5, 6]:

$$Z_{\text{eff}} = \sqrt[b]{a_1 Z_1^{\,b} + a_2 Z_2^{\,b} + ...} \tag{1}$$

with

$$a_i = \frac{n_i(Z_i)}{\sum_i n_i(Z_i)}, \qquad n_i = N_A Z_i$$

where a_1, a_2,… are the fractional contents of electrons belonging to different elements of atomic number Z_1, Z_2, ….etc in the composite, n_i is the number of electrons, in one mole, belonging to each element Z_i and N_A is the Avogadro's number. The values of *b* are in the range from 2.94 to 3.5.

The total mass attenuation coefficient of a mixture or compound $(\mu/\rho)_m$ has been calculated by WinXCom, based on the mixture rule [7], where

$$\left(\frac{\mu}{\rho}\right)_m = \sum_i^n w_i \left(\frac{\mu}{\rho}\right)_i \tag{2}$$

$(\mu/\rho)_i$ is the mass attenuation coefficient for the individual element in each component and w_i is the fractional weight of the element in each component. This equation is valid when the effects of molecular binding, chemical and crystalline environment are negligible. Berger and Hubbell developed XCOM for calculating the total mass absorption coefficients or photon interaction cross- sections for any element, compounds or mixtures in a wide range of photon energies (from 1keV to 100 GeV). Recently, XCOM was transformed to the Windows platform by Gerward et al. [8], called WinXCom and our calculations were extracted using this software.

3. RESULTS AND DISCUSSIONS

In this study, the *(*100-*x)*B_2O_3-*x*Li_2O glass system (where x=5, 10, 15, 20, 25, 30, 35 and 40 mole %) was converted to weight fraction and given in table (1). For an example LiB_5 sample refers to the composition $95B_2O_3$-$5Li_2O$.

Table (1). Chemical composition of samples and compound mole fraction of each in the mixture of the studied glass systems

Sample	B_2O_3 (Mol. %)	Li_2O (Mol. %)
LiB_5	95	5
LiB_{10}	90	10
LiB_{15}	85	15
LiB_{20}	80	20
LiB_{25}	75	25
LiB_{30}	70	30
LiB_{35}	65	35
LiB_{40}	60	40

The total mass attenuation coefficients, of the studied glass systems were calculated at two photon energies 0.662 (^{137}Cs-source) and 1.25 MeV (average energy of ^{60}Co-source) using the WinXCom software on the basis of mixture rule.

3.1 Photoelectric mass absorption cross section (μ_m^{ph})

Based on our calculations, it was found that the photoelectric cross section (μ_m^{ph}) of the studied glass system at 0.662 and 1.25 MeV showed a decrease with increasing the Li_2O concentrations (see Fig. 1).

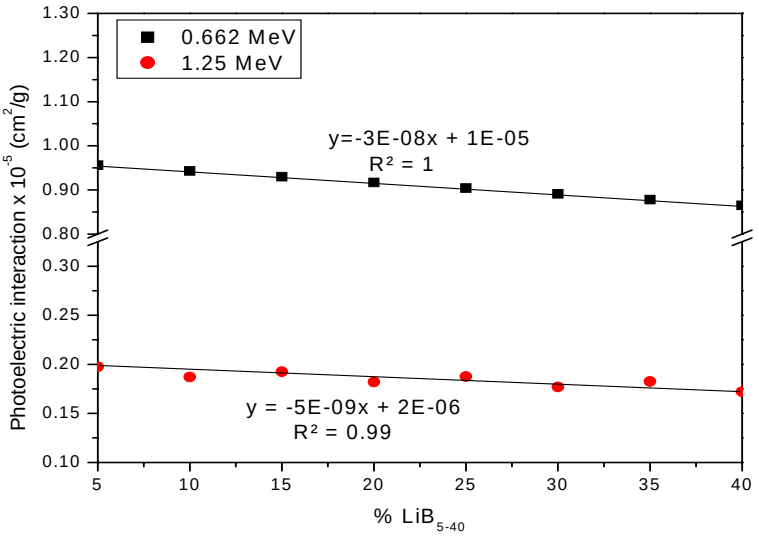

Fig. (1). The photoelectric mass absorption coefficient of (100-*x*) B_2O_3-*x*Li_2O glass system (where x=5, 10, 15, 20, 25, 30, 35 and 40 mole %).

It is clear from Fig. 1 that the values of μ_m^{ph} at low photon energy (0.662 MeV) are higher than those at high energy (1.25 MeV). In addition, the slope of the straight line between μ_m^{ph} and *x* at 0.662 MeV is higher than that at 1.25 MeV. Therefore, the effect of increasing Li_2O, and accordingly decreasing the B_2O_3 concentrations, showed a decrease in the μ_m^{ph} values of the studied glass systems at both energies.

3.2 Compton and coherent scattering

Compton scattering mass attenuation coefficients (μ_m^{cs}) of the studied glass system were calculated using WinXcom software. Results are given in Fig. 2 where μ_m^{cs} values show an observed decrease with increasing Li_2O concentration. Also, values of μ_m^{cs} at 0.662 MeV are higher than those at 1.25 MeV. Therefore, both μ_m^{ph} and μ_m^{cs} values are more effective at low energy value, i.e at 0.662 MeV.

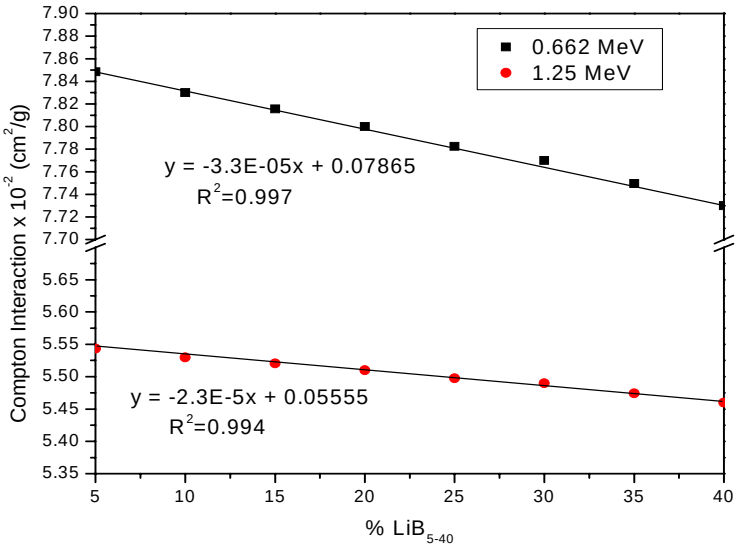

Fig. (2) The Compton scattering, interaction of *(100-x)* B_2O_3-*x*Li_2O glass system (where x=5, 10, 15, 20, 25, 30, 35 and 40 mole %).

The Coherent scattering mass attenuation coefficients (μ_m^{ch}) of the studied glass system were also calculated and results are represented in Fig. 3. μ_m^{ch} shows (see Fig.3) a decrease with increasing Li_2O concentration. The rate of increase in μ_m^{ch} is obvious at energy of 0.662 MeV where values of μ_m^{ch} are higher than those at 1.25 MeV.

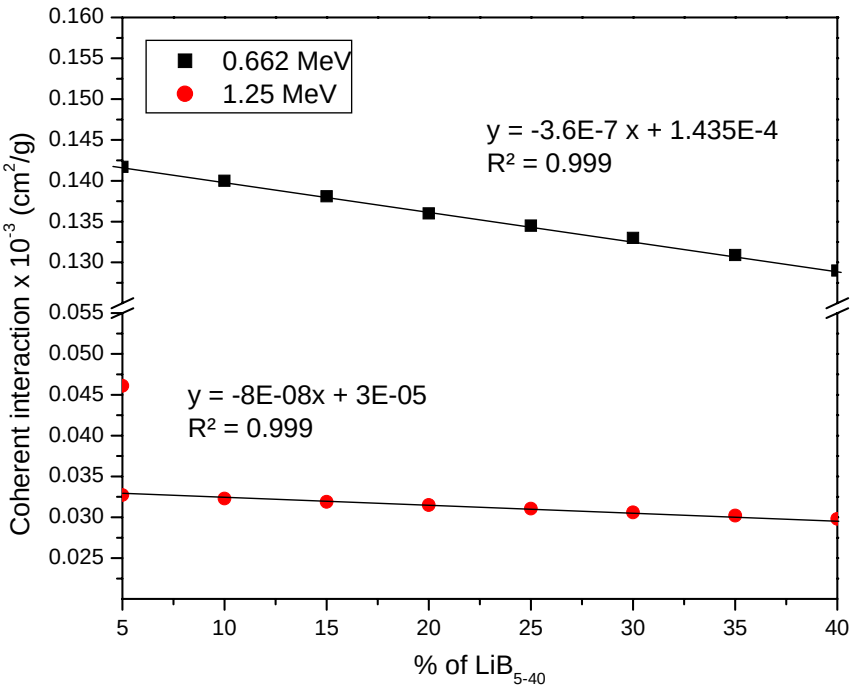

Fig. (3) The coherent scattering mass attenuation coefficient of (100-*x*) B_2O_3-*x*Li_2O glass system (where x=5, 10, 15, 20, 25, 30, 35 and 40 Mol. %).

From the above calculations of photoelectric, Compton and coherent interaction, the total mass absorption coefficient were calculated and illustrated in Table 2.

Table (2). Total absorption coefficient values of the studied glass system.

Sample	Energy	Coherent	Compton (cm^2/g)	Photoelectri	Sum
LiB_5	0.60	1.42×10^{-4}	7.85×10^{-2}	9.56×10^{-6}	7.86×10^{-2}
	1.25	3.27×10^{-5}	5.54×10^{-2}	1.98×10^{-6}	5.55×10^{-2}
LiB_{10}	0.60	1.40×10^{-4}	7.83×10^{-2}	9.43×10^{-6}	7.84×10^{-2}
	1.25	3.23×10^{-5}	5.53×10^{-2}	1.87×10^{-6}	5.53×10^{-2}
LiB_{15}	0.60	1.38×10^{-4}	7.82×10^{-2}	9.30×10^{-6}	7.83×10^{-2}
	1.25	3.19×10^{-5}	5.52×10^{-2}	1.93×10^{-6}	5.52×10^{-2}
LiB_{20}	0.60	1.36×10^{-4}	7.80×10^{-2}	9.17×10^{-6}	7.81×10^{-2}
	1.25	3.15×10^{-5}	5.51×10^{-2}	1.82×10^{-6}	5.51×10^{-2}
LiB_{25}	0.60	1.35×10^{-4}	7.78×10^{-2}	9.04×10^{-6}	7.80×10^{-2}
	1.25	3.11×10^{-5}	5.50×10^{-2}	1.88×10^{-6}	5.50×10^{-2}
LiB_{30}	0.60	1.33×10^{-4}	7.77×10^{-2}	8.91×10^{-6}	7.78×10^{-2}
	1.25	3.06×10^{-5}	5.49×10^{-2}	1.77×10^{-6}	5.49×10^{-2}
LiB_{35}	0.60	1.31×10^{-4}	7.75×10^{-2}	8.78×10^{-6}	7.76×10^{-2}
	1.25	3.02×10^{-5}	5.48×10^{-2}	1.83×10^{-6}	5.48×10^{-2}
LiB_{40}	0.60	1.29×10^{-4}	7.73×10^{-2}	8.65×10^{-6}	7.74×10^{-2}
	1.25	2.98×10^{-5}	5.46×10^{-2}	1.72×10^{-6}	5.46×10^{-2}

From table (2), one can notice that the total absorption coefficient closes to the Compton interaction values. To confirm the obtained values of the attenuation coefficient of the studied glass, the effective atomic number (**Z_{eff}**) should be calculated and compared the obtained data by the attenuation coefficient of the element with Z has the same or near Z_{eff}.

4. Z_{EFF} –CALCULATION

Z_{eff} was calculated for the studied glass samples [$LiB_{(5-40)}$] and given in Table 3 using Eq. (2). Column 1 gives the glass composition, element under study is given under column 2, the atomic weight, *A* and atomic number *Z* are given under columns 3 and 4, respectively. Weight fraction, *w*, and the total number of electrons per gm, $N_A Zw/A$ are displayed under columns 5 and 6 respectively. The fraction number of electrons due to each element in the composition is then calculated and given under column 7 and denoted by *a*.

The values of aZ^b were then calculated and given under the last two columns where *x* takes the values 2.94 and 3.5. Finally, values of Z_{eff} were calculated and given in the last row of each glass composition. For example, Z_{eff} values of LiB_5 glass composition were found to be 7.33 and 7.39 with a percentage difference of about 0.8% and of an average of 7.36.

Table (3). Z_{eff} calculation for our studied glass samples [$LiB_{(5-40)}$].

	Element	**A**	**Z**	***W***	**N_AZ W/A**	**a**	**a $Z^{2.94}$**	**a $Z^{3.5}$**
LiB_5	B	10.81	5	0.295	8.19×10^{22}	0.279	31.719	78.118
	O	16	8	0.684	2.06×10^{23}	0.702	317.203	1016.407
	Li	6.941	3	0.021	5.47×10^{21}	0.019	0.472	0.872
	Sum			1	2.93×10^{23}	1	349.394	1095.397
	Z_{eff}						**7.329**	**7.387**
LiB_{10}	B	10.81	5	0.27781	7.738×10^{22}	0.264	29.991	73.861
	O	16	8	0.67318	2.027×10^{23}	0.692	312.833	1002.404
	Li	6.941	3	0.049	1.275×10^{22}	0.043	1.101	2.037
	Sum			1	2.928×10^{22}	1	343.925	1078.302
	Z_{eff}						**7.290**	**7.354**
LiB_{15}	B	10.81	5	0.265	7.35×10^{22}	0.252	28.576	70.376
	O	16	8	0.674	2.03×10^{23}	0.694	313.582	1004.804
	Li	6.941	3	0.061	1.59×10^{22}	0.054	1.374	2.542
	Sum			1	2.92×10^{23}	1	343.532	1077.722
	Z_{eff}						**7.287**	**7.352**
LiB_{20}	B	10.81	5	0.245	6.824×10^{22}	0.234	26.573	65.442
	O	16	8	0.65714	1.979×10^{23}	0.679	306.809	983.105
	Si	6.941	3	0.09742	2.536×10^{22}	0.087	2.199	4.068
	Sum			1	2.915×10^{22}	1	335.582	1052.616
	Z_{eff}						**7.230**	**7.303**
LiB_{25}	B	10.81	5	0.235	6.52×10^{22}	0.224	25.412	62.584
	O	16	8	0.664	2.00×10^{23}	0.686	309.937	993.125
	Li	6.941	3	0.101	2.63×10^{22}	0.090	2.283	4.223
	Sum			1	2.91×10^{23}	1	337.632	1059.931
	Z_{eff}						**7.245**	**7.318**
	Element	**A**	**Z**	***W***	**N_AZ W/A**	**a**	**a $Z^{2.94}$**	**a $Z^{3.5}$**
LiB_{30}	B	10.81	5	0.21347	5.946×10^{22}	0.205	23.243	57.241
	O	16	8	0.64128	1.931×10^{23}	0.665	300.562	963.084
	Li	6.941	3	0.1452	3.779×10^{22}	0.130	3.290	6.0873
	Sum			1	2.903×10^{23}	1	327.095	1026.412
	Z_{eff}						**7.167**	**7.251**
LiB_{35}	B	10.81	5	0.205	5.68×10^{22}	0.196	22.227	54.740
	O	16	8	0.654	1.97×10^{23}	0.678	306.268	981.368
	Li	6.941	3	0.141	3.67×10^{22}	0.126	3.197	5.915
	Sum			1	2.90×10^{22}	1	331.692	1042.023
	Z_{eff}						**7.201**	**7.282**
LiB_{40}	B	10.81	5	0.18194	5.068×10^{22}	0.175	19.892	48.989
	O	16	8	0.62565	1.884×10^{23}	0.652	294.451	943.504
	Li	6.941	3	0.19242	5.008×10^{22}	0.173	4.378	8.100
	Sum			1	2.891×10^{23}	1	318.721	1000.593
	Z_{eff}						**7.104**	**7.198**

The variation of the mean values of Z_{eff} of the present glass system with Li_2O is given in Fig. 4. It is clear that (see Fig. 4), Z_{eff} decreases with increasing the Li_2O concentration and their values range from 7.15 to 7.36. This variation is represented by an excellent linearity form with R^2=0.99.

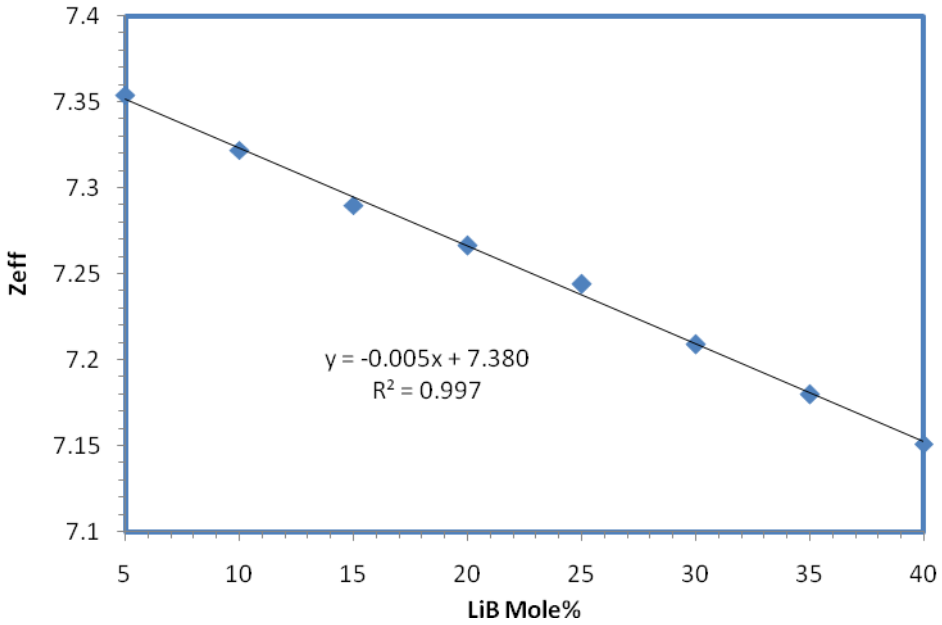

Fig(4) The effective atomic number of (100-*x*) B_2O_3-*x*Li_2O glass system (where x=5, 10, 15, 20, 25, 30, 35 and 40 mole %).

From the Z_{eff} calculations, one can notice that, the Z_{eff} for the studied glass are decreased from 7.35 to 7.15. So, the attenuation coefficient can be compared by an element closes to this range as Nitrogen atom [9] which has an attenuation coefficient value of 0.081 and 0.057 at gamma energies of 0.66 and 1.25 MeV respectively which is in a good agreement with our data (see table 2). Z_{eff} of LiB glass system have the same as soft tissue (Z_{eff} = 7.30 ± 1.25%) [10], which is recommended for dose measurements using insertion of LiB TL-detectors in various phantoms [1].

5. CONCLUSION

The total mass attenuation coefficients and partial interactions at photon energies 0.662 and 1.25 MeV *(*100-*x)* B_2O_3-*x*Li_2O glass system (where x=5, 10, 15, 20, 25, 30, 35 and 40 mole %) have been investigated using the WinXCom software. Results showed that total mass attenuation coefficients decreased with increasing Li_2O concentration, due to a decrease in Compton scattering of glass samples which contribute dominantly to the total interaction. Although, the coherent scattering showed a decrease with increasing Li_2O concentrations but it has lower values than Compton scattering. The photoelectric interaction has a slight influence in these glass samples on comparison to the effects of other two interactions. In addition, the Z_{eff} values of our studied glasses showed a decrease with increasing Li_2O

concentration and found to have values from 7.15 to 7.35. Results recommend Li_2O-B_2O_3 glass system as a TL γ-dosimeter especially at low Li_2O content. In addition the low Li_2O content in the glass system makes it very close to tissue equivalent material. Therefore, it is recommended to use low Li_2O content in Li_2O-B_2O_3 glass system as good gamma detectors at energy of 0.66 MeV.

6. REFERENCE

(1) A. El-Adawy, N. E. Khaled, A. R. El-Sersy, A. Hussein, and H. Donya, *Appl. Radiat. Isot.*, **68 – 6** (2010) 1132.

(2) N.E.Khaled, A.R.El-Sersy, H. M. El-samman, A.Hussein, A. El-Adawy and H. Donya, *World Acad. of Sci. Eng. and Techn.,* 76 (2011) 894.

(3) H. Donya, H.M. El-Samman, A. El-Adawy A. Hussein, A.R. El-Sersy and. N.E. Khaled , Tenth Radiation Physics & Protection Conference*, EG1100464,* 42(33) (2011) 135 ***www.iaea.org/inis/collection/NCLCollectionStore/Public/42/076/42076638.pdf***

(4) A.R. El-Sersy, A. Hussein, H.M. El-Samman, N.E. Khaled, , A. El-Adawy and H. Donya, *J. of Anal. and Nucl. Chem.*, **288** (2010) 65.

(5) P.R. González, , C. Furetta, B. E. Calvo, M. I. Gaso, E. Cruz-Zaragoza , Nucl. Inst. & Meth. Phys. Res. B **260** (2007) 685.

(6) C. Furetta, B.E. Calvo, M.I. Gaso, E. Cruz-Zaragoza*, Mod. Phys. Lett. B*, **22**(2008) 1997.

(7) D.F. Jackson, D.J. Hawkes, *Phys. Rep.* **70** (1981) 169.

(8) L. Gerward, N. Guilbert, K.B. Jensen, H. Levring, *Radiat. Phys. Chem.* **60** (2001) 23.

(9) http://physics.nist.gov/PhysRefData/XrayMassCoef/tab3.html (2013).

(10) Faiz M. Khan, "The Physics of Radiation Therapy" Lippincott Williams & Wilkins , 3rd ed., 2003.

Application of Virtual Wedge in Electron Beams of Mevatron Linear Accelerator

Ahmed L. El-Attar[1], Mahmoud A. Hefni[1], Moamen M. Aly[2], Mohamed I. El-Said[2] and Mostafa A. Hashem[2]

[1] *Physics Department, Faculty of Science, Assiut University*

[2] *Radiotherapy and Nuclear Medicine Department, South Egypt Cancer Institute, Assiut* University

ABSTRACT

In the year, 1997 Siemens introduced the virtual wedge (VW) in its linear accelerators for the use in photon beams radiation treatment. The idea was that a dose profile similar to that of a physical wedge can be obtained by moving one of the accelerator jaws at a constant speed and changing the dose rate. The application of VW is restricted for the photon beams Therefore, in this paper we developed the use of VW in electron beams of energies 7, 10, 12 and 14 MeV generated from a Siemens Mevatron linear accelerator. Dosimetric parameters including percentage depth doses (PDDs) and dose profiles for 10 × 10 cm^2 and 15 × 15 cm^2 applicators were measured. In addition, comparison between depth doses for open and wedged fields for all applicators and energies was made. This study showed that using the principles of VW in electron beams is visible and no difference in PDDs of VW beams compared with open beams.

Keywords: *virtual wedge, electron beam, radiotherapy.*

INTRODUCTION

The wedged fields are often used in many clinical situations to get homogeneous dose distribution around target volume[1]. In the year, 1975 Kutting and Ziegler developed a polystyrol wedge filters to improve the dose distribution in electron therapy[2], and in the year 1998 Eugene et. al. purposed the use of wedged electron fields to utilizing multiple electron beams using intensity modulation to improve the dose distribution[3]. The use of virtual wedge filters is a well-established method for dose inhomogeneity compensation in photon therapy[4]. The technique of the virtual wedge achieves wedge-shaped dose distributions by computer-controlled movement of one of the collimator jaws under simultaneous adjustment of dose rate. In this paper, we present a simple model based on using the principles of photon VW to operate VW in electron beams.

METHODS AND MATERIALS

1.Calculation model

The basic dosimetric principles of photon VW have been presented by van Santvoort[5]. The monitor unit (MU) in the wedge direction can be analytically described by an exponential function (1)[6-9],(1)

$$MU(Y) = MU(0)e^{(c\mu Y \tan\alpha)}$$

where Y is the distance away from the central axis, MU(Y) is the number of monitor units given at position Y, MU(0) is the number of monitor units at the central axis, μ is a generic effective linear attenuation coefficient in water for the nominal beam energy, and α is the desired wedge angle. c = c (E) is a factory-set attenuation calibration factor near unity, used to more accurately specify μ for the specific beam. The wedge angle α can be set to any desired value when treating a patient.

For Siemens linear accelerator, the virtual wedge is only implemented in the direction of Y-jaws. For each Y-jaw, the maximum open position is 20 cm, and the maximum to pass the central axis is 10 cm. Since only one jaw is employed in the wedge operation, the maximum range of the moving jaw is +20 to -10 (30) cm.

2.Virtual wedge implementation

The option of irradiation using virtual wedge in the electron mode is not available in the linear accelerator. Therefore, a way to implement this option was developed. For each applicator the secondary collimator opens for a larger field size to cover the upper aperture of the applicator. This large field size was divided to smaller fields (segments) by closing the jaw in the direction of the desired wedge angle. The number of MU per each segment was calculated using the equation (1) and delivered. This process was repeated until the jaw reaching the original location.

3.Measurements

The beam profiles and depth doses, measured for 7, 10, 12 and 14 MeV, were carried out using Kodak X-Omat V films which is a well established method for electron beam dosimetry[4]. These films were then used for the measurement of dose distributions in wedged fields[10]. Measurements of percentage depth dose (PDD) and beam profiles with film were carried out by removing the film from its envelope in a dark room, sandwiching it between two slabs of solid water with the edges sealed using black tape. The film place parallel to the electron beam, as shown in Figure (1), and additional solid water is add on bath sides until there is at least 5 cm of excess phantom on each side of the field to ensure reaching a good electron equilibrium around the film. Finally, the film assembly is align to the surface of the phantom and entice assembly is tighten with a clamp to prevent artifacts which might arise due to air pockets between the film and the phantom. The X-Omat films were irradiated with VW angles, 15°, 30°, 45°, and 60° for applicator sizes 10 × 10 cm^2 and 15 ×15 cm^2. The surface of the film was placed at the target to surface distance (TSD) of 100 cm and beam profiles at depths d_{max}, $d_{90\%}$, $d_{80\%}$, $d_{70\%}$, $d_{60\%}$ and $d_{50\%}$ cm and percentage depth doses were read out using laser densitometer scanner (DynaScan dosimetry system, CMS Associates Inc.).

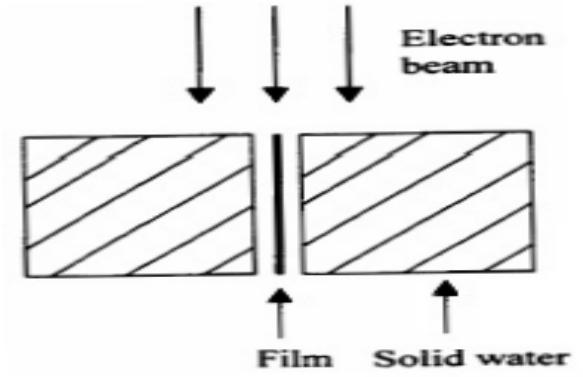

Figure (1): PDD and Beam profiles measurements setup with film and solid water.

RESULTS AND DISCUSSION

Figure (2) displays the percentage depth doses for open and virtual wedge angles of 15°, 30°, 45°, and 60° with the applicator size of 15 × 15 cm^2 at TSD of 100 cm for 7, 10, 12 and 14 MeV electron beams. It is clear that there is no change in the PDDs due to the use of virtual wedge even at different wedge angles, compared to the open PDD. These results are in a good agreement with[11, 12] where they found that down to 10 cm, in case of photon beams, the PDD for open and virtual wedge were identical. This can be justifying due to the absence of any hardening materials in the beam direction that could alter the PDD.

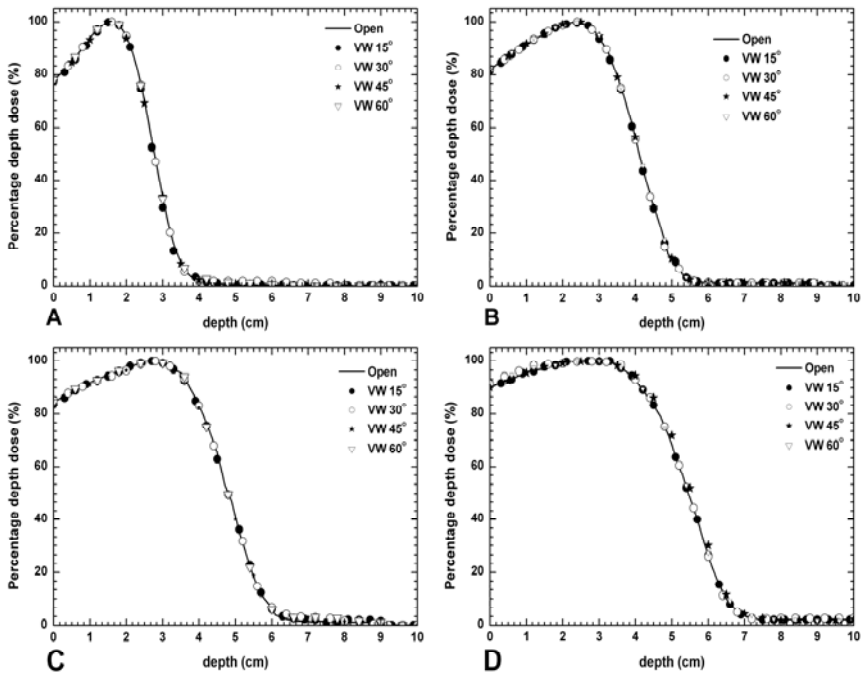

Figure (2): The percentage depth dose of 15 × 15 cm^2 applicator at TSD of 100 cm for open and 15°, 30°, 45°, and 60° virtual wedges for (A) 7 MeV, (B) 10 MeV, (C) 12 MeV and (D) 14 MeV electron beams.

Off-axis profiles for the open and wedged (15°, 30°, 45° and 60°) fields in the wedges direction at the depth of maximum dose, d_{max} and TSD of 100 cm for the applicator sizes of 10 × 10 cm^2 and 15 × 15 cm^2 in the 7 and 14 MeV electron beams were presented in figures (3) and (4) respectively.

Off-axis profiles in the wedge direction showed a small change with the electron beam energy at the same virtual wedge angle, which found to be similar to those found in photon beams[13]. However, the profiles shape and tilt were overlapped for each virtual wedge angle (15^o, 30^o, 45^o, and 60^o) and energy (7, 10, 12, and 14 MeV) while changing the applicator size (10 × 10 cm^2 and 15 × 15 cm^2). The Penumbra values (Penumbra is the average distance separating the 80% and 20% isodose lines) for VW fields were less than open fields for all energies and applicator sizes.

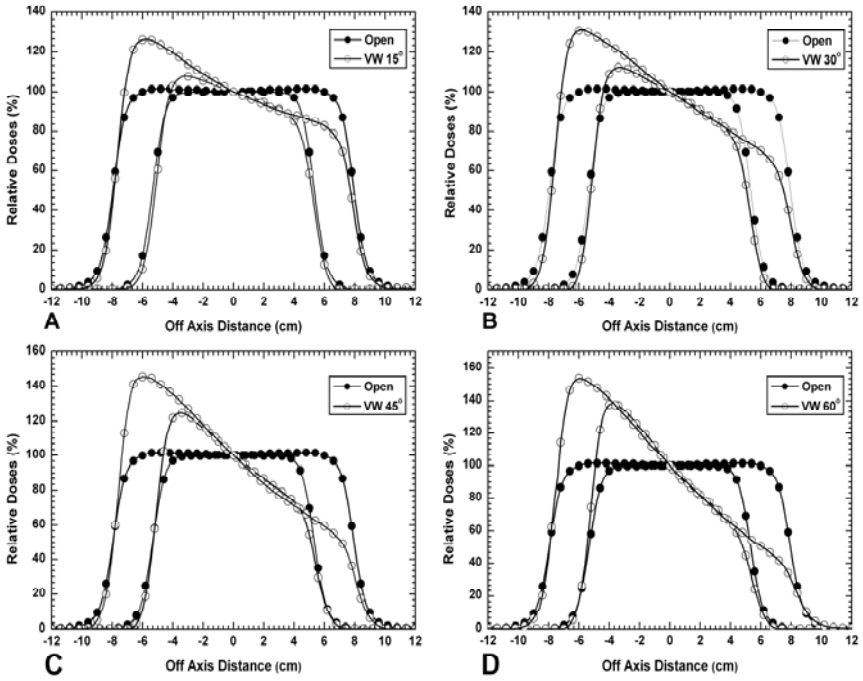

Figure (3): Off-axis profiles of applicator sizes 10 × 10 cm^2 and 15 × 15 cm^2 at the depth of d_{max} while TSD equal to 100 cm for open and (A) 15°, (B) 30°, (C) 45° and (D) 60° virtual wedge angles in 7 MeV electron beam.

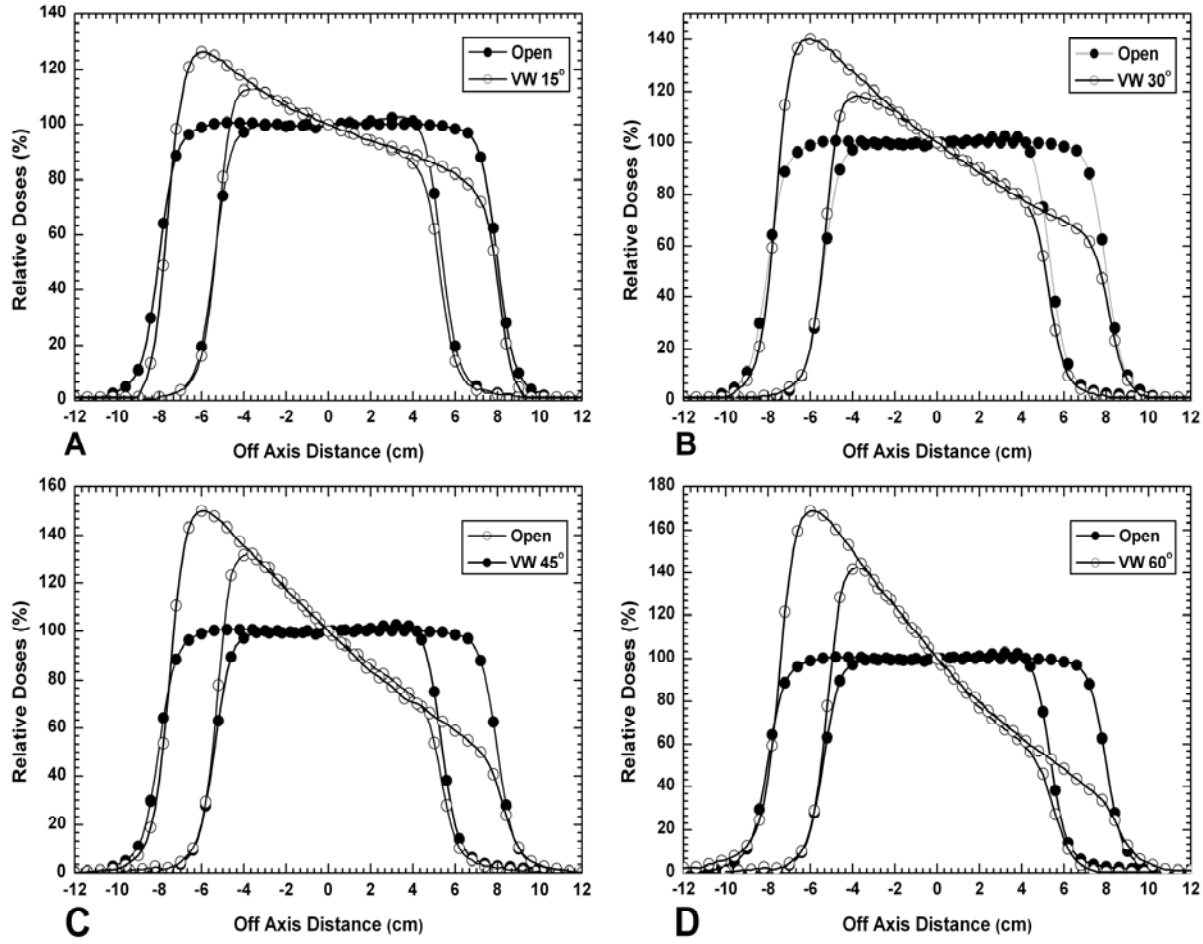

Figure (4): Off-axis profiles of applicator sizes 10 × 10 cm^2 and 15 × 15 cm^2 at the depth of d_{max} while TSD equal to 100 cm for open and (A) 15°, (B) 30°, (C) 45° and (D) 60° virtual wedge angles in 14 MeV electron beam.

Table (1) show the penumbra values for open and (15°, 30°, 45° and 60°) wedges at the depth of d_{max} and TSD of 100 cm in 7, 10, 12 and 14 MeV beams with applicator sizes of 10 × 10 cm^2 and 15 × 15 cm^2.

The electron open field penumbra (20%–80% intensity) decreased with higher energies. For the same energy, it has been found that the penumbra decreased with increase wedge angle. At high energies, the beam is more forward scattered, with less lateral scattering, giving rise to a narrow penumbra. This is expected because high-energy electrons are subject to less scattering[14].

Table (1): Penumbra values of applicator sizes 10 × 10 cm^2 and 15 × 15 cm^2 at the depth of d_{max} while TSD equal to 100 cm for open and 15°, 30°, 45° and 60° virtual wedge angles in 7 MeV, 10 MeV, 12 MeV, 14 MeV electron beams.

		7 MeV	10 MeV	12 MeV	14 MeV
Open	10 × 10 cm^2	1.17	1.15	1.13	1.12
	15 × 15 cm^2	1.21	1.19	1.18	1.17
Wedge 15^0	10 × 10 cm^2	0.96	0.94	0.93	0.91
	15 × 15 cm^2	0.99	0.96	0.91	0.90
Wedge 30^0	10 × 10 cm^2	0.92	0.9	0.88	0.87
	15 × 15 cm^2	0.94	0.91	0.90	0.89
Wedge 45^0	10 × 10 cm^2	0.85	0.82	0.81	0.79
	15 × 15 cm^2	0.92	0.89	0.87	0.86
Wedge 60^0	10 × 10 cm^2	0.82	0.81	0.79	0.75
	15 × 15 cm^2	0.84	0.82	0.81	0.79

Figures (5) and (6) show the isodose distributions crossing the central axis for 7 MeV and 14 MeV beams respectively, for open and, 15^o, 45^o, and 60^o virtual wedge angles in 15 × 15 cm^2 field sizes at 100 cm TSD. It is clear the effect of using the virtual wedge on the isodose curves.

Experimental Study of Using Wax Wedge Filter in Electron Beams

Mahmoud A. Hefni[1], Ahmed L. El-Attar[1], Moamen M.O. Aly[2], Mohamed I. El-Said[2], and Mostafa A. Hashem[2]

[1] *Physics Department, Faculty of Science, Assiut University*

[2] *Radiotherapy and Nuclear Medicine Department, South Egypt Cancer Institute, Assiut University*

ABSTRACT

Wedged beams are often been used in clinical photon radiotherapy to compensate missing tissues and dose gradients. In this work, we designed a wedge filter made of wax to be implemented in electron beams radiotherapy. Measurements were carried out for a hexahedral high-energy electron beams (5-14 MeV) generated by Siemens Mevatron linear accelerator by using radiographic film dosimetry for off-axis dose profiles and depth doses measurements. This study showed that there was a large difference between open and wedged PDD and this difference was decreased with electron beams energy increase. Therefore, we recommend using wax wedge filters with higher electron energies, and take into account the increase in the surface dose and the decrease of the depth of maximum dose when used with low electron energies

Keywords*: physical wedge, electron wedge, dose gradient*

INTRODUCTION

Treatment with megavoltage electron beams is ideal for irradiating shallow seated tumors because of their short range in tissues[1]. The homogeneous dose distribution is usually obtained by means of setting appropriate weights to individual beams and/or by modifying the dose distribution of the individual beams by using wedges or compensators[2]. The treatment of adjacent fields using the electron beams is a lengthy and complicated process[3]. However, the treatment of extended areas with electrons often requires the use of two or more adjacent fields. In such cases, unacceptably large dose variations may arise at the junction of the fields. These dose variations come from the presence of large bulges in the low value isodose curves created by electron beam divergence and lateral scattering in tissues. Overlapping of these bulges creates a high dose region at depth, while the constriction of the isodose curves near the surface may produce a low-dose region, depending critically on the field separation[4]. To overcome this problem, several authors have proposed techniques for matching electron beam edges in such a way as to make the overlap region as uniform as possible.

In the year 1975 H. Kuttig et al were used polystyrol wedge filters to obtain a uniform dose distributions during electron therapy[5]. B. Lachance et al were described a method to modify an electron beam to produce a wide penumbra and yield an excellent dose uniformity

at the junction between adjacent electron fields using a Lipowitz metal block placed on top of the electron applicator's insertion plate and positioned to stop part of the electron beam[6]. M. G. Karlsson et al were used photon MLC to increase the penumbra for electron fields[7-10]. E. P. Lief et al were used electron over photon radiation, by exploiting the rapid fall-off in dose with depth to create wedged electron fields using intensity modulation[11]. In the year, 2012 H. Mosalaei et al were developed this technique to reduce electron beam penumbra by adding low-energy intensity-modulated radiation therapy (IMRT) photons (4 MV)[1]. In this work, we proposed a wedge filter made of paraffin wax to compensate dose gradients of electron beams, and to assist in solving the adjacent fields' problem.

MATERIALS AND METHODS

We designed a wedge filter made of paraffin wax. It was mounted in a U shaped wooden frame to protect wedge from damages and movement during the experiment as shown in Figure (1). The wax wedge position was on top of the applicator at source to wedge distance(SWD) of 56 cm. The wedge filter has been used as a universal wedge hence it was used for all applicator sizes; where the wedge filter was centered in respect to the beam central axis.

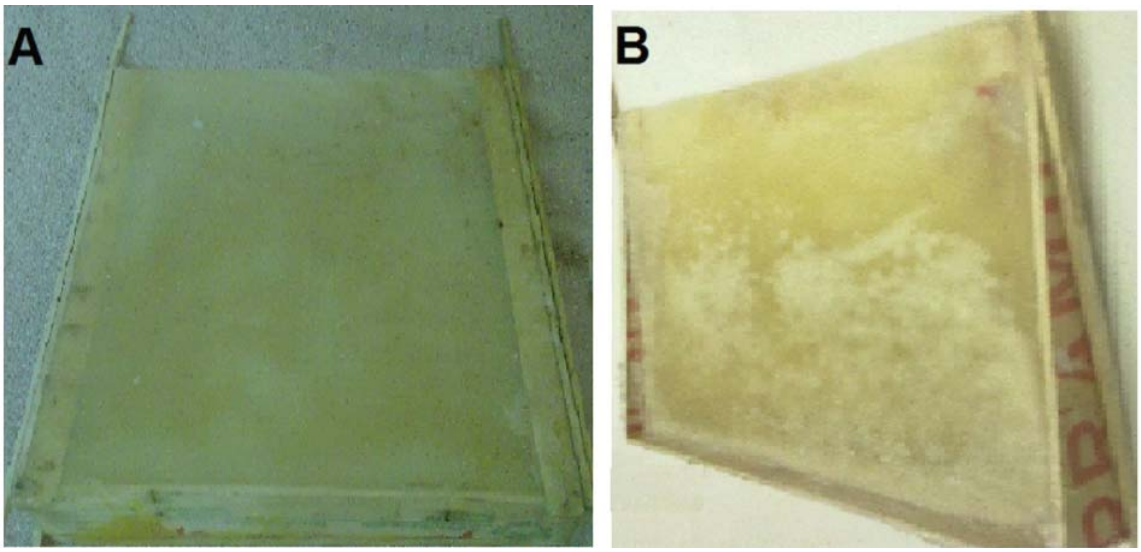

Figure (1): Wedge filter made of wax (A) backside (B) front side.

The beam profiles and percentage depth doses were carried out using Kodak X-Omat V films for electron energies 5, 7, 8, 10, 12 and 14 MeV, , which is a well-established method for electron beam dosimetry[12]. These films were used for the measurement of dose distributions in wedged fields[13]. Measurements of percentage depth dose (PDD) and beam profiles with film were carried out by removing the film from its envelope in a dark room, sandwiching it between two slabs of solid water with the edges sealed using black tape. The film placed parallel to the electron beam central axis, and additional solid water is add on both sides until there is at least 5 cm of excess phantom on each side of the field to ensure reaching a good electron equilibrium around the film. Finally, the film assembly is align to the surface of the phantom and entice assembly is tighten with a clamp to prevent artifacts which might arise due to air pockets between the film and the phantom. The X-Omat films were irradiated

with the universal wedge for applicator sizes 10 × 10 cm^2, 15 × 15 cm^2 and 20 ×20 cm^2. The surface of the film was placed at the target to surface distance (TSD) of 100 cm and beam profiles at depths d_{max}, $d_{90\%}$, $d_{80\%}$, $d_{70\%}$, $d_{60\%}$ and $d_{50\%}$ cm and percentage depth doses were read out using laser densitometer scanner (DynaScan dosimetry system, CMS Associates Inc.).

The most probable energy (E_{p0}) at the phantom surface for the reference field size was calculated using the following equation (1)[14].

$$E_{p0} = C_1 + C_2 R_p + C_3 R_p^2 \quad (1)$$

Where C_1=0.22 MeV, C_2=1.98 MeV cm^{-1}, C_3=0.0025 MeV cm^{-2} and R_p is the practical range in centimeters.

The mean energy of the electron field in the phantom surface was calculated by equation (2)[15, 16].

$$E_{0(mean)} = C_4 R_{50} \quad (2)$$

Where C_1=2.33 MeV cm^{-1} and R_{50} is (the depth at which the dose is 50% of the maximum dose)

RESULTS AND DISCUSSION

Figure (2) displays the percentage depth dose (PDD), or the depth dependence of dose for open and wedged fields for 5, 7, 10 and 14 MeV electron beams at 15 × 15 cm^2 applicator size. It shows that the open field has a larger PDDs than wedged fields. However, surface doses for wedged fields were larger than those of open fields, and depth of maximum dose (d_{max}) for wedged Wax fields were less when compared with those for open fields.

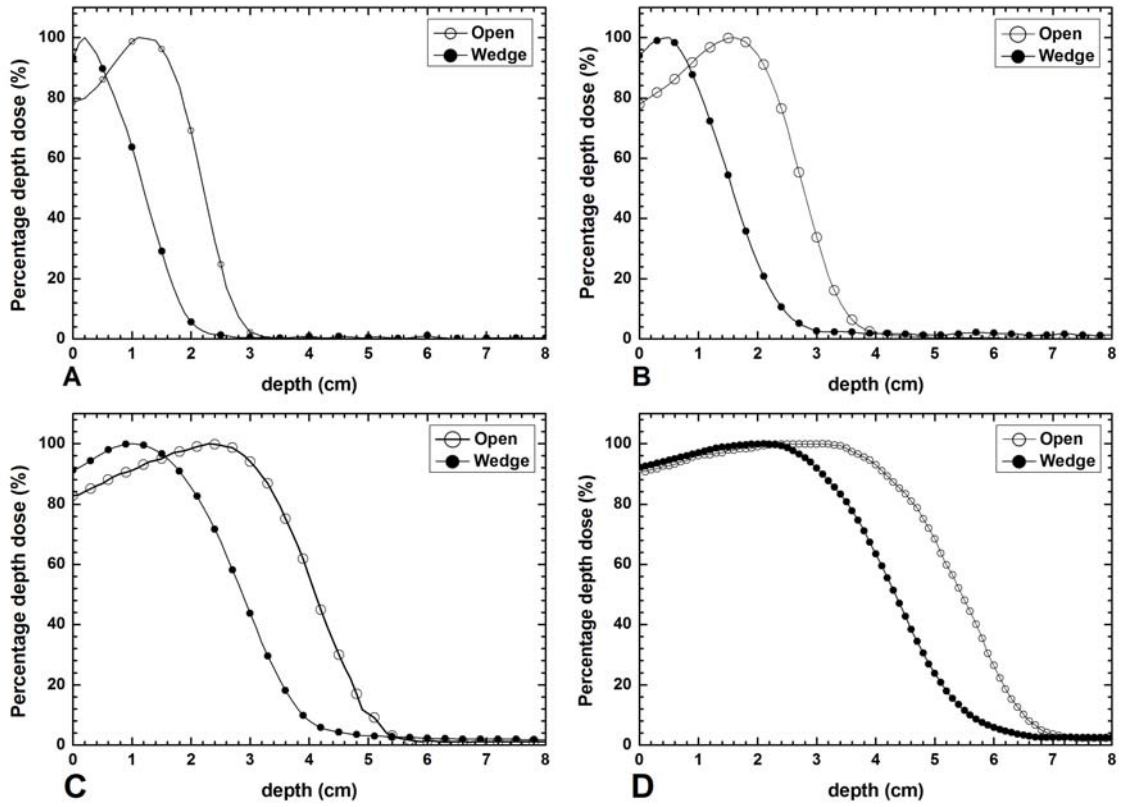

Figure (2): The percentage depth dose of 15 × 15 cm^2 applicator at TSD of 100 cm for open and wedged beams for (A) 5 MeV, (B) 7 MeV, (C) 10 MeV and (D) 14 MeV electron beams.

Figure (2) show the difference in PDDs between open and wedged Wax field decreases with the electron beam increases. This has pointed out by Ekstrand and Dixon[17-19], who showed that the beam obliquity tends to shift d_{max} toward the surface, and decrease the depth of penetration. In addition, Wedge's material (paraffin wax) was used in electron beam therapy as Bolus, to flatten out an irregular surface, reduced the penetration of the electrons and increased the surface dose[16].

R_p and R_{50} measured from the PDDs were used to calculate the most probable energy and the mean energy of open and wedged electron field using equation (1) and equation (2) for 5, 7, 8, 10, 12 and 14 MeV, and all data were tabulated in table (1).

Table (1): Calculation of the most probable energy and the mean energy of the electron field 15 × 15 cm^2 for open and wedged beams in 5, 7, 8, 10, 12, 14 MeV electron beams using equations (1) and (2).

Energy	Filed (15×15) cm^2	R_{max}	R_{50}	R_p	E_{p0}	$E_{0(mean)}$	$\frac{E_{p0}(wedge)}{E_{p0}(open)}$ %	$\frac{E_{0(mean)}(wedge)}{E_{0(mean)}(open)}$ %
5 MeV	**Open**	1.1	2.2	2.8	5.78	5.13	**70.38**	**54.09**
	Wedge	0.2	1.19	1.94	4.07	2.77		
7 MeV	**Open**	1.6	2.78	3.5	7.18	6.48	**72.22**	**56.12**
	Wedge	0.5	1.56	2.5	5.19	3.63		
8 MeV	**Open**	1.8	3.15	4	8.18	7.34	**75.58**	**68.25**
	Wedge	0.7	2.15	3	6.18	5.01		
10 MeV	**Open**	2.3	4.1	5.1	10.38	9.55	**76.86**	**69.76**
	Wedge	1	2.86	3.9	7.98	6.66		
12 MeV	**Open**	2.7	4.8	5.9	11.99	11.18	**81.59**	**75.00**
	Wedge	1.7	3.6	4.8	9.78	8.39		
14 MeV	**Open**	3.1	5.45	6.6	13.40	12.70	**83.49**	**79.38**
	Wedge	2.1	4.326	5.5	11.19	10.08		

Table (1): Calculation of the most probable energy and the mean energy of the electron field 15 × 15 cm^2 for open and wedged beams in 5, 7, 8, 10, 12, 14 MeV electron beams using equations (1) and (2).

Table (1) shows that the depth of maximum dose shift toward the surface about 1 cm for all energies and this explains that the change in the depth of maximum dose related material wedge[16]. The most probable energy and the mean energy for wedged filed decreased by 29.62 % and 45.91% for 5-MeVand by 16.51% and 20.62% for 14-MeV, respectively, when compared with those for open field. The variation in most probable energy and mean energy decreases with increasing electron beam.

Figure (3) shows off-axis profiles at d_{max} cm depth for wedged field with 10 × 10 cm^2, 15 × 15 cm^2 and 20 × 20 cm^2 applicators in the wedge direction for 5, 7, 12 and 14 MeV electron beams. The off-axis profiles for wax wedge match well with field size change for all energies from 5-MeV to 14-MeV. The OARs with changing the field sizes were shown the accuracy of wedge design, and confirmed its validity for all fields and for all electron beams.

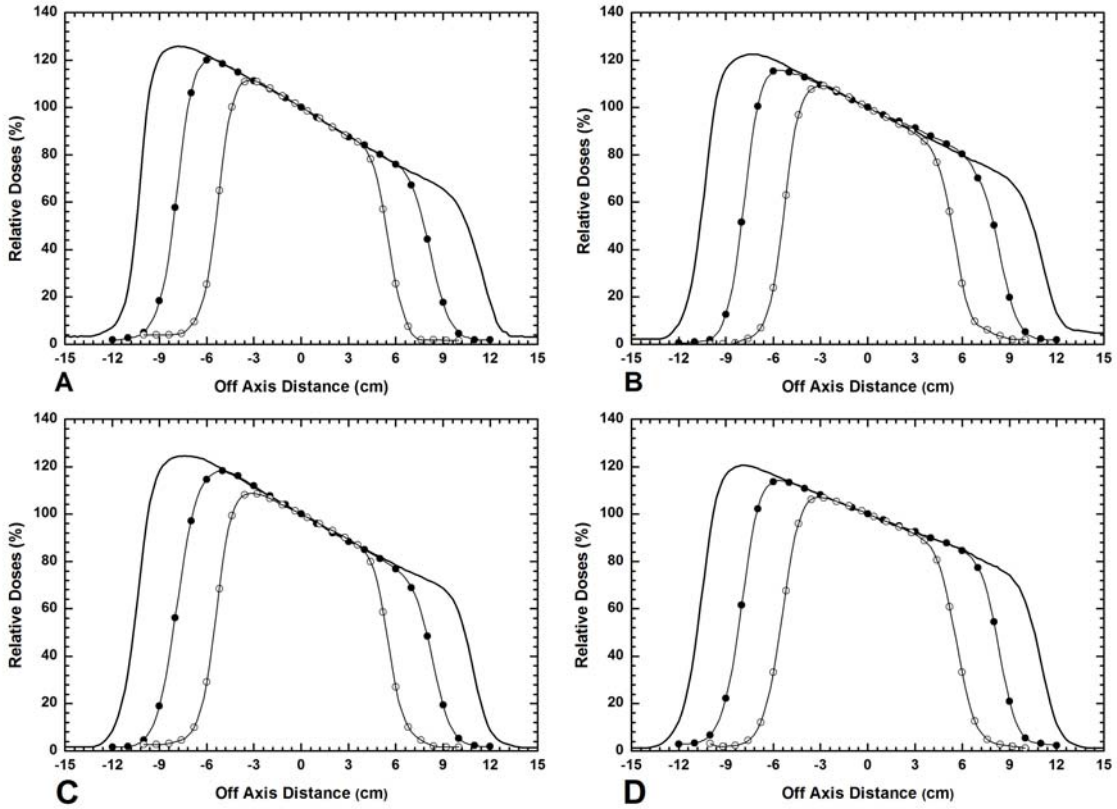

Figure (3): Off-axis profiles of 10 × 10 cm^2, 15 × 15 cm^2 and 20 × 20 cm^2 applicators for wedged beams at the depth of d_{max} while TSD equal to 100 cm for (A) 5 MeV, (B) 7 MeV, (C) 10 MeV and (D) 14 MeV electron beams.

Figures (4), (5) and (6) display the isodose distributions along the central axis for 5, 7 and 14 MeV beams respectively, for wedged field of 15 × 15 cm^2 applicator at 100 cm TSD. Those figures show that the wedge effect displays in practical therapeutic range and the wedge effect decrease with dose decrease.

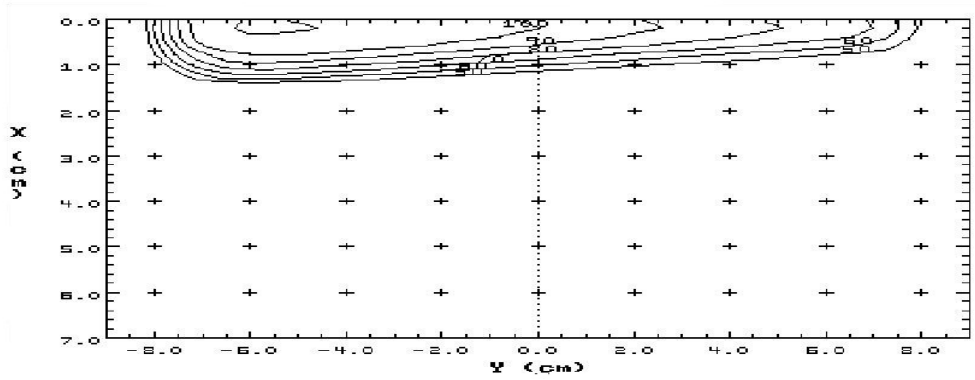

Figure (4): The isodose curves of 15 × 15 cm^2 applicator at TSD of 100 cm for Wax wedge for 5-MeV beam.

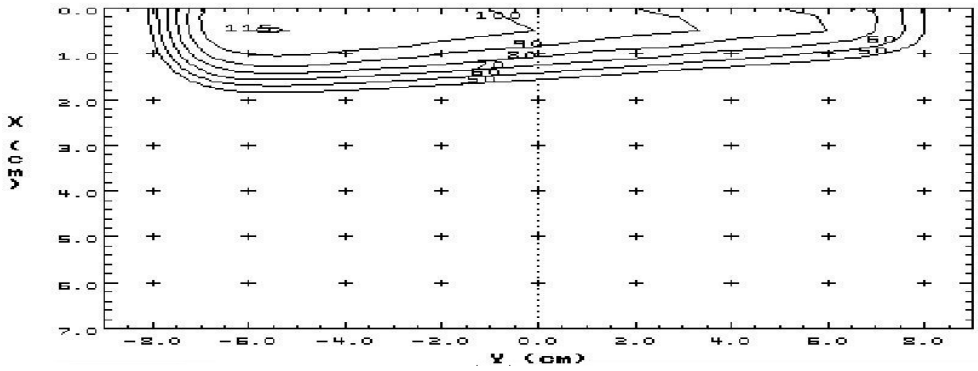

Figure (5): The isodose curves of 15 × 15 cm^2 applicator at TSD of 100 cm for Wax wedge for 7 MeV beam.

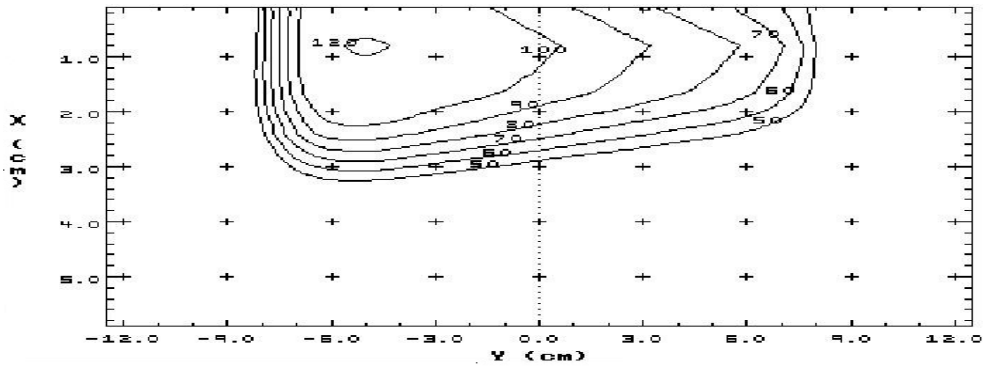

Figure (6): The isodose curves of 15 × 15 cm^2 applicator at TSD of 100 cm for Wax wedge for 14 MeV beam

CONCLUSION

We have presented a comprehensive and direct comparison of dosimetric characteristics of a universal wax wedge filter. There was a large difference between open and wedged PDD and this difference was decreased with electron beams energy increase. The Dose profiles in the wedge direction matched very well for all studied field sizes. Therefore, we recommend using wax wedge filters with higher electron energies, and take into account the increase in the surface dose and the decrease of the depth of maximum dose when used with low electron energies.

REFERENCE

(1) H. Mosalaei, S. Karnas, S. Shah, S. Van Doodewaard, T. Foster and J. Chen, Medical Dosimetry **37** (1), 76-83 (2012).

(2) P. F. Kukołowicz and K. Kamiński, Reports of Practical Oncology and Radiotherapy **11** (4), 183-189 (2006).

(3) F. Bagne, Physics in Medicine and Biology **23** (6), 1186 (1978).

(4) *Radiation oncology physics : a handbook for teachers and students*. (International Atomic Energy Agency, Vienna :, 2005).
(5) H. Kuttig and F. Ziegler, Strahlentherapie **150** (4), 383-388 (1975).
(6) B. Lachance, D. Tremblay and J. Pouliot, Medical Physics **24** (4), 485-495 (1997).
(7) M. Karlsson and B. Zackrisson, Radiotherapy and Oncology **29** (3), 317-326 (1993).
(8) B. Zackrisson and M. Karlsson, Radiother Oncol **39** (3), 261-270 (1996).
(9) J. M. Moran, M. K. Martel, I. A. Bruinvis and B. A. Fraass, Medical Physics **24** (9), 1491-1498 (1997).
(10) M. G. Karlsson, M. Karlsson and B. Zackrisson, Physics in Medicine and Biology **43** (5), 1159-1169 (1998).
(11) E. P. Lief, Y.-C. Lo and J. L. Humm, International journal of radiation oncology, biology, physics **40** (1), 233-243 (1998).
(12) K.Chełmiński, J. Rostkowska and M. Kania, Reports of Practical Oncology and Radiotherapy **10** (6), 293-300 (2005).
(13) K. Chełmiński, W. Bulski, J. Rostkowska and M. Kania, Reports of Practical Oncology and Radiotherapy **11** (2), 67-75 (2006).
(14) N. Khaledy, A. Arbabi and D. Sardari, Journal of Medical Physics **36** (4), 213-219 (2011).
(15) F. M. Khan, K. P. Doppke, K. R. Hogstrom, G. J. Kutcher, R. Nath, S. C. Prasad, J. A. Purdy, M. Rozenfeld and B. L. Werner, Medical Physics **18** (1), 73-109 (1991).
(16) F. M. Khan, *Physics of Radiation Therapy*, 4th ed. (Lippincott Williams & Wilkins, 2010).
(17) M. Müller and R. Zenker, Welding International **2** (2), 180-183 (1988).
(18) F. M. Khan, *The Physics of Radiation Therapy*, 3ed ed. (Lippincott Williams & Wilkins, 2003).
(19) Journal of the ICRU **4** (1), 39-48 (2004).

Measurements of U and Ra Activities in Drinking Water Samples and of Rn in Dwellings in Morocco. Calculation of Equivalent Effective Doses.

A. Choukri and O. K. Hakam
Laboratoire de Polymères, Rayonnements et Environnement, Equipe de Physique et Techniques Nucléaires, Faculté des Sciences, P.B 133, Kenitra, Morocco.
e-mai: choukrimajid@yahoo.com

ABSTRACT

Activities of uranium and radium isotopes were measured in some drinking water samples collected from wells, springs and tap water samples. The obtained results show that the 238U activity, is relatively higher in wells than in springs and 226Ra activity is more higher in hot springs. The results are similar to those published for other non polluting regions of the world and don't present any risk for public health in Morocco. In parallel measurements of indoor radon showed that the calculated effective dose for dwellings are comparable to those obtained in other regions in the word. The risks related to these activities could be avoided by simple precautions such the continuous ventilation.

Key words *: Natural radioactivity/ Indoor Radon / Drinking water/ Radioprotection*

INTRODUCTION

The natural radioactivity comes mainly from the primordial radio-nuclides in soils (40K and the 4n and 4n+2 series). Further, some cosmogenic radionuclides and/or radionuclides originated from a pollution can be found in natural waters used for drinking. The natural polluting radio-elements can rise from industrial wastes, geological erosion of U-bearing rocks or excessive utilization of agricultural fertilizers. Concentrations of natural radio-elements in water depend on the physico-chemical conditions and on the geological, geographical and socio-economical environment.

The natural radioactivity of groundwater varies greatly. High concentrations of natural radioactive elements have been found not only in water from U mines, but also in mineral water and in some drilled wells. The knowledge of U and Ra concentrations in drinking water is important because an appreciable fraction of the absorbed U and Ra is deposited in human bone, with the corresponding contribution to the internal dose.

Radon gas (222Rn) is commonly found in the environment and is known to be one of the principal sources of natural radiation exposure among human beings. Most of this exposure occurs inside homes, where many hours are spent each day and where the volumic activity of radon is usually higher than outdoors.

In this work, we have measured the activities of principal U and Ra isotopes such 234U, 238U, 226Ra and 228Ra in some drinking water samples, the volumic activities of Rn in some indoor dwillings and workplaces in Morocco. Then we have calculate from these results the equivalent doses and we have comparative them to Annual Limits of Incorporation by ingestion recommended by the International Commission of Radioprotection.

EXPERIMENTAL

Twenty liters of water are collected in a polyethylene tank and immediately slightly acidified to pH 2-3 with concentrated HNO3. After filtration, an iron carrier (FeCl3) and a known amount of 232U-228Th equilibrated spike solution are added. U and Th are coprecipitated with Fe(OH)3 by addition of NH4OH as described in (1,2). A known quantity of barium in BaCl2 form is then added. Ra isotopes are co-precipitated with BaSO4 formed by addition of H2SO4. The two precipitates are recovered by centrifugation and/or filtration.

Hydroxides containing U and Th are soluble in acid medium whereas BaSO4 coprecipitated with Ra is not soluble in this medium. The two fractions are separated by filtration or centrifugation.

After complete mixing and oxidation, U and Th are separated and purified on a single resin exchange column using a combinaison of acids and organic solvents. The are extracted separately with TTA (1-(2-thenoyl)-3,3,3-trifluoroacetone) in toluene in a nitric media at pH 3 and 1, respectively. The two organic phases containing U and Th are evaporated onto aluminium foils and flamed to remove any trace of carbon. The thin sources are, at the end, ready for alpha spectrometry.

Ra is extracted from the water samples by precipitation with BaSO4 after removal of U and Th as described above. The obtained powder is dried and sealed into a plastic ferrule whose form is compatible with the dimensions of the used well Germanium detector. The gamma spectrum is measured after 20 days which is necessary to ensure radioactive equilibrium between Ra isotopes and their daughters. Ra activity is measured by gamma spectrometry using a 220 cm3 low-background well type gamma ray detector in the Laboratoire Souterrain de Modane (LSM-Centre National de la Recherche Scientifique (CNRS-France)/Commissariat à l'Energie Atomique).

For radon, the passive time–integrated method of using a solid state nuclear track detector (LR-115 type II) was employed. These films, cut in pieces of 3.4×2.5 cm2, were placed in detector holders and enclosed in heat-scaled polyethylene bags. Calibration measurements were made giving a calibration factor of 0.58 tracks.cm-2/kBq.h.m-3 at the reference "removed thickness" of 6 μm (2,3). After exposure, the films were chemically etched in sodium hydroxide (2.5N) at 60°C for 120 minutes. The tracks produced were counted with an optical microscope and the background was then subtracted. After normalizing the track density to a removed thickness of 6 μm, the number of tracks per cm2 was correlated to the volumic activity of radon. Figure 1 show the relationships established between the volumic activity of 222Rn and the density of counted tracks.

In houses, detectors are exposed in the most frequented room. They are generally hung on the ceiling by a support. Detectors are got back after an exposure time of about 3 months. If the result of the first measure is below 5 Bq/m3, a priori abnormal situation, or exceeds 400 Bq/m3, a second measure is realized to confirm the result. Detectors are then developed and counted following the procedure described by Hakam (2)

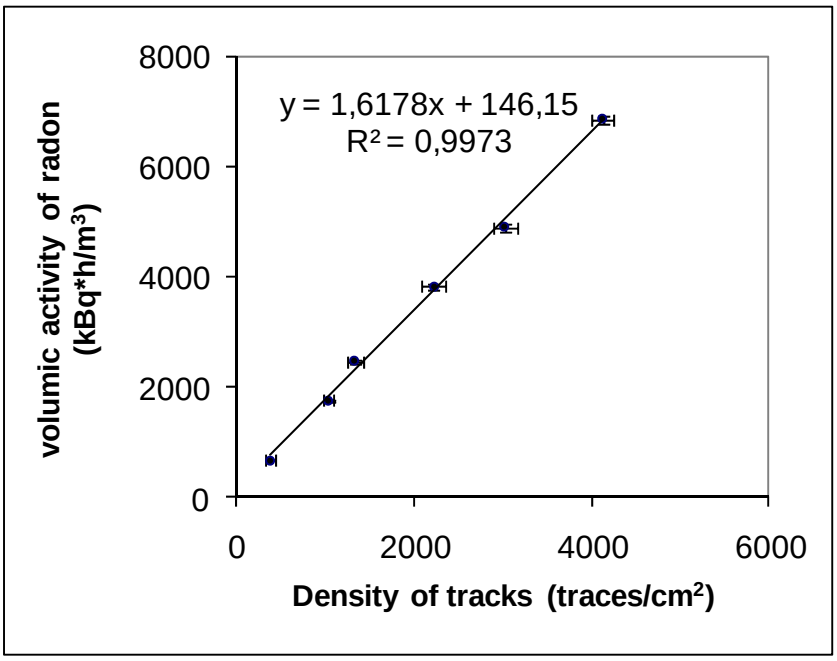

Figure 1: Calibration curve of cellulose nitrate films LR-115 type II

RESULTS AND DISCUSSION

The activities of uranium isotopes (^{234}U, ^{238}U) and radium isotopes (^{226}Ra,^{228}Ra), for the analyzed samples, are given in table 1. The equivalent doses in analyzed waters and their comparison to the Incorporation Annual Limits recommended by the International Commission of Radioprotection are given in table 2.

In springs, both Ra and U distributions are affected by temperature, salinity, and redox condition. High temperature tends to decrease U but to increase Ra concentrations. The decline of U concentration may result from the retrograde stability of uranyl carbonate complexes (4). High temperature may increase Ra concentrations by reducing adsorption coefficients for the divalent Ra ions (5). Although solid solutions with celestite, barite, or other alkaline-earth sulphates or carbonates may control soluble Ra concentrations in some cases (6). The aqueous chemistry of Ra may also be greatly influenced by redox state of the environment, but the effect is opposite to that for U. In geothermal sources where the temperature and the concentration of the chlorine are very elevated and the reducing potential is very weak, the ^{226}Ra / ^{238}U activity ratios are often very large. Zukin et al. (7), and Herczeg et al. (8) have found in samples of geothermal origin, the ratios in the order of 10^3 to 10^4. Indeed, in a reducing medium where U is much less mobile than Ra, the disappearance of sulphates allows more important concentrations of Ra in solution (9).

The data are similar to those published for other regions of the word. Though much discussion has taken place in recent years about what constitutes a generally acceptable level of individual risk in the word. A consensus exists for substances to witch large numbers of people are exposed involuntarily via media such as food and water. The Annual Limits of Incorporation (LAI) by ingestion recommended par the International Commission of Radioprotection (CIPR) are 5.10^4 Bq/year for ^{238}U, 4.10^4 Bq/year for ^{234}U, 7.10^3 Bq/year for ^{226}Ra and 9.10^3 Bq/year for ^{228}Ra. Table 2 gives the equivalent annual dose to the mean activity values for each water source assuming an individual annual consummation of 900 l of water by year. This calculation show that all measured activities are inferior to the maximum contaminant levels recommended by the International Commission of Radioprotection and they don't present any risk for public health in Morocco.

Table 1: ^{234}U, ^{238}U, ^{226}Ra and ^{228}Ra activities in analyzed samples

n°	Site	location	^{234}U (mBq l^{-1})		^{238}U (mBq l^{-1})		^{226}Ra (mBq l^{-1})		^{228}Ra (mBq l^{-1})	
Hot springs										
1	Sidi Harazem	Fez	36.02	2.56	5.19	0.52	89.10	1.20	16.20	1.10
2	Aïn Allah	Fez	25.70	2.38	5.40	0.58	30.00	0.60	3.10	0.10
3	My Yacoub	Fez	11.87	1.08	6.45	0.75	36.96	1.2	6.20	1.0
4	Oulmes	Oulmes	2.44	0.27	0.59	0.09	12.48	3	6.50	1.90
5	Sidi Ali	Oulmes	4.92	0.74	5.07	0.76	9.10	0.60	3.30	0.60
6	Ouled Reguia	F.B. Salah	41.12	2.29	17.88	1.17	12.00	2.10	9.60	1.60
Cold springs										
7	Foum el Anser	Beni Mellal	10.62	1.20	2.19	0.36	10.50	0.47	3.30	0.60
8	Ain Asserdoun	Beni Mellal	15.13	1.23	2.85	0.32	2.45	0.25	0.75	0.19
9	Tirhboula	Beni Mellal	22.41	1.37	2.70	0.24	9.05	0.49	2.40	0.50
Wells										
10	Settat	Settat	166.45	27.10	164.80	26.80	10.83	0.50	17.26	1.26
11	Beni Yakhlef	Khouribga	4.37	0.28	4.46	0.32	5.10	0.30	1.00	0.20

12	Ourghida	Khouribga	24.33	1.98	22.53	1.84	25.00	1.00	5	1
13	Lahmina	Khouribga	30.39	2.27	26.20	1.98	15.10	1.40	0.60	0.40
14	Beni Mellal	Beni Mellal	13.19	0.99	6.25	0.53	1.00	0.20	1.20	0.30
15	Ouled Reguia	F.B. Salah	61.21	4.17	60.60	4.13	6.31	0.32	4.80	0.50
16	Beni Amir	F.B. Salah	44.12	3.64	45.48	3.75	5.42	0.38	4.90	0.60
Tap water										
17	Kenitra	Kenitra	2.85	0.32	2.50	0.30	0.46	0.06	0.77	0.04
18	Khouribga	khouribga	21.67	1.90	15.70	1.41	34.60	1.50	7.70	1.40
19	K. Tadla	K. Tadla	15.06	1.06	7.24	0.56	40.60	1.70	5.40	2.20
20	F.B. Salah	F.B. Salah	24.68	1.76	12.92	0.98	45.80	0.90	12.40	1.00
21	Beni Mellal	Beni Mellal	12.80	1.67	8.31	1.24	2.12	0.29	<0.40	

Table 2: Equivalent doses in analyzed waters and their comparison to the Incorporation Annual Limits recommended by the International Commission of Radioprotection

Source	**Mean activity** (mBq l^{-1})	**Annual equivalent dose** (Bq/year)	**% LAI**
Hot springs	^{234}U 20.35	18.3	0.05
	^{238}U 6.76	6.08	0.01
	^{226}Ra 865.7	779	11
	^{228}Ra 120	108	1.2
Cold springs	^{234}U 16	14.4	0.04
	^{238}U 2.58	2.3	0.005
	^{226}Ra 7.3	6.6	0.09
	^{228}Ra 2.15	1.94	0.02
Wells	^{234}U 49.3	44.4	0.11
	^{238}U 47.2	42.5	0.09
	^{226}Ra 9.82	8.8	0.13
	^{228}Ra 4.97	4.5	0.05
Tap waters	^{234}U 15.41	13.87	0.04
	^{238}U 9.33	8.4	0.02
	^{226}Ra 24.72	22.2	0.31
	^{228}Ra 5.33	4.8	0.05

For radon, the measurements were performed in 9 dwellings and 7 enclosed work areas in some regions of Morocco. Results for dwellings are given in table 1 and these for enclosed

work areas are given in table 3. The exposure period of films in dwellings and in enclosed work areas varied between 2 and 4 months. The given results are an average of at least 2 measures by locality and at least in two houses.

The effective dose per unit exposure to radon and radon progeny was obtained using the so-called dose conversion convention as defined by ICRP (10,11). This approach compared the detriment per unit exposure to radon and its progeny with the total detriment associated with unit effective dose. The values given were 5 mSv per WLM (Working level month) for workers and 4 mSv per WLM for members of the public. 1 Bq/m^{3}of radon during 1 year = 4.4 10^{-3} WLM at home and 1 Bq/m^3 of radon during 1 year = 1.26 10^{-3} WLM at work assuming 7000 h per year indoors or 2000 hours per year at work and an equilibrium factor of 0.4.

Table 3 show the relatively higher indoor volumic activities of ^{222}Rn in Youssoufia and khouribga towns situated in regions rich in phosphate deposits. Measurements at the geophysical observatory of Berchid show that the volumic activity of radon increases with depth, this is most probably due to decreased ventilation.

The radon would be the second cause of death by lung cancer (after the tobacco). In 1990, the European Commission fixed two limits, the one for the existing houses (400 Bq/m^3), the other one for the future constructions (200 Bq/m^3). In 1993, the CIPR proposes a range between a low value (200 Bq/m^3 corresponding to an effective dose value of 3 mSv/year) and a high value (600 Bq/m^3 corresponding to an effective dose value of 10 mSv/year) beyond which it considers that it is justified almost always to act. The effective dose was different between homes and workplaces largely because of the different number of hours spent at each. For workplaces the corresponding range of permit concentrations of radon was 500–1500 Bq/m^3. In 1996, the European directive N 96/29, imposes the inventory of all the workplaces susceptible to provoke an increased exposure to radon. The first occupations concerned by the exposure in the radon were the miners.

Table 3: Volumic activities of ^{222}Rn and effective doses in indoor dwellings

Town	Volumic activity of ^{222}Rn (Bq/m^3)	Effective dose (mSv/year)
Berchid	76 ± 8	1.34 ± 0.14
Casablanca	31 ± 3	0.55 ± 0.05
El Jadida	47 ± 4	0.83 ± 0.07
Ouarzazate	99 ± 5	1.74 ± 0.09
Oujda	83 ± 7	1.46 ± 0.12
Rabat	64 ± 5	1.13 ± 0.09
Kénitra	59 ± 6	1.04 ± 0.11
Youssoufia	124 ± 8	2.18 ± 0.14
Khouribga	136 ± 9	2.39 ± 0.16

Table 4: Volumic activities of ^{222}Rn and effective doses in enclosed work areas.

Enclosed work area	Volumic activity (Bq/m^3)	Effective dose (mSv/year)
Laboratory of nuclear physics (Rabat)	60 ± 4	0.38 ± 0.03
Local for practical nuclear studies (Faculty of Sciences, Rabat)	68 ± 6	0.43 ± 0.04
Factory 1	435 ± 4	2.74 ± 0.03
Factory 2	142 ± 15	0.90 ± 0.09
Geophysical Observatory of Berchid (Ground level)	63 ± 5	0.40 ± 0.03
Geophysical Observatory of Berchid (Cave at –12 meters)	1884 ± 199	11.90 ± 1.25

Our measures sow that volumic activities of radon vary in Houses, between 31 and 136 Bq/m^3 with an average value of 80 Bq/m^3. This value is comparable to those found in the other regions of the word. In Enclosed work area, they vary between 60 Bq/m^3 in an ordinary area to 1884 Bq/m^3 at not airy underground level of 12 m. For example, values of 4150 and 5122 have been found also in Two deep cellars in Orléans in France (12).

The calculated effective dose in houses varies between 0.55 and 2.39 mSv/year with an average value of about 1.41 mSv/year. In enclosed areas it varies between 0.38 and 11.9 mSv/year with an average value of about 2.8 mSv/year. Thus the radon concentration levels found in this study are below the action level recommended by the ICRP.

The relationships between volumic activities of indoor radon and seasonal variations have already confirmed by Hakam et al. (2,13) (see table 5).

Table 5: Seasonal variation study of Radon volumic activity

Exposition season	Volumic activity (Bq/m^3)
Summer	37 ± 2
Autumn	60 ± 4
Winter	95 ± 7
Spring	66 ± 4

The data of this table show a maximal value of 95 Bq/m^3 in winter and a minimal value of 37 Bq/m^3 in summer, that is a report of 2.5. This difference results especially from an important aeration in summer. Both seasons Spring and Autumn are respectively characterized by average concentrations of radon of 66 Bq/m^3 and 60 Bq/m^3.

These seasonal characters are marked themselves by variations during the day, maximal during the night and minimal during the day. This is explained by the closure of doors and windows during night, preventing the renewal of air in the house.

Houses can be classified in two categories following the nature of building materials, stones on one hand and other materials on the other hand (bricks, perpend, concrete). We observed a difference between houses in stones and the other constructions. The volumic activity of the radon is 47 Bq/m^3 in a house in stones and 31 Bq/m^3 in the other construction not in stones. These values are obtained during the same period of exposure in two nearly houses in El Jadida region.

As the main source of radon in houses is the basement, we can expect to observe differences between dwellings results in the various floors of a building. This aspect is shown by the data collected in the various floors of a building situated in the Kénitra city. We so measured radon volumic activities varying from 67 Bq/m^3 in the first floor to 32 Bq/m^3 in the fourth floor (table 6). Thus the activity of the radon decreases with the height.

Table 6: Radon volumic activities according to the height

floor	Volumic activity (Bq/m^3)
1st	67
2nd	54
3th	47
4th	32

In order to check the effect of the depth on the variation of the Radon volumic activity, we took advantage of our access to the geophysical observatory of Berchid to make our measures at three underground levels. The obtained results are given in the table 7.

Table 7: Radon volumic activities According to the depth

Depth		Volumic activity (Bq/m^3)
Ground Level	Office	58 ± 6
	Room	68 ± 8
The cellar	1st level (-4m)	1208 ± 184
	2nd level (-8m)	1499 ± 100
	3th level (-12m)	1884 ± 119

We notice a big difference between the activities of the radon of the ground floor and those in the different levels of the cellar. This explains by the fact that the cellar is closed in a continuous way and is not equipped with a system of aeration.

CONCLUSION

For water the obtained results show comparable results to those reported in previous works for different regions in the world. The calculated equivalent dose to mean activity for each radio-isotope in each source of analyzed drinking water are inferior to the Annual Limits of Incorporation by ingestion recommended by the International Commission of Radioprotection. we can not generalize the obtained results for all drinking waters in Morocco because of the limited analyzed samples number. Although they gave a general idea of U and Ra radio-isotopes activity repartition in wells, springs and tap water samples which could be used to orient the next samplings in order to establish a global distribution map of radio-elements in drinking waters of Morocco.

For radon, The measurements performed in 9 dwellings and 7 enclosed work areas in different regions of Morocco show that:

- The obtained values of volumic activities of radon in dwellings and in enclosed work areas and the calculated effective dose are comparable to those obtained in the other regions in the word and they are below the action level recommended by the ICRP (3 to 10 mSv/year corresponding to volumic activities from 200 to 600 Bq/m^3 for houses and from 500 to 1500 Bq/m^3 for workplaces)
- The relatively higher volumic activities of ^{222}Rn in Youssoufia and khouribga towns are obtained because Youssoufia and khouribga are situated in regions rich in phosphate deposits.
- The volumic activity of radon increases with depth, this is most probably due to decreased ventilation.
- A maximal value of radon volumic activity was measured in winter and a minimal value of this activity was measured in summer. This difference results especially from an important aeration in summer. The use of air conditioners in summer and the possible natural ventilation in winter help to keep concentration levels of indoor radon low.
- The measured volumic activities of radon depend on some parameters such type of construction, the height of building and the depth of the underground.
- The radon concentration levels found in this study are below the action level recommended by the ICRP.

To protect human health, efforts are always necessary to reach the effective dose of 1 mSv / year recommended by ICRP for the public in his publication 60 (1991) and confirmed in the later publications.

REFERENCES

(1) Choukri, A., Reyss, J.-L., Turpin, L., Berrada, M.: Radiochemical separation of U and Th isotopes in phosphate rich samples for age determination. Radiochim. Acta 65, 137-139 (1994).

(2) Hakam O.-K., Choukri A., Reyss J.-L. and Lferde M. "Activities and activity ratios of U and Ra radio-isotopes in drinking wells, springs and tap water samples in Morocco." Journal of Radiochem. Acta 88, 55-60 (2000).

(3) Hakam O., Lferde M. and Berrada M. (1995a), "Calibration of a solid state nuclear track detector for the measurements of radon concentration in air." Appl. Radiat. Isot. Vol.46, *N°6/7*, pp. 483-484.

(4) Langmuir, D.: Uranium solution-mineral equilibria at low temperatures with applications to sedimentary ore deposits. Geochim. Cosmochim. Acta 42, 547-569 (1978).

(5) Ames, L. L., McGarrah, J. E., Walker, B. A.: Sorption of uranium and radium by biotite, muscovite, and phlogopite. Clays Clay Minerals 31, 343-351 (1983).

(6) Langmuir, D., Melchior, D. C.: The geochemistry of calcium, strontium, barium and radiumsulphates in some deep brines from the Palo Duro Basin, Texas. Geochim. Cosmochim. Acta 49, 2423-2432 (1985).

(7) Zukin, J. G., Harmond, D. E., Ku, T. L., Elders, W. A.: Uranium-thorium series isotopes in brines and reservoir rocks from two deep well holes in the Salton Sea geothermal field, Southeastern California. Geochim. Cosmochim. Acta 51, 1719-1731 (1987).

(8) Herczeg, A. L., Simpson, H. J., Anderson, R. F.: Uranium and radium mobility in groundwaters and brines within the Delaware Basin, Southeastern New Mexico. Chem. Geol. 72, 181-196 (1988).

(9) Beaucaire, C., Toulhoat, P.: Redox chemistry of uranium and iron, radium geochemistry, and uranium isotopes in the groundwaters of the Lodèvre basin. Massif Central, France. Appl. Geochem. 2, 471-426 (1987).

(10) ICRP (1993). Protection against Rn-222 at home and at work. ICRP Publication 65. Ann. ICRP 23(2), Pergamon, Oxford..

(11) ICRP (1994). Human Respiratory Tract Model for Radiological Protection ICRP Publication 66

(12) Anne-Marie Pieux-Gilède, Gare au radon en toutes régions Revue "Sortir du nucléaire" n° 22, juillet 2003, p. 34

(13) Hakam O., Choukri A., Moutia Z., Lferde M. & Reyss J.-L. (2001), " Mesure des activités spécifique de l'uranium (^{234}U,^{238}U), du radium (^{226}Ra,^{228}Ra) dans des échantillons d'eau potable et du radon dans l'air de quelques habitations au Maroc." Journal Maghrébin de Physique, volume 1, n° 2, pp. 115-121

Investigation of Natural Radioactivity in the Tap and Spring Water in Yaounde Town, Cameroon

R. Marie Lydie[1,2], O.K. Hakam[1,3], and A. Choukri[1,3*]

[1]*Equipe de Physique et Techniques Nucléaires, Laboratory Polymers, Radiations and Environment, Faculty of Sciences, University of Ibn Tofail, Kenitra, Morocco.*

[2]*National Radiation Protection Agency of Cameroun (ANRP)*

[3]*Moroccan Radiation Protection Association (AMR)*

**Corresponding Author: choukrimajid@yahoo.com*

ABSTRACT

The natural radionuclide concentrations in the tap and springs water in Yaounde town, capital of Cameroon with a population of 3.5 million inhabitants were estimated by gamma spectrometry, using both well calibrated Canberra NaI(Tl) and HPGe detector systems. Tap water samples were collected during the dry and the rainy seasons, respectively in December 2002 and July 2003 and spring water samples were collected in August 2010. The radionuclides observed with regularity belonged to the series decay naturally occurring radionuclides headed by ^{238}U and ^{232}Th as well as the non-series nuclide ^{40}K. Assuming an individual daily consumption of 1 litre of water, the average annual intake for these populations is 3821 Bq/y for tap water and 1161 Bq/y for spring water.

***Key words**: Natural Radionuclides/ Concentration/ Annual intake /Gamma spectrometry.*

INTRODUCTION

There are different isotopes of uranium but ^{238}U is the predominant contributor to natural radioactivity. The average ^{238}U content in the earth's crust has been estimated to be 2.7 mg/kg and the concentration may be as high as 120 mg/kg in phosphate rocks [(1)]. Meanwhile, the average ^{232}Th content of the earth's crust is about 9.6 mg/kg [(2)]. Enhanced levels of uranium, thorium and their fission products might be present in water in areas that are rich in natural radioactivity. Several radionuclides coming from the radioactive decay chain starting from ^{238}U and ^{235}U are highly radiotoxic. The most radiotoxic and most important among them is radium, which is a known carcinogen and exists in several isotopic forms. The predominant radium isotopes in ground water are ^{226}Ra, an alpha emitter with a half-life of 1600 years, and ^{228}Ra, a beta emitter with a half-life of 5.8 years [(3)]. When radium is taken into the body, its metabolic behaviour is similar to that of calcium and an appreciable fraction being distributed almost uniformly in soft tissues [(4)].

The purpose of the present work is firstly to investigate the types and concentrations of natural radionuclides in the reservoir and tap water of Yaounde town in Cameroon, and secondly to estimate the annual intake for these populations submitted to the consumption of this water.

MATERIALS AND METHODS

Sampling

Yaounde town lies at the latitude of 3°52'N and longitude of 11°31'E, covering a total area of 297 km^2, with an average altitude 740 m. The study area was partitioned into 14 units in which 9 were tap water sampling locations and 5 were spring water locations. The major bedrock types of the river Nyong where the tap water comes from include gneiss, pegmatite, pegmatite schist and undifferentiated schist [5]. Tap and spring water studied are used for drinking, washing clothes, cleaning of food, for irrigation, and for various domestic uses. The sampling locations were chosen based on such factors as population density, hospital, educational institutions, etc. The water taps were first turned on at full capacity for several minutes to purge the plumbing system of any water which might have been there for some time. The taps were turned down to a low rate to reduce turbulence and thus, reduce radon loss [6]. After the water samples were collected as mentioned above, they were transferred to 1 litre kegs prior to processing for γ-spectrometry analysis. The springs water was equally collected using 1 litre plastic kegs.

All the samples of water were acidified with 11 M of (H_3O^+, Cl^-) at the rate of 10 ml per litre of sample as soon as possible after sampling to avoid absorption of radionuclides on to the walls of the containers as documented by the International Atomic Energy Agency [7]. Marinelli beakers of 1 litre volume capacity previously washed, rinsed with a dilute sulphuric acid and dried to avoid contamination were filled with known volume of the various water samples and later firmly sealed for, at least, four weeks to ensure that no loss of radon occurs thereby ensuring a state of secular equilibrium to be reached between radium isotopes and their respective daughters. From each location, four samples were made from water collected.

Instrumentation

The first Gamma-counting equipment was a Canberra sodium iodide thallium activated NaI(Tl) crystal detector model GC2018-7500, serial number b 87063. This crystal used has an excellent energy resolution; with a typical measurement time was 36000 seconds. The second Gamma counting system was a Canberra High Purity Germanium (HPGe) detector, model Gx3019-7500SL, serial number 11026235; with a counting time of 86400 seconds. Because of the cosmic radiation that continuously bombards the earth's atmosphere and the existence of natural radioactivity in environment, radiation detectors records some background signal which varies with the size and type of the detector as well as the extent of shield. Hence the knowledge of the net peak area (without the background) under the full-energy peak that appears in its spectrum is important to apply the peak efficiency data for any detector. In gamma spectrometry, the pulse height scale must be calibrated in terms of absolute gamma-ray energy if various peaks in the spectrum are to be properly identified. Also, any measurement of absolute gamma-ray emission rates requires knowledge of the detector efficiency. Thus, the detector system has to be calibrated in terms of energy and absolute efficiency. The energy and the International Atomic Energy Agency (IAEA), Vienna, Austria. The techniques used are well described elsewhere. The photopeaks observed with regularity in the water samples were identified to belong to the naturally occurring series decay radionuclides headed by ^{238}U and ^{232}Th. Other radionuclides, if present appeared rather infrequently at low levels or efficiency calibrations were done using a well calibrated standard

water source supplied by occurred at levels below the maximum detectable limits (MDL), statistically determined at two-standard deviation analytical error.

The activity concentrations of ^{226}Ra and ^{228}Ra were indirectly obtained from the γ-rays emitted by their progenies which were in secular equilibrium with them. ^{226}Ra concentration was determined by measuring the 609.3 keV γ-rays from ^{214}Bi; the 583.0 keV γ-rays of ^{208}Tl was used to determine that of ^{228}Ra. While that of ^{40}K was estimated directly by its γ-line of 1460.8 keV. The gamma spectroscopy analysis with NaI(Tl) crystal was carried out by a sophisticated spectra-analysis program, SAMPO 90 [8] which matched γ-energies at various energy levels to a library of possible isotopes. Another sophisticated spectra-analysis program named Genie 2000 was used for the HPGe detector. The activities of the radionuclides were calculated from the difference between net peak and net background areas, accumulation time, absolute peak efficiency, absolute γ-ray emission probability (γ-ray intensity) and the sample volume. Triplicate analyses were conducted on all the water samples to check on the reproducibility of results and the stability of the counting system. The overall uncertainty in the measured concentrations was estimated from the parameters contained in the above mentioned relation, the calibration procedure, the peak area determination and the background. Each radionuclide activity per unit volume A, in each water sample was evaluated using the relation:

$$A = \frac{N}{\varepsilon \times I_\gamma \times V \times t_c} \qquad \textbf{[1]}$$

N: net peak area of the radionuclide of interest
ε : efficiency of the detector for the energy E_γ
I_γ : intensity per decay for the energy E_γ
V: volume of the water sample
t_c : total counting time in seconds

RESULTS AND DISCUSSIONS

Table 1 shows the summary of ^{40}K, ^{226}Ra and ^{228}Ra activity concentrations, table 2 shows the evaluation of the annual intake of ^{226}Ra and ^{228}Ra by ingestion of studied waters, which is represented in figure 1.

Table 1. Mean specific activity content (BqL^{-1}) in tap and springs water in Yaounde town.

Type of Water sample	Number of Samples	Radionuclides					
		^{40}K		^{226}Ra		^{228}Ra	
		Range	Mean	Range	Mean	Range	Mean
Tap water (dry season)	36	74 -138.6	111 ± 17	8.4 - 13.8	11.4 ± 3.7	0.3 - 1.6	1 ± 0.3
Tap water(rainy season)	36	23.3 - 85.8	51 ± 10	4.3 - 12.2	9 ± 3.5	0.2 - 1.1	0.7 ± 0.2
Spring water(rainy season)	20	1.3 - 5.11	2.65 ± 0.36	1.7 - 5.2	3.2 ± 0.6	< 0.0002	< 0.0002

Table 2. Annual intake (Bq/y) for tap and spring water in Yaounde town

Radionuclides	^{226}Ra			^{228}Ra		
Water samples	Tap		Spring	Tap		Spring
Season	Dry	Rainy	Rainy	Dry	Rainy	Rainy
I_i ($Bq.d^{-1}$)	11.40	9.14	3.18	1.02	0.68	< 0.0002
Ii (Bq/Season)	1038	2504	872	93	186	< 0.055
Ii (Bq/y)	3542		1161	279		< 0.073
Annual intake (Bq/y)	**Tap water** : 3542 + 279 = **3821 Bq/y** **Spring water :** 1161 + 0.073 = **1161 Bq/y**					

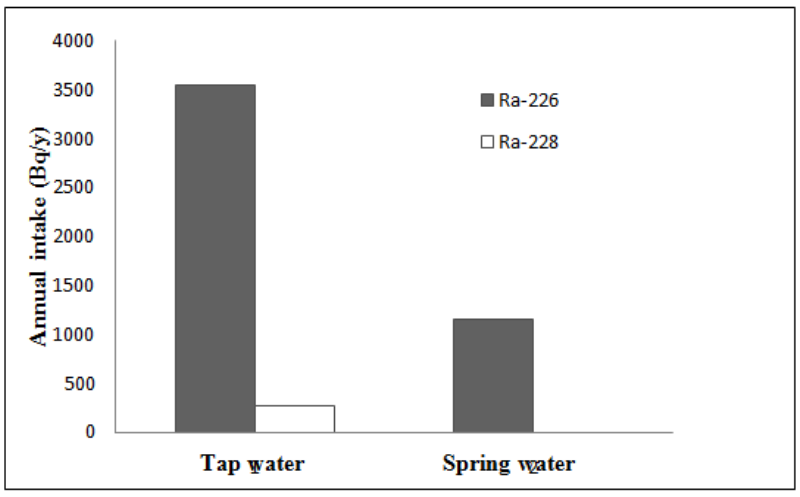

Figure1. The annual intake of ^{226}Ra and ^{228}Ra by ingestion of studied waters

The mean concentration of ^{226}Ra agreed with a range of values obtained by many investigators namely Mc Curdy and Russel in 1981: 0.08 - 36.4 BqL^{-1} in imported bottled water [9], and Dana in1987 : 1.5 -124 BqL^{-1} in public water supplies in North Carolina [10]. The ^{228}Ra concentrations recorded for this work fell within the wide range of values 0.05- 4.6 BqL^{-1} quoted for the USA's imported bottled water by Mc Curdy and Russel[9]. The concentration values are relatively low during the rainy season; this could be due to the dilution effects of rain water since the river Nyong where tap water studied comes. The mean specific activity of uranium in this type of water samples is lower than the results 10.4 ± 1.7 BqL^{-1} obtained by Tchokossa in 1998 in the reservoir water of Mukuro in Nigeria [11]. ^{228}Ra activity is not too different to the result 620 ± 10 $mBqL^{-1}$ obtained by Hakam et al in 2001 in the drinking water from Fez locality in Morocco [12]. While they are higher than 0.20 - 135 $pCiL^{-1}$ equivalent to 0.007 - 0.05 BqL^{-1}, obtained by Nour Khalifa in 2004 in tap water from Qena locality in Egypt [13]. They are still within the range of 0.00 - 8.75 BqL^{-1} reported by David et al in 1981, quoted by Mc Curdy and Russel [9] for domestic bottled water marketed and consumed in USA. The specific activity due to natural thorium is relatively low in all the water samples investigated; this is because ^{238}U is more mobile than ^{232}Th. Slight variation in the radioactivity content in water of the same type and from the same source can be observed in different locations and even worldwide, mainly due to potential changes occurring in the pipe during transportation of tap water, the oxidation state of the water, the concentration of suitable complexing agents which can increase the solubility of uranium or thorium.

The higher levels of ^{40}K observed in all water samples are a function of the geological formation of the area [14]. The mineralogy of this area is dominated by orthoclase which generates more ^{40}K through the hydrolysis reactions. However, because ^{40}K is an essential biologic element which is under close metabolic control, variations in dietary composition have little effect on the body content or on the radiation dose received [15]. This is the reason for which the activity of ^{40}K can't be used to evaluate the annual intake.

CONCLUSION AND RECOMMENDATIONS

The results has indicated that the average specific activity concentration of ^{40}K, ^{226}Ra and ^{228}Ra in the tap and spring water in this area, are comparable to those reported in previous works throughout the world. This study has shown that the naturally occurring radionuclides in studied samples differ in quantity from location to location. These observations demonstrate that the radionuclide concentrations are a function of the geology of the area and it could be greatly influenced by the water transportation, precipitation and other numerous factors. The annual intake by the populations of Yaounde town as a result of both ^{226}Ra and ^{228}Ra in these drinking waters is estimated to be for tap water 3821 Bq/y and for spring water 1161 Bq/y, assuming an individual daily consumption of 1 litre of water. In fact, high radiation doses as well as low radiation doses could induce serious health effects. People can then filter this tap water before consumption, because by filtrating, the radioactive substances that couldn't be dissolved have been eliminated.

ACKNOWLEDGEMENTS

Gamma spectrometry analysis was realized first in the laboratory of radioprotection, Obafemi Awolowo University of Ile-Ife Nigeria and secondly in the spectrometry laboratories of CNESTEN-Morocco. The authors are deeply grateful for this support.

References

(1) S. Padam, N. Rana, A. Naqvi, and D. Srivastava; Levels of Uranium in Water from some Indian Cities Determined by Fission Track Analysis, Radiation Measurements; 26, 683-687 (1996).

(2) B.R. Firestone, S.V. Shirley, M.C. Baglin, Y.S. Frank Chu, and J. Zipkin; The 8th Edition of the Table of Isotopes, CD-ROM, John Wiley & Sons, Inc.(1996).

(3) G. J. Marovic, Sencar, Z. Franic, and N. Lokobaner; Radium-226 in Thermal and Mineral Springs of Croatia and Associated Health Risk, Journal of Environmental Radioactivity; 33, 309-317 (1996).

(4) M. E. Wreen, P.W. Durbin, B. Howard, J. Lipsztein, J. Rundo, E.T.Still, and D.I.Willis; Metabolism of Ingested U and Ra, Health Physics; 48, 601-633 (1985).

(5) G. Olivié-Lauquet, T. Allard, J. Bertaux, and J.P. Muller; Crystal-chemistry of Suspended Matter in a Tropical Hydrosystem Nyong basin (Cameroon, Africa). Chem. Geol.; 170, 113-131 (2000).

(6) J. E. Watson; Ground-Water Concentration of ^{226}Ra and ^{222}Rn in North Carolina Phosphate Lands, Health Physics; 52, 361-365 (1986).

(7) International Atomic Energy Agency; Summary Report on the post accident review meeting on the Chernobyl accident, Safety Ser. 75-INSAG-1, IAEA, Vienna (1986).

(8) P. A. Aarnio, M.T. Nikkinen, and J.T. Routti; SAMPO 90 High Resolution Interactive Gamma-Spectrum Analysis Including Automation with Macros, Journal of Radioanalytical and Nuclear Chemistry; vol 160, N°1, 286-296 (1992).

(9) D.E. McCurdy, and A.M. Russel; The Concentration of ^{226}Ra and ^{228}Rn in Domestic and Imported Bottled Water, Health Physics; 40, 250-253 (1981).

(10) P.L. Dana; The Relationship between Water System Size and ^{222}Rn concentration in North Carolina Public Water Supplies, Health Physics; 50, 33-71 (1987).

(11) P.Tchokossa; Measurement of Natural Radionuclide Concentrations in the Community Water Supplies in Ife Central and East Ife Local Government Areas, Nigeria, M.Sc. thesis, Obafemi Awolowo University, Ile-Ife (1998).

(12) O.K. Hakam, A. Choukri, J.L. Reyss, and M. Lferde; Determination and Comparison of Uranium and Radium Isotopes Activities and Activity Ratios in Samples from some Natural Water Sources in Morocco, Journal of Environment Radioactivity; 1-15 (2001).

(13) A. Nour Khalifa; Natural Radioactivity of Ground and Drinking Water in some Areas of Upper Egypt, Journal of Engineering and Environmental Sciences, 28 Turkish; 345-354 (2004).

(14) J. E. Watson; Ground-Water Concentration of ^{226}Ra and ^{222}Rn in North Carolina Phosphate Lands, Health Physics; 52, 361-365 (1986).

(15) National Council on Radiation Protection and Measurement; Environmental Radiation Measurements, NCRP Report N°50, NCRP, W

Low Magnitude Occupational Radiation Exposures – Are They Safe or Unsafe

Ramamoorthy Ravichandran
Medical Physics Unit, Dept.of Radiotherapy, Royal Hospital, Muscat, Oman

INTRODUCTION

Man has always been exposed to ionizing radiation from natural sources and background exposure varies with the locations. No deleterious effects have been uniquely correlated, either they are not produced at low levels of exposure or their frequency is too low to be statistically observable. Direct source of information on radiation hazards in man is obviously based on follow up of population groups exposed to certain levels of radiation. Harmful effects of ionizing radiations are traced to documented exposures; for radiologists during 1920s and 30s, miners exposed to airborne radioactivity, workers in the radium industry, follow-up data of Japanese nuclear bomb survivors of Hiroshima and Nagasaki, the Marshallese accident in 1954, and the victims of the limited number of accidents at nuclear installations including Chernobyl. Mostly these information are from situations involving higher doses and dose rates.

Ionizing radiations have been used extensively on the peaceful applications of atomic energy in general and medical applications in particular have shown to outweigh benefits over the risks. Personnel, low magnitude of exposures are encountered during routine work in handling radiation sources. In the light of present knowledge there is need to reassess the quantum of actual risk instead of projected risk based on long time models.

EFFECTS OF LOW DOSES

The United Nations Scientific Committee on the Effects of Atomic Radiation (UNSCEAR) described models for dose-response relationships and micro-dosimetric arguments for defining low doses. The definition of low doses could also be based on direct observations in experimental or epidemiological studies. Through measurement of cell damage or death using human lymphocytes, linear and quadratic terms have been fitted the response and low doses have been judged to be 20-40 mSv. Data derived from epidemiological studies, mainly the atomic bomb survivors, suggests that for solid tumours and leukaemia, 200 mSv could be considered the upper limit for low dose exposure. Mechanistic models give quantitative estimates considering cellular repair, transformation, survival, energy deposition, cellular and track structures.

RISK AT LOW DOSES

The established model for determining carcinogenic effects at low doses in radiation protection is based on the hypothesis that the cancer incidence increases proportionally with radiation dose. A so-called linear no threshold model (LNT) has major implication of no-threshold for stochastic effects regardless of how low they are. Some risk potential for carcinogenisis must be accepted at any level of protection. Therefore, current belief is that

exposure to ionizing radiation, no matter how small, carries a risk of detriment with the risk being proportional to the dose accumulated. UNSCEAR models involve excess relative risk (ERR) depending on gender and age-at exposure, and another model the 'attained-age-model', the ERR depends on gender and attained age, i.e. the age at death or incidence of cancer.

RECOMMENDED DOSE LIMITS FOR OCCUPATIONAL WORKERS

Dose limits of ICRP 60 (1990) apply to occupational and public exposures; based on the evaluation of detriment from continuous exposure over a working life time of 47 years (18-65 years). Consideration based on 'just short of unacceptable' assuming a maximum risk figure of 1:1000 (10^{-3} per year) mortalities. With available database, the Health Physics Society recommends 'against' quantitative estimation of health risks below an individual dose of 50 mSv (5 Rem) in one year; or a life time dose of 100 mSv (10 Rem) above that received from natural sources. Though the recommended annual dose equivalent limit is 20 mSv, recent survey showed a mean cumulative dose of 19.4 mSv from pooled analysis of nuclear workers from 15 countries.

Another study indicated cumulated doses 0-20mSv, 20-100 mSv, >100mSv in 87.3%, 10.8% and 1.9% of monitored radiation workers respectively. This is far low compared to the dose received from background radiations, at the rate of about 2.4 to 3.0 mSv/year.

EPIDEMIOLOGICAL STUDIES

Epidemiological studies expressed difficulties in quantifying the risk after exposure to 50 mSv, as the additional increase in death due to cancer is 0.5%. Another important study of atomic bomb survivors estimated 75000 subjects with radiation dose less than 200 mGy which implies that this dose does not increase the risk.

Considerable debate is on the possibility of a dose below which there is no excess risk. The threshold discussion is probably even more relevant after low dose rate exposure since protracted exposure might theoretically allow for molecular repair. Life span study (LSS) considers threshold being 0 Sv, gives an upper limit to the confidence interval of 60 mSv. Linear no threshold (LNT) model states that any exposure to ionizing radiation, no matter how small, carries with it a commensurate risk of detriment (i.e fatal cancer or heritable genetic effect), with risk being proportional to the dose accumulated.

HEALTH EFFECTS AT LOW DOSES

It is reported that the LNT hypothesis for cancer risk appears scientifically unfounded and invalid in favour of a threshold or hormesis. This is consistent with data both from animal studies and human epidemiological observations on low-dose induced cancer.. It has been postulated that by exposing cells to a low dose of ionizing radiation would make them less susceptible to a later high dose exposure. Animal studies have shown prolonged latency periods for leukaemia and more efficient DNA repair in mice previously exposed to an adapting dose compared to those not pre-irradiated. Even a beneficial effect of low dose of ionizing radiation, termed hormesis, has been discussed and the belief is that metabolic

detoxification and cell repair benefits from doses in the range of 1-50 mSv. It has even been suggested that atomic bomb survivors have had a beneficial effect (hormesis) of the exposure to ionizing radiation.

Supportive data in the last two decades relating to health effects of low-level ionizing radiation (LLIR) are available from large epidemiologic data sets such as those acquired from study of atomic bomb survivors, nuclear industry workers, and medically exposed patient cohorts. Epidemiological data on residents exposed to high back ground (BG) natural radiations, and radiation workers (Table-1) showed reduced life time risk of cancer with statistical significance, which supports the claim that low quantities of radiations make subjects healthier. Most current estimates of the health impact of population exposures to low-level ionizing radiations (LLIR) continue to use a 'risk per person per rem' extrapolation which tacitly assumes that proportionally scaled high level exposures will accurately reflect the epidemiologic consequences of LLIR. Hormeticists argue that these scaled epidemiologic extrapolations are invalid and that the majority of the available experimental data on LLIR do not support a significantly adverse health effect; rather much of the data suggest some theoretical and experimental 'benfits' accruing from such exposures. There are two other low-dose phenomena, 1) The bystander effect tends to 'exaggerate' the effect of low doses, by communicating damage from hit to non-hit cells, while 2) the adaptive response confers 'resistance' to a subsequent dose by a low initial priming dose.

PROTECTIVE RESPONSES

Increasing evidence in the literature over the past 25 years indicates that adaptive protection responses occur in mammalian cells in vivo and in vitro after single as well as protracted exposures to X- or gamma radiation at low doses. Protective responses occur in various ways. They appear to depend on mammalian species, individual genomes, cell types, cell cycle, and cell metabolism. Adaptive protection categories after single low-dose, low-LET irradiation, are as follows. Since DNA damage and cancer in mammals arise mainly from non-radiogenic sources, it is justified to relate the low-dose induced various adaptive protection mechanisms mainly to non-radiogenic, i.e. ''spontaneous'' DNA damage and cancer in addition to their potential effect against radiogenic damage and cancer. Graphs summarizing the application of the model of risk evaluation after single low-dose irradiation are shown in Fig.1. This illustrate that low-doses induce adaptive protection against DNA damage and its accumulation in tissue, mainly from endogenous, i.e. ''spontaneous'' sources, and that these can counterbalance radiation effects. The net risk of cancer becomes lower than predicted by the LNT-hypothesis, or even negative with more benefit than damage to the low-dose exposed system.

Table- Effects of low level radiations in humans

No.	High background natural radiations		Occupational Exposures	
	Related studies	Epidemiological observations	Related Studies	Epidemiological observations
1	Chinese study high background 2.28mGy/Yr	Lower Cancer mortality	Canadian study in nuclear power station	58% lower cancer mortality
2	Indian study higher BG in 5 cities 600-800 μSv/yr	Less Cancer incidence -ve correlation to radiation dose	British nuclear power workers	Less cancer frequency compared to others
3	US Study on variable BG radiations & Ca mortality	-ve correlation with lung cancer	US study on plutonium plants	70% lower cancer mortality
4	US Study, radon levels and lung cancer incidence	-ve correlation with lung cancer	US study on ship yard nuclear workers	Lower mortality rates than non-nuclear
5	UK study with radon levels and lung cancer	-ve risk for cancer incidence Survivors with disease free	Nuclear workers, Rocket-dyne USA Pooled study from 7 reports	Workers showed low Rates of cancer death
6	Indian Study, Kerala BG radiation 4-70mGy/year		15 countries pooled study, no effects	No effect of low level radiations Cumulative mean dose 19.5mSV
7	Japanese Atom bomb survivors[9] < 200 mGy			

Recently Italian researchers claimed that low dose radiation exposure at levels considered safe by regulatory bodies can induce biological and cellular changes that might offset the hazards of radiation due to protective mechanisms. Therefore low radiation exposures are not as harmful as was thought so far. At low doses reduction of damage from endogenous sources by adaptive protection may be equal to or outweigh radiogenic damage induction. Data from interventional cardiologists who were exposed to median radiation exposure 4.7mSv/Y; and lifetime exposure ranging from 20mSv to 100mSv, working in cardiac cath.lab compared with matched unexposed controls documented adaptive responses with low dose radiations.

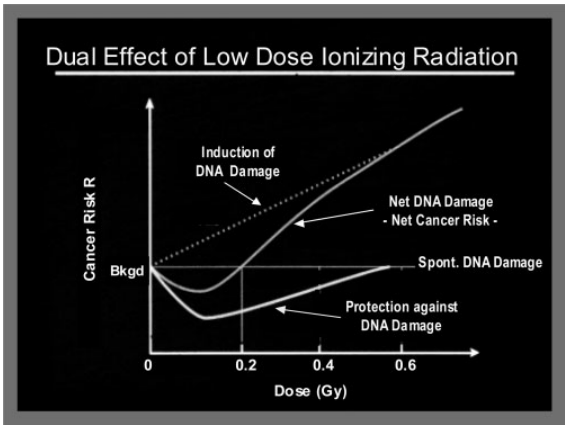

Fig.1 Net Cancer Risk lower than expected by LNT model (Reproduced with permission [14])

2 recent studies brought out clearly that a) there is growth inhibition in cells in the absence of radiations and b) a 'stress response' seen when cells were grown under reduced radiation conditions. The possibility of ecological studies of environmental exposure to ionizing radiation to contribute to our knowledge on effects of low dose exposure is limited. The effects of natural background radiation are low and other risk factors will distort the results. Advances in molecular biology and genetics will hopefully increase the likelihood of finding the "true" effect of ionizing radiation at low doses. Research will focus on understanding cellular processes responsible for recognizing and repairing normal oxidative damage and radiation-induced damage. If the damage and repair induced by low dose radiation is the same as for other oxidative damage, it is possible that there are thresholds of damage that the body can handle. On the other hand, if the damage from ionizing radiation is different from normal oxidative damage, then its repair, and the hazard associated with it, may be unique and a threshold will never be identified. It appears, therefore, that radiation is necessary for 'normal growth'? It is therefore becoming necessary to institute awareness, to enlighten the people about the myths and realities of radiation effects.

Acknowledgement:

Author extend his sincere thanks to Prof. Feinendegen for kind permission to use some of his research data.

REFERENCES

(1) United Nations Scientific Committee on the Effects of Atomic Radiation: UNSCEAR 1993, 2000, 2006.
(2) ICRP-60. International Commission on Radiological Protection. 1990, Vol 21, Publication 60.
(3) Pierce DA, Shimizu Y, Preston DL, Vaeth M, Mabuchi K. Radiat Res (1996) 146: 1-27.
(4) Ritz B, Morgenstern H, Froines J, Young BB. Amer.J.Ind. Med. (1999), 35:21–31.
(5) Pierce DA, Preston DL Radiat Res (2000) 154: 178-86.
(6) Preston D, Ron E, Tokuokas, Funamutos, Nishi N, Soda M, Maduchi K. Radiat.Res. (2007), 168, 1-64.

(7) Radiation protection 125. Proc.Scientific Seminar, Luxembuorg, Nov,2000.
(8) Macklis RM, and Beresford B Radiation Hormesis. J. Nucl. Med. (1991), 32: 350-359.
(9) Devasagayam TPA, Kesavan PC. In. Advances in Medical Physics. New Delhi. 2000; 280-287.
(10) Raghu Ram K.N, Rajan B, Akiba S, Jayalekshmi P, et al. Health Phys. (2009), 96, 55– 66.
(11) Cardis E, Gilbert E, Carpenter L, Howe G, Kato I, Armstrong BK et al.. Radiat.Res. (1995), 142, 117-132.
(12) Sawant SG, Pehrson GR, Metting NF, Hall EJ. Radiat. Res. (2001) 156, 177–180.
(13) Biologic Effects of Ionizing Radiation (BEIR) VII: Washington, DC 20001, 2002.
(14) Feinendegen LE. The Brit. J. Radiol. (2005), 78, 3–7.
(15) Russo GL, Picano E. Euro.Heart.J (2012), 33,423-424.
(16) Smith, Battle G, Yair G, Navarrette, Guilmettee A, Raymond. Health Phys. 2011, 100, 263-265.

Evaluation of the Ventilation and Air Cleaning System Design Concepts for Safety Requirements during Fire Conditions in Nuclear Applications

Samia Rashad, Mohamed El –Fawal and Magy Kandil
Nuclear and Radiological Regulatory Authority , ENRRA Cairo, Egypt

ABSTRACT

The ventilation and air cleaning system in the nuclear or radiological installations is one of the essential nuclear safety concerns. It is responsible for confining the radioactive materials involved behind suitable barriers during normal and abnormal conditions. It must be designed to prevent the release of harmful products (radioactive gases, or airborne radioactive materials) from the system or facility, impacting the public or workers, and doing environmental damage. There are two important safety functions common to all ventilation and air cleaning system in nuclear facilities. They are: a) the requirements to maintain the pressure of the ventilated volume below that of surrounding, relatively non-active areas, in order to inhibit the spread of contamination during normal and abnormal conditions, and b) the need to treat the ventilated gas so as to minimize the release of any radioactive or toxic materials. Keeping the two important safety functions is achieved by applying the fire protection for the ventilation system to achieve safety and adequate protection in nuclear applications facilities during fire and accidental criticality conditions.The main purpose of this research is to assist ventilation engineers and experts in nuclear installations for safe operation and maintaining ventilation and air cleaning system during fire accident in nuclear facilities. The research focuses on fire prevention and protection of the ventilation systems in nuclear facilities. High-Efficiency particulate air (HEPA) filters are extremely susceptible to damage when exposed to the effects of fire, smoke, and water; it is the intent of this research to provide the designer with the experience gained over the years from hard lessons learned in protecting HEPA filters from fire. It describes briefly and evaluates the design safety features, constituents and working conditions of ventilation and air cleaning system in nuclear and radioactive industry.This paper provides and evaluates different design concepts or approaches for the ventilation and air cleaning system (VACS) that can be used to achieve safety and adequate protection in nuclear applications facilities during fire and accidental criticality conditions. Various anticipated events or accidents causing hazards in nuclear fuel cycle facilities, e.g. routine hazards, fires, accidental criticality and iodine release have been reviewed and discussed. Also it describes the possible fire protection approaches with their functional classifications and their engineered and administrative safety features. Finally a conclusion on the selection of the best design concept is recommended.

Key Words: *Ventilation and Air Cleaning System/ Safety Requirements/ Fire and Accidental Criticality Conditions*

INTRODUCTION

Concern about fires a potential agent of common cause failure in nuclear power plants has increased greatly since the serve fire at Browns Ferry in March 1975. This accident led to shutdown of the plant for 550 days and considerations of the basic design. the probability of incidents leading to core melt has been investigated by postulating various failure scenarios; the results have been reported on in a reactor safety study. The conditional frequency of core melt as a result of fires could have been as high as 0.03, while the unconditional frequency was 10^{-5} incidents per reactor year [1].

The goals of the fire protection scenarios are to minimize the potential for:

- The occurrence of a fire or related events;
- A fire that causes an unacceptable on - site or off - site release of hazardous or radiological material that will threaten the health and safety of employees, the public or the environment;
- Unacceptable interruptions as a result of fire and related hazards;
- Property losses from a fire and related events exceeding the prescribed limits ; and
- Critical process controls and safety class systems being damaged as a result of a fire and related events.

There are two important safety features common to all ventilation and air cleaning systems **(VACS)** in nuclear facilities[2] . They are: a) the requirements to maintain the pressure of the ventilated volume below that of surrounding, relatively non-active areas, in order to inhibit the spread of contamination during normal and abnormal conditions, and b) the need to treat the ventilated gas so as to minimize the release of any radioactive or toxic materials.

In addition, ventilation systems are designed for a reliable continuous operation and are constructed for easy testing, servicing and repair and easily accessible in accordance with the radiological protection principles [3]. It is possible to exchange components requiring servicing, e.g. fans, dampers, valves, measuring probes, without major structural building measures and without having to dismantle any components of safety related facilities. In addition ventilation systems and components in Air-Conditioning are designed to withstand the influences from those design basis accidents for the mitigation of which these facilities are required.

The design of the support and suspension stability of ventilation systems and components are induced vibrations from design basis accidents if, otherwise, secondary damages could occur to equipment that are required for ensuring safe enclosure of radioactive substances or are required in taking the reactor plant to the safe condition and keeping it in this safe conditions.(These requirements may also be met by providing special measures that limit the effects of vibrations on the components.)

The openings required for the external air supply or for the exhaust air in those buildings that are specified to be designed against pressure surges from external explosions shall be equipped with pressure surge protectors, e.g., pressure surge valves or labyrinth systems, provided, this is necessary for the protection of the components in these buildings. The surfaces of ventilation systems that are exposed to contamination is normally designed such that, either, the contamination remains negligibly small or a decontamination is possible.

The design of the components of ventilation systems, e.g. ducts, flaps and measuring probes, shall be with regard to materials and their construction, they will

withstand the maximum pressures and pressure differences, the relative humidity as well as the choice of conditions of temperature, corrosion and radiation expected during specified normal operation. The design shall take the characteristics of organic insulation materials into consideration. With regard to a possible failure of the negative pressure control and to an inadvertent closing of the ventilation valves of the containment vessel, measures shall be taken that will effectively prevent the occurrence of impermissible pressures inside the containment under all operating conditions of the ventilation systems[4].

The operating center of the external air supply facility in the restricted-access area shall normally be separated from the rest of the restricted-access area by pressure equalization locks. The structural enclosure of the restricted-access area shall be sufficiently air tight such that it is possible to achieve the guide values specified in [3] for negative pressures of the inner atmosphere required for maintaining a directed air current.

Doors shall be hung such that any existing pressure differences pull the doors shut, provided, there are no reasons of overriding importance, e.g., escape routes and pressure related design. The venting of combustible and harmful gases and fumes shall be based on sound engineering practice. All electrical power consumers of the ventilation systems, e.g. ventilators, may be connected to the auxiliary power supply facility, provided does not specify otherwise.

This Paper presents, discuss and evaluates different design concepts or approaches for the ventilation and air cleaning system that can be used to provide safety and adequate protection in nuclear facilities e.g. nuclear fuel fabrication plants and radwaste storage facilities [9], during fire and accidental criticality conditions. The Paper provides a summary of the recent international requirements for ventilation and air cleaning system protection, a discussion of selected fire protection considerations in designing nuclear facilities, and a description of the possible protection concepts with functional classifications, and conclusions on selection of the best design concept. It is the intent of this Paper to provide the regulatory body experts and inspectors of the ventilation system with the background necessary to fully evaluate the ventilation and air cleaning system fire protection design concepts in a nuclear facility. However the Paper is not intended to provide all of the design requirements, but to allow the filter media selection to be based on a comprehensive understanding of the different design concepts.

The Ventilation and Air Cleaning System Design

One of the most important tasks of the VACS is to limit the undesirable movement of radioactive material (i.e., contamination) inside and outside the nuclear facility [5]. The normal flow movement is from areas of least contamination to highest contamination. Filtration systems are used to prevent the contamination from entering exhaust plenums and exiting the building. A schematic diagram for VACS of a nuclear facility is shown in Fig.1. It consists of supply and exhaust systems and the filters are intended to prevent the contamination spread out of the building in the event accidental reverse flow [6].

The definitions of the different elements in fig .1.can be represented in the following:

(1) Vent air

Vent air is the air removed from a room or compartment.

(2) Separation efficiency of a filter

The separation efficiency of a filter with respect to a particular substance to be deposited on

the filter is equal to the ratio of the mass of the substance retained by the filter to the mass of the substance fed into the filter.

(3) External air

External air is the air drawn in from the outer atmosphere.

(4) Decontamination factor

The decontamination factor of a filter with respect to a particular substance to be deposited on the filter is equal to the concentration of this substance in the air fed into the filter divided by the concentration of this substance in the air vented from the filter.

(5) Pressure zone of a ventilation system

A pressure zone of a ventilation system is a zone made up of contiguous rooms and room groups at the same pressure level.

(6) Exhaust air

Exhaust air is the vent air released to the outer atmosphere.

(7) K-factor of an iodine adsorber

The K-factor of an iodine adsorber is equal to the common logarithm of the decontamination factor of the iodine adsorber divided by the retention time of the air in the iodine adsorber.

(The K-factor is dependent on the type of test medium and on the test conditions).

(8) Leakage air

Leakage air is the air that seeps in or out in an uncontrolled way.

(9) Train of the air conditioning system

A train of the air conditioning system is a contiguous arrangement of components in direction of the air current.

(10) Air exchange rate of a room

The air exchange rate of a room is the quotient of the volumetric air current into the room over the free air volume of the room.

(11) Redundancy

Redundancy is the existence of more functioning technical means than are necessary for the fulfillment of the planned function.

(12) Recirculated air

Recirculated air is the air circulated inside, or returned to, a confined region.

(13) Volumetric air current of a ventilation, air conditioning or filtration facility

The volumetric air current of a ventilation, air conditioning or filtration facility is equal to the air or gas volume passing through this facility or component in a given time period divided by this same time period [7].

(14) Supply air

Supply air is the air fed into a room.

(15) Secondary air

Secondary air is the supply air of a room that has first passed through another room.

The High Efficiency Particulate Air (HEPA) filters in the inlet to the exhaust plenum are expected to reduce the contamination entering the exhaust ducts, thus minimizing the buildup of contamination in the exhaust system. A typical HEPA filter design configuration used in nuclear facilities is shown in Fig.2. [8]

In the nuclear facilities, the supply and exhaust air handling units are selected and balanced to maintain the required air movement, to prevent undesired contamination

migration. Also, the exhaust system will handle slightly more air than the supply system to account for in leakage through doors and building joints. During accident conditions the ventilation systems usually automatically respond to maintain the required negative pressure differential. If an exhaust fan fails to run, a standby fan will automatically start or supply fans will shut down as necessary. While this is often discussed as maintaining negative pressure differential, it is positive in-flow that is critical. This differentiation becomes very important during a fire where bi-directional flow can occur in doors and openings[9].

Nuclear Facility Fire History

Fires in nuclear facilities have been caused by a variety of energy sources, including electrical energy and spontaneous combustion of pyrophoric metals. While fixed fire suppression systems or operator intervention have limited the size and consequences of most of these fires, some did propagate and cause significant damage and material release. There have been numerous occurrences of fire in nuclear facilities since the beginning of the Browns ferry in march 1975 many lessons learned from those fires. Some lessons have been learned at great expense. A brief history is discussed here in the hope that the lessons will not be forgotten or ignored by facility designers, operators and special for regulation inspectors .

Summary of fire events in nuclear power plants in the USA (United States American) and the FRG (Federal German) is represented in Table .1. in order to provide some idea of the fire records, causes and fire fighting activities in the two country.

History of Fire Involving Confinement Ventilation Systems

The following is a partial list of fires [10,11] known to have occurred in nuclear facilities, involving nuclear materials, and having some interaction with the facility confinement ventilation system or some other significance. These come from U.S. Atomic Energy Commission (AEC) Serious Accident Reports. The AEC was a predecessor of the U.S. Department of Energy.

1. Fire in Ventilating System Filters. U.S., July 27, 1955
2. Serious Ventilating System Incidents. U.S, November 8, 1956
3. Fire in British Windscale Facility. U. S., October 15, 1957
4. Explosion in Glove-Box Line of Plutonium Facility, . U. S ,October 28, 1957
5. Small Metallic Plutonium Fire Leads to Major Property Damage Loss. U.S. Nov., 27, 1957
6. Filter Fire ,U.S., December 2, 1958 and March 9, 1959
7. Drybox Explosion Disperses Polonium Contamination. U.S., October 8, 1959
8. Ventilating Air Filter Clogs During Fire. U.S., October 28, 1959
9. Plastic Windows and a $125,000 Sprinkler Head. U.S., October 29, 1959
10. Radiochemical Plant Explosion releases Plutonium Contamination Outside Facility. U.S., March 30, 1960
11. Sprinkler Protection Have Reduced $200,000 Radiochemistry Building Fire Loss. U.S., April 5, 1961
12. Polyester Fibrous Glass Duct Fire causes $43K Damage. U.S., January 31, 1964.
13. Filter Box Fire. U.S., February 7, 1964
14. Fire and the Reaction of Nitric Acid with Plutonium Ion Exchange Resin Leads to Major Property Damage. U.S., December 4, 1964
15. Explosion Within Glovebox Disperses Contamination. U.S., January 11, 1965

16. Burning Plutonium Chips Explode in Carbon Tetrachloride Degreasing Bath. U.S., March 12, 1965
17. Cutting Wheel residues in Plutonium Waste Cause Explosion. U.S., December 17, 1965
18. Hazardous Solvent Causes Explosion in a Glovebox. U.S., February 1966
19. Maintenance on Plutonium Machining Coolant Lines Leads to $17,500 Fire. Building 776/777, Rocky Flats, 1965, U.S., March 4, 1966
20. Fire During Glovebox Cleanup Leads to $23,000 Damage Via Contamination Spread. U.S., July 8, 1966
21. Fire Damages Hot Cell Window. U.S., November 4, 1966
22. Glovebox Explosion Causes $42,000 Damage and Plutonium 238 Contamination Spread. U.S., August 26, 1968
23. Waste Incinerator Incident Affirms Fire-Resistive Filter Value. U.S., July 31, 1968
24. Fire - Rocky Flats Plant - May 11, 1969. U.S., December 1, 1969
25. Incinerator Fire at Rocky Flats, July 2,1980. Investigation Report, July 31, 1980
26. Fire in TRISTAN Experiment at HFBR at BNL, March 31, 19945
27. Cerro Grande fire effects on HEPA filters at LANL May 4, 2000
28. Cutting Operations Ignite Residue In Bottom Of Glovebox, Rocky Flats Environmental Technology Site, Building 371, May 6, 2003

From the previous fire accidents involving ventilation systems and filters the following points can be outlined : Suppressing fire in ventilation systems is difficult due to the reactivity of the dust in the ductwork with water. Oxides generated by filters combustion in air of NaK, may carry by the ventilating system to a combustible filter. For unknown reasons, the NaK may began splattering and igniting the filters. The fire may involve a combustible filter under the hood and traveled through the exhaust system, reaching the main filter bank inside the nuclear building. A fire may occur on the inside of a cavern drybox designed although it is prepared for working with high levels of radioactivity. The fire spread to other areas within the cavern involving plastics and wood.

A fire may occur in a filter box on the roof of a nuclear facility. The burning filters can be manually removed from the box by firefighters who then can use carbon dioxide and dry chemical fire extinguishers to extinguish the fire. The fire causes rupturing the glovebox and dispersing plutonium throughout the glovebox line (there is no direct impact on HEPA filters).

During operations to remove the paint from the inside of a glovebox in preparation for its disposal, fire may involve flammable solvents occurred in the airlock for the glovebox system. And the fire can be put out by firefighters using solid carbon dioxide. Contamination is spread throughout the ventilation system ductwork and over two floors of the building. The initial fire may release a significant quantity of flammable vapors into the confinement ventilation system, which subsequently ignite and explode.

As a result of all these events, fire-resistant HEPA filters are researched, developed, and put into service in the nuclear industry. And the major recommendation is the use of fire resistive “absolute” filters.

Design Concepts of Ventilation systems

The major issues that must be addressed by the designers to successfully implement an all-HEPA filter design are:

- Design Data : There is little empirical design data on the performance of HEPA filters during fires. The data that is available is based on HEPA filters that were fabricated prior to the pricing pressure for clean rooms and DOE budget cuts.
-Life Expectancy : There has been an issue raised on the life expectancy of HEPA filters. Resolution of this issue may affect the final design and operating approach for a design based solely on HEPA filtration.
-Active Components : The integrity of the filtration system is dependent on active components to shift airflow between filter sets. The design of these components is expected to require additional effort by the design team.
-Housing Protection : No acceptable method to adequately reliable fire protection of the HEPA filter housings from direct fire effects has been identified.
-Pre filter Credit : It is possible to credit the pre filters to mitigate the smoke loading on the HEPA filters. If so, the pre filters are expected to be safety class and additional design data would need to be developed.
- Administrative Controls : The robustness of the filtration system is sensitive to the administrative controls that limit transient combustible loading and concept configuration controls to maintain the planned fixed combustible loading. This requirement will require special efforts by the design team and the facility operator.

1. Different Design Concepts of Ventilation systems

For the VACS system to successfully mitigate radioactive contamination spread during accidental conditions, it will require the following engineering safety requirements:

a) Air handling equipment to maintain the building at a negative pressure during and following the fire
b) Filtration media that allows ventilation flow during and following the fire (i.e., does not plug)
c) Control of the air temperatures approaching the filtration media, to avoid filter media failure by excessive temperature
d) Filtration media that do not collapse as a result of smoke loading during a severe fire.
e) Screens or water sprays that prevent hot brands from damaging filters

To accomplish the above five requirements efficiently, different design concepts or approaches for the VACS system are proposed as shown in Table 1. One or more approach could be implemented. In the following sections, different engineered and administrative safety design concepts or approaches for the VACS as well as its design requirements have been discussed and evaluated. These concepts can be used to provide adequate protection during fire and accidental criticality conditions in nuclear facilities.

Concept 1 : This approach Provides the utilization of a full HEPA filters protection system as well as the automatic water spray system is used to reduce the effect of plugging [11]. There have been several studies and standards that discuss the protection of HEPA filters by active water spray components. While most demonstrate successful protection, some indicate that water sprays can also accelerate filter plugging. In addition, the seal failure temperature (122°C for urethane [12]) is very close to the upper value of the fire detectors (121°C [13]), so excessive exposure may occur without spray system activation. Thus, the successful protection of HEPA filters by active water spray is problematic. It is possible that these issues can be resolved, but not with high certainty.

During fire accidents, the generated smoke, soot and dust aerosols due to fire, will enter the exhaust system and transfer to the filtration system where it will deposit on the

filters causing filter plugging. The quantity of smoke generated during a typical multi-room fire is expected to blind most HEPA filters media. The blinding can have two possible outcomes. (1) The air movement through the facility is reduced, compromising the negative pressure containment and allowing contamination to leave the building though doors and other openings; or (2) the filters collapse allowing the contamination to bypass the filtration media and exit the building through the filter plenum.

Concept 2: In this approach, there is adequate face area of HEPA filter media, to preclude unacceptable plugging during a fire and adequate dilution to preclude excessive temperatures at the filters. The two concepts are very similar and rely on the integrity of the HEPA filters. . In this concept, the philosophy behind it is very simple. It provides enough HEPA filter face area and any possible fire can be accommodated. To make such a system work will require some method to prevent hot brands from damaging the HEPA filters. This could be accomplished by fire screens. It is expected, but not confirmed, that the entire filter bank capacity cannot be on-line at one time, since the efficiency of the HEPA filters will drop for some particle sizes at low flow rates [14]. Thus, to make a large face area concept work it may be necessary to install a switching system to transfer airflow from "plugged" to "clean" filters.

For both concept 1 and 2, the filter housings must be protected from direct (external) fire effects, since the Concepts only provide for internal fire protection. This external protection might be accomplished by redundant parallel trains separated by fire rated construction, high-integrity, automatic fire suppression, or any other high reliability method. Without such protection a fire in the room containing HEPA housing has the potential to allow an unacceptable release

Concept 3 relies on the building safety class suppression system to prevent the fire from becoming too large for the ventilation system to handle. In this approach, fire propagation to more than 3 rooms must be prevented. Demonstrating that a fire in 2 rooms will not result in excessive temperatures at the HEPA filters, or unacceptable plugging.

Concept 4, a mix of HEPA and sand filters and exhaust system that is sized to accommodate the design basis fire accidents. It is a successful design concept that is used at many nuclear fuel cycle facilities [15]. With the exception of the exhaust fans, all of the Safety Class features are passive, thus the concept is very robust and flexible. Recent cost estimates for an integrated sand filter design are not available. The cost estimates for recent VACS designs have been for standalone attachments to facilities that have multiple stages of HEPA filtration. Thus, the estimates do not show the cost savings associated with reducing the complexity of the ventilation and air cleaning system. The major issues that must be addressed by the designer to successfully implement a combined HEPA filter and sand filter design are: -

Design Standard: No formal design standard has been published , so it will be necessary for the RB to generate a design basis .

- Seismic Qualification: There is limited information on how sand filters perform during earthquakes. The RB will need to generate empirical data and analysis to demonstrate that sand filters will perform adequately during seismic events.

Concept 5, this concept provides the utilization of radioiodine charcoal filters combined with the full HEPA filter concept. It is demonstrated especially for radioiodine removal in fuel processing plants either in normal operation or during accidental criticality conditions.

2. Comparison between the different Concepts of Ventilation systems

In the design of nuclear facilities, several automatic responses to fire events are considered. The earliest approach is to shut off the supply air and close inlet dampers when a fire is detected. This has the effect of reducing the airflow through the facility, thus reducing the oxygen supply to the fire and limiting the fire size. If a significant fire size reduction is achieved the temperatures in the fire compartment will drop. The more recent approach is to maintain or increase flow during a fire event. This has the effect of reducing room temperatures and pressure by diluting the heated combustion gases as shown in Fig. 4 . As shown in the figure, it is possible, although undesirable, to optimize the air movement or flow through the building to control the fire compartment temperature and pressure.

The first concept (full reliance on the HEPA filter spray system) relies on active components to be successful. As mentioned above, the difference between the specified detector temperature range and the filter failure temperature is minimal, thus the system may not activate on demand. This shortcoming is considered a potentially irreconcilable issue representing a very high potential risk. This high risk merits exclusion of this design concept from further consideration. In addition, there is limited test data demonstrating the robustness of this design approach. However this concept has been approved by the DNFSB [15, 16]**.**

The second concept can be readily constructed. While there is some uncertainty in the smoke plugging data, excess capacity can compensate for this shortcoming. In addition, it is expected that active safety class components may be needed to switch the flow prior to filter plugging. The flexibility of this design is limited and the costs for this Concept have not been developed.

Concept 3, In it there are no nuclear facilities that rely on (Safety class building suppression system) so the concept has not been reviewed by RB authorities. However this concept was never fully developed into a final design. Thus, it is uncertain if RB authorities would accept this concept. Based on the lack of demonstrated success using concept 3, the risk is considered very high and further consideration of this Concept is not recommended.

Concept 4, it is a successful design concept that is used at multiple nuclear fuel cycle facilities [15]. With the exception of the exhaust fans, all of the Safety Class features are passive, thus the concept is very robust and flexible. Recent cost estimates for an integrated sand filter design are not available. The cost estimates for recent VACS designs have been for standalone attachments to facilities that have multiple stages of HEPA filtration. Thus, the estimates do not show the cost savings associated with reducing the complexity of the ventilation and air cleaning system.

The major issues that must be addressed by the designer to successfully implement a combined HEPA filter and Sand filter design are: .

–Design Stand: No formal design standard has been published, so it will be necessary for the RB to generate a design basis .

–Seismic Qualification: There is limited information on how sand filters perform during earthquakes. The RB will need to generate empirical data and analysis to demonstrate that sand filters will perform adequately during seismic events.

The restricted supply air approach (i.e., ventilation controlled) has several disadvantages. If the flow is not restricted adequately, it is possible that the flow reduction could increase, rather than decrease the fire temperatures. In addition this approach seldom will extinguish the fire, thus significant smoldering combustion is expected. This type of combustion produces carbon monoxide, rather than carbon dioxide, that has the potential to explosively ignite (i.e., back draft). Thus, while restricting the supply air will often result in a less severe

fire, the approach has an inherent instability (i.e., explosion potential) that can cause significant consequences.

The high air supply approach reduces the air temperature, as shown in Fig.4, in smaller and less severe fires. Thus, the likelihood of these fires growing until they cause measurable contamination releases is reduced. Since such fires are generally anticipated (frequency > 1E-2/yr) [6], this is very desirable. This approach is possible because the combustion rate of most fuels is limited by the evolution of combustible gases (i.e., fuel surface controlled). The ventilation has other advantages. These include: removal of smoke allows fire fighters to be more effective, and removal of heat reduces compartment pressure and minimizes damage of equipment and containers.

Concept 5 is a matter of safety concerns, where radioiodine removal either during normal operation or criticality, is performed through out a combined units of charcoal and HEPA filter assemblies. Since the aim is to collect all the iodine in one off-gas stream so as not to have to set up numerous iodine removal devices, as much iodine as possible should be removed from the feed solution to the dissolver off-gas. In order to do this, the iodine must be maintained in or converted into the highly volatile elemental form. Radioiodine releases during normal or accidental conditions could be reduced by using of modular and mobile filter units, which are particularly useful for localized extraction and air cleaning operation**.**

To evaluate the above concepts, the importance of the various design features need to be ranked. In developing ranking criteria functional classification process can be useful. This process identifies the following levels of protective features:

- Safety Class (SC) – Controls that reduce the unmitigated public risk to below the evaluation guidelines
- Safety Significant – Controls that reduce the unmitigated worker risk to acceptable level or provide defense-in-depth to a safety class protective feature
- Design Feature – Controls that provide for a significant reduction in risk, but are not required being safety class or safety significant.

Table 2 provides a ranking of the importance of the design features for the different ventilation concepts. In performing this ranking the functional classification level of safety significant and design features were combined into a category considered important to safety (IS). An additional category Operating Feature (OF) was also created. Features in this category might limit risk but are not required for facility risk to be considered acceptable. There were several features that must be safety class for all possible concepts. These include the building structure, the exhaust fans, the supply system filtration (or backflow prevention) and the exhaust filtration. Thus at least Five features must be safety class. In evaluating each concept the respective number of SC features is 10, 11, 11,6 and 6. as shown in Table 3. Thus, the sand filter approach requires the fewest SC features.

In selecting between the different proposed design concepts, the evaluation metrics are: construction cost, operating cost, and risks. The designers focus on the potential risk metric since cost estimates can be readily developed once the design and operating costs are understood. There are many factors or parameters that contribute to the design risk metric. These are:

- State-of-the-art for design concept
- Robustness of the design approach
- Extent of design data available
- Flexibility of the design
- Acceptance by reviewers, and

- Complexity of the design concept .

Table 3 summarizes the potential risks for the proposed VACS concepts.

In judging complexity of the number and type of protective controls that will be used, it is preferable to use engineered controls (i.e., structures, systems and components, SSC) rather than administrative controls. Where engineered controls are used passive is preferable, since they usually have the greatest reliability. Active controls can be further separated into two sets, those requiring a change of state following the accident initiator and those that do not. The order of preference is thus:

1- Passive SSC (e.g., building structure) .
2- Active SSC not requiring a change of state (e.g., continuously operating exhaust fan)
3- Active SSC that must change state after the event initiatory occurs (e.g., emergency generator)
4- Administrative controls

CONCLUSIONS

The Paper provides and evaluates different design concepts for the VACS system proposed to provide adequate fire protection at the nuclear facilities:

1. Two approaches are considered viable: an all-HEPA filter system that relies on dilution to prevent excessive temperatures during a fire, and a system that relies on a combination of HEPA filters and a sand filter. The other Concepts are reliance on the HEPA filter water spray fire suppression system, and a building-wide safety class fire suppression system. Both of these latter Concepts are considered to have an unacceptably high potential risk. .
2. The all-HEPA filter VACS system concept will require multiple passive and active safety class components to limit fire risk. Some of these would include building structure, exhaust fans, exhaust filtration, supply filtration (or backflow protection), fire screens, and active control dampers to redirect flow when filters plug.
3. The sand filter VACS system concept will require the fewest number of safety class components to limit the fire risk. The major safety class components would include the building structure, exhaust fans, external ventilation ducts and the filter. With the exception of the exhaust fans all of these components will be passive, thus the system can be considered very flexible and reliable. .
4. Charcoal filters in a modular, mobile and reliable units combined with the all HEPA filter concept could be used in nuclear facilities during normal operations and in case of accidental criticality conditions. .
5. Both the all-HEPA filter and the sand filter VACS system concepts can be successfully constructed and operated to achieve the desired risk profile. Since both have advantages, the selection between these concepts is best made by balancing construction costs, operating costs and the potential risk.

REFERENCES

(1) S. M. Rashad, A. Z.Hussein, F. H. Hammad, " Comparative study of fire protection guidelines in nuclear power plants", proceedings of an international symposium on fire protection and fire fighting in nuclear installations organized by IAEA, 1989.

(2) Standard for Fire Protection for Facilities Handling Radioactive Materials. 1998. Quincy: MA. National Fire Protection Association. NFPA 801.
(3) J.G.Wilhelm, "Iodine Filters in Nuclear Installations" Commission of the European Communities, October 1982.
(4) Standard for Fire Protection for Facilities Handling Radioactive Materials. 1998. Quincy: MA. National Fire Protection Association. NFPA 801.
(5) D. J. Will,e et. al; " Safety Review of the Hanford Spent Nuclear Fuel Project During the Design and Construction Phase" DNFSB/TECH-30, February 2011 .
(6) D. A. Coutts, J. M. East, J. W. Lightner, W. R. Mangiante, J. K. Norkus, and J. R. Schornhorst. 1998. Actinide Packaging and Storage Facility Fire Studies Summary Paper. Aiken: SC. Westinghouse Savannah River Company. (July) WSRC-TR-98-00255.
(7) Hall, Jr., John R. 1994. "The U.S. Experience with Smoke Detectors: Who Has Them? How Well Do They Work? When Don't They Work?" NFPA Journal. (September/October) 36-46.
(8) Viera, Diane L. 1992. "Fire Doors: A Potential Weak Link in the Protection Chain" Fire Technology. (May) pp 177-80. .
(9) DOE TECHNICAL STANDARDS NOVEMBER 2003.
(10) W. M. Shields, F. Bamdad, and A.K. Gwal," Fire Protection at Defense Nuclear Facilities"DNFSB/TECH-27, June 2000.
(11) Hall, Jr., John R. 1993. "The U.S. Experience with Sprinklers: Who Has Them? How Well Do They Work?" NFPA Journal. (November/December) 44-55 .
(12) Fire Protection Design Criteria. 1999. Washington: DC. U.S. Department of Energy. (July) DOE-STD-1066-99. .
(13) National Fire Alarm Code®. 1999. Quincy: MA. National Fire Protection Association. NFPA 72
(14) Burchsted, C. A., J. E. Kahn, and A. B. Fuller. 1969. Nuclear Air Cleaning Handbook. Oak Ridge, TN: Oak Ridge National Laboratory. ERDA 76-21.
(15) Zavadoski, Roger W., and Dudley Thompson. 1999. HEPA Filters Used in the Department of Energy's Hazardous Facilities. Washington: DC. Defense Nuclear Facilities Safety Board. (May) DNFSB/TECH-23.
(16) Zavadoski, Roger W., and Dudley Thompson. 2000. Improving Operation and Performance of Confinement Ventilation Systems at Hazardous Facilities of the Department of Energy. Washington: DC. Defense Nuclear Facilities Safety Board.. DNFSB/TECH-26, February 2000. (17) Preparation Guide for U.S. Department of Energy Nonreactor Nuclear Facility Safety Analysis Papers. Washington: DC. Department of Energy, DOE-STD-3009-94, June 2012.

Table 1. Fire Events in Nulear Power plants in the USA and FER.

Item	USA	FRG
No of recorded incidents	354	59
No of operating plants	104	18
Reactor-years	952	182
Events per plant per year	0.17	0.32*
Causes of fire (%)		
Component failure	5.9	
Oil leakage		30.4
Welding	1.5	
Electrical failure	17.5	22.1
Heating	11.9	6.8
Explosion	7.8	
Component and electrically failure	9.1	
Component failure and	11.25	
Over heated material		
Others	21	13.6
Fire fighting(%)		
Shift personnel		
Fire brigade (plant)	27.6	25.6
Fire brigade(civic)	7.7	57.7
Automatic system	12.7	6.7
	5.9	
others	46.1	10

*This includes fires in parts of the plant relevant to nuclear safety.

Table 2.: Proposed VACS concepts and their design features

VACS Concept	Design Features
I II III IV V	- Full HEPA filters protection and demonstrate that the automatic water spray system reduces t he effect of plugging. - Adequate face area to preclude unacceptable plugging during a fire and adequate dilution to preclude excessive temperatures at the filters. - Using safety class building suppression system for preventing fire propagation to more than 3 rooms. Demonstrate that a fire in 2 rooms will not result in excessive temperatures at the HEPA filters, or unacceptable plugging. – Combined HEPA and sand filter with exhaust system that is sized to accommodate the design basis fire. -Charcoal filter for Radioiodine absorbing combined with the full HEPA filter approach.

Table 3: Summary of potential risks for VACS design concepts.

VACS Design parameters	Concept 1: ALL-HEPA	Concept 4: HEPA & Sand Filter	Concept 5: Charcoal & HEPA
State of the art for design concept.	-	+	+
Robustness of the design approach Extent of			+
design data available.	-	+	+
Flexibility of the design.		+	+
Acceptance by reviewers	-	+	+
Complexity.	-	+	+
Extent of passive features.	-	+	+
Design standard at component level.	+	+	+
System design standard.	-	-	+
Seismic integrity fully demonstrated.			

Table 4: Ranking of design features for proposed VACS protective concepts

Function	SSC	Item Description	HEPA			Concept 4	Concept 5
			Concept 1	Concept 2	Concept 3	HEPA & sand filter	Charcoal & HEPA
Containment	Building structure	Exterior	SC	SC	SC	SC	SC
		Fire barriers	IS	SC	SC	O-F	O-F
		Fire partitions	O-F	O-F	SC	O-F	O-F
	Ventilation	Supply fans	O-F	O-F	O-F	O-F	O-F
		Exhaust fans	SC	SC	SC	SC	SC
		Fire dampers	O-F	O-F	SC	O-F	O-F
	Control dampers	Supply	O-F	SC	OF	O-F	O-F
		Exhaust	SC	SC	O-F	SC	SC
	Ductwork	Internal to building	SC	SC	IS	IS	IS
		External to building	SC	SC	IS	SC	SC
	Filtration	Supply HEPA	SC	SC	SC	SC	SC
		Exhaust HEPA	SC	SC	SC	O-F	O-F
		Sand filter	…	…	…	SC	…
Fire protection	HEPA	Automatic spray	SC	IS	IS	…	…
		Manual spray	O-F	O-F	O-F	O-F	O-F
		Fire screen	SC	SC	SC	…	…
		Demister	SC	SC	SC	…	…
	Building wide	Sprinkler	O-F	O-F	SC	O-F	O-F
		Detection	O-F	O-F	SC	O-F	O-F
Iodine retention			…	…	…	…	SC
Number of safety class SSCs			10		11	6	6

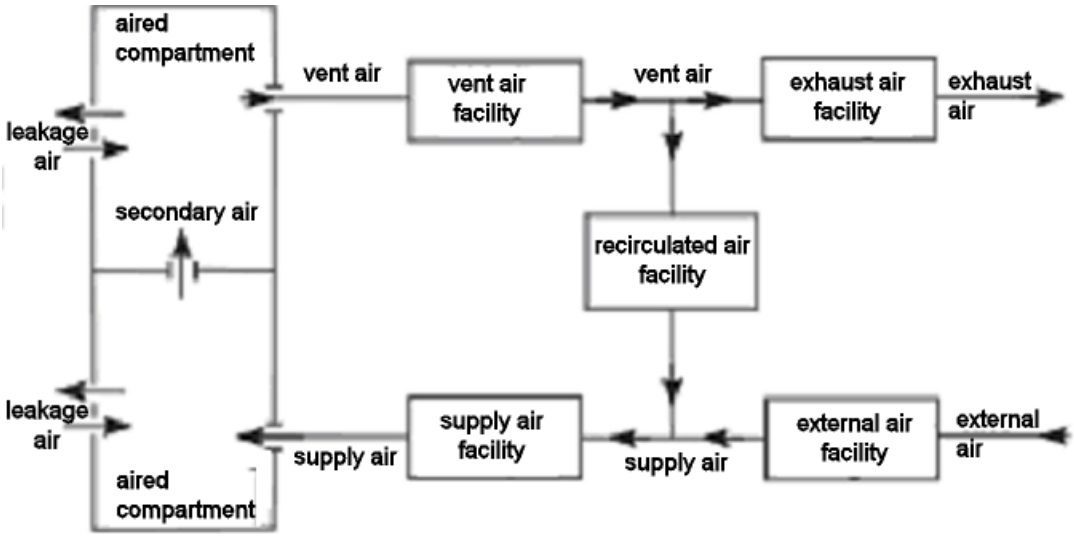

Fig. 1 . A schematic diagram for ventilation and air cleaning system of a nuclear facility

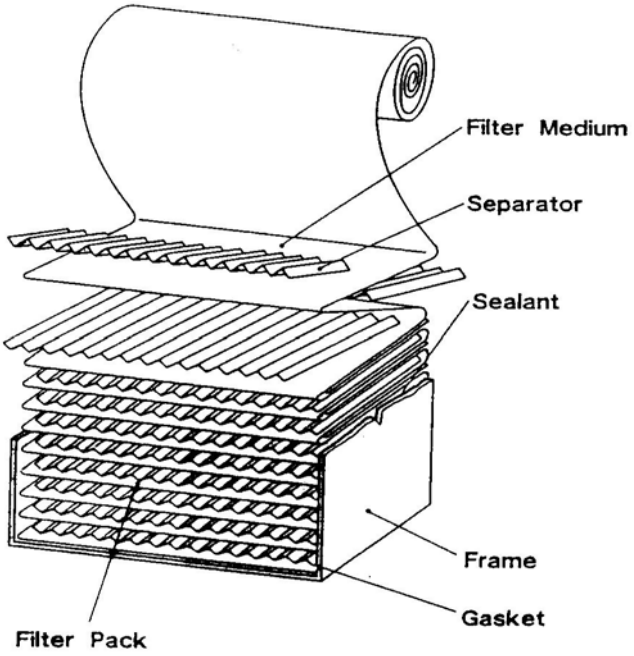

Fig. 2. A typical HEPA filter design configuration used in nuclear facilities

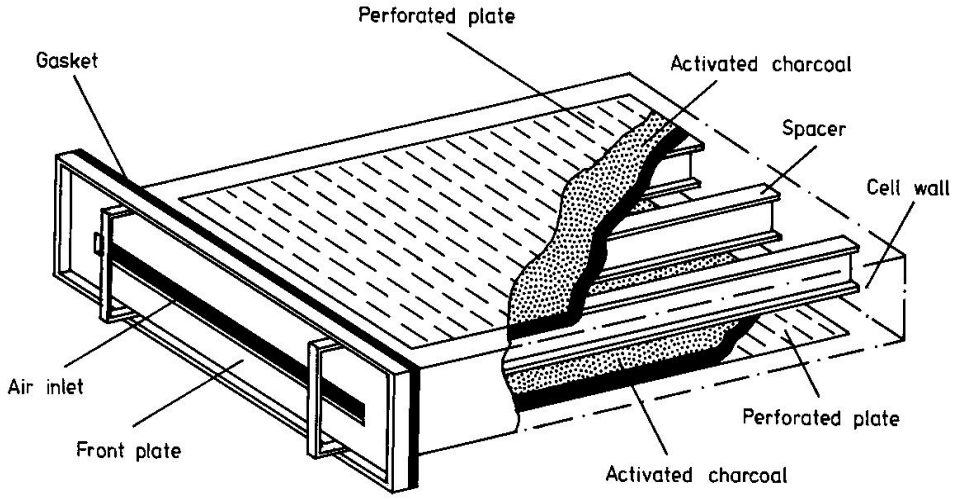

Fig.3. A Typical charcoal filters for Iodine retention in a nuclear facility

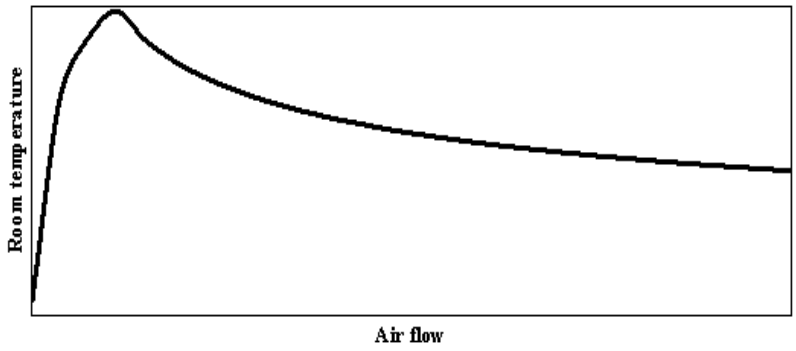

Fig.4. Ventilation effect on room temperature

Charge transport and X-ray dosimetry performance of a single crystal CVD diamond device fabricated with pulsed laser deposited electrodes

Mohamed A.E. Abdel-Rahman[1/2], Annika Lohstroh[2], Imalka Jayawardena[3] and Peter Bryant[2]

[1] *Military Technical college, Cairo, Egypt*

[2] *Department of Physics, University of Surrey, Guildford, Surrey GU2 7XH, South East Physics Network (SEPnet), United Kingdom*

[3] Advanced Technology Institute, University of Surrey, Guildford, Surrey, United Kingdom

e-mail: marahman_e@yahoo.com

ABSTRACT

The deposition of amorphous Carbon mixed with Nickel (C/Ni) as electrodes for a diamond radiation detector using Pulsed Laser Deposition (PLD) was demonstrated previously as a novel technique for producing near-tissue equivalent X-ray dosimeters based on polycrystalline diamond. In this study, we present the first characterisation of a single crystal CVD diamond sandwich detector (of 80 nm thickness) fabricated with this method, labelled SC-C/Ni. To examine the performance of PLD C/Ni as an electrical contact, alpha spectroscopy and x-ray induced photocurrents were studied as a function of applied bias voltage at room temperature and compared to those of polycrystalline CVD diamond detectors (PC-C/Ni); the spectroscopy data allows us to separate electron and hole contributions to the charge transport, whereas the X-ray data was investigated in terms of, linearity and dose rate dependence, sensitivity, signal to noise ratio, photoconductive gain, reproducibility and time response (rise and fall-off times). In the case of electron sensitive alpha induced signals, a charge collection efficiency (CCE) higher than 90 % has been observed at a bias of -40 V and 100 % CCE at -300 V, with an energy resolution of ~3 % for 5.49 MeV alpha particles. The hole sample showed very poor spectroscopy performance for hole sensitive signals up to 200 Volt; this inhibited a similar numerical analysis to be carried out in a meaningful way. The dosimetric characteristic show a high signal to noise ratio (SNR) of ~7.3×10^3, an approximately linear relationship between the photocurrent and the dose rate and a sensitivity of 4.87 μC/Gy.mm^3. The photoconductive gain is estimated to around 20, this gain might be supported by hole trapping effects as indicated in the alpha spectroscopy. The observed rise and fall-off times are less than 2 and 0.56 seconds, respectively – and mainly reflect the switching time of the X-ray tube used.The reproducibility of (0.504 %) approaches the value recommended by the IAEA (~ 0.5 %) and hence minor improvements in processing parameters and device geometry have the potential to fulfil this requirement.

Keywords: *CVD diamond, radiation detector, alpha spectroscopy, dosimetric characteristics, carbon electrode, PLD*

INTRODUCTION

The radiation hardness and the corrosion resistance of diamond allow it to be used for measuring radiation in difficult circumstances / hostile environments such as in nuclear waste monitoring [1]. The strong atomic bonding in the crystal structure is an advantage in diamond, which gives the material the ability to measure high intensity ionizing radiation with a long device life time.

Diamond is an attractive material for radiation detection purposes especially when used in medical applications. One of its advantages is its near tissue equivalence [1-6] where its atomic number is comparable to that of human tissue (Z=6 for diamond and Z≈7.5 for human tissues). Thus the energy absorbed by diamond is similar to that absorbed by human tissue, which reduces the need for correction mechanisms as with other semiconductor materials [6]. Its high bandgap (5.5 eV) [1, 3, 7-9] ensures a low dark current and hence a low background noise. It also has a high electron and hole mobility [2, 3, 7, 8], which permits a fast time response of the signal.

It is preferable to use electrical contacts with low thickness and low atomic number in medical applications. For this reason, carbon is considered the optimum choice as electrical contact. Pulsed Laser Deposition (PLD) of amorphous carbon and carbon/metal mixtures allow us to control the electrical properties of the electrode layer by the variation of deposition parameters. Amorphous carbon films (containing a high proportion of sp^3 bonds) are called diamond-like carbon (DLC) as they have similar properties to diamond. Of particular interest in this context are radiation hardness, tissue equivalence, non-toxicity and chemical inertness [2, 3]. Therefore the development of DLC as electrode films will help applications in medical x-ray dosimetry. The deposition by laser helps the formation of a layer of carbon with a high quality and a low percentage of sp^2 hybridization [3], which in turn reduces the conductivity of the material and consequently reduces the dark current. The quality of this film depends on the ratio of sp^3/sp^2 bonded carbon in the film that can be influenced by many preparation parameters such as the laser fluence, number of laser shots used, pulse duration, and nature of the graphite target [4].

In this work, spectroscopic and dosimetric characterization results of a single crystal CVD diamond (SC-C/Ni) with a mixed C/Ni contact was fabricated using pulsed laser ablation of a mixed graphite/Nickel target in an attempt to remove the dose rate dependence in polycrystalline CVD diamond detector (PC-C/Ni), which published in a previous report [10], and a comparison drawn to the previous polycrystalline device. Finally using alpha particle spectroscopy the electron and hole transport properties were separately investigated for SC-C/Ni device confirming the results of some of the measurements undertaken using x-rays.

DEVICE FABRICATION

Due to the superior properties of the polycrystalline diamond with a contact of C/Ni (at.80:20) in a previous report [10] , Poly-C/Ni, investigated as x-ray dosimeters, another device with the same electrical contact (C/Ni (at.80:20) was produced using the same technique, on a single crystal CVD diamond material. This device was labelled SC-C/Ni. The description of the device fabrication has been published previously and can be found in detail in [10]. A single crystal electronic grade chemical vapour deposited diamond sample (area 4 x 4 mm^2, 0.4 mm thickness) was procured from Element Six Limited and with C/Ni contacts of

80 nm thickness were produced in sandwich geometry on both sides sample as described in [10].

Prior to the electrode deposition, the base material was chemically treated for oxidation before DLC deposition to improve the surface properties and ensure an oxygen terminated surface with high resistivity. For the oxidation of the material 5 grams of potassium nitrate (KNO_3) were mixed with 20 mL of concentrated sulphuric acid (H_2SO_4) and heated to a temperature of 300 ^{0}C [11]. The sample is then submerged in the boiling solution for 5 minutes; the sample is washed with de-ionized water and then acetone. This was then followed by washing it in isopropanol and finally another wash by using de-ionized water.

The main set-up, as shown in figure (1), is simply composed of two components, the vacuum (growth) chamber and a source which is a high-power laser. The former has multiple sample holders and a rotating target holder is housed inside the vacuum chamber (typically operated at 6×10^{-6} Torr). A 25 ns pulsed KrF excimer laser (Lambda- Physik LPX 210i) operating at 248 nm is focused through a quartz window onto the target to evaporate the material and form a plasma plume which then deposits a thin film on the surface of the sample. The deposited material is amorphous in nature. By ablating an sp2 rich target with short laser pulses a plasma plume with energetic species (ions, small carbon clusters) are formed. Due to the lack of a background gas, the carbon deposited on the substrate is also highly energetic in nature and leads to the formation of an amorphous film that is more Diamond like in nature [12].

The focused laser beam falls on the carbon target surface (which is 6 cm away from the samples) with an angle of 45^o with respect to the normal of the target surface. Before any deposition the target is cleaned for 10 minutes while rotating with a speed of 40 rpm to improve the adhesion of the deposited thin film, on to the crystal (sample) through the removal of any contamination present on the top layer of the target surface. During the deposition process, the target is also rotated at the same speed. Deposition of each film was carried out using 2500 laser shots.

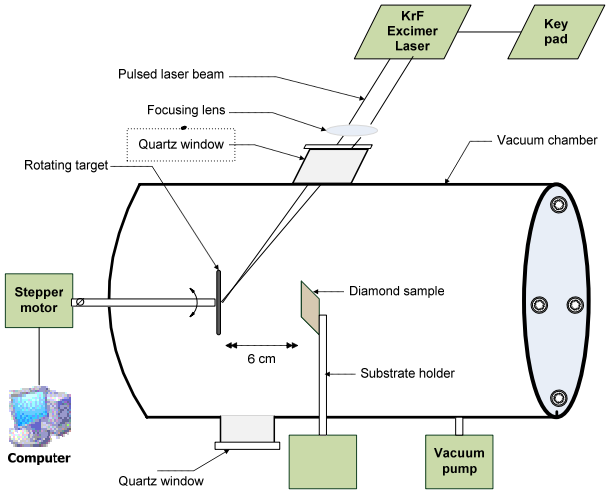

Figure (1): Schematic diagram of the thin film deposition on the single-crystal diamond using the Pulsed Laser Deposition (PLD) technique.

In order to determine the optimum fluence required for the carbon to adhere to the diamond sample and to give a film with a good quality, four different fluence values were investigated on low cost SiO_2 samples. The values of the fluence used were 3, 4, 5 and 6 J/cm^2. It was found that the increase of the fluence results in the increase of stress which results in poor adhesion (adherence) of the deposited layer. A fluence of 4 J/cm^2 (focused to a spot size of 2×0.5 mm^2) was found to be the optimum and was achieved using 40 mJ of energy per pulse with a repetition rate of 10 Hz.

The target used for the fabrication was C/Ni: 80:20 (at. %). The C/Ni contact deposited on the centre of the sample on both sides using a shadow mask with dimensions 2×2 mm^2. The entire procedure is repeated for the other face of the crystal. The shadow mask used in the second deposition is a mirror image of the first one to keep the symmetry of the deposited devices on both sides of the crystal as shown in figure (2).

After contact deposition, the SC-C/Ni device was annealed at 600 ^oC for 10 minutes, to increase electron delocalization through graphitization leading to better electrical properties [12]. This was achieved using a Lenton low pressure furnace operated with 100 sccm of Helium. The ramp rate of the heating oven is in the 15-20 ^oC/min range. Then the sample was mounted on a printed circuit board (PCB), using a small dot of Colloidal Graphite Epoxy on the centre of the deposited square. A gold wire (thickness of 24 μm) was attached to the contact on the top using Conductive Silver Epoxy. The other end of the gold wires was connected to their corresponding copper pads on the PCB using silver paint. The pads are connected with standard electrical wires connected to a BNC bulkhead connector.

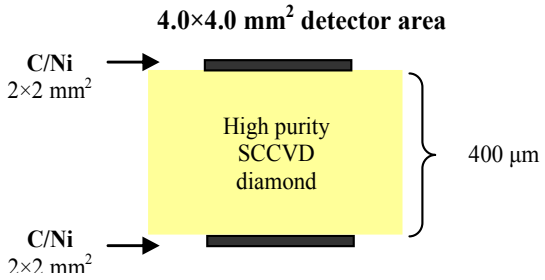

Figure (2): Schematic diagram of the SC-C/Ni diamond detector.

In this work, the alpha response of the SC-C/Ni device will be reported. Alpha spectra were acquired and used to measure the energy resolution, charge collection efficiency (*CCE*) and mobility-lifetime ($\mu\tau$) product. This was performed using a 3.5 kBq ^{241}Am alpha source with a mean energy of 5.49 MeV.

The diamond device was irradiated in a vacuum chamber with alpha particles from the ^{241}Am source as shown in figure (3). These measurements were performed in the dark, at room temperature with pressure less than 10^{-1} mbar. The benefit of performing these measurements in a vacuum is to avoid the loss of energy from the alpha particles due to attenuation in air. The device was connected to a charge sensitive preamplifier (ORTEC 142) and the output signal connected to a shaping amplifier (ORTEC 570), followed by a multi-channel analyzer (MCA, DSP-spect). During the irradiation with alpha particles, a high voltage was applied to the detector via the preamplifier as shown in figure (3). The pre-amplifier is disconnected from the detector and directly connected to a 2.31 pf capacitor and pulser during the energy

calibration. This allows an absolute system calibration of the electronics in the system to be performed.

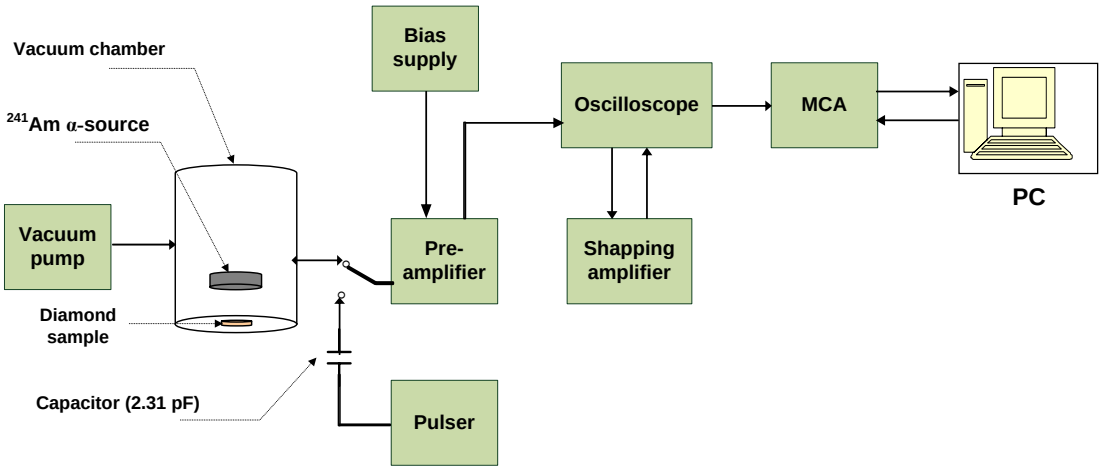

Figure (3): Schematic diagram of the α-spectroscopic set-up for the SC-C/Ni diamond device irradiated by 3.5 kBq ^{241}Am α-source of 5.49 MeV.

Alpha spectroscopy of the SC-C/Ni

The range of a 5.49 MeV alpha particles within diamond is of the order of 15 μm [13] (and as such very close to the surface of the detector). For this reason when irradiating the surface of the detector where a positive bias is applied, the majority of the signal produced within the device will be from holes. This is due to the electron hole pairs being produced close to the anode and as such the holes travel though almost the entire thickness of the device till they reach the cathode whereas the electrons move through only a small portion of the device till they reach the anode. It is therefore possible to investigate the properties of electrons and holes separately by changing the applied bias to the irradiated surface.

Alpha spectra

Figure (4) shows the spectra of the ^{241}Am of 5.49 MeV alpha particles (3.5 kBq) acquired with the SC-C/Ni diamond device at different bias voltages (negative and positive bias, drift of electrons and holes, respectively) ranging from 50 to 200 V. With an increase in negative bias voltage the centroid peak is shifted to a higher energy position and the resolution is improved.

However, at a positive bias (hole transport) the behaviour of the device is clearly different i.e. the centroid channel number (peak position) is far lower than that of an equivalent negative bias. This gives the impression that the charge collection efficiency increases more slowly with increasing positive bias and has not yet reached the plateau level at 300V. Furthermore, there is no significant change in the peak amplitude with the bias and there is an increase in peak broadening as shown in figure (4). This contrast is believed to be due to the polarization effects.

All these observations give the impression that the electron transport properties for SC-C/Ni are superior compared to holes. It should be noted that the experiments were repeated twice to investigate the reproducibility of the measurements. The repeat measurements

showed reasonable reproducibility for this sample.

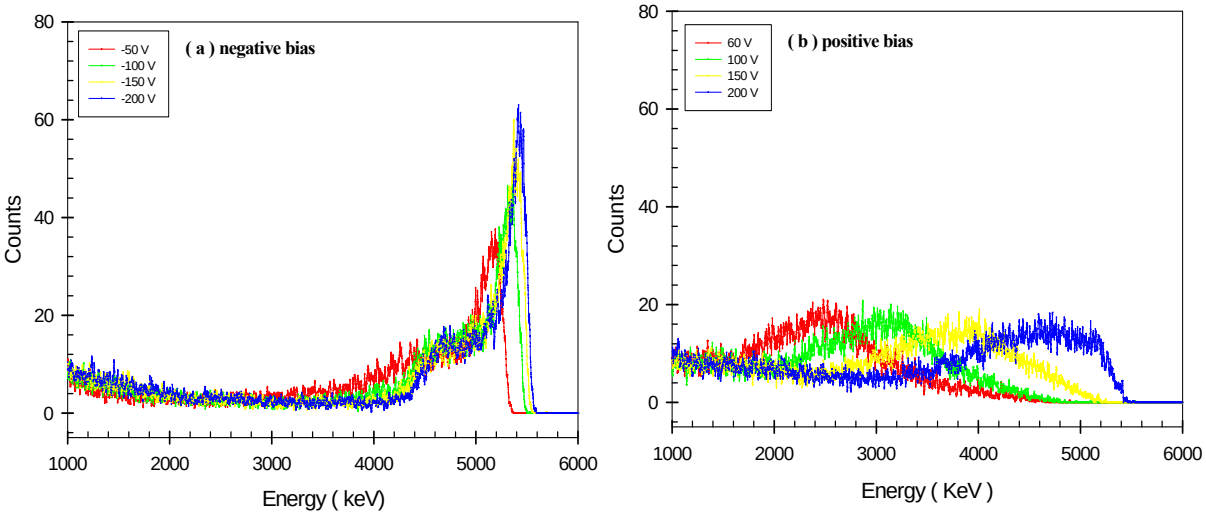

Figure (4): Alpha spectra of the SC-C/Ni diamond device under ^{241}Am α-source at (a) negative (b) positive bias.

Energy resolution

Because of the asymmetry in the shape of the peak, the results of the Gaussian fit (used to determine the centroid location and FWHM) are sensitive to where you define the region of interest (ROI) included in the fit. In this particular case various ranges were chosen for the ROI and it was found that the maximum variation in both the centroid position and FWHM are ~ 0.5%.

By fitting Gaussian curves to the main peaks of the diamond spectra, the FWHM of 160 keV for negative bias (for electron transport) and consequently $\Delta E/E_\alpha \approx 3$ %, was found at -150 V. As for the positive bias, as a result of the broadening peaks, as shown in figure (4), it is seen that the value of the FWHM is higher than its corresponding value at the negative bias and it reaches a value of around 400 keV ($\Delta E/E_\alpha \approx 8.5$ %) at 150 V. It should be noted that even at high voltages the FWHM of the spectra is still large. The relatively broad width of the FWHM, which reduces the energy resolution, for hole transport is caused by a high density of hole traps, combined with a non uniform distribution for the electric field.

The measured values of the FWHM, at negative bias, are consistent with the typical value (~3%) suggested by Galbiati et al [15] for a single crystal diamond having DLC/Pt/Au contacts when exposed to a ^{241}Am 5.49 MeV alpha source. The comparison shows a good agreement between the experimental and the published data.

Charge Collection Efficiency and Mobility-lifetime product

The CCE of a radiation detector can be calculated according to the Hecht equation [19]:

$$CCE = \frac{\mu\tau V}{d^2}\left[1-\exp\left(\frac{-d^2}{\mu\tau V}\right)\right].$$

where $\mu\tau$ is the mobility – lifetime product of the charge carriers, V is the detector bias and d is the detector thickness. Figure (5) shows the obtained CCE and the corresponding Hecht equation fit for both electrons (negative bias) and holes (positive bias).

It is clear from figure (5) that at negative bias (electron drift) high CCEs > 90% are obtained over a wide range of bias starting from -40 V and a max CCE of ~100% is observed. Additionally, a high mobility-lifetime ($\mu_e\tau_e$) product is estimated (~1.16×10^{-4} ±3.4×10^{-5} $cm^2.V^{-1}$).

As for positive bias (hole drift), it is obvious that the *CCE* plot differs from that which is obtained at negative bias. The CCE increases with bias reaching a maximum *CCE* value of ~89%. A significant lower mobility-lifetime ($\mu_h\tau_h$) product of ~1.55×10^{-5} ±1.1×10^{-6} ($cm^2.V^{-1}$) is obtained for holes, which indicates that the transport properties of the holes are worse than that of the electrons.

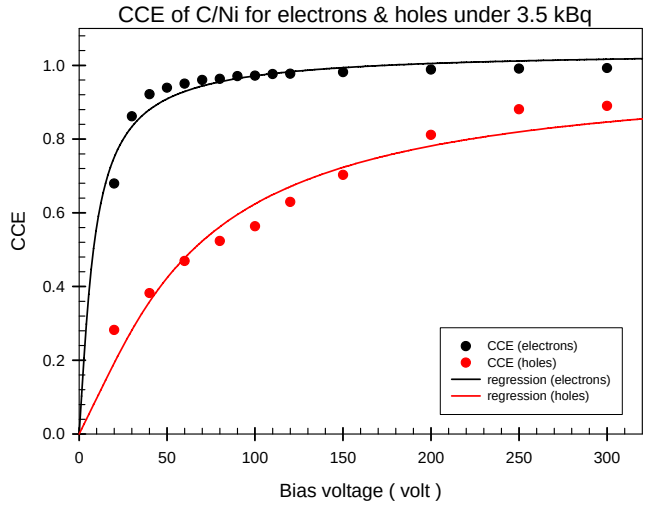

Figure (5): The *CCE* and the Hecht plot of the SC-C/Ni diamond device as a function of both negative and positive bias.

Although generally it is reported that the hole mobility in diamond is higher than the electron mobility however in this device the CCE of electrons is higher than of holes. This could be related to a high density of hole traps. All the previous observations confirm that the electron transport properties in this device are better than that of the hole transport ones.

Electrical characterisation and x-ray measurements

I-V characteristics

The I-V characteristic of the SC-C/Ni diamond device was investigated in both dark conditions and under X-ray irradiation as illustrated in figure (6). The broad beam X-ray irradiation of the device was carried out in air using a 50 kVp X-ray tube with a molybdenum reflection target (Oxford instruments XF50 11). The irradiated curves were obtained at two different dose rates of 1.5 and 2.45 Gy/min which were set by varying the anode current. The quoted values correspond to the air kerma near the sample position calibrated by a 0.6 cm^3 ionization chamber of model number NE2571A; this gives a crude approximation of the energy deposited in the samples neglecting differences due to air ionization and scattering, and absorption effects by the sample mounting material.

The bias voltage is applied through the top contact and varied from -150 V to 0 then from 0 to +150 V in steps of 2 V. All current measurements were performed using a Keithley 487 Pico ampere meter which was adjusted to record the current after 30 seconds stabilisation time, in

order to measure the equilibrium current. The device was pre-irradiated with an x-ray dose of ~10 Gy before any measurements were taken.
It is obvious from figure (6) that in the SC-C/Ni device the dark current has a relatively low value (below 30 and 18 pA at -150 V and +150 V, respectively) resulting in a minimum resistivity of $\sim 5\times10^{12}$ Ω.cm - deduced from the highest dark current at -150 V. Additionally, there is a slight difference in the I-V plot at negative and positive bias of the SC-C/Ni device.

The dark current observed in SC-C/Ni could be attributed to the presence of defects, either presented in the bulk material or at the contact-material interface. The above results may indicate that the defects may be introduced in the carbon-diamond interface during the deposition of C/Ni onto the diamond sample. These defects create energy levels within the bandgap of the device. These defect levels increase the transition probability of electrons from valance band (VB) to conduction band (CB) via thermal excitation. A valence band electron can be thermally excited readily to a defect level and subsequently to the CB there by generating a free electron-hole pair. This kind of defect assisted in the thermal generation of electron hole pairs, which increase the magnitude of the dark current. Another possible explanation could be the C/Ni deposition process changed the sp^3 bonds between the carbon atoms in the diamond surface, below the contacted area, into a sp^2 bonds which is more stable at room temperature. As such this surface area could be changed to a graphite film, which has a high conductivity leading to a reduction in the surface resistance after annealing which could contribute to the electrical conduction of the dark current. It is believed that the addition of nickel to the carbon could be participated in part of the darkcurrent value due to its high conductivity. The amorphous carbon upon annealing is highly conductive. Again proof of this has been given in [12] where excellent electrical properties were achieved in both pure carbon and Ni doped films through annealing at lower temperatures than the ones used for this work. The significant increase in the current signal with increasing bias voltage can be interpreted as described in previous reports [20-23] where the higher the bias voltage, the greater the charge collection in the device and hence the rapid rate of e-h recombination phenomenon can be overcome. However the dark current increases.

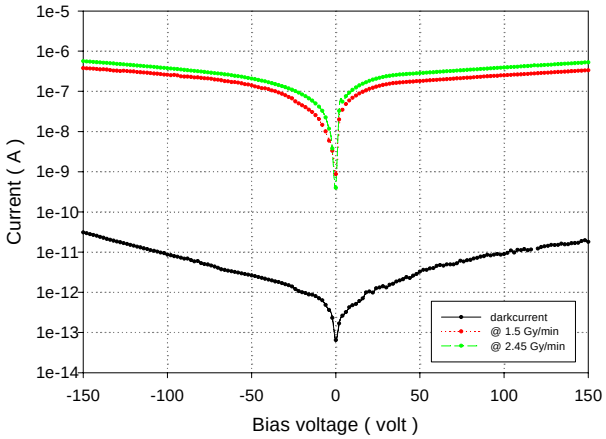

Figure (6): I-V characteristics of the SC-C/Ni diamond detectorboth in dark conditions and under different dose rates of 1.5 and 2.45 Gy/min.

Under x-ray irradiation increasing the dose rate results in a shift to higher currents – as seen in figure (6). Additionally, the photocurrent plots in the SC-C/Ni show a similar behaviour starting from bias voltages higher than 50 V and less than -50 V (the induced current at a positive bias is approximately the same at a negative bias - within 7 %). However, the two curves look systematically different in the range of -50 to 50 V. Furthermore, figure (6) shows a high difference ratio between the irradiated plots and the dark current plot and a SNR is higher than 1000, satisfying the recommendations of the IAEA for dosimetry [24].
All current measurements for the subsequent characterisation for this device was performed at 50 V bias voltages because it provided the best SNR whilst at the same time providing the optimum signal in terms of time response and stability.

Signal amplitude
Performing a linear regression on the data points obtained from the dose rate dependence of the SC-C/Ni diamond device, as seen in figure (8), the value for the device sensitivity was calculated to be ~7.8 μC/Gy, corresponding to a specific sensitivity of 4.87 μC/Gy.mm^3. This is a larger sensitivity compared to Poly-C/Ni, which has been published in a previous report [10] as 65 nC/Gy.. This is attributed to the lower density of defects in the single crystal material leading to a higher CCE than in polycrystalline samples [26].
A high sensitivity value was also reported by Cirrone et al. [25] with a value of 1.19 μC/Gy for commercial CVD diamond, produced by De Beers, using 6 MV photon beams..
Photoconductive gain or the charge collection efficiency (CCE), of an ionizing radiation detector, is considered one of the most important parameters that can determine the efficiency of the device in use for radiation detection. Generally, when the detector is irradiated, a current ($I_{generated}$) will be generated in the detector, which sequentially induces a current ($I_{measured}$) in the external circuit. The photoconductive gain value is known as the ratio between the current measured by the current meter and the theoretical current generated within the detector as a result of irradiation, i.e. dose rate. The expected value of the theoretical current can be calculated from the equation:

$$I_{generated} = \frac{D\rho e v}{w}$$

Where: D, ρ,e,v and w are the dose rate, density of diamond, elementary charge, sensitive volume and the energy required to produce e-h pair in diamond (13.2 eV in natural diamond) respectively.
Table (1) shows the generated current within the crystal and the measured current in the external circuit and from these two values the photoconductive gain is calculated. All these measurements were performed at a bias and a dose rate of 50 V and 1.5 Gy/min, respectively.
It is obvious from table (1) that SC-C/Ni has a high photoconductive gain. The gain value of the SC-C/Ni (~20) is approximately 450 times greater than the typical value of Poly-C/Ni (~44×10^{-3}) as mentioned in a previous report [10]. The high photoconductive gain in SC-C/Ni could be attributed to the sensitization effects. This effect appears only when a particular type of trap exists in the crystal which has the ability to capture only one type of carrier (electron or hole), while the other type remains free [27, 28]. When ionizing radiation of energy greater than the band gap (5.5 eV) is incident on the diamond crystal, an electron-hole pair is generated (i.e. electrons in the conduction band and holes in the valence band). For example, if holes are captured immediately in the traps, the corresponding electrons remain free in the conduction band and contribute to the conductivity until they recombine with the thermally de-trapped holes, thereby increasing the average lifetime of the electrons and thus increasing

the photoconductive gain of the device [27, 28]. The α-spectroscopy of this sample showed that α-spectra are only observed under a negative bias which suggests that holes suffer from a larger amount of trapping than electrons. This supports the assumption of the photoconductive gain by Sensitizing effect.

Table (1): The gain factor, sensitivity, specific sensitivity and SNR of SC-C/Ni were obtained with irradiation by a dose rate of 1.5 Gy/min and under bias.

Device	Bias voltage (V)	$I_{measured}$ (A)	SD	I_{dark} (A)	$I_{generated}$ (A)	Gain factor	Sensitivity μC/Gy	Specific Sensitivity μC/Gy.mm^3	SNR
SC-C/Ni	50	2.12×10^{-7}	1.1×10^{-9}	2.9×10^{-11}	1.06×10^{-8}	~20	7.8	4.87	7.2×10^{3}

A very high photoconductive gain was obtained in previous reports with values from 6×10^{4} to 10^{5}

Using the data obtained from table (1) to measure both the average currents under irradiation and dark current a significant high signal to noise ratio (SNR) was observed for the SC-C/Ni device. The SNR is satisfactory as per the recommendations of the IAEA (>1000) i.e. ~7.2×10^{3}. This value is more than two times greater than the Poly-C/Ni (~3.3×10^{3}) value. The SNR of the SC-C/Ni is between a value reported by Galbiati et al. [15] who found a SNR of 3.3×10^{4} for single crystal CVD diamond with argon magnetron sputtered DLC/Pt/Au contacts on both sides when exposed to Co-60 γ-rays at 100 V and a SNR of 776 found in another report [30] for single crystal diamond with a contact of nickel on one side and gold on the other side.

Time response (Rise and fall-off times)

The aim of this section is to present the rise and fall-off times of the SC-C/Ni diamond samples. The rise time, $\tau_{10\%-90\%}$, is the time between 10% and 90% of the steady state current. The fall-off time is calculated by measuring the time between 90% and 10% of the steady state current. All measurements were achieved under irradiation by a dose rate and at a bias voltage of 1.5 Gy/min and 50 V, respectively. For a good estimate of the time to reach the stable detector current, a Keithley electrometer was set to record the current with a sampling time of 0.4 seconds.

Figure (7) shows that a rise time of about 2 seconds and fall-off time of ~0.56 seconds are observed. These values are slightly higher (slower) than the time response of the Poly-C/Ni (the minimum time value measured in polycrystalline sample was ~0.4 sec [10]) device. This is attributed to priming effects, from thermal detrapping of the shallow trapping level defects. The current plateau is inclined due to filling of the trapping levels in the band gap of the material until it saturates when an equilibrium rate of trapping and detrapping is achieved. A fast time response is required of any radiation detector as it leads to the ability to detect sudden changes in the x-ray irradiation.

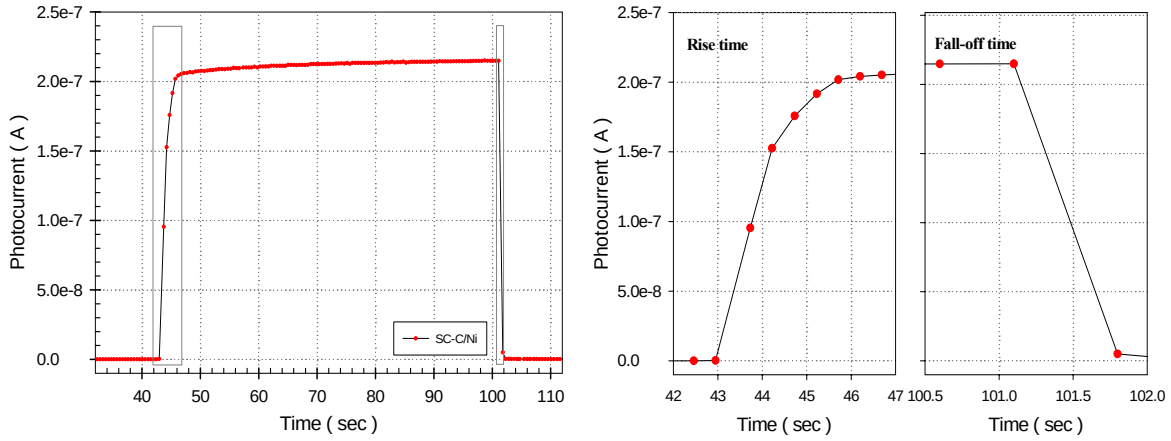

Figure (7): (a) Time response and (b) magnified rise and fall-off times of the SC-C/Ni at bias voltage and dose rate of 50 V and 1.5 Gy/min, respectively.

The measured values of the rise and fall-off times for the SC-C/Ni are consistent with the typical values reported by Descamps et al. [26] (1.29 and 0.78 seconds, respectively) for synthetic single crystal CVD diamond and (2.08 and 1.58 seconds, respectively) for PTW natural diamond under irradiation with medical linear accelerators. The authors acknowledge that part of these values could be limited by the electronic device set-up. A fast time response was obtained in a previous report by Galbiati et al [15] with a value of 0.2 seconds for a single crystal CVD diamond with DLC/Pt/Au contacts when the Co-60 γ-ray source was switched on or switched off. He suggests that this fast response shows that there is no memory or pumping effect.

Reproducibility

Reproducibility (or repeatability) is considered one of the main parameters that should be fulfilled for use in dosimetric applications. It should be less than 0.5% as recommended by the International Atomic Energy Agency (IAEA) [24]. The stability and the reproducibility of the current response were estimated by taking the percentage ratio of the standard deviation (SD) to the average photocurrent value under exposure of a fixed test dose rate of 1.5 Gy/min and 50 V bias voltages.

$$(\text{Reproducibility} = \left[\left(\frac{SD}{average}\right)\%\right])$$

Looking at the obtained data in table (2) a reproducibility close to that recommended by the IAEA (~ 0.504%) is obtained for the SC-C/Ni. It should be noted that this value is consistent with the results obtained from Poly-C/Ni under the same conditions. This is indicative of a low fluctuation in the signals. This value is consistent with the results reported by Galbiati et al. [15] (~0.32 %) for a single crystal diamond with a deposition of DLC/Pt/Au on both sides under irradiation by Co-60 γ-rays at an electric field of 0.2 V/μm.

Table (2): Reproducibility of the SC-C/Ni diamond device under fixed bias voltage and dose rate of 50 V and 1.5 Gy/min, respectively

Sample	No. of re-use	Average current (A)	SD	Reproducibility %
SC-C/Ni	1st	2.149e-7	1.102e-9	0.51
	2nd	2.155e-7	1.056e-9	0.48
	3rd	2.156e-7	1.137e-9	0.52
	Σ	2.154e-7	1.098e-9	**0.504**

1.8 Linearity and dose rate dependence

This section is used to discuss the linearity of the photocurrent as a function of the irradiated dose rates for the SC-C/Ni diamond device. The dose rates are changed from 15.5 to 245.5 (cGy/min) at fixed bias voltages of 50 V.

The linearity of a radiation detector, i.e. the variation of the current I as a function of the irradiated dose rate (D), can be expressed using the Fowler relationship [31]:

$$I = I_{dark} + RD^{\Delta}$$

Where: I_{dark} is the dark current. The exponent Δ, sometimes referred to as the fitting coefficient, or the linearity index is a constant showing the deviation from linearity. It usually varies between 0.5 and 1.0 if all the traps in the crystal have the same capture cross section. The measured value of Δ is expected to equal one if all the traps are distributed uniformly or quasi uniformly inside the diamond material. Additionally, the value of Δ can exceed one, if the traps in the crystal have different capture cross sections or are distributed non-uniformly.

Measuring Δ is particularly important in the case of x-ray dosimetry, because it determines a corrective factor needed to calculate absorbed dose. In the case of Δ equals one, the integrated photocurrent of the device does not depend on the dose rate, which is an advantage in dosimetry applications.

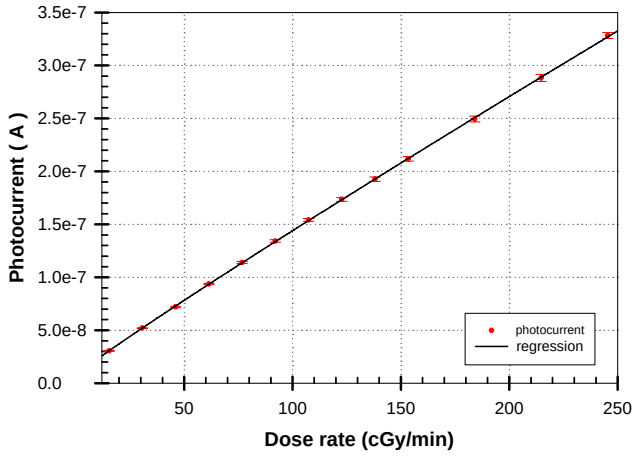

Figure (8): Dose rate dependence of the SC-C/Ni at different dose rates ranging from 15.5 to 245.5 cGy/min. The measurements were performed under 50V bias voltage.

Figure (8) shows the linearity of the photocurrent as a function of the dose rate for the SC-C/Ni device. A linear relationship was observed between the current and the dose rate for the SC-C/Ni device with Δ value of 0.97 obtained, as compared to the Poly-C/Ni (~0.86) [10] device. This value indicates two things; firstly there is an approximately uniform distribution of the traps within the single crystal device and secondly, by using a single crystal, the diamond device with C/Ni contact shows a linear current response with dose rate obtained. The comparison of the Δ values from the polycrystalline samples and the single crystal sample (SC-C/Ni) showed that Δ is changing according to the nature of the detector material.
The measured value of Δ for the SC-C/Ni is consistent with the typical values reported by Descamps et al. [26] (0.98) for SC CVD diamond, with an electrical contact of 50 nm gold, using a linear accelerator with 6 MV x-ray photons at varying dose rates from 1 to 6 Gy/min. Furthermore the measured values are consistent with De Angelis et al. [32] with value of 0.98 for PTW natural diamond using 6 MV photon beam at varying dose rates from 0.9 to 4.65 Gy/min was measured at 100 V.

CONCLUSIONS

The purpose of this study was to develop a near-tissue equivalent dosimeter for X-rays based on free standing single crystal diamond with C/Ni electrodes deposited using PLD. In the SC-C/Ni sample the dark current was low (below 30 pA between -150 V and +150 V) with high resistivity of ~5×10^{12} Ω.cm.
The linear current response with dose rate improved with a Δ value change of 0.86 to 0.97. This suggests that Δ is changing according to the nature of the detector material.
The sensitivity and specific sensitivity of the SC-C/Ni device showed a value of ~7.8 μC/Gy and 4.87 μC/Gy.mm^3, respectively. The higher sensitivity in SC-C/Ni than in Poly-C/Ni is believe to be due to the lower density of defects than in the polycrystalline sample and the higher CCE in the single crystal sample (SC-C/Ni) as seen in alpha spectroscopy. The gain value of the SC-C/Ni (~20) device is approximately 450 times greater than the typical value of Poly-C/Ni. The high photoconductive gain in SC-C/Ni could be attributed to the sensitization effects, with the alpha spectroscopy of this sample suggesting that holes suffer from a greater quantity of trapping than electrons. This suggests that the gain originates from the electrons rather than the holes.
A reproducibility close to that recommended by the IAEA (~ 0.504%) is obtained for the SC-C/Ni. The SNR was satisfactory as per the recommendations of the IAEA (>1000) i.e. ~7.3×10^3. The SC-C/Ni device shows a fast time response, with rise and fall-off times of ~2 and ~0.56 seconds, respectively.
Spectroscopic response of a SC-C/Ni detector to alpha particles has been studied. In the case of electron drift, a CCE higher than 90 % has been observed at a bias of -40 V and 100 % CCE at -300 V. In the case of hole drift, a lower CCE of 89 % was observed at bias of 300 V. The SC-C/Ni showed a superior electron energy resolution of ~3 % to 5.49 MeV alpha particles than the corresponding value for hole drift which was ~8.5 %. Additionally, a mobility-lifetime ($\mu_e\tau_e$) product for electrons was estimated at ~1.16×10^{-4} cm^2.V^{-1} and a mobility-lifetime ($\mu_h\tau_h$) product for holes at ~1.55×10^{-5} cm^2.V^{-1}. These observations suggest that the electron transport properties for SC-C/Ni is superior to that of hole transport. This is believed to be due to the presence of deep (hole) traps within the material.

REFERENCES

(1) Bergonzo, P., Brambilla, A., Tromson, D., Mer, C., Guizard, B., Marshall, R. D., Foulon, F., *CVD diamond for nuclear detection applications.* Nuclear Instruments and Methods in Physics Research Section A: Accelerators, Spectrometers, Detectors and Associated Equipment, 2002. **476**(3): p. 694-700.

(2) Robertson, J., *Mechanical properties and coordinations of amorphous carbons.* Physical Review Letters, 1992. **68**(2): p. 220.

(3) Gutiérrez, A., Díaz, J., López, M. F., *X-ray absorption spectroscopy study of pulsed-laser-evaporated amorphous carbon films.* Applied Physics A: Material Science & Processing, 1995. **61**(2): p. 111-114.

(4) Diaz, J., Gago, J. A. Martin, Ferrer, S., Comin, F., Abello, L., Lucazeau, G., *Raman spectroscopy of carbon films grown by pulsed laser evaporation of graphite.* Diamond and Related Materials, 1992. **1**(7): p. 824-827.

(5) Almaviva, S., Marinelli, M., Milani, E., Prestopino, G., Tucciarone, A., Verona, C., Verona-Rinati, G., Angelone, M., Pillon, M., *Extreme UV photodetectors based on CVD single crystal diamond in a p-type/intrinsic/metal configuration.* Diamond and Related Materials, 2009. **18**(1): p. 101-105.

(6) Kuzmany, H., Pfeiffer, R., Salk, N., Günther, B., *The mystery of the 1140 cm-1 Raman line in nanocrystalline diamond films.* Carbon, 2004. **42**(5-6): p. 911-917.

(7) Ferrari, A.C., Robertson J. , *Resonant Raman spectroscopy of disordered, amorphous, and diamondlike carbon.* Physical Review B, 2001. **64, 075414**.

(8) Di Benedetto, R., Marinelli, Marco, Messina, G., Milani, E., Pace, E., Paoletti, A., Pini, A., Santangelo, S., Scuderi, S., Tucciarone, A., Verona-Rinati, G., Bonanno, G., *Influence of metal-diamond interfaces on the response of UV photoconductors.* Diamond and Related Materials, 2001. **10**(3-7): p. 698-705.

(9) Fidanzio, A., Azario, L., Viola, P., Ascarelli, P., Cappelli, E., Conte, G., Piermattei, A., *Photon and electron beam dosimetry with a CVD diamond detector.* Nuclear Instruments and Methods in Physics Research Section A: Accelerators, Spectrometers, Detectors and Associated Equipment, 2004. **524**(1-3): p. 115-123.

(10) Abdel-Rahman, M.A.E., et al., *The X-ray detection performance of polycrystalline CVD diamond with pulsed laser deposited carbon electrodes.* Diamond and Related Materials, 2012. **22**(0): p. 70-76.

(11) Galbiati, A., et al., *Performance of Monocrystalline Diamond Radiation Detectors Fabricated Using TiW, Cr/Au and a Novel Ohmic DLC/Pt/Au Electrical Contact.* IEEE Transactions on Nuclear Science, 2009. **56**(4): p. 1863-1874.

(12) Jayawardena, K.D.G.I., Tan, Y. Y., Fryar, J., Shiozawa, H., Silva, S. R. P., Henley, S. J., Fuge, G. M., Truscott, B. S., Ashfold, M. N. R., *Highly conductive nanoclustered carbon:nickel films grown by pulsed laser deposition.* Carbon, 2011. **49**(12): p. 3781-3788.

(13) Biersack, J.P., Haggmark, L. G., *A Monte Carlo computer program for the transport of energetic ions in amorphous targets.* Nuclear Instruments and Methods, 1980. **174**(1-2): p. 257-269.

(14) Lohstroh, A., Sellin, P. J., Wang, S. G., Davies, A. W., Parkin, J. M., *Mapping of Polarization and Detrapping Effects in Synthetic Single Crystal Chemical Vapor Deposited Diamond by Ion Beam Induced Charge Imaging*. 2007, Surrey Scholarship Online.

(15) Galbiati, A.B., GB), *CONTACTS ON DIAMOND*. 2010: United States.

(16) M. Pomorski, E.B., M. Ciobanu, A. Martemyianov, P. Moritz, M. Rebisz, B. Marczewska, *Characterisation of single crystal CVD diamond particle detectors for hadron physics experiments.* physica status solidi (a), 2005. **202**(11): p. 2199-2205.
(17) M. Pomorski, E.B., A. Caragheorgheopol, M. Ciobanu, M. Kiscaron, A. Martemiyanov, C. Nebel, P. Moritz, *Development of single-crystal CVD-diamond detectors for spectroscopy and timing.* physica status solidi (a), 2006. **203**(12): p. 3152-3160.
(18) Trammell, R., Walter, F. J., *The effects of carrier trapping in semiconductor gamma-ray spectrometers.* Nuclear Instruments and Methods, 1969. **76**(2): p. 317-321.
(19) Hecht K., Z. Phys., 1932(77): p. 235
(20) Iwakaji, Y., Kanasugi, M., Maida, O., Takeda, Y., Saitoh, Y., Ito, T., *Characterization of soft-X-ray detectors fabricated with high-quality CVD diamond thin films.* Applied Surface Science, 2008. **254**(19): p. 6277-6280.
(21) Matsubara, H., Saitoh, Y., Maida, O., Teraji, T., Kobayashi, K., Ito, T., *High-performance diamond soft-X-ray detectors with internal amplification function.* Diamond and Related Materials, 2007. **16**(4-7): p. 1044-1048.
(22) Pauling, L., *Electronic Processes in Ionic Crystals. By N. F. Mott and R. W. Gurney.* The Journal of Physical Chemistry, 1941. **45**(7): p. 1142-1142.
(23) Boer, K.W., *Survey of Semiconductor Physics*. Barriers, Junctions, Surfaces and devices. Vol. vol. II. 1992, New York: Van Norstrand Reinhold.
(24) Agency, I.A.E., *Calibration of dosimeters used in radiotherapy* in *Technical reports series -- no. 374.* 1994: Vienna.
(25) Cirrone, G.A.P., Cuttone, G., Lo Nigro, S., Mongelli, V., Raffaele, L., Sabini, M. G., *Dosimetric characterization of CVD diamonds in photon, electron and proton beams.* Nuclear Physics B - Proceedings Supplements, 2006. **150**: p. 330-333.
(26) Descamps, C., Tromson, D., Tranchant, N., Isambert, A., Bridier, A., De Angelis, C., Onori, S., Bucciolini, M., Bergonzo, P., *Clinical studies of optimised single crystal and polycrystalline diamonds for radiotherapy dosimetry.* Radiation Measurements, 2008. **43**(2-6): p. 933-938.
(27) Schirru, F., Kupriyanov, I., Marczewska, B., Nowak, T., *Radiation detector performances of nitrogen doped HPHT diamond films.* physica status solidi (a), 2008. **205**(9): p. 2216-2220.
(28) McKeag, R.D., Marshall, R. Duncan, Baral, Bhaswar, Chan, Simon S. M., Jackman, Richard B., *Photoconductive properties of thin film diamond.* Diamond and Related Materials, 1997. **6**(2-4): p. 374-380.
(29) A. Lohstroh, P.J.S., F. Boroumand, J. Morse, *High gain observed in X-ray induced currents in synthetic single crystal diamonds.* physica status solidi (a), 2007. **204**(9): p. 3011-3016.
(30) Tranchant, N., Tromson, D., Descamps, C., Isambert, A., Hamrita, H., Bergonzo, P., Nesladek, M., *High mobility single crystal diamond detectors for dosimetry: Application to radiotherapy.* Diamond and Related Materials, 2008. **17**(7-10): p. 1297-1301.
(31) Fowler, J.F., *Solid state electrical conduction dosimeters*. ,edited by Attix, Roesch, and Tochlin, Radiation Dosimetry II (Academic Press Inc., 1966), Chapter 14, p. 308.
(32) De Angelis, C.O., S.; Pacilio, M.; Cirrone, G. A. P.; Cuttone, G.; Raffaele, L.; Bucciolini, M.; Mazzocchi, S., *An investigation of the operating characteristics of two PTW diamond detectors in photon and electron beams.* Medical Physics, 2002. **29**(2): p. 248-254.

Parameters Affecting ^{137}Cs Migration within Soil Profile

Sefien S.M. Ibrahim A.S., Abdelmalik W.E.Y.
Radiation Protection Department N.R.C., A.E.A., Cairo EGYPT 13759

ABSTRACT

Some studies have been carried out on the adsorption, distribution and migration of ^{137}Cs within soils of the area in the vicinity of the Nuclear Research Centre, Egypt, and Ismailia Canal. The soil physicochemical and mineralogical characteristics were carried out and indicated that the soil samples consisted mainly of sand fraction (quartz) and silt fractions (semctite minerals). The kinetics of caesium adsorption and its adsorption isotherms for the tested soils were also studied. The sorption of ^{137}Cs on soil minerals markedly affects its migration rate. The natural background of both locations of study indicated that the amounts of ^{137}Cs present in the reactor site were found to be originated from the fallout and from the external contamination which affected the background level. The ^{137}Cs activity at the canal site was found to be 20.01 Bq/m^2.cm, while that around the reactor site were found to be 231.15 Bq/m^2.cm which may be originating from the fallout and from external contamination which affect the background level at that location. The activity in the canal soil which amounted to 20.01 Bq/m^2/cm (0.87 Bq/kg) is about that of background.Based on the distribution data, the vertical distribution of ^{137}Cs has been studied for soil in both locations (the vicinity of the Nuclear Research Centre (NRC) and Ismailia canal). The vertical migration rates of ^{137}Cs were calculated for soil samples selected from different locations. These rates were found to be 0.056 and 0.031 cm/year for the reactor and canal site respectively.

Key words: *Background / ^{137}Cs Activity/Soil/Migration Studied*

INTRODUCTION

Baseline information of radiation dose and radionuclide distribution in the aquatic and terrestrial environment is essential in understanding the human exposure to radiation and the calculation of the exposure dose and its radiation damage [1, 2]. As the reactor in the Egyptian Nuclear Research Centre (NRC) is located in the vicinity of Ismailia Canal (IC), it is considered as an important and interesting site to collect the information about the migration of radionuclide that might reach the surrounding ecology.

The migration of radionuclide in different types of soil, both vertical and horizontal, is very important issues in tracing of radioactive contamination of the natural environment. Such studies despite its purely scientific aspect has also a very practical objective, namely; it allows to predict possible sites of accumulating of radionuclide This should also help to determine the accessibility of the isotopes to plants and more generally to food chain.[3,4,5]. Others studied the concentration and the distribution of Cs^{137} in ecosystems and agricultural areas [8, 9]. The mineralogical compositions (sand, silt and clay) affect the behaviour of ^{137}Cs with soil.

The background activity of ^{137}Cs isotope in most of Egyptian soils has been found to be less than 1 Bq/kg [5]. The natural radioactivity in Ismailia Canal and other locations in Egypt[6,7].

Several investigations have shown that the behaviour of ^{137}Cs isotope on the soil materials is greatly affected by the mineral composition of the soil [2, 3, 4]. The caesium migration within the soil layer may be affected by the adsorption kinetics [6]. Such studies despite its purely scientific aspect has also a very practical objective, namely, it allows predicting possible sites of cumulating of radionuclide. This should also help to determine the accessibility of isotopes to plants and, more generally, to food chains [7, 8, 9].

This work presents results of studies carried out on different soil profiles at the Nuclear Research Centre (N.R.C.) location and from area near to Ismailia canal. Concentrations of ^{137}Cs isotope were measured in particular layers of the profiles selected. The samples were separated into fractions and laboratory tests of adsorption kinetics of ^{137}Cs were conducted. The adsorption isotherms were also plotted. A special attention was paid to the effect of mineral composition of the soils on the ^{137}Cs migration rate.

EXPERIMENTAL

Sampling Procedure

The sampling spots were concentrated in two areas, firstly around the reactor area and spread away around it in circle of about 0.5 km radius. These locations had not been farmed for the last 15 years and were scarcely overgrown with short plants. Secondly at Ismailia canal area (active agricultural and industrial area) far from the reactor by about 5km to the west.

Before sampling, the soil surface was cleaned of the over ground plant parts and larger organic pieces. Profiles of the soil were taken from the surface and down to 40 cm depth. The sampling procedure included collecting of soil layers, each of 20x30 cm area. The topmost and the second layers were 2 and 3 cm thick then subsequent 5 cm thick respectively [12]. The samples taken from each profile level were stored in polyethylene bags. Samples were dried in a drying oven at 80 ^{o}C and then screened on a 1 mm sieve to remove stones and larger organic fragments.

Particle Size Distribution

Each soil layer was washed on a 0.25 mm sieve onto a 1 dm^3 glass measuring cylinder. Then the cylinder was filled up with water and the contents mixed. The separation of soil into size fractions was carried out following sedimentation method at 25 ^{o}C. Under these conditions, and using stock's equation [13], four size fractions were separated: 0.2-0.1, 0.1-0.05, 0.05-0.02, and less than 0.02mm. The sedimentation times of these fractions, from a height of 10 cm, were 4.4, 15.5 and 57.1 and more than 57.1 seconds, respectively. The extracted fractions of the sample were rinsed with distilled water and then dried at 100^{o}C for further investigations.

$$d = \sqrt{\frac{18\mu v}{(\rho_s - \rho_l)g}}$$

Where

d= equivalent diameter of a particles freely setting freely in water under gravity.

ρ_l = liquid density

ρ_s = Soil density

v = The sedimentation velocity of particles constituting a given fraction and it is equal to x/t where x is the distance and t is the time.

g = Acceleration due to gravity.

μ = water viscosity.

Chemical Analysis

The following chemical parameters of the soil profiles were determined such as; exchangeable hydrogen ions concentration (measured as the pH value of suspended soil sample in a 1M KCl solution using a ERH-110 combined electrode and a pH-meter Hi-8417-Hanna instruments), the organic matter content was determined using roasting method. Exchangeable cations were assayed in a buffered 1N ammonium acetate solution using the conventional batch method, as well as the major cations composition for each profile depth using methods described in standard soil analysis [12, 14].

Gamma Spectrometric Measurements

Known mass (1kg) of the homogenized soils samples were placed in 0.5 dm^3 Marinelli bottle mounted on 1.0 inch CsI(Tl) crystal attached to URSA portable spectrometer connected to 4096-channel pulse height analyze. The detector resolution has a full width at half maximum (FWHM) of 0.9 keV at 0.122 MeV, 1.2 keV at 0.661 MeV and 1.9 keV at 1.33 Mev peaks, and its efficiency is1.8% for ^{137}Cs peak. Caesium activity measurements were calculated using of a GAMMA VISION II, ver. 4.11 computer program. Each spectrometric measurement lasted for 24 hours [5].

Adsorption Experiments

Measurements of caesium sorption were carried out using soil fractions of 0.2-0.1, 0.1-0.05 and 0.05-0.02 mm size for samples collected from the two sites. An amount of 0.5 gm of the soil fractions were added in plastic bottles to 25 cm^3 CsC1 solutions of concentration ranged from $8x10^{-9}$ to $8x10^{-4}$ mol/dm^3, traced with Cs^{137}, at 25 ^oC (laboratory temperature). Before the addition of the soil 1.0 cm^3 aliquots of the solutions were taken and their activities measured (A_o). When the soil was added the suspensions were stirred continuously and after 60 minutes the soil suspensions were centrifuged at 2000 rpm for 15 minutes. Then 1.0 cm^3 aliquots were taken from the supernatants and their radioactivity levels were measured again (A_L). The concentration of caesium adsorbed on the soil (C_s) was calculated based on the radioactivity difference before and after the adsorption using the following relationship [12]:

$$C_s = \frac{C_o . V_L (1 - \frac{A_L}{A_o})}{m}$$

Where

C_s = concentration of Cs^+ adsorbed on the solid surface, mol/g,

C_o = initial concentration of Cs in solution before adsorption, mol/dm^3,

V_L= volume of solution, dm^3,

A_L = activity of solution at adsorption equilibrium, Bq,
A_o = initial activity of solution, Bq,
m = mass of soil, g.

The kinetics of caesium adsorption was investigated ,using the above technique, by withdrawing 1,0 cm^3 aliquots for the radioactive assay after 1, 3, 5, 10, 15, 20, 25, 30, 40, 50 and 60 minutes from the moment of the addition of the soil. The initial CsC1 concentration was $8x10^{-6}$ mol/dm^3. The kinetic curves are shown in Figs 1 and 2.

RESULTS AND DISCUSSION

Tables 1 and 2 show the results of the physicochemical investigations of the two locations from these tables it can be seen that the soil of the same site and from different depths do not differ significantly .In addition, the soil of both sites are almost similar concentrations of exchangeable cations, only Ca^{2+} and exchangeable hydrogen vary clearly .this leads to differences in the values of the sorption capacities. The largest difference were observed in the C_{org} content in the first two centimetre depth in the both sites which in turn results in different permeability of thee two layers . Varying in particle size distribution, and in soils chemical composition, results in differences in soil sorption capacities.

The total ^{137}Cs activity in the profiles collected from the reactor site area amounted to 271.15 $Bq/m^2.cm$, while in the canal area was 20.01 $Bq/m^2.cm$ and this value is markedly lower than the average natural radioactive background in Egyptian soil. As it can be seen from Table 1, the canal site soil is composed mainly of fine mineral particles of a size below 0.1 mm which are subject to washing away together with caesium adsorbed on their surfaces.

In order to investigate the sorption properties of minerals occurring in the tested soils , the dominated components were extracted from the samples based on their particle size and confirmed by X-ray diffraction identification[15] .This minerals were then used for the adsorption test of Cs^+ from CsCl solution traced with ^{137}Cs .

Figure 1 shows the kinetics of caesium adsorption on size fractions that were separated from the Ismailia Canal site. Fig. 2 presents the adsorption kinetics of ^{137}Cs on semctite (smallest particle size fraction) and sand (largest particle size fraction) from the reactor site. It can be concluded from the two figures that the adsorption equilibrium was reached within several minutes after contacting the soil with the CsC1 solution. It is evident that the equilibrium was achieved most rapidly on sand from the reactor soil and on the large size fraction from the canal site soil with the particle size ranging from 0.2 to 0.1mm. In the light of the laboratory tests, the retention of Cs^+ on the surface layers of the reactor site soil seems to be caused by efficient sorption of Cs^+ on semctite portion.

It was found that the caesium uptake follow the Freundlich isotherm equation [16]

$$C_s = kC_{eq}^{(1/n)}$$

Where Cs=Concentration of caesium on solid phase.
C_{eq}=Concentration of caesium in solution at equilibrium.
k,n=are constants.

It can be found from the adsorption isotherms, (Fig. 3) that semctite particles exhibit the largest caesium sorption capacity. It can also be seen from the isotherms that sand, when present in soil, can adsorb caesium only in small quantities.

The migration of Cs, bonded with fine mineral grains and soil colloids, together with infiltrating water is a consequence of the strongest adsorption of Cs on the fine fractions. Fine solid particles are also more tractable to migration in soil due to the biological activity of

growing plant roots as well as of small organisms and animals living in soil[17]. As a result of the above processes caesium can migrate carried by soil particles. Also, the very fine caesium-carrying particles can be easily blown around by winds and washed away by percolating water. It is very likely that such processes are involved in the migration of caesium in the reactor soil.

Soil minerals, especially mica, shale and semctite exhibit a stratified structure[15]. Caesium, introduced onto soil surface initially is bonded reversibly on the surface of the minerals but in the course of time, caesium becomes irreversibly bonded due to slow diffusion and ion exchange with, e.g., K^+ and Ca^{+2} ions, in the interlayer spaces inside those stratified minerals [15]. Thus, the irreversibly bonded caesium is immobilized on the mineral surfaces and its migration in soil will occur only when there are favourable conditions to the co-migration of the soil particles on which Cs is strongly adsorbed.

The above discussions presented differences in possible migration pathways of caesium and the varying physicochemical properties of the two tested soils result in different average vertical migration rates of Cs^+ in these soils [18, 19]. The vertical migration rates were obtained from the following formula

$$V_{av.} = \frac{d_{1/2}}{t}$$

where $d_{l/2}$ is the thickness of a soil layer containing half of the total caesium activity in a tested profile (cm), and t is the migration time (years), it was assumed that the migration time was 18 years counting from the period of the first sample collected in 1990 . The vertical migration rates were found to be 0.056 and 0.03 cm/year for the reactor site soil and the canal site respectively. Such low values of the average migration rate cause ^{137}Cs to remain in the upper layers of the soils up to a depth of a few centimetres. This proves that ^{137}Cs to a large extent is permanently bonded with soil minerals through the chemical interaction rather than a physical one.

The results confirm the assumption that the migration rate of Cs^+ in soil is affected primarily by the mineral composition of soil since the mineral fraction determines the way caesium is bonded[17,18,]. When minerals contain a stratified structure is present in soil the migration rate of Cs decreases with time. As a result it is frequently observed that the migration of the newly contaminated caesium is faster than the migration of Cs originating from the global fallout because the process of caesium immobilization takes many years. Blocking of the active sites by caesium liberated from fallout can be one of the factors that differentiate the migration rates of caesium from new contamination sources and that from the fallout in the 1990's. Subsequently, the new contamination caesium can migrate faster to deeper layers of soil where it can finally adsorb on free adsorption sites. However, even in case of fast and strong adsorption on soil minerals caesium is able to migrate constantly, in very small quantities deeper into soil. This is a result of natural processes like precipitation or biological activity of living organisms. The migration rate depends not only on the sorption properties of the soil but, of course, on the size of soil particles [19].

On the other hand figure 4 presents the natural background of the ^{137}Cs activities in the particular layers of the soil profiles. It can be clearly seen that the ^{137}Cs activity distribution differs substantially between the tested profiles. In case of the canal site soil the distribution is rather uniform up to a depth of 30 cm except 0-2 and 2-5 cm layers. In these two, topmost layers the caesium activity level was twice as high as in the remaining samples. This Cs^+ migration agreed with work conducted by other investigator on Ismailia canal site [2].The activity in the 0-2 cm layer constitutes 14% of the total caesium activity in the profile. The

phenomenon of caesium retention in the topmost layer of soil is even more clearly seen in reactor site soil profile where the activity of ^{137}Cs in the 0-2 cm layer amounted to 58% of the total caesium activity in this profile. In order to determine the percent content of ^{137}Cs originating from any recent change above the fallout, a sample from a reactor area collected at 1990 (about 18 years ago) was subjected also to radio analysis for ^{137}Cs .

The result of gamma measurements of the samples collected in year 2008 showed that the ^{137} Cs content in the first layer collected from the reactor site is 10.25 Bq/Kg considering the half life time and the decay equation, this value which expected to be present if it was counted in year 1990 would amounted to 15.23 Bq/Kg . While the gamma measurements carried in 2008 on samples collected from the same location in year 1990 contained 6.08 Bq/Kg ^{137}Cs. By considering the half life time and the decay equation, this value which is expected to be present if it was counted in year1990 would amounted to 9.22 Bq/Kg, which assumed to be due to the natural fallout only. The difference in activity between the two samples if they were collected and counted at the same time in 1990 is 5.81 Bq/Kg ,this difference may be arise from some external source of contamination. This difference reaches by natural decay to 3.83 Bq/Kg in 2008. This value is confirmed by the difference between the measured values of the two reactor samples counted in year 2008 which is found to be3.87 Bq/Kg.

Taking into account that the average soil density 2.3 g/cm^3 therefore, 1 m^{2}x1cm soil has mass 23 Kg. This leads that the ^{137}Cs activity in the surface reactor area at the year 2008 is 231.15 Bq/ cm^2/cm, but the calculated and expected value due to fall out is only 140 Bq/ cm^2/cm which mean that 91.31 Bq/m^2/cm caused by external source of activity which representing 39% of the total Caesium activity in the reactor site. This result is summarized in table 3. Sample collected from the canal at the same time contained ^{137}Cs amounted to 0.87 Bq/Kg. Taking into consideration that the canal area is far from the reactor site and hardly subjected to any external contamination and in the same time it is a cultivated zone.

CONCLUSIONS

In conclusion, one should point out that the vertical migration of caesium in soil is a very slow process. The migration rates ranged from a fraction of millimetres to few millimetres per year and consequently Cs remains retained in the upper layers of soil, in a zone reaching plant roots. Because of strong adsorption on soil minerals, caesium does not occur in soil in the ionic form. For this reason, only a very small amount of Cs can be absorbed by plants and then transferred to further links of the food chains. Model measurements confirmed that the retention of Cs in soil is affected primarily by soil minerals. Semctite separated from the reactor soil exhibited the strongest sorption ability among the tested minerals. The strong retention of Cs on semctite is most likely responsible for a larger accumulation of the isotope in the reactor soil compared with the canal site .It was found that in the reactor soil, there was 58% of the total activity of Cs in its 0-2 cm profile layer while in the canal site soil profile, in the topmost layer; there was only about 14% of the total caesium activity. Also the study showed that 39% of the Cs present in the reactor site is due to man made contamination, but the total activity still in the acceptable limits[5].

REFERENCES

(1) Quindes L.S.,FermandeZ P.L., Sota J. and Comaz L., Health physics, 62(2),194, (1994)
(2) W.E.Y. Abdel Malik .,Elzahaby A.S.and Bawdy S.A.,Isotope and rad.Res.,34(3) , 357-367 (2002)
(3) IAEA "Measurement of Radionuclides in Food and the Environment" A Guidebook, Technical Reports, Ser. No. 295, IAEA, Vienna, , p. 5. (1989)
(4) G.Lujaniene et al , Nukleonika 50,1. 23-29 (2005)
(5) Juri Ayub, j. et al, , The Natural Radiation Environment—8th International Symposium (2008)
(6) W.E.Y. Abdel Malik et al , Radiochimica Acta 61,109-111(1993)
(7) S.M.Sefien "Radiation Background and Heavy Metal Concentration in the Egyptian Aquatic Ecology." Ph.D. Thesis submitted to University collage for women, Physics dept, Ain Shams University (.2005)
(8) G.Arapis et al , 8th Intr.Conf.on Environmental Science and Technology Lemnos island, Greece 8-10 Sep.(2003)
(9) Grzegorzporeba et al , Geochronometria,– Journal on Methods and Applications of Absolute Chronology Vol. 22, pp 67-72, (2003)
(10) K.Niesiobedzka , Polish Journal of Environmental Studies Vol.9,2,133-136 (2000)
(11) Sohsah,M.A.M et al ,Isotope&Rad.Res.,19,2,115-122(1987)
(12) C.A.Black "Methods of soil analysis." American Society of Agronomy ,Inc., Publisher Madison,Wisconsin,USA (1965)
(13) R.E.Means "Physical properties of soil." Charles E. Merrill Publishing Co.(1963)
(14) American Public Health Association "Standard methods for the examination of water and waste water" 19th Edition (2005)
(15) Grim, R.E., "Clay Minerolgy" .Mc.graw –Hill book company New york (1968)
(16) Friedrich Helfferich "Ion Exchange" Dover Publications ,Inc.NewYork (1995)
(17) J.C.Igwe et al "Kinetics of Radionuclides and Heavy metals Behavior in Soils: Implications for plant growth",African Journal of Biotechnology Vol. 4 (13), pp. 1541-1547, December, (2005)
(18) Palensky et al , Health physics Vol. 94, No. 6, June (2008)
(19) Donatas Butkus1, et al ,J. of Envi. Eng. and Landscape Management, 16(1), 23–29(2008)

Table 1. Soil fraction composition of the tested soil sites

PROFILE DEPTH cm	REACTOR SITE YIELD OF SIZE FRACTIONS %				PROFILE DEPTH cm	CANAL SITE YIELD OF SIZE FRACTIONS %			
	0.2-0.1 mm	0.1-0.05 mm	0.05-0.02 mm	<0.002 mm		0.2-0.1 mm	0.1-0.05 mm	0.05-0.02 mm	<0.002 mm
0-2	22	48	30	8	**0-2**	5	65	30	10
2-5	19	40	41	14	**2-3**	11	58	31	12
5-10	19	40	41	16	**3-5**	7	60	33	13
10-15	19	39	42	14	**5-10**	5	65	30	15
15-20	20	39	41	13	**10-15**	6	63	31	13
20-25	25	34	41	14	**15-20**	7	62	31	13
25-30	23	34	43	16	**20-25**	5	63	32	19
30-35	23	31	46	18	**25-30**	4	63	33	18
35-40	23	30	47	22	**30-35**	5	65	30	17
40-45	23	23	54	33	**35-40**	6	63	31	15

Table 2. Chemical properties of the tested soils

PROFILE DEPTH cm	pH (KCl)	$C_{org.}$	Exchangeable cations meq/ 100g of soil						
			Ca^{+2}	Mg^{+2}	K^{+}	Na^{+}	Hh*	Sum of basic cations	Sorption capacity meq/100 g
REACTOR SITE									
0-2	4.7	1.92	4.15	0.88	0.79	0.05	3.30	5.87	9.17
2-5	4.3	0.87	3.84	0.73	0.44	0.04	3.30	5.05	8.35
5-10	4.3	0.66	3.76	0.68	0.35	0.04	3.15	4.83	7.98
10-15	4.2	0.54	4.27	0.76	0.25	0.07	3.15	5.35	8.50
15-20	4.3	0.69	3.69	0.71	0.27	0.06	3.15	5.00	8.15
20-25	4.3	0.66	3.84	0.67	0.30	0.05	3.15	4.86	8.01
25-30	4.3	0.27	5.12	0.98	0.26	0.05	2.55	6.41	8.96
30-35	4.5	0.21	5.34	1.00	0.29	0.09	2.10	6.72	8.82
35-40	4.6	0.12	5.17	0.97	0.27	0.06	1.65	6.47	8.12
40-45	4.8	0.09	4.98	0.95	0.21	0.06	1.35	6.20	7.55
CANAL SITE									
0-2	5.0	5.10	6.41	1.02	0.78	0.07	7.20	8. 28	15.48
2-3	3.5	2.34	4.49	0.50	0.43	0.08	8.85	5.50	14.35
3-5	3.5	1.50	3.97	0.41	0.33	0.08	8.85	4.79	13.64
5-10	3.5	1.35	3.62	0.31	0.22	0.10	8.85	4.25	13.10
10-15	3.4	0.84	2.94	0.20	0.13	0.12	7.50	3.39	10.89
15-20	3.4	0.72	2.84	0.17	0.14	0.11	7.95	3.26	11.21
20-25	3.4	0.60	2.83	0.14	0.14	0.11	7.95	3.22	11.17
25-30	3.5	0.54	3.97	0.20	0.17	0.15	8.25	4.49	12.74
30-35	3.3	0.78	5.59	0.26	0.24	0.20	9.30	6.29	15.59
35-40	3.4	0.72	6.74	0.41	0.41	0.35	9.00	7.91	16.91

** Exchangeable hydrogen ion concentration*

Table 3:Cs^{137} activity in reactor samples collected in years 1990 and 2012 , and from Canal site collected in year 2012

Year of sampling and locations	Cs^{137} Activity * ($Bq/m^2/cm$)	Cs^{137} Activity in 1990** ($Bq/m^2/cm$)
Reactor site 2012	231.15	350.29
Reactor site 1990	139.84	212.06
Difference in Cs^{137} Activity ($Bq/m^2/cm$)	91.31	138.23
Canal site 2008	20.01	--

* *Natural Cs137 activity counted in 1990 and 2012*

** *Calculated natural Cs137 activity in 1990 based on the measured activity in 2012 .and decay equation.*

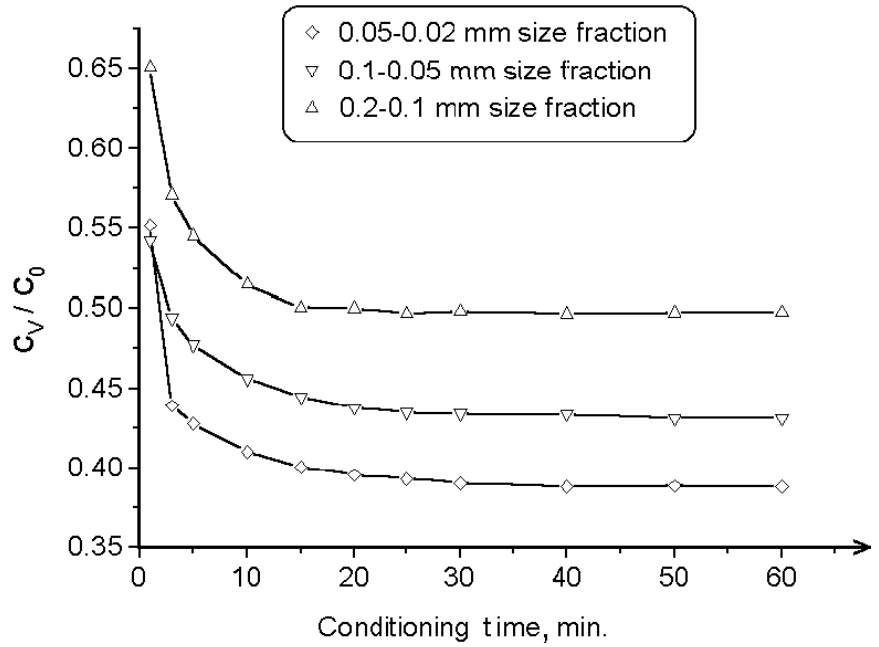

Fig.1. Adsorption kinetics of Cs^+ on different size fractions (0.20- 0-0.1 mm, 0.1- 0.05 mm, 0.05-0.02 mm) extracted from the canal site. Initial concentration of CsC1 solution: $C_o = 8.0 \times 10^{-6}$ mol/dm^3.

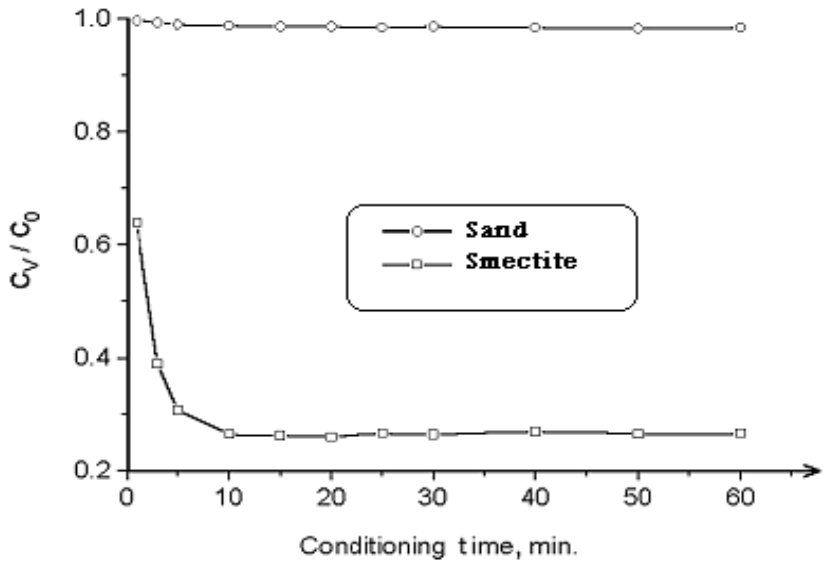

Fig.2. Adsorption kinetics of Cs^+ on semctite and sand, extracted from the reactor Site soil. Initial CsCl solution concentration: $C_o = 8x10^{-6}$ mol/dm^3

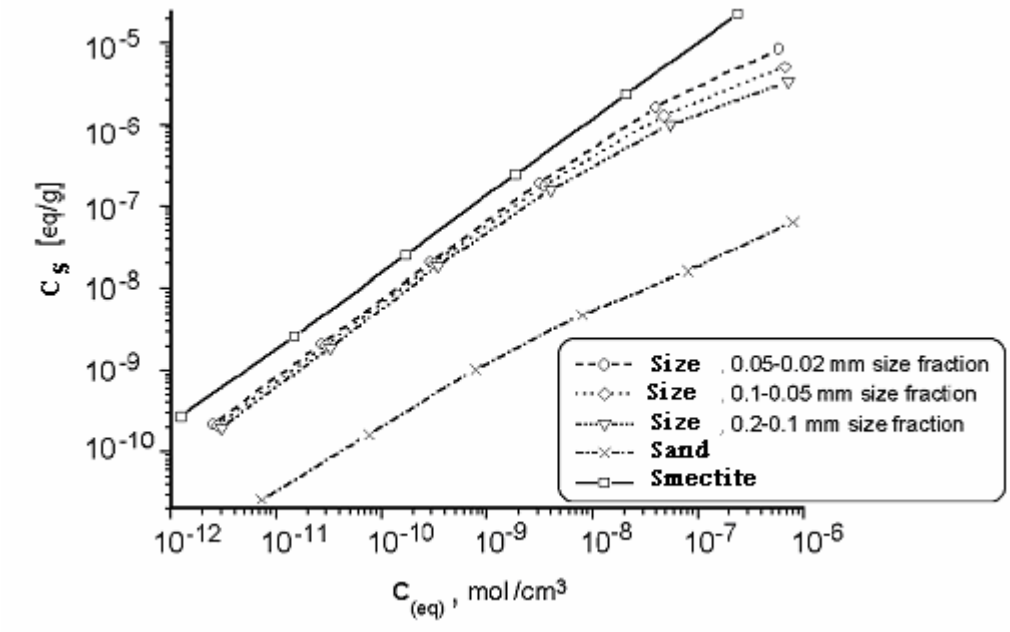

Fig.3 Adsorption isotherm of Cs^+ on minerals fractions separated from the tested soils

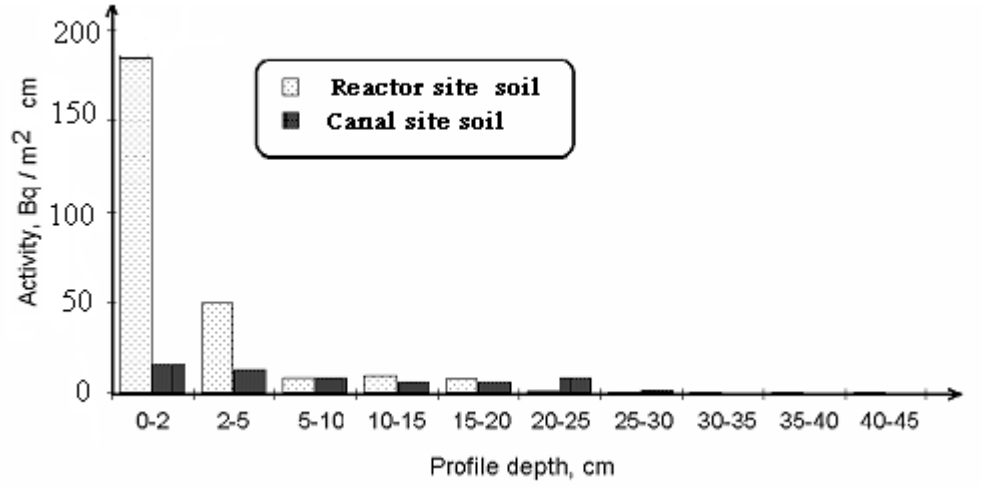

Fig.4 Distribution of ^{137}Cs activity at different depths in the two tested soil profiles

Effect of Treated and Untreated potato periderm on the Removal of ^{60}Co and $^{(152+154)}$Eu from Radioactive Waste Solutions

H. A. Omar[1] and M.S. Sayed[2]

[1]*Radiation Protection Department, Nuclear Research Centre, AEA, Cairo, Egypt*

[2]*Department of Radiation Protection and Safety, Hot Labs Center, Atomic Energy Authority.*

ABSTRACT

The potential of potato periderm and potato periderm ash to remove ^{60}Co and $^{152+154}$Eu ions from aqueous solution has been studied. Potato periderm either in the form of raw material or its prepared oxidized material were used in the removal of ^{60}Co and $^{152+154}$Eu from aqueous radioactive waste solution. Characterization of the studied material were done using Fourier Transform Infrared (FTIR), X-ray diffraction (XRD), surface area, thermogravimetric analysis (TGA) and differential thermal analysis (DTA). Experimental studies were conducted to evaluate and optimize the various process variables e.g. shaking time, pH, initial ion concentration and the effect of interfering ions. Sorption data have been interpreted in terms of Freundlich and Langmiur models. The thermodynamic parameters of the sorption system have been determined at different temperatures. The negative values of ΔH^o showed that the sorption is exothermic where as the negative values of ΔG^o showed the spontaneity of the sorption process and it is more favorable at higher temperature.

***Key words**: adsorption, ^{60}Co and $^{152+154}$Eu, Liquid radioactive waste, Potatoperiderm ash*

INTRODUCTION

Removal of radioactive nuclides from nuclear liquid waste effluent is an important environmental concern in nuclear waste management(1). Environmental radioactive contamination can be caused by the accidental emissions from any stage of nuclear fuel cycle, fallout from nuclear testing or radiochemical laboratories wastes(2). ^{60}Co and $^{152+154}$Eu are some of the most important nuclear fission products present in the radioactive waste, from the bio-toxicity point of view due to their sufficient long half life and higher solubility in aqueous systems(3). Hence, during the last several decades, considerable efforts have been directed towards the development of improved processes for the removal and recovery of ^{60}Co and $^{152+154}$Eu from nuclear waste streams(4). The removal of ^{60}Co and $^{152+154}$Eu from radioactive waste solution was usually achieved by physico-chemical processes such as coprecipitation, ion exchange, solvent extraction, electrochemical processes and membrane processes(5). However, these methods are relatively expensive involving either elaborate, costly equipment or high cost operation and energy requirements. Sorption characteristics of ^{60}Co and $^{152+154}$Eu on bentonite and other natural minerals have been also studied(6). Biological and agriculture

systems have great potential for waste-remediation because they are easily obtained, low cost and prevent further chemical pollution to the environment[7]. Hence, biotechnology has gained a lot of importance in a variety of industrial process as well as for environmental management. Studies on the uptake of metal ions by the various agriculture wastes including apple wastes, olive stone waste, rice husk, orange peal cellulose and peat were reported in some literatures[8-12]. Some of these natural materials contain various and interesting functional groups such as carboxyl, hydroxyl, amidocyanogen and so on. Potato periderm (solanum tubersum) consists of cellulose, hemi- cellulose, pectin substances, proteins and other low molecular weight compounds like starch[13]. Potato periderm has shown very high affinity for many metal ions [14]. The present work aimed to use agricultural waste as potato periderm to remove radioactive isotopes from aqueous solution under several parameters such as contact time, pH, adsorbent dose, concentration of adsorbat, competing ions and temperature.

EXPERIMENTAL

All chemicals and reagents used in this work were of analytical grade. The pH values were adjusted using NaOH and HCl. Deionized water was used in all experiments.

Radioactive tracers:

^{60}Co and $^{152+154}$Eu used in this work were prepared from nuclear installation. The radioactivity of ^{60}Co and $^{152+154}$Eu were assayed radiometrically. In this concern a known volume was taken from aqueous solution before and after contacting with solid phase and its γ-activity was measured, using a well type NaI crystal connected to a multichannel (Giene, 2000). All measurements were carried out in triplicate.

Biosorbent preparation:

Potato periderm wastes were supplied from different sources. The potato periderm (P) was washed with water and with deionized water and dried in an oven at 105^{o}C for 72 h, its weight represented 12% of the wet original matrix. Ball-mill was utilized to turn dried samples into smaller particles and sieved into two mesh size, 315-500 μm and 500-700μm.

Method of carbonization:

Potato periderm wastes were prepared firstly by stirring one part of material with 1.8 part per weight of concentrated sulfuric acid, then keep in an air oven at 150$\pm$5^{o}C for 24 hours. The resulted carbonized material was washed with distilled water to remove the free acid, secondly washed with 1% sodium bicarbonate solution until effervescence stopped, and finally soaked in 1% sodium bicarbonate solution overnight to remove any residual acid[15]. The material; was then washed with distilled water and dried at 105$\pm$5^{o}C as modified potato preiderm (PC).

Characterization of the material*:*

The specific surface areas of the studied samples (P) and (PC) were determined using Nova SA instrument 3200. A Fourier transform infrared (FTIR) spectrometer from Perkin Elmer 1600 was used to analyze the matrices in the wave number range 600– 4000 cm^{-1}. Differential thermal analysis DTA and thermogravimetric analysis TGA were carried out by using TA 50 Shimadzu, Japan. Temperature was cycled at a constant rate of 20^{o}C/min from ambient temperature to 800 ^{o}C under nitrogen atmosphere. X-ray powder diffraction (XRD) data were obtained by Philips PW 1730 instrument supplied with (P) and (PC) using CoKα radiation.

Characteristics of liquid radioactive waste*:*

Table 1 showed the chemical composition of simulated low level radioactive liquid waste (LLLW). The main objectives of the treatment of the radioactive waste are to reduce the

waste volume and to produce stabilized leach resistant product suitable for storage and disposa

Table 1: Chemical composition of the simulated LLLW

ions / conc.	Total hardness	Ca:Mg	SO_4^{-2}	Cl^-	NO_3^-	PO_4^{3-}	Oxalate	Detergent	^{60}Co	$^{152+154}Eu$
g/l	0.003	1:1	0.03	0.02	0.06	0.001	0.001	0.01	0.0059	0.00023

Batch sorption studies*:*

Batch equilibrium experiments were conducted by adding 0.35g of P or PC, to a series of Erlenmeyer flasks containing 20 ml solutions of $1x10^{-3}$ M initial metal concentrations. The initial solution pH was adjusted using 0.1MHCl or 0.1M NaOH. After 2 h of contact time, the samples were separated from radioactive solution by centrifugation at 2000 rpm for 10 min. at room temperature (24 ± 1^oC) was sufficient to attain equilibrium. The activity of ^{60}Co and $^{152+154}Eu$ in the supernatant solution was determined by using multichannel analyzer connected to NaI crystal and calculated using the following equation:

$$q = V/M (C_0-C_t) \quad (1)$$

where q is the metal uptake (mg/g), C_0 and C_t the initial and equilibrium activity in the solution (counts/min), respectively. V is the solution volume (l), and M is the mass of sorbent (g).

RESULTS and DISCUSSION

Characterization of the studied material

The measured specific surface areas for both P and PC were 130.24 and 308.75 $m^2.g^{-1}$ respectively. Infrared analysis was used to characterize the structure of both P and PC as shown in Fig.1. The spectrum of P and PC showed a characteristic band a 3400 cm^{-1}, which corresponding to stretching of OH and another band at 2750 cm^{-1} , which corresponding to the C-H stretching . A very strong band at 1688 cm^{-1} indicated the presence of carbonyl group. Additional peaks at 1220 and 585 cm^{-1} appeared in the spectrum represent C-H stretching and C-O stretching respectively. By comparing the two IR spectra, a sharpness of the functional groups as –OH and carboxlic groups resulted from chemical carbonization[16].

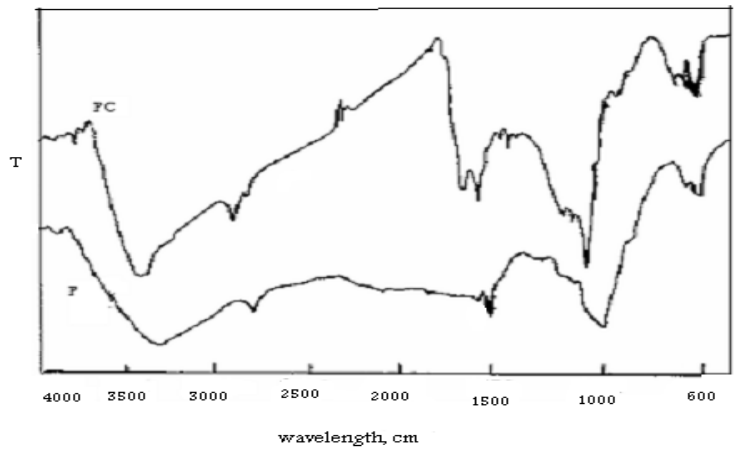

Figure 1: IR spectra of PC and P samples

X-ray diffraction analysis was conducted to monitor the phases present in samples PC and P, it was clear from Fig.2, that the used matrices were mainly amorphous in the range 5-70 (2θ) [17].

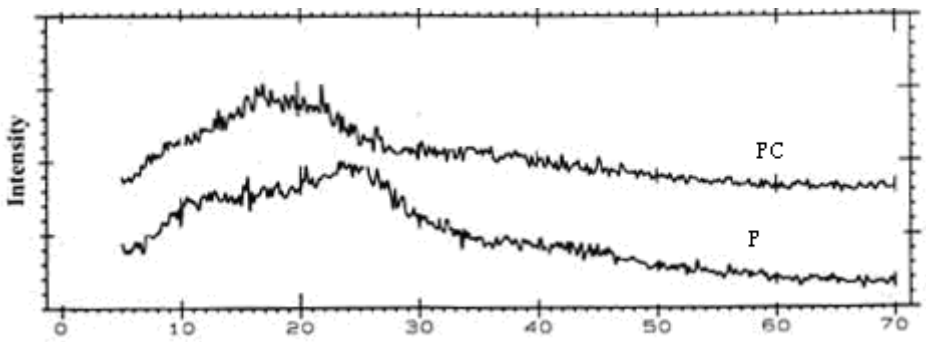

Figure 2: XRD pattern of PC and P samples

The TGA of PC is presented in Fig.3 which showed a weight loss about 4 - 7% between 25-150^{o}C. These may attribute to the evaporation of the adsorbed water. Between 450-550 ^{o}C a weight loss about 7-40 % may be attributed to the removal of the embedded water and transformation to ash.

The DTA diagram of PC was presented in Fig.4 showed a very small endothermic peak could be related to the heat needed to evaporate the adsorbed water at 95^{o}C. Also an exothermic peak was observed at 450-550^{o}C may be due to the transformation of the remainder potato periderm fibers into the ash form[18].

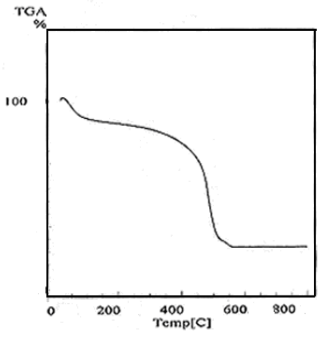

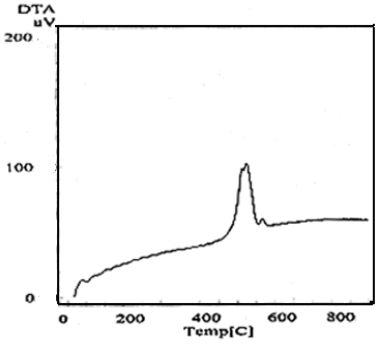

Figure 3: TGA diagram of PC

Figure 4: DTA diagram of PC

Effect of shaking time

The effect of shaking time on uptake of ^{60}Co and $^{152+154}Eu$ onto samples P and PC are shown in Fig.5, at initial metal concentrations of 10^{-3}M and at room temperature (25 ± 1°C). The figure showed that, the uptake was firstly at 90 (min.) rapid (35- 40 % for P and 75-90 % for PC) probably due to easily available exchangeable sites located on surface of P and PC followed by subsequent slow process suggested that intra pore diffusion was also involved in the sorption. It was stated that the plateau portion of the curve corresponded to pore diffusion and linear portion of the curve reflects surface layer diffusion[19]. From Fig. 5 PC sample has higher initial adsorption rate for ^{60}Co, $^{152+154}Eu$ and the adsorption equilibrium reached after 120 min. The first-order rate equation of the Lagergren is one of the most widely used for the sorption of a solute from the liquid solution and is represented as[20]:

$$\ln (1 - F) = Kt + C \qquad (2)$$

Where t is the adsorption time, K the adsorption rate constant and C is a constant. F is given as:

$$F = q_t / q_e \qquad (3)$$

Where q_t and q_e are the amount of adsorption at time t and equilibrium, respectively. The experimental results for Fig.5 can be converted into the plots of –ln (1 – F) versus t as shown in Fig. 6 and tabulated in Table 2,

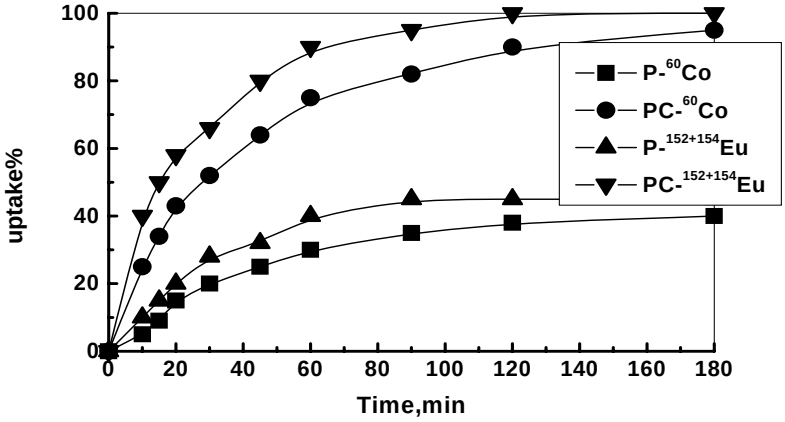

Figure 5: Effect of contact time on the uptake of ^{60}Co and $^{152+154}$Eu onto P and PC

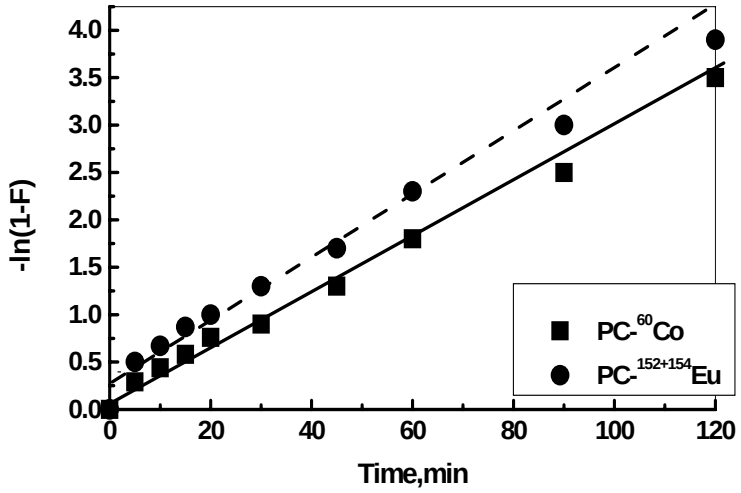

Figure 6: Lagergren plot for the uptake ^{60}Co and $^{152+154}$Eu onto PC

Table 2: The first order kinetic constants for the sorption of ^{60}Co and $^{152+154}$Eu on P and PC

Sorbent type	Experimental q_e (mol	K (min^{-1})	R^2
PC-^{60}Co	0.50	0.0276	0.997
PC-$^{152+254}$Eu	0.52	0.0633	0.966

Effect of sorbent mass

Fig. 7 shows the sorption behavior of ^{60}Co and $^{152+154}Eu$ onto PC as a function of its mass. The amount of adsorbent in the studied samples was varied from 0.02 to 0.4 gm. The percent uptake increased with increasing the amount of adsorbent up to 0.35 gm. This increases in sorption may be due to the ease exchange of ^{60}Co and $^{152+154}Eu$ with the H^+ in either–OH or –COOH groups of the studied matrices[21].

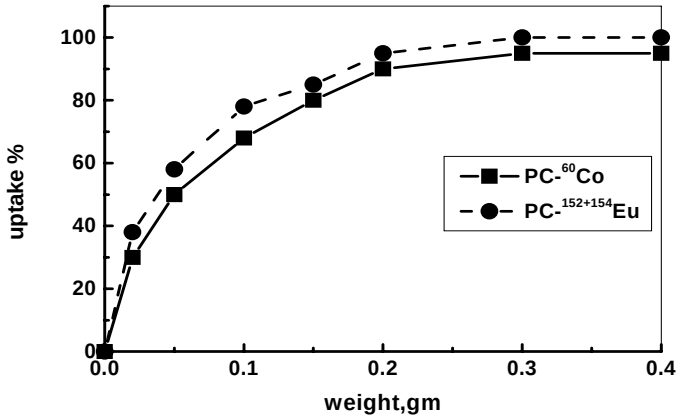

Figure7: Effect of different PC weights on the uptake of ^{60}Co and $^{152+154}Eu$

Effect of pH value

Fig.8 shows the effect of initial pH on the uptake of ^{60}Co and $^{152+154}Eu$ from the studied samples at pH range from 2.5 to 8. The figure showed the percent uptake of ^{60}Co and $^{152+154}Eu$ onto P and PC samples were low at lower pH values, and reached its maximum values at pH 4 and 5.5, respectively. The decrease in the uptake of ^{60}Co and $^{152+154}Eu$ at low pH, acidic medium (2-4), can be explained by the fact that at this low pH range the proton concentration $[H^+]$ is high and the studied ^{60}Co and $^{152+154}Eu$ are present in solution as free cations, so proton can compete with metal cations for attacking the active surface sites of the studied material. At pH range (4 - 5.5), the carboxylic acid groups of either P and PC slowly deprotonate and favor binding of metal ions takes place. This behavior may be explained by the presence of polygalacturonic acids on the external part of the cellular wall of Salanum Tuber Osum (potato periderm) and also due to the presence of starch and protein in the plasmatic membrane [22,23]. The maximum uptake of ^{60}Co and $^{152+154}Eu$ by PC indicated that PC exhibited behavior similar to that of Zwitter ion type exchanger at the studied pH range. The decrease in uptake of ^{60}Co and $^{152+154}Eu$ on either P and PC with increasing the pH medium, alkaline medium (7.5 – 8), was attributed to the formation of $Co(OH)_3$ and $Eu(OH)_3$. The mentioned negatively charged species suffer repulsive forces with the active surface sites, hence showed low adsorption.

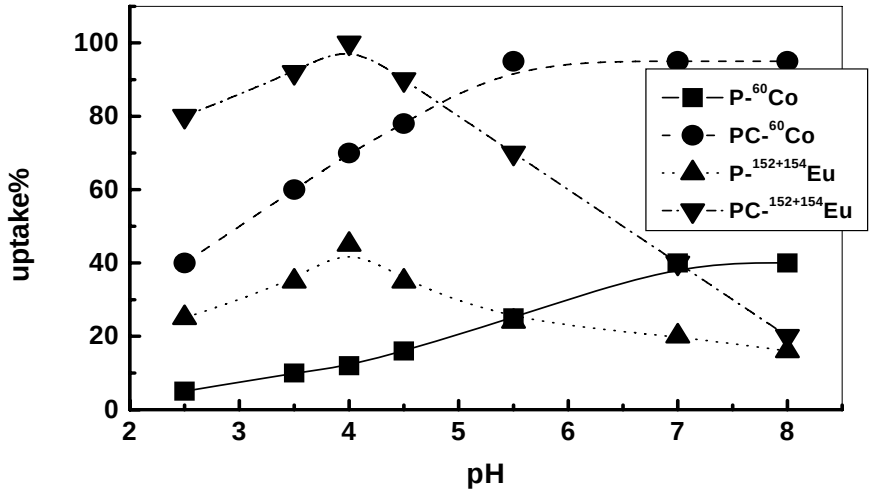

Figure 8: Effect of pH variation on the uptake of ^{60} Co and $^{152+154}$Eu by PC.

Effect of initial ^{60}Co and $^{152+154}$Eu concentration

The effect of variation Co and Eu concentrations on their sorption onto PC samples were studied under the optimized conditions of shaking time, pH and the amount of adsorbent. The Co^{+2} and Eu^{+3} concentrations have been tested, at room temperature (25±1°C), in the concentration range of 10^{-4} to $5x10^{-2}$ M. The adsorption showed in Fig.9 was almost constant up to 10^{-3}M of cobalt and europium, beyond this concentration the adsorption decreased gradually with the increase of cobalt or europium concentration in the aqueous solution. This may be due to the fast mobility of either cobalt or europium ions up to 10^{-3}M concentration which probably cause the increase of interaction of these ions with PC sample. On the basis of these results, $1x10^{-3}$ M/l concentration from both ions was used for all further studies. The results were also subjected to analysis in terms of Freundlich and Langmuir adsorption isotherms. The data were found to fit both the two isotherm equations. However the Freundlich adsorption isotherm was capable of describing the data over the entire concentration range, while the Langmuir adsorption isotherm was capable for describing the data in the concentration range from $1x10^{-4}$ to $5x10^{-3}$ M. The Freundlich isotherm was tested in the linearized form:

$$\log q_e = \log K_F + (1/n) \log M \qquad (4)$$

Where, K_F and 1/n are characteristic constants for the adsorption system, the values of K_F and 1/n were deduced respectively from the intercept and the slope of the straight line resulted from plotting log q_e versus log M, where M either Co or Eu concentration ion. The results have been cleared in Figure 10 and tabulated in Table 3. The values of (1/n) <1 signify that strong adsorption forces were operative on the adsorbent surface. According to the statistical theory of adsorption which showed that this type of isotherm with 1/n<1 corresponds either to a heterogeneous surface with no interaction between adsorbed atoms or molecules, or to a

homogeneous surface on which there are repulsive forces between the adsorbed species. In the present case the isotherm of Co^{+2} and Eu^{+3} necessarily due to a heterogeneous surface structure [24].
The modified Langmuir model tested in this study is:

$$C_e/q_e = 1/K_L Q_o + C_e/Q_o \qquad (5)$$

Where, K_L and Q_o are the Langmuir constants, their values were related to the physical properties of the system and reflected the energy of adsorption and the solute adsorptivity respectively, Q_o is generally called the monolayer capacity. On plotting C_e/q_e versus C_e a straight line was obtained, in the Co^{+2} and Eu^{+3} concentration range from $1x10^{-4}$ to $5x10^{-3}$ M. From Fig.11, Q_o and K_L were obtained from the slope and intercept of the straight line. The values were tabulated in Table 3. The validity of the Langmuir isotherm over the specified concentration range indicated monolayer coverage of the surface of samples by cobalt and europium.

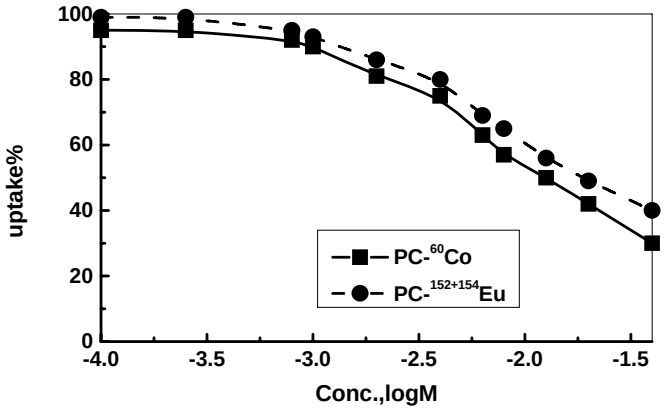

Figure 9: Effect of different ion concentrations on the uptake of ^{60}Co and $^{152+154}Eu$ by PC.

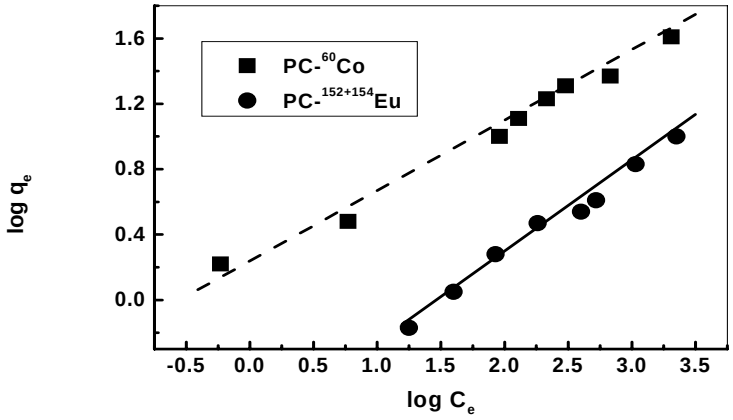

Figure 10: Freundlich isotherm for ^{60}Co and $^{152+154}Eu$ sorption on PC.

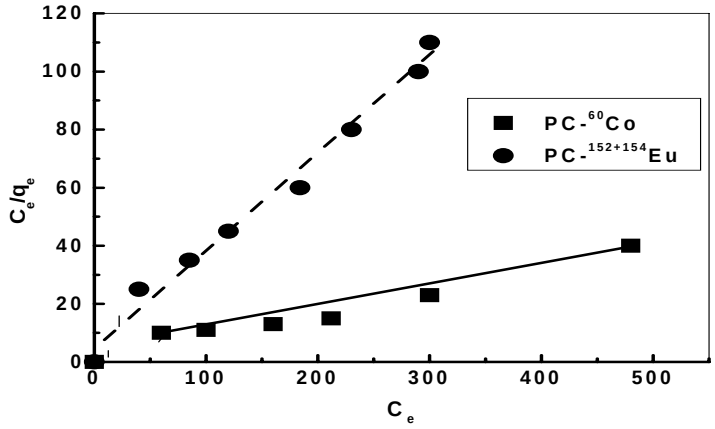

Figure 11: Langmiur isotherm for ^{60}Co and $^{152+154}$Eu sorption on PC.

Table 3: Langmiur and Freundlich parameters for sorption of ^{60}Co and $^{152+154}$Eu on PC.

Ions	Langmiur			Freundlich		
	Q_o mg/g	K_L	R^2	1/n	K_F	R^2
PC-Co	45.87	0.118	0.963	0.406	1.780	0.989
PC-Eu	91.74	0.635	0.916	0.695	4.953	0.993

Effect of temperature

Temperature has two major effects on adsorption process. Increasing temperature is known to increase the rate of diffusion of the adsobate molecules across the external boundary layer and in the internal pores of the adsorbent particle, owing to the decrease in velocity of the solution. In addition, changing the temperature will change the equilibrium capacity of the adsorbent for the particular adsorbate[25].

The effect of temperature on the adsorption of ^{60}Co on PC was studied using different initial concentrations ranging between $1x10^{-3}$ and $2x10^{-2}$M. Figure 12 showed the effect of different temperatures as 298, 308 and 313 K, while other parameters were kept constant. The increase in the temperature increased the amount of ^{60}Co sorbed on PC sample. This may be due to the attraction of the particles at higher temperature, thus, increasing the surface area available as ion exchange[26]. At $1x10^{-3}$M concentration, the K_d value at 298 K was 514.2 and reached 1847.5 at 313 K, while the cobalt uptake was increased from 90% (0.0303 mmol/g) at 298 K to 97% (0.0327mmol/g) at 313K . The thermodynamic parameters such as free energy change (ΔG^o), enthalpy change (ΔH^o) and entropy change (ΔS^o) for the adsorption process were calculated using the following equations to know the nature of adsorption:.

$$\Delta G^o = - RT \ln K_d \qquad (6)$$

$$\ln K_d = (\Delta S^o)/ R - (\Delta H^o)/ RT \quad (7)$$

$$\Delta G^o = \Delta H - T \Delta S \quad (8)$$

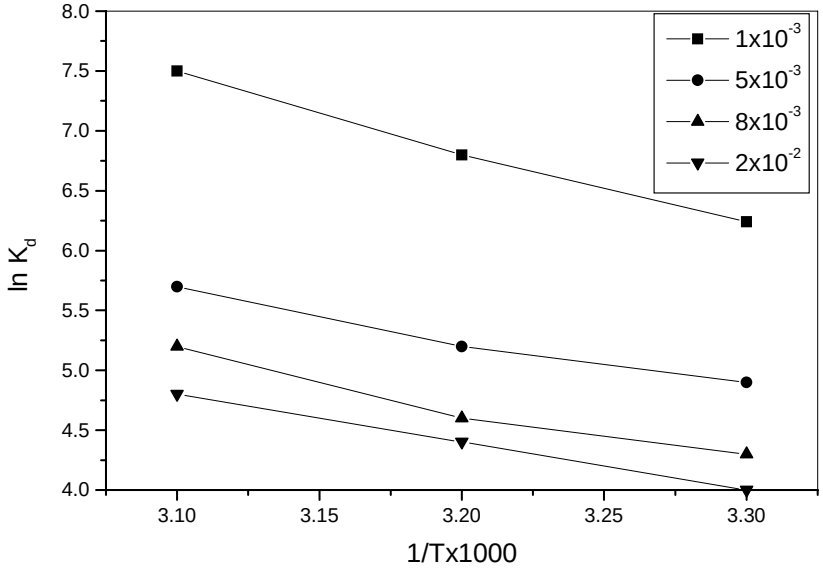

Figure 12: Variation of 1/T and lnKd on the uptake of ^{60}Co on PC sample.

Table 4 Thermodynamic parameters of the adsorption isotherms of ^{60}Co onto PC

Conc. of Co^{+2} M	T	%uptake	Ln K_d KJ/mol	ΔS^0 KJ/mol	ΔH^0 KJ/mol	ΔG^0 KJ/mol
10^{-3}	298	90	6.24			-15.46
	308	93	6.63	3.28	0.77	-16.97
	318	97	7.52			-19.88
	298	70	4.98			-12.11
$5x10^{-3}$	308	76	5.2	2.19	0.49	-13.31
	318	84	5.7			-15.07
	298	56	4.28			-10.60
$8x10^{-3}$	308	64	4.62	2.23	0.52	-11.83
	318	75	5.14			-13.60
	298	50	4.05			-10.02
$2x10^{-2}$	308	56	4.45	2.08	0.48	-11.40
	318	69	4.85			-12.62

Effect of competing ions

Fig.13 studies the effect of foreign ion as Na^{+}, K^{+}, Ca^{2+}, SO^{2-}_{4} and PO^{2-}_{3} on the sorption capacity of Co^{+2} on PC samples. These ions are mostly present in the simulated radioactive liquid waste Table 1. The results showed that sorption of Co^{+2} was severely interfered by SO^{2-}_{4} and PO^{2-}_{3} than other cations due to chemical similarity between either Co and Ca producing 34.3% lower in sorption of the desired ions. It was observed also that the solubility products of $CaSO_4$ and $Ca_3(PO_4)_2$ are $2.4x10^{-5}$ and $1x10^{-6}$ M respectively due to it's lower value so these ions which prefers to precipitate in solution cause lowering in sorption of Co^{+2} capacity[27].

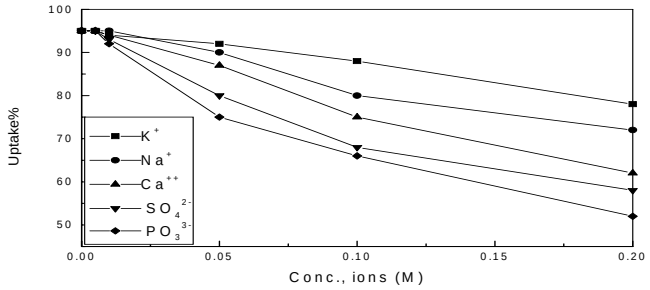

Figure 13: Effect of different competing ions on the uptake of ^{60}Co onto PC.

CONCLUSION

Chemically modified potato periderm was suitable for treatment of radioactive waste containing either cobalt or europium. The maximum capacity was 0.85 and 0.90 $molKg^{-1}$. The higher value of the specific surface area of PC was 308 $m^2.g^{-1}$ than P 130 $m^2.g^{-1}$ indicated that, the higher fraction of mesopores of PC than P which contributed to the difference in adsorption capacity. The kinetics of
Co^{+2} and Eu^{+3} adsorption on PC showed that an agitation time of 2 h is needed to reach equilibrium values with the experimental system used. The first-order rate equation of the Lagergren described the kinetic of adsorption. The amount of adsorbent PC in the studied PC samples was 0.05 gm. The maximum adsorption capacity of Co^{+2} and Eu^{+3} on PC was occurred in the pH 5.5 and 4.0 respectively. The adsorption process was exothermic in nature and decreases with increase in ionic strength. The data obtained from studying at different concentrations were fitted to Langmiur and Freundlich models. The thermodynamic parameters were calculated to predict the theoretical behavior of Co^{+2} adsorption onto PC.

REFERENCES

(1) Technical Report Series No. 408, Application of Ion exchange process for the treatment of Radioactive waste and management of spent ion exchangers, IAEA, Viena, 2002.
(2) R.C. Marlay, Radioactivity releases to the environment by nuclear power plants, locally and for total fuel cycle, MIT Energy Laboratory Report No. MTI-EL-79-014, March 1979.
(3) L.D. Danilin, and V.S. Drozhhin; J. Radiochemistry, 49(3) 319-322 (2007).
(4) J.Lehto and R. Harjula; Radiochem. Acta 86, 65-70 (1999).
(5) J.I. Davila, M. Solache Rios and J.E. Nunez Monreal; J. Nuclear Material, 362, Issue1, 53-59 (2007).
(6) S. Babel, and T.A. Kurniawan;J. of Hazardous Material, 97, Issue 1-3 (28) 219-243 (2003).
(7) R.Turpeinen, Interactions between metals, microbes and plants bioremediation of As and Pb contaminated soil, Department of Ecological and Environmental University of Helsinki (2007).
(8) S.H. Lee, and H.W. Yang; J. Separation Science and Technology, 32(8) 1371-1387 (1997).
(9) N.Fiol, I. Villaescusa, M. Martinez, N. Miralles, J. Poch and J.Serarols; Separation Science and Technology, 50 , 132-140 (2006).
(10) A.H. Mahvi, M. Maleki, and A. Eslami; American J. of applied sciences, 4, 321-326 (2004).
(11) X. Li, Y.Tang, Z.Xuan, Y.Liu and F.Luo;, J. Separation and Purification technology, 55,69-75 (2007).
(12) H.A. Omar, M.Aziz and K.Shakir; J. Radiochemical Acta, 95, 17-24 (2007).
(13) P.E. Kolattukudy, and V.P. Agrawal, Lipids, 9:170.(1974).
(14) A.Saeed, M.Iqbal, and M.W. Akhtar; J. Hazard. Mater. B 117, 65-73(2005).
(15) A.A.El-Hendawy; J.Carbon,41,713-722 (2003).
(16) Nyquist, R.N and Kagel, R.O.; Academic Press; New York; 1997.
(17) D.S. OrlovSoil Chemistry, OxfordL IBH, New Delhi, 1992.
(18) F. Stengele, and W.S. Kloss; J. of Thermal Analysis and Calorimetry,51, 219-230 (1998).
(19) T.S. Anirudhan, and M.Ramachandran; J. of Colloid and interface science, 299, 116-124 (2006).
(20) S.Lagergren, Sevenska Handl, B.K.; Water Research; 32, 3062 (1998).
(21) S.P. Mihra, and D.Tiwari; J. Radioanal. Nucl. Chem.,251,1,47-53 (2002).
(22) M.V. Balarama Krishna, S.V. Rao, and V.K. Manchanda; J. Separation and Purification Technology, 38,149-161 (2004).
(23) T. Aman, A.A. kazi, Mu.SAbri and Q.Bano; J. Colloids Surf. Biointerfaces,1,63(1)116-121 (2008).
(24) M. Gardea-TorresdeyHejazi, K. Tiemann and J.G. Parsons; J. Hazard. Mater. B 91, 95-112. (2002).
(25) Z.Reddad, C. Gerente, Y.Andres and P. LeCloirec, ; J.Environ. Sci. Technol., 36,2067-2073 (2002).
(26) A.M. El Kamash; Arab J. of Nuclear Science and Applications, 41,72-88(2008).
(27) F.T. Edward, and Michael, Streat; J.Chem. Tech. Biotechnol. 33A, 180 (1983).
(28) M.S. Murali, and J.N. Mathur; J. Radioanal. Nucl. Chem., 254, (1)129-136 (2002).

Statistical treatment of hazards result from radioactive material in metal scrap

E.F. Salem, S.M. Rashad
Nuclear law and License department Egypt nuclear and radiological regulatory authority
Sayeda_f@yahoo.com
Nasr City-P.O. Box 7551, Cairo, Egypt

ABSTRACT

Radioactive sources have a wide range of uses in medicine and industry. Radioactive materials entering the public domain in an uncontrolled manner may creating a serious risk of radiation exposure for workers and the public as well as excessive costs for plant decontamination and waste of product to be borne by the metal industry. This paper describes the major accidents that had happened in the last decades due to radioactive material in metal scrap, provides assessment of associated hazards and lessons learned. This will help Regulatory Authority to introduce measures capable to avoid the recurrence of similar events. The study highlights the situation for metal scrap incidents in Egypt.

1- INTRODUCTION

Nowadays, scrap metal is an important source material for the metal production industry contributing a large fraction (about 50% for steel) of the final product. This fact shows the hugeness importance of the metal scrap as raw material resources for human race. There have been several accidents over the past decades involving orphan radioactive sources or other radioactive material that were inadvertently collected as scrap metal that was destined for recycling. In the USA alone, over 5,000 incidents were recorded in 2004 that involved various types of radioactive metal scrap [1]. According to the forecast of the United Nations Economic Commission for Europe (UNECE) it is expected that the number of incidents with radioactive scrap will increase despite of the efforts, on the world scale, to avert such incidents. The melting of an orphan source with scrap metal or its rupturing when mixed with scrap metal has also resulted in contaminated recycled metal and wastes. If radioactive substances found in metal scrap and not detected in time, in the process of melting they may be incorporated into ferrous or nonferrous metals and various articles manufactured from them. This may lead to hazardous consequences for the health of the workers and the population and radioactive contamination of the environment. Also leads to negative economic, trade and social consequences. According to the data of the international Atomic Energy Agency (IAEA) for a ten-year period, until 1998, in the world there have occurred average 30 incidents per year when radioactive sources have been melted in metallurgical enterprises during the process of reprocessing of metal scrap [1] . During 2004, only in the USA, about 250 cases man-made radioactive sources were found in metal scrap (orphan, abandoned, lost or stolen). In Bulgaria for the period 1998-2006 were registered a total of 125 incidents with radioactive scrap, i.e. on the average 14 cases for this 9 year period. In 120 of

the cases components with increased content of natural radionuclides were found, while in 5 cases orphan radioactive sources were found (Cs-137 and Co-60).In all of these cases no radioactive consequences were established for the Bulgarian population and the environment, but nevertheless such type of incidents should not be allowed to occur, which requires implementing preventive and response measures on a national scale. Reducing the magnitude of the problem by prevention, detection and subsequent reaction requires the cooperative efforts of all concerned parties, that is, the scrap metal carriers, the authorities.

2- CATEGORIZATION OF RADIOACTIVE SOURCES

The categorization system set out five categories. This number is considered sufficient to enable the practical application of the scheme, without unwarranted precision [15]. The categorization system is based on the resulting ratio A/D, where A the source activity and D its dangerous factor [5]. Table (1) illustrates the category of radioactive source according to hazard strength. Within this categorization system, sources in Category 1 are considered to be the most 'dangerous' because they can pose a very high risk to human health if not managed safely and securely. An exposure of only a few minutes to an unshielded Category 1 source may be fatal. At the lower end of the categorization system, sources in Category 5 are the least dangerous; however, even these sources could give rise to doses in excess of the dose limits if not properly controlled, and therefore need to be kept under appropriate regulatory control.

Table (2) Categorization of sources according to deterministic effects:

Category	A/D	Risk due to direct exposure
1	A/D> 1000	Extremely dangerous
2	1000>A/D> 10	Very dangerous
3	10>A/D> 1	Dangerous
4	1>A/D> 0.01	Les dangerous
5	0.01>A/D> Exemption level (EL)	No dangerous

3- ASSESSMENTS THE ORIGINS OF RADIOACTIVE SCRAP METAL

Radioactive scrap metal can occur in a number of different ways. Some of the main origins are :(a) Demolition or decommissioning of industrial facilities processing raw materials containing naturally occurring radionuclides. These industries include phosphate ore processing and oil and gas recovery and processing. The pipes and metal vessels from such facilities are sometimes lined with significant deposits of naturally occurring radionuclides and they may, on occasions, be mistakenly collected as scrap metal. (b) Decommissioning of nuclear installations (such as nuclear power plants and other nuclear fuel cycle facilities) and other facilities. This can produce significant amounts of various metals. A fraction of this material is radioactively activated or contaminated and is normally decontaminated or disposed of as radioactive waste but, on occasions, it may be mistakenly released for recycling. Material from decommissioning or demolition containing artificial or naturally occurring radionuclides at levels below the regulatory clearance level may be released with the approval of regulatory authorities for possible recycling. (c) Loss of sources. Sealed radioactive sources are sometimes lost or mislaid. They may be collected as scrap metal, often with the sealed sources

still housed within their protective containers. Industrial radiography sources are used for testing welds on pipework and may be lost in the field. The loss of radioactive sources used in medicine sometimes occurs through poor accounting. d) Delivering as metal scrap of devices, goods and articles containing radioactive materials or radioactive sources remaining out of regulatory control or containing naturally occurring radionuclides.

4- INTERNATIONAL DATABASES

4-1- Iaea Illicit Trafficking Database (Itdb):

From January 1993 to December 2011, a total of 2164 incidents were reported to the ITDB by participating States and some non-participating States. 399 incidents involved unauthorized possession and related criminal activities. Incidents included in this category involved illegal possession, movement or attempts to illegally trade in or use nuclear material or radioactive sources. Sixteen incidents in this category involved high enriched uranium (HEU) or plutonium. There were 588 incidents reported that involved the theft or loss of nuclear or other radioactive material and a total of 1124 cases involving other unauthorized activities, including the unauthorized disposal of radioactive materials or discovery of uncontrolled sources see figure(1).

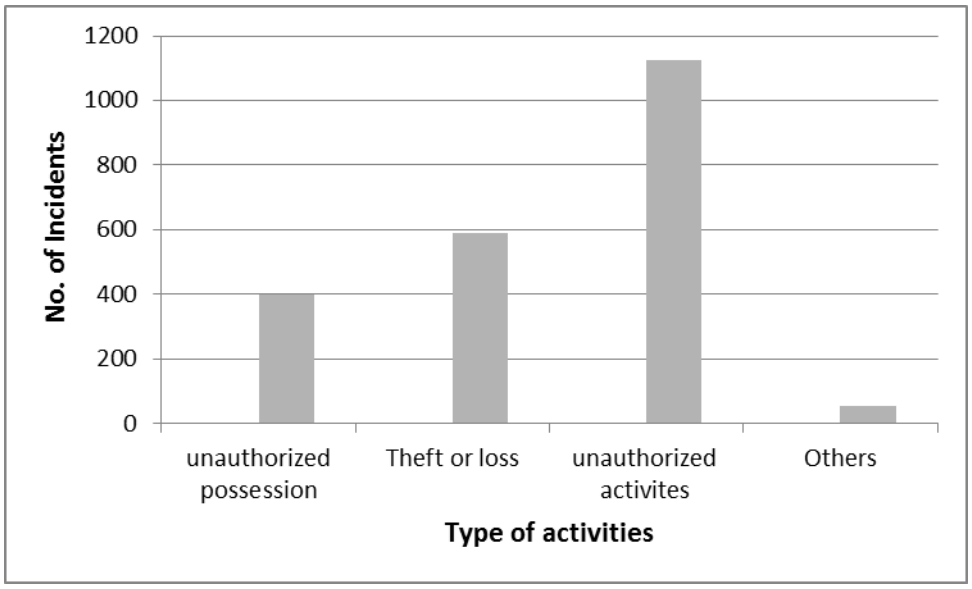

Figure (1) IAEA ITDB (1993-2011) : 2164 cases

The majority of incidents involving 'other unauthorized activities or events', fall into one of three categories: the unauthorized disposal (e.g. radioactive sources entering the scrap metal industry), unauthorized movement (e.g. scrap metals contaminated with radioactive material being shipped across international borders) or the discovery of radioactive material (e.g. uncontrolled radioactive sources). The occurrence of such incidents can indicate deficiencies in the systems to control, secure and properly dispose of radioactive material [17]. Figure (2) represented the number of incidents involving 'other unauthorized activities that were happened in the period 1993 to 2011. It is clear that the number of incidents from 1993 to 1999

represent 5% from the total incidents, where 95 % in the period 2000 to 2011.There is evidence that this rise is related to the increased number of radiation portal monitoring systems that have been deployed at national borders and scrap metal facilities.

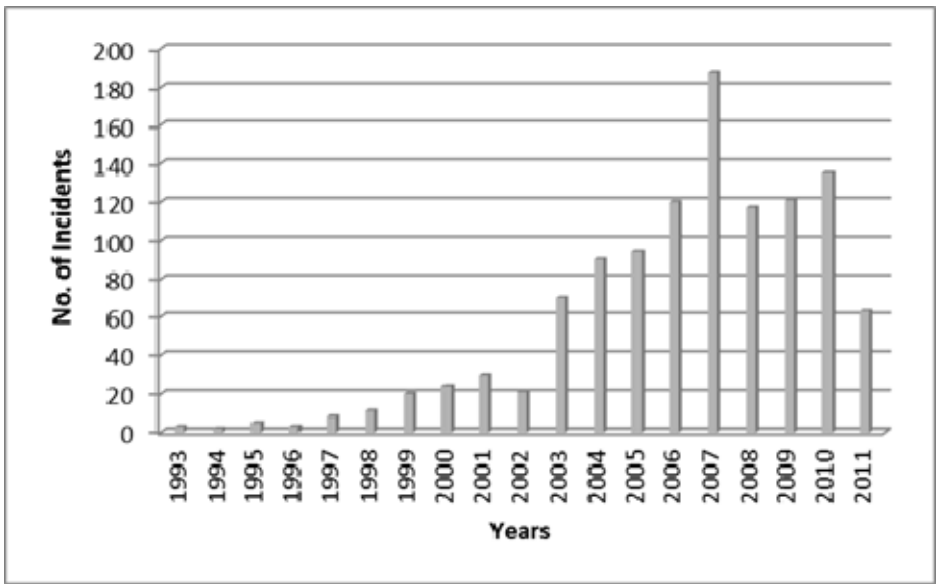

Figure (2) number of incidents involving 'other unauthorized activities in the period 1993 – 2011

4.2- The US NRC Records:

U.S. Nuclear Regulatory Commission (NRC) has reported that it has lost track of over 1,500 sealed sources since 1996, more than half the number have never been traced. In fact, the U.S. National Nuclear Security Administration (NNSA) has a major ongoing programme for the recovery of orphaned sources. A European Union (E.U.) study estimated that about 70 sources are "orphaned" every year. A recent European Commission report estimated that about 30,000 disused sources in the E.U. that were held in local storage at the users' premises were at risk of being lost from regulatory control [12].

5-STATISTICAL NALYSIS OF MAJOR RADIOACTIVE METAL SCRAP ACIDENTS

The metal recycling industry itself recognizes the harm which it could suffer if consumers become concerned about the safety of their products. The British Metals Federation wants no detectable radiation permitted in their products above normal background levels. In the US, steel manufacturers there are concerned about the impact on their industry. The industry maintains zero tolerance level for allowing radioactive contaminants into steel smelters, but it has been plagued by illegal dumping. The US Steel Manufacturers Association reports 50 incidents in which materials released for recycling were contaminated at levels higher than the free release threshold [13]. Significantly, in the US the industry's concerns may be winning

through with recent reports that the US Energy Secretary has imposed a moratorium on the release of further contaminated scrap for recycling Exactly how many orphan sources there are in the world is not known, but the numbers are thought to be substantial. Based on the data of the NRC (USA) annually about 200 incidents have been reported with theft, loss of abandoned radioactive sources [1]. In the USA alone, over 5,000 incidents were recorded in 2004 that involved various types of radioactive metal scrap .UK record 20 incidents turning up scrap yard in the period of 1997-2000. At the period 1998 –2006 Bulgaria recorded 125 radioactive metal scrap incidents. Since January 1997- October 1999, 113 incidents were recorded in Italy. During the period from 1983 to 1998 there are around sixty two reported incidents with melted radioactive sources in different countries in the world [1]. The data demonstrate that the two radionuclides most commonly implicated in melting incidents are Cs-137 (48.8%) and Co-60 (26.7%), as in figure (3). In 1983 -1996 there were 25 confirmed accidental melting of radioactive sources at U.S. mills [3]. Disposal and cleanup cost plant where a melting occurred average of $10 million at one mill up to $23 million [3]. Table (3) represents the major accidents with radioactive sources in scrap metal, the causes and their consequences.

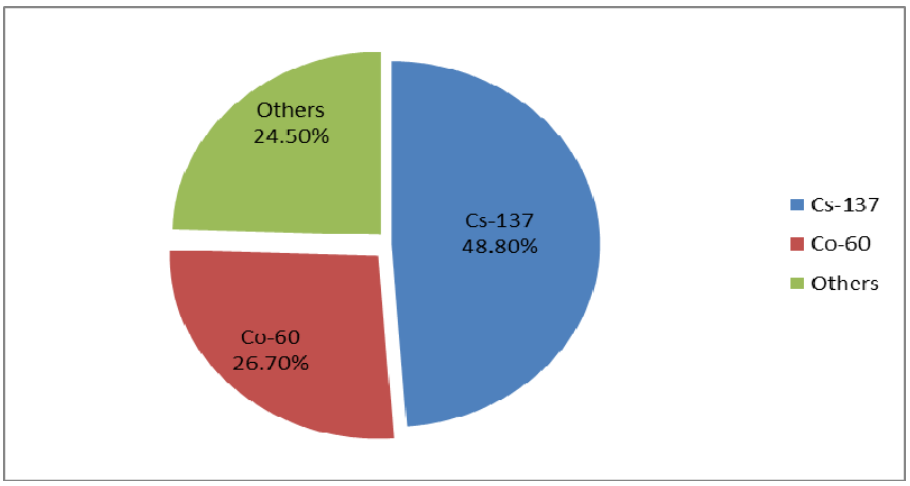

Figure (3) Scrap metal accidents according to the radionuclide type

Table (2) Magor Accidents Involving Radioactive Sources In Scrap Metal

Date and place	Radionuclide	Consequences
Juarez, Mexico 1983	Co-60 37 TBq	75 people received doses between 0.25 and 7 Gy, 814 houses demolished and 16000 m3of soil waste and 4500 tonnes of metal waste were collected
Goiania, Brazil 1987	Cs-137 (50 TBq)	4 people died and 21 people with dose above 1 Gy, 200 people form 41 houses were evacuated and 7 houses were demolished and 3500m^3 of wastes were collected.
Jilin, Xinzhou, PR China, 1992	cobalt-60 (10curie)	3 fatalities and 5 injuries
Tammiku, Estonia 1994	Cs-137 (7.4 TBq)	1 people died from radiation exposure and 4- suffered significant deterministic effect

Istanbul, Turkey 1998	Co-60 (3.3 TBq; 23.5 TBq; 21.3 TBq)	18 people hospitalized: 5 with doses of about 3 Gy, 1 with a dose of about 2 Gy and others with doses below 1 Gy
Los Barrios, Spain 1998	Cs-137	The radiological consequences of this event were minimal, with six people having slight levels of caesium-137 contamination. However, the economic, political and social consequences were major. The estimated total costs for clean-up, waste storage, and interruption of business at the affected Companies exceeded $25 million US dollars.
Samut Prakarn Thailand, 2000	Co-60 (15.7 TBq)	10 people received high doses, 3 (all workers at a scrapyard) died. Source recovered intact
UK, 2000	Pu-238 (140 GBq) melted in foundry	The doses involved were negligible but the clean-up and disposal costs are several million US dollars.
Nigeria, 2002	Am-241/Be (721 GBq, 18 GBq)	Sources detected in a scrap metal, shipment in Europe
Mayapuri, India 2010	C0-60 it was dismantled and was cut into eleven pieces	6 people was hospital as a result of radiation exposure and one died.

From table (2) it is clear that Mexico accident and Goiana accident still the worst accidents until now. Mexico accident provides an example of a combination of causes: Illegal importation of the Co-60 sources in 1979 preventing regulatory oversight and the authorities were unaware of it with long term insecure storage before use until 1983 and loss of staff key and member of staff had no knowledge of the hazard [5]. The accident required a large-scale cleanup program both in Ciudad Juárez. In most cases of scrap metal radioactive accident the radiological consequences were minimal, however the economic cost for decontamination process were major.

5.1-Risk assessment due to radioactive metal scraps accidents

It is noticed that the commonly sources in melting accident are Co-60. Cs-137, Am/Be and Pu-238. Table (3) demonstrates the dangerous index (A/D) and the risk due to direct exposure.

Table (3): Risk due to direct exposure:

Source	Activity (A)	D value	A/D	category	Risk due to direct exposure
Co-60	37(TBq)	0.03	1233.33	1	Extremely dangerous
Am-241/Be	0.721(TBq)	0.06	12.85	2	Very dangerous
Cs-137	50(TBq)	0.1	500	2	Very dangerous
Pu-238	0.140(TBq)	0.06	2.33	3	dangerous

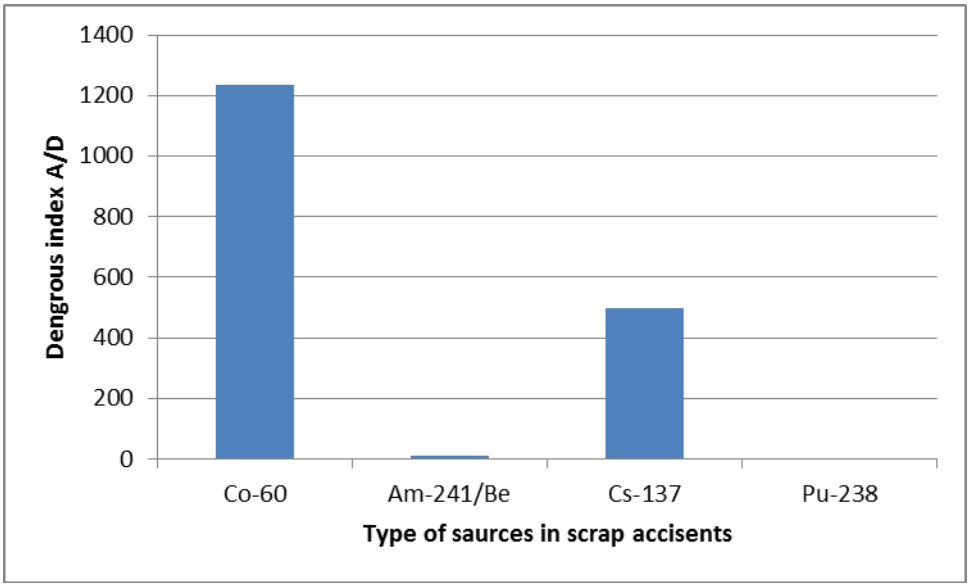

Figure (4) the relation between dangerous index and risk due to exposure

Figure (4) indicates that Co-60 and Cs-137 are major dangerous source cause and hazard.

6- REPORTED SCRAP METAL INCIDENTS IN EGYPT AND THE NEED TO IMPROVE THE REGULATORY CONTROL REGIME

In 1998 radioactive cesium-137 was found in exporting scrap metal to Amsterdam, the Netherlands. The license was withdrawn from the exported company, which reported that the shipment was radiation-free in violation of the truth [16]. A Container of neutron source which used to measure moisture in the soil was found at scrap dealer in Sabteia District – Cairo in 2001. The source quoted by the Atomic Energy Authority. In recent incidents were detected by regulatory inspectors from Atomic Energy Authority. There was detection of high radiation level from Cars carrying a load out from the border of Damietta Port two times. It was doubt in both cases that the contamination may be due to the Cargo on the Cars. More investigations showed that the contamination was due to cobalt-60, the first was in a small steel area from the trailer (0.5 mSv/h on the surface of the contaminated area), and the second was in the steel center of the wheel of the Car with activity 0.04µCi (3 µSv/h). This indicates that lost Cobalt-60 source not follow up and was melted during the metal recycling industry, resulted a contaminated metal.

In Oct-2012 detection gate monitoring Damietta Port Maritime warning voice recording readings from natural background radiation during the passage of truck carrying 8 tons of supplies (Pipes - Tubes - Motors) made of iron coming from India. Alarm was confirmed by a detection device and multi-channel analysis radioactivity and make sure that the contamination was due to cobalt-60. Detection monitoring reading was 300 count/sec and survey meter reading was 0.5 µSv. The truck was prevented from entering and returned to the country of origin. The government should establish a policy and strategy for the control of

radioactive material recovered in the metal recycling. The policy and strategy should be developed in cooperation with the metal recycling and production industries, the regulatory body and organizations for the management of radioactive waste. An obligation to notify of any temporary or permanent disuse of sources or their removal from operational use, would allow the regulatory authority to perform a closer follow up of all sources no longer in use and prevent loss of control of these sources [7]. National regulatory requirements should include an obligation to report missing and found sources and abnormal events with radiation sources. If radioactive scrap metal is discovered, the scrap metal owner (national or foreign), is obliged to cover all expenses associated with the recovery and disposal of the material and any clean-up costs. Basically Regulatory Authority should take into consideration geographical identification of all radioactive sources used in the country in the different practices. All radioactive materials are sent for storage at the radioactive waste repository operated by the country radioactive waste organization and the information is recorded by the Nuclear and Radiological Regulatory Authority. Regulatory authority should bound scrap yard places, stimulates owners to introduce a system of radioactive detection, to effective control the possibility to receive an orphan source and give license according to safety requirements. The operator of a metal recycling and production facility should establish a response plan. The response plan should be consistent with the national radiation emergency plan. The objective of the response plan should be to ensure the protection of workers, members of the public and the environment. The response plan should be documented, exercised, kept under review and updated as necessary.

CONCLUSION

The root causes of the radioactive scrap metal accidents are lack of regulatory control and theft from unsecured building for reprocessing as scrap metal. Reducing the probability of loss of control of orphan sources requires in most countries establishment of a national specific strategy focused on improving regulatory controls regimes. Reports and analyses of incidents involving radioactive scrap metal are valuable to the national and international scrap metal community as a means of learning from the experiences of others; where IAEA implemented unified system for information exchange web site. Increasing number of radiation portal monitoring systems that have been deployed at national borders to cover portals all over the country.

REFERENCES

(1) BULGARIAN NUCLEAR REGULATORY AGENCY “Prevention, Detection and Response to Radiation Emergency in Case of Discovering of Radioactive Material in Metal Scrap” safety guide, PP - 4/2010.

(2) United Nation “Recommendations of monitoring and response procedures for radioactive scrap metal” , New York and Geneva, 2006.

(3) Jose de Jullio Rozental “Two Decades of Radiological Accidents Direct Causes,Roots Causes and Consequences", Brazilian Archives of Biology and Technology, An International Journal, (2002): Vol.45 Special n : pp. 125-133.

(4) Dr. Eugenio GIL, “Orphan sources extending radiobiological protection outside the regulatory framework” second European IRPA congress on radiation protection Paris, May 15-19, 2006.

(5) John Croft “The lessons to be learned from incidents and accidents, United Kingdom,2004.

(6) Greta Joy Dicus "MATERIALS SAFETY AND REGULATION Commissioner U.S. Nuclear Regulatory Commission" Presentation to the Regulatory Information Conference Washington, DC April 2, 1997.
(7) P. Ortiz, M. Oresegun, J. Wheatley "Lessons from Major Radiation Accidents" IAEA, T-21-1, P-11-230
(8) IAEA "Reducing Risks in the Scrap Metal Industry Sealed Radioactive Sources",IAEA/PI/A.83 / 05-09511 , 2005.
(9) IAEA "THE RADIOLOGICAL ACCIDENT IN TAMMIKU", VIENNA, 1998
(10) IAEA, Safety Standards "Control of Orphan Sources and Other Radioactive Material in the Metal Recycling and Production Industries" Specific Safety Guide No. SSG-17, 2012.
(11) Johnston's Archive "Database of radiological incidents and related events", 2008.
(12) R. RAMACHANDRAN "Radiation shock "FRONTLINE, Volume 27 - Issue 10 May. 08-21, 2010, INDIA'S NATIONAL MAGAZINE from the publishers of THE HINDU.
(13) Nuclear Free Localized Authorities Radioactive Scrap Metal.mht, 2000.
(14) Nuclear Safety web editors IAEA," Illicit Trafficking Database (ITDB)"2012
(15) IAEA, Safety Guide No.RS-G-1.9 "Categorization of Radioactive Sources", 2005
(16) Dr, Ahmed Gomaa, Seminar of nuclear and radiological incidents, which was held in Collaboration between the Academy of Scientific Research and Technology and the Faculty of Science- University of the Suez Canal 2-12 2000.
(17) IAEA ILLICIT TRAFFICKING DATABASE (ITDB, fact sheet 20011

Developing a Science and Technology Centre for Supporting the Launching of a Nuclear Power Programme[0]

I. Badawy
Department of Nuclear Safeguards and Physical Protection
Egyptian Nuclear and Radiological Regulatory Authority
Cairo, Egypt
Email: isma.sam@hotmail.com

ABSTRACT

The present investigation aims at developing a science and technology centre for supporting the launching of a nuclear power [NP] programme in a developing country with a relatively high economic growth rate. The development approach is based on enhancing the roles and functions of the proposed centre with respect to the main pillars that would have effect on the safe, secure and peaceful uses of the nuclear energy -particularly- in the field of electricity generation and sea-water desalination. The study underlines the importance of incorporating advanced research and development work, concepts and services provided by the proposed centre to the NP programme, to the regulatory systems of the concerned State and to the national nuclear industry in the fields of nuclear safety, radiation safety, nuclear safeguards, nuclear security and other related scientific and technical fields including human resources and nuclear knowledge management.

Key Words: *Nuclear safety/Safeguards/Security/Human resources/ Knowledge management.*

INTRODUCTION

Nowadays, nuclear energy is becoming a competitive and economic source of energy compared with fossil fuel resources, and may be considered as the only energy source of non green-house gas emissions that can replace fossil fuels while satisfying the world increasing demand for energy. Highly industrialized countries with operating nuclear power plants [NPPs] are developing and expanding their nuclear programmes "Nuclear Renaissance". Developing nations -especially with relatively high economic growth rates- are trying to develop and/or launch nuclear power programmes for peaceful uses of atomic energy[1-3].

It is essential that each concerned State would establish, maintain and develop its own effective nuclear regulatory systems and efficient licensing processes for attaining the highest possible levels of nuclear safety, nuclear safeguards, nuclear security and all other

---

[*] The present paper describes an investigation that is initiated by the author. It does not necessarily represent the policy of the Egyptian Government or the Atomic Energy Authority of Egypt.

effective parameters of the nuclear field. Also, it is necessary to ensure independent and efficient regulation of the nuclear industry in the country, and the development of NP programmes for electricity generation, sea-water desalination and other peaceful uses of atomic energy. Therefore, the concerned government of a State -as well as the population at large- could be assured that the nuclear activities in the country are safe and consistent with both the national and international standards while satisfying its national interests and needs[3-4].

It seems very important that specialized science and technology support services would be considered as main factors for safe, secure and peaceful nuclear energy. This would include the development of highly specialized human resources [HR] and knowledge management systems for both the concerned "State" regulatory organizations and the operating organizations. The technology and science organization(s) [TSO(s)] that can supply such services could be designed as an integral part of the national regulatory system in a State or could be a separate organization according to its policies. In this respect, the roles, functions and quality of the scientific and technical expertise -that could be provided by the proposed centre to support the launching of a nuclear power programme, to promote the tasks of the national nuclear regulatory systems and the nuclear industry would be of fundamental importance[5-7].

In the present study, a proposed TSO is developed as a "Separate" Science and Technology Centre or "Institute". It is designed as "Official" and "Neutral", for providing scientific and technical basis for decisions regarding the safety and security of nuclear activities and concerning the use of nuclear materials [NMs] and other radioactive materials [RMs] as well.

DEVELOPMENT OF A SUPPORT ORGANIZATION

1. TSO Roles and Functions

As a matter of fact, scientific research and development [R&D] work played a vital role in launching nuclear power programmes in the world. It is known that no developed or developing country has ever initiated a nuclear power programme without first having established a nuclear R&D organization. Successful technology transfer requires the existence and participation of national R&D as part of the national infrastructure. The effective introduction of nuclear technology into a country has usually been accomplished -at least partly- through nuclear research institutes and/or research centres as an initial step towards establishing a nuclear power programme. Such institutes -not only- provided education in and adaptation of nuclear science and technology, but also promoted the formation of an overall scientific and technological infrastructure within the country and offering a supporting role and performing "Applied" R&D work in nuclear power generation. A national nuclear power plant [NPP] programme for electricity generation may be represented as shown in Fig. 1.[5-7].

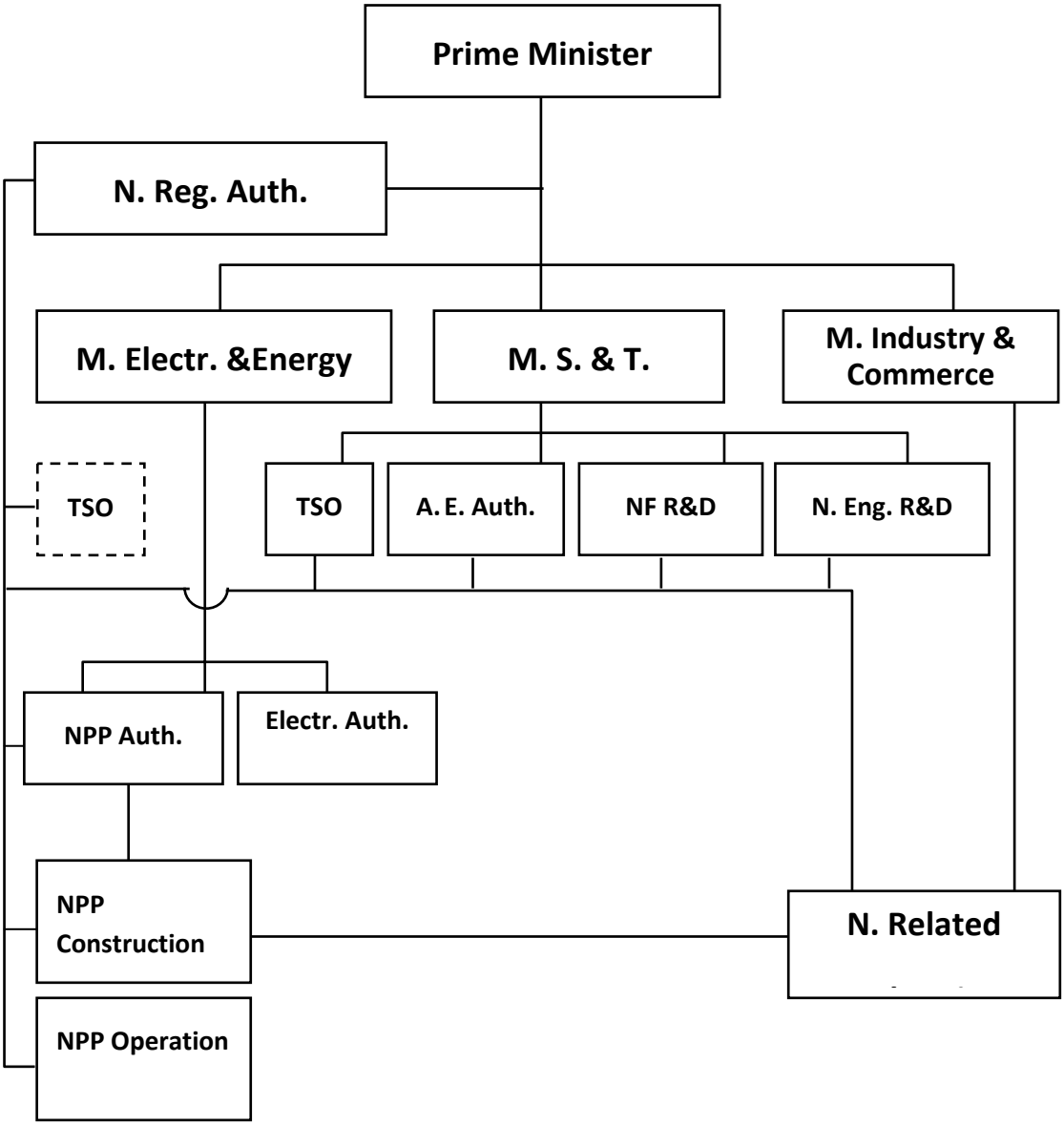

Figure 1. A proposed example of an organization diagram including a TSO for a nuclear power programme for electricity generation.

NB:

M.	Ministry	Auth.	Authority
N.	Nuclear	A.	Atomic
Electr.	Electricity	E.	Energy
S.	Science	O.	Organization

The process of establishing and/or developing a highly specialized TSO is designed to satisfy the needs for launching a nuclear power programme in a developing country with a relatively high economic growth rate. It would be essential to consider incorporating advanced R&D work in the fields of the main nuclear safety pillars (and other related fields). Namely, these are the nuclear engineering safety, radiation protection, environmental radiation protection, nuclear safeguards [SG], physical protection [PP] of NMs and

installations under the umbrella of the national nuclear security regime of the concerned State; and the radiation monitoring. The roles and functional structure of the proposed TSO is shown in Fig. 2.[5-10].

Also, it would be necessary to investigate innovative concepts, approaches and measures in the direction of enhancing nuclear safety, in parallel with the ongoing national and/or international technological innovations in nuclear power generation while attaining the ultimate goal of achieving sustained global nuclear safety and security[7-10].

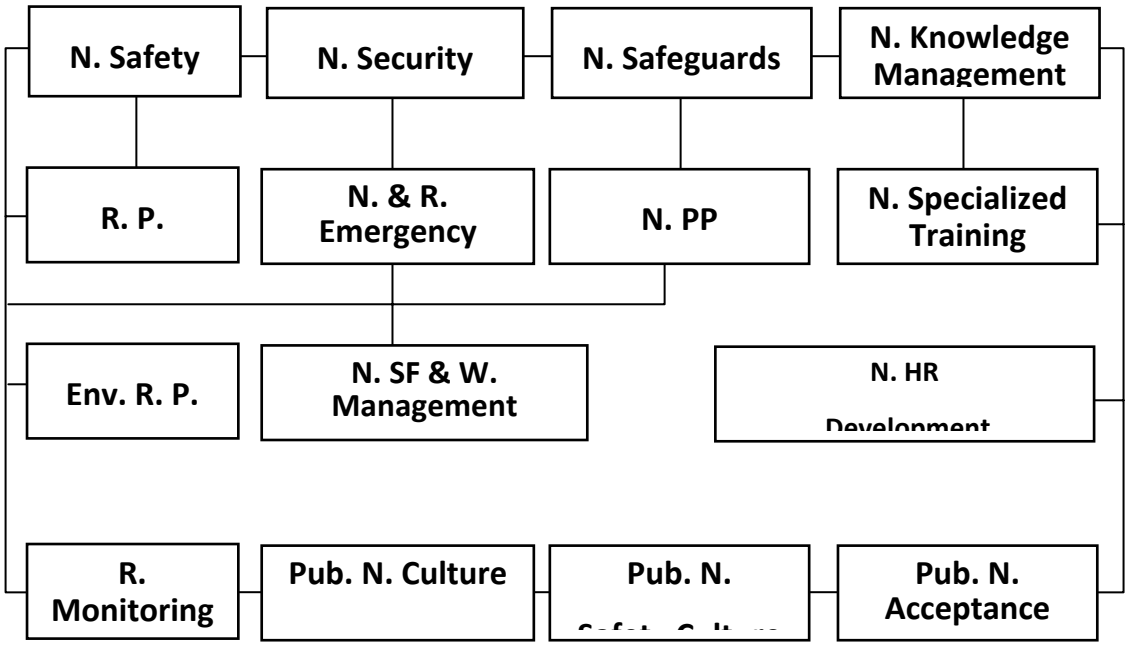

Figure 2. Schematic representation of the functional structure of a proposed Science and Technology Centre for supporting the launching of a nuclear power programme.

NB:

N.	Nuclear	SG	Nuclear Safeguards
R.	Radiation	PP	Physical Protection
P.	Protection	Pub.	Public
Env.	Environmental	W.	Waste
SF	Spent Fuel	HR	Human Resources
WF	Work Force		

2. Specialized Laboratories

Establishment and development of specialized scientific laboratories, e.g., for Destructive Assay Techniques "DA" and Non-destructive Assay Techniques "NDA", Quality Assurance Techniques "QA",…etc, for advanced nuclear measurements and methods are of great importance for precise verification and measurernent of NMs, processes, operations,...etc, for calibration techniques of nuclear instruments and for performing R&D work in the fields of the nuclear safety pillars (item 2.1.). At a certain stage, upgrading of provisions of one of such laboratories could approach higher levels as of a "Reference Laboratory" at the national or regional scale (e.g., for environmental radiation measurements, NMs,… trace analysis,… etc)[10-11].

EXTENDED SUPPORT

1. Knowledge Management

The expected growth in the nuclear field represents a great challenge -especially- for developing countries which are in hard need of acquiring advanced nuclear knowledge and technology as well. Each State should have its own national strategy for development. In practice, the implementation of such a strategy would need the collective efforts of specialized and efficient HR for implementing the different phases of the nuclear projects[5,6,12].

Some of the most important parameters that may contribute in the national development of a country are the advanced science and technology institutions, knowledge management, national education system, the highly specialized learning and training institutions, R&D centres and laboratories where information aquiring and knowledge transfer are fundamental tools for improving the HR in the nuclear field and for ensuring the continuity of the work force [WF]. Moreover, an important task of national interest is to enhance the safety culture related to the peaceful applications of nuclear energy for public awareness and public nuclear acceptance[5,6,12].

2. Workforce Development

The planned introduction and expected growth of nuclear power in a country will have to reflect the needed size and qualification of nuclear WF [NWF] for the operating organizations and the staff of the national nuclear regulatory body as well. Sufficient qualified WF should be provided in propper time to carry out the functions in such a manner to attain the goal with credible assurance of the quality of work. At the earliest stages, use of outside (or foreign) experts may be made to assist in the performance of the functions. But it is essential to aim at developing the national competence in as many technical areas as possible[5,6,12].

An important role of the proposed TSO is to participate in NWF development, e.g., by offering specialized courses, seminars, on-the job practical training in laboratories,...etc. Also, an equally important task for the TSO would be achieved by implementing a continuous training regime for the NWF to ensure establishing the continuity of the first generation,

maintaining of the second generation of nuclear specialists/experts and for preparing NWF replacement in proper time[6,12].

The TSO -acting as an information gathering/distribution centre for nuclear science and technology- could also offer an essential role in knowledge transfer for the NWF and HR in the national industries that are related to nuclear activities. This would aim at enhancing the national participation in the NP programme[6,12].

CONCLUSION

The launching of a national nuclear power programme –in a developing country with a relatively high economic growth rate- for electricity generation and sea-water desalination is a greet step forward in the direction of national sustained development.

The proposed establishment and/or development of the roles and functions of a national "Science and Technology Centre" or "Institute" is strongly recommended in the present investigation for offering specialized support services to the nuclear power programme for ensuring safe, secure and peaceful nuclear energy.

It may be concluded that the proposed centre would be designed as an Official Separate and Neutral Science and Technology R&D centre. Its main roles and functions are directed towards providing highly specialized scientific and technical basis for decisions concerning the nuclear activities and the proper use of nuclear materials and other radioactive materials. Such high quality R&D centre specialized in nuclear safety, safeguards and security; and all other effective parameters of the nuclear field would be extremely important in supporting the nuclear power programme with advanced services, concepts and systems. Also, it would be of effective help in finding solutions to the national nuclear regulatory systems and the national nuclear related industry as well.

ACKNOWLEDGEMENT

The author expresses his thanks and gratitude to the Egyptian Nuclear and Radiological Regulatory Authority for supporting the publishing of the present paper.

REFERENCES

(1) IAEA, International Data File; "Nuclear Share of Electricity generation, IAEA Bulletin, No. 39/2, Vienna-Austria (1997).
(2) IAEA, Sustainable Development and Nuclear Power, IAEA Publication IAEA/P1/55E, Vienna-Austria (1997).
(3) EL-BARADEl, M., Nuclear Power Changing Picture, IAEA Bulletin No 49/1, pp 18-21, Vienna-Austria (2007).
(4) WANG, J. L. and HANSEN, C. J., Revising Nuclear Renaissance, IAEA Bulletin No. 49/1, pp 22-23, Vienna-Austria (2007).
(5) BADAWY, I., Transferring Nuclear Knowledge; An International Partnership, International Conf. on Knowledge Management in Nuclear Facilities, IAEA-153, I/P10, [Extended Synopsis] Vienna-Austria (2007) & Egyptian Atomic Energy Authority,

External Report, No. ARE- AEA/Rep. 480, Cairo-Egypt (2008).
(6) IAEA, Manpower Development for Nuclear Power; a Guide, IAEA Technical Report Series No. 200, JAEA/STI/DOC/10/200, Vienna-Austria (1980).
(7) BADAWY, I., Nuclear Safety Pillars in Nuclear Power Plants; Concepts and Technology, Proc. Al-Azhar Eng. Tenth International Conf. [AEIC 2008] Cairo-Egypt, 24-26 (2008), publ. in Al-Azhar Univ. Eng. Journal "JADES, Special Issue, Vol. 3, No. 12, pp 228-237, Dec. 2008.
(8) TANIGUCHI, T and NILSSON, A., Hot Spot - Weak Links; Strengthening Nuclear Security in a Changing World, IAEA Bulletin, 46/1, pp 57-61, Vienna-Austria (2004).
(9) BADAWY, I., An Integrated Approach for Securing a Nuclear Power Plant for Electricity Generation, International Symposium on Nuclear Security, IAEA-CN-166, Session 8/062, Vienna-Austria (2009) [To be Published].
(10) BADAWY, I., ETAL., A Real Time System of Accounting and Control of Nuclear Materials and Radioactive Sources, IAEA Symp. on International Safeguards; IAEA-CN-148/145P, Vienna-Austria (2006).
(11) IAEA, Safeguards Techniques and Equipment, IAEA International Nuclear Verification, Series No. 1 (Revised), IAEA, Vienna-Austria (2003).
(12) IAEA, Managing Human Resources in the Nuclear Power Industry: Lessons Learned, IAEA/TECDOC Series No.1364, Vienna-Austria (2003).

"Education and training in radiological protection for diagnostic and interventional procedures" ICRP 113 in brief

S. Salama[(1)], Jamal H. Alshoufi[(2)] and M. A. Gomaa[(1)]
[(1)] *Egyptian Atomic Energy Authority, Cairo Egypt* - [(2)] *Syria-Damas*
topazgemss@yahoo.com

ABSTRACT

The international commission on radiological protection (ICRP) is the primary body in protection against ionizing radiation. Among its latest publication is ICRP publication 113 "education and training in radiological protection for diagnostic and interventional procedures". This document introduces diagnostic and interventional medical procedures using ionizing radiations in deep details. The document is approved by the commission in October 2010 and translated into Arabic at December 2011. This work is a continuation of the efforts series to translate some of the most important of the radiological protection references into the Arabic; aiming to maximize the benefit. The previous translation include "WHO handbook on indoor radon: a public health perspective, issued by world health organization 2009" and "Radiation Protection in Medicine, ICRP Publication 105 2007 that translated into Arabic with support of Arab atomic energy authority at 2011.

ICRP -113 text

The ICRP-113 text is composed of abstract, guest editorial, preface, executive summary, six chapters. ICRP Publication 113 includes four. The publication is summarized to provide the experience gained.

ICRP-113 executive summary

This guide is assumed to be considered by who related to medical field by education, training and/or diagnosis and treatment with radiation as the regulators, health authorities, medical institutions, professional bodies, medical industry beside to universities and other academic institutions.

It is a comprehensive approach to education and training in the field of radiation protection in medicine including the proposed content, objectives to be achieved, the required management, and the proposed time to train the medical professionals. The guide does not contain specific materials for training, but it includes detailed data of web sites that present. The responsibilities of authorities that perform RP are cleared. The training must be subject to the supervision and follow-up. The number of medical procedures and diagnostic interventional use ionizing radiation are rise continuously. The current procedures become routinely and repetitive hence, increase radiation doses of patients and staff.

The guide Provide the necessary instructions on education and training of radiation protection program that should be used by:

A. Regulatory bodies, health authorities, medical institutions and professional.
B. Industries which produces and markets equipment used in these procedures.
C. Finally, universities and other academic institutions responsible for the education of professionals involved in the use of ionizing radiation in the field of health care.

The term "education" refers to the transfer of knowledge while the "training" term refers to the necessity to provide instructions and guidance on the knowledge of radiation protection; in order to justify the medical radiation exposures and optimize the applied procedures. This is most importance in specific applications result in high radiation exposures (e.g. computed tomography, fluoroscopy). Thus, the participants should have the ability to develop the performance of the medical practice.

This guide provided advice on accreditation and certification of the recommended education and training. The "accreditation" means that an organization has been approved by an authorized body to provide education or training on the radiological protection aspects of the use of diagnostic or interventional radiation procedures in medicine. In order to give permission it must meet the standards set by the competent authority. The term "certification" means that an individual medical or clinical professional has successfully completed the education or training provided by an accredited organization for the diagnostic or interventional procedures to be practiced. There are two major problems on the RP; the lack of consensus views of experts on the topics met the RP requirements and the appropriate time for this training.

ICRP-113 chapters

1. Training requirements for healthcare professionals

Training objectives should be achieved. The medical exposure must be justified. The medical profession should understand the radiation hazards to avoid. Lack of knowledge may result in more ionizing radiation. The physician or other regulated healthcare practitioner providing the justification for the applied exposure, should be aware of the risks / benefits of the procedures involved. Education in RP needs to be given to medical referrers, after that transfer Knowledge and experience for him.

Medical and other healthcare professionals involved more directly in the use of ionizing radiation should receive education and training in RP at the start of their career and this program should continue. The deterministic effects on the skin need to be avoided. Special training in RP must give to interventional cardiologists.

Medical physicists working in RP, nuclear medicine and diagnostic radiology should receive the highest level of RP training with certification.

Knowledge of the risks and precautions is required to minimize the exposure of healthcare professionals, professionals assisting in fluoroscopic procedures, maintenance engineers, applications specialists and nurses.

2. RP training and courses for non-radiation specialists

There are essential requirements for RP courses should be satisfied. Medical professionals are perceived. Training activities should be evaluate and analyze. Examination systems are performed to test competency. The certificate should be obtained before a professional is involved in practicing. Follow-up will occurred to maintain the accreditation of organizations providing training.

There are different RP to correspond with different categories of medical and clinical staff. The training material must be relevant. The practice optimization should be cleared. The training is depending on the involvement of the different professionals in medical exposures. Practical training should be done in an environment similar to that the participants will be practice. Adequate resources of a training program should take account of all aspects involved at the present and at the future.

With respect to lecturers and trainers they should be experts in the RP practice, by official certification. Training team should involve radiological professionals in related topics. Trainers must have sufficient knowledge of the procedures performed by the medical specialists. Evaluation systems online is necessary to develop.

Continuing education is enabling development of the professional skills at the practice. Computer-based tools are good for this type of education. RP training should be updated at least each 3 years and at unregularly time if there is a significant change in radiology technique or radiation risk.

.

3. Responsibilities for training provision

It must be specify certain roles of different organizations. RP should be promoted by; the regulatory and health authorities, professional bodies and scientific societies. Hence, Universities have main role. Education and training at medical schools should be updated and evaluated to satisfy RP requirements. For the relevant regulatory and health authorities they must strength the defects of the training and issue the official certificates. Minimum aspects of optimization and practical RP need to be given for the medical staff. The professional bodies and scientific societies should enforce the program and encourage the lectures. Finally, equipment manufacturers have a responsibility to develop and make available appropriate tools, ensure that maintenance engineers and should give a good training for new technologies.

Chapter (1): ICRP-13 -Introduction

The number of medical procedures and diagnostic interventional that use ionizing radiation are in steady increase recently. The patients are receiving higher doses now. So, there are an urgent need for reviewing the education of medical staff, the topics of the RP and study the ways to apply.

1.1. Need for a greater awareness of radiological protection

Some people are exposed in diagnostic and interventional medical procedures. The doses are high. Radiation doses to patients need to be optimized to prevent the deterministic effects. Medical radiation procedures must justify. The procedures benefits / risks must be analyzed. The shortages of the medical staff in RP need to be avoided. This report provides recommendations and sets out guidance that should be considered. The courses need to perceive. The program time is strictly limited. This will allow individuals be persuaded of the attending advantages. Some information material of the training should be published on the internet.

1.2. Education and training in radiological protection

It is appropriate to include basic RP education in medical and dental degrees. The definition of a referrer is a medical doctor, dentist, or other health professional who is entitled

to refer individuals for medical exposures to a practitioner, in accordance with national requirements. The justification should confirmed by a radiation specialist.
Professionals should receive education and training in RP throughout their professional life. Medical physicists, radiographers and radiologists should work closely. The radiological equipment manufacturers have an important role for optimization. They have a responsibility to aware the users of the dosimetric implemented in the procedures, to inform them about the proper application, to make available appropriate tools that are built into radiological equipment and to facilitate easy determination and recording of exposure with reasonable accuracy.

1.3. Knowledge that radiological protection education and training should provide

There are potential health effects from radiation exposure. Avoiding deterministic effects and minimizing the probability of stochastic effects is the main purpose. Deterministic effects are occurred if the radiation dose is above a certain threshold while stochastic effects increase proportionally with the dose.

There is potential for radiation effects in the embryo/fetus. Possible damage to the developing central nervous system may occur, particularly from the 8^{th} week to the 15^{th} after conception and to a lesser extent at (16^{th} - 25^{th}) week. These deterministic effects have relatively high threshold radiation doses (>100 mSv) and should not occur for optimized diagnostic procedures. With regard to stochastic effects, there is an increase in the probability of leukemia and other cancers that may occur later in childhood from irradiation during all stages of fetal development. Stochastic effects cannot be eliminated totally but could be reduced. Management ensures the optimization of RP. The authors introduce examples of the need to manage radiation dose with some details for pregnant patients, interventional procedures, CT procedures, digital radiology procedures and doses to operators.

1.4. Recommendations in ICRP Publications 103 and 105

The objective is to increase the proficiency of medical professionals in managing patient and staff. The radiation doses are commensurate with the clinical task as recommended in (103 and 105) publication. Publication 103 ensured that the final responsibility for the medical exposure of patients lies with the physician. Publication 105 cleared RP training requirements for the medical staff, due to his responsibilities.

1.5. Training in interpretation of images

The medical exposure must be justified. An interpretation of the radiation images is a key of justification.

Chapter (2): Healthcare professionals to be trained

Physicians need to evaluate the risks to benefits when requesting medical exposures. More attention must be taken when dealing with pregnant patients.

2.1. Consequences of failure to deliver training in radiological protection

The medical are necessary to understand the hazards to avoid any unnecessary risks. The lack of knowledge may lead to pregnant women not receiving enough medical care. It is necessary to optimize the procedures. Techniques used should be developed to help in optimization. Digital radiology, as an example, has the potential to reduce patient doses, if used by an expert. The need for medical doctors employing fluoroscopically-guided procedures to be both trained and certified for this practice is very important to avoid unnecessary exposures.

2.2. Categories of healthcare professionals requiring education and training

In order to facilitate specification of the RP training required by different medical and healthcare professionals, categories that cover the majority of those involved are seventeen; radiologists, nuclear medicine specialists, cardiologists and interventionists from other specialties, other medical specialists using x rays, other medical specialties using nuclear medicine, other physicians who assist with radiation procedures, dentists, medical referrers, medical physicists, radiographers, maintenance engineers and clinical applications specialists, other healthcare professionals, nurses, dental care professionals, chiropractors, radio pharmacists and radionuclide laboratory staff and finally the regulators.

2.3. Training for healthcare professionals

2.3.1. Medical professionals involved directly with the use of radiation

The training and certification in RP of diagnostic radiologists and nuclear medicine specialists is involve (30–50) h. ICRP proposed a second level of RP training for interventional radiologists and cardiologists. It is considers that provision of more RP training for interventional cardiologists and those directing cardiac CT. Less training is given to other medical specialists such as vascular surgeons, urologists, endoscopists, and orthopedics surgeons before they direct fluoroscopically-guided invasive techniques. Occupational health doctors who review dose and health records of radiation workers and other medical specialties who are closely involved with the operators, such as anaesthetists, will require training on the basic aspects of RP.

2.3.2. Medical prescribing diagnostic exposures and medical students

The medical professionals who refer for diagnostic examinations and procedures need to pass a certain level of education in RP. Referrers need to be familiar with imaging and referral criteria. Education on the fundamentals of diagnostic techniques with ionizing radiation should integrate in the medical degree. Other healthcare professionals need to recognize some instruction in radiation hazards

2.3.3. Other healthcare professionals

Training for healthcare professionals in RP will be related to their specific jobs and roles. Radiographers, nuclear medicine technologists and x-ray technologists need substantial training in RP. Maintenance engineers understand how the settings of the x-ray systems and adjustments that they may make influence the radiation doses to patients. Nurses and healthcare assisting in fluoroscopic procedures require knowledge.

Chapter (3): Priorities in topics to be included in training

This chapter focuses on topics of education and training should be included in RP, depend on the role of the physician or healthcare professional.

Objectives of training must be cleared. The optimization is a key in the success of RP. High doses may increase leading to incidence and mortality while doses (<0.1 Sv) is low in risk. The risk of death in the daily practice of clinical medicine is higher than that may came from a diagnostic or interventional radiation procedure. The danger of stochastic phenomena is third-order concern. Ignorance of real consequences for radiation exposure leads to the risk. Trainees must ensure the optimization of RP is correct in procedures and intervention, both logically and ethically. Table (3.1.and 3.2.) gives recommended radiological protection training requirements for different categories of physicians and dentists. There are different

levels for different categories. Training requirements are vary depending on the roles of individuals. The medical applications should be linked and update.

The practical application of RP, accidental procedures and unintended doses to patients should be included and number of hours to be considered. Medical physicists should know the training areas at the highest level in the RP and in QA, developments in techniques, equipment and legislative requirements. The components of the course should be adapted to achieve the objectives. The practical exercises of the training course should be in the range (20–40%) of the total time or higher.

Chapter (4): Training opportunities and suggested methodologies

This chapter provides recommendations on training for a selection of staff categories and discusses developing.

Training programs need to be devised in formal education and examination system to test competency. The physicians have a significant role to play in the justification and optimization. Training on RP of patients needs to be expanded, particularly in digital radiology and new equipment. Radionuclide laboratory workers should not be confused with other categories. Staff from regulatory authorities should be senior medical physicists or equivalent.

Delivery of training is important. The objective of any training is to acquire knowledge and skills. Practical training should be given in a similar environment to that the participants will be practicing. Training should be provided by a professional team. Each trainer should be an expert in his practice. He should be aware about national legislation, responsibilities of individuals and organizations and have a clear perception about the practicalities in the work that the training has to cover.

There is not reference amount of training till now. This guide gives just recommendations. Pre and post-training evaluations are recommended; theoretically and practically. Self assessment examination systems need to be encouraged to become more helpful, to confirm successful the training completion and hence, to allow the accreditation via several evaluation methods. The type of radiation work undertaken, level of the risk, frequency of the procedure and the probability of occurrence of over-exposures to the patient or to staff need to be considered. The practice of interventional cardiology must be performed carefully; du to it is involving high localized radiation doses to patients; may induce skin injuries.

Chapter (5): Certification of training

The accreditation of organizations and advice on the certification of individuals are the main topic of this chapter. Criteria for accreditation must be studied in details. Feedback from participants could rise from surveys of participant responses at the end of training activities as global. Software is a good and fast method. Accredited bodies should also be registered. The certificates of the diplomas should include the basic details. The certification of RP should be limited in time and renewal because the other details are changeable.

Various organizations have an important role in radiological protection training as universities, training institutions and scientific societies. Their courses on RP are attractive for medical staff. Regulatory and health authorities have the capability to enforce some levels of RP training and to maintain a register of the certified professionals. Some international organizations give recommendations on; the content, number of hours, criteria for accreditation, certification and offer the training material on their websites. The radiology

industry has a role to play in RP training for the new technologies to promote the advances in RP to alert operators of the new modalities that impact on patient doses.

Financing of training must be fully studied by organizations. The infrastructure availability and the financial requirements have to be taken into account. The co-operation of international organizations could be helpful to initiate the activities and provision of training materials. If certification in RP is required for practices it must be obtained before starting share in the practice. The healthcare providers need to provide the resources available to train their own professionals in RP.

Annex a. Examples of suggested content for training Courses

(A.1) is represents nuclear medicine that cleared in categories 2 at (table 3.1) and 10 (table 3.2). The following subjects should be included in training and education regarding optimization of RP while administering radiopharmaceuticals to patients for diagnostic purposes. (A.1) include (3) items; that are: additional radiological protection aspects for therapeutic nuclear medicine procedures, protection of personnel working in nuclear medicine and radiological protection for personnel working in PET/CT.

(A.2) is represents interventional radiology that cleared in categories 1 at (table 3.1). It is related with those working in interventional radiology as: X-ray systems for interventional radiology, dosimetric quantities specific for interventional radiology, radiological risks in interventional radiology, radiological protection of staff in interventional radiology, radiological protection of patients in interventional radiology, quality assurance in interventional radiology and optimization of the procedures with regard to radiation dose in interventional radiology.

(A.3) is represents interventional cardiology that cleared in category 3 at (table 3.1). (A.3) is related with those working in interventional cardiology and should have the knowledge to do the following; X-ray systems for interventional cardiology, dosimetric quantities specific for interventional cardiology, radiological risks in interventional cardiology, radiological protection of staff in interventional cardiology, radiological protection of patients in interventional cardiology, quality assurance in interventional cardiology and optimization of the procedures in interventional cardiology.

(A.4) is represents interventional cardiology that cleared in categories 4 at (table 3.1) and 12 at (table 3.2). (A.4) is connected to that theatre fluoroscopy using mobile equipment at X-ray systems, radiological protection of staff and radiological protection of patients.

Annex b. Outline of specific educational objectives for paediatric radiology that are: General, equipment, and installation considerations, Reduction of exposure, Risk factors, Patient dosimetry: diagnostic reference levels, Protection of personnel and parents, International recommendations and Nuclear medicine considerations.

Annex (c) gives examples of some sources of training material while annex (d) introduce references containing information of interest for the present report.

Finally, efforts to translate international documents into Arabic are wider day after day to implicit: role of UN organizations (UNSCEAR, IAEA, WHO), role of IOMP branches (ICRP-105), role of AAEA, ICRP-105 and ICRP-113 and role of individual efforts (SS-9, SS-6, that performed with Gomaa translations).

CONCLUSION

ICRP-113 should be published among who is interested in diagnoses and treatment of radiation. It is recommended to translate the guide into different languages; aiming to maximize the value.

REFERENCES

1. Annals of the ICRP, ICRP 113, education and training in radiological protection for diagnostic and interventional procedures, Elsevier, Ann. ICRP 39 (5), 2009.
2. Annals of the ICRP, ICRP publication105, Radiological Protection in Medicine (in Arabic),Arab Authority for Atomic EnergyTunisia, 2011.
3. WHO handbook on indoor radon, a public health perspective, the world health organization, France, 2009.
4. IAEA, International Atomic Energy Agency
5. UNSCEAR, The United Nations Scientific Committee on the Effects of Atomic Radiation
    1. SS-9
    2. SS-6

Legal Elements For Nuclear Security: Egyptian Nuclear Law As A Case Study

A. M. Ali
Nuclear Law Dept. Nuclear and Radiation Regulatory Authority(NRRA).Cairo .Egypt.
adel_m_ali@yahoo.com

ABSTRACT

This paper deals with the legal bases for nuclear security. First, It analysis the international legal framework for nuclear security. Second, it analysis the legal bases for the import–export control. The legal aspects related with illicit trafficking (IT) were also reviewed. Third, It deals with the Egyptian nuclear law no. 7 and its executive regulation. The Egyptian legal regime for nuclear security and the role of State System for Accounting and Control of Nuclear Materials (SSAC) in realizing the nuclear security were also discussed. The purpose of the paper is to evaluate the Egyptian legal framework for nuclear security.

Key Words: *nuclear security, Nuclear law, Egyptian nuclear law*

INTRODUCTION

The term 'nuclear security' is generally accepted to mean "the prevention and detection of, and response to, theft, sabotage, unauthorized access, illegal transfer or other malicious acts involving nuclear material, other radioactive substances or their associated facilities." ([1]) The State responsibility is to establish and maintain legislative and regulatory framework for nuclear security, define what the nuclear security and establish or designate a competent authority responsible to implement and control framework for nuclear security ([2]). The operators' responsibility is to implement and enforce the laws and regulations, establish guidance documents implementing security requirements of national laws and regulations relevant to their specific activities, establish and implement security plans and procedures based on the national laws and regulations. There is a new international nuclear security framework is emerging ([3]) based on obligations contained in the Convention on the Physical Protection of Nuclear Material (CPPNM) and its Amendment, the International Convention for the Suppression of Acts of Nuclear Terrorism, the relevant Security Council resolutions and the non-binding Code of Conduct for the Safety and Security of Sources and its supplementary Guidance ([4]).

PART I : THE INTERNATIONAL LEGAL FRAMEWORK FOR NUCLEAR SECURITY

The international legal framework for nuclear security consists of many treaties in particular, the Convention on the Physical Protection of Nuclear Material (CPPNM) and the 2005 Amendment there to, the Convention on Early Notification in the Event of a Nuclear Accident, the Convention on Assistance in the Case of a Nuclear Accident or Radiological Emergency, and the International Convention for the Suppression of Acts of Nuclear Terrorism that concluded under the auspices of the United Nations. Non-binding legal

instruments also promulgated under IAEA auspices, including the Nuclear Security Recommendations on Physical Protection of Nuclear Material and Nuclear Facilities (INFCIRC/225/Revision 5) and the Code of Conduct on the Safety and Security of Radioactive Sources([5])

FIRST: THE LEGALLY BINDING INTERNATIONAL INSTRUMENTS

Over the past three decades a number of international instruments have been developed both to help strengthen physical protection in individual States and to encourage greater consistency in requirements and procedures among States in this important area.

1- CONVENTION ON THE PHYSICAL PROTECTION OF NUCLEAR MATERIAL (CPPNM)

The most important legal instrument is the CPPNM of 26 October 1979 and adopted on 3 March 1980. In force since February 1987 till August 2012, the CPPNM has 145 parties and 45 signatories. The CPPNM sets forth a range of measures to ensure the protection of nuclear material (basically, enriched uranium and plutonium), primarily in international transport. However, the Convention also contains important provisions covering the domestic use of these materials. The CPPNM focuses primarily on nuclear material being shipped in international commerce, but it also contains other important requirements related to domestic physical security measures. In summary, the CPPNM requires Parties to:

(a) Make certain physical protection arrangements and ensure specific defined levels of physical protection for international shipments of nuclear material;

(b) Co-operate in the recovery and subsequent protection of stolen nuclear material;

(c) Make specified acts (e.g. thefts of nuclear material and threats or attempts to use nuclear material to harm the public) punishable offences under national law;

(d) Prosecute or extradite those accused of committing such acts.

1.1. REQUIREMENTS FOR PPNM

General requirements for PPNM may be listed as follow:

1- Physical protection measures can be implemented by the State itself, by an authorized person (e.g. the operator) or by any other entities authorized by the State

2- The State (through the regulatory body or otherwise) should verify continued compliance with physical protection requirements through periodic inspections and other monitoring procedures.

3- The designated authority should be provided adequate authority to enforce physical security requirements.

4- Essential for an effective physical protection system is the establishment by legislation of a well designed and well supported State system for recording and monitoring the quantities and locations of the nuclear material under the State's jurisdiction or control.

5- Legislation should contain provisions requiring the development and implementation of emergency plans for responding to the unauthorized removal and subsequent unauthorized use of nuclear material, the sabotage of nuclear facilities and attempts to perpetrate such acts.

6- Protecting the confidentiality of information whose unauthorized disclosure could compromise the physical protection of nuclear material and nuclear facilities(PPNMF) ([6]).

1.2.REQUIREMENTS FOR PROTECTION OF NUCLEAR MATERIAL AT THE SHIPPING

1-taking into account the category of nuclear material and its location use, storage and during transport.
2-Whether the weather conditions prevailing in the country or on the road transport.
3 -When you consider the necessary measures to provide physical protection of nuclear material against theft or other, the State must take into account the natural self-protection of radioactive materials.
4-The physical protection requirements set on the concept of defense in depth to be prevention and protection measures for each facility which handled a nuclear materials.
5- An assessment of the likelihood of sabotage to the means of transport.
6-To ensure that the shipping arrangements in accordance with international regulations for both the receiving State or other States that the shipments will pass([7]).

The CPPNM has been promoting during 2005, within the framework of the Conference which the States parties agreed on the amendment, so as to provide further protection of nuclear facilities and materials during use, storage and transport within the State for peaceful purposes. The amendment also provides to expand the scope of cooperation between States on the identification of nuclear materials stolen or smuggled and recovery, and mitigation of any radiological consequences would result from acts of sabotages, as well as related crime prevention and combat it. CPPNM Amendment was adopted on 8 July 2005. As August 2012, the CPPNM Amendment had been formally approved by only 48 states and has not yet entered into force. Under the convention's amendment provision in Article 20 (2), the Amendment will enter into force only after two thirds of the parties have formally approved. With its current large membership of 145 states parties, the CPPNM therefore requires 95 States to approve the Amendment. Given that it has taken some five years for only about a third of the necessary States to approve the Amendment, considerable delay in implementing this important instrument seems likely([8]).

The national legislation, in the area of Nuclear Security, should contain provisions realizing the nuclear security and provide for protecting the confidentiality of information. It also should set forth the regulatory functions essential for protecting public health, safety and the environment. A fundamental element of an acceptable national framework for the development of nuclear energy is the creation or maintenance of a regulatory body with the legal powers and technical competence necessary in order to ensure that operators of nuclear facilities and users of nuclear material and ionizing radiation operate and use them safely and securely.

2- INTERNATIONAL CONVENTION FOR THE SUPPRESSION OF ACTS OF NUCLEAR TERRORISM ([9])

In April 2005, the General Assembly approved to the International Convention for the Suppression of Acts of Nuclear Terrorism. It deals in detail the crimes relating to possession and use of radioactive material or a radioactive devices and nuclear facilities or destruction of the illegal and deliberate([10]).

The Nuclear Terrorism Convention has a broader scope than the CPPNM and the Amendment thereto as follow:

1.It criminalizes acts involving 'radioactive material', which includes not only nuclear material, but also other radioactive material, as defined by the Convention.
2.It also brings under its scope, nuclear material and facilities used or retained for military purposes, which are explicitly excluded from the scope of the CPPNM and of its 2005 Amendment.
3.States Parties are obliged to establish their jurisdiction and to make the offences listed in Article 2 punishable under their domestic law.
4.States Parties are also obliged to cooperate and provide for mutual assistance, notably in relation to criminal investigations and extradition.

Article 7 States that parties are obliged to take appropriate measures in order to inform, where appropriate, international organizations in respect of the commission of offences set forth in Article 2 as well as preparations to commit such offences about which they have learned. Article 7.1 obliged the States Parties to inform the UN Secretary-General of their competent authorities and liaison points responsible for sending and receiving the information referred to in Article 7. The Secretary-General shall communicate such information regarding competent authorities and liaison points to all States Parties and the IAEA. Such authorities and liaison points must be accessible on a continuous basis. The States Parties according to article 7.4 shall make every effort to adopt appropriate measures to ensure the protection of radioactive material taking into account relevant IAEA recommendations and functions. The convention is primarily an international criminal law instrument that defines certain acts as criminal offences and obliges States Parties to establish their jurisdiction over such offences, to render them punishable under their domestic law.

3-THE CONVENTION ON EARLY NOTIFICATION OF A NUCLEAR ACCIDENT AND THE CONVENTION ON ASSISTANCE IN THE CASE OF A NUCLEAR ACCIDENT OR RADIOLOGICAL EMERGENCY

The Early Notification and Assistance Conventions were adopted immediately following the Chernobyl accident in 1986. The IAEA General Conference adopted the two Conventions at a special session on 26 September 1986. The Early Notification Convention entered into force on 27 October 1986 and the Assistance Convention entered into force on 26 February 1987, and each has now112 and 107 States Parties. While conceived and adopted as safety instruments, the Early Notification and Assistance Conventions strengthen the international response to nuclear accidents or radiological emergencies, including a terrorist or other malicious act by, respectively, providing a mechanism for rapid information exchange and a mechanism for mutual assistance with a view to minimizing the consequences of such accidents or emergencies and protecting life, property and the environment against the effects of radioactive releases([11]).

4-UN SECURITY COUNCIL RESOLUTIONS ADOPTED UNDER CHAPTER VII Of The UN CHARTER

Day after the terrorist attacks on the United States of America on 9/11/ 2001, the Security Council of the United Nations unanimously adopted resolution No. (1373/2001) which states, inter provisions that all countries should criminalize assistance for terrorist activities, and refuse to provide financial support and safe resort for terrorists and exchange information on groups that are planning to launch terrorist attacks([12]). It also established at the same time the Counter-Terrorism Committee, which consists of 15 members to follow up the

implementation of the resolution. In an effort to revitalize the work of the Committee, the Security Council adopted Resolution No.1535 in 2004, that established the Executive Directorate of the Counter-Terrorism Committee to provide expert advice to the Committee in all areas covered by resolution 1373, and to facilitate the provision of technical assistance to the states, as well as closer cooperation and coordination within the United Nation organizations and among regional bodies and intergovernmental([13]).

Following a Security Council debate on weapons of mass destruction on 22 April 2004, and in connection with its continuous efforts to elaborate a comprehensive counter-terrorism regime, the Security Council unanimously adopted UNSCR 1540 (2004) on 28 April 2004 by which it decided that all States shall refrain from supporting by any means non-State actors that attempt to acquire, use or transfer nuclear, chemical or biological weapons and their delivery systems. Both UNSCR 1373 (2001) and UNSCR 1540 (2004) were adopted under Chapter VII of the UN Charter and are therefore binding on all States. In UNSCR 1887 (2009), the Security Council, among other things, reaffirmed resolution 1540 (2004) and the need for its full implementation ([14]).

SECOND: LEGALLY NON-BINDING INTERNATIONAL INSTRUMENTS

1. NUCLEAR SECURITY RECOMMENDATIONS ON PHYSICAL PROTECTION OF NUCLEAR MATERIAL AND NUCLEAR FACILITIES

Non-binding instruments concluded under the auspices of the IAEA such as Nuclear Security Recommendations on Physical Protection of Nuclear Material and Nuclear Facilities(INFCIRC/225/Revision 5). Following the publication in 1972 of Recommendations for the Physical Protection of Nuclear Material, these recommendations were revised by the IAEA and the revised version was published in 1975 as INFCIRC/225. These guidelines have published in 1972 before the conclusion of CPPNM, and included elements of the texts of the Convention. The document was revised in 1977, 1989, 1993, 1998 and 2010. INFCIRC/225/Revision 5 reflects the recommendations of the national experts to assist States in implementing a comprehensive physical protection regime in respect of nuclear facilities and nuclear material, including any obligations they may have under international agreements, such as the 2005 Amendment to the CPPNM.

The guidelines developed elements and protection requirements such as:

1 - Elements of a national system of physical protection and nuclear facilities.

2- Requirements for the Physical Protection of Nuclear Materials, used and stored, from unauthorized access.

3- Requirements for physical protection of nuclear facilities from sabotage and terrorist operations involving nuclear material being used, stored, and transported.

4 - Requirements for physical protection of nuclear material during the transport ([15]).

2- THE CODE OF CONDUCT ON THE SAFETY AND SECURITY OF RADIOACTIVE SOURCES AND THE SUPPLEMENTARY GUIDANCE ON THE IMPORT AND EXPORT OF RADIOACTIVE SOURCES ([16]).

The objectives of the Code and Guidance are, through the development, harmonization and implementation of national policies, laws and regulations, and through the fostering of international cooperation, to (i) achieve and maintain a high level of safety and security of radioactive sources; (ii) prevent unauthorized access or damage to, and loss, theft or

unauthorized transfer of such sources so as to reduce the likelihood of accidental harmful exposure to such sources or the malicious use of such sources to cause harm to individuals, society or the environment; and (iii) mitigate or minimize the radiological consequences of accidents or malicious acts involving a radioactive source.

The Code applies to all radioactive sources listed in Annex I that may pose a significant risk to individuals, society and the environment. The Code does not apply to nuclear material as defined in the CPPNM, except for sources incorporating plutonium-239. The Code does not apply to radioactive sources within military or defence programmes. The Guidance applies to the Category 1 and 2 sources within the scope of the Code. The Code establishes guidance for each State regarding the legislation and regulations that should be in place. It further recommends that the regulatory body be granted appropriate authority and resources, and sets out a number of functions that the regulatory body should have. The Code provides recommendations on the import and export of radioactive sources (supplemented by the Guidance).

PART II : IMPORT AND EXPORT CONTROLS OF NUCLEAR MATERIAL OR RADIOACTIVE SOURCES

Export and import controls play a central role in preventing the unauthorized acquisition of licensed material. It must be implemented within a State's general legal framework for regulating foreign commerce. A State's basic law for nuclear export and import controls should focus on a few important objectives such as to ensure that transfers of nuclear material, equipment and technology take place in a secure, safe and environmentally responsible manner and such transfers do not directly or indirectly using nuclear material for unauthorized purposes. National nuclear law should reflect the fact that sanctions for non-compliance should be commensurate with the seriousness of the non- compliance and should authorize a range of penalties

FIRST: THE IMPORTANCE OF EXPORT AND IMPORT CONTROLS

There is an importance of all state to issue a legal framework to control the export and import of the nuclear materials and equipments for many reasons as follows ([17]):

1- Nuclear export and import controls also support a State's fundamental regulatory task of preventing unauthorized persons in that State from acquiring material and technology that they are unable to manage safely and securely

2- It is providing a barrier against nuclear explosives development and nuclear terrorism,

3- Export and import controls are also necessary in order that a State may comply with its obligation under multilateral treaties and conventions such as the NPT, particularly under Article I (for nuclear weapon States) and Article II (for non-nuclear-weapon States), not to assist non-nuclear-weapon States in acquiring nuclear weapons or to seek or receive assistance in acquiring them([18]). Also, export controls are essential for meeting the NPT Article III.2 obligation not to provide source or special fissionable material, or equipment or material especially designed or prepared for the processing, use or production of source or special fissionable material to a non-nuclear-weapon State, even for peaceful purposes, unless the source or special fissionable material is subject to IAEA safeguards([19]). Parallel commitments and obligations are provided for in other treaties:

a)Article 4 of the CPPNM to permit exports and imports of material covered by the convention only after receiving assurances that the material will be protected at levels described in Annex I to the convention([20]).

b)Article 27 of the Joint Convention requires Contracting Parties to participate in the transboundary movement of covered material only when specified conditions are met([21]).

So, establishing an adequate legislative framework for nuclear export and import controls is important for all States. Even States that are neither exporters nor importers of nuclear material or technology need a basis for controlling any nuclear transfers through their territories([22]).

1. IMPORT, TRANSIT AND EXPORT OF RADIOACTIVE SOURCES

Many of radioactive sources are used in industry, agriculture and medicine. A large number of portable sealed sources, most of them of low activity, are used in industry and medicine; consequently, it is not surprising that, in spite of inventory keeping and controls, some sources are lost. The construction of most sealed sources is quite robust, so that accidents involving lost sources are usually due to human error. The regulatory body should control over the sources and determine which activities and which sources can be exempted from regulatory control. The national nuclear law should also contain provisions regulate and control the import, transit and export of radioactive sources. Categorizes 1 and 2 according to code of conduct is supplementary guidance on the import and export of radioactive sources. The legislation should identify and assign clear responsibilities to assure the safety and security of the radioactive sources. It should require the finders of such orphan sources to report them to the regulatory body and to assign to the regulatory body the responsibility to develop a national strategy for recovery orphan sources.

Each state intends to import or export of radioactive sources takes into account the following rules:

1- Not to approve on the import of radioactive material unless authorized for a recipient and the receipt the source under its national law, and the availability of technical and managerial capacity, resources and appropriate regulatory structure necessary for a secure disposal of radioactive sources in a secure way.
2- Not to approve the export of radioactive material unless it had a notification in advance that the receiving State is authorized to receipt and possession of source, and have available the technical capacity and appropriate administrative and supervisory resources and structure necessary for a secure disposal of radioactive sources in a secure way.
3- The state that authorized to the import or export of radioactive source, should take the appropriate steps to ensure that the import or export is in a manner consistent with international standards for the safe transport of radioactive materials, especially to maintain the continuity of control during the process of international transport([23])

2. THE BASIC REQUIREMENTS FOR THE ISSUANCE OF EXPORT OR IMPORT LICENSES

As with all other activities involving nuclear material and technology, a transfer of such commodities and information across national boundaries should be permitted only after the issuance of a license (or permit or other authorization) that clearly states the essential features of the transfer. These include: the identity of the licensee; the precise subject matter of the transfer (in terms of the types and quantities of material or the character of technology); the destination of the transfer; the end use or (if different from the destination) the end user of the

material; the duration of the license; and any relevant limitations or conditions (such as the mode of transport and the required physical protection measures).
The following are some typical requirements:
(a) That the receiving State have made a binding commitment to use transferred material and information for peaceful purposes only;
(b) That international safeguards be applied to the transferred item;
(c) That the receiving State place all its nuclear material and nuclear facilities under international safeguards (the full scope safeguards requirement);
(d) That retransfers of previously transferred material and technology to a third State be subject to a right of prior approval by the supplying State;
(e) That the levels of physical protection that will apply to the international transport of nuclear material be consistent with those given in Annex I to the CPPNM (Article 4 of the CPPNM);
(f) That, in the case of certain material, the State of destination have received prior notification of and have consented to the transfer such as the Joint Convention ([24]) in Article 27(1)(i);
(g) That, in the case of certain material, the State of destination have the administrative and technical capacity and the regulatory structure needed to manage the material in a safe and secure manner such as , Article 27(1)(iii) of the Joint Convention([25]).
(h)That transfers of certain material be not to the Antarctic region such as the Article 27(2) of the Joint Convention([26]) .

SECOND: NUCLEAR SECURITY AND THE ILLICIT TRAFFICKING

One of the most serious of threats is IT and nuclear terrorism([27]). Among the factors that have helped it appears are:
1- Some groups and political actors try to achieve its objectives independently and not through the existing institutions of power.
2- Increasing numbers of non-governmental organizations and the financial impact and potential of growing in international relations, such as terrorist groups and organized crime groups across national borders, and movements of ethnic separatism and religious extremism([28]).

THE NATIONAL LAW AND THE ILLICIT TRAFFICKING

A widely accepted working definition of IT reads as follows:**"A situation which relates to the unauthorized receipt, provision, use, transfer or disposal of nuclear materials, whether intentional or unintentional and with or without crossing international borders".** IT of nuclear materials defined as the movement of sensitive nuclear materials from the viewpoint of non-proliferation (ie, uranium enriched at 20% or more and plutonium, in addition to facilities fuel cycle that can be accessed illegally), within the State of origin or transported illegally to another State. The latter is the most dangerous from the standpoint of the non-proliferation ([29]). Thus an IT situation may arise when physical protection measures have failed.

The General objective of the law in this field to reduce to a minimum the possibility of smuggling of nuclear or radioactive materials in to the country or through the country and to have an effective plan to react in case of an illicit traffic event in the state.

Provisions that are contained in export and import control legislation regarding IT should be carefully reviewed to ensure their consistency with the laws dealing with physical

protection. Discrepancies in the scope of coverage, requirements, definitions or procedures between, on the one hand, export and import control legislation and, on the other hand, legislation against illicit trafficking, can lead to inefficiency and confusion in these two closely related fields. A State's export and import control laws should authorize relevant governmental agencies and officials to provide relevant information to the IAEA's Illicit Trafficking Database (ITDB)for the purpose of helping the international community to prevent unauthorized transfers of potentially dangerous material and technology

In fact the existence of a regulatory authority empowered to establish effective physical protection on one hand and accountancy and control measures on the other hand enhances the states capability to prevent, intercept and respond to illicit use of nuclear materials. Design and implementation of a system of physical protection is the responsibility of the state. That system is entrusted to take the necessary steps to minimize the possibilities of unauthorized removal of nuclear material or sabotage, undertake the necessary measures to locate and recover missing materials as rapidly as possible and minimize the effect of sabotage.

SSAC are complementary measures contributing to the prevention of illicit uses of nuclear materials. This is realized through the establishment of SSAC which should comprise a set of requirements and procedures applicable to all nuclear materials to ensure that such material is not diverted to unauthorized uses.

PART III : THE EGYPTIAN NUCLEAR LAW NO. 7 FOR REGULATING THE NUCLEAR AND RADIATION ACTIVITIES AND ITS EXECUTIVE REGULATION

As we mentioned, the State should establish and maintain a legislative and regulatory framework to govern physical protection. The legislation should designate a regulatory body responsible for the implementation of the legislative and regulatory framework.

FIRST: THE EGYPTIAN NUCLEAR LAW FOR REGULATING THE NUCLEAR AND RADIOACTIVE ACTIVITIES LAW NO. 7 ; 2010

Egypt started its legal framework to regulate the peaceful uses of nuclear energy by the law no 59 in the year 1960.. It also issued many republican decrees regulating the uses of nuclear energy. In September 2006, Egypt decided to study all alternatives for energy production. So, in 2007, it also decided to review its legal framework and drafting a unified nuclear law. In March 2010, Egyptian nuclear law was issued to regulate the nuclear and radioactive activities; It called law no. 7 for the year 2010. It contains provisions govern all the elements of national nuclear legislation according to many of the IAEA documents. The Egyptian nuclear law also establishes (in chapter no.3) a legislative framework for the licenses of the nuclear facilities. It also regulate the safe management of all nuclear materials and radiation sources to ensure that individuals, society and the environment are protected against radiological hazards. It also contains provisions regulate and control the import, transit and export of radioactive materials. It contains provision to put used sources under regulatory control. The Egyptian nuclear law provides for the regulatory body to issue the regulations contain requirements for every stage of the licenses. The law contains provisions (in chapter no. 5) to regulate nuclear safeguards and realizing the nuclear security.

1.THE LAW AND PHYSICAL PROTECTION

The objectives of physical protection legislation are, inter alia:

(a) To provide for the implementation of the State's relevant international obligations such as the CPPNM;
(b)To establish or designate a regulatory body with the powers and resources necessary for implementing the legislative and regulatory framework relating to physical protection;
(c) To promulgate a clear and comprehensive set of basic obligations that authorized persons must fulfill in order to ensure the effective physical protection of nuclear material and facilities;
(d) To establish the requirements that must be met in order to protect against the unauthorized removal of nuclear material in use and storage, and during transport;
(e) To establish the requirements that must be met in order to protect against the sabotage of nuclear facilities and against sabotage involving nuclear material in use and storage, and during transport;
(f) To establish the requirements for the preparation and exercise of contingency plans for a rapid response to any cases of the unauthorized removal of nuclear material, including the location and recovery of missing or stolen nuclear material (and in the event of sabotage) ([30])**.**

Although Egypt is not a state party to the CPPNM , the law contained the most of the physical protection recommendations. In Article (9), the law stated that "Be the Ministries of Interior, Foreign Affairs and the competent ministry to both the civil aviation and transport, the Suez Canal Authority, and the General Intelligence Service, and the Atomic Energy Authority and other relevant authorities, respective, responsible for taking the necessary measures to ensure the protection of radioactive materials in the framework of international transportation in accordance with the provisions set forth in international conventions governing it and be into force in Egypt([31]).

The law stated in part III Chapter II entitled licensee in Article (38) item 6 that "The licensee shall exercise nuclear or radiological activity with develop and implement measures and procedures required in significant nuclear security of nuclear materials and facilities and radioactive sources, and that against different threats.". The law in Article (41)stated that the licensee shall establish a security system for nuclear or radiation facility or nuclear materials and radioactive sources of his or her possessing and to fulfill all the requirements specified by the ENRRA to achieve the required levels of protection".

The following are some general requirements that may be considered for inclusion in legislation ([32]):
(a) A categorization of nuclear material.
(b) A provision that primary responsibility rests with the holders of the relevant licenses or with the holders of other authorizing documents (e.g. operators or shippers).
(c) A provision that the responsibility for physical protection during international transport should be the subject of agreement between the States concerned, with a clear definition of the point at which the responsibility is transferred from one State to another.
(d) A provision that the operator or some other authorized person should prepare plans for effectively countering the design basis threat through, inter alia, the actions of an emergency response force.
(e) A provision that the State's system for physical protection should ensure that competent authorities consider the following in establishing detailed requirements for physical protection:
— The category and location of the nuclear material (and whether the material is being used, stored or transported);

— The need for taking into account possible radiological consequences when establishing physical protection requirements against sabotage;
— The value of defence in depth through a combination of preventive and protective measures based on the appropriate facility design, hardware (security devices) and procedures (including the use of guards);
— Whether there is a credible threat of the malevolent dispersal of nuclear material.

Although general requirements may be codified in legislation, detailed requirements are typically promulgated by the regulatory body in regulations or rules.

2.THE LAW AND THE ILLICIT TRAFFICKING

The law establishes the legal base against IT in articles 31,55&62. In article (31) the licensee shall notify the ENRRA in writing immediately after knowing the loss or theft of any shipment containing radioactive materials, in accordance with rules and procedures prescribed by the Executive Regulations of this law. Under the title of Import, export, transport and transit, the Article (55) stated that "Prohibited, without the approval of the ENRRA in accordance with the conditions and standards set by the import, export or transfer any radioactive materials or any components or products of radiological nature and unlike X-ray machines for use in the medical field"([33]). The article (107) punished by imprisonment for a term not exceeding five years and a fine of not less than one hundred thousand pounds and not exceeding four hundred thousand pounds Whoever violates deliberately none of the provisions of articles 55 of this law, and ruled in the case of conviction export the seized items at the expense of the defendant.

Chapter sixth from part III, titled "Possession, handling and production licenses of nuclear materials and radioactive sources inclusion in Article (62) that states "Prohibited without a license from the ENRRA in accordance with the rules, conditions and procedures specified by the possession, handling or production or bring nuclear materials or radioactive sources. The issuance of the license referred to, and in accordance with the requirements of the need for a period determined by the ENRRA and be subject to renewal unless there requires review of the license during the duration of effect. In all cases, prohibits the natural person or a representative of the legal person possessing, trading or production or bring materials or sources referred to in his personal capacity([34]).The article (108) punished by imprisonment for a period not less than one year and a fine of not less than ten thousand pounds and not exceeding fifty thousand pounds every person who violates any of the provisions of articles (31, 53, 14, 74, 50, 15, 52, 45, 58, 61.66, 37) of the Act.
The law also establishes a system for nuclear security in article 77 to control procedures and measures to combat illicit trafficking in materials and sources.

3. THE LAW AND OFFENCES

There is a need to the law to include two kinds of sanctions: first, a range of administrative sanctions for the unauthorized removal or use of nuclear material and for non-compliance with physical protection requirements; and, second, for more serious violations (such as sabotage), a range of criminal sanctions. The Egyptian law punished the violators by imprisonment and fine for non-compliance with nuclear security, prevent illicit trafficking and physical protection requirements(Articles 106,107,108)

SECOND: THE EXECUTIVE REGULATION OF THE LAW NO.7 AND THE NUCLEAR SECURITY

The second Chapter of the executive regulation for The Egyptian nuclear law no. 7 that regulating the nuclear and radiation activities in the state included many articles related to Nuclear Security.

1.THE EXECUTIVE REGULATION AND PHYSICAL PROTECTION

In the article (12) one of the requirements for license of the nuclear facilities is an initial plan for the physical protection and security of nuclear installations. In Article (94)The ENRRA shall specify the requirements for the physical protection of nuclear materials used and stored and is being transmitted and nuclear facilities and that are resistant to withdraw without the permission of nuclear material or sabotage of the facility, respectively. Article (95)stated that "Borne by the licensee or owner of the facility or activity bear the primary responsibility for providing security toward nuclear facilities and activities, radiological and nuclear materials and nuclear fuel and radioactive sources, including radioactive waste and spent nuclear fuel. Article (99) The ENRRA shall review inventory and classification of nuclear materials and radioactive sources state into categories determined by rules and regulations, standards and technical regulations from the perspective of the nuclear security of nuclear materials and review the measures to be taken regarding each category of protection commensurate with its gravity within the principle of the cost analysis for yield to enhance security (the gradient approach). Article (98)The licensee shall implement the adopted of the Authority system to give full protection and security of nuclear facility or nuclear activity and subject those systems to control of the ENRRA directly to confirm the effectiveness of that system, including the inspection of all components of the system used, if necessary. Article (102) ENRRA to cooperate or consult with relevant organizations and institutions at home in matters concerning the operations of the physical protection and development, as well as foreign bodies in the case of cooperation for the recovery of any materials were stolen or loss through the official bodies and in coordination with the Supreme Committee for Nuclear and Radiological Emergencies.

2.THE EXECUTIVE REGULATION AND NUCLEAR SECURITY

Article (93) stated that "The Egyptian regime of nuclear security has the authority to ensure the availability of protection systems for nuclear and radiation installations, as well as of nuclear materials and radioactive sources used or stored and in particular what is being transferred internationally and has the audit be conducted of the systems or field inspection. The licensee of any facility or nuclear activity or radiological, according to Article (96), shall identifies sources of threat that could harm the safety of property, plant and environment such as theft, sabotage, and should develop plans to ensure confront that threat. Article (97) included that "The licensee shall develop systems and plans nuclear security required under the cost analysis for yield to enhance security (the gradient approach) to counter all kinds of threats expected of the facility or activity nuclear or radiological or nuclear materials and view a report of nuclear security to ENRRA for approval".

Article (100)The ENRRA shall confidentiality of any information or documents have confidentiality and maintain on physical protection systems also identify confidentiality requirements associated with this matter and associated documentation accurate information or details that could lead disclosure without permission to prejudice the physical protection of nuclear material and nuclear facilities that are subject to protection and confidentiality. Article

(101)determine the kind of the restrictions imposed on the preview of sensitive information by restricting who require the nature of their work found, and information that relate to what is going to be gaps in the physical protection systems should provide maximum protection.

3.THE EXECUTIVE REGULATION AND LICENSE OF POSSESSION OR HANDLING OR PRODUCTION OF NUCLEAR MATERIAL

Chapter VI of Part II of the executive regulation deal with the Possession or handling or production 'license of nuclear material. The Article (31) stated that possessing or handling licenses or production of nuclear materials are subject to the rules and the following conditions: 1 - Submitted to the Chief of ENRRA immediately the data and information on the handling of nuclear materials within the Arab Republic of Egypt or in any place under its control or supervision, as well as data and information on import and export of such materials, so as to meet the requirements of the IAEA contained safeguards agreement, including design information of the facility.

2 - Early notification to the head of ENRRA the design information of the facility and any change happening on this information before 6 months of its occurrence.

3– The ENRRA, in coordination with nuclear installations or locations outside facilities, prepare a document (facility attachment) specify in detail how to apply the procedures relating to the activities of the Egyptian regime of accounting and control of nuclear materials within each facility or location and is approved by the ENRRA Board of Directors in the finalized form.

4 – To get out of the regulatory of the ENRRA on nuclear material, required the approval of the Egyptian regime of accounting and control of nuclear material.

Article (32) stated that "the issuance of a license for possession, handling or production of nuclear materials with the following procedures:

1 -The applicant provides a written request is accredited to the President of ENRRA meets the following data and documents: -

A-The name of the facility and public statements about the location and / or outside locations, and the name and address of the person responsible and described.

B- Describe the site or outside sites and the approximate area and full address and telephone and fax numbers and e-mail.

C- General description of the activity of the facility (or outside sites) and the quality and quantities of nuclear material to be acquired or handled or produced and the purpose of the activity.

D- Description of the system (or systems) of measurement to determine the types and quantities of nuclear material under the possessed or traded or produced and any change thereof.

E- Provide an information document for the design and adoption of correctness of the information came from.

F- Description of the accounting system of nuclear materials, including models of the records and reports used.

G- The presence of an trained responsible person on accounting and control of nuclear material.

H- Approval to accept inspections by the ENRRA and the IAEA until the completion of the facility attachment according to the requirements set by the systems and standards, rules and requirements issued by the ENRRA.

I - Approval of correctness of the data in the license application.

J- Payment of the prescribed fees.
k- Deciding on the license application within thirty days from the date of completion([35]).

4. THE EXECUTIVE REGULATION AND THE EXPORT AND IMPORT

Part V Regarding the import, export and transport of radioactive sources / radioactive materials, in Chapter I titled Conditions for obtaining approval, the Article (61) stated that "the approval to import radioactive sources / radioactive materials will be subject to the following conditions: -

1 - Obtain a license for the handling and use of radioactive sources / radioactive materials to be imported or obtain a license operation to gamma irradiation facilities and electronic and ionic accelerators.

2 - Provide all the technical data for the device and belongings which will contain radioactive sources / radioactive materials and obtain the approval of ENRRA with the conformity to safety specifications.

3 - Apply procedures and radiation protection requirements through an expert or official protection certified and registered so special Authority records and determine technical regulations issued by the ENRRA obligations.

4 - Provide a statement from the body requested the approval of the re-export of radioactive sources / radioactive materials that have expired for work or discarded to the imported state or disposed it through the radioactive waste management facility.

In Article (62) the ENRRA obliged to establish a record codifies approvals to import radioactive sources / radioactive material.

5.EGYPTIAN NUCLEAR SECURIT SYSTEM AND SSAC

Egypt started its SSAC with the presidential decree no 152 in 2006([36]). The same obligations included in the nuclear safeguards chapter from the nuclear law. Article (71) stated that the ENRRA shall implement all the actions of the Egyptian SSAC in a manner that ensures accounting for and control of all nuclear material in Egypt or in any place under its jurisdiction or control or supervision and to meet the basic technical requirements according to the application of safeguards. The article (73) obliged the bodies and persons subject to the provisions of this Act shall submit to the ENRRA data, information and documents on the activities related to the work of nuclear safeguards, in accordance with the rules and procedures specified by the ENRRA in this regard. Article (74) gives the ENRRA the right to enter into any site and in the inspection and measurement and inventory, sampling and other necessary to validate the data, information and documents submitted by the licensee entity or sites outside as to the ENRRA put containment and surveillance systems.

In chapter III from part V titled" Nuclear security", the Article (77) stated that " the organizational structure of the ENRRA shall Established a system for nuclear security of nuclear and radiological installations and activities, nuclear materials, nuclear fuel and radioactive sources, including radioactive waste and spent nuclear fuel, to ensure the achievement of the following:

- Follow-up the types of threats expected that must be reservists in the design of nuclear security systems in the country, and analysis on the national level, and determine the appropriate means to meet them.
- Review the design of nuclear security systems and evaluate the performance of these systems during operation in the light of possible threats and appropriate means to meet them.

- Develop appropriate category of nuclear material and radioactive sources from the perspective of nuclear security, and the measures that are required in each category to protect materials and sources referred to in order to ensure proportionality between the seriousness and the level of protection required.
- Approval on the import and export operations.
- Control procedures and measures to combat illicit trafficking in materials and sources.
- Create a database of nuclear materials and radioactive sources in the country in all fields so as to ensure compatibility with the data related to the Egyptian system of accounting and control of nuclear material.
- Sure to provide the necessary protection for nuclear and radiological facilities, as well as nuclear materials and radioactive sources used, stored and what is being transferred by any means, including international transportation, and through the implementation of administrative and technical measures necessary.

The law also obliged the applying of the provisions of this article, by coordination with the Ministry of Interior, Foreign Affairs, the competent ministry to both transport and civil aviation bodies concerned to import and export, the General Intelligence Service, the Suez Canal Authority, the Atomic Energy Authority, the nuclear power plants to generate electricity Authority, the nuclear materials Authority and other ministries and relevant agencies, Within the limits of their respective jurisdiction. This will help these authorities in requesting radiation monitoring to detect any IT. Exit portals of all facilities in which radioactive sources or nuclear materials are handled or used or stored should be provided with suitable radioactive monitors to detect any unlawful acquisition, or theft of any amount of radioactive materials or any radioactive source on the spot.

According to the law (article 72’73’74’75’76) The SSAC have the jurisdiction to:-
a- Ensure that the nuclear materials are imported, exported, produced, transferred, stored, used or disposed of only by an authorized party through the license or approval by ENRRA.
b- Ensure that the licensee are well known of their responsibilities and applicable procedures and requirements associated to the nuclear security.
c- Maintain an updated data base system of all nuclear materials present in the country. In case of radioactive sources, it is a usual practice to apply adequate security measures, using the graded approach, to assure that the radioactive sources are under adequate and effective control.

Some experts considered the accountancy measures are also complementary to the effective control over radioactive sources. This could be achieved by applying registration systems for following up of the radioactive sources. In order to discover illicit trafficking or inadvertent movement of radioactive materials, the following steps are required: detection of any abnormal radiation level, verification of such detection, localization of the origin of the radiation, radiation safety measurement, and identification of the radioactive material ([37])

THE CONCLUSIONS

The aim of the international security system in the nuclear field to be transfers of nuclear materials, equipment and technology to safe and secure manner to humans and the environment. It also aims to help ensure that such transfers, directly or indirectly to the illegal use of nuclear materials. Many cases of illicit trafficking in nuclear materials led to the recognition of the need to strengthen the international system of physical protection.

Therefore, need to make every state possession of nuclear materials a crime punishable under national law, and enforcement of laws and regulations pertaining to this matter in order to achieve deterrence of such acts. It also should cooperate each State with other States and international bodies through the exchange of information on this subject, as well as plans or attempts to procure nuclear material illegally([38]).

The CPPNM sets forth a range of measures to ensure the protection of nuclear material (basically, enriched uranium and plutonium), primarily in international transport. However, the Convention also contains important provisions covering the domestic use of these materials. In force since February 1987, the CPPNM has 142 parties and 45 signatories.

As of early 2010, the CPPNM Amendment had been formally approved by only 34 states. Under the convention's amendment provision in Article 20 (2), the Amendment
will enter into force only after two-thirds of the parties have formally aprovied with its current large membership of 142 states parties, the CPPNM therefore requires 95 States to approve the Amendment. Given that it has taken some five years for only about a third of the necessary States to approve the Amendment, considerable delay in implementing this important instrument seems likely.

EVALUATION OF THE EGYPTIAN NUCLEAR LAW

The purpose of this work is to evaluate the legal situation in the country for the combat of IT in the framework of the international law rules and the Egyptian law. we must emphasized that the security is a matter of national sovereignty so, although it has common features, the Legislation, Regulation etc, and associated processes are vary from State to State. The General objective of the law in this field to reduce to a minimum the possibility of smuggling of nuclear or radioactive materials in to the country or through the country and to have an effective plan to react in case of an illicit traffic event in the state. State must enact state legislation to a system of physical protection of nuclear material is laying the groundwork that could reduce the vulnerability of nuclear materials to theft or loss or destruction, and ease of facilitating information and providing technical and financial assistance, for the recovery of stolen or lost and to reduce the radiation effects of sabotage or terrorist operations.

The Egyptian legislative framework provides legal bases for nuclear security of nuclear and radioactive material. The law contains provisions govern all these objectives above. It also contains a chapter to establish a regulatory body with the legal powers and technical competence necessary in order to ensure that operators of nuclear facilities and users of nuclear material and ionizing radiation sources operate and use them safely and securely. It provides the regulatory body with legal authority to issue a regulation of physical protection that should include many principles. The law also establishes a legislative framework for the safe management of all radiation sources. It also contains provisions regulate and control the import, transit and export of radioactive sources. It contains provision to put used sources under regulatory control. The Egyptian nuclear law contains provisions for nuclear safeguards and realizing the nuclear security. It also provides for the regulatory body to issue the regulations contain requirements for nuclear security. As well as, it reflected the all elements that should be included in the national law in the area of nuclear security.

A State's nuclear export and import control legislation should be consistent with applicable international agreements to which that State is a Party. The Egyptian nuclear law is

applied all Egyptian obligations according to the international treaties and conventions associated with the nuclear security which Egypt is a state party.

Because of the law criminalized the possession, handling or production or bring nuclear materials or radioactive sources without a license from the ENRRA in accordance with the rules, conditions and procedure, the Article (106) Punishable by imprisonment for a term not less than five years and no t more than seven years and a fine of not less than twenty thousand pounds and not exceeding one hundred thousand pounds Whoever violates any of the provisions of articles (25, 26 first paragraph, 49, 53, 62) of this law.

The law addresses specifically the illicit trafficking as an illegal act against the illicit trafficking and consequently there is penalty in case of an event of such nature occurs. Customs have radiation monitors to detect the traffic of nuclear or radioactive material. This law provides a legal base against the IT although it doesn't represent a serious threat at present in Egypt. It is very important to put at the border enter/exit points, as well as at air and sea ports in Egypt radiation detecting portals to enable the customs officials to detect and prevent any unlawful movement of nuclear materials or radioactive sources across the borders.

As the establishment of any legal system in terms of effectiveness requires the availability of three elements:

1- Set of Principles and the principles and objectives underlying the system.
2- A set of rights and obligations to achieve the objectives of the system, and accepted by the people of the system.
3 - An institution or a body that is on the application and implementation of the legal system.

To confront the IT,([39])efforts need to intensify to prevent illicit trafficking of nuclear materials by:

1-Reinforcing the defense first such as the storage of nuclear materials in a safe and guaranteed.
2-Take effective measures for the prevention and control.
3-Tighten national controls on exports and import of radioactive materials.
4-Increase the international cooperation in this field, because it cannot resolve this problem without the consolidation of cooperation between the countries, especially universal adherence to the NPT and the implementation of effective mechanisms and provisions, as well as to join the convention for the protection of nuclear material([40]).

REFRENCES

[1]- "International legal framework for Nuclear Security", IAEA International Law Series No. 4 VIENNA, (2011).p5
[2]- "Nuclear Security", Global Reach. IAEA BULLETIN 48/1 September (2006)
[3]- Carlton Stoiber, "Nuclear Security: An Emerging Domain of International Nuclear Law", Nuclear Inter Jura Proceedings. 1-4 October 2007, Bruxelles. (2007)pp852-865

[4]-For more details see: Carlton Stoiber, "Nuclear Security: Legal Aspects of physical protection, Combating Illicit Trafficking and Nuclear Terrorism". Chapter in " International Nuclear Law : History, Evaluation and Outlook" OECD Nuclear Energy Agency. Paris. (2010) p.219-242.

[5]- The fifth and latest revision of INFCIRC/225 has been issued by the IAEA together with two other publications aimed at assisting States in implementing a comprehensive nuclear security regime. IAEA Nuclear Security Series No. 14 provides Nuclear Security Recommendations on Radioactive Material and Associated Facilities, while IAEA Nuclear Security Series No. 15 is entitled Nuclear Security recommendations on Nuclear and Other Radioactive Material out of Regulatory Control.
[6] - Carlton Stoiber, Alec Baer, Norbert Pelzer and Wolfram Tonhauser."Handbook on nuclear law" 2003, PP.152-155
[7]- Carlton Stoiber,"Handbook on nuclear law" Op.Cit,p.127
[8]- Annual Report 2005, GC (50)/4, IAEA, Reports 2005.
[9]- For the text and status see
http://treaties.un.org/Pages/ViewDetailsIII.aspx?&src=TREATY&mtdsg_no=XVIII~15&
chapter=18&Temp=mtdsg3&lang=en.
[10]- Ibid
[11]- For the text see http://www.iaea.org/Publications/Documents/Conventions/cenna.htl;
for the status see
http://www.iaea.org/Publications/Documents/Conventions/cenna_status.pdf.
[12]- Walter Gehr, The Universal legal framework Against Nuclear Terrorism. Nuclear Inter Jura 2007 Proceedings. Op.Cit . pp869--881
[13]- Annual Report 2005, GC (50)/4, IAEA, Reports 2005
[14]- Bruno Demeyere, Sanctioning Illicit trafficking in Nuclear Materials and other Radioactive Substances through Individual Criminal Responsibility. Nuclear Inter Jura 2007 Proceedings. Op.Cit . pp869--881
[15]- Annual Report 2005, GC (50)/4, IAEA, Reports 2005.
[16]- For the text of the Code and Guidance see:
http://www.iaea.org/Publications/Documents/Infcircs/2005/infcirc663.pdf and for status see
http://www.iaea.org/Publications/Documents/Treaties/codeconduct_status.pdf.
[17]- Carlton Stoiber, Handbook on nuclear law, Op.Cit PP 137- 138
[18]- Treaty on the Non-Proliferation of Nuclear Weapons (NPT), International Atomic Energy Agency (IAEA) INFCIRC 140.
[19]- The structure and content of agreements between the agency and states required in connection with the treaty on the non-proliferation of nuclear weapons, International Atomic Energy Agency (IAEA) INFCIRC 153.
[20]-The convention on the physical protection of nuclear material and nuclear facilities, International Atomic Energy Agency (IAEA), INFCIRC 247/Rev.1.
[21] - Joint convention on the safety of spent fuel management and on the safety of radioactive waste management, International Atomic Energy Agency (IAEA), INFCIRC 546.
[22]-Carlton Stoiber, "Handbook on nuclear law", Op.Cit, PP 137-138
[23]- Code of Conduct on the Safety and Security of Radioactive Sources, IAEA, COODEOC/Vienna (2004).
[24]- Joint convention on the safety of spent fuel management and on the safety of radioactive waste management, International Atomic Energy Agency (IAEA), INFCIRC 546.
[25]- Ibid
[26]- Ibid
[27]- For more details about the Illicit Trafficking see:
Barry Kellman and Savid S. Gualtieri, Barricading the nuclear window – regime to curtail nuclear smuggling, University of Illinois Law Review.Volume 1996, No. 3
[28]- Vladimer Orlov, Illicit trafficking and the new agenda,, IAEA Bulletin No., 2 2004. pp.53-55.
[29]- Carlton Stoiber, "Handbook on nuclear law" Op.Cit,p143
[30] -Ibid, PP 148-149
[31]- Ibid.
[32]-Ibid. P.151
[33]- Ibid.
[34]- Ibid.
[35]- Ibid.
[36]- Presidential decree no. 152 for the year 2006. Official Gazette-no 20 , 20 May 2006.

[37]- M. Barakat, M. H. Nassef, and S. A. El Mongy, Measures Against-Illicit Trafficking of Nuclear Materials and Other Radioactive Sources. Presented in 9 th conference of Nuclear Science and Applications. Organized with The Egyptian Association for Nuclear Science, held from 11-14 February 2008. Cairo, Egypt.
[38]- IAEA Bulletin, 2004, Vol. 46, No. 1.
[39]- Scott Spence, " Legal aspects of the control and repression of illicit trafficking of nuclear and other radioactive materials: Is there a need for an international convention?" Nuclear Law. Vol. 2012/1.pp67-107.
[40]- IAEA Bulletin, 2004, Vol. 46, No. 1.

ICRP Recommendations to the Protection of People Living in Long-Term Contaminated Areas ICRP publication 111in brief

S. Salama[(1)], M. A. Gomaa[(1)] and S. Rashad[(2)]
[(1)] *Egyptian Atomic Energy Authority, Cairo Egypt-* [(2)] *ENNRA*
topazgemss@yahoo.com

ABSTRACT

The main aim of the present study is to through some lights on ICRP free release publication at 4 April 2011-Internationally Known as ICRP-publication 111. The title of the publication is (application of the commission's recommendations to the protection of people living in long-term contaminated areas after a nuclear accident or a radiation emergency). Nuclear accidents or a radiation emergency may cause contamination. The contamination may be spread on a large area. There are people living in these areas. For many factors the people refuse to leave their homes. They want to stay along their life as in the case of the normal conditions. So, it is important to facilitate their stay and make it safe. This is not easy. But it is possible without neglect the radiation hazard. The radiation hazard is effective on the life fields. It is harmful in plants, animals, foods, water, milk and the buildings it self. With considering the radiological protection principles the living of the people for a long time could be a fact of the life and will be more easy and safe. Optimization principle has priority to apply. This publication achieves these purposes.The ICRP-111 is translated into Arabic at August 2012. This work is a continuation of the efforts series to translate some of the most important of the ICRP radiological protection references into the Arabic; aiming to maximize the benefit. The previous translations include, ICRP-105 (radiation protection in medicine) and ICRP -113 (education and training in radiological protection for diagnostic and interventional procedures).

ICRP -111 text

The ICRP-111 text is composed of abstract, editorial (after the emergency), preface, executive summary, six chapters. The publication is summarized to clear the possibility of living on the contaminated land, with restrictions and to provide the experience gained.

ICRP-111 executive summary

This guide is assumed to be considered by who supposed to protect the people living in long-term contaminated areas resulting from either a nuclear accident or a radiation

emergency. The commission considers this situation as an "existing exposure situation". ICRP-111 develops the role of stakeholders. It is reinforces the principle of optimization of protection to be applied in a similar way to all exposure situations with restrictions on individual doses. Many recommendations developed in this report are broadly applicable with the necessary adaptations to other existing exposure situations. The decision to allow people who wish to live in contaminated areas to do so is taken by the authorities. These are complex situations which cannot be managed with radiation protection considerations alone. The level of exposure is mainly driven by individual behavior, so it should be controlled. Past experience of the management of contaminated areas has demonstrated that the involvement of local professionals. The priority of protection strategies implemented by authorities is to protect people with the highest exposures and in parallel to reduce all individual exposures associated with the event to as low as reasonably achievable. Stakeholder engagement is a key to the development and implementation of radiological protection strategies for most existing exposure situations.

ICRP-111 chapters

1. INTRODUCTION

In Publication 103, the commission described the general principles of protection in three different types of exposure situation: planned emergency, and existing which becomes practices and interventions. The present report provides guidance on the application of the commission's recommendations for the protection of people living in long-term contaminated areas resulting from either a nuclear accident or a radiation emergency. Radiation exposure due to long-lived radioactive residues in the environment must be controlled. The transition from an emergency exposure situation to an existing exposure situation may occur at different times within the contaminated areas.

2. LIVING IN CONTAMINATED AREAS

Chapter 2 considers the effects of a nuclear accident or a radiation emergency on the affected population. This includes the pathways of human exposure, the types of exposed populations, the characteristics of exposures and the experience from past events. Daily life of the inhabitants is affected within the contaminated areas. The relevant dimensions such as health, environmental, economic, social, psychological, cultural, ethical, political, etc. are affected.

2.1. Exposure pathways

The types of existing exposure situation considered in this report are the result of dispersive events that lead to radioactive contamination over relatively extended areas. Following contamination of the environment, several exposure pathways can be distinguished: external exposure due to deposited radionuclides and intake via consumption or inhalation of contaminated material. Radionuclide intake by humans may arise from

consumption of vegetables, milk, meat and fish. The use of an average individual is not appropriate for the management of exposure in a contaminated area. Exposure from ingestion of contaminated foodstuffs may result from both chronic and episodic intakes according to the relative importance of locally produced foodstuffs in the diet.

2.2. Characteristics of exposures

Day-to-day life or work in contaminated areas leads to some exposure. Individual exposures are affected by location, profession or occupation and individual habits. Twenty years after the Chernobyl accident, typical average daily intake due to ^{137}Cs for an adult in the contaminated areas is in the range of (10-20) Bq and in the range of a few hundred Bq is common at neighbors. For the sake of controlling exposure, different exposed groups of populations are considered to assess the overall dose impact. A good knowledge of the radiological situation and the basic radiation protection advice are necessary for affected populations.

2.3. Experience from past events

Past events have provided significant experience of practical value. It is used in developing appropriate management approaches to address long-term post-accident radiological, social, economic, and political issues.

3. APPLICATION OF THE COMMISSION'S SYSTEM TO THE PROTECTION OF PEOPLE LIVING IN CONTAMINATED AREAS

Chapter 3 discusses the application of the commission's recommendations in the type of existing exposure situation. It is includes consideration of justification and optimization of protection strategies and introduce application of reference levels to reduce individual dose distributions.

3.1. Justification of protection strategies

Living or working in a contaminated area is considered as an existing exposure situation. For such situations, the fundamental protection principles include the justification of implementing protection strategies. The principle of justification is a source-related principle, ensuring that any decision that alters the radiation exposure situation should do more good than harm. Justification of protection strategies goes far beyond the scope of radiological protection as they may also have various economic, political, environmental, social, and psychological consequences. Justification is concerned with the cumulative benefits and impacts of individual protective actions composing the protection strategy. The responsibility for ensuring an overall benefit to society as well as to individuals when populations are allowed to stay in contaminated areas lies with governments or national authorities.

3.2. Optimization of protection strategies

Reference levels are used during the optimization process to plan protection strategies that estimate residual doses lower than these levels. Dose limits are not applied. Protection strategies are made up of a series of protective actions directed at the relevant exposure pathways. New protective actions are needed to avoid severely inequitable outcomes of this

optimization procedure, there should be restrictions on the doses or risks to people from a particular source through the application of dose or risk reference levels. Due to its judgmental nature, there is a strong need for transparency of the optimization process. Protection strategies have to be prepared by authorities as part of national planning arrangements. These plans should take self-help protective actions into account.

The optimization process faces many specific challenges, notably: consumer vs producer interest, local population vs national and international population and the multiple decisions taken by the inhabitants in their day-to-day life. The optimization process can be implemented step by step. It is possible to reduce exposures progressively to levels comparable with those in normal situations. Optimization of protection strategies is the process of developing the strategy's form, scale and duration. The aim is to obtain not only a positive net benefit but also a maximized net benefit. The optimization of protection is an iterative process aiming to reduce future exposures. It takes into account both technical and socio-economic factors. Comparison of justified protection strategies is a key feature of the optimization process. It is not relevant to determine a dose level below which the optimization process should stop.

3.3. Reference levels to restrict individual exposures

It is defined as the level of dose or risk above which it is judged to be inappropriate to plan to allow exposures to occur, and below which optimization of protection should be implemented. The reference levels are recommended to set in terms of (mSv/year). The reference level is set at the end of the emergency exposure situation phase. The radiological protection measures need to be implemented. These measures include the need or not to establish protection strategies and ensure the radiation source is under control. Authorities implement the necessary protective measures to allow people to continue living in contaminated areas instead of abandoning them. The appropriate reference levels are chosen in the (1–20) mSv range. It is necessary to maintain exposures close or similar to those in normal situations.

4. IMPLEMENTATION OF PROTECTION STRATEGIES

Chapter 4 considers practical aspects of the implementation of protection strategies both by authorities and the affected population. The radiological management is depending on the level of contamination, its space and time distribution. The regulatory authorities should establish the conditions and means to allow the effective engagement of the affected population in the protection strategies. Mechanisms for engaging with stakeholders are driven by national and cultural characteristics.

4.1. Protective actions implemented by authorities

The priority of protection strategies implemented by authorities is to protect people with the highest exposures and in parallel to reduce all individual exposures. This assessment can support by radiation monitoring. The individual dose distribution is necessary to investigate the main exposure pathways. Radiological protection strategies must include clean-up of buildings, remediation of soil and vegetation, changes in animal husbandry, environment monitoring, produce clean foodstuffs and waste management. Human activities are affected by the radionuclides present and its distribution in the environment.

Identification of the highest doses is important to protect specific groups of people. Authorities have to set up infrastructures to support all protection strategies, including self-help strategies. An infrastructure is based on three keys: a radiation monitoring system, a health surveillance strategy and the transmission of practical knowledge within the population.

4.2. Protective actions implemented by the affected population

Self-help protective is aiming to characterize the radiological situation. Inhabitants need to manage the situation by establishing local mapping of their living places to evaluate the external exposure. Inhabitants can act according to the radiological quality of the foodstuffs consumed each day to evaluate internal exposure. This supposes that they have access to the measurements of local products. Applied agricultural techniques are recommended to limit transfer of radionuclides from soil to plants. Information and training help people to manage their radiological situation and monitoring equipment. Authorities should facilitate the setting-up of local forums involving representatives of the affected population and relevant experts. Stakeholder engagement is a key to develop radiological protection strategies.

5. RADIATION MONITORING AND HEALTH SURVEILLANCE

Chapter 5 covers radiation monitoring and health surveillance. Individual monitoring is an important requirement, coupled with an information program.

5. 1. Radiation monitoring

The key objective of monitoring systems is to assess current levels of human exposure (both external and internal), environmental levels of contamination and to allow the prediction of their evolution in the future. The monitoring system allows identification of population groups receiving elevated doses and better orientation of radiation protection strategies. So, the monitoring system should be designed to provide regularly updated information.

5. 2. Health surveillance:

The exposed population should have an initial medical evaluation. The epidemiological studies aim to identify adverse health effects in an at-risk group. Medical monitoring refers to screening of the entire affected population in order to detect specific preclinical disease with the purpose of delaying or preventing the development of disease among those individuals.

6. MANAGEMENT OF CONTAMINATED FOODSTUFFS AND OTHER COMMODITIES

Chapter 6 deals with the management of contaminated foodstuffs and other commodities. The management of contaminated foodstuffs and other commodities produced in areas affected by a nuclear accident or a radiation emergency has the priority. Protection strategies work to reduce exposure from the ingestion of foodstuffs produced in long-term contaminated areas to levels as low as reasonably achievable, taking economic and social conditions into

account. Relevant stakeholders (authorities, farmers unions, food industry, food distribution, consumer non-governmental organizations, etc.) should be shared.

6.1. Management inside the contaminated areas

A fraction of the diet of the local population may include local agricultural produced. Authorities should provide relevant information and set contamination criteria based on directly measurable levels of contamination (expressed in Bq/kg or Bq/L), taking into account the proportion of locally produced food in the diet. More restrictions on the sale of contaminated foodstuffs, without detailed studies, may cause loss its ratio at the market, hence affect to the local economy.

6.2. Management of exportations outside the contaminated areas

Protection of populations living outside contaminated areas is mainly driven by the control of trade. Due to some reasons foodstuffs coming from outside the contaminated areas may contain some contamination, even though it is well below the contamination criteria. The placement of contaminated foodstuffs on the market should be governed by the codex guideline levels for use in international trade. Traceability of food is an important factor to maintain the consumer confidence. Protection strategies should be developed to meet the established reference level and the strategy should be further optimized at all levels where it is possible to intervene.

6.3. Management of other commodities

Beside to foodstuffs other commodities may be contaminated. These commodities include agricultural products (wood, paper and oil) or products recycled from contaminated materials (scrap metal). The contamination levels for the use of contaminated commodities inside the contaminated areas should be derived from the annual dose reference level on the basis of realistic exposure scenarios. Trade of contaminated commodities or consumer products manufactured with contaminated material outside the contaminated territory should be in accordance with the rules or recommendations for international trade. Optimization strategies recommended to be developed with the time to face such these situations.

Annex A

Finally, Annex A summarizes past experience of long-term contaminated areas resulting from radiation emergencies and nuclear accidents, including the radiological criteria followed in carrying out remediation measures. These experiences are resulting from nuclear tests (Bikini, Maralinga), nuclear accidents (Kyshtym, Palomares, Chernobyl) and/or a radiological source accident (Goiaˆnia). It is illustrate the potential importance of ingestion of contaminated foodstuffs several decades after the event at the source of the problems when large rural areas are affected. Management of these foodstuffs to protect the local population against chronic internal exposure and to maintain the viability of local productions is essential.

According to historical occurrence Bikini, Maralinga, Kyshtym, Palomares, Chernobyl/Commonwealth of independent states countries, Chernobyl/Norway, Chernobyl/UK and Goiaˆnia, Brazil are introduced in deep details with learned lessons.

CONCLUSION

ICRP-111 insures the possibility of living in long-term contaminated areas after a nuclear accident or a radiation emergency without major problems or effective radiation hazard by following the updated regulations and considering some restrictions. Related authorities have responsibility to allow people to continue living in these areas or not. It is applicable to facilitate the people stay at these areas and make it safe with considering the radiological protection principles. The living of the people in contaminated areas for a long time could be a fact of the life and will be more easy and safe if optimization principle is applied in a creative ways.

REFERENCES

(1) Annals of the ICRP, ICRP 111, Application of the Commission's Recommendations to the Protection of People Living in Long-term Contaminated Areas after a Nuclear Accident or a Radiation Emergency, Elsevier, Ann. ICRP 39 (5), April 2011.
(2) Annals of the ICRP, ICRP publication105, Radiological Protection in Medicine (in Arabic), Arab Authority for Atomic Energy, Tunisia, 2011.
(3) WHO handbook on indoor radon, a public health perspective, the world health organization, France, 2009.
(4) Safety series No 9, IAEA, 1982.
(5) Safety series No 115, 1996 (Arabic Version).
(6) Updating International Basic Safety Standards 2007.
(7) Annals of the ICRP, ICRP 113, education and training in radiological protection for diagnostic and interventional procedures, Elsevier, Ann. ICRP 39 (5), 2009.

Heath Effects Sequence of Meet Halfa Radiological Accident After Twelve Years

M.H.Shabon
Nuclear and Radiation Regulatory Authority(NRRA).Cairo .Egypt.

ABSTRACT

The accident of Meet-Halfa developed consequent upon the loss of an industrial gamma radiography source. The source was found by a farmer resident of Meet-Halfa who took it to his house occupied by his family. The sequence of events developed over a period of seven weeks from the time the source was found on May 5, 2000, till the day of its retrieval from the house by the national authorities on June 26. The protracted exposure patterns of the family members during the period of source possession are not precisely known, however these exposures resulted in two fatalities, clinical forms of bone marrow depression, and several skin burns of different severities. The recent sequences of the accident is as follows:-
The three survived siblings married and get good children. That mean there is no hereditary stochastic effects. The sister died at 2007 with 72 years old with senility and no specific disease. The youngest daughter amputate the left thumb and index fingers at 2001. The elder son amputate the terminal phalanx of the right thumb at 2009. The youngest daughter amputate the right index finger at 2009. The elder son graft the burn at the lower right quadrant of the abdomen for more than 20 times (3 of them were in the Mansheat Al-Bakry Millitary Hospital), but there is residual of burn untill now. Sever abdominal hernia in the elder son due to necroses in the right quadrant abdominal muscles. Grafting for these muscles occur but failed.

INTRODUCTION

Nature of the Accident

The accident of Meet-Halfa developed consequent upon the loss of an industrial gamma radiography source. The source was found by a farmer resident of Meet-Halfa who took it to his house occupied by his family . The sequence of events developed over a period of seven weeks from the time the source was found on May 5, 2000, till the day of its retrieval from the house by the national authorities on June 26.

The protracted exposure patterns of the family members during the period of source possession are not precisely known, however these exposures resulted in two fatalities, clinical forms of bone marrow depression, and several skin burns of different severities.

CHRONOLOGY OF EVENTS

Possession of the Radiological Source.

On May 5, a resident from Meet-Halfa village found an industrial gamma radiography source that had been lost sometime before from an operator working for pipe welding testing company. Ignorant of the real nature of the strange looking metal object, the man took the source home where he lived with his wife, sister, two sons and two daughters. All seven

members of the family were fascinated by the object and firmly believed it was of precious metal.

During the weeks that followed, the source was handled by the family members with varying frequencies and durations. It was placed in different places for various periods, mainly in a cardboard box on top of a closet in the utility room. The family members were subject to protracted radiation exposures of different intensities. Determination of the nature, magnitude, extent and duration of the radiation exposure involved in such circumstances is very difficult to achieve.

Development of Events

On June 5, a message was received at the Infectious Disease office at the Ministry of Health in Cairo, from the Public Health Department at Qaluobiya; reporting the death of a nine years old child from Meet- Halfa village. The clinical condition prior to death was that of marked bone marrow failure and extensive inflammatory skin lesions. No indication of the exact diagnosis was given.

On June 10, a fact-finding mission from the Ministry of Health discovered four cases with similar signs and symptoms among family members of the deceased boy. The diagnosis of an inflammatory or viral cutaneous lesion associated with bone marrow depression was coined to the condition. All family members were admitted to Imbaba Fever hospital for observation.

On June 16, the father died from bone marrow failure associated with extensive inflammatory skin lesions. The remaining members of the family were further transferred to Abassiah Fever hospital for further studies. All laboratory investigations related to inflammatory or viral conditions of the skin proved negative.

Response of National Authorities.

On June 25, a task group from the Ministry of public Health was sent to Meet Halfa on a fact finding mission. The results of the mission revealed high radiation levels around the family house. The responsible authorities were immediately notified.

On June 26, experts from the Division of Chemical Warfare (armed forces) and from the Atomic Energy Authority (AEA) carried out detailed radiological survey of the family house and its surroundings at Meet-Halfa. A radiological industrial source was eventually found in a cardboard box above the closet in the utility room.

The source was controlled, retrieved, contained in a suitable lead container and transported under protective guidance to the Atomic Energy Authority laboratories at Inchas where it was placed in one of the hot cells. A radiological survey was further conducted at Meet-Halfa, and the village was declared free of high radiation levels.

On June 26, it became evident that the death of the younger son and the father, and the clinical conditions of the remaining members of the family were caused by the radiation exposures they received during the time they lived in the house in possession of the source from May 5 until June 10, the time they were admitted to Imbaba Fever hospital. on June 26, when the diagnosis of radiation effects was ascertained, the female members of the family were transferred to Naser Medical Institute to be placed under direct supervision of an expert

group from the National Cancer Institute. The elder boy of the family, being an army recruit was transferred to Maadi Military Hospital.

The source was Iridium 192. The half life of Iridium192 is 74 days. Calculating the decay process, the source activity would be 31.5 Curies on May 5 the day the source was found and became in possession of the family. On June 26, the day the source was retrieved, its activity would be 19.34 Curies. Iridium192 has a complicated gamma spectrum from 0.136 –1.062 MeV. The specific gamma ray emission (Gamma Factor) of Iridium192 is 0.13 mSv per hour at one meter per Giga Bq (10^9 Bq). (150 – 93 mSv per hour at one meter).

The Exposed Groups.

Family members. Thesewere in possession of the source from May 5, to June 10. This included the father (Sixty years), the wife (fifty years), the sister (Sixty five years), the older son (twenty two years), the younger son (nine years), the older daughter (seventeen years), and the younger daughter (thirteen years). The younger son died on June 5, and the father died on June 16.

According to detailed investigation revealed that the number of family associates including neighbors and relatives does not exceed 50 individuals. Because of the prudence and discretion of the farmer, very few associates knew of the radiological source hidden in the cardboard box on top of that closet in the utility room

Radiation Dose Estimates of Exposed Groups.

Using the Gamma Factor of 0.13 mSv per hour at one meter for one Giga Bq and the activity of the source of 31.5 Ci on May 5, and 19.34 Ci on June 26; the effective doses were 151 mSv per hr at one meter and 93 mSv per hr at on meter on the dates indicated respectively.

The exposures were protracted and subject to several known variables including frequency, mode, duration and exact dose rate at time of exposure. This particular situation renders precise dose estimates to the exposed groups very difficult to achieve and subject to a wide margin of error.

Dose Estimates to Family Members. Dose estimates to this members family would be based on the type and severity of the biological effects incurred to each individual. The biological indicators used for dosimetric purposes would include such criteria as degree and extent of skin burns, changes of peripheral blood cells, severity of bone marrow affection, gastrointestinal disturbances and cytogenetic findings.

Taking into account the dose rate on May 5, and on June 26; and considering the acute effects acquired by the members of the family, it would be rational to postulate a cumulative dose of 7.5 – 8 Gy to the father, and a cumulative dose of 5.5-6 Gy to the younger son. Both died from bone marrow failure, severe skin burns and gastrointestinal manifestations.

Cumulative doses to the wife and sister approximate to about 3.5-4Gy; and to the older son would be about 4.5 Gy localized to the lower right quadrant of the abdomen. The cumulative dose to the elder daughter reached 4 Gy to the whole body affecting bone marrow

deposits. The cumulative dose to the younger daughter is of the same magnitude, with characteristic localization to the skin of both hands, Rt. Knee and Rt. thigh.

Dose estimates to radiation survey groups. These include a total of 70-100 individuals. These groups were exposed to low level radiation during the survey operations. Personal dose-meters carried by some individuals during the survey procedures gave readings between 1-15 mSv.

Dose estimates to family associates. As previously mentioned, the number of family associates was about 50 individuals. The exposure doses to this group would range between 0.5 and 5 mSv.

Radiation Dose Estimates to Exposed Groups

(Protracted Exposure)

A- Family Members

Members	Dose (Gy)	Members	Dose (Gy)
Father	7.5-8 Total Body	Sister	3.5 – 4 Total Body
Younger Son	5-6 Total Body	Wife	3.5 – 4 Total Body
Elder Son	3.5 – 4 Localized	Younger Daughter	3.5 – 4 Localized
		Elder Daughter	3.5 – 4 Total Body

B- Radiation Survey Groups

Number	Dose (mSv)
70-100 individuals	1-15 mSv

C- Family Associates

Number	Dose (mSv)
50 individuals	1- 5 mSv

MEDICAL ASPECTS.

The Early Phase.

The essential features of this case study are the radiation effects induced after accidental protracted overexposure from cumulative doses acquired over five to six weeks. The determination of the nature, magnitude, extent, duration and frequency of the exposure in this case is very difficult to achieve.

The prodromal signs and symptoms reported by the members of the family were generalized malaise, fatigue, and skin ulceration. The early laboratory investigations indicated decreased peripheral blood counts, signs of bone marrow depression and infected skin lesions. The diagnosis of viral or infective cutaneous condition was suggested.

The younger son died on the June 5, followed by the father's death on June 16. The death in both cases was attributed to bone marrow aplasia, severe infected skin lesions, and signs of gastrointestinal disturbance. The cause of death from acute radiation injury induced by accidental protracted overexposure was ascertained only after the Iridium192 source was retrieved from the family house on June 26. The clinical manifestations of the remaining five members of the family were finally diagnosed as being radiation induced. In order to provide adequate medical care for the five members of the family, the sister, the wife and the two daughters were transferred to Naser Medical Institute Hospital. On June 26, and the elder son was admitted at Maadi Military Hospital.

Clinical and Laboratory Investigations.

At both medical facilities, similar clinical investigations were performed, and the same treatment protocols were adopted. The clinical and laboratory investigations comprised complete clinical examination including the skin, hair, oral cavity and genitals, X-Ray of chest, electrocardiogram, abdominal ultrasonic, complete total and differential blood count, liver and kidney function tests, blood chemistry, bone marrow examination and cytogenetic studies of blood cells.

Bone marrow: All bone marrow examinations for the five patients showed evidence of bone marrow hypocellularity of all cell lines, particularly evident in the myeloid, lymphocyte, and megakaryocyte cell lines. Differences in severity were observed among the patients.

Hematological data. Early laboratory finding after admission revealed different degrees of leucopaenia, anaemia and decreased platelet counts. During hospitalization blood counts were performed daily for the first week, every other day during the second week and twice during the third week . This was followed by weekly counts during the outpatient follow up. The data for peripheral blood counts for each patient at specific selected times over two months covering the period of hospitalization from June 26 to July 20, and extending as out patient follow up till August 25, are given in figures 1-5 (a,b,c).

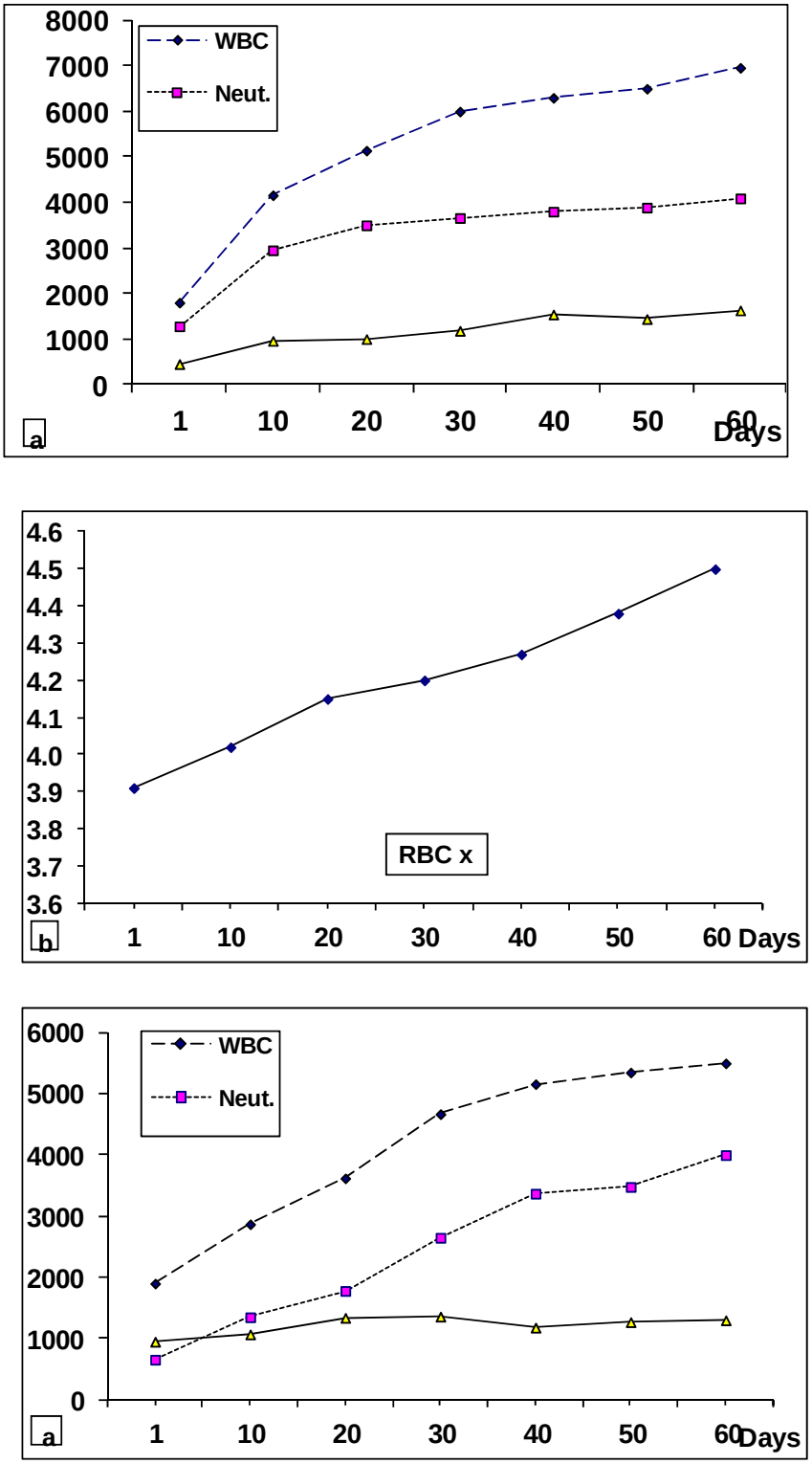

Figure 1 (a,b,c) show data for haematological findings (total WBCs, Neutrophiles, Lymphocytes, RBCs and Platelet counts) for the sister, over a period of sixty days

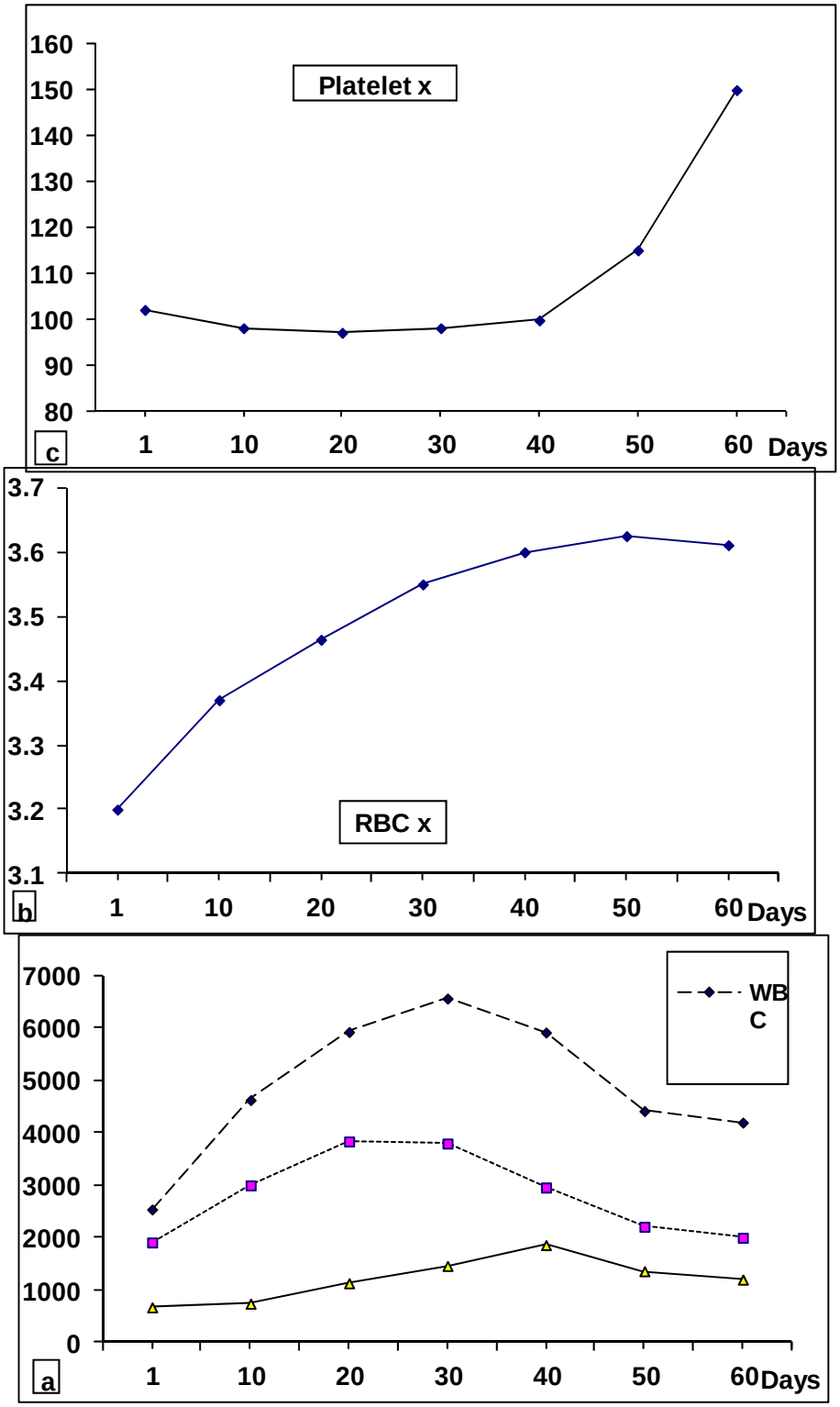

Figure 2 (a,b,c) show data for haematological findings (total WBCs, Neutrophiles, Lymphocytes, RBCs and Platelet counts) for the wife, over a period of sixty days.

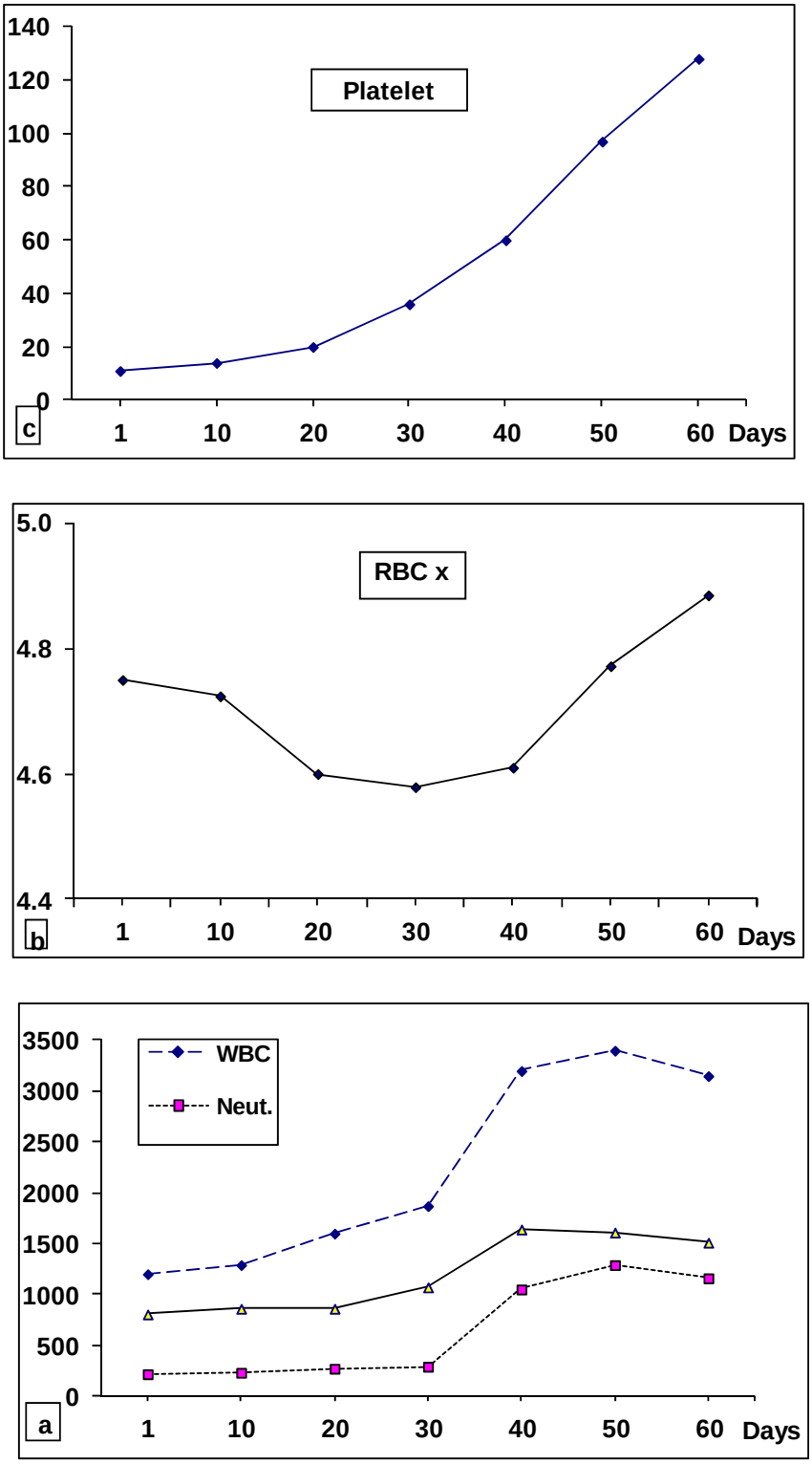

Figure 3 (a,b,c) show data for haematological findings (total WBCs, Neutrophiles, Lymphocytes, RBCs and Platelet counts) for <u>elder son</u>, over a period of sixty days

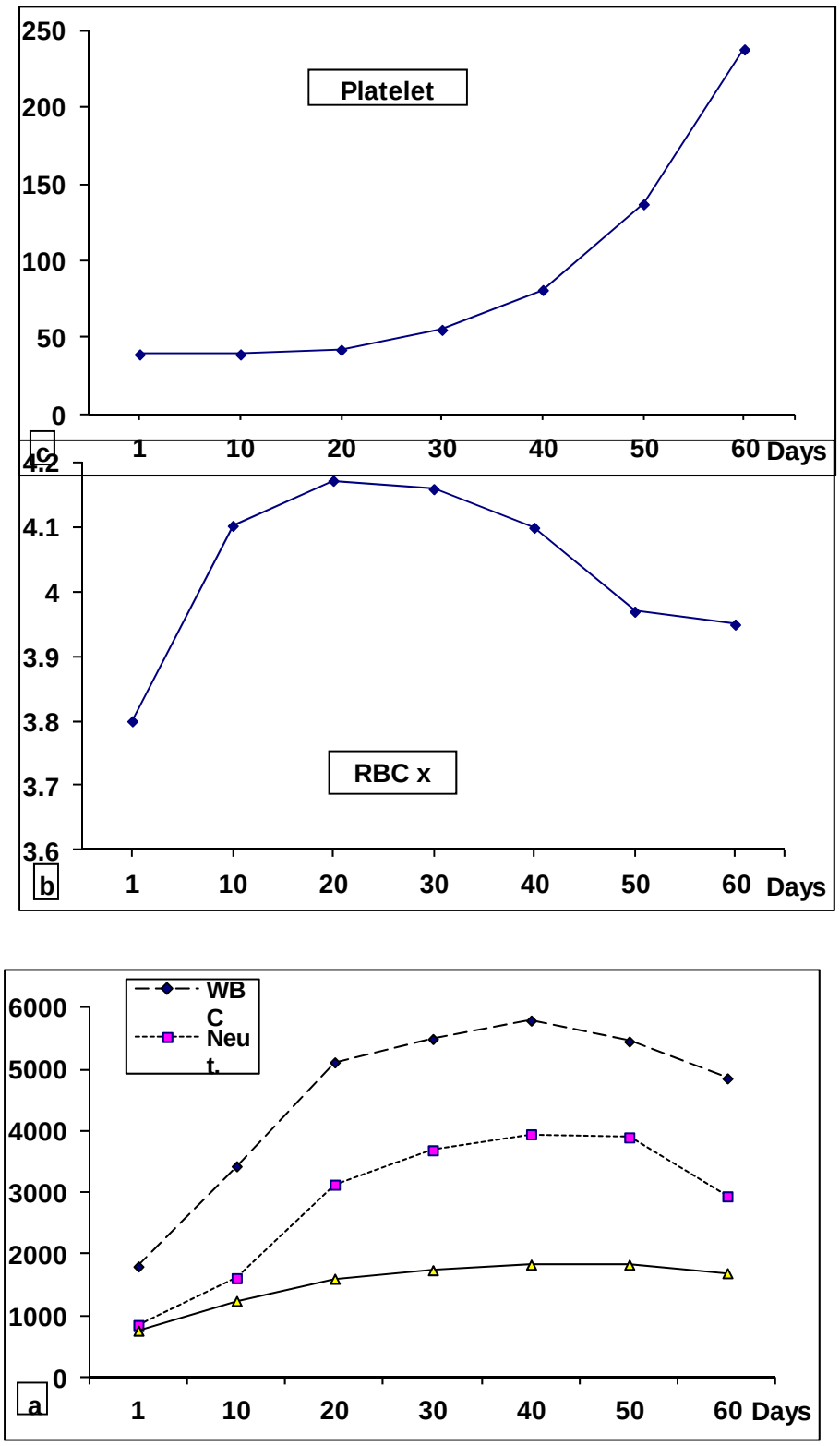

Figure 4 (a,b,c) show data for haematological findings (total WBCs, Neutrophiles, Lymphocytes, RBCs and Platelet counts) for elder daughter, over a period of sixty days.

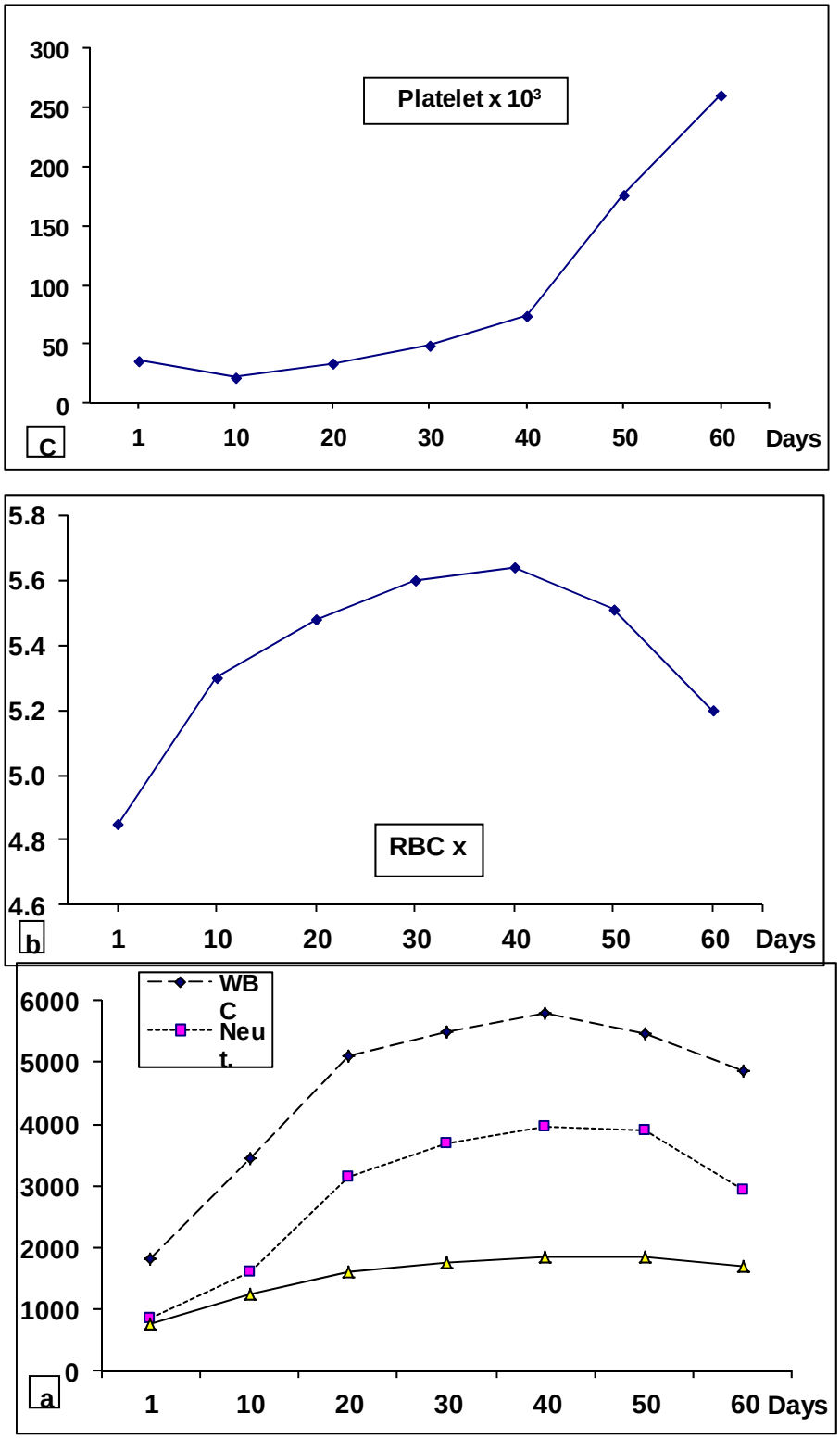

Figure 5 (a,b,c) show data for haematological findings (total WBCs, Neutrophiles, Lymphocytes, RBCs and Platelet counts) for younger daughter, over a period of sixty days.

Skin burns. The elder son suffered extensive skin burns of varying degrees affecting the lower right quadrant of the abdomen and extending laterally. The thumb and index finger showed evidence of healing radiation ulcers. Severe stomatitis and rash were reported. The younger daughter showed severe burns and contractures of both hands mainly involving the palms, index and thumb of left and right hands, deep localized ulcer of right knee, and deep localized ulcer at upper outer aspect of the right thigh. The wife showed a healing ulcer at the distal end of the Rt. Index finger. No other significant findings were observed. Photographs of skin lesions are shown.

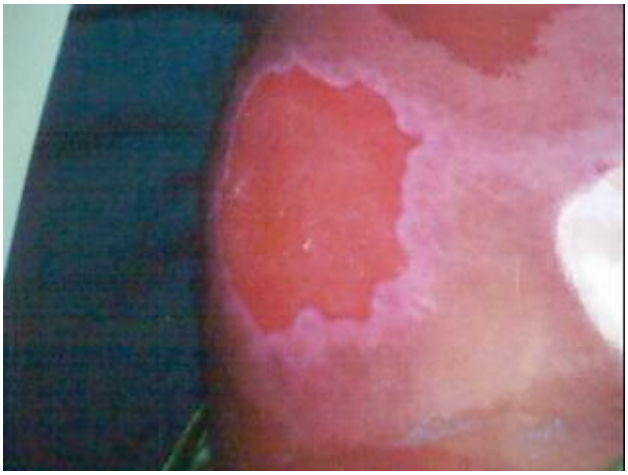

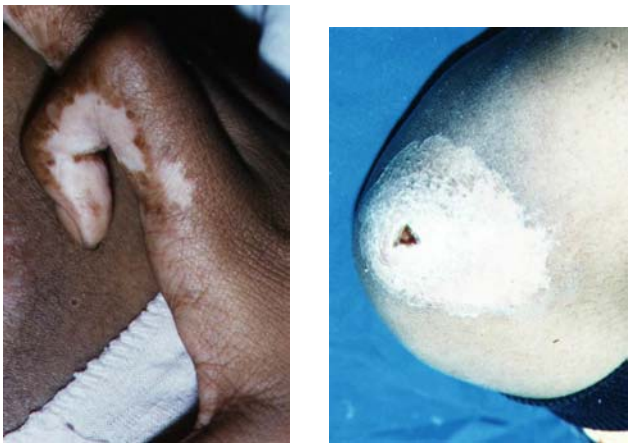

Cytogenetic studies. Reports of cytogenetic studies of blood cells for all five patients indicated no evidence of any abnormality. Such results appeared questionable, since it was expected that some radiation induced dicentrics or other abnormalities would appear in the cytogenetic examinations. However, in this situation, the accidental protracted exposure may have resulted in non uniform doses to only a portion of the body from low LET radiation from a point source. The lymphocytes present in the radiation field received a radiation dose. Exposed and non-exposed lymphocytes became mixed as blood circulates. If only a small portion of the body was exposed (e.g. fingers, extremity or localized part of body, the number of lymphocytes receiving radiation damage are too few to provide a reasonable probability of detecting cytogenetic evidence to be used for dosimetric purposes.

Psychological Implications.

Various degrees of psychological manifestations were evident during the events of the accident. The main causes of these manifestations were absence of exact credible information about the accident, ignorance of the nature of radiation effects, and uncertainties regarding the chances of recovery and the consequences of exposure and the delayed effects. These psychological patterns affected mainly the surviving members of the family. However, several village residents were concerned about radioactive pollution, and anxious about contagious possibilities. These psychological implications were an outstanding feature during the early

phases of the accident events. The remaining psychological symptoms concerned the surviving members of the family regarding the chances of total recovery, and means of support after the father's death.

Medical Management.

The treatment protocols adopted for the five patients were essentially similar, however, certain medications were used according to specific patient needs. The main lines of medical management included the following:

- Patient isolation in laminar air flow tent.
- Administration of excellent hygiene with daily baths,
- Maintaining high quality nursing-mouth and respiratory care.
- Complete control of portals of infection.
- Well balanced food and fluid intake.
- Maintain proper electrolyte balance
- Administration of Granulocyte Colony Stimulating Factor (Neopogen 10 microgram / kg/day)
- Liberal use of Antibiotics (ceprafloxacid 500mg/12hrs) or (Augmentine 650 mg/8hrs)
- Platelet transfusion for the elder daughter.
- Hormonal treatment to control menstruation for the elder daughter.
- Multivitamins.
- Antifungal and Antimicotic drugs when needed
- Attending to the skin lesions with suitable medication and dressings.
- Skin grafting for the elder boy which failed on two trials. A third trial is contemplated.

RECENT SEQUENCES

1- **The three survived siblings married and get good children. That mean there is no hereditary stochastic effects.**
2- **The sister died at 2007 with 72 years old with** senility **and no specific disease.**
3- **The youngest daughter amputate the left thumb and index fingers at 2001.**
4- **The elder son amputate the terminal phalanx of the right thumb at 2009.**
5- **The youngest daughter amputate the right index finger at 2009.**
6- **The elder son graft the burn at the lower right quadrant of the abdomen for more than 20 times (3 of them were in the Mansheat Al-Bakry Millitary Hospital), but there is residual of burn untill now.**
7- **Sever abdominal hernia in the elder son due to necroses in the right quadrant abdominal muscles. Grafting for these muscles occur but failed.**

The following photos are for the elder son showing the remaining abdominal ulcer in the lower right quadrant of the abdomen; sever abdominal hernia and the right thumb after amputation of the terminal phalanx.

LESSONS LEARNED.

Any radiation accident will add knowledge and experience. Accident from lost, stolen or neglected sources are particularly special because the radiation exposure patterns of the individuals involved and the scenario of the accident are always different.

The accident of Meet-Halfa provide several aspects and defines generic lessons to be learned by the regulatory authorities, source operators, manufacturers and all individuals responsible for the safety of radiation sources. Some of these important aspects that should be considered as lessons learned are: Proper implementation of the codes of practice, minimizing the probability of human error, by repeated educational training programmes, minimizing the probability of source malfunction by performance of repeated maintenance, stringent supervision over the logistics involved in importing, licensing, transportation and – recording of sources and formulation of a proper system for dealing with spent sources.

REFERENCES

(1) R. A. Allen et al., United Kingdom Atomic Energy Authority, Radioisotope Data, (1961).
(2) International Atomic Energy Agency – Technical Reports series No.260, (1986).
(3) The Radiological Accident in Goiana, IAEA, (1988).
(4) The Radiological Accident in San Salvador, IAEA, (1990).
(5) The Medical Basis of Radiation Accident Preparedness II, Editors Robert C. Ricks and Shirley Fry (1990).
(6) The Medical Basis of Radiation Accident Preparedness III, 1991 Editors Robert C. Ricks, Mary Ellen Berger and a Frederick. O, Hara (1991).
(7) International Atomic Energy Agency, Manual on Gamma Radiography, (1992).
(8) Lessons learned from Accidents in Industrial Radiography – IAEA – Safety Report Series, No.7, (1998).
(9) International Atomic Energy Agency, Radiation Protection and Safety in Industrial Radiography, Safety Report Series, No.13, (1999).
(10) Major Radiation Accidents Worldwide (1944-2000) Radiation Accident Registries, REAC/TS, (2000).
(11) Atomic Energy Authority Report, Cairo, Egypt, (July 2000).
(12) Ministry of Health Report, Cairo, Egypt, (July 2000).

Estimation of the Radiation Hazard Indices from the Natural Radioactivity of Building Materials.

Shams A.M. Issa[a], M.A.M. Uosif[a], M.A. Hefni[b], A.H. El-Kamel[b] and Asmaa Makram[b]
[a]*Physics Department, Faculty of Sciences, Al-Azhar University (Assiut branch), Egypt*
[b]*Physics Department, Faculty of Sciences, Assiut University, Egypt*
shams_issa@yahoo.com

ABSTRACT

The activity concentrations of uranium, thorium and potassium can vary from material to material and it should be measured as the radiation is hazardous for human health. Thus first studies have been planned to obtain radioactivity of building material used in the Tema city region of Egypt. The radioactivity of some building materials used in this region has been measured using a γ-ray spectrometry, which contains a NaI (Tl) detector connected to MCA. The specific activity for ^{226}Ra, ^{232}Th and ^{40}K, from the selected building materials, were in the range 7±0.4–64±3.2, 4±0.2–55±2.7 and 116±5.8– 404±20 Bqkg^{-1}, respectively. Absorbed dose rate in air, annual effective dose, radium equivalent activities, external hazard index and excess lifetime cancer risk associated with the natural radionuclide are calculated to assess the radiation hazard of the natural radioactivity in the building materials.

Key word: *Natural radionuclides, building materials and hazard index.*

INTRODUCTION

Human beings are continuously exposed in their houses and ionizing radiation emitted by from building materials. Materials derived from rock and soil contains mainly the natural radionuclides of the uranium (^{238}U) and thorium (^{232}Th) series, and ^{40}K. These radionuclides can cause external and internal radiation exposure to occupants. The external exposure is caused by direct gamma radiation. The internal radiation exposure, affecting the respiratory tract, is due to radon and radon decay products which emanate from building materials (1). Knowledge of the basic radiological parameters such as radioactive content in building materials is important in the assessment of possible radiation exposure to the population. This knowledge is essential for the development of standards and guidelines for the use of these materials.

MATERIALS AND METHODS

Sampling and sample preparation

In order to obtain samples used as building materials in Tema city which located in upper Egypt, manufacturers, building material suppliers and sites where houses and buildings were under construction in thirteen regions were visited; the samples were obtained from these locations; 2 red clay-brick, one lime-brick, 2 gravel, 3 clay-brick and 4 sand samples were

collected from seven regions. Building material samples were oven dried at a temperature of 110 °C for 12 h and sieved through a 200 mesh. The dried samples were transferred to polyethylene Marinelli beakers of 197 cm^3 capacity. Each sample was left for at least 4 weeks to reach secular equilibrium between radium and thorium, and their progenies (2, 3).

Gamma spectrometric analysis

Activity measurements have been performed by gamma ray spectrometer, employing a scintillation detector (3×3 inch). It is hermetically sealed assembly, which includes a NaI (Tl) crystal, coupled to PC-MCA Canberra Accuspec. To reduce gamma ray background, a cylindrical lead shield (100 mm thick) with a fixed bottom and movable cover shielded the detector. The lead shield contained an inner concentric cylinder of copper (0.3 mm thick) in order to absorb X-rays generated in the lead. In order to determine the background distribution in the environment around the detector an empty sealed beaker was counted in the same manner and in the same geometry as the samples. The measurement time of activity or background was 43200s. The background spectra were used to correct the net peak area of gamma rays of measured isotopes. A dedicated software program (4).

The ^{226}Ra radionuclide was estimated from the 609.3 keV (46.1%) γ-peak of ^{214}Bi, 351.9 keV (36.7%), 1120.3 keV (15%), 1728.6 keV (3.05%) and 1764 keV (15.9%) γ-peak of ^{214}Pb. The 186 keV photon peak of ^{226}Ra was not used because of the interfering peak of ^{235}U with energy of 185.7 keV. ^{232}Th radionuclide was estimated from the 911.2 keV (29%) γ -peak of ^{228}Ac and 238.6 keV (43.6%) γ -peak of ^{212}Pb. ^{40}K radionuclide was estimated using 1,461 keV (10.7%) γ -peak from ^{40}K itself. The below detectable limit (BDL) were 25.2 $Bqkg^{-1}$ for ^{40}K, 6.5 $Bqkg^{-1}$ for ^{226}Ra and 5.7 $Bqkg^{-1}$ for ^{232}Th. All procedures were described in previous publications (5).

RESULTS AND DISSECTION

Radioactivity measurements

The results for the activity concentrations of natural radionuclides ^{226}Ra, ^{232}Th and ^{40}K in the building material samples are summarized in Table 1. The highest values of ^{226}Ra, ^{232}Th were found in Red Clay-brick, while the highest value of ^{40}K was found in Lime-brick.

Table 1: Activity concentration Bqkg^{-1}of ^{226}Ra, ^{232}Th and ^{40}K in samples.

	^{226}Ra	^{232}Th	^{40}K
Red Clay-brick 1	42±2.1	43±0.2	178±8.9
Red Clay-brick 2	204±10.2	221±11.1	346±17.3
Red Clay-brick 3	35±1.7	24±1.2	258±12.9
Lime-brick	48±2.5	1±0.3	872±43.6
Clay- brick 1	64±3.2	24±1.2	203±10.2
Clay- brick 2	33±1.7	37±2.8	404±20.2
Clay- brick 3	64±3.2	24±0.3	203±8.6
Gravel 1	47±2.3	16±0.8	321±16.1
Gravel 2	9±1.2	4±0.8	123±7.4
Sand 1	52±2.6	55±2.7	167±8.3
Sand 2	19±1	7±0.3	128±6.4
Sand 3	10±0.5	4±0.2	116±5.8
Sand 4	17±1	70±0.3	121±6

Radium equivalent activity (Ra_{eq})

To compare the radiological effects of the building material samples, which contain ^{226}Ra, ^{232}Th and ^{40}K, a common index is required to obtain the sum of activities. This index is usually called the radium equivalent activity (Ra_{eq}) as given in the following expression (6).

$$\mathbf{Ra_{eq} = A_{Ra} + 1.43A_{Th} + 0.077A_K} \qquad \mathbf{(1)}$$

where, A_{Ra}, A_{Th} and A_K are the activity concentrations of ^{226}Ra, ^{232}Th and ^{40}K in Bqkg^{-1},respectively. It has been assumed that 370 Bqkg^{-1} of ^{226}Ra, 259BqBq.kg^{-1} of ^{232}Th and 4810 Bqkg^{-1} of ^{40}K produce the same gamma doses in Eq. (1). The maximum value of Ra_{eq} in building materials samples is required to be less than the limit value of 370 Bqkg^{-1} recommended by the Organization for Economic Cooperation and Development for safe use, i.e., to keep the external dose below 1.5mSvy^{-1}. Table (2) shows that, the values of Ra_{eq} are less than the 370 Bqkg^{-1}, except for Red Clay-brick 2.

Air-absorbed dose rates (D)

The absorbed dose rates in outdoor (D) due to gamma radiations in air at 1m above the ground surface for the uniform distribution of the naturally occurring radionuclides (^{226}Ra, ^{232}Th and ^{40}K) were calculated based on guidelines provided by (7). The conversion factors used to compute absorbed γ-dose rate (D) in air per unit activity concentration in Bq/kg (dry-weight) corresponds to 0.427 nGyh^{-1} for ^{226}Ra (of U- series), 0.662 nGyh^{-1} for ^{232} Th and 0.043 nGyh^{-1} for ^{40}K.

$$\mathbf{D = 0.427C_{Ra} + 0.662\ C_{Th} + 0.043\ C_K \quad nGyh^{-1},} \qquad \mathbf{(2)}$$

Where C_{Ra}, C_{Th} and C_K are the concentration in (BqKg^{-1}) of radium, thorium and potassium respectively. Table 2 gives the results for the absorbed dose rate in air for building materials samples.

Table (2): Radium equivalent, the dose rate, hazard index, annual effective dose rate and excess lifetime cancer risk.

	Ra_{eq} Bq/kg	D nGy/h	H_{ex} nGy/h	A. Eff. µSv/y	ELCR
Red Clay-brick 1	117.2	52.8	0.3	64.1	2.2E-04
Red Clay-brick 2	546.7	242.2	1.5	293.9	1.0E-03
Red Clay-brick 3	89.2	41.4	0.2	50.3	1.8E-04
Lime-brick	116.6	59.1	0.3	71.8	2.5E-04
Clay- brick 1	114.0	52.5	0.3	63.8	2.2E-04
Clay- brick 2	117.0	54.4	0.3	66.1	2.3E-04
Clay- brick 3	114.0	52.5	0.3	63.8	2.2E-04
Gravel 1	94.6	44.8	0.3	54.3	1.9E-04
Gravel 2	24.2	11.7	0.1	14.2	5.0E-05
Sand 1	143.5	64.2	0.4	77.9	2.7E-04
Sand 2	38.9	18.3	0.1	22.3	7.8E-05
Sand 3	24.7	11.9	0.1	14.4	5.0E-05
Sand 4	37.2	17.8	0.1	21.6	5.5E-05

External radiation hazard (H_{ex})

The external hazard index is an other criterion to assess the radiological suitability of a material. It is defined as follows (8):

$$H_{ex} = C_{Ra}/370 + C_{Th}/259 + C_K/4810 \quad (3)$$

where C_{Ra}, C_{Th} and C_K are the activity concentration of ^{226}Ra, ^{232}Th and ^{40}K, respectively, in $Bqkg^{-1}$ .The values of the indices should be <1. It is observed in Table 2 that the values of H_{ex} is below the criterion value (<1), except for Red Clay-brick 2.

Annual effective dose (A. eff.)

Annual estimated average effective dose equivalent received by a member was calculated using a conversion factor of 0.7 $SvGy^{-1}$, which was used to convert the absorbed rate to human effective dose equivalent with an outdoor occupancy of 20% and 80% for indoors (9). The annual effective dose was determined as follows:

$$\text{Annual effective dose rate} = D \times T \times F \quad (4)$$

Where D is the calculated dose rate (in $nGyh^{-1}$), T is the outdoor occupancy time (0.8x24 h x365.25 d≈7013 hy^{-1}), and F is the conversion factor ($0.7x10^{-6}$ $SvGy^{-1}$). The experimental results of annual effective dose rate are presented in table 2. The International Commission on Radiological Protection (ICRP) has recommended the annual effective dose equivalent limit of 1 $mSvy^{-1}$ for the individual members of the public and 20 $mSvy^{-1}$ for the radiation workers (10).

Excess lifetime cancer risk (ELCR):

Excess lifetime cancer risk (ELCR) was calculated using the following equation and presented in Table 2.

$$ELCR = AEDE \times DL \times RF \quad (5)$$

where AEDE, DL and RF is the annual effective dose equivalent, duration of life(70 years) and risk factor (Sv^{-1}), fatal cancer risk per sievert. For stochastic effects, ICRP60 uses values of 0.05 for the public (11). The calculated value of ELCR showed that, the highest value ware in Red Clay-brick 2.

CONCLUSION

The specific radioactivity values of ^{226}Ra, $^{232}Th$and ^{40}K measured in commonly used building materials used for the construction purposes in Tema city, upper Egypt have been determined by gamma-ray spectrometer. For each sample in this study, the specific activity, radium equivalent activity, annual radiation dose, external hazard and excess lifetime cancer risk have been determined to assess the radiological hazards from the building materials. The calculated radium equivalent activity (Ra_{eq}) values for all the building materials examined are lower than the recommended maximum level of radium equivalent of 370 $Bqkg^{-1}$, except in Red Clay-brick 2.

The external (H_{ex}) hazard index has been determined to be less than the recommended value, except in Red Clay-brick 2. The values obtained in the study are with in the recommended safety limit, showing that the building materials do not pose any significant radiation hazard

and hence the use of these materials in the construction of dwelling is considered safe for the inhabitants. This study can be used as a reference for more extensive studies of the same subject in future.

ACKNOWLEDGMENT

This work was carried out using the nuclear analytical facilities at the Physics Department, Faculty of Sciences, Al-Azhar University, Assiut, Egypt.

REFERENCES

(1) European Commission). Radiation Protection 112. Radiological Protection Principles Concerning the Natural Radioactivity of Building Materials. Direc- torate-General Environment, Nuclear Safety and Civil Protection, (1999).
(2) American Society for Testing Materials (ASTM). Standard method for sampling surface soils for radionuclides. Report No. C. ASTM, 983, (1983).
(3) American Society for Testing Materials (ASTM). Recommended practice for investigation and sampling soil and rock for engineering purposes. Report No. D Ann. Book of ASTM Standards (04.08) 420, ASTM, 109, (1986).
(4) GENIE-2000, Basic Spectroscopy (Standalone) V1.2A Copyright (c), Canberra Industries, (1997).
(5) Shams A. M. Issa, M. A. M. Uosif and L. M. Abd El-Salam; Radiation Protection Dosimetry; 150, 488-495, (2011).
(6) Beretka, J., Mathew, P.J.; Health Phys; 48, 87–95, (1985).
(7) Yu. K.N, Z.J,Guan., M.J, Stoks., E.C, Young; J.Environ. Radioactivity; 17, 931, (1992).
(8) UNSCEAR; In: Sources and Effects of Ionizing Radiation, Report of the General Assembly with Scientific Annexes, vol. 1 (New York); (2000).
(9) United Nations Scientific Committee on the Effect of Atomic Radiation. Sources and effects of ionizing radiation. Report to the general assembly (NY: United Nations) (1993).
(10) International Commission on Radiological Protection (ICRP), 1993. ICRP Publication 65, Annals of the ICRP 23(2). Pergamon Press, Oxford.
(11) V. Ramasamy, G.Suresh , V.Meenakshisundaram and V.Ponnusamy; Applied Radiation and Isotopes; 69 184–195, (2011)

Comparison of $^{230}Th/^{234}U$ Dating Results Obtained on Fossil Mollusk Shell from Morocco and Fossil Coral Samples from Egypt. Research of Methodological Criteria to Valid the Measured Age.

A. Choukri[a], **O. K. Hakam**[a] and **J. L . Reyss**[b]

[a] *Laboratoire de Polymères, Rayonnements et Environnement, Equipe de Physique et Techniques Nucléaires, Faculté des Sciences, P.B 133, Kenitra, Morocco.*

[b] *Laboratoire des Sciences de Climat et de l'Environnement, Domaine du CNRS, Avenue de la Terrasse 91 1958, Gif sur Yvette, France.*

e-mai: choukrimajid@yahoo.com

ABSTRACT.

Radiochemical ages of 126 unrecrystallized coral samples from the Egyptian shoreline and 125 fossil mollusk shell samples from the Atlantic coast of Moroccan High Atlas are discussed.
For corals, the obtained ages are in good agreement with the ages reported previously on urecristallized corals except in some sites where some samples are affected by a cementation of younger aragonite.
For mollusk shells, the obtained ages are in the most of cases, rejuvenated. This rejuvenation is due eventually to a post-incorporation of secondary uranium that is responsible of the wide dispersion of apparent ages of mollusk shells.

Key words *: Sea level/fossil mollusc shells/corals/Quaternary.*

INTRODUCTION

The Egyptian coast of the Red Sea is characterized by fringing reefs, since at least the middle Pleistocene. The arid to hyperarid climate of the eastern Sahara desert certainly varied according to the glacial-interglacial cycles but the tropical latitudes (24°-30° N) appear to have favoured reef development during every interglacial highstand of sea-level (1-4).

The Pleistocene reefs of the Red Sea have been among the first references concerning raised reefs (5-7). A few Sudanese, Djibouti and Egyptian coral reefs were dated before 1980 (8-10) while more published dates appeared with the last decade, many of them producing extremely wide ranges of ages for the lower raised reefs confidently referred to late Pleistocene times: from 150 to 50 ka. The most recent detailed studies of Egyptian reefs (11,12) interpreted the younger dates as clues for 5c and 5a reefs being part of above sea-level outcrops, despite the absence of effective upheaval of the 5e reef. On the other hand, an assumed rift tectonic activity during Holocene times (rift shoulder surrection or diapirism induced to mistake a late Pleistocene (5e) reef for a raised Holocene reef (13) and to refer the gypsum residual tables (culminating more than 3 m above the present littoral sabkhas) to Holocene salinas or sabkhas.

In case of absence of corals and in spite of the seminal paper by Kaufman et al. (14) demonstrating that U-series ages derived from fossil mollusk are extremely unreliable, these samples have been used to determine the sea level fluctuation ages and to establish the stratigraphic scale of palaeoenvironmental change for some costs in the word. In the Western Mediterranean Basin, following an early study by Stearns and Thurber (15) in Morocco, a large body of U-series data, derived from several species of mollusk, has accumulate as a result of work by Bernat et al. (16), Goy et al. (17), Hillaire-Marcel et al. (18, 19), Causse et al. (20), Hearty et al. (21), El Gharbaoui et al. (22), Szabo and Rosholt, (23), Reyss et al. (24), Choukri (25) and Choukri et al. (26) amongst others.

In contrast to unrecrystallized corals regarded as ideal dating materiel in the marine environment, chronological data obtained on mollusk shells are often questionable because of open-system conditions. As a matter of fact, mollusk shells contain little authigenic U: their bulk U content essentially represents early diagenetic uptake (14, 23, 26). Kaufman et al. (14) ascribed the failure in reliability of mollusk shells dating to the postmortem migration of uranium into mollusk shells. The uranium concentrations of fossil shells are usually higher than of living mollusk shells and the $^{234}U/^{238}U$ ratios are, in the most of cases, higher than was possible if their uranium was incorporated from seawater conducting so to the rejuvenation of fossil samples.

In this work, we have analyzed 125 mollusk shell samples collected from the Atlantic coast of Moroccan High Atlas at the north of Agadir City in Morocco and 126 untecristallizer fossil coral samples from the Egyptian shoreline of the north-western Red Sea. This great number allowed a significant comparison of $^{230}Th/^{234}U$ ages for samples coming from cups assumed to be geologically developed during the emerged high sea level corresponding to Holocene, 5e and 7 and/or 9 climatic stages in two different regions of the word.

INVESTIGATION AREAS AND SAMPLING

126 coral samples were collected from the emerged coral reef terraces on the Egyptian shoreline of northwestern Red Sea extending over 500 km from the Ras Gharib-Ras Shukeir depression (28°10') in the north to Wadi Lahami (north of Ras Banas, 24°10') in the south (Fig. 1). The Egyptian coasts of the north-western Red Sea and Gulf of Suez are characterized by a series of spectacular Quaternary reef-terraces which have been geologically studied by several authors (3,8,11). Holocene Coral samples were taken from terraces situated at positions between 0 and 1 m relatively to the actual sea water level. Coral samples corresponding to the 5e climatic stage (27) were taken between 4 and 8 m except in the Zeit area known to be a tilted block rotated after Pleiocene deposition where samples were taken from terraces situated between 12 and 18 m. The older Coral samples corresponding eventually to 7 and/or 9 climatic stages were collected from apparent sections of terraces situated under the 5e terraces.

125 mollusk shell samples were collected on the Atlantic coast of Moroccan High Atlas in the north of Agadir city from Agadir Harbour in the south to Tamri village in the north extending over about 50 km (Fig. 2). The studied area is known by its geological importance and its fossil mollusc shells wealth and diversity. Several geological sections on the Coast of High Atlas at the north of Agadir City have been previously described (15, 22, 25, 28-30). Some of our radiochemical results have been used in a pervious work to prove the

rejuvenation of the mollusk shell ages before developing two models to establish relationships between the real and apparent ages related to the U post-incorporation mode. The collected samples belong to a variety of species that could be fossilized in the same place.

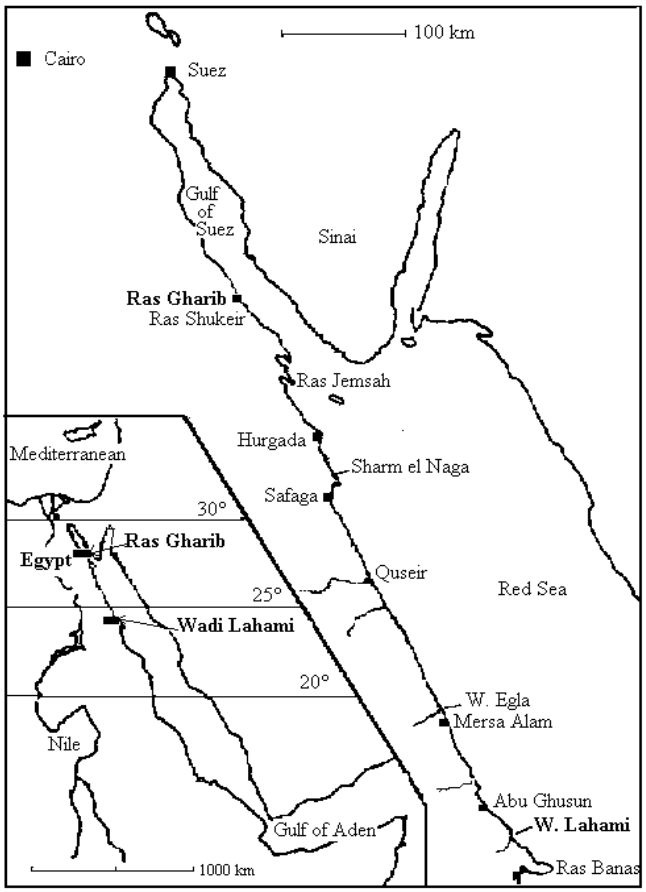

Fig.1. Localization map of studied sites on the Egyptian coast

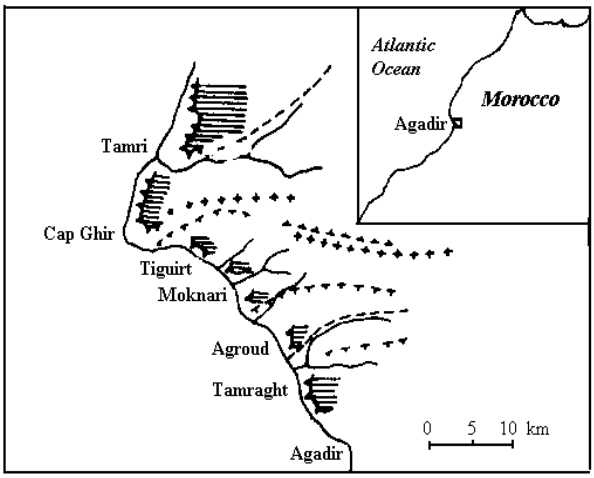

Fig. 2. Localization map of studied sites on the Moroccan coast

RESULTS AND DISCUSSION

Discussion of coral samples results

The results (ages, ^{238}U content, $^{234}U/^{238}U$ activity ratio) of radiochemical analysis obtained on coral and fossil mollusc shells samples are compared in given histograms. A study of Radiochemical data obtained by alpha spectrometry on unrecristallized fossil coral samples from the Egyptian shoreline of the north-western Red Sea has have already been realised previously (31). Radiochemical data obtained by alpha spectrometry on fossil mollusk shell samples from 5e shorelines on the Atlantic coast of High Atlas in Morocco have been also discussed (32).

The obtained ages on coral samples vary between 108.2 ka and 131.6 ka with an average of 122.2 ka. The results concerning the same sea level that have been reported by Edwards (33), Bard et al. (34) and Hamelin et al. (35) are in the range of our results. Except for samples from the Zeit area, the reef terrace is between 2 and 6 m above the present sea-level. This position is similar to the highest sea level from the last interglacial in the Caribbean and Bermuda islands as interpreted by Lambeck and Nakada (36) according to the glacio-isostatic rebound. This work proves that the large tectonic motions which affected the studied area after the Oligocene ceased since at least the last interglacial period.

On coasts tectonically stable, two sea levels are often established: the Holocene and 5e sea levels (dated respectively at about 6 ka and 122 ka). In addition to these two sea levels, an older sea level has been sometimes found (3,4). The deposits corresponding to this later was formed during sea water stagnation's before the last interglacial and a part or all of these formations have been destroyed or masked by repeated phases of erosion. The ages reported previously for these deposits are generally comprised between 170 and > 300 ka. The ages larger than 300 ka are not precise because they are beyond the dating limit of the method used.

Discussion of mollusc shell samples results

In the same way as for coral samples, results obtained for fossil mollusk shell samples from cups supposed formed during the three different stages (Holocene, 5e, 7 and/or 9) called, according to the Moroccan stratigraphy nomenclature, Mellahien, Ouljien and Harounien. In contrast to coral samples, the criteria of calcite cannot be used to cheque the closed system assumption which is the principal condition to valid the measured age. The measured calcite rates in analyzed mollusk shell samples are in the range of 0 to 100 % in independently of their species and of their origin. As for corals, the analyzed mollusk shell samples do not contain detrital material.

All the samples from the Mellahien climatic stage were taken from cups not higher than 2 m above the actual sea water. Ages measured are 0 ka for modern samples and between 6.3 and 9.7 ka with an average value of 7.51 ka for samples from the Holocene. The latter is in good agreement with Holocene ages from corals and with the previously measurements of mollusk shell samples.

All mollusc shell samples for 5e level sea were taken at altitudes between 4 and 8 m above the actual sea water on the Atlantic coast of High Atlas. The ages vary between 36.2 and 146 ka for the 5e sea level, while the ages obtained for unrecrystallized coral samples are about 122-125 ka. These results show that the ages of mollusk shell samples could be rejuvenated by a posterior incorporation of secondary uranium from the surrounding environment during the fossilization period (37).

The samples for older sea levels than 5e were taken at altitudes between 16 and 24 m above the present sea level. Deposits at these positions were recognized by some authors Weisrock (28), Stearns et al. (15), and Brebion et al. (29) at the Atlantic coast as Harounian sea level which correspond to 7 and/or 9 climatic stages. The average of ages reported previously for this level is about 260 ka (22,25,28,30). The 21 calculated ages vary between 180 and 511 ka and are in good agreement with the ages reported previously and with the average value obtained in this work for the same levels by means of coral samples.

Comparison of coral and mollusc shell samples results

The histograms of figures 3 to 6 allow a statistical comparison of the obtained ages for every level by means of both dated materials. A briefly discussion of statistical distribution of radiochemical results in coral samples from the Egyptian shoreline of the north-western Red Sea and in fossil mollusk shells from the Atlantic coast of High Atlas in Morocco and their Implications for $^{230}Th/^{234}U$ dating has already been reported (38).

The histograms of figure 3 allow the age comparison obtained in both regions for the level Holocene. They are, in spite of their small distance, comparable and the difference is also due to the uncertainties of determination of the age by alpha spectrometry. On the histogram of the mollusk shells, we also presented the results of the actual mollusc shells whose gave 0 ka.

The histograms of figure 4 allow a comparison of a significant number of ages obtained by coral samples and mollusc shell samples for the same level at two different regions.

Regarding the coral samples, the ages of this level were possible to determine. Except the rejuvenated ages because of the posterior cementation of recent aragonite, all results are in a good agreement with other studies on unrecristallised coral samples in some regions of the word. The rejuvenated ages could be avoided by detecting the secondary cementation of the recent aragonite which brings some uranium responsible for this rejuvenation.

For mollusc shell samples, the range of 5e level age is large between 36 and 146 ka, while the ages obtained for unrecrystallised coral samples are about 122 ka. These results show that the ages of mollusc shell samples could be rejuvenated by a posterior incorporation of secondary uranium from the surrounding environment during the fossilization period. They are obviously affected by the variability of values of ^{238}U contents and $^{234}U/^{238}U$ activity ratios.

The average of the obtained ages from mollusc shell samples could not be used to determine an age for the studied level because of the rejuvenation of some of them. The obtained results must be confronted to a geological context before attributing it to the formation having livered the sample.

The histograms of figure 5 show a statistical distribution of older sea levels than 5e often attributed to the 7 and/or 9 level. The ranges are in the two cases dispersed and cannot supply precise statistical ages for these levels. Furthermore, when the age exceeds 200 ka, the $^{230}Th/^{234}U$ ratio activity used to calculate the age aims gradually towards 1 and the method becomes very sensitive to the small variations, what gives wide intervals of uncertainties and contributes to obtain a wide spectre of results either for corals, or for the mollusc shells.

Nevertheless, both ranges tend to show the existence of, at least, two age groups: between 180 and 260 ka often attributed to the 7 level, between 300 and 340 ka often attributed to the 9 level and the ages oldest that 400 ka. If we take into account the reasoning made for the mollusc shells for 5e level, these ages could be also rejuvenated and the real ages could be older than apparent ages.

We have presented, separately for corals and mollusc shells, all the ages measured for the high marine levels: Holocene, 5e, 7 and/old 9 in the same histogram (figure 6).

The figure 6(a) shows that it is possible to distinguish statistically groups of age corresponding to the Holocene, the highest marine level during the last interglacial period (5 e) and two under groups corresponding possibly to older high marine levels than 5e (levels 7 and 9).

Contrary to the figure 6(a), the figure 6(b) does not allow a statistical study of the existence of these levels because of the rejuvenation of mollusc shell samples ages due to the secondary incorporation of uranium during their fossilisation.

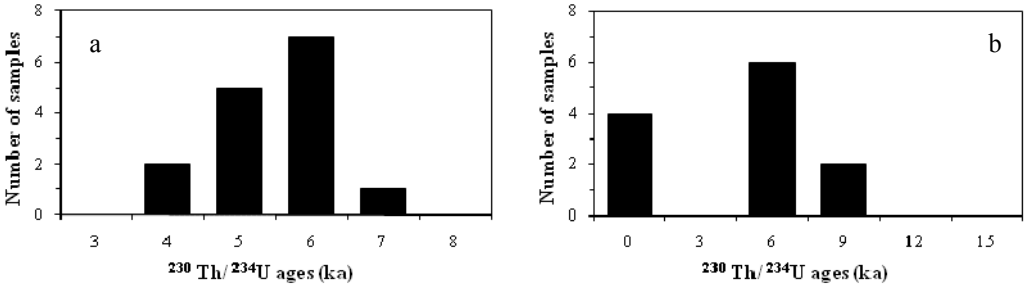

Fig. 3. Distribution histograms of ages in Holocene samples (a: corals, b : mollusc shells)

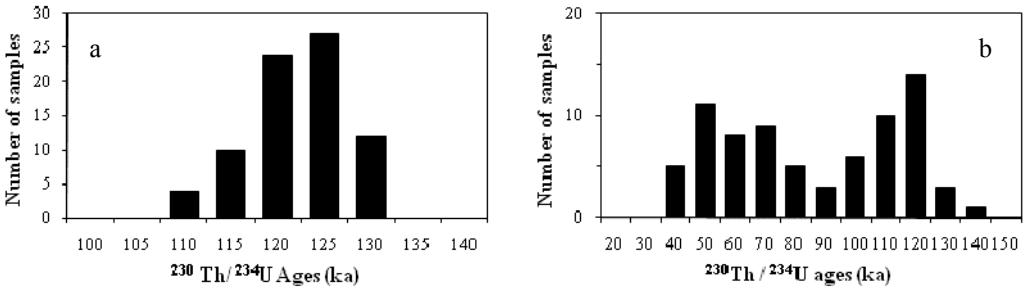

Fig. 4. Distribution histogram of ages in 5e sea level samples (a: corals, b : mollusc shells)

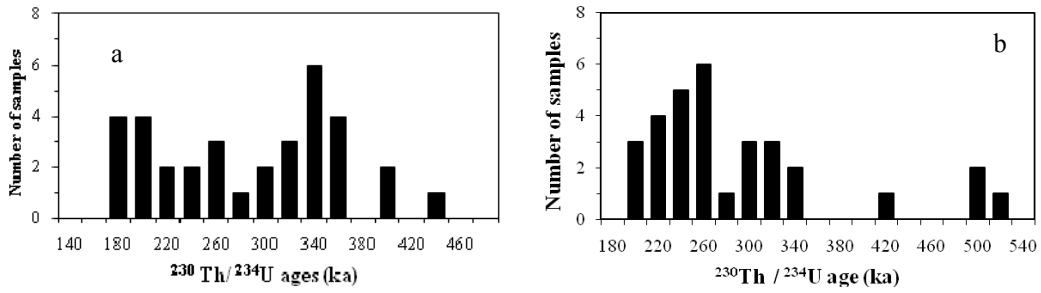

Fig. 5. Distribution histogram of ages in 7 and/or 9 level samples (a: corals, b : mollusc shells)

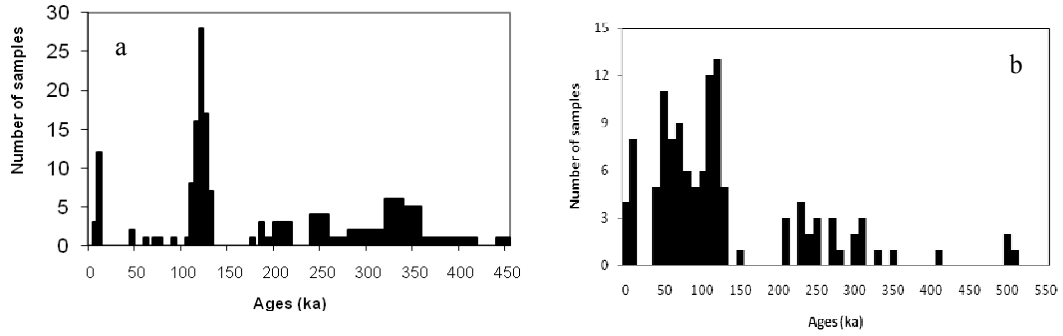

Fig. 6. Distribution histogram of all ages (a: corals, b : mollusc shells)

CONCLUSION

A study of radiochemical analysis results of 126 unrecrystallized coral samples from the Egyptian shoreline of northwestern Red Sea and on 125 fossil mollusk shell samples from the Atlantic coast of Moroccan High Atlas at the Nord of Agadir City obtained by alpha spectrometry have allowed to conclude that:

The unrecristallized corals constitute the reliable means of determining the timing of Pleistocene sea level fluctuations in the past. A statistical study of the measured ages allowed to distinguish statistically groups of age corresponding to the Holocene, the highest marine level during the last interglacial period (5e) and two under groups corresponding possibly to older high marine levels than 5e (levels 7 and 9). The average of obtained ages for each level are in good agreement with the previous measurements on the unrecristallized corals on some regions of the word. Precautions on the ground are necessary to avoid samples showing a secondary cementation of a recent aragonite which is responsible of the rejuvenation of the sample ages affected by this cementation.

For mollusc shells, the dispersed ages often found for the Ouljian level on the Moroccan coasts, do not correspond to real ages, but only to a rejuvenated ages due to a posterior incorporation of secondary uranium during the burial period. This incorporation could be continuous during the burial as it could be episodical, which explains the range of rejuvenated ages obtained sometimes for the same level. The degree of reliability of the dating

varies from a site to another according to its position and its conservation with respect to inland waters and sea water.

Contrary to the corals where some methodological indications could inform about the validity of the age, no methodological criterion is still well established. Precautions must be taken during the sampling to be able to confront the measured age to the geologic context of the formation having delivered the analyzed sample.

REFERENCES

(1) Plaziat, J. C., Baltzer, F., Choukri, A., Conchon, O., Freytet, P., Orszag-Sperber, F., Raguideau, A., Reyss, J. L., 1998. Quaternary marine and continental sedimentation in the N Red sea and Gulf of Suez (Egyptian coast). Influences of rift tectonics, climatic changes and sea-level fluctuations." In Purser B.H. & Bosence D.W. J. Eds., Sedimentation and tectonics of rift basins *:* Red Sea-Gulf of Aden, Chapman and Hall, Londres. ISBN 0412 73490 7, 537-573.

(2) Plaziat, J. C., Baltzer, F., Choukri, A., Conchon, O., Freytet, P., Orszag-Sperber, F., Raguideau, A., Reyss J. L., 1995. Quaternary changes in the Egyptian shoreline of the NW Red sea and gulf of Suez. Quaternary International 27, 11-21.

(3) Plaziat, J. C., Reyss, J. L., Choukri, A., Orszag-Sperber, F., Baltzer, F., Purser, B. H., 1998. Mise en évidence, sur la côte récifale d'Egypte, d'une régression interrompant brièvement le plus haut niveau du Dernier Interglaciaire (5 e) : un nouvel indice de variations glacio-eustatiques à haute fréquence au Pléistocène ?. Bull. Soc. Géol. France 169, 115-125.

(4) Plaziat, J.-C., Reyss, J.-L., Choukri, A., Cazala C., 2008. Diagenetic rejuvenation of raised coral reefs and precision of dating. The contribution of the Red Sea reefs to the question of reliability of the Uranium-series datings of middle to late Pleistocene key reef-terraces of the world.- Carnets de Géologie / Notebooks on Geology, Brest, Article 2008/04 (CG2008_A04)

(5) Darwin, C., 1842. The structure and distribution of coral reefs. Smith Elder and co, London, 214 p.; Project Gutenberg, Release #2690 (June 2001), URL: http://digital.library.upenn.edu/webbin/gutbook/lookup?num=2690

(6) Newton R.B., 1899. On some Pliocene and Pleistocene shells from Egypt.- *Geological Magazine*, Cambridge, (n.s.), vol. 6, 402-407.

(7) Sandford, K. S., Arkell, W.J.,1939. Paleolithic man and the Nile valley in Lower Egypt.- *Oriental Institute Publications*, Chicago, vol. XLVI; *Prehistoric Survey of Egypt and Western Asia*, Chicago.

(8) Butzer, K.W., Hansen, C. L.,1968. The coastal plain of mersa alam. *In*: butzer k.w. & hansen C.L. (eds.), Desert and river in Nubia: Geomorphology and prehistoric environments at the Aswan Reservoir. University of Wisconsin Press, Madison, p. 395-432.

(9) Veeh, H.H., Giegengack R., 1970. Uranium-series ages of corals from the Red Sea. *Nature*, London, vol. 226, n° 5241, p. 155-156.

(10) Faure, H., Hoang, C.T., Lalou, C., 1980. Datations $^{230}Th/^{234}U$ des calcaires coralliens et mouvements verticaux à Djibouti.- *Bulletin de la Société géologique de France*, Paris, (7° série), t. XXII, n° 6, 959-962.

(11) Gvirtzman, G., Buchbinder, B., Sneh, A., Nir, Y., Friedman, G.M., 1977. Morphology of the Red Sea fringing reefs, a result of the erosional pattern of the last-glacial low-stand sea level and the following Holocene recolonization, *2ème Symposium Intern. Sur les coraux et récifs coralliens fossiles. Mém. B.R.G.M.* 89, 480-491

(12) El Moursi, M., Hoang, C.T., Fahmy El Fayoumi, I., Hegab, O., Faure, M., 1994. Pleistocene evolution of the Red Sea coastal plain, Egypt: evidence from Uranium-series dating of emerged reef terraces. Quat. Sci. Rev. 13, 345–359

(13) Ibrahim, A., Rouchy, J. M., Maurin, A., Guerlorget O., Perthuisot, J. P., 1986. Mouvements halocinétiques récents dans le Golf de Suez: l'exemple de la Pénisule de Gemsah, *Bull. Soc. Géol. France* 8,177-183.

(14) Kaufman, A., Broecker, W. S., Ku, T. L., Thurber, D. L., 1971. The status of U-series methods dating. Geochimica Acta 35, 1115-1183.

(15) Stearns, C. E., Thurber, D. L., 1965. $^{230}Th/^{234}U$ Dates of the late Plioctocene Marine Fossils from Mediterranean and Moroccan Littoral. Quatenaria 7, 29-41.

(16) Bernat, M., Bousquet, J. C., Dars, R., 1978. -Io-U dating of the Oulgian stage from torre garcia (southern spain). Nature 275, 302-303.

(17) Goy, J. L., Zazo, C., Hillaire-Marcel, C., Causse, C., 1986. Stratigraphie et chronologie (U/Th) du Tyrrhénien Sud-Est de l'Espagne. Zeitschrift für Geomorphologie, 71-82.

(18) Hillaire-Marcel, C., Carro, O., Causse, C., Goy, J. L., Zazo, C., 1986. Th/U dating of Strombus bubonius bearing marine terraces in south-eastern Spain. Geology 14, 613-616.

(19) Hillaire-Marcel, C., Gariépy, C., Ghaleb, B., Goy J. L., Zazo, C., Barcelo, J. C., 1996. U-Series Measurement in Tyrrhenian deposit from Mallorca-Further evidence for two Last-Interglacial high sea levels in the Balearic Islands. Quaternary Science Reviews 15, 53-62.

(20) Causse, C., Goy, J. L., Zazo, C., Hillaire-Marcel, C., 1993. Potentiel chronologique (Th/U) de faunes Pléistocènes méditerranéennes: exemple des terrasses marines des régions de Murcie et Alicante (Sud-Est de l'Espagne). Geodinamica Acta 6 (2), 121-134.

(21) Hearty, P. J., Hollin, J. T., Dumas, B., 1986. Geochronology of Pleistocene littoral deposits on the Alicate and Almeria coasts of Spain. In: Zazo C. Ed., Late Quaternary sea Level Changes in Spain. Tab. Sobre Neogeno-cuaternario, Madrid, Spain, v. 10, 95-107.

(22) El-Gharbaoui, A., Choukri, A., Berrada, M., Falaki, H., Reyss, J. L., 1994. Datation de deux niveaux marins sur la côte du Haut Atlas atlantique à 275 000 ans et 120 000 ans. Cahiers de Géographie du Québec 38 (104), 241-247.

(23) Szabo, B. J., Rosholt, J. N., 1969. Uranium-series dating of Pleistocene molluscan shells from southern California- An open system model. Journ. of Geophys. Res. 74 3253-3260.

(24) Reyss, J. L., Choukri, A., Plaziat, J. C., Purser, B. H., 1993. Datations radiochimiques des récifs coralliens de la rive occidentale du Nord de la Mer Rouge, premières implications stratigraphiques et tectoniques. C. R. Acad. Sci. Paris 317, 487-491.

(25) Choukri, A., 1994. Application des méthodes de datation par les séries d'uranium à l'identification des hauts niveaux marins sur la côte égyptienne de la mer rouge en

moyen de coraux, radioles d'oursins et coquilles, et sur la côte atlantique du Haut Atlas au Maroc, au moyen de coquilles." Thèse d'Etat, Univ. Med V, Rabat, pp. 192.

(26) Choukri, A., Reyss, J. L., Plaziat, J. C., Orszag-Sperber, F., Berrada, M., 1995. Reliability of Sea Level Dating using Th/U Method for Mollusks from the west coast of red sea and from the Atlantic coast of Moroccan High Atlas. Appl. Radiat. Isot. 46, n° 6/7, 653-654.

(27) Martinson, D. G., Pisias, N. G., Hays, J. D., Imbrie, J., Moore, T. C., Schackleton, N. J., 1987. Age dating and the orbital theory of ice ages: development of a high-resolution from 0 to 300 000-years chronostratigraphy. Quaternary Research 27, 1-29.

(28) Weisrock, A., 1980. Geomorphologie et Pleoenvironnements de l'Atlas atlantique (Maroc). Thèse d'Etat, Paris I, pp. 931.

(29) Brebion, P., Hoang, C.T., Weisrock, A., 1984. Intérêt des coupes d'Agadir-port pour l'étude du pléistocène supérieur marin du Maroc." Paris, Bull. Mus natn. Hist. nat., 4° sér., 6 section C, n° 2, 129-151.

(30) Meghraoui, M., Outtani, F., Choukri, A., De Lamotte, D. F., 1998. Coastal Tectonics across the South Atlas Thrust Front and the Agadir Active Zone, Morocco. In: Stewart, I. S. & Vita-Finzi, C.(eds) Coastal Tectonics. Geological Society, London, Special Publications 146, 239-253.

(31) Choukri, A., Hakam, O. K., Reyss, J. L., Plaziat J. C., 2007. Radiochemical dates obtained by alpha spectrometry on fossil mollusk shell from the 5e Atlantic shoreline of the High Atlas, Morocco, *Applied Radiation and Isotopes 65, 883-890*.

(32) Choukri, A., Hakam, O. K., Reyss, J. L., Plaziat, J. C., 2007. Radiochemical data obtained by _ spectrometry on unrecrystallized fossil coral samples from the Egyptian shoreline of the north-western Red Sea." *Radiation Measurements 42, 271-280*

(33) Edwards, R. L., 1988. High precision of thorium-230 ages of corals and the Timing of sea level fluctuations in the late Quaternary. PhD Thesis, California Institute of Technology, pp. 347.

(34) Bard, E., Hamelin, B., Fairbanks, R. G., 1990. U-ages obtained by mass spectrometry in corals from Barbados, Sea Level during the past 130.000 years. Nature 345, 405-410.

(35) Hamelin, B., Bard, E., Zindler A., Fairbanks R. G., 1991. $^{234}U/^{238}U$ mass spectrometry of corals: how accurate is the U-Th age of the last interglacial period?. Earth Plan. Sci. Lett. 106, 169-180.

(36) Lambeck, K., Nakada, M., 1992. Constraints on the age and duration of the last interglacial period and on sea-level variations. Nature 357, 125-128.

(37) Choukri, A., Jahjouh, E., Semghouli, S., Hakam, O. K., Reyss, J. L., 2001. Influence of uranium post-incorporation on the fossil mollusk shell age rejuvenation: Application to the study of the marine level variation in the past." Physical & Chemical News 1, 92-96.

(38) Choukri, A., Reyss, J. L., Hakam, O. K., Plaziat, J. C., 2002. A statistical study of ^{238}U and $^{234}U/^{238}U$ distributions in coral samples from the Egyptian shoreline of the north-western Red Sea and in fossil mollusk shells from the Atlantic coast of High Atlas in Morocco: Implications for $^{230}Th/^{234}U$ dating." Journal of Radiochemica Acta 90, 329-336.

Measurement of Natural Radioactivity in Beach Sediments From Aden Coast on Gulf of Aden, South of Yemen.

S. Harb*, A. H. El-Kamel, A. M. Zahran ** , A. Abbady*, and F.A.A AS-SUBAIHI**.**

** Physics department, Faculty of Science, Qena 83523, South Valley University.Eygpt*

***Physics department, Faculty of Science Assiut University, Egypt*

ABSTRACT

The distribution of natural gamma emitting ^{238}U, ^{232}Th and ^{40}K radionuclides in beach sediments along Aden coast on Gulf of Aden, South of Yemen has been carried out using a NaI(Tl) gamma ray spectrometric technique. The mean activity concentrations of measured radionuclides were compared with other literature values. The absorbed dose rate, annual effective dose equivalent, external hazard index and representative level index were calculated and compared with internationally recommended values.

Keywords: *Radionuclides, absorbed dose rate, hazard indices, representative level*

INTRODUCTION

The naturally occurring radionuclides are relatively and uniformly distributed in the seas and the oceans. Human activities like mining and milling of mineral ores, ore processing and enrichment, nuclear fuel fabrication and handling of the fuel cycle tail end products cause release of additional amounts of natural radionuclides into the environment. Also, the discharge into the sea of low level waste from nuclear industry has become a source of contamination in the marine coastal environment of countries possessing nuclear power plants and nuclear reprocessing plants (Akram, *et al.*, 2007).

Most of the radioactivity deposited on surface sediments is washed by rains and drained through rivers to the oceans. Part of the ground deposited activity is absorbed in the soils and percolates with the underground waters to the oceans. Radionuclides reaching the ocean become part of the marine ecosystem (water, sediments, and biota) and may transfer through seawater-sediment-biota interface to human beings (Akram, *et al.*, 2006). Accumulation of such substances in the marine costal environment raises many problems concerning safety of biotic life, food chain and ultimately humans. To address these problems, assessment of radioactivity concentration in the marine environment is essential. It is necessary to quantify the distribution of radionuclides in the main marine constituents (sea water, sea sediments and marine organisms) and to assess radiological impacts of the detected radionuclides on human health. Beach sediments are mineral deposits formed through weathering and erosion of either igneous or metamorphic rocks. Among the rock constituent minerals are some natural radionuclides that contribute to ionizing radiation exposure on Earth. Natural radioactivity in soils comes from U and Th series and natural K.

The study of the distribution of primordial radionuclides allows the understanding of the radiological implication of these elements due to the gamma-ray exposure of the body and irradiation of lung tissue from inhalation of radon and its daughters (Uosif, *et al.*, 2008).

During the last few decades, the coastal environment of Aden coast Gulf of Aden, South of Yemen has experienced intense developments in industry, tourism, transport, urbanization and aquaculture.

This paper reports the activity concentrations of natural radionuclides ^{238}U, ^{232}Th and ^{40}K, for beach sediments of Aden coast on Gulf of Aden, South of Yemen. The objective of this paper is to evaluate the radiological hazards due to natural radioactivity associated with beach sediments by calculating the absorbed dose rate, annual effective dose rate, representative level index and external hazard index.

MATERIALS AND METHODS

This study took place in Aden coast, South of Yemen is on Gulf of Aden (figure 1). The total study area spread over from Kawa (Lat: 12º 44' 472"N; Long 44º 28'367"E) to Alalam beach (Lat: 12º 50' 759"N; Long 45º04'452"E), which covers an area about 150km. The tidal range is 1.2-1.5m for spring tides and 0.3-0.6m for neap tides.

Sample collection and preparation: Beach sediment samples were collected during January 2012. The total study area covers about 150km, from which at the distance of 2-3km interval, 44 sampling locations [S_1-S_{44}] are selected. The exact position of each sampling site was recorded using Hand held GARMIN GPS (Global Positioning System, Model no 12).The samples were collected from 10-20m away from the high tide, when it makes towards the road side. Five samples were collected from each site covering an area of one meter square, at a depth of 5cm and packed in plastic pouches.

The collected samples were dried in an oven at 100-110ºC for about 24h and sieved through a 2-mm mesh-size sieve to remove stone, pebbles and other macro-impurities. The homogenized sample was placed in a 400g airtight PVC container. The inner lid was placed in and closed tightly with outer cap. The container was sealed hermetically and externally using cellophane tape and kept aside for about a month to ensure equilibrium between Ra and its daughter products before being taken for gamma ray spectrometric analysis (Ramasamy, *et al.,* 2004).

Gamma spectroscopic analysis: To estimate the activity levels of the ^{238}U, ^{232}Th and ^{40}K in the samples, a gamma ray spectrometer in Environmental Radioactivity Measurements Laboratory (ERML), physics department, Faculty of Science, University of south valley, Qena. was used in the present investigations. NaI(Tl) crystal detector of size 3" X 3" along with a 8K multi channel analyzer was used to record the gamma spectra.

The energy calibration of the spectrometer was performed using the 1-l Marinelli calibration sources, which contained well-known standard sources (^{137}Cs, ^{60}Co, ^{57}Co, and ^{241}Am).

The absolute efficiency of the detector was determined accurately to evaluate the radionuclide concentrations precisely. This was undertaken using multinuclide standard sources distributed in a sand matrix to be homoconditioned with the investigated soil samples. These standards were obtained from Radioactivity Measurements Laboratory (ERML), physics department, Faculty of Science, University of south valley, Qena. With the counting time of 10,000 seconds for each sample, the below detectable limit (BDL) limits were 21.2Bqkg^{-1} for ^{40}K, 5.5 Bqkg^{-1}for ^{238}U and ^{232}Th.

To determine the radioactivity concentration in the soil samples, each sample was placed on the NaI(Tl) detector and counted for the same counting time (12 h). It was found that the detected gamma lines belong to the naturally occurring series radionuclides and a non-series natural radionuclide ^{40}K.

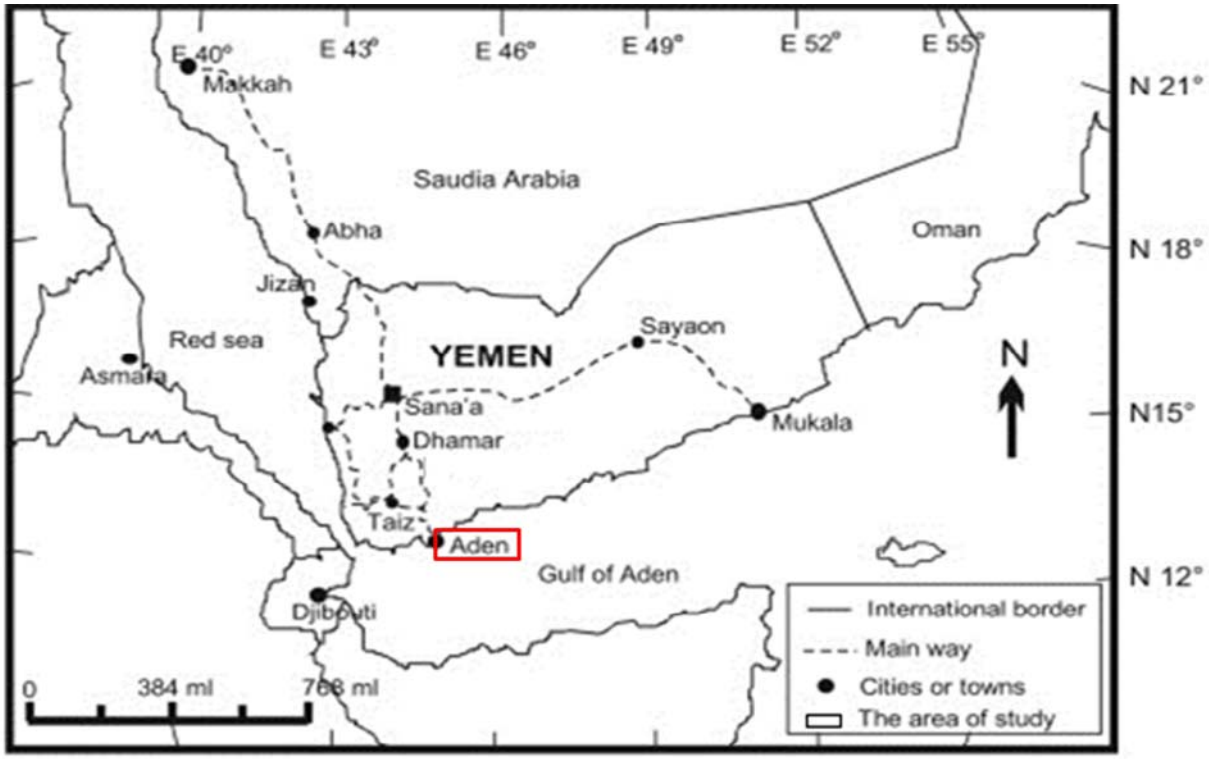

Fig.1: Geographic location of Aden coast Gulf of Aden, South of Yemen where the beach sediment samples were collected.

Calculation of elemental concentration

Count rates for each detected photo peak and activity for each of the detected nuclides are calculated. The specific activity (in Bq.kg-1), A_{Ei} of a nuclide i. and for a peak at energy E, is given by:

$$A_{Ei} = \frac{NP}{t_c . I_\gamma (E_\gamma) . \varepsilon (E_\gamma) . M} \quad (1)$$

Where *NP* is the number of count in a given peak area corrected for background peaks of a peak at energy *E,* $\varepsilon(E_\gamma)$ the detection efficiency at energy E, t_c is the counting lifetime, $I_\gamma(E_\gamma)$ the number of gammas per disintegration of this nuclide for a transition at energy *E,* and *M* the mass in kg of the measured sample.

Under the assumption that secular equilibrium was reached between ^{232}Th and ^{238}U and their decay products, the γ-ray transitions to measure the concentration of the assigned nuclides in the series (EML, 1990) are as follows:
(a) ^{214}Bi (609.31, 1120.3 and 1764.49 keV), ^{214}Pb (295.22 and 351.93 keV) for uranium-238.
(b) ^{208}Tl (583.19 and 2614.53 keV), ^{212}Pb (238.63Kev), ^{228}Ac (911.20keV) for the thorium series
(c) ^{40}K (1460.83 keV) for potassium.

Calculation of radiological effects:

Dose rate calculation: The absorbed dose rate was calculated from the measured activities of ^{238}U, ^{232}Th and ^{40}K in the surface sediment samples using the below formula (Papaefthymiou, *et al.,* 2008).

$$\mathbf{D\ (nGy\ h^{-1}) = 0.462\ C_U + 0.604 C_{Th} + 0.042 C_K} \qquad \mathbf{(2)}$$

Where D is the absorbed dose rate (nGy h^{-1}). C_U , C_{Th} and C_K are the activity concentrations (Bqkg^{-1}) of ^{238}U, ^{232}Th and ^{40}K respectively.
To estimate the annual effective dose rates, the conversion coefficient from absorbed dose to effective dose, 0.7SvGy^{-1} and outdoor occupancy factor of 0.2 proposed by UNSCEAR, 2000 were used. The effective dose rate in units of mSv y^{-1} was calculated by the following formula

$$\mathbf{Effective\ dose\ rate\ (m\ Sv\ y^{-1}) = D\ (nGy\ h^{-1})\ x\ 8760\ h\ x\ 0.2\ x\ 0.7\ SvGy^{-1}\ x\ 10^{-6}} \qquad \mathbf{(3)}$$

Calculation of hazard indexes: The external hazard index, H_{ex} , is defined as (Marija Jankovic *et al.,* 2008).

$$\mathbf{H_{ex} = (C_U/370 + C_{Th}/259 + C_K/4810) \leq 1} \qquad \mathbf{(4)}$$

An additional hazard index so called representative level index is calculated by using the formula (V.Ramasamy *et al.,* 2009).

$$\mathbf{I_{\iota r} = (C_U/150 + C_{Th}/100 + C_K/1500)} \qquad \mathbf{(5)}$$

Where C_U , C_{Th} and C_K are the specific activities (Bqkg^{-1}) of ^{238}U, ^{232}Th and ^{40}K, respectively. The value of these indexes must be less than unity in order to keep the radiation hazard insignificant.

RESULTS AND DISCUSSION

The results of analysis of activity concentration of ^{238}U, ^{232}Th and ^{40}K radionuclides in beach sediment samples for different locations of the study area are presented in table 1. Activity is reported in Bqkg^{-1} on the basis of the sediment's dry weight. The measured activity concentrations range from 9.41±0.365 to 120.11±4.6 Bqkg^{-1} for ^{238}U, 5.12±0.3 to 109.59±6.6Bqkg^{-1} for ^{232}Th and 179.66±15.4 Bqkg^{-1} to 1183.05±102 Bqkg^{-1} for ^{40}K.

The maximum activity concentration of ^{238}U (120.113±4.6 Bqkg^{-1}) and ^{232}Th (109.59±6.6 Bqkg^{-1}) were observed in Amran and Al-Akil station beach (S-4) and (S-38), which is two of the famous historical and tourism places. The highest activity concentration of ^{40}K (1183.05±102Bqkg^{-1}) was found in Amran beach (S-4) nearer to little Aden city. The lowest concentration of all radionuclides was found at Road sea Bridge beach (S-31) (table 1), which may be due to high composition of Si (M arija Jankovic, *et al.,*2008).
Table 3 presents the absorbed dose rate, annual effective dose equivalent, external hazard index and representative level index values. The calculated absorbed gamma dose rate varied from 142.29 nGy h^{-1} (S-4, Amran beach) to 14.98 nGy h^{-1} (S- 31, Road sea Bridge beach) with a mean of 78.01 nGy h^{-1} . The mean absorbed dose rate is found to be 1.53 times the world average value (51 nGy h^{-1}: UNSCEAR, 2000). The calculated values of annual effective dose rate ranging from 0.073 to 0.69 mSv, with a mean value of 0.38 mSv, which is lower than the world average value of 0.48mSv (UNSCEAR, 2000). The calculated value of external hazard index ranges from 0.08 to 0.82.The representative level index value being 0.23 to 2.26, with the average of 1.22, higher than the world average (0.66 Bq kg^{-1}: V.Ramasamy *et al.,* 2009).

Large variation among the radioactivity concentration for different sites has been observed. It may be due to geological condition and drainage pattern of the study area. According to Harb (2008), large variation of radionuclides in beach sediments may be due to the continuous wave action, as the waves reaches up to about 10m from the waterline during high tide and results in the fresh deposition of heavy minerals along the seashore. The high values could be explained as due to the presence of black sands, which are enriched in the mineral monazite containing a significant amount of ^{232}Th. The enrichment occurs because of the specific gravity of monazite allows its concentration along beaches where lighter materials are swept away (Uosif, *et al.,* 2008). The mean activity concentrations of ^{238}U, ^{232}Th and ^{40}K is 1.8, 1.9 and 1.7 times the world average values (UNSCEAR, 2000). Table 2 shows the comparison of observed activity concentration of ^{238}U, ^{232}Th and ^{40}K in the present samples with literature values of different beaches.

Table 1: Geographical location and activity concentration of ^{238}U, ^{232}Th and ^{40}K in the beach sediment samples of Aden coast on Gulf of Aden, South of Yemen.

S. no	Name of the site	Latitude	Longitude	Activity concentration (Bq/ kg)		
				^{238}U	^{232}Th	^{40}K
1	Kawa	12°44’.472	44°28’.367	69.74±2.68	77.56±4.7	1137.7±97.8
2	Mashhor	12°48’.395	44°33’.239	104.78±4.1	69.82±4.2	1076.4±92.6
3	Al-mansa	12°48’.302	44°40’.451	85.66±3.29	56.35±3.4	984.24±84.7
4	Amran	12°45’.273	44°43’.665	57.18±2.20	109.59±6.6	1183.1±102
5	Amran*	12°45’.277	44°44’.100	13.3375	14.32±0.87	291.45±25.1
6	Ras-Amran	12°44’.863	44°43’.162	18.33±0.71	36.89±2.25	542.64±46.7
7	Fakam	12°46’.351	44°47’.882	67.43±2.61	69.35±4.2	1063.1±91.4
8	Fakam*	12°44’.939	44°49’.648	15.1±0.58	47.51±2.9	444.17±38.2
9	Nasser houses	12°44’.163	44°52’.558	10.4±0.40	24.52±1.49	336.73±28.9
10	Al-adeer	12°44’.109	44°50’.055	34.1±1.31	31.63±1.93	451.38±38.8

11	Al-adeer Rest.	12°43’.988	44°53’.091	34.5±1.33	38.35±2.33	283.02±24.3
12	Koad-Anamer	12°44’.966	44°53’.468	20.7±0.81	29.1±1.77	236.69±20.4
13	Koad-Anamer*	12°45’.091	44°53’.957	14.98±0.58	17.13±1.04	390.54±33.6
14	Al-hisa	12°44’.789	44°54’.372	61.78±2.38	22.84±1.39	326.20±28.1
15	Br-Bra	12°44’.814	44°54’.839	22.57±0.87	49.11±2.99	354.67±30.5
16	Bridge	12°46’.459	44°53’.450	95.9±3.69	63.37±3.86	592.71±50.9
17	Al-farsi	12°47’.170	44°53’.698	37.26±1.10	35.39±2.15	616.56±53.1
18	Al-farsi*	12°46’.811	44°53’.679	22.66±0.68	35.99±2.19	794.46±68.3
19	Army comb	12°47’.901	44°53’.963	53.4±1.53	50.443±3.07	270.09±23.2
20	Gas station	12°48’.210	44°54’.154	47.097±1.8	48.6854±2.9	564.77±48.6
21	Iron factory	12°48’.474	44°54’.341	53.788±2.1	49.3226±3.0	478.89±41.2
22	Radio-station	12°48’.911	44°54’.744	60.66±2.3	42.291±2.58	689.23±59.3
23	Radio-station*	12°49’.105	44°54’.946	32.82±1.6	53.288±3.2	614.73±52.9
24	Power station	12°49’.458	44°55’.951	71.20±2.75	58.593±3.56	804.07±69.2
25	Ashaab city	12°49’.532	44°56’.243	47.66±1.8	65.27±3.98	751.15±69.6
26	Al-haswa Bridge	12°53’.955	44°58’.726	46.81±1.8	52.8038±3.2	688.55±59.2
27	Al-kasir Hotel	12°49’.642	44°57’.085	58.9±2.2	78.35±4.78	794.27±68.3
28	Anma City	12°49’.980	45°02’.914	69.94±2.6	43.96±2.60	739.21±63.6
29	haswa Mahmyia	12°49’.599	44°58’.058	54.44±2.1	60.86±3.70	664.10±57.1
30	haswa Mahmyia*	12°49’.469	44°58’.588	56.85±2.2	44.501±2.70	679.06±58.4
31	Roadsea Bridge	12°50’.564	45°00’.233	9.41±0.363	5.120±0.30	179.66±15.4
32	Labor Island	12°48’.656	45°01’.419	28.02±1.0	49.303±3.0	341.17±29.3
33	Al-arosa Rest.	12°46’.646	44°58’.764	26.16±1.0	9.598±0.58	226.09±19.4
34	Al-feel Gulf	12°46’.527	44°59’.076	29.17±1.1	36.124±2.21	474.04±40.8
35	Goldmor	12°49’.640	44°57’.084	51.87±2.0	28.3202±1.7	527.44±45.4
36	Golden club	12°46’.054	44°59’.374	50.5±1.9	30.39±1.8	781.46±67.2
37	Seara	12°46’.601	45°02’.758	93.32±3.59	50.37±3.1	721.89±62.1
38	Al-Akil station	12°47’.643	45°02’.383	120.11±4.6	49.27±3.01	931.32±80.1
39	Mercureo Hotel	12°48’.206	45°02’.478	51.57±1.98	102.91±6.28	1006.9±86.1
40	Aden University	12°48’.854	45°02’.619	26.92±1.03	20.21±1.23	922.65±79.4
41	Kornish Kahtan	12°49’.431	45°02’.747	21.80±0.8	82.56±5.03	796.48±68.5

42	Aden airport	12°49'.979	45°02'.914	25.93±1.0	41.17±2.5	775.36±66.7
43	Al-areish	12°50'.854	45°03'.216	41.90±1.6	80.056±4.88	1135.1±97.6
44	Al-alim	12°50'.759	45°04'.452	21.80±0.6	82.56±5.03	796.48±68.5
Aden Beach			Mean	46.32817	48.755	646.8159
			Minimum	9.41±0.36	5.12±0.30	179.66±15.4
			Maximum	120.11±4.6	109.59±6.6	1183.1±102

Table 2: Comparison of activity concentrations of ^{238}U, ^{232}Th and ^{40}K in beach sediment samples of Aden coast on Gulf of Aden, South of Yemen and other studies in different beaches of the world.

S. no	Location	Mean activity concentration (Bq/ kg)			Reference
		^{238}U	^{232}Th	^{40}K	
1	World	25	25	370	UNSCEAR2000
2	India	28.67	63.83	327.6	UNSCEAR2000
3	Beach sand Egypt	------	177	815	Uosif et al (2008)
4	Beach sand Read sea coast Egypt	23.1	7.2	338	Harb (2008)
5	Hungary	28.67	27.96	302.4	UNSCEAR2000
6	Kuwait	36	6	227	Al-Azmi (2002)
7	Nigeria	16	24	35	Arogunjo et al (2004)
8	Kalpakkam in Tamiln adu India	112	1455.8	351	Kannan et al (2002)
9	Ulla l in Karna taka , India	374	158	158	Radhakrishna et al (1993)
10	North east coast of Tamiln adu, India	7.82	24.52	274.87	Ramasamy et al (2009)
11	Aden coast on Gulf of Aden, south Yemen	46.32817	48.755	646.8159	Present study

Table 3: The Absorbed dose rate, Annual effective dose rate and Hazard indices of all sites

Site number	Absorbed dose rate (nGy h^{-1})	Annual effective dose rate(m Sv y^{-1})	Hazard indices	
			H_{ex}	Iγr
1	126.8561	0.622305	0.724514	1.9991
2	135.7909	0.666136	0.776562	2.11437
3	114.9546	0.563921	0.653743	1.790827
4	142.2989	0.698061	0.823632	2.265818
5	25.23639	0.1238	0.141306	0.400214
6	53.54431	0.262667	0.304809	0.852915
7	117.6911	0.577345	0.671031	1.85178
8	54.31315	0.266439	0.316507	0.871674
9	33.76149	0.16562	0.192811	0.539084
10	53.7837	0.263841	0.307934	0.844074
11	51.0126	0.250247	0.300292	0.802525
12	37.07291	0.181865	0.217455	0.58665
13	33.67471	0.165195	0.187848	0.531601
14	56.04537	0.274936	0.323019	0.857844
15	54.98382	0.269729	0.324336	0.877978
16	107.4817	0.527262	0.627124	1.668268
17	64.48495	0.316337	0.365525	1.013337
18	65.5799	0.321709	0.365405	1.040698
19	66.48999	0.326173	0.395282	1.040603
20	74.88584	0.36736	0.432683	1.177358
21	74.75433	0.366715	0.435369	1.171073
22	82.51668	0.404794	0.470524	1.286802
23	73.16886	0.358937	0.422259	1.161521
24	102.0573	0.500652	0.585837	1.596669
25	92.99306	0.456187	0.536999	1.47124
26	82.44107	0.404423	0.473552	1.299171
27	107.8615	0.529125	0.626636	1.705209
28	89.91965	0.44111	0.512493	1.398812
29	89.80941	0.440569	0.520222	1.414367
30	81.66686	0.400625	0.466662	1.276762
31	14.98583	0.073514	0.082553	0.233711
32	57.05694	0.279899	0.337039	0.907329
33	24.67547	0.121048	0.137483	0.376346
34	55.20959	0.270836	0.316892	0.871798
35	63.2227	0.310145	0.359194	0.980641
36	74.48744	0.365406	0.416169	1.161246
37	103.859	0.509491	0.59679	1.60713
38	124.3679	0.610099	0.70849	1.914352
39	128.2731	0.629256	0.746051	2.044165
40	63.40239	0.311027	0.342652	0.996783
41	93.39749	0.458171	0.543318	1.502039
42	69.41608	0.340528	0.390265	1.101548

43	115.3858	0.566037	0.658329	1.836624
44	23.07392	0.113191	0.133421	0.370737
Average	78.0179	0.382725	0.447928	1.227615
Minimum	14.98583	0.073514	0.082553	0.233711
Maximum	142.2989	0.698061	0.823632	2.265818

CONCLUSION

The data obtained in the present work cover a wide area in the Aden coast on Gulf of Aden south of Yemen, which can be considered as the base-line of the region. The lowest concentration of uranium (9.41±0.36 Bq Kg-1) was observed in Road sea Bridge beach sediment, and the highest (120.11±4.6 Bq Kg-1) in Al-Akil station sediment. Similarly, the lowest (5.12±0.30 Bq Kg-1) and highest (109.59±6.6 Bq Kg-1) levels of ^{232}Th were found in Road sea Bridge sediment and Amran sediment. This indicates that the radioactive minerals are distributed erratically. The lowest (179.66±15.4 Bq Kg-1) and highest (1183.1±102 Bq Kg-1) levels of ^{40}K were found in Road sea Bridge sediment and Amran sediment, respectively. Similarly, The total absorbed radionuclides from ambient air ranges from 14.98 nGy h-1 to 142.29 nGy h-1 with an average of 78.01nGy h-1. The highest dose rates were found in Amran, which were higher than the international recommended limit. Values of annual effective dose range from 0.073 mSv/year to 0.69 mSv/year with an average of 0.38 mSv/year which were higher than the international recommended limit. Values of I_{yr} range from 0.23 Bq/kg to 2.26 Bq/kg with an average of 1.22 Bq/kg which were higher than the international recommended limit. While the Hazard index values range from 0.082to 0.82 which were lower than the international recommended limit. Therefore the present study has pointed out the area under study need further studies in order to better understand the origin and distribution of naturally occurring radionuclide.

REFERENCE

(1) **Akram**, M., Qureshi, M.Riffat, N. Ahmad and T.J. Solaija, 2007. Determination of gamma-emitting radionuclides in the inter-tidal sediments off Baluchistan (Pakistan) coast, Arabian Sea. Radiation Protection Dosimetry. 123: 268-273.

(2) **Akram**, M., M. Riffat, Qureshi, N. Ahmad and T.J. Solaija, 2006. Gamma-emitting radionuclides in the shallow marine sediments off the Sindh Coast, Arabian Sea. Radiation Protection Dosimetry, 118:440-447.

(3) **Arogunjo**, A.M., I.P.Farai and I.A. Fuwape, 2004. Dose rate assessment of terrestrial gamma radiation in the delta region of Nigeria. Radiation Protection Dosimetry, 108: 73-77.

(4) **Ramasamy**, V. *et al.,* 2009. Natural Measurement of Natural Radioactivity In Beach Sediments From North East Coast of Tamilnadu, India. Applied Sciences, Engineering and Technology 1(2): 54-58.

(5) **Kannan**, V., M.P. Rajan., M.A.R.Iyengar and R.Ramesh, 2002. Distribution of natural and anthropogenic radionuclides in soil and beach sand samples of Kalpakkam (India) using hyper pure germanium (HPGe) gamma ray spectrometry. Applied Radiation and Isotopes, 57: 109-119

(6) **Papaefthymiou**, H. and M. Psichoudaki, 2008. Natural radioactivity measurements in the city of Ptolemais.Journal of Environmental Radioactivity. 99: 1011-1017

(7) **Radhakrishna**, A.P., H.M. Somashekarappa, Y. Narayana and K.A. Siddappa, 1993. New natural background radiation area on the South West Coast of India. Health Physics, 65: 390-395.

(8) **Ramasamy**, V., S. Murugesan and S. Mullainathan, 2004. Gamma-ray spectrometric analysis of primordial radionuclides in sediments of Cauvery River in Tamilnadu, India. Ecologica, 2: 83-88.

(9) **Saad**, H.R. and D.Al-Azmi, 2002. Radioactivity concentrations in sediments and their correlation to the coastal structure in Kuwait. Applied Radiation and Isotopes, 56: 991-997

(10) **United Nations** Scientific Committee on the Effects of Atomic Radiation, 2000. Sources, effects and risks of ionizing radiation, report to the General Assembly, with annexes. (New York, NY: United Nations) (UNSCEAR 2000).

(11) **Uosif**, M.A.M., A.El-Taher and Adel G.E. Abbady, 2008. Radiological significance beach sand used for climate therapy from Safaga, Egypt. Radiation Protection Dosimetry, 131:331-339

Correlation Between The Concentrations of The Heavy Minerals and The Terrestrial Radioactivity at El Massaid and El Kharrouba, Sinai, Egypt

Y. A. Abdel-Razek, A. A. Abu-Diab, and A. F. Bakhit
Nuclear Materials Authority
ya_sien@hotmail.com

ABSTRACT

Two areas at El Massaid beach and El Kharrouba sand dunes were studied to investigate the concentrations of the heavy minerals and the terrestrial radioactivity in the sands at these areas. The value of the percentage concentration of the heavy minerals in the sands at El Massaid beach ranged between 3.56 % and 14.68 % with an average of 7.10 % while the value of the percentage concentration of the heavy minerals in the sands at El Kharrouba was in the rang 1.06 and 9.23 % with an average of 4.58 %. These values declare economic concentrations of the heavy minerals. The average of the total activity concentration in the sands at El Massaid beach due to the terrestrial radionuclides ^{238}U, ^{232}Th, ^{40}K and ^{226}Ra was 50.37 Bq/kg and the average of the total activity concentration in the sands at El Kharrouba sand dunes was 112.3 Bq/kg. However, the variation of the activity concentration in the sands at both El Massaid and El Kharrouba showed positive relations with the variation of the percentage concentration of the heavy minerals. Also, the orthoclase feldspar reflected the typical concentration of potassium in the beach sands.The average annual effective dose due the probable use of the sands at El Massaid beach and El Kharrouba sand dunes were estimated to be 0.616 and 0.662 mSv, respetively. These values are lower than the reported worldwide public effective dose. Generally, the low exposures from the terrestrial radioactivity in the sands at El Massaid beach and at El Karrouba indicate the safe use of these sands as building materials.

Key Words: *Black sands/ Public exposure/ Radon gas/ Effective dose.*

1. INTRODUCTION

The Egyptian black sands occur along the northern coastal plain from Abu Qir in the west to Rafah in the east. The area of these sands is considered as one of the important mineral resources in Egypt. The detritus of these deposits were originally derived from the metamorphic rocks composing the Ethiopian plateau, beside the minor contribution from the igneous rocks of the south Sudan and the Red Sea mountains range. They consist of heavy economic minerals such as magnetite, ilmenite, hematite, zircon, rutile, monazite and garnet beside other gangue minerals called the green silicates. Magnetite and ilmenite is the main constituent in the heavy economic part. Minor traces of heavy economic minerals like casseterite, gold and sillimanite are present. Two of these heavy economic minerals, zircon and monazite, are radioactive beside xenotime and uranothorite[(1)].

However, the sands at the coastal plain contain some lighter minerals as the orthoclase feldspar which has the potassium as a major constituent.

One studied sand dunes area at El Kharrouba is located on north Sinai coastal plain, 10 km east of El Arish city. It is bounded from the north by the Mediterranean Sea shoreline and from the south by El Arish-Rafah Highway (Fig. 1). The El Kharrouba Coast Guard Asphaltic Road crosses the area perpendicular on the Mediterranean Sea shoreline and divides it into two sectors. The studied sand dunes extend for about 2 km parallel to the shoreline with a width of about 1.25 km and cover an area of about 2.5 km^2.

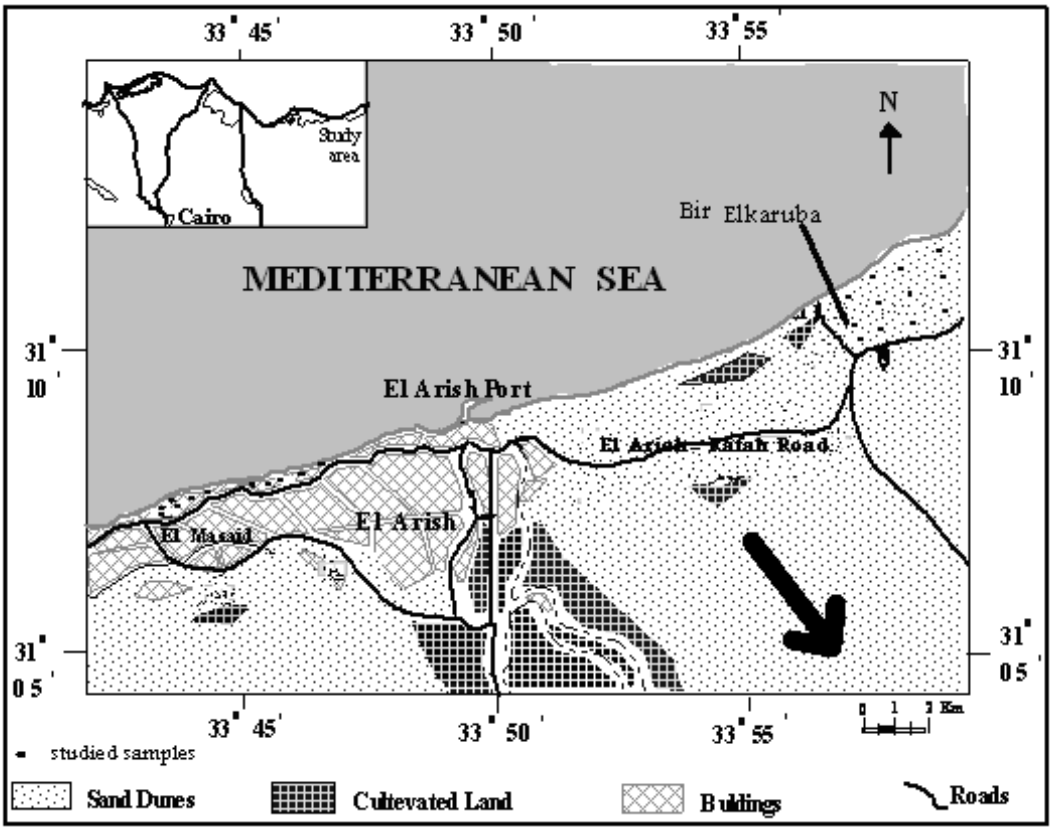

Fig. (1): Location of the two studied areas at El Massaid and El Kharrouba. The bold arrow represents the direction of the air winds.

The other area is located at El Mssaid beach about 10 km to the west of El Arish city. The area is chosen to be parallel to the shore line with a 3 km long before El Massaid resort, Fig. (1).

It was obvious that the occurrence of the dune deposits on the two studied areas introduces a number of negative impacts especially, the radiation hazard. The radiation hazards, caused by the black sand deposits, increase with their concentration in the beach sands. The radiation hazards are mainly due to the presence of monazite and to less extent to zircon minerals along with the orthoclase mineral contained in the black sand deposits.

These minerals contain radionuclides of the ^{238}U and ^{232}Th series besides the non-series radionuclide ^{40}K[(2)].

This study aims to investigate the correlation between the concentration of the heavy minerals in the beach sands at El Kharrouba and El Massaid areas and the terrestrial radioactivity at these areas. Also, the study intends to evaluate the radiation exposure due to these sands.

2. EXPERIMENTAL METHODS AND TECHNIQUES

2.1. Sample locations

Twenty three samples were collected for the studied areas. Eleven samples (1-11) were collected from the beach sands at El Massaid close to the shore line, Fig. (2). The remaining samples (12-23) were collected from El Kharrouba sand dunes along three paths parallel to the shore line. The first path extends at a distance of about 100m from the shore line, Fig. (3).

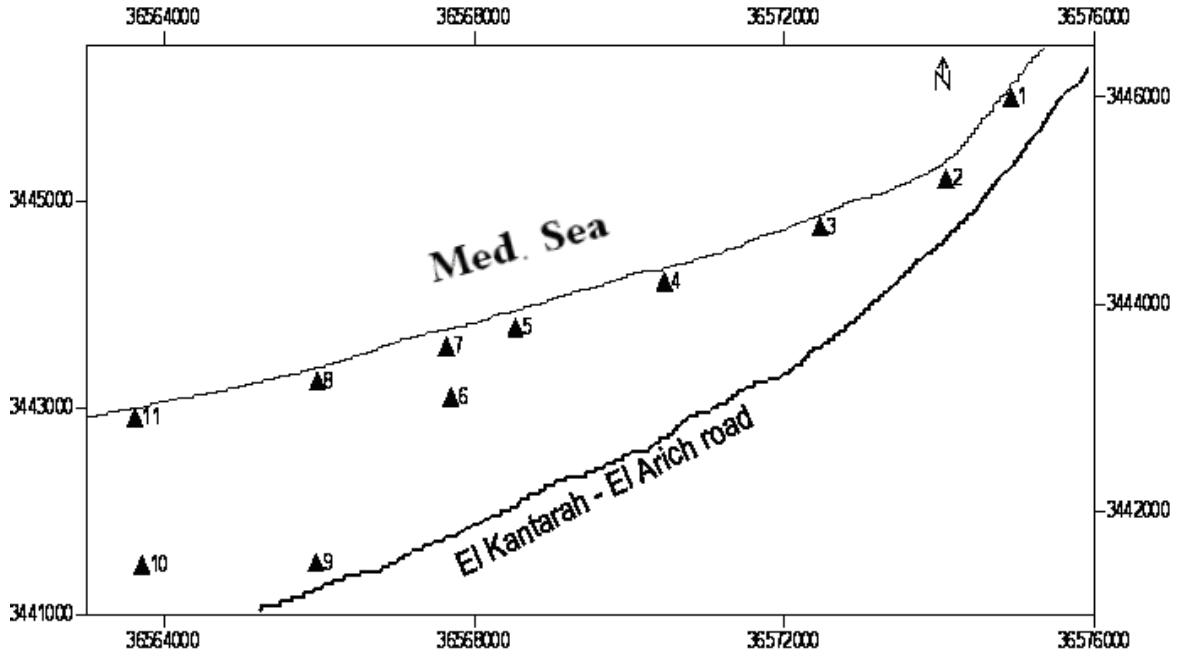

Fig. (2): Distribution of sample locations at El Massaid beach.

2.2. Determination of the percentage concentration of the total heavy minerals in the sands at El Massaid beach and El Kharrouba sand dunes

To determine the heavy mineral contents of the studied beach sands, sands collected from the hole at each monitoring station were splitted by quartering using Jon's splitter to get a representative sample. The 50g sample was put in a carrot shape funnel (250cm^3). Bromoform (sp. Gr. 2.85 gm/cm^3) was added to the sample in a quantity enough to make the solid/liquid ratio suitable to give a complete freedom for all the particles to sink or float. After a suitable time at rest, the sample was separated into a float layer and a sink layer with clear liquid layer in-between. The sink of the total heavy fraction was taken on filter paper in a precipitating funnel and the float or the light fraction was taken on another filter paper in another precipitating funnel. After complete filtration, the remaining bromoform in the bore spaces of mineral grains and the thin film coating the grains of both heavy and light fractions was washed with acetone. Both light and heavy fractions were dried and weighed. The percentage of each of heavy and light fractions was calculated relative to the original representative sample[3].

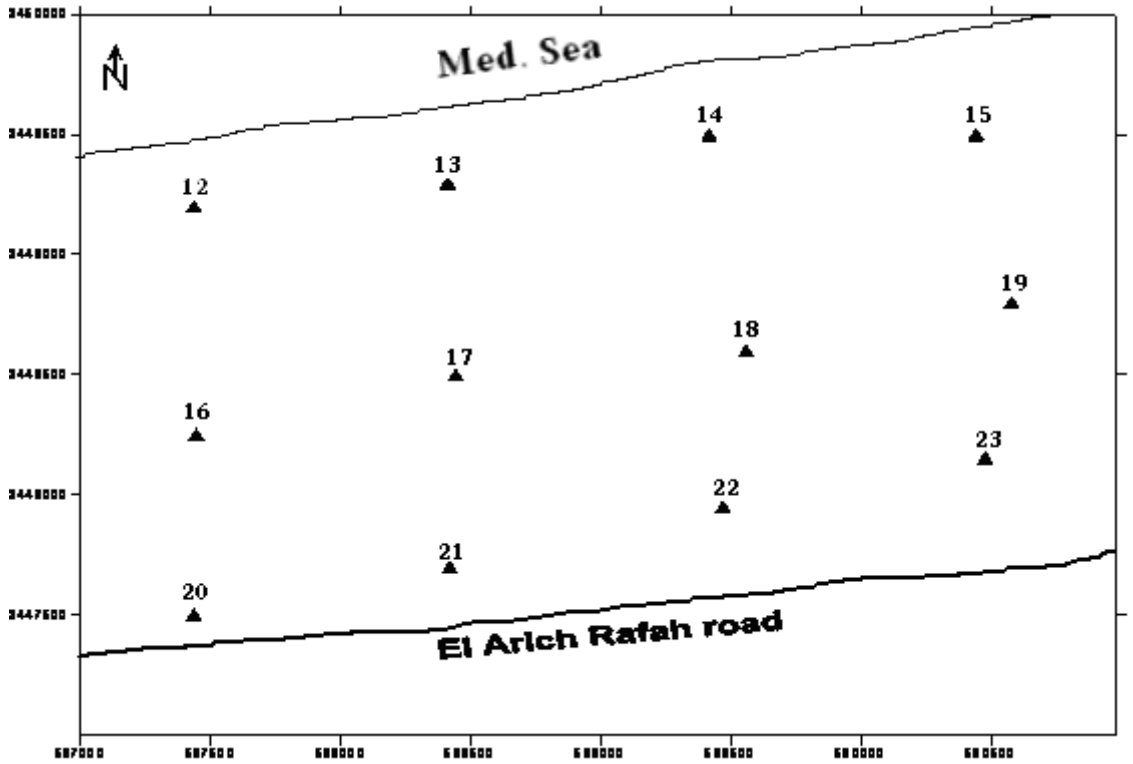

Fig. (3): Distribution of sample locations at El Kharrouba sand dunes.

2.3. Radiometric measurements

About 300-350g from each sample was packed in a plastic container, sealed well and stored for about 30 days before analysis. This prevents the escape of radiogenic gases ^{222}Rn and ^{220}Rn and allows the in-growth of uranium ^{238}U and thorium ^{232}Th decay products to reach secular equilibrium. After attainment of secular equilibrium, each of the prepared samples was measured in the laboratory for their U, Th, Ra and K contents using a high efficiency multichannel analyzer of γ-ray spectrometer (NaI detector). Each sample was counted for 1000s. The radiometric measurement for the studied radionuclides was carried out through four energy regions of interest (ROIs). Since uranium and thorium are not γ-emitters, they were measured indirectly through the γ-ray photons emitted from their decay products, ^{234}Th (81-108keV) for ^{238}U, ^{212}Pb (221-273keV) for ^{232}Th, and radium was measured from the γ-ray photon emitted by ^{214}Pb (327-390keV) whereas potassium was measured directly from the γ-ray photon emitted by ^{40}K (1319-1471keV). Consequently, they are expressed as equivalent U (eU), equivalent thorium (eTh) and equivalent radium (eRa). The chosen energy regions for U, Th, Ra and K were determined from the indicated energy lines of the spectra generated by means of laboratory uranium, thorium, radium and potassium reference standard samples provided by the IAEA.

This technique was carried out at laboratory of γ-ray spectrometry of the Egyptian Nuclear Materials Authority (ENMA). Its probable measurement error was about 10%[4].

The values of eU and eTh in ppm as well as K in percent were converted to activity concentrations, (Bq/kg), using the conversion factors given by the International Atomic Energy Agency[5]. The activity concentration of a sample containing 1 ppm by weight of ^{238}U is 12.35 (Bq/kg), 1 ppm of ^{232}Th is 4.06 (Bq/kg), 1 ppm of ^{226}Ra is 11.1 (Bq/kg) and 1 % of ^{40}K is 313 (Bq/kg).

3. RESULTS AND DISCUSSIONS

3.1. Relation between the concentration of heavy minerals and the activity concentration in the beach sands at El Massaid and in the sand dunes at El Kharrouba

Table (1) represents the values of the percentage weight of the total heavy minerals, T.H. (%), in the beach sands at a) El Massaid and in the sand dunes at b) El Kharrouba. From the table, the average of the concentration of heavy minerals over the eleven location at El Massaid beach is higher than the average concentration of heavy minerals in the sands at El Kharroba. However, the average values of the percentage total heavy minerals in the sands at both El Massaid beach and El Kharrouba dunes are higher the threshold value of the economic concentration (~2%).

Also, Table (1) represents the activity concentration (Bq/kg) of the radionuclides; ^{238}U, ^{232}Th, ^{40}K and ^{226}Ra besides the total activity concentration in the sands collected from a) El Massaid beach and b) El Kharrouba sand dunes.

The average activity concentration of both ^{238}U and ^{232}Th is much below the worldwide average of 33 and 45(Bq/kg),respectively[6]. The activity concentration of ^{40}K in the sands at El Massaid beach and in the sand dunes at El Kharrouba reflects a particular characteristic of the sands originated from the beach deposits; below 400 (Bq/kg)[6].

Also, from Table (1), the average activity concentrations of ^{238}U and ^{232}Th in the sand dunes at El Kharrouba are higher than these concentrations in the sands at El Massaid beach. However, Barakat[1] concluded that the values of the percentage concentrations of the radioactive minerals; monazite and zircon in the sand dunes are higher than their values in the sands along the Mediterranean coastal plains at Egypt.

On the other hand, the activity concentration of ^{40}K in the sand dunes at El Kharrouba is higher than that in the beach sands at El Massaid. This is due to the fact that air winds displace the lighter sands, feldspars, which have the potassium as a major constituent down the beach to build up the sand dunes and leave the heavier non-radioactive mineral sands; magnetite and ilmenite.

These arguments are reflected in Figs. (4a and b) which reveal the linear proportionality of the variation of the activity concentration with the variation of the percentage concentration of the total heavy minerals in the sands at both El Massaid beach and El Kharrouba dunes.

The slope of the regression line for El Massaid beach sands is 4.41 i.e. 1% of total heavy minerals in these sands adds 4.41 Bq/kg to the total activity concentration at El Massaid area while the slope of the regression line for El Kharrouba sand dunes is 21.84 i.e. 1% of the total heavy minerals adds 21.84 Bq/kg to the total activity concentration in the sands at El Kharrouba dunes. Again, the higher value of the slope of the regression line for El Kharrouba sands is ascribed to the higher concentrations of the radioactive minerals; monazite and zircon in these sands.

Table (1): Percentage of the heavy minerals, (T.H. %), activity concentration (Bq/kg) of ^{238}U, ^{232}Th, ^{40}K, ^{226}Ra and the total activity concentration in the sands at a) El Massaid beach and b) El Kharrouba sand dunes.

So. N.	T.H. (%)	^{238}U (Bq/kg)	^{232}Th (Bq/kg)	^{40}K (Bq/kg)	^{226}Ra (Bq/kg)	Total (Bq/kg)
a) El Massaid beach						
1	4.35	24.70	4.06	0.00	0.00	28.76
2	9.25	12.35	8.12	46.95	0.00	67.42
3	4.51	24.70	4.06	0.00	0.00	28.76
4	11.14	37.05	24.36	0.00	22.20	83.61
5	5.84	24.70	8.12	0.00	0.00	32.82
6	6.25	24.70	8.12	0.00	11.10	43.92
7	9.65	37.05	16.24	0.00	11.10	64.39
8	14.68	24.70	4.06	68.86	0.00	97.62
9	3.56	37.05	4.06	0.00	0.00	41.11
10	3.94	24.70	8.12	0.00	0.00	32.82
11	4.88	24.70	8.12	0.00	0.00	32.82
Ave.	7.10	26.95	8.86	10.53	4.04	50.37
b) El Kharrouba sand dunes						
12	2.67	37.05	12.18	3.13	11.10	63.46
13	8.68	37.05	12.18	140.9	11.10	201.2
14	1.51	37.05	8.12	0.00	0.00	45.17
15	5.05	37.05	8.12	78.25	11.10	134.5
16	1.88	37.05	8.12	15.65	0.00	60.82
17	8.28	24.70	8.12	147.1	11.10	191.0
18	1.06	12.35	8.12	0.00	0.00	20.47
19	9.23	49.40	8.12	150.2	0.00	207.8
20	7.37	24.70	12.18	128.3	11.10	176.3
21	1.31	37.05	8.12	0.00	0.00	45.17
22	3.25	12.35	12.18	53.21	11.10	88.84
23	4.66	24.70	4.06	84.51	0.00	113.3
Ave.	4.58	30.88	9.14	66.77	5.55	112.3

The intercepts of the regression lines for the studied sands give the values of the total activity concentrations in the light sands at El Massaid beach and El Kharrouba dunes, Figs. (4a and b). The higher value of the intercept for El Kharrouba sand dunes relative to the intercept for El Massaid beach sands is ascribed to the displacement of the lighter potassium minerals from the beach towards the sand dunes by the effect of air winds, Fig. (1).

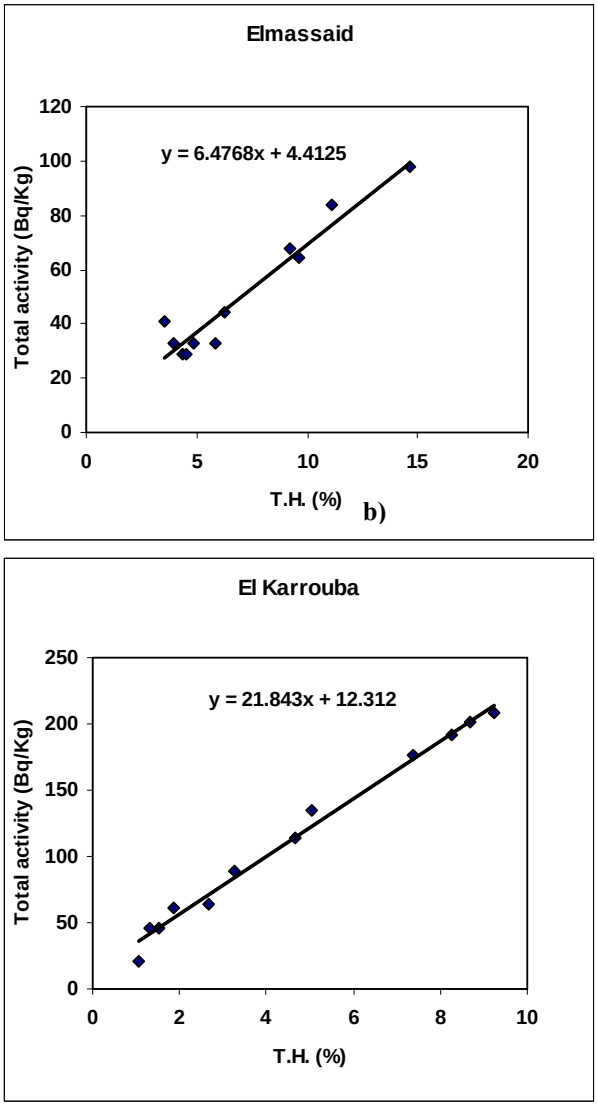

Fig. (4): Variation of the total activity concentration (Bq/kg) with the percentage weight of the total heavy minerals in the sands from a) El Massaid beach and b) El Kharrouba dunes.

3.2. Public exposure from sands at El Massaid beach and El Kharrouba sand dunes

3.2.1. External exposure

3.2.1.1. Absorbed dose

The conversion factor used to calculate the absorbed dose rate *D* is given as[7]:

$$D\ (\mathrm{nGyh^{-1}}) = 0.427\mathrm{U} + 0.662\mathrm{Th} + 0.043\mathrm{K} \qquad (1)$$

where

U, Th and K are the mean activities of ^{238}U, ^{232}Th and ^{40}K in (Bq/kg), respectively, Table (1).

Table (2) represents the absorbed dose *D* (nGy/h) estimated at 1m above the sands at 11 locations at El Massaid beach and at 1m above the sand dunes at 12 locations at El Kharrouba using equation (1). From the table, the average value of *D* at El Massaid beach is lower than the average value at El Kharrouba sand dunes. However, direct measurements of absorbed dose rates in air have been carried out in many countries of the world. The population-

weighted average is 59 nGy h^{-1}. The average values range from 18 to 93 nGy h^{-1}. A typical range of variability for measured absorbed dose rates in air is from 10 to 200 nGy h^{-1}. The population-weighted values give absorbed dose rate in air outdoor from terrestrial gamma radiation of 60 nGy h^{-1} [6].

3.2.1.2. External effective dose

The committee (UNSCEAR, 2000)[6] proposed occupancy factors 0.8 and 0.2 for the indoor and outdoor, respectively. Besides, the ratios of indoor to outdoor exposures are ranged from 0.6 to 2.3, with a population–weighted value of 1.4. The indoor exposures are 40% greater than the outdoor exposures. Values are less than one are in Thailand, and United States and Iceland, where wood frame construction is common. High values of the ratio (>2) result from high levels indoors in Sweden and Hong Kong. Low values outdoors relative to indoors are in the Netherlands.

Table (2): Absorbed dose rate *D* (nGy/h) at 1m over the sands, the annual effective outdoor external dose $E_{ex,\,out}$, the annual effective indoor external dose $E_{ex,\,indoor}$ and the total effective external dose due to the sands at a) El Massaid beach and b) El Kharrouba sand dunes.

L. N.	*D* (nGy/h)	$E_{ex,\,out}$ (mSv/y)	$E_{ex\,,\,indoor}$ (mSv/y)	$E_{ex,\,total}$ (mSv/y)
a) El Massaid beach				
1	13.2	0.016	0.091	0.107
2	12.7	0.016	0.087	0.103
3	13.2	0.016	0.091	0.107
4	31.9	0.039	0.219	0.259
5	15.9	0.020	0.109	0.129
6	15.9	0.020	0.109	0.129
7	26.6	0.033	0.182	0.215
8	16.2	0.020	0.111	0.131
9	18.5	0.023	0.127	0.150
10	15.9	0.020	0.109	0.129
11	15.9	0.020	0.109	0.129
Ave.	17.8	0.022	0.122	0.144
b) El Kharrouba sand dunes				
12	32.9	0.040	0.226	0.267
13	16.9	0.021	0.116	0.137
14	24.6	0.030	0.169	0.199
15	10.6	0.013	0.073	0.086
16	15.6	0.019	0.107	0.126
17	21.2	0.026	0.146	0.172
18	22.2	0.027	0.153	0.180
19	21.2	0.026	0.146	0.172
20	29.9	0.037	0.206	0.242
21	21.9	0.027	0.150	0.177
22	24.1	0.030	0.166	0.195
23	24.0	0.029	0.165	0.194
Ave.	22.1	0.027	0.226	0.179

The annual effective doses are determined as follows[6]:
Outdoor effective dose $E_{ex,\ out}$ (mSv/y)=

$$\boldsymbol{D\ (nGyh^{-1})\ x\ 8760\ h\ x\ 0.2\ x\ 0.7\ x\ 10^{-6}} \qquad \textbf{(2)}$$

Indoor effective dose $E_{ex,\ indoor}$ (mSv/y)=

$$\boldsymbol{D\ (nGyh^{-1})\ x\ 1.4\ x\ \ 8760\ h\ x\ 0.8\ x\ 0.7\ x\ 10^{-6}} \qquad \textbf{(3)}$$

Table (2) represents the annual outdoor effective dose $E_{ex,\ out}$ (mSv/y) for the public due to the terrestrial radioactivity at El Massaid beach and at El Kharrouba sand dunes estimated using equation (2). The average values of $E_{ex,\ out}$ at these locations are 0.022 (mSv/y) and 0.027 (mSv/y), respectively. These values are much lower than the worldwide average of the outdoor external effective doses, 0.07 (mSv/y)[6].
Indoor exposure due to gamma rays, is mainly determined by the materials of construction, the indoor exposure is greater than the outdoor exposure, if earth materials have been used, the source geometry changes from half-space to more surrounding configuration indoors, when the duration of occupancy is taken into account indoor exposure becomes more significant, building constructed of wood decrease the indoor exposures.
Table (2) represents the annual indoor effective dose $E_{ex,\ indoor}$ (mSv/y) for the public due to the regular uses of sands collected from El Massaid beach and from El Kharrouba sand dunes estimated using equation (3). The average values of $E_{ex,\ indoor}$ due to the sands from the studied areas are 0.122 and 0.226 (mSv/y), respectively. These averages are lower than the worldwide average, 0.41 (mSv/y)[6].

3.2.1.3. Total external effective dose

Table (2) represents the total annual effective external dose $E_{ex,\ total}$ (mSv/y) which is the sum of $E_{ex,\ out}$ and $E_{ex,\ indoor}$ for the public due to the sands collected from El Massaid beach and El Kharrouba dunes. The average values of $E_{ex,\ total}$ are 0.616 and 0.662 (mSv/y), respectively. The worldwide average of the annual effective dose is 0.48 mSv range, with the results for individual countries being within 0.3-0.6 mSv range[6].

3.2.2. Internal exposure to radon gas

3.2.2.1. Radon flux due to a building element

The estimation of the diffusive entry rate from building materials, the flux density rate from one side of a building element such as wall and floor is given by the following expression[6]:

$$\boldsymbol{J_{Db} = {}^{226}Ra\ \lambda_{Rn}\ f\ \rho_s\ L\ \tanh(d/L)} \qquad \textbf{(4)}$$

where,
^{226}Ra : is the activity concentration of ^{226}R in the sands (Bq kg^{-1}), Table (1),
J_{Db} : is the flux density of radon from a building element (Bq m^{-2} s^{-1}),
f : is the emanation coefficient of the sand grains,
ρ_s : is the density of the building element kg/m^3,
L : is the diffusion length in concrete that equals to 18 cm,
d : is the wall half-thickness of the slab (10 cm).

The parameters of the standard house and building materials are represented in Table (3).

Table (3): Parameters of the standard house and building materials used in this study [6].

Area (m^2)	Volume (m^3)	f	ρ_s (kg m^{-3})	λ_{Rn} (s^{-1})	d (m)	L (m)
450	250	0.1	1600	$2.1x10^{-6}$	0.1	0.18

Table (4) represents the estimated values of J_{Db} at the studied locations. From the table, the average value of radon flux, J_{Db} (Bq m^{-2} s^{-1}), from a building element made of sands from El Massaid beach into the air of a reference house is $1.18x10^{-4}$ while this value is $1.5x10^{-4}$ when the building element is made of sands collected from El Kharrouba sand dunes.

3.2.2.2. Indoor radon concentration

Indoor radon concentration in spaces other than tunnels is estimated using the formula[8]:

$$C_{Rn,\,indoor} = (J_{Db} \times S_B/V) / \lambda_v + C_{Rn,\,out} \qquad (5)$$

where,

$C_{Rn.\,indoor}$: is the indoor radon activity concentration in a reference house (Bq m^{-3}),
J_{Db} : is the flux density of radon from a building element (Bq m^{-2} h^{-1}),
S_B : is the emanating surface area ($450m^2$),
V : is the volume of the reference house that equal ($250m^3$),
λ_v : is the ventilation rate chosen to equal (1 h^{-1})[6],
$C_{Rn,\,out}$: is the worldwide average of the outdoor radon activity concentration, 10Bq m^{-3} [7].

Table (4) represents the indoor radon gas concentration $C_{Rn,\,indoor}$ Bq/m^3 in the air of a reference house due to the use of sands collected from El Massaid beach or El Kharrouba sand dunes. The average values of the indoor radon gas concentration due to the sands from the two areas are 10.8 and 11.1 Bq/m^3, respectively. However, the values of $C_{Rn,\,indoor}$ are much below the worldwide variability range of 30-40 Bq/m^3 [6].

3.2.2.3. Internal effective dose due to radon gas

For the representative concentrations of radon the equilibrium factors of 0.4 outdoors and 0.6 indoors, the annual effective doses (mSv/y) are derived from the following equations[6]:

Outdoor annual effective dose $E_{Rn,\,out}$:

$$10\ (Bqm^{-3}) \times 0.4 \times 8760h \times 0.2 \times 9nSv\ (Bq\ h\ m^{-3})^{-1} \times 10^{-6} = 0.063\ (mSv/y) \qquad (6)$$

Indoor annual effective dose $E_{Rn,\,indoor}$

$$= C_{Rn}\ (Bqm^{-3}) \times 0.6 \times 8760h \times 0.8 \times 9nSv\ (Bq\ h\ m^{-3})^{-1} \times 10^{-6} \qquad (7)$$

Table (4): Radon flux density J_{Db} (Bq m^{-2} h^{-1}), $C_{Rn.\ indoor}$ (Bq m^{-3}), the total annual effective dose due to radon gas $E_{Rn,\ total}$ (mSv/y) and the total annual effective dose due the public uses of sands from a) El Masaid beach and b) El Kharrouba sand dunes

.

L. N.	J_{Db} (Bq m^{-2} s^{-1})	$C_{Rn,\ indoor}$ (Bq m^{-3})	$E_{Rn.\ indoor}$ (mSv/y)	$E_{Rn,\ total}$ (mSv/y)	E_{Total} (mSv/y)
a) El Massaid beach					
1	0.0000	10.000	0.378	0.441	0.548
2	0.0000	10.000	0.378	0.441	0.544
3	0.0000	10.000	0.378	0.441	0.548
4	0.0007	14.385	0.544	0.607	0.866
5	0.0000	10.000	0.378	0.441	0.570
6	0.0003	12.193	0.461	0.524	0.653
7	0.0003	12.193	0.461	0.524	0.739
8	0.0000	10.000	0.378	0.441	0.572
9	0.0000	10.000	0.378	0.441	0.591
10	0.0000	10.000	0.378	0.441	0.570
11	0.0000	10.000	0.378	0.441	0.570
Ave.	1.18x10^{-4}	10.797	0.408	0.471	0.616
b) El Kharrouba sand dunes					
12	0.0000	10.000	0.378	0.441	0.708
13	0.0000	10.000	0.378	0.441	0.578
14	0.0003	12.193	0.461	0.524	0.723
15	0.0000	10.000	0.378	0.441	0.528
16	0.0003	12.193	0.461	0.524	0.651
17	0.0000	10.000	0.378	0.441	0.613
18	0.0003	12.193	0.461	0.524	0.704
19	0.0000	10.000	0.378	0.441	0.613
20	0.0003	12.193	0.461	0.524	0.767
21	0.0000	10.000	0.378	0.441	0.618
22	0.0003	12.193	0.461	0.524	0.720
23	0.0003	12.193	0.461	0.524	0.719
Ave.	1.5x10^{-4}	11.096	0.419	0.483	0.662

The outdoor annual effective dose due the inhalation of radon gas and its decay products $E_{Rn,\ out}$ at El Massaid and El Kharrouba areas is constant and equals 0.063 mSv, Equation (6). Table (4) represents the indoor annual effective dose $E_{Rn,\ indoor}$ and the total annual effective dose from radon gas and its decay products $E_{Rn,\ total}$ which is the sum of $E_{Rn,\ out}$ and $E_{Rn,\ indoor}$. The average values of the total annual effective dose due to radon $E_{Rn,\ total}$ at El Massaid and El Kharrouba area are 0.471 and 0.483 (mSv), respectively. These values are lower than the recommended action limit in the range 3-10 mSv[9].

From Table (4), the average of the total annual effective dose E_{Total} from both external and internal public exposure due to the use of the sands from El Massaid beach is 0.616 (mSv) while the average of E_{Total} due to El Kharrouba sand dunes is 0.662 (mSv). These values are lower than the reported public effective dose[6].

Generally, the low exposures from the terrestrial radioactivity in the sands at El Massaid beach and at El Karrouba indicate the safe use of these sands as building materials.

4. CONCLUSIONS

The heavy minerals in the sands at both El Massaid beach and El Kharrouba dunes are estimated to have economic concentrations. The variation of the activity concentration in the sands at both El Massaid and El Kharrouba showed positive relations with the variation of the percentage concentration of the heavy minerals due to the presence of radioactive minerals monazite and zircon. The orthoclase feldspar reflected the typical concentration of potassium in the beach sands. The average values of the annual effective dose due the probable use of the sands at El Massaid beach and El Kharrouba sand dunes were lower than the worldwide average indicating the safe use of these sands as building materials.

RERERENCES

(1) M.G. Barakat, (2004): Sedimentological studies and evaluation of some black sands deposition on the northern coast of Egypt. M.Sc.Thesis, Faculty of Science, Alexandria University

(2) UNSCEAR (1993): Exposures from natural sources of radiation. United Nations Scientific Committee on the Effects of Atomic Radiation, Report to the General Assembly, Annex A, pp. 33-89.

(3) Y. A. Abdel-Razek and A. F. Bakhit, (2009): Comparison Between the Measurements of Radon Gas Concentrations and γ-ray Intensities in Exploring the Black Sands At El-Burullus Beach. Arab. J. Nucl. Sci. & Aplicat. 42, 214, Oct (2009).

(4) M. Matolin, (1991): Construction and use of spectrometric calibration pads for laboratory γ-ray spectrometry, NMA, Egypt. A Report to the Government of the Arab Republic of Egypt. Project EGY/4/030-03, IAEA (1991), 14p.

(5) IAEA (1989): Construction and use of calibration facilities for radiometric field equipment. International Atomic Energy Agency, IAEA Technical Reports Series No. 309, IAEA, Vienna.

(6) UNSCEAR (2000): Exposures from natural sources of radiation. United Nations Scientific Committee on the Effects of Atomic Radiation, Report to the General Assembly, Annex A, pp. 83-156.

(7) UNSCEAR (1988): Exposures from natural sources of radiation. United Nations Scientific Committee on the Effects of Atomic Radiation, Report to the General Assembly, Annex A, pp. 49-134.

(8) **8**-UNSCESR, (1982): Exposures to radon and thoron and their decay products. United Nations Scientific Committee on the Effects of Atomic Radiation, Report to the General Assembly, Annex D, pp. 141-210.

(9) ICRP (1993): Protection against ^{222}Rn at home and at work. ICRP Publication 65. Annals of the ICRP 23 (4). Pergamon Press, Oxford, UK, 45p.